

Membrane Fouling Mechanisms in a Membrane-Coupled Anaerobic Baffled Reactor (ABR) Treating a Complex Wastewater

Sudhir Pillay
MSc

Submitted in fulfillment of the academic requirements for the degree of
Doctor of Philosophy
In the School of Chemical Engineering
University of KwaZulu-Natal, Durban

July 2011

DECLARATION

I, **Sudhir Pillay**, confirm that

- (i) This thesis is my own work and has been generated by me as the result of my own original research except where otherwise indicated.
- (ii) I have acknowledged all main sources of assistance. Where the thesis is based on work done jointly by myself and others, I have made it clear what was done by others and what I have contributed myself.
- (iii) This thesis has not been submitted for any degree or examination at any other academic institute.
- (iv) This thesis does not contain work of others, including writing, data, pictures, graphs or other information, unless specifically acknowledged as being sourced from other persons. This also includes text, graphics or tables copied and pasted from the internet which are acknowledged in the reference section.
- (v) Where I have reproduced a publication of which I am an author, co-author or editor, I have indicated in which part of the publication was actually written by myself alone and have fully referenced such publications.

Signed:

(Mr. Sudhir Pillay)

Place: University of KwaZulu-Natal

As the candidate's supervisors, we have approved this thesis for submission

Dr KM Foxon

Prof .CA Buckley

ACKNOWLEDGEMENTS

I would like to thank my supervisors, Prof. Chris Buckley and Dr. Katherine ‘Kitty’ Foxon for their support and unwavering faith in my ability to complete this degree. Thanks Chris for the many impromptu meetings on university and faraway places. I am continuously learning from you and I appreciate your guidance. There are three things that I distinctly remember from our time together that will stay with me for the rest of my life:

- The first is making me memorise the five essential requirements for a Masters and PhD degree (*understand the nature of the problem, be conversant with the literature, master the necessary techniques, apply the appropriate methodology, understand the implications of your results and for a PhD, you must make a contribution to the knowledge base*). It is the first question that Chris asks when you start post-graduate studies and you are expected to know it at a drop of a hat.
- The second is that *it is just a PhD or MSc* (depending on who Chris talks to). This statement is not the most reassuring of statements when you are doing post-graduate studies or when something does not work according to plan. But the statement is true; there are other things to life and your work does not have to win a Nobel Prize.
- And lastly, *never burn bridges between yourself and other people because you never know when you may need their assistance*. It seems everyone in the water field knows Chris Buckley or has worked together with him. When I had unusual requests (buckets of faeces, sludge, pipe cleaning devices or membranes), Chris usually called one of his contacts and arranged for me to pick it up.

Thanks Kitty for all the supervision and patience from the start of my MSc to the end of my PhD. I know sometimes that I am unconventional in my professional approach and I thank you for keeping me grounded. I also promise to stop peeking in your office while you are busy to ask for help (especially when I did not arrange a meeting).

The research results presented in this thesis emanate from a project funded by the European Union *EUROMBRA* Project and the South African Water Research Commission, Project K5/1661 entitled:

The Development of an Anaerobic Membrane Bioreactor (Pillay *et al.*, 2011a).

I would like to acknowledge all persons involved in this project and thank them for their assistance and input:

Prof. CA Buckley, Mr. CJ Brouckaert, Dr. KM Foxon, Dr. S Pollet, Mr. J Kapuku and Dr. G Gugliemi.

The financing of the study by European Union *EUROMBRA* Project and the Water Research Commission is gratefully acknowledged as is the contribution of the members of the Steering Committee.

I would like to express my thanks to the following people and organisations:

- eThekwini Municipality for arranging places for me to collect faeces – the most valuable resource in our laboratory.
- Bremen Overseas Research and Development Association (BORDA) staff and workers especially Mr. Andreas Schmidt and Ms. Susmita Sinha.
- National Research Foundation for funding.
- Mr. Olivier Lorrain from Polymem for supplying hollow-fibre modules.
- Mr. Tim Young from Aquator for supplying Kubota modules.
- Prof. Lingam Pillay from Durban University of Technology for supplying woven-fibre modules.
- Technical and support staff at the University of KwaZulu-Natal. Many thanks to Mr. Danny Singh, Mr. Ken Jack, Mr. Les Henwood, Mrs. Rekha Maharaj, Mr. Preyothan Nayager, Mr. Sadha Naidoo and Mr. Conrad Sydney.
- Prof. TorOve Leiknes, project manager of the *EUROMBRA* Project. Thanks to him and his team from Norwegian University of Technology for inviting me to come to your laboratories. It was a good (and cold) experience. I miss your constant ‘threats’ of inviting me to defend my dissertation in Norway. I was also blown away by your hospitality and your leadership.
- Dr. Giuseppe Gugliemi from University of Trento, Italy for helping me to develop a biochemical model for the anaerobic baffled reactor. Many thanks to you and Martina for showing me around Italy.
- Dr. Valerie Naidoo, Mr. Jay Bhagwan and Dr. Heidi Snyman from the Water Research Commission, South Africa. I would like to thank Mr. Jay Bhagwan for being a mentor and role model to me. I would also like to thank Dr. Valerie Naidoo for her patience and understanding during this work.
- Prof. Corinne Cabassud and her team from the Institut National des Sciences Appliquées de Toulouse. I would like to thank Prof. Cabassud for giving me some useful literature on anaerobic membrane bioreactors and providing the methodology for the *EUROMBRA* Project. I would also like to thank Dr. Benoit Teychenne for showing me his laboratory set-up which I tried to replicate in our laboratory, Dr. Marlene Stricot for her hospitality and Mr. Valetin Yvenat for aiding me in equipment set-up, and data capture and analysis. You guys saved me a lot of time and effort.

-
- People from the Marianhill home from where I sampled. I may have not known your names but you always knew I was the toilet emptying man with the old, green Land Rover. Your toilet was the best to sample. Thanks for allowing us to come by whenever we wanted to. I miss your hospitality as much as you will probably miss my service.
 - To Mr. Scebi Mkhize, Mr. Mluleki Mnguni and Mr. Mikey Gunes for coming with me to Marianhill to collect faeces. Scebi, you are the best shit shoveller in the world. Nobody I worked with could empty a pit toilet as fast and efficiently as you could. I tried many times but you always filled the bucket faster than me and with less spilt.
 - Many thanks to my colleagues and friends at university: Mr. Wolf Raber, Mr. Diego Avesani, Dr. Tom Bond, Dr. Elisa Roma, Mr. David Hawksworth, Mr. Farai Mhlanga, Mr. Elly Obwaka, Mrs. Anusha Singh, Mrs. Merlien Reddy, Ms. Kavisha Nandhlal, Mr. Shameer Hareeparsad, Mr. Rinay Bhowmath, Mr. David Lockat, Mr. Lars Schöbitz, Mr. Brian Satola, Mr. Babatunde Bakare, Mr. Ashlee Reddy, Mr. Tarik Bodasingh, Mr. Alain Smith, Mr. Sandile Mbatha, Dr. Caleb Narasigadu, Dr. Lakesh Maharaj and Dr. Sershen Naidoo. Special thanks to Mrs. Chika Nwaneri for supplying me with a bucket of fresh poo whenever I needed it.
 - To my brother, Dr. Che Pillay and my sister-in-law, Dr. Marianna Ciacciariello. Thanks for reading some bits. You were always available to help me academically and financially. Also thanks to my other brother, Mr. Zubin Pillay, the one who decided against an academic life and the richest amongst us. Thanks for the numerous ‘loans’ and the car. I’ll pay it back someday. To my mom, thank you for helping me in all different ways through my life. I hope I get my doctorate before you. If a 60 year old mother, who works full-time, cooks, cleans and still washes my clothes gets a doctorate before me, I will be very disappointed in myself.
 - And finally thanks to the crazy bunch of international students who worked with me. To my adopted French son, Dr. Xavier Courtial, daddy misses you very much. To Dr. Linda Gaulke, it was a pleasure to be your colleague. To Mr. Nicolaus Reynaud, it was pleasure travelling and working with you in South Africa, India and Indonesia. To Ms. Sandra Hildbrand, thanks for your love and support. You are the most caring and loving partner I have ever had. Any lady who possesses the willpower to forget about her own injuries and can drag me out of a bus wreckage is worth keeping. And last, to my dearest friend and the best co-worker I have ever had, Dr. Samuel Pollet. Never in my life has someone encompassed the phrase *work hard, play hard* as well as you. You have shown me more of my own country than I knew possible and your enthusiasm for work was unmatched. Without you, the thesis would have never been completed. Many thanks and bisous!

ABSTRACT

This thesis presents a chemical and mathematical analysis of membranes filtration systems coupled to an anaerobic baffled reactor (ABR). The purpose of this investigation was to gain an understanding of the mechanisms involved in fouling in membranes coupled to an ABR and to use this understanding to develop a guideline for the implementation of a membrane polishing step to ABR sanitation applications. The research objective was derived from previous research at the Pollution Research Group which showed that although the ABR was a robust sanitation technology capable of superior performance over conventional septic tanks, the ABR effluent still requires nutrient and pathogen disinfection polishing to meet local discharge regulations. A similar situation has been reported in some ABR sanitation applications designed by the non-profit organisation BORDA (*Bremen Overseas Research and Development Association*). In these BORDA plants – called DEWATS (*DEcentralised WAstewater Treatment System*) units – the effluent from an ABR is treated by a combination of polishing steps. This includes constructed wetlands, ponds systems and/or anaerobic filters polishing steps. However, these polishing steps can have a large land area footprint and inconsistent pathogen removal has been reported in some plants.

In this thesis, membrane technology was evaluated as an alternate polishing step for ABR sanitation applications as it could be easily incorporated into the design of the ABR (fitted into the last compartment) with little or no change to the overall design. Moreover, membrane technology can be applied at lower land area footprint (than constructed wetlands or ponds) and has proven disinfection capabilities.

One of the challenges in this work was to operate membrane modules without gas scouring and using gravitational water heads to drive the membrane filtration process – in line with decentralised applications (no energy). Moreover, the conditions for membrane filtration were different to aerobic and other anaerobic membrane systems in that the membrane filtration step is at the back end of the ABR where the concentration of suspended solids and biodegradable substances are expected to be low. The novelty of this approach is that the mechanisms governing fouling will be different to other membranes systems (due to differences in membrane tank conditions, and the design and operation of modules).

This thesis presents and analyses the operating data from membrane filtration units treating the effluent from a laboratory-scale ABR system (200 L capacity). The laboratory ABR was fed with a complex synthetic wastewater comprised of ventilated improved pit latrine sludge, representative of black wastewater (faeces and urine), and was operated at different conditions

(phases). Specific membrane challenge experiments were performed during each of these phases of laboratory ABR operation and the results used to gain insight into the fouling mechanisms of membranes coupled to this system. The methods used to characterise the fouling in this thesis were stipulated by project partners from a larger international project – EUROMBRA - into which this work fits.

The principal findings of this research were:

- The laboratory ABR used in this thesis was not well-designed to the feed wastewater. The feed wastewater, made from diluted VIP sludge, had a low biodegradability content. Consequently, the large non-biodegradable portion built up in the reactor which sometimes required desludging or clogged overflow pipes to the ABR train. The main mechanism of treatment in this ABR plant occurred through solids retention and accumulation.
- A standardised test cell technique was used to determine the fouling propensities of the soluble fraction of different sludge sources. The results showed that the samples from starved pilot ABR had the lowest fouling propensity whilst the sample from a conventional anaerobic digester had the highest propensity. Gel-like fouling layers developed from compartment 3 (and to lesser extent from compartments 2 and 4) of the starved ABR which contained biogranules. Although these solutions had low fouling propensities, the layer was highly compressible. The tests also showed that the effluent from a laboratory ABR had similar fouling propensities to other samples (both aerobic and anaerobic) tested. The results could not be statistically validated due to non-linearity of data indicating that improvements to the technique are required.
- Different fouling mechanisms were observed between hollow-fibre and flat-sheet modules treating the same laboratory ABR effluent. This difference was hypothesised to be the result of membrane surface-bulk fluid interactions with an irremovable gel layer formation in the flat-sheet modules and removable ‘cake-like’ fouling in the hollow-fibre modules. The differences observed were thought to be the result of differences in membrane pore shape and surface topography.
- The fluxes of the modules tested were low (less than $1 \text{ L}\cdot\text{m}^{-2}\cdot\text{h}^{-1}$) under gravitational pressures suggesting that membrane polishing is better suited to small-scale ABR applications.

It was concluded that membrane performance, particularly the type of foulant responsible for fouling, differed according to the module type used. Hence, a situation where one module type can be used for all ABR sanitation applications does not exist. Modules should be rather chosen

for performance over time (higher quality product with reduced production versus a lesser quality product with higher production) and/or intended purpose of discharge (into a water body or less restricted agricultural irrigation). The practical experience gained from this study was used to design a membrane sump for a full-scale experimental DEWATS plant.

TABLE OF CONTENTS

DECLARATION.....	i
ACKNOWLEDGEMENTS.....	ii
ABSTRACT	v
TABLE OF CONTENTS.....	viii
LIST OF ABBREVIATIONS	xvii
LIST OF NOTATIONS	xiv
LIST OF FIGURES	xx
LIST OF TABLES	xli
CHAPTER 1: INTRODUCTION.....	1-1
1.1 INTRODUCTION	1-2
1.2 THE EUROMBRA PROJECT	1-4
1.3 CONTEXT OF THIS RESEARCH WITHIN THE EUROMBRA PROJECT	1-5
1.4 OBJECTIVES AND AIMS OF STUDY.....	1-7
1.5 PRODUCTS OF THE STUDY.....	1-8
1.6 THESIS OUTLINE	1-8
CHAPTER 2: LITERATURE REVIEW.....	2-1
2.1 ANAEROBIC DIGESTION	2-1
2.1.1 ADVANTAGES OF ANAEROBIC DIGESTION	2-2
2.1.2 THE CONVERSION PROCESS IN ANAEROBIC SYSTEMS	2-2
2.1.3 WATERBORNE ANAEROBIC SANITATION SYSTEMS	2-7
2.1.4 POST TREATMENT OPTIONS FOR ANAEROBIC SYSTEMS	2-14
2.1.4.1 Facultative Ponds.....	2-15
2.1.4.2 Overland Flow System	2-15

2.1.4.3	Trickling Filter (aerobic)	2-15
2.1.4.4	Anaerobic Filter	2-16
2.1.4.5	Constructed Wetland	2-17
2.1.5	THE ANAEROBIC BAFFLED REACTOR	2-19
2.1.5.1	Basic Design	2-19
2.1.5.2	Historical Overview of the Anaerobic Baffled Reactor.....	2-20
2.1.5.3	Start-up	2-20
2.1.5.4	Low-Strength Treatment.....	2-21
2.1.5.5	Shock Loadings (Organic and Hydraulic)	2-23
2.1.5.6	Effect of Temperature.....	2-24
2.1.5.7	Application of Anaerobic Baffled Reactors in Sanitation	2-25
2.2	MEMBRANE FILTRATION	2-33
2.2.1	PROCESS DESCRIPTION	2-34
2.2.2	MEMBRANE MATERIALS	2-35
2.2.3	MODULE CONFIGURATIONS	2-35
2.2.4	PROCESS TERMINOLOGY.....	2-37
2.2.5	EMPIRICAL MODELS	2-39
2.2.6	CONCENTRATION POLARISATION	2-40
2.2.7	MEMBRANE FOULING.....	2-42
2.2.7.1	Mixed Liquor Suspended Solids.....	2-43
2.2.7.2	Colloidal Particles.....	2-45
2.2.7.3	Extracellular Polymeric Substances	2-47
2.2.8	MEMBRANE CONFIGURATION	2-50
2.2.9	CRITICAL AND SUSTAINABLE FLUX CONCEPTS	2-53
2.2.10	MEMBRANE CLEANING.....	2-54
2.3	ANAEROBIC MEMBRANE BIOREACTORS	2-55
2.4	PATHOGEN REMOVAL BY MEMBRANE PROCESSES	2-60
2.5	CONCLUDING REMARKS	2-61
2.5.1	ABR.....	2-61
2.5.2	MEMBRANES.....	2-62
2.5.3	CHALLENGE	2-62
2.5.4	TECHNOLOGICAL GAPS	2-63

CHAPTER 3: DESIGN, CONSTRUCTION AND OPERATION OF LABORATORY SYSTEM

3.1	DESIGN AND CONSTRUCTION OF ABR.....	3-1
------------	--	------------

3.2	OPERATION OF ANAEROBIC BAFFLED REACTOR.....	3-4
3.2.1	FEEDING MODE	3-4
3.2.2	HYDRAULIC RETENTION TIME AND ORGANIC LOADING RATE	3-4
3.3	MEMBRANE FILTRATION SYSTEM	3-5
3.3.1	HOLLOW-FIBRE UNIT.....	3-5
3.3.2	FLAT-SHEET MEMBRANE UNIT	3-7
3.3.3	MEASUREMENT OF TMP IN MEMBRANE UNITS.....	3-10
3.4	FEED COLLECTION AND HANDLING	3-13
3.4.1	SYNTHETIC BLACKWATER	3-14
3.4.2	GREYWATER	3-17
3.5	FEED PREPARATION	3-18
3.5.1	SYNTHETIC DOMESTIC WASTEWATER.....	3-18
3.5.2	SYNTHETIC BLACKWATER	3-19
3.6	COMPARISON OF LABORATORY FEED WITH ACTUAL WASTEWATERS	3-20
3.7	MATERIALS AND METHODS.....	3-21
3.7.1	SAMPLING.....	3-22
3.7.2	FEED WASTEWATER	3-22
3.7.3	FEED TANK OVERFLOW	3-23
3.7.4	ABR EFFLUENT SAMPLES	3-23
3.7.5	MEMBRANE PERMEATE	3-23
3.8	OPERATIONAL AND MAINTENANCE ISSUES.....	3-24
3.8.1	ABR.....	3-24
3.8.2	MEMBRANE UNITS	3-25
3.8.3	POWER OUTAGES.....	3-26
3.8.4	RELOCATION OF FACULTIES	3-26
3.8.5	CONSTRUCTION DISTURBANCES	3-26
3.9	TERMINOLOGY	3-27
 CHAPTER 4: BENCH-SCALE EXPERIMENTS		4-1
4.1	THEORETICAL BACKGROUND	4-2
4.2	SAMPLING AND HANDLING	4-5
4.3	METHODOLOGY	4-5
4.3.1	EXPERIMENTAL SET UP	4-6
4.3.2	FRACTIONATION OF SOLUBLE PHASE	4-7
4.3.3	OPERATION OF TEST CELL	4-7

4.3.4	ANALYSES PERFORMED	4-9
4.4	RESULTS AND DISCUSSION.....	4-10
4.4.1	PERMEATE FLUX.....	4-10
4.4.2	DETERMINATION OF THE PRODUCT OF $\alpha.C_s$	4-14
4.5	DISCUSSION.....	4-36
4.6	CONCLUSIONS.....	4-38

CHAPTER 5: HOLLOW FIBRE FILTRATION 5-1

5.1	SHORT-TERM TMP-STEP EXPERIMENTS.....	5-1
5.1.1	INTRODUCTION.....	5-1
5.1.2	METHODOLOGY	5-2
5.1.2.1	Membrane Feed.....	5-2
5.1.2.2	Membrane Units	5-3
5.1.2.3	Filtration Experiment.....	5-3
5.1.2.4	Data Acquisition and Interpretation.....	5-5
5.1.2.5	Physico-Chemical Analyses	5-6
5.1.3	RESULTS AND DISCUSSION.....	5-6
5.1.3.1	Phase I Effluent	5-6
5.1.3.2	Phase III Effluent.....	5-11
5.1.3.3	Phase V Effluent.....	5-15
5.1.3.4	Phase VI Effluent.....	5-18
5.1.4	SUMMARY OF TMP STEP EXPERIMENTS.....	5-22
5.2	SHORT-TERM FILTRATION AT CONSTANT TMP	5-26
5.2.1	INTRODUCTION.....	5-26
5.2.2	METHODOLOGY	5-26
5.2.3	RESULTS AND DISCUSSION.....	5-27
5.2.4	CONCLUSIONS	5-29
5.3	LONG-TERM FILTRATION AT CONSTANT TMP	5-30
5.3.1	INTRODUCTION.....	5-30
5.3.2	METHODOLOGY	5-30
5.3.3	RESULTS AND DISCUSSION.....	5-31
5.3.4	CONCLUSIONS	5-33
5.4	MEDIUM-TERM FILTRATION OF ABR EFFLUENT	5-33
5.4.1	INTRODUCTION.....	5-34
5.4.2	METHODOLOGY	5-34
5.4.3	RESULTS AND DISCUSSION.....	5-34

5.4.4	CONCLUSIONS	5-35
5.5	SHORT-TERM FILTRATION USING TMP RELAXATION	5-35
5.5.1	INTRODUCTION	5-36
5.5.2	METHODOLOGY	5-36
5.5.3	RESULTS.....	5-37
5.5.4	CONCLUSIONS	5-37
5.6	MEDIUM-TERM FILTRATION OF SETTLED ABR EFFLUENT.....	5-38
5.6.1	INTRODUCTION	5-38
5.6.2	METHODOLOGY	5-38
5.6.3	RESULTS AND DISCUSSION.....	5-39
5.6.4	CONCLUSIONS	5-39
5.7	MEDIUM-TERM FILTRATION OF SOLUBLE ABR EFFLUENT	5-41
5.7.1	INTRODUCTION	5-41
5.7.2	METHODOLOGY	5-41
5.7.3	RESULTS.....	5-42
5.7.4	CONCLUSIONS	5-42
5.8	SUMMARY OF HOLLOW FIBRE FILTRATION EXPERIMENTS	5-43
 CHAPTER 6: FLAT SHEET FILTRATION		6-1
6.1	LONG TERM FILTRATION WITH ABR EFFLUENT	6-1
6.1.1	INTRODUCTION	6-2
6.1.2	METHODOLOGY	6-2
6.1.3	RESULTS AND DISCUSSION.....	6-5
6.1.4	CONCLUSIONS	6-15
6.2	MEDIUM TERM FILTRATION OF SUPERNATANT FROM SETTLED ABR EFFLUENT.....	6-15
6.2.1	INTRODUCTION	6-15
6.2.2	METHODOLOGY	6-16
6.2.3	RESULTS AND DISCUSSION.....	6-16
6.2.4	CONCLUSIONS	6-21
6.3	MEDIUM-TERM FILTRATION OF SOLUBLE ABR EFFLUENT	6-22
6.3.1	INTRODUCTION	6-22
6.3.2	METHODOLOGY	6-22
6.3.3	RESULTS AND DISCUSSION.....	6-23
6.3.4	CONCLUSIONS	6-28
6.4	SUMMARY OF FLAT-SHEET FILTRATION.....	6-28

CHAPTER 7: DISCUSSION AND CONCLUSIONS	7-1
7.1 INTRODUCTION	7-1
7.2 TECHNOLOGICAL GAP.....	7-1
7.3 DESIGN AND OPERATION OF THE PLANT.....	7-1
7.4 OPERATION OF ABR SYSTEM.....	7-2
7.5 QUANTIFYING FOULING PROPENSITY IN TEST CELLS	7-3
7.6 HOLLOW FIBRE MEMBRANE PERFORMANCE.....	7-6
7.7 FLAT SHEET MEMBRANE PERFORMANCE.....	7-8
7.8 EFFECT OF PORE SIZE AND SURFACE MORPHOLOGY ON FOULING LAYER DEVELOPMENT	7-8
7.9 CONTEXT OF OBSERVED FOULING BEHAVIOUR IN RELATION TO LITERATURE.....	7-20
7.10 IMPLICATIONS OF STUDY FOR DEWATS APPLICATION	7-23
7.11 MAIN CONCLUSIONS.....	7-25
CHAPTER 8: RECOMMENDATIONS.....	8-1
8.1 STANDARD TEST CELL TECHNIQUE.....	8-1
8.2 FUTURE RESEARCH.....	8-1
APPENDIX I: LIST OF EUROMBRA PARTNERS	I-1
APPENDIX II: OPERATION OF THE ANAEROBIC BAFFLED REACTOR.....	II-1
A 2.1 INTRODUCTION	II-1
A 2.2 PHASE I	II-3
A 2.2.1 FLOW RATE, DOWN-TIME AND INCIDENTS	II-3
A 2.2.2 ABR PERFORMANCE	II-4
A 2.3 PHASE II.....	II-4
A 2.3.1 FLOW RATE, DOWN-TIME AND INCIDENTS	II-5
A 2.3.2 ABR PERFORMANCE	II-5
A 2.4 PHASE III	II-6
A 2.4.1 FLOW RATE, DOWN-TIME AND INCIDENTS	II-6
A 2.4.2 ABR PERFORMANCE	II-7
A 2.5 PHASE IV	II-8
A 2.5.1 FLOW RATE, DOWN-TIME AND INCIDENTS	II-9

A 2.5.2	ABR PERFORMANCE	II-10
A 2.6	PHASE V	II-11
A 2.6.1	FLOW RATE, DOWN-TIME AND INCIDENTS	II-11
A 2.6.2	ABR PERFORMANCE	II-12
A 2.7	PHASE VI	II-13
A 2.7.1	FLOW RATE, DOWN-TIME AND INCIDENTS	II-13
A 2.7.2	ABR PERFORMANCE	II-14
A 2.8	PHASE VII	II-15
A 2.8.1	FLOW RATE, DOWN-TIME AND INCIDENTS	II-15
A 2.8.2	ABR PERFORMANCE	II-16
A 2.9	SUMMARY OF RESULTS	II-16

APPENDIX III: FOULING ABILITY OF FLAT SHEET

	MEMBRANE APPARATUS	III-1
A 3.1	APPARATUS AND EQUIPMENT	III-1
A 3.2	REAGENTS AND MATERIALS	III-1
A 3.3	PROCEDURE	III-2
A 3.4	DATA INTERPRETATION	III-3
A 3.5	LINEAR REGRESSION ANALYSIS OF t/V VERSUS V PLOTS	III-8

APPENDIX IV: ANALYTICAL METHODS..... IV-1

A 4.1	pH.....	IV-1
A 4.2	TEMPERATURE	IV-1
A 4.3	CHEMICAL OXYGEN DEMAND (COD).....	IV-1
A 4.3.1	PRINCIPLE	IV-1
A 4.3.2	APPARATUS.....	IV-1
A 4.3.3	SAMPLE HANDLING and STORAGE	IV-2
A 4.3.4	PREPARATION OF REAGENTS.....	IV-2
A 4.3.5	PROCEDURE	IV-3
A 4.4	TOTAL SOLIDS (TS).....	IV-4
A 4.4.1	PRINCIPLE	IV-4
A 4.4.2	APPARATUS.....	IV-4
A 4.4.3	SAMPLE HANDLING AND STORAGE	IV-4
A 4.4.4	PROCEDURE:	IV-5
A 4.5	VOLATILE SOLIDS (VS).....	IV-5
A 4.5.1	PRINCIPLE	IV-5

A 4.5.2	APPARATUS	IV-5
A 4.5.3	SAMPLE STORAGE AND HANDLING	IV-5
A 4.5.4	PROCEDURE:	IV-6
A 4.6	TOTAL SUSPENDED SOLIDS (TSS)	IV-6
A 4.6.1	PRINCIPLE	IV-6
A 4.6.2	APPARATUS	IV-6
A 4.6.3	SAMPLE HANDLING AND STORAGE	IV-6
A 4.6.4	PROCEDURE:	IV-7
A 4.7	VOLATILE SUSPENDED SOLIDS (VSS).....	IV-7
A 4.7.1	PRINCIPLE	IV-7
A 4.7.2	SAMPLE HANDLING AND STORAGE	IV-7
A 4.7.3	APPARATUS	IV-8
A 4.7.4	PROCEDURE	IV-8
A 4.8	EPS EXTRACTION AND DETERMINATION	IV-8
A 4.8.1	SEPARATION OF SOLUBLE FRACTION	IV-8
A 4.8.2	EXTRACTION OF BOUND EPS.....	IV-9
A 4.9	PROTEIN CONCENTRATION	IV-12
A 4.9.1	APPARATUS.....	IV-12
A 4.9.2	SAMPLE HANDLING AND STORAGE	IV-12
A 4.9.3	REAGENTS	IV-12
A 4.9.4	PROCEDURE	IV-13
A 4.9.5	CALIBRATION CURVE.....	IV-13
A 4.10	CARBOHYDRATE CONCENTRATION.....	IV-13
A 4.10.1	APPARATUS.....	IV-13
A 4.10.2	SAMPLE HANDLING AND STORAGE	IV-14
A 4.10.3	REAGENTS	IV-14
A 4.10.4	PROCEDURE	IV-14
A 4.10.5	CALIBRATION CURVE.....	IV-15
 APPENDIX V: NEWLANDS MASHU PLANT		V-1
A 5.1	INTRODUCTION	V-1
A 5.2	THE BORDA NEWLANDS MASHU PLANT	V-2

APPENDIX VI: TECHNOLOGY TRANSFER	VI-1
A 6.1 CONFERENCE PROCEEDINGS	VI-1
A 6.2 PUBLICATIONS.....	VI-1
A 6.3 INTERNATIONAL COLLABORATION	VI-2
A 6.4 LOCAL COLLABORATION	VI-2

LIST OF ABBREVIATIONS

<i>ABR</i>	Anaerobic baffled reactor
<i>AF</i>	Anaerobic filter
<i>AnMBR</i>	Anaerobic membrane bioreactor
<i>BOD</i>	Biochemical oxygen demand
<i>BORDA</i>	Bremen Overseas Research and Development Association
<i>CFU</i>	Colony forming units
<i>COD</i>	Chemical oxygen demand
<i>CSLM</i>	Confoccal scanning laser microscopy
<i>DEWATS</i>	Decentralised wastewater treatment system
<i>DNA</i>	Deoxyribonucleic acid
<i>DOM</i>	Dissolved organic matter
<i>DUT</i>	Durban University of Technology
<i>DWAF</i>	Department of Water Affairs and Forestry (of South Africa)
<i>EDTA</i>	Ethylenediamine tetraacetic acid
<i>EGBS</i>	Expanded granular sludge blanket
<i>EPA</i>	Environmental Protection Agency
<i>EPS</i>	Extracellular polymeric substances (preferred term – see page 2-47)
<i>EU</i>	European Union
<i>GTZ-GATE</i>	Deutsche Gesellschaft für Technische Zusammenarbeit - German Appropriate Technology Exchange
<i>HRT</i>	Hydraulic retention time
<i>INSA</i>	Institut National des Sciences Appliquées
<i>MBR</i>	Membrane bioreactor
<i>MDG</i>	Millennium Development Goals
<i>MF</i>	Microfiltration
<i>MLSS</i>	Mixed liquor suspended solids
<i>MWCO</i>	Molecular weight cut-off
<i>NF</i>	Nanofiltration
<i>NWML</i>	Nominal molecular weight limit
<i>OHPA</i>	Obligate hydrogen-producing acetogens
<i>OLR</i>	Organic loading rate
<i>PRG</i>	Pollution Research Group
<i>RBC</i>	Rotating biological contactor
<i>RO</i>	Reverse Osmosis
<i>RPM</i>	Revolutions per minute

<i>SEM</i>	Scanning electron microscope
<i>SI</i>	Système International
<i>SMP</i>	Soluble microbial products (not the preferred term – see EPS)
<i>SRB</i>	Sulphate-reducing bacteria
<i>SRT</i>	Sludge retention time
<i>SS</i>	Suspended solids
<i>SVI</i>	Sludge volume index
<i>TKN</i>	Total Kjeldhal nitrogen
<i>TMP</i>	Transmembrane pressure
<i>TOC</i>	Total organic carbon
<i>TS</i>	Total solids
<i>TSS</i>	Total suspended solids
<i>UASB</i>	Upflow anaerobic sludge blanket
<i>UCT</i>	University of Cape Town (South Africa)
<i>UD</i>	Urine diversion toilet
<i>UF</i>	Ultrafiltration
<i>UKZN</i>	University of KwaZulu-Natal (South Africa)
<i>UN</i>	United Nations
<i>USEPA</i>	United States Environmental Protection Agency
<i>VFA</i>	Volatile fatty acids
<i>VIP</i>	Ventilated improved pit latrine
<i>VS</i>	Volatile solids
<i>VSS</i>	Volatile suspended solids
<i>WFD</i>	Water Framework Directive
<i>WHO</i>	World Health Organisation
<i>WRC</i>	Water Research Commission (of South Africa)

LIST OF NOTATIONS

c	Solute concentration in the boundary layer
$ca.$	Calculated average
c_g	Constant gel concentration
c_m	Concentration at the membrane surface
c_p	Solute concentration in the permeate
C_s	Quantity of accumulated matter on the membrane per volume of filtrated water (mg/L)
CWF	Clean water flux
D	Diffusion coefficient of the solute
Da	Daltons
G	Gravity force
J_{lim}	Limiting flux
J_p	Permeate flux ($L.m^{-2}.h^{-1}$)
J_{p20}	Permeate flux at 20°C
K_s	Half-saturation constant
L_p	Membrane permeability ($L.m^{-2}.h^{-1}.Pa^{-1}$ or $L.m^{-2}.h^{-1}.bar^{-1}$)
L_{p0}	Initial membrane permeability ($L.m^{-2}.h^{-1}.Pa^{-1}$ or $L.m^{-2}.h^{-1}.bar^{-1}$)
m	Mass of cake per unit area (kg/m^2)
R_c	Cake resistance (m^{-1})
R_f	Fouling resistance (m^{-1})
R_m	Clean membrane resistance (m^{-1})
R_t	Total membrane resistance (m^{-1})
S	Membrane area (m^2)
t	Filtration time (s)
T	Temperature (°C)
TMP	Transmembrane pressure (Pa)
V_c	Fouling velocity ($m^{-1}.h^{-1}$)
Greek	
α	Specific cake resistance (m/kg)
μ	Permeate viscosity (Pa.s)
μ_{20}	Permeate viscosity at 20°C (Pa.s)
$\mu_{(temp\ exp)}$	Permeate viscosity at experimental temperature (Pa.s)

LIST OF FIGURES

CHAPTER 1

- Figure 1.1: Research students involved in ABR research at the Pollution Research Group. The WRC projects which dealt with that research are included..... 1-2
- Figure 1.2: Breakdown of chapters in this thesis. The interdependence of chapters is indicated by arrows..... 1-9

CHAPTER 2

- Figure 2.1: Diagram illustrating substrate conversion patterns and the micro-organisms involved in the anaerobic digestion of complex macromolecules (from Bell, 2000)..... 2-4
- Figure 2.2: Schematic cross-section through a conventional septic tank used for the treatment of domestic sewage (adapted from City of Cape Town, 2011). 2-8
- Figure 2.3: Schematic representation of a conventional UASB and a UASB septic tank (adapted from Seghezzi, 2004). 2-10
- Figure 2.4: Schematic representation of anaerobic filter (AF) used in BORDA designed DEWATS plants (taken from Gutterer *et al.*, 2009). The AF is usually operated in the upflow mode after an ABR or an un-compartmentalised septic tank..... 2-17
- Figure 2.5: Schematic diagram of the ABR with cut-away, showing hanging and standing baffles (from Foxon *et al.*, 2004). 2-19
- Figure 2.6: Schematic configuration of BORDA DEWAT plants. Picture taken from Gutterer *et al.* (2009). 2-27
- Figure 2.7: Pictures of BORDA DEWATS plants worldwide. The pictures show different components of various DEWATS plants at community scale (pictures by PRG, 2008 to 2010). 2-28

Figure 2.8: Schematic representation of the flow pattern in the laboratory systems used by Nguyen <i>et al.</i> (2007). Plastic cylinders represented the upflow region of each unit. (a) 2-chambered septic tank and (b) 6-compartment ABR. The systems were fed with blackwater from the same collection vessel.	2-30
Figure 2.9: Classification of pressure driven membrane processes, * MWCO [molecular weight cut-off (Daltons)] (from Evenblij, 2006).....	2-34
Figure 2.10: Filtration mode applicable to hollow fibre and tubular membranes. During inside/out mode, the feed flows in the bore of the membrane. During outside/in mode, the permeate flows inside the bore of the membrane.	2-36
Figure 2.11: Fouling mechanisms: (a) complete blocking, (b) standard blocking, (c) intermediate blocking, (d) cake filtration (taken from Judd, 2006).	2-40
Figure 2.12: Definition of bound and soluble EPS. EPS may originate from bacterial synthesis, hydrolysis and lysis or from attachment (taken from Nielsen and Jahn, 1999).....	2-48
Figure 2.13: Schematic representation of a) submerged (internal) MBR and b) recirculated (external) MBR (from Ueda, 2001). The representation shows the set up for an aerobic MBR. Aeration and air scouring would not occur inside an AnMBR.	2-51
Figure 2.14: Schematic representation of dead-end and cross-flow filtration (from Evenblij, 2006).	2-52
Figure 2.15: Comparison of transition flux and limiting flux with permeate flux against TMP for pure and real fluids (taken from Cabassud <i>et al.</i> , 2006).....	2-54

CHAPTER 3

Figure 3.1: Schematic representation of the ABR plant showing external dimensions. The feed tank and the compartment boxes were built from 3 mm stainless steel sheets. Diagrams are not drawn to scale.....	3-1
--	-----

Figure 3.2: Schematic representation of laboratory ABR with membrane post-treatment.....	3-2
Figure 3.3: The inside view of the laboratory-scale ABR compartment. Downflow pipes act as hanging baffles whilst upflow pipes act as standing baffles. The siphon breaker acts to limit scum from moving to the next compartment and prevents the clogging the pipes.....	3-3
Figure 3.4: Schematic comparison of ABR designs from (a) Project K5/1248 (Foxon <i>et al.</i> , 2006) with (b) the laboratory ABR used in this thesis showing flow patterns. In Project K5/1248, the pilot ABR had hanging and standing baffles with clearly defined downflow and upflow regions. In contrast, the laboratory ABR used in this study removed the ‘downflow’ section of the old design; flow through sludge bed in each box compartment occurred through slanted pipes welded at the bottom of each box. The diagrams are not drawn to scale.	3-3
Figure 3.5: Hollow-fibre ultrafiltration and microfiltration membrane modules provided by Polymem, France.....	3-6
Figure 3.6: Schematic representation of the external MBR used in this study. (1) ABR effluent container, (2) peristaltic pump, (3) height-adjustable feed funnel, (4) feed funnel overflow, (5) membrane feed line, (6) water column stand pipe, (7) decant valves, (8) siphon breaker, (9) permeate line, (10) mass balance. The diagram is not drawn to scale.	3-6
Figure 3.7: Pictures of the Kubota (left) and fabric (right) membranes (PRG, 2009).	3-8
Figure 3.8: The microstructure detail of the Kubota membrane (Taken from: Ministry of the Environment - Global Environment Centre, 2007).	3-8
Figure 3.9: SEM image of the fabric membrane showing woven fibres (PRG, 2010).	3-9
Figure 3.10: Schematic of the membrane pilot used to house flat-sheet membranes (PRG, 2009).....	3-9

Figure 3.11: Schematic representation of the configurations used to measure the hydraulic head in the hollow-fibre membrane unit. (a) Configuration used when hydraulic heads under 500 mm water were required. (b) Configuration used when hydraulic heads over 500 mm water were required. Key: (1) ABR effluent feed line, (2) feed funnel overflow, (3) height-adjustable feed funnel, (4) membrane feed line, (5) decant valves, (6) water column stand pipe, (7) siphon breaker, (8) permeate line, (9) mass balance. The diagram is not drawn to scale.	3-11
Figure 3.12: Photograph of the flat-sheet membrane unit during a clean water filtration test. The hydraulic head was determined by the difference in elevation from the permeate line to the middle of the membrane module. (a) Height from liquid level in box to the middle of the membrane module. (b) Height from middle of the membrane module to the floor. (c) Height from floor to permeate pipe.	3-12
Figure 3.13: A view of the housing settlements where VIP waste is collected. a) Marianhill, b) a township in Tongaat. Both areas are serviced with VIP toilets (PRG, 2007).	3-15
Figure 3.14: Contents of a VIP toilet in the Marianhill area. The pit consists of a semi-solid mixture of faeces and urine. Other non-desirable materials, such as glass, plastic and even tablets are found in the waste. Larger items, such as bricks and bottles, are removed from the toilet before sampling (PRG, 2007).	3-15
Figure 3.15: Sampling of a household VIP pit from Marianhill. a) Plastic buckets (100 L) with sealable lids are used to collect VIP sludge, b) the pit is sealed once sampling is complete by placing the concrete slab over the pit (PRG, 2007).	3-16
Figure 3.16: Pit emptying in Magwaveni, Tongaat (approximately 35 km from Durban). VIP sludge is manually removed from pit latrines and transported to a vehicle via refuse bins (PRG, 2007).	3-16

Figure 3.17: The bins are transported to a nearby wastewater treatment facility where the waste is screened and pumped into the head of works. It is at this point where samples for feeding the ABR were taken (PRG, 2007).....	3-17
Figure 3.18: a) Greywater storage containers at the Old Mutual test site. The eThekweni Municipality delivered approximately 200 L of greywater to the site and poured it into the storage containers, b) Wire mesh on the storage container which prevents undesirable material from entering the containers (PRG, 2006).	3-18
Figure 3.19: Sludge from VIP toilets that had been mixed with a shovel (large bucket). In the smaller bucket, undesirable material such as glass and plastic have been removed from the waste and placed in an autoclave bag for sterilisation. The pre-mixed VIP waste is further homogenised in a mechanical blender.	3-19
Figure 3.20: Photograph of feed wastewater sample taken from the middle of the feed tank (PRG, 2008).....	3-23
Figure 3.21: Photograph of the laboratory ABR effluent from the collection container after the outlet pipe of the last ABR compartment (PRG, 2008).....	3-24
 CHAPTER 4	
Figure 4.1: A typical non-linear t/V versus V curve showing three regions which correspond to pore blocking, cake filtration and cake filtration with clogging and/or cake compression (Boerlage <i>et al.</i> , 2003). It is common practice to determine the MFI from the gradient of the linear portion of the curve.	4-4
Figure 4.2: Picture of fouling ability of flat sheet membrane apparatus (FAFS) recommended by <i>EUROMBRA</i> partners.	4-6
Figure 4.3: Breakdown of filtration experiments performed on Amicon® membranes using the soluble phase from different biomasses.	4-8

Figure 4.4: Plots of flux at 20°C as a function of constant TMP for supernatant samples of (a) sludge from compartment 2 of ABR (n = 2), (b) sludge from compartment 3 of ABR (n = 2), (c) sludge from compartment 4 of ABR (n = 2), and (d) sludge from an activated sludge plant on Amicon® membrane 1 (n = 2). Error bars represent the standard deviation for each TMP step under dead-end conditions. In certain instances, the error bars are too small to be visible.	4-11
Figure 4.5: Plots of flux at 20°C as a function of constant TMP for supernatant from (a) raw supernatant (1 281 mg COD/L) (n = 1) and (b) diluted supernatant from an anaerobic digester (258 mg COD/L) (n = 2) at a local wastewater treatment facility on Amicon® membrane 2. Error bars represent the standard deviation for each TMP step under dead-end conditions.	4-12
Figure 4.6: Plots of flux at 20°C as a function of constant TMP for supernatant from the laboratory ABR treating (a) synthetic domestic wastewater and (b) diluted VIP sludge on Amicon® membrane 3 and 4, respectively. Error bars represent the standard deviation for each TMP step under dead-end conditions.	4-14
Figure 4.7: Timeline of filtration experiments performed on the Amicon® membrane 1 using supernatant from different sludge sources. For each experiment, duplicate filtration experiments were performed with chemical cleaning and clean water tests (CWF) performed after each supernatant filtration cycle.	4-15
Figure 4.8: Plots of t/V versus V for (a) Run 1 and (b) Run 2 of the membrane filtration of supernatant from compartment 2 of the pilot ABR at 50 kPa. Regions A and B on each graph represent approximate location of blocking and cake filtration, respectively.	4-16
Figure 4.9: Plots of clean water flux (CWF) before and after compartment 2 supernatant filtration for (a) Run 1 and (b) Run 2. Each point represents the average flux for a specific TMP whilst error bars represent the standard deviation for that point. In some instances the error bars are too small to be visible.	4-17

Figure 4.10: Picture of the fouling layer after compartment 2 supernatant membrane filtration. The fouling layer was thin and easily removed by rinsing and chemical cleaning.	4-18
Figure 4.11: Plots of t/V versus V for (a) Run 1 and (b) Run 2 of the membrane filtration of supernatant from compartment 3 of the pilot ABR at 50 kPa. Regions A, B and C on each graph represent the approximate location of blocking filtration, cake filtration and cake filtration with blocking and/or compression, respectively.....	4-18
Figure 4.12: Plots of clean water flux (CWF) before and after membrane filtration of compartment 3 supernatant for (a) Run 1 and (b) Run 2. Each point represents the average flux for a specific TMP whilst error bars represent the standard deviation for that point. In some instances the error bars are too small to be visible.....	4-19
Figure 4.13: Picture of the fouling layer after compartment 3 supernatant membrane filtration. The fouling layer was viscous and gel like and could not be easily removed by rinsing and chemical cleaning.	4-20
Figure 4.14: Plots of t/V versus V for (a) Run 1 and (b) Run 2 of the membrane filtration of supernatant from compartment 4 of the pilot ABR at 50 kPa. Regions A and B on each graph represent approximate location of blocking and cake filtration, respectively.....	4-22
Figure 4.15: Plots of clean water flux (CWF) before and after membrane filtration of compartment 4 supernatant for (a) Run 1 and (b) Run 2. Each point represents the average flux for a specific TMP whilst error bars represent the standard deviation for that point. In some instances the error bars are too small to be visible. For comparison, the CWF for the virgin membrane (1) and at the beginning of the compartment 2 supernatant test (2) have been included.....	4-23
Figure 4.16: Picture of the fouling layer after membrane filtration of compartment 4 supernatant. The fouling layer was thin and evenly distributed around the membrane.	4-23

Figure 4.17: Plots of t/V versus V for (a) Run 1 and (b) Run 2 of the membrane filtration of supernatant from an activated sludge tank at 50 kPa.	4-24
Figure 4.18: Plots of clean water flux (CWF) before and after membrane filtration of activated sludge supernatant for (a) Run 1 and (b) Run 2. Each point represents the average flux for a specific TMP whilst error bars represent the standard deviation for that point. In some instances the error bars are too small to be noticed.....	4-25
Figure 4.19: Picture of the fouling layer after membrane filtration of the soluble component of activated sludge. The fouling layer was thin and evenly distributed around the membrane.	4-25
Figure 4.20: Timeline of filtration experiments performed on Amicon® membrane 2 using supernatant from an anaerobic digester. For the first experiment, only one run was performed. For the second experiment, triplicate experiments were performed with chemical cleaning and clean water tests (CWF) performed after each supernatant filtration cycle.....	4-26
Figure 4.21: Plots of t/V versus V for the membrane filtration of supernatant from an anaerobic digester at 50 kPa. The area highlighted in the plot shows the points which were used to calculate the lower and upper limits of the product of $\alpha \cdot C_s$	4-27
Figure 4.22: Plots of clean water flux (CWF) before and after membrane filtration of anaerobic sludge supernatant. Each point represents the average flux for a specific TMP whilst error bars represent the standard deviation for that point. In some instances the error bars are too small to be visible.	4-28
Figure 4.23: Plots of t/V versus V for (a) Run 1, (b) Run 2 and (c) Run 3 of the membrane filtration of diluted supernatant from an anaerobic digester at 50 kPa on Amicon® membrane 2.	4-29
Figure 4.24: Plots of clean water flux (CWF) before and after membrane filtration of diluted anaerobic sludge supernatant. Each point represents the average flux for a specific TMP whilst error bars represent the standard deviation for that point. In some instances the error bars are too small to be visible.....	4-30

Figure 4.25: Plots of t/V versus V for (a) Run 1, (b) Run 2 and (c) Run 3 of the membrane filtration of supernatant from an ABR treating a synthetic domestic wastewater at 50 kPa on the Amicon® membrane 3. 4-31

Figure 4.26: Plots of clean water flux (CWF) before and after membrane filtration of supernatant from an ABR treating a synthetic domestic wastewater on Amicon® membrane 3. Each point represents the average flux for a specific TMP whilst error bars represent the standard deviation for that point. In some instances the error bars are too small to be visible. 4-32

Figure 4.27: Plots of t/V versus V for (a) Run 1, (b) Run 2 and (c) Run 3 of the membrane filtration of supernatant from an ABR treating diluted VIP sludge at 50 kPa on the Amicon® membrane 4. 4-34

Figure 4.28: Plots of clean water flux (CWF) before and after the membrane filtration of supernatant from an ABR treating diluted VIP sludge on Amicon® membrane 4. Each point represents the average flux for a specific TMP whilst error bars represent the standard deviation for that point. In some instances the error bars are too small to be noticed. 4-35

Figure 4.29: SEM micrograph from compartment 3 of pilot ABR treating domestic wastewater reproduced from WRC Project K5/1248 (Foxon *et al.*, 2006). The granules surface is covered with gas cavities (GC) which lead to inner structure bound by EPS containing different metabolic groups (Pillay *et al.*, 2006). 4-37

CHAPTER 5

Figure 5.1: Schematic representation of the protocol used for assessing Polymem performance based on practical definition of fouling (refer to section 2.2.7). 5-4

-
- Figure 5.2: Variation of flux with pressure during Phase I effluent for a) flux-TMP graph of the Polymem MF module and b) flux-TMP graph of the Polymem UF module. Each data point (●) represents the average flux over each pressure step. The error bars represent the standard deviation for each TMP step. In some instances, the error bars are too small to be visible. 5-7
- Figure 5.3: Fouling resistance (R_f) as a function of TMP over progressive increases in TMP for the Polymem MF module during Phase I. The encircled areas represent the asymptote of R_f for a particular TMP step. 5-8
- Figure 5.4: Fouling resistance (R_f) as a function of TMP over progressive increases in TMP for the Polymem UF module during Phase I. The encircled areas represent the asymptote of R_f for a particular TMP step. 5-9
- Figure 5.5: Fouling velocity (or fouling rate) for Polymem MF and UF modules as a function of TMP during Phase I. The points were calculated by from the slope of R_f over filtration time. Outliers have been excluded from plot. 5-9
- Figure 5.6: Variation of clean water permeate flux (CWF) with TMP during Phase I for a) Polymem MF module and b) Polymem UF module. The data points (Δ) represent the average clean water flux over a specific TMP whilst the error bars represent the standard deviation for a specific period. In some instances, the error bars are too small to be visible. 5-10
- Figure 5.7: Variation of flux with pressure during Phase III for a) flux-TMP graph of the Polymem MF module and b) flux-TMP graph of the Polymem UF module. Each data point (●) represents the average flux over each pressure step. The error bars represent the standard deviation for each TMP step. In some instances, the error bars are too small to be visible. 5-11
- Figure 5.8: Fouling resistance (R_f) as a function of TMP over progressive increases in TMP for the Polymem MF module during Phase III. The encircled areas represent the asymptote of R_f for a particular TMP step. 5-12

Figure 5.9: Fouling resistance (R_f) as a function of TMP over progressive increases in TMP for the Polymem UF module during Phase III. The encircled area represents the asymptote of R_f for a particular TMP step.	5-12
Figure 5.10: Fouling velocity (or fouling rate) as a function of TMP for Polymem MF and UF modules during Phase III. The points were calculated by determining the slope of R_f over filtration time. Outliers have been excluded from plot.....	5-13
Figure 5.11: Variation of clean water permeate flux (CWF) with TMP during Phase III for a) Polymem MF module and b) Polymem UF module. The data points (Δ) represent the average clean water flux over a specific TMP whilst the error bars represent the standard deviation for a specific. In some instances, the error bars are too small to be visible.	5-14
Figure 5.12: Variation of flux with pressure during Phase V for a) flux-TMP graph of the Polymem MF module and b) flux-TMP graph of the Polymem UF module. Each data point (\bullet) represents the average flux over each pressure step. The error bars represent the standard deviation for each TMP step. In some instances, the error bars are too small to be visible.....	5-15
Figure 5.13 Fouling resistance (R_f) as a function of TMP over progressive increases in TMP for the Polymem UF module during Phase V.	5-16
Figure 5.14: Fouling resistance (R_f) as a function of TMP over progressive increases in TMP for the Polymem UF module during Phase V.	5-16
Figure 5.15: Fouling velocity (or fouling rate) for Polymem MF and UF modules as a function of TMP during Phase V. The points were calculated by determining the slope of R_f over filtration time.	5-17
Figure 5.16: Variation of clean water permeate flux (CWF) with TMP during Phase V for a) Polymem MF module and b) Polymem UF module. The data points (Δ) represent the average clean water flux over a specific TMP whilst the error bars represent the standard deviation for a specific period. In some instances, the error bars are too small to be visible.	5-18

Figure 5.17: Variation of flux with pressure during Phase VI for a) flux-TMP graph of the Polymem MF module and b) flux-TMP graph of the Polymem UF module. Each data point (●) represents the average flux over each pressure step. The error bars represent the standard deviation for each TMP step. In some instances, the error bars are too small to be visible.....	5-19
Figure 5.18: Fouling resistance (R_f) as a function of TMP over progressive increases in TMP for the Polymem MF module during Phase VI.	5-19
Figure 5.19: Fouling resistance (R_f) as a function of TMP over progressive increases in TMP for the Polymem UF module during Phase VI.	5-20
Figure 5.20: Fouling velocity (or fouling rate) for Polymem MF and UF modules as a function of TMP during Phase VI. The points were calculated by determining the slope of R_f over filtration time.	5-20
Figure 5.21: Variation of clean water permeate flux (CWF) with TMP during Phase VI for a) Polymem MF module and b) Polymem UF module. The data points (Δ) represent the average clean water flux over a specific TMP whilst the error bars represent the standard deviation for a specific period. In some instances, the error bars are too small to be visible.	5-21
Figure 5.22: Permeate versus TMP for Polymem microfiltration and ultrafiltration modules during TMP step experiments at different feed COD concentrations. Each point represents the average flux over each TMP whilst error bars represent the standard deviation. In some instances, the error bars are too small to be noticed.....	5-22
Figure 5.23: Plot of average fouling resistance (R_f) versus TMP for Polymem microfiltration and ultrafiltration modules. The errors bars represent the standard deviation for each TMP step.	5-23
Figure 5.24: Photographs of the Polymem ultrafiltration module being cleaned after fouling experiment.....	5-24

Figure 5.25: Relationship between membrane permeability and total COD during each series of experiments for the Polymem microfiltration and ultrafiltration module.	5-24
Figure 5.26: Comparison of membrane permeability of the Polymem microfiltration and ultrafiltration module during various phases of membrane testing.....	5-25
Figure 5.27: Variation in flux at a constant TMP of 4 kPa over 4h for Polymem MF and UF modules treating laboratory ABR effluent. The dashed lines (---) represent the calculated average clean water flux (CWF) before effluent filtration at 4 kPa.	5-27
Figure 5.28: Schematic representation of the total COD concentration through the membrane coupled ABR during 4 h filtration.	5-28
Figure 5.29: Variation of clean water permeate flux (CWF) with TMP during Phase VI for a) Polymem MF module and b) Polymem UF module. The data points (Δ) represent the average clean water flux over a specific TMP whilst the error bars represent the standard deviation for a specific period.	5-29
Figure 5.30: The evolution of flux over time for the Polymem UF module treating ABR effluent. Data points (\bullet and \bullet) represent a 16 point moving average of the flux at a specific time whilst error bars represent the standard deviation for each point. The module was operated at constant TMP at 3 kPa (\bullet) for 34 d after which the TMP was increased to 6 kPa (\bullet). Horizontal dashed lines (--) represent potential performance affecting incidents such as TMP relaxation whilst the solid vertical black line (—) represents the transition from 3 kPa to 6 kPa.	5-32
Figure 5.31: Variation of clean water permeate flux (CWF) before and after effluent filtration and after physical cleaning (Polymem UF module). The data points (Δ) represent the average clean water flux over a specific TMP whilst the error bars represent the standard deviation for a specific period.	5-33
Figure 5.32: The simultaneous variation of flux against time for the Polymem microfiltration module treating ABR effluent at 3 kPa. Data points represent a 16 point moving average of the flux over a specific time.	5-35

Figure 5.33: Real time flux for the Polymem microfiltration module operated with and without TMP relaxation.....	5-37
Figure 5.34: The simultaneous variation of flux against time for the Polymem ultrafiltration module treating laboratory ABR effluent and the supernatant of settled ABR effluent. Data points represent the flux (presented as 12-point and 16-point moving average for the ABR effluent and the supernatant of settled ABR effluent, respectively) over a specific time.....	5-40
Figure 5.35: Variation of clean water permeate flux (CWF) before and after supernatant filtration and after physical cleaning. The data points (Δ) represent the average clean water flux over a specific TMP whilst the error bars represent the standard deviation for a specific period.....	5-40
Figure 5.36: The simultaneous variation of flux against time for the Polymem ultrafiltration module treating (a) the soluble component of ABR effluent, (b) untreated ABR effluent and (c) the supernatant of settled ABR effluent. Data points represent the average flux over a specific time. Error bars represent the standard deviation for flux over a time period.	5-42

CHAPTER 6

Figure 6.1: Photograph of the inside of the membrane feed box showing modules immersed in tap water. The permeate pipes, hose supplying tap water and overflow drain are also shown in photograph (PRG, 2009).	6-3
Figure 6.2: Photograph of the flat sheet system showing permeate lines, membrane feed line and overflow. Unlike the Polymem system (Chapter 5), the flat sheet system was not completely airtight (PRG, 2009).	6-4
Figure 6.3: Variation of clean water flux (CWF) with TMP for Kubota and fabric modules before laboratory ABR effluent filtration. The data points represent the average flux over a specific time period.	6-6

Figure 6.4: The simultaneous variation of flux versus time for Kubota and fabric modules treating laboratory ABR effluent. a) Flux-time profile of modules over 80 d. b) Magnified view of area marked by □ in (a). Data points represent the actual flux at a specific time.....	6-6
Figure 6.5: A magnified view of the simultaneous variation of flux versus time for Kubota and fabric modules treating laboratory ABR effluent. The plot shows the steady state flux for each TMP and module tested.	6-7
Figure 6.6: Variation of clean water flux (CWF) with TMP for Kubota and fabric modules after laboratory ABR effluent filtration. The data points represent the average flux over a specific time period.	6-9
Figure 6.7: Photographs of the fouling layer on a) Kubota module and b) fabric module after laboratory ABR effluent filtration. The fouling layer had a gel like structure and was difficult to remove using physical cleaning techniques (PRG, 2009).....	6-9
Figure 6.8: The simultaneous variation of flux versus time for Kubota and fabric modules treating laboratory ABR effluent. Effluent and permeate samples were collected on day 1, 7 and 17 (grey solid lines) and were analysed for total COD, soluble protein and soluble carbohydrate. On day 79 the fouling layer was removed and analysed for protein, carbohydrate and COD content.....	6-10
Figure 6.9: Flow diagram showing the feeding system to the membrane from the laboratory ABR effluent container.	6-12
Figure 6.10: Variation of clean water flux (CWF) with TMP for Kubota and fabric modules before laboratory ABR effluent filtration. The data points represent the flux over a specific time period.....	6-17

Figure 6.11: The simultaneous variation of flux versus time for Kubota and fabric modules treating the supernatant from settled laboratory ABR effluent. a) Flux-time profile of flat sheet modules over 8 d. b) Magnified view of (a) with flux presented a maximum of $5 \text{ L.m}^{-2}.\text{h}^{-1}$. The thick grey dashed line represents the combined average flux of flat sheet modules during the 8 d filtration test. Data points represent the actual flux at a specific time.....	6-18
Figure 6.12: Variation of clean water flux (CWF) with TMP for Kubota and fabric modules after filtration of supernatant from settled laboratory ABR effluent. The data points represent the average flux over a specific time period.....	6-20
Figure 6.13: Variation of clean water flux (CWF) with TMP for Kubota and fabric modules before microfiltered ABR effluent filtration. The data points represent the average flux over a specific time period.	6-24
Figure 6.14: The simultaneous variation of flux versus time for Kubota and fabric modules treating the soluble component of the laboratory ABR effluent. a) Flux-time profile of modules over 8 d. b) Magnified view of (a) with flux presented at a maximum of $20 \text{ L.m}^{-2}.\text{h}^{-1}$. The vertical grey line (—) represents the time of the incident whilst the horizontal dashed black line (---) represents the flux plateau from previous experiments. Data points represent the actual flux at a specific time.....	6-25
Figure 6.15: Variation of clean water flux (CWF) with TMP for Kubota and fabric modules after laboratory ABR effluent filtration. The data points represent the flux over a specific time period.....	6-27

CHAPTER 7

Figure 7.1: SEM micrograph showing surface view of a single hollow fibre from the Polymem ultrafiltration module operated at constant TMP (Chapter 5). The module was cleaned with tap water before SEM examination. The area in the background is the adhesive used to place the fibre on an aluminium stub for SEM viewing (PRG, 2010). Magnification = $125 \times$	7-11
---	------

Figure 7.2: SEM micrograph showing cross section view of inner morphology of a freeze fractured hollow fibre from the Polymem ultrafiltration module operated at constant TMP. The module was cleaned with tap water before SEM examination (PRG, 2010). Magnification = 300 ×.....	7-11
Figure 7.3: SEM micrograph showing high magnification (× 12 640) of the inner surface of a single hollow fibre from the Polymem ultrafiltration module. The insert located on the top left corner of micrograph shows the approximate location (encircled area) on the hollow-fibre from which this micrograph was taken (PRG, 2010).	7-12
Figure 7.4: SEM micrograph showing the smooth outer surface skin with relatively evenly distributed pores (nominal pore of 0.08 μm) of a single hollow fibre from the Polymem ultrafiltration module (PRG, 2010). The insert located on the top left corner of micrograph shows the approximate location (shown by arrow) on the hollow-fibre from which this micrograph was taken. Magnification = × 5 000.....	7-12
Figure 7.5: SEM micrograph showing high magnification (× 71 350) of the inner surface of a single hollow fibre from the Polymem ultrafiltration module. The SEM micrograph shows the pore structure on the membrane surface on the Polymem ultrafiltration module (PRG, 2010). Manufacturer stated pore size = 0.08 μm.	7-13
Figure 7.6: SEM micrograph of surface view of a fabric microfiltration membrane constructed by the Durban University of Technology. The membrane was constructed from spun polyester filaments and used in filtration experiments in Chapter 6 (PRG, 2010). Magnification = 150 ×.....	7-13
Figure 7.7: SEM micrograph showing a filament strand of the spun fibres making up the microfiltration fabric membrane (made by DUT) at high magnification (3 190 ×) (PRG, 2010). Much more space exists between strands than the other modules.	7-14

Figure 7.8: SEM micrograph of the surface topography of a cleaned microfiltration Kubota membrane (Chapter 6) (PRG, 2010). The surface is more porous than the Polymem modules. Manufacturer stated pore size = 0.4 μm . Magnification = 2 870 \times	7-14
Figure 7.9: SEM micrograph showing a high magnification of the surface topography of a cleaned microfiltration Kubota membrane. Magnification = 31 880 \times	7-15
Figure 7.10: Proposed mechanism of fouling layer development in hollow fibre modules treating effluent from an ABR treating complex particulate wastewater. (a) Pressure applied with flux at its highest. (b) Colloids loosely adhered to pores which are normal to the outer surface of the module, decrease in flux. (c) Colloids and aggregates held together by soluble binding constituent and permeate flow is restricted. (d) Build-up of cake until flow becomes impeded.	7-16
Figure 7.11: Proposed mechanism of fouling layer development in flat sheet modules treating effluent from an ABR treating complex particulate wastewater. (a) Bulk fluid transported to membrane under TMP. (b) Adsorption and/or pore blocking of rough membrane surface by colloids. The porous nature of membrane surface also facilitates adherence of foulants through greater surface area. (c) Binding of protein layer and subsequent concentration polarisation gel like layer formed. Transport through the layer occurs through diffusion (Judd, 2006).....	7-18

APPENDIX II

Figure II.1: Time-line of study showing different periods of operation for the laboratory ABR from 30 June 2007 to 5 October 2009. Phases III to VI were performed by Kapuku (2011).	II-2
Figure II.2: Cumulative flow treated, incidents and downtime during Phase II (30 June 2007 to 23 March 2008). Grey areas represent reactor downtime whilst dashed lines (---) indicate potentially performance affecting incidents such as desludging.....	II-3
Figure II.3: Cumulative flow treated, incidents and downtime during Phase II (28 March 2008 to 30 July 2008). Grey areas represent reactor downtime.....	II-5

Figure II.4: Cumulative flow treated, incidents and downtime during Phase III (3 August 2008 to 3 September 2008). Grey areas represent reactor downtime whilst dashed lines (---) indicate potentially performance-affecting incidents such as desludging.	II-7
Figure II.5: Cumulative flow treated, incidents and downtime during Phase IV (4 September 2008 to 2 October 2008). Grey areas represent reactor downtime whilst dashed lines (---) indicate potentially performance-affecting incidents such as desludging.	II-9
Figure II.6: Cumulative flow treated, incidents and downtime during Phase V (3 October 2008 to 23 October 2008). Grey areas represent reactor downtime whilst dashed lines (---) indicate potentially performance-affecting incidents such as desludging.	II-11
Figure II.7: Cumulative flow treated, incidents and downtime during Phase VI (24 October 2008 to 6 November 2008). Grey areas represent reactor downtime whilst dashed lines (---) indicate potentially performance-affecting incidents such as desludging.	II-13
Figure II.8: Cumulative flow treated, incidents and downtime during Phase VII (4 June 2009 to 5 October 2009). Grey areas represent reactor downtime whilst dashed lines (---) indicate potentially performance-affecting incidents such as desludging.....	II-15
Figure II.9: Feed, overflow and effluent total COD concentrations for the laboratory ABR treating a synthetic blackwater (diluted VIP sludge) from 30 June 2007 to 5 October 2009. The light blue dashed line (---) represents the transition in operating parameters.	II-20
Figure II.10: Phases III to VI in Figure 4.9 showing feed, overflow and effluent total COD (tCOD) concentrations for the laboratory ABR treating a synthetic blackwater (diluted VIP sludge) from 2 August 2008 to 6 November 2008. The light blue dashed line (---) represents the transition in operating parameters.....	II-20

Figure II.11: The removal of COD from the feed tank to overflow (flow from feed tank to compartments) to effluent. The percentage values above grey arrows indicate percentage COD removal from either feed tank to overflow or overflow to effluent. The percentage value in grey box represents the COD removal from feed to effluent. II-21

Figure II.12: Photographs of the biogas dome from a DEWATS plant in Indonesia (PRG, 2007) and China (BORDA, 2007). II-22

APPENDIX III

Figure III.1: Determination of the permeability (L_{po}) from the graph of flux (J) versus TMP (from Cabassud *et al.*, 2006). III-5

Figure III.2: Evolution of the cake resistance and TMP over time (from Cabassud *et al.*, 2006). III-6

Figure III.3: A typical plot of fouling velocity against constant TMP which can be used to compare the fouling potential of biological fluids from different sludge sources (from Cabassud *et al.*, 2006). III-7

Figure III.4: Linear regression of points from t/V versus V plots in **Chapter 4** for the pilot ABR supernatant samples on Amicon membrane 1. III-10

Figure III.5: Linear regression of points from t/V versus V plots in **Chapter 4** for the activated sludge samples on Amicon membrane 1. III-11

Figure III.6: Linear regression of points from t/V versus V plots in **Chapter 4** for the activated sludge samples on Amicon membrane 2. III-11

Figure III.7: Linear regression of points from t/V versus V plots in **Chapter 4** for the effluent samples from the laboratory ABR. Plots (a) to (c) represent samples from the ABR treating a synthetic domestic wastewater on Amicon membrane 3. Plots (d) to (f) represent samples from the ABR treating a synthetic domestic wastewater on Amicon membrane 4. III-12

APPENDIX IV

- Figure IV.1: Picture guideline of the separation process used in this project. Not included in the guide is the extraction process with cation exchange resin. IV-11
- Figure IV.2: Plot of BSA concentration against absorbance at 750 nm (spec 1, spectrophotometer at the School of Biological and Conservation Science; spec 2 and 3 represent readings from Merck spectrophotometer). IV-14
- Figure IV.3: Plot of D glucose versus absorbance at 490 nm for two different spectrophotometers (Spec 1, School of Biological and Conservation Science; Spec 2, Merck spectrophotometer at our laboratory). IV-15

APPENDIX V

- Figure V.1: Photograph of the site showing the experimental Newlands Mashu plant designed by BORDA (PRG, 2010). V-2
- Figure V.2: Inside of the DEWATS plant showing the settler, three ABR trains and AF compartments (nearest compartments). The larger sized ABR compartments can be seen in the left of the picture (fewer walls) (PRG, 2010). V-3
- Figure V.3: Downflow pipes in the AF chamber. Concrete slabs have been placed at the bottom and filled with graded material. V-4
- Figure V.4: Membrane evaluation sump designed by Dr. S Pollet. The sump has two sides; a wet side for immersing membrane modules and a dry side for collecting permeate. The sump was designed to the water level of the effluent pipes after the AFs and excavated to the depth of the settler ABR AF. Membranes will operate under a gravitational head in the wet chamber. V-4

LIST OF TABLES

CHAPTER 2

Table 2.1: Advantages and disadvantages of anaerobic wastewater treatment (adapted from Seghezzi <i>et al.</i> , 1998).	2-3
Table 2.2: Comparison of UASB septic tank performances. The numbers in parenthesis represent standard deviation. Data adapted from Al Jamal and Mahmoud (2009).	2-11
Table 2.3: Historical modifications of the ABR (adapted from Barber and Stuckey, 1999).	2-20
Table 2.4: Average removal efficiencies reported by Nguyen <i>et al.</i> (2007) in a 2-compartment septic tank and a 6-compartment ABR treating blackwater and operated at different HRTs.	2-29
Table 2.5: Removal of selected parameters through a BORDA DEWATS plant treating domestic wastewater in Nepal (adapted from Singh <i>et al.</i> , 2009).	2-33
Table 2.6: Membrane configurations and application in different separation processes (from Baker, 2000).	2-36
Table 2.7: Fouling definitions used in MBR study (modified* from Judd, 2006 and 2007).	2-43
Table 2.8: Influence of changing MLSS concentration on MBR fouling (adapted from Judd, 2006).	2-44
Table 2.9: Effluent concentrations from ABRs treating various wastewaters.	2-63

CHAPTER 3

Table 3.1: Characteristics of hollow fibre membranes used during study.	3-5
Table 3.2: Comparison of physico-chemical properties of sanitation wastewater in relation to the feed used in this study.	3-21

Table 3.3: Table of responsibilities of feeding, sampling, analyses and data collation for the laboratory ABR treating diluted VIP sludge.	3-22
Table 3.4: Table of responsibilities for different analytical method used during this study.	3-22
Table 3.5: Standard terminology and the context in which it is used in this thesis (Chapters 4 to 7).....	3-28
Table 3.6: Location of standard terminology (Table 3.6) used in this thesis and the location of this terminology in thesis.	3-29

CHAPTER 4

Table 4.1: Summary of chemical results obtained from membrane filtrations of diluted and undiluted anaerobic sludge supernatant.	4-12
Table 4.2: Physico-chemical results of the different soluble fractions of each sludge source.....	4-21
Table 4.3: Lower and upper confidence values (95% confidence level) for the product of $\alpha.C_s$ at 50 kPa (reference TMP).	4-36
Table 4.4: Cost of experimental equipment used to evaluate fouling propensity. Cost based on 2006 prices (US\$ 1 = ZAR 7.8) and excludes value added tax. Cost of pressure reservoir and weighing balance has not been included.....	4-39

CHAPTER 5

Table 5.1: Summary of ABR effluent characteristics during short term TMP-step filtration. Polymem ultrafiltration and microfiltration modules were tested using the TMP step method during these phases. The values represent the average and standard deviation (except pH value which is represented as a median) with numbers in parentheses representing the sample replicates.....	5-6
---	-----

CHAPTER 6

Table 6.1:	Feed and effluent characteristics for Phase VII (4 June 2009 to 5 October 2009). Calculations of averages and standard deviations are presented for all measurements except for the pH value which is reported as a median value. The number in parenthesis represents the number of samples over the operating period.	6-2
Table 6.2:	Calculated cumulative volumes of Kubota and fabric modules operated at 3 and 6 kPa over 80 d*.	6-8
Table 6.3:	Chemical composition of ABR effluent, membrane box and permeate samples from Kubota and fabric modules operated at 3 and 6 kPa for days 1, 7 and 17. Analyses were performed in duplicate or triplicate (unless otherwise stated).	6-11
Table 6.4:	Chemical composition of manually removed fouling layer from Kubota and fabric modules operated at 3 and 6 kPa for day 79. Analyses were performed in duplicate or triplicate (unless otherwise stated). Cumulative volumes of permeate were calculated using flow rates between sampling days and divided by the effective filtration area for each module.	6-14
Table 6.5:	Calculated cumulative volumes of Kubota and fabric modules operated at 3 and 6 kPa over 8 d treating the supernatant from settled ABR effluent. Cumulative volumes of permeate were calculated using flow rates between sampling days and divided by the effective filtration area for each module. For comparison, the cumulative volumes of the modules treating ABR effluent from section 7.1 have also been included.	6-19
Table 6.6:	Chemical composition of settled ABR supernatant, membrane box and permeate samples from Kubota and fabric modules operated at 3 and 6 kPa for day 7 (9 June 2009). Analyses were performed in duplicate or triplicate (unless otherwise stated).	6-19
Table 6.7:	Chemical composition of the fouling layer from Kubota and fabric modules operated at 3 and 6 kPa (10 June 2009). Analyses were performed in duplicate or triplicate (unless otherwise stated).	6-21

Table 6.8: Chemical composition of microfiltered laboratory ABR effluent, membrane box and permeate samples from Kubota and fabric modules operated at 3 and 6 kPa for day 7 (9 June 2009). Analyses were performed in duplicate or triplicate (unless otherwise stated).....	6-26
---	------

Table 6.9: Chemical composition of the fouling layer from Kubota and fabric modules operated at 3 and 6 kPa for day 7 (9 September 2009). Analyses were performed in duplicate or triplicate (unless otherwise stated). The volume produced takes into consideration the effective filtration area of each module.....	6-28
--	------

APPENDIX I

Table I.1: List of participants in the <i>EUROMBRA</i> Project.	I-1
--	-----

APPENDIX II

Table II.1: Details of membrane investigations.	II-2
--	------

Table II.2: Feed and effluent characteristics for Phase I (30 June 2007 to 23 March 2008). Calculations of averages and standard deviations are presented for all measurements except for the pH value, which is reported as a median value. The number in parenthesis represents the number of samples over the operating period.	II-4
---	------

Table II.3: Feed and effluent characteristics for Phase II (27 March 2008 to 30 July 2008). Calculations of averages and standard deviations are presented for all measurements except for the pH values which are reported as a median values. The number in parenthesis represents the number of samples over the operating period.....	II-6
---	------

Table II.4: Feed and effluent characteristics for Phase III (3 August 2008 to 3 September 2008). Calculations of averages and standard deviations are presented for all measurements except for the pH value, which is reported as a median value. The number in parenthesis represents the number of samples over the operating period.	II-8
---	------

Table II.5: Feed and effluent characteristics for Phase IV (4 September 2008 to 2 October 2008). Calculations of averages and standard deviations are presented for all measurements except for the pH value, which is reported as a median value. The number in parenthesis represents the number of samples over the operating period. II-10

Table II.7: Feed and effluent characteristics for Phase VI (24 October 2008 to 6 November 2008). Calculations of averages and standard deviations are presented for all measurements except for the pH value, which is reported as a median value. The number in parenthesis represents the number of samples over the operating period. II-14

Table II.8: Feed and effluent characteristics for Phase VII (4 June 2009 to 5 October 2009). Calculations of averages and standard deviations are presented for all measurements except for the pH value, which is reported as a median value. The number in parenthesis represents the number of samples over the operating period. II-16

Table II.9: Average measurements of COD for feed wastewater (COD in) and the effluent (COD out) of the ABR train at various phases of laboratory ABR operation. II-17

Table II.10: Average measurements of TS for feed (TS in) and effluent (TS out) during various phases of laboratory ABR operation. II-18

Table II.11: Average measurements of VS for feed (VS in) and effluent (VS out) at various phases of laboratory ABR operation. II-18

CHAPTER 1 : INTRODUCTION

The anaerobic baffled reactor (ABR) has been investigated as a wastewater treatment system for over a decade at the Pollution Research Group (PRG), University of KwaZulu-Natal. Early research focussed on the treatment of high-strength organic loads such as that from the textile industry (Bell, 2000). Research was then expanded to domestic wastewater treatment where the particular attributes of the system, namely, its efficient chemical oxygen demand (COD) removal, potential to operate without power and its resilience to organic and hydraulic shock loadings, is well-suited to the decentralised approach required in densely populated informal areas.

A comprehensive study was conducted within the Pollution Research Group to evaluate the technology for this particular purpose (Foxon *et al.*, 2006). Two PhD, three MSc Eng and two MSc degrees were awarded from research emanating from that study (Foxon *et al.*, 2006; Foxon, 2009) (Figure 1.1). The results from that research showed that the ABR displays hydraulic and biological advantages relative to its nearest competitor, the septic tank (Foxon *et al.*, 2006). However, effluent polishing is required to remove pathogens and nutrients (Foxon *et al.*, 2006). The next logical technological step would therefore be to incorporate an appropriate polishing step with ABR technology. Importantly, this step should adhere to the requirements of a *decentralised sanitation approach* (easily maintained, consistent treatment efficiency and no energy usage).

A number of DEWATS (*DE*centralised *W*astewater *T*reatment *S*ystem) plants designed by the non-profit organisation BORDA (*B*remen *O*verseas *R*esearch and *D*evelopment *A*ssociation) (<http://www.borda-net.org/index.php?id=81>) use ABR technology for sanitation at a household or community level (Sasse, 1998). In these plants, the ABR forms the core treatment system with effluent polishing achieved through a combination of anaerobic filters and/or constructed wetlands and ponds (Sasse, 1998; Gutterer *et al.*, 2009). In some instances, the polishing step is unable to reduce the pathogen load to an acceptable level for discharge. Moreover, in densely congregated informal communities, the lack of space may limit the construction of wetlands for effluent polishing. For this reason, a range of polishing technologies should be available for consideration.

In this thesis, the use of membrane technology as a polishing step was evaluated. Membrane separation is a well established process in conventional wastewater treatment systems and its use is seen as advantageous as it can produce a consistent and superior quality effluent with a low land area footprint. The aim of this study was therefore to investigate the application of

membrane technology in conjunction with ABR technology. Although there is an appreciable quantity of literature dedicated to membrane processes under aerobic conditions, the body of knowledge that exists for anaerobic membrane systems is significantly smaller and non-existent with regards to ABR technology. This research formed part of a larger European Union project called *EUROMBRA* (Leiknes, 2006; <http://www.mbr-network.eu/mbr-projects/proj-desc-eurombra.php>) which was concerned with providing solutions to membrane-related challenges.

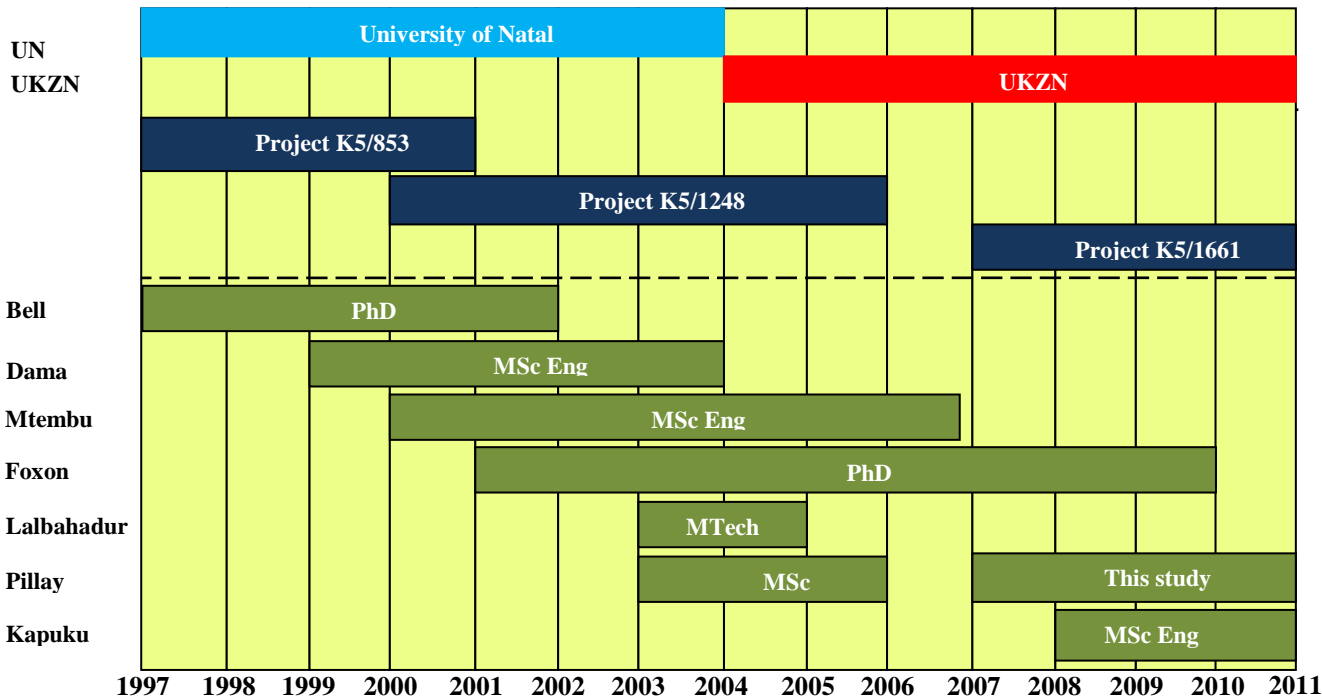


Figure 1.1: Research students involved in ABR research at the Pollution Research Group. The WRC projects which dealt with that research are included.

The remainder of this chapter describes the need for improved sanitation within the South African context, the context of the *EUROMBRA* Project within this thesis, background to the thesis and objectives of this thesis.

1.1 INTRODUCTION

The delivery of basic water and sanitation is a national development priority and is well placed within the context of the Millennium Development Goals (MDG), a framework for global development with time-bound targets by which progress can be measured (United Nations, 2006). Among the goals are to halve the number of people without sustainable access to drinking water and basic sanitation by 2015.

The South African government implemented a free basic water programme in 1994 whereby each household is entitled to 200 litres per day (L/d) [Department of Water Affairs (DWAF, 2003)]. The provision is based on the World Health Organisation (WHO) standard which is considered sufficient to maintain good health and productivity. A similar strategy has produced a dramatic decline in waterborne infections in developed countries (Genthe and Seager, 1996). The programme has been largely successful with an estimated 15.5 million people supplied with free basic water since the programme started.

Whilst significant progress has been made with regards to the supply of potable water, far less progress has been made with regards to the delivery of basic sanitation services. In 2007, an estimated 15 million South Africans still did not have access to basic sanitation (Water Wheel, 2008). South Africa is not the only country experiencing this problem. A report on the status on the Millennium Development Goals revealed that several developing countries are behind their projected sanitation targets (UN, 2006). In South Africa, the slower sanitation delivery has been attributed to the strong prioritisation of potable water supply (in comparison to sanitation delivery) by both unserved communities and the government (Muller, 2002). Moreover, there is a perceived difficulty in providing sanitation at the household level (Muller, 2002).

Providing sanitation services to previously unserved communities is a challenge. In the past, the conventional wisdom was to implement conventional centralised wastewater treatment systems (Parkinson and Tayler, 2003). Whilst these systems are appropriate for urban areas with a large concentration of people, service provision to peri-urban areas is difficult, especially when these areas are highly populated and fall outside the sewered network (Parkinson and Tayler, 2003). In such cases, “economies of scale do not exist” such that centralised wastewater technologies require comparatively more investment costs (than a decentralised system) which are unaffordable to the majority of the peri-urban poor (Parkinson and Tayler, 2003). Moreover, a large infrastructural investment is required within a limited timeframe, trained personnel are required for construction, operation and maintenance, and the systems are costly to operate. The financial investment required for such systems may be beyond the reach of most developing countries as even in developed countries these systems are directly cross-subsidised and have low chances of being financially sustainable (Hauff and Lens, 2001). In South Africa, there already exists a critical shortage of trained and skilled staff in centralised wastewater treatment works with a small proportion of plants operated and maintained adequately (evidence cited in Eales, 2008). For this reason, many decision-makers are keen on adopting a decentralised approach to managing wastewater treatment and disposal. This approach involves the treatment of wastewater close to the source such that large savings in investment cost of sewerage systems

and pumping costs can be achieved (Lettinga *et al.*, 2001; Parkinson and Tayler, 2003). Moreover, they are likely to be less costly to construct and operate (Parkinson and Tayler, 2003) and there is potential to use reuse the treated wastewater for various activities near the source. This approach is in line with the Bellagio Principles for water sustainability set out in Italy (<http://www.iisd.org/measure/principles/progress/bellagio.asp>) (International Institute For Sustainable Development, 1997).

In South Africa, sanitation provision outside the sewer network is usually in form of on-site dry toilets, such as a urine diversion (UD) or ventilated improved pit (VIP) latrine toilet with approximately 8% of the population serviced with the latter system (Eales, 2008). However, many communities prefer flushing toilets over dry sanitation. Thus, there is a technological gap for waterborne sanitation options that are both practical and sustainable for these areas.

1.2 THE EUROMBRA PROJECT

In 2005, the European Union (EU), encouraged by the Water Framework Directive (WFD), initiated the project entitled *Membrane Bioreactor Technology (MBR) with an EU Perspective for Advanced Wastewater Treatment for the 21st Century (EUROMBRA)* (Leiknes, 2006). The group consisted of several leaders in membrane research in industry and academic institutions. The project team is made primarily of research partners from the EU, with one research group from South Africa (UKZN) and another from Australia (a list of participants can be viewed in **Appendix I**). The vision of the project was to develop sustainable solutions for municipal wastewater treatment based on membrane technology.

Membrane technology is seen as a key process in future wastewater re-use strategies as it can produce a high-quality effluent that could potentially be free of bacteria and viruses (Cicek *et al.*, 1998; Madaeni, 1999). The membrane product can then be returned to the environment or re-used for various applications without any detrimental effects. With respect to the *EUROMBRA* Project, most of the research was directed towards upgrading conventional wastewater treatment systems, such as the activated sludge process, with membrane technology. The membrane bioreactor (MBR), a combination of membrane filtration with a biological step, has attracted great attention with respect to the activated sludge process as it can replace the clarification and settlement stages with a single step (Chang *et al.*, 2002). Other advantages include a smaller land area footprint, less sludge production and superior effluent quality (Le Clech *et al.*, 2005; Fan *et al.*, 2006). Despite these advantages, the wider application of MBR systems is restricted because of the inherent membrane fouling phenomena (Chang *et al.*, 2002; Le Clech *et al.*, 2005). Excessive membrane fouling can result in a severe

loss of performance and the use of costly and time-consuming cleaning procedures. In some instances, the fouling is so severe that acceptable operation cannot be maintained and membrane replacement is required (Baker and Dudley, 1998; Chang *et al.*, 2002). As a result, the capital and operational costs of MBRs are at present greater than conventional processes.

One of the major obstacles in attempting to solve the membrane fouling problem is the diversity of methodologies used to characterise fouling which restricts the comparison between groups. Many of the solutions that are available for MBR systems differ in several aspects depending on the type of wastewater being treated, the type and design of membrane systems used, recommended operating regimes and ranges, strategies to achieve economical and sustainable operation, and footprint (Leiknes, 2006). Another problem is related to the differences in the analytical techniques (both physical and chemical) that are used to characterise the biomass and identify the membrane foulants (Evenblij *et al.*, 2005; Rosenberger *et al.*, 2005). Consequently, contradictory information on the substances which are responsible for fouling are often cited in literature (Rosenberger *et al.*, 2005).

The *EUROMBRA* Project was initiated between various leaders in membrane research to try to solve the lack of standardisation and to provide *a comparison of concerted and cohesive research effort, explicitly linking key limiting phenomena, such as fouling, observed and quantified on various scales* (Leiknes, 2006). Techniques to characterise membrane fouling, biomass and possible membrane foulants were standardised among research groups to present a clearer understanding of the processes limiting membrane performance.

1.3 CONTEXT OF THIS RESEARCH WITHIN THE *EUROMBRA* PROJECT

To date, the majority of MBR research has been focussed on activated sludge membrane technology. The reason being that municipal wastewater in most developed countries is treated by the conventional activated sludge process. Therefore, most new technological advances have been focussed on integrating or upgrading existing treatment systems. Anaerobic wastewater treatment processes, however, are becoming increasingly popular for the treatment of various wastewaters, especially in developing countries (van Haandel and Lettinga, 1994; Foresti, 2002; Franklin, 2001; Rao *et al.*, 2010; Show *et al.*, 2010). They offer numerous advantages over conventional activated sludge process, including the production of biogas, lower sludge production, higher organic loadings, lower space requirements for a similar organic loading, and lower chemical and nutrient requirements (van Haandel and Lettinga, 1994; Rittmann and McCarty, 2001). Many problems associated with anaerobic treatment, such as the slow growth

of methanogenic organisms and their susceptibility to adverse environmental conditions, have been overcome through novel reactor design, *inoculating* or *seeding* reactors to limit the start-up period and acclimatisation of micro-organisms to toxic materials.

One of the recent advances (over the last three decades) in reactor design is the ABR (Bachmann *et al.*, 1983). The reactor consists of a number of vertical baffles, which compartmentalise the reactor, allowing high solids retention and treatment rates. The design also allows for the separation of the various phases of anaerobic catabolism, which confer greater protection against shock and hydraulic loadings, environmental conditions and toxic materials (Barber and Stuckey, 1999; Bell, 2000). The ABR has been previously studied and proposed as an on-site sanitation technology for low-income areas that are not served by the local waterborne sanitation system and are not appropriate for dry on-site sanitation systems (Foxon *et al.*, 2006). The results from that study revealed that organic removal was higher than those reported for septic tanks under similar hydraulic regimes. Other advantages included a relatively fast recovery from shock and hydraulic loadings, and low sludge production (no desludging was required over the 5-year study). In addition, the effluent from the ABR has the potential to be re-used in agricultural irrigation as no nutrient removal occurs under anaerobic conditions. The main drawback of ABR technology, however, is that anaerobic digestion alone is not effective in removing pathogen and indicator organisms and the effluent requires post-treatment.

In this thesis, membrane technology was investigated as a possible post-treatment option as it could potentially offer superior quality effluent despite varying load conditions and at reduced land area footprint. The effluent could then be re-used for various activities, including urban horticulture, thereby encouraging efficient water usage.

One of the challenges faced in this thesis was the understanding of membrane processes under anaerobic conditions. Whilst there is a large number of publications regarding the use of aerobic MBR, published articles relating to anaerobic MBR (AnMBR) for domestic wastewater treatment or membrane effluent polishing from an anaerobic system are scarce. The reason for the few papers is that conventional MBR processes commonly use air to scour the membranes to minimise fouling (air scouring cannot be used in anaerobic systems as oxygen is toxic to the process). Other challenges faced in this thesis include membrane operation under gravitational pressures (to conform to the decentralised approach – low energy) and that fouling processes in an ABR will be different to aerobic systems and other anaerobic systems.

The contribution of this research is therefore to investigate the application of membrane technology under anaerobic conditions, with the specific application being a gravity-driven membrane filtration step coupled to an ABR. In contrast to other membrane filtration systems, the membrane filtration step is at the back end of the ABR where the concentration of suspended solids is expected to be low. The novelty of this research is that the processes governing fouling will be different to aerobic systems and other anaerobic systems (due to design of the system). Moreover, membrane filtration will be performed using gravitational pressure to eliminate the need for pumping (and thus energy). This situation presents a unique challenge in that membranes must be operated under constant transmembrane pressure (TMP) mode (which is thought to result in more significant fouling compared to the constant flux mode – Defrance and Jaffrin, 1999) using low hydrostatic pressure heads and no gas scouring. Although this is not the only documented use of membranes in this manner, the use of the membranes for effluent polishing from a pre-treatment step, specifically an ABR is. Thus, the fouling behaviour will be very different to aerobic and other anaerobic systems coupled to membranes.

1.4 OBJECTIVES AND AIMS OF STUDY

The primary objective of the thesis was to understand membrane processes under anaerobic conditions, more specifically, when associated with an ABR pre-treatment step.

The specific aims of the project as set out at the beginning of the thesis were:

- To build, operate and monitor the performance of a laboratory-scale ABR for the pre-treatment of *complex wastewater* (wastewater containing particulates – not easily degraded as a soluble feed).
- To use a standardised test cell technique recommended by *EUROMBRA* partners to determine the fouling propensity of the soluble fraction of anaerobic fluids in comparison to aerobic ones.
- To operate membranes under gravity pressures and without gas scouring.
- To assess the effect of operating conditions on the productivity of different membrane modules using a *practical approach* (refer to section 2.2.7 for a definition).
- To determine the treatment efficiency of membranes treating an ABR effluent.
- To compare hollow-fibre and flat-sheet membrane processes treating ABR effluent.
- To use a *compositional approach* to identify foulants in the ABR effluent (refer to section 2.2.7 for a definition).
- Use standardised chemical techniques to characterise fouling.

1.5 PRODUCTS OF THE STUDY

The products from this study will provide technical information for water authorities, designers and operators of decentralised membrane polishing operation and strategies. Moreover, it will provide insight to the fouling behaviour in an anaerobic system, in particular an ABR plant. Useful information on the anaerobic degradation of complex particulate matter in an ABR system will also be generated.

The limitation of this study is related to the characteristics of the feed. The project team did not have access to a sufficient amount of domestic wastewater for the long-term operation of an ABR-membrane filtration plant. Thus, the decision was undertaken to use ventilated improved pit latrine (VIP) sludge as a high-strength, complex ‘synthetic’ wastewater representative of blackwater. Some biodegradation would have occurred in the pits before samples were taken (Bakare, 2011). The feed was chosen as it was could be easily obtained throughout the year and would be more representative of blackwater than a soluble synthetic feed. Consequently, membrane experiments *cannot be extrapolated* to future field-scale ABRs treating domestic wastewater. The project did, however, generate a considerable amount of scientific information regarding the operation of membrane modules at low gravitational pressures under anaerobic conditions, the results of which could be used to develop a strategy for field-based membrane coupled ABR systems.

1.6 THESIS OUTLINE

Figure 1.2 illustrates the breakdown of the remaining chapters in the thesis.

Chapter 1 highlights the need for an appropriate polishing step to ABR based sanitation technologies. Membrane technology is considered as a possible polishing step for these plants. However, there is a lack of scientific knowledge regarding the use of membrane technology and the processes governing membrane performance for this specific application. This investigation was performed on a laboratory ABR treating a complex synthetic wastewater in the Biochemical Engineering laboratory at the University of KwaZulu-Natal. The limitation of this approach is that membrane filtration experiments cannot be extended to field-based systems.

In **Chapter 2**, the background for the subsequent chapters is presented and the technological gaps are highlighted.

Chapter 3 provides the details of the laboratory system used in this thesis.

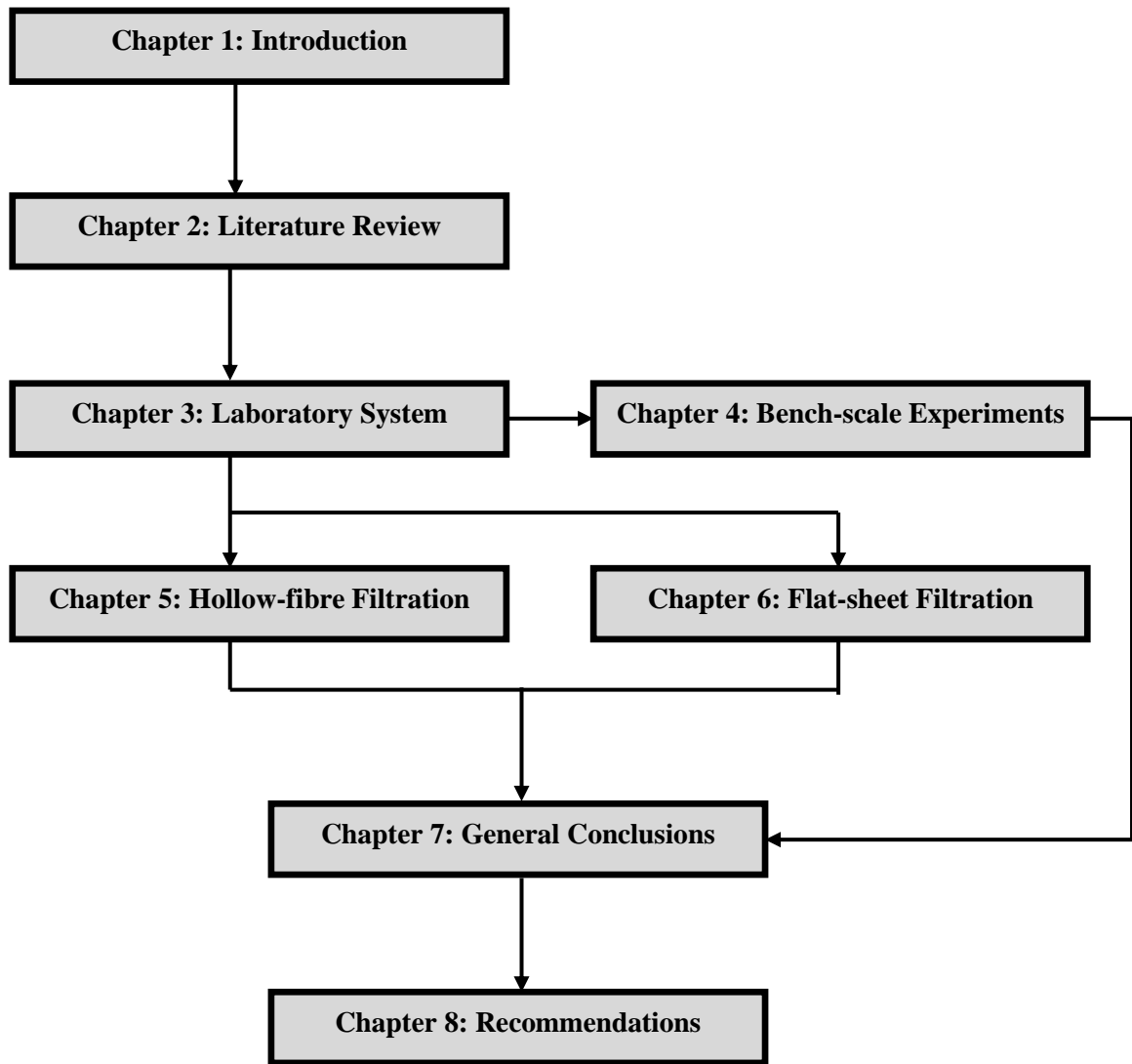


Figure 1.2: Breakdown of chapters in this thesis. The interdependence of chapters is indicated by arrows.

Specific membrane experiments performed are reported in **Chapters 4 to 6**. Each of these chapters is defined by its own goals more specific to the particular investigation.

In **Chapter 4**, a recommended test cell technique was used to elucidate fouling propensities of anaerobic and aerobic membrane feed sources. The results are discussed in view of the suitability of the technique to quantify membrane fouling propensity between these sources.

Chapter 5 presents laboratory-based membrane experiments of hollow-fibre modules coupled to an ABR. Specific membrane experiments were performed to elucidate the mechanism of fouling for this module type. The results of **Chapter 5** are interlinked with **Chapter 6** which

presents a parallel investigation performed with flat-sheet modules on the same membranefeed (laboratory ABR effluent).

Lastly an overall conclusion and remarks on the membrane fouling mechanisms of different module types treating ABR effluent is presented in **Chapter 7**. The recommendations are given in **Chapter 8**.

CHAPTER 2 : LITERATURE REVIEW

Membrane bioreactor (MBR) technology is based on the coupling of two distinct processes; a biological treatment step followed by membrane filtration. In this thesis, anaerobic digestion was used as a pre-treatment step for membrane polishing. The background information and the principles behind anaerobic digestion and membrane filtration are presented in section 2.1 and section 2.2, respectively. Section 2.3 presents a review of the operation of anaerobic membrane bioreactors treating domestic wastewater. Section 2.4 presents a review of pathogen removal in membrane bioreactor. The concluding remarks from this chapter are presented in section 2.5.

2.1 ANAEROBIC DIGESTION

Anaerobic digestion has been used for over a century to treat wastewater (McCarty, 1981; McCarty and Smith, 1986). The process involves the breakdown of organic matter into methane and carbon dioxide (in the absence of oxygen) through a complex series of reactions which are mediated by a consortium of interacting micro-organisms (Hawkes *et al.*, 1978; McInerney, 1999). In spite of its early introduction, the process has not been broadly implemented as the main biological wastewater treatment step (Seghezzi *et al.*, 1998; Kassam *et al.*, 2003). There are a number of reasons for this. First, there were concerns over the reliability of the process to treat large and increasing wastewater volumes especially in industrialised and densely populated areas (Lubberding, 1998). More importantly, there was also a lack of fundamental understanding and experience of anaerobic processes (Rittmann and McCarty, 2001). Consequently, doubts remained over its suitability to treat the wastewater effectively especially low-strength wastewater (Foresti, 2002). Such scepticism of the process has consequently resulted in a preference of centralised aerobic systems, such as activated sludge processes, over anaerobic systems (Rittmann and McCarty, 2001; Leitão *et al.*, 2006). Increases in energy prices have resulted in higher operation and maintenance costs of centralised aerobic systems reducing the attractiveness of the technology (Aiyuk *et al.*, 2004; van Haandel and Lettinga, 1994), especially in developing countries where the finance and skill for the operation and maintenance of these plants is limited (Aiyuk *et al.*, 2006; Eales, 2008). This has directed research towards alternative, cost-effective and energy-saving treatment systems, such as anaerobic treatment. Through experience and a better understanding of the basic principles of the process, it has been shown that anaerobic systems can offer several advantages over aerobic systems, thereby producing an economical and viable alternative for wastewater treatment (Lettinga, 1995; Rittmann and McCarty, 2001).

2.1.1 ADVANTAGES OF ANAEROBIC DIGESTION

A summary of the advantages and disadvantages of anaerobic treatment is presented in Table 2.1. The most obvious advantage of anaerobic digestion is the generation of biogas, specifically methane. The biogas can be harvested for electrical or heating purposes and can be channelled into the running of a treatment plant. In contrast, aerobic systems have a relatively high energy requirement (Leitão *et al.*, 2006) as oxygen must be mechanically supplied at a cost (van Haandel and Lettinga, 1994).

Methane harvesting and its utilisation is an economic advantage that has been realised by many municipal treatment facilities. In some instances, the methane harvested from the anaerobic treatment of sludge from municipal plants employing secondary aerobic treatment satisfies the energy requirements to operate the entire plant, including the aeration tanks (Rittmann and McCarty, 2001). If anaerobic treatment could be used for all or most of the wastewater treatment, there exists potential for energy exportation via the treatment facility instead of energy consumption (Rittmann and McCarty, 2001). From a sanitation viewpoint, the process offers another advantage over centralised aerobic systems in that it could be performed in the *decentralised* mode (treated and disposed on-site) which has the potential to reduce waterborne infrastructure costs (evidence cited in Aiyuk *et al.*, 2006).

Many substantial developments have been made over the years to overcome the problems associated with the operation of anaerobic reactors. These include increasing the retention and the protection of anaerobic micro-organisms through novel reactor design and inoculating the reactor before start-up. Indeed, many anaerobic reactors have become well-established for the treatment of various wastewaters, including low-strength wastewater such as domestic wastewater (Aiyuk *et al.*, 2006). The upflow anaerobic sludge blanket (UASB) reactor and its variants are good examples of this (Seghezzo *et al.*, 1998). Post-treatment, however, is still required to reach certain discharge guidelines (van Haandel and Lettinga, 1994).

2.1.2 THE CONVERSION PROCESS IN ANAEROBIC SYSTEMS

The conversion of complex organic waste into methane occurs (in the absence of oxygen) through the interaction of several groups of micro-organisms, often linked by their individual substrate and product specificities (Pohland, 1992). A schematic representation of the chemical pathway of the methane fermentation reactions is shown in Figure. The process involves the degradation of complex organics (polysaccharides, proteins, lipids) into simpler compounds such as carbohydrates, amino acids and fatty acids through a series of successive steps that ultimately lead to the formation of methane (Pohland, 1992). The process is not a sequence of independent reactions. Instead, it involves both indirect and direct symbiotic interactions among

Table 2.1: Advantages and disadvantages of anaerobic wastewater treatment (adapted from Seghezzi *et al.*, 1998).

Advantages	<p><i>Simplicity and flexibility.</i> The construction of anaerobic reactors is relatively simple, and can be applied on either a large or small scale.</p> <p><i>Low energy consumption in low-rate digesters.</i> The process is generally a net producer of energy in the form of methane. Energy input for aeration is not required as in aerobic systems.</p> <p><i>Low decay rate.</i> Anaerobic micro-organisms can remain viable for months, whereas aerobic micro-organisms decay within a few weeks. This is important for industries with seasonal activity.</p> <p><i>Low sludge production.</i> Sludge production is much lower in anaerobic systems compared to aerobic systems due to a lower yield co-efficient.</p> <p><i>Low nutrient and chemical requirement.</i> Smaller biomass production occurs in anaerobic systems, and thus the nutrient requirements can be proportionally less.</p> <p><i>High organic loading possible.</i> Anaerobic systems are not limited by the supply of oxygen making them attractive for treating industrial wastewater with high organic loading.</p> <p><i>Low space requirement.</i> The area needed for a reactor is proportionally smaller as it is able to treat wastewater with a high organic loading.</p> <p><i>Decentralised operation possible.</i> No energy requirement and low sludge production.</p>
Disadvantages	<p><i>Long start-up.</i> Lower energy yield results in smaller microbial yields and slower growth yields. Due to slow growth rate, start-up time is longer than aerobic systems.</p> <p><i>High microbial sensitivity.</i> Methanogens are sensitive to pH, temperature and assumed to have less resistance towards toxic compounds.</p> <p><i>Odour production.</i> Production of sulphides, especially when there are high concentrations of sulphate in the influent, results in a strong, unpleasant smell.</p> <p><i>High buffer requirement for pH control.</i> The desired pH range for an anaerobic reactor is between 6.5 and 7.6. Chemical addition may be necessary to control pH in wastewaters (mostly industrial wastewaters) with insufficient natural buffering capacity.</p> <p><i>Low pathogen and nutrient removal.</i> Anaerobic digestion results in partial removal of pathogens and incomplete nutrient removal. Post-treatment of anaerobic effluent is required to meet discharge guidelines.</p>

different anaerobic microbial species (Lubberding, 1998). These anaerobic micro-organisms can be categorised into four major metabolic groups that are generally accepted as being present in anaerobic systems (Zinder *et al.*, 1984a; van Haandel and Lettinga, 1994; Lubberding, 1998; Anderson *et al.*, 2003). These include *hydrolysis*, *acidogenesis*, *acetogenesis* and *methanogenesis*.

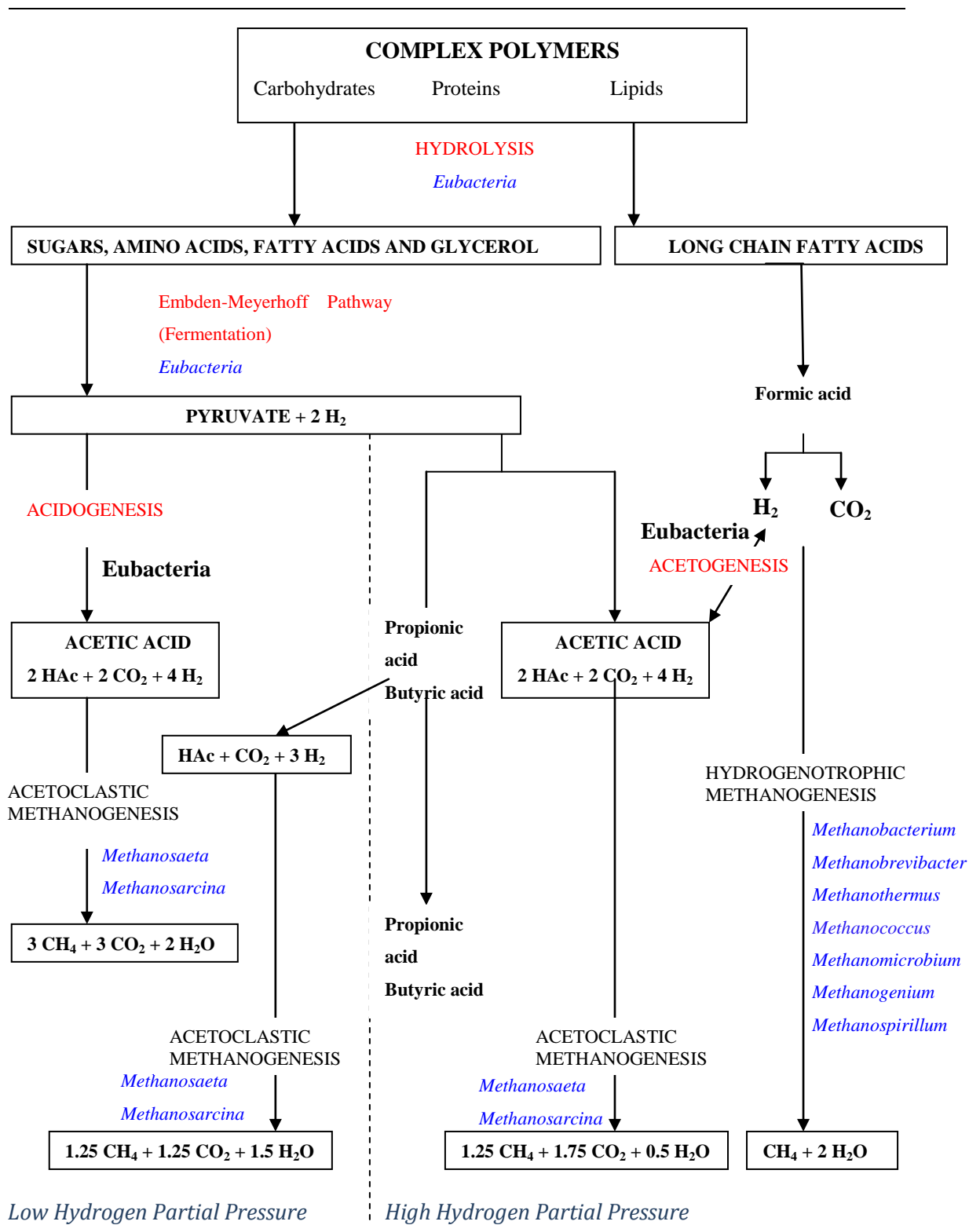


Figure 2.1: Diagram illustrating substrate conversion patterns and the micro-organisms involved in the anaerobic digestion of complex macromolecules (from Bell, 2000).

Often the first two or three groups (*hydrolysis*, *acidogenesis* and *acetogenesis*) are considered as a single metabolic group that operate in fermentative reactions whilst the last, methane producing step is called methanogenic fermentation (Gunnerson and Stuckey, 1986; van Haandel and Lettinga, 1994).

2.1.2.1 Hydrolysis

Hydrolysis is the first step in anaerobic digestion and involves the degradation of complex organic polymers (proteins, cellulose, lignin, lipids) by a consortium of micro-organisms into smaller, intermediate organic monomers. The monomers generated include sugars, such as mono- and disaccharides, fatty acids and amino acids (Pohland, 1992; van Haandel and Lettinga, 1994). The hydrolytic process is catalysed by a number of *extracellular* or *exocellular enzymes* (enzymes produced to the outside of the cell), such as cellulases, proteases, and lipases, which are secreted by relatively fast-growing fermentative bacteria (Bitton, 1994). The role of these enzymes is to facilitate the digestion process by converting the complex polymers into soluble monomers which can then be taken up by cells. By doing so, the substrate formed from the complex polymers becomes available to other metabolic groups (Bitton, 1994; van Haandel and Lettinga, 1994; Anderson *et al.*, 2003). Hence, the terms *solubilisation* or *liquidification* are commonly used as synonyms for this step (van Haandel and Lettinga, 1994). This step is usually the *rate-limiting* step when the feed consists of complex particulate matter (van Lier *et al.*, 2008). This is not due to the lack of enzyme activity but rather to the available surface area of particulates to enzyme activity and the overall structure of the solid substrate (evidence cited in van Lier *et al.*, 2008).

2.1.2.2 Acidogenesis

Acidogenesis, the second step of the digestion process, involves the utilisation of the soluble products formed through hydrolysis. The products formed by acidogenic bacteria include organic acids (acetic, propionic formic, lactic, butyric, and succinic acids), alcohols and ketones, acetate, carbon dioxide, and hydrogen (Bitton, 1994). *Facultative bacteria* are often included in this group and are thought to play an important role in the digestion process by utilising dissolved oxygen that would otherwise be toxic (van Haandel and Lettinga, 1994).

2.1.2.3 Acetogenesis

In acetogenesis, a group of bacteria produce acetate, carbon dioxide and hydrogen from fatty acids, alcohols and even aromatic compounds. The by-products generated by this step are the only substrates that are efficiently used by methane-producing micro-organisms. Acetogens are differentiated into two distinct metabolic groups: obligate hydrogen-producing acetogens (OHPA) and homoacetogens (Anderson *et al.*, 2003). The OHPA produce acetate from

consuming the major fatty acid intermediates (propionic acid, butyric acid) from acidogenesis (Bitton, 1994; Anderson *et al.*, 2003). In contrast, homoacetogens produce acetic acid from hydrogen and carbon dioxide which has the importance of keeping the hydrogen partial pressures low and making OHPA fatty acid oxidation reactions thermodynamically feasible (Lubberding, 1998).

2.1.2.4 Methanogenesis

Methanogenesis involves production of methane as a metabolic by-product by a distinct group of microbes called methanogens. Without these microbes, the ultimate degradation of organic matter would not occur (Anderson *et al.*, 2003). As methanogens are slow-growing, this step is often recognised as being rate-limiting particularly when the feed contains high concentrations of soluble organic compounds. Furthermore, methanogens are highly sensitive to pH change outside their optimum (approximately pH 6.5 to 7.6) meaning that the process is susceptible to excessive acid production from earlier steps.

Two groups of methanogens have been described in literature; *acetoclastic methanogens* and *hydrogenotrophic methanogens* (Anderson *et al.*, 2003). Their classification into either group is based on their substrate specificity (Figure 2.1). Hydrogenotrophic methanogens metabolise hydrogen and carbon dioxide to produce methane. Approximately 30% of the methane produced in anaerobic reactors occurs via this pathway. Although it represents only a relatively small fraction of methane produced, this pathway is critical to the efficiency of the digestion process as it utilises hydrogen produced during previous steps (hydrolysis and acidogenesis) (Gunnerson and Stuckey, 1986). The micro-organisms therefore play a similar role to OHPA in maintaining low hydrogen partial pressures.

Acetoclastic methanogens produce methane from acetate in a pathway known as *acetotrophic methanogenesis*. This pathway is responsible for approximately two-thirds (65 to 75%) of the methane produced in anaerobic systems (Bitton, 1994; van Haandel and Lettinga, 1994; Lubberding, 1998; Anderson *et al.*, 2003). However, only two genera of methanogens are able to utilise acetate efficiently; *Methanosarcina* and *Methanosaeta* (formerly *Methanothrix*). The genera have different affinities for acetate and thus acetate concentrations have considerable influence over the genera that predominates in an anaerobic system (Zinder *et al.*, 1984b). At high acetate concentrations, the more versatile *Methanosarcina* is favoured, whilst at low concentrations, *Methanosaeta* dominates. This shift in genera predominance is brought about by differences in specific growth rates and substrate affinity for acetate. *Methanosarcina* has a higher maximum specific growth rate (or shorter doubling time) but a relatively lower substrate

affinity for acetate [half-saturation constant values (K_s) = 200 to 400 mg/L; higher K_s value means lower affinity for acetate]. *Methanosaeta*, on the other hand, has a high affinity for acetate ($K_s = 20$ mg/L) but a lower maximum specific growth rate. Thus, *Methanosarcina* is able to grow faster than *Methanosaeta* but only in an environment with a relatively high acetate concentration. In contrast, the slower growing *Methanosaeta* has preference for environments with relatively low acetate concentrations.

2.1.3 WATERBORNE ANAEROBIC SANITATION SYSTEMS

In decentralised sanitation, two situations are distinguished based on the separation of wastewater streams (Kujawa-Roelveld and Zeeman, 2006). The first involves the treatment of total *domestic wastewater* which is composed of all wastewater produced by households including sanitation, washing and cleaning activities (cooking, showering, and laundry). The second involves the separation and management of the domestic wastewater stream into *blackwater* and *greywater* components. Blackwater is generated from human and animal excreta (faeces and urine) and includes toilet flushing water (Kujawa-Roelveld and Zeeman, 2006). Greywater is a more voluminous stream generated from domestic activities such as washing, cleaning and showering, and represents less of health threat than blackwater (Parkinson and Tayler, 2003). In conventional centralised treatment systems, these streams are combined, sometimes with the rain-water and effluent from industrial streams using the sewered system, and treated. In this case, the wastewater is referred to as *sewage* (van Haandel and Lettinga, 1994). From a technological point of view, source separation of domestic wastewater streams and treating the streams individually is the most logical option. However, this is not always applied as more complex piping is required at a household level (Kujawa-Roelveld and Zeeman, 2006).

The wastewater stream to be treated on-site by an anaerobic treatment system will be composed of total domestic wastewater or one of its components. In this section, only anaerobic systems treating domestic wastewater containing a blackwater stream are reviewed. Emphasis is placed on on-site waterborne treatment systems that serve individual households, communities or a combination of both. These waterborne options therefore represent the technological competitors of anaerobic baffled reactor (ABR) technology.

2.1.3.1 Septic Tank

The history of the septic tanks dates back to 1891 when WD Scott constructed the first septic tank to retain sewage solids. The system has been used on-site for over 100 years to treat sewage and is the simplest and most widely used anaerobic process (Jewel, 1987). The general structure consists of a buried tank constructed out of concrete, metal or fibreglass, and a

subsurface drainage system, which treats the effluent as it percolates into the soil. Wastewater (blackwater and greywater) enters the reactor with grease and oil forming a floating *scum layer* (Wright, 1999) (Figure 2.2). This layer is often trapped by vertical baffles to prevent it from being discharged (McKinney, 1962) This feature is not necessary for residential septic tanks but rather for those institutions which generate wastewater with a high fat content (restaurants, hotels) or other foreign materials (hospitals) (Wright, 1999).

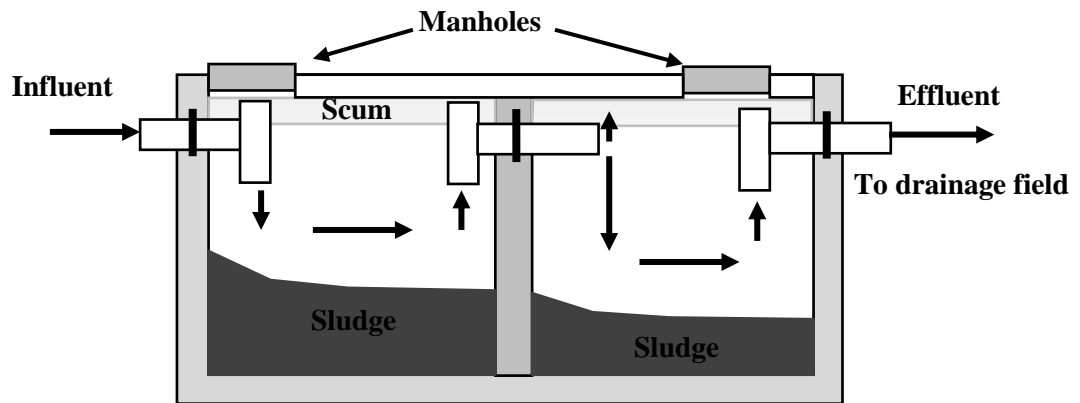


Figure 2.2: Schematic cross-section through a conventional septic tank used for the treatment of domestic sewage (adapted from City of Cape Town, 2011).

The primary function of the tank is to settle suspended matter, treat incoming wastewater by anaerobic digestion and accumulate inert particles (Kujawa-Roeleveld and Zeeman, 2006). Anaerobic sludge or *septage* is produced at the bottom of the tank through sedimentation of settleable material. Eventually, the sludge becomes compacted by the weight of accumulated solids with layers of sludge developing at the bottom of the tank. The septage builds-up in the system and eventually has to be disposed of either by land application or introduced with wastewater to be treated by treatment works (Bitton, 1994).

The average retention time of wastewater within the tank varies between 1 to 4 d (McKinney, 1962; Bitton, 1994) with biochemical oxygen demand (BOD) and suspended solids removals between 65 to 80% and 70 to 90% attainable, respectively (Wright, 1999). The system does not reduce the pathogen load in the incoming wastewater significantly with a large number of viruses, bacteria, protozoa and helminths present in the effluent, scum and sludge (Wright, 1999). Another disadvantage of the septic tank is that retention of solids is affected by gas production in the septage layer.

Polishing of the septic tank effluent usually takes place in the drainage field which the effluent enters through a series of perforated pipes. The drainage field consists of either a soakaway (trench, bed, seepage pit, mound or fill) or an artificially drained system (Wright, 1999). The soil acts as a filter, removing any remaining solids and microbial contaminants in the effluent as it moves towards groundwater (Wright, 1999). The drainage field is an integral part of the septic tank process and its functioning is dependent on a number of factors, such as wastewater characteristics, rate of wastewater loading, geology, and soil characteristics (Bitton, 1994). It is not uncommon, however, for groundwater contamination to occur as not all pollutants are removed (Yates, 1985; Greg and Michael, 1994; Scandura and Sobsey, 1997). According to Bitton (1994), septic tank effluents are responsible for a large proportion of waterborne disease outbreaks from contaminated groundwater and are probably the major contributors to enteric viruses found in subsurface environments. In South Africa, certain municipalities do not allow the construction of drainage fields due to bad experiences in the past. Instead, these municipalities pump out the effluent and combine it with municipal wastewater at the nearest wastewater treatment plant or dispose of it by land application (surface spreading or infiltration in open trenches) (Wright, 1999). This can incur high costs to the municipality and may present a hazard as the emptier assumes that the tank has been properly constructed which is not always the case (Wright, 1999).

2.1.3.2 Upflow Anaerobic Sludge Blanket

The upflow anaerobic sludge blanket (UASB) reactor was developed in the early seventies by Lettinga and colleagues (van Haandel and Lettinga, 1994; Lettinga and Hulshoff Pol, 1991; Seghezze *et al.*, 1998; Rittmann and McCarty, 2001). The reactor has been the most successful and widely-used reactor type in industrial and domestic wastewater applications (Rittmann and McCarty, 2001; Foresti, 2002). The successful application of the reactor at various scales in domestic wastewater treatment has been shown in hot climates, such as Brazil, Mexico, Cuba and India, where temperatures higher than 20°C are important for the digestion process (Verstraete and Vandevivere, 1999; Passig *et al.*, 2000; Chernicharo and Nascimento, 2001; Florencio *et al.*, 2001; Rodriguez *et al.*, 2001; Foresti, 2002; Torres and Foresti, 2001; Khalil *et al.*, 2008).

The reactor consists of a sludge blanket at the bottom of the reactor and an upper liquid layer (Figure 2.3). Good wastewater-biomass contact in UASB systems is achieved through an even flow distribution at the bottom sludge layer at a satisfactory upflow velocity coupled with the natural turbulence created by gas production (Lettinga and Hulshoff Pol, 1998; Seghezze, 2004). The incoming wastewater is treated as it flows upwards through the sludge

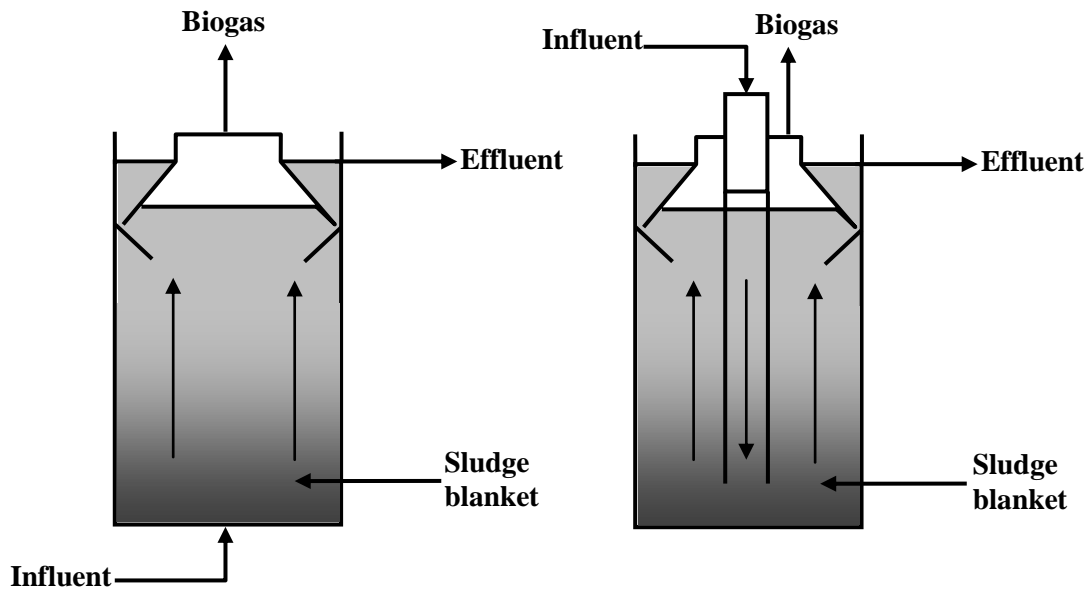


Figure 2.3: Schematic representation of a conventional UASB and a UASB-septic tank (adapted from Seghezzeo, 2004).

bed which consists of a floating layer of active microbial flocs (Bitton, 1994). The sludge is formed through the accumulation of solids and bacterial growth and its establishment is critical to successful operation (Seghezzeo, 2004). Over time these microbial flocs will grow and form well-defined, compact, spherical granules which generally consist of a small ash content and a mixed population of anaerobic microbes (Rittmann and McCarty, 2001). The granular sludge has good settling properties and is not easily washed out the system (Seghezzeo, 2004) thus enhancing retention of sludge – the major advantage of the UASB system (MacLeod *et al.*, 1990). Moreover, the granular sludge is not easily broken up and can withstand high mixing forces (Lettinga *et al.*, 1980). Although these characteristics have made the UASB the most successful anaerobic reactor in wastewater treatment, the process is heavily dependent on the formation and integrity of granules which may not always reach desirable levels (Schmidt and Ahring, 1996; Ghangrekar *et al.*, 2005; Bhunia and Ghangrekar, 2007).

There are numerous studies in which the application of UASB reactors is used in the treatment of sewage (Behling *et al.*, 1997; Seghezzeo *et al.*, 1998, Kalker *et al.*, 1999; Seghezzeo, 2004; Álvarez *et al.*, 2006). This section will only focus on those treating domestic wastewater using a decentralised approach.

Those UASB reactors that have been developed for decentralised applications are usually hybrid septic tanks that can serve single households or large communities (Table 2.2). In an early

Table 2.2: Comparison of UASB-septic tank performances. The numbers in parenthesis represent standard deviation. Data adapted from Al-Jamal and Mahmoud (2009).

Reactor	Wastewater	Temperature (°C)	HRT (days)	OLR (kg COD/m ³ .d)	Removal (%)				Reference
					COD _{tot}	COD _{ss}	COD _{col}	COD _{dis}	
UASB-septic tank	Blackwater	11.7 (4.0)	4.3	0.40	60	77	ND	6 ^b	Bogte <i>et al.</i> (1993)
UASB-septic tank	Greywater	13.8 (3.7)	1.8	0.53	31	9	ND	47 ^b	Bogte <i>et al.</i> (1993)
UASB-septic tank	Greywater	12.9 (2.4)	2.4	0.34	4	6	ND		Bogte <i>et al.</i> (1993)
UASB-septic tank	Blackwater	>20	15	0.23 (0.06)	90-93	ND	ND	ND	Lettinga <i>et al.</i> (1993)
UASB-septic tank	Domestic	>20	1.4	0.96	67-77	ND	ND	ND	Lettinga <i>et al.</i> (1993)
UASB-septic tank ^a	Synthetic blackwater	10	4.4 (4.2) + 1.4	0.301 (0.155)	94 (3.3)	98 (2.6)	50 (32)	71 (19)	Luostarinen and Rintala (2005)
UASB-septic tank ^a	Kitchen + blackwater	10	3.4 (0) + 1.4 (0.28)	0.62 (0.19) + 0.46 (0.29)	91 (4.1)	98 (1.3)	28 (38)	ND	Luostarinen and Rintala (2007)
UASB-septic tank ^a	Blackwater	20	3.4 (0.53) + 1.3 (0.23)	0.56 (0.15) + 0.32 (0.17)	88 (9.2)	96 (4.0)	38 (39)		
UASB-septic tank ^a	Blackwater	10	2.9 + 1.3 (0.22)	0.46 (0.14) + 0.18 (0.01)	92 (3.9)	98 (2.2)	35 (45)	ND	Luostarinen and Rintala (2007)
UASB-septic tank	Blackwater	20	2.9 + 1.3 (0.22)	0.37 (0.12) + 0.17 (0.01)	91 (4.6)	98 (1.9)	11 (55)		
UASB-septic tank	Blackwater	14-18	7.2	0.741-0.968	71	75	ND	44 ^b	Luostarinen <i>et al.</i> (2007)
UASB-septic tank	Domestic	24	2	0.63	56	87	34	20	Al-Shaya and Mahmoud (2008)
UASB-septic tank	Domestic	24	4	0.32	58	90	31	22	Al-Shaya and Mahmoud (2008)
UASB-septic tank	Domestic	17.34	2	0.45 (0.12)	51	83	20	24	Al-Jamal and Mahmoud (2009)
UASB-septic tank	Domestic	17.34	4	0.23 (0.06)	54	87	10	28	Al-Jamal and Mahmoud (2009)
UASB-septic tank	Domestic	12-36	0.25-1.0	0.18-0.72	31-77	ND	ND	ND	Moussavi <i>et al.</i> (2010)

^a, two-phased septic UASB –septic tank, ^b, COD_{colloidal+dissolved}

Abbreviations: COD_{col}, colloidal COD; COD_{dis}, dissolved COD; COD_{ss}, suspended solids COD; COD_{tot}, total COD; ND, not determined.

study, Lettinga and colleagues investigated an UASB-septic tank reactor in the Netherlands and Indonesia. The system is similar to a septic tank except it operated in the upflow mode as an UASB reactor and different to a conventional UASB in that it accumulates the stabilised sludge (Kujawa-Roeleveld and Zeeman, 2006). Treatment performance was also reported to be better than a septic tank (Zeeman, 1997). In the Netherlands, a feasibility study of on-site anaerobic treatment of domestic wastewater using UASB-septic tanks was conducted by Bogte *et al.* (1993). Three UASB-type reactors (1.2 m³) were tested in different rural locations treating blackwater. The process was shown to be highly dependent on the reactor temperature. At temperatures below 12°C, settling was the main mechanism of digestion. Above 12°C, organic matter was degraded by increased microbial activity. COD and BOD removal efficiencies ranged between 33% and 60% respectively for two of the reactors tested at above 12°C. The complete conversion of volatile fatty acids (VFA) into biogas was achieved during warm months (temperatures above 15°C). This period also corresponded to average efficiencies for COD and BOD removal of 60% and 72%, respectively, while the maximum gas production reached 300 L/d.

A similar system was tested by Lettinga *et al.* (1993) in Bandung, Indonesia to treat blackwater and a combination of blackwater and greywater. Treatment efficiencies in UASB-septic tanks in Indonesia were higher (COD, BOD, total suspended solids – TSS - removal efficiencies of 63 to 93%, 82 to 95%, and 74 to 97% respectively) than those reported in Netherlands (Lettinga *et al.*, 1993).

Much of the earlier work by Lettinga's Wageningen research group was extended by Luostarinen and co-workers in Finland. The latter have been investigating the UASB-septic tank for a number of household wastewaters with emphasis on the performance at low temperatures. In one of their earlier works, a two-phase UASB-septic tank treated a synthetic blackwater and a dairy parlour wastewater at low temperatures (10 to 20°C) (Luostarinen and Rintala, 2005). The reactors were found to be an appropriate pre-treatment system for the treatment of these wastewaters. Total COD removal (at all temperatures) was above 90% and greater than 80% for the synthetic blackwater and dairy parlour wastewater, respectively. The removals of TSS and dissolved COD were above 90% and approximately 70% respectively for both wastewaters regardless of temperature. A single-phased reactor was found to be sufficient for blackwater treatment (in terms of COD removal) whilst a two-phased process was required for the treatment of dairy parlour wastewater. In the reactor treating blackwater, nutrients were removed with TSS which was indicative of the feed wastewater characteristics (synthetic feed made from primary sludge from a municipal treatment facility which contained a high

concentration of bound nutrients) and not reactor performance as only limited dissolved nutrient removal occurs under anaerobic digestion.

The two-phase UASB-septic tank was also used to treat a mixture of blackwater and kitchen wastewater (Luostarinen and Rintala, 2007). As was the case with other studies by the research group, temperatures were low (10 and 20°C). Removal efficiencies of 90 and 95% were attained for COD and TSS, respectively, with a low concentration of residual dissolved COD in the final effluent (110-113 mg/L). The study revealed that a two-stage digestion process is required for high removals at low temperature using the blackwater/kitchen water mixture while a single-phased process is adequate for only the blackwater stream at the same temperature.

The effect of temperature on the UASB-septic tank process was given more precedence in another study by Luostarinen and co-workers (2007) where three reactors were used to treat blackwater. A larger UASB-septic tank reactor had a volume of 1.2 m³ and had been previously used by Bogte *et al.* (1993) in the first years of a 13-year study. The other two reactors were smaller, identical in size to each other (0.2 m³) and operated at similar loadings at 15 and 25°C respectively. The study showed sludgeacclimatisation had occurred over the years in the larger reactor to lower temperature with same sludge used to inoculate one of the smaller reactors. Despite this seeding, the two smaller UASB-septic tanks had similar suspended solids COD removals. In the larger reactor, solids retention was the main mechanism of treatment in cold periods as indicated by the reduced suspended solids COD wash-out and dissolved COD washing out of the system. In warmer periods, the conversion of COD to methane was increased and decreased suspended solids COD removal was observed (Luostarinen *et al.*, 2007). The reactor operated at 25°C also showed dissolved COD removal. The effluent of the UASB-septic tanks did not meet local (Dutch) discharge regulations (Luostarinen *et al.*, 2007).

In Palestine, UASB-septic tanks have also been investigated for on-site domestic wastewater treatment. Many of the earlier studies were performed together with Lettinga's group in Wageningen University (Mahmoud *et al.*, 2003). In 2008, the treatment of high-strength domestic wastewater (total COD > 1 000 mg/L) in a single-stage UASB reactor and a UASB-digester system was compared (Mahmoud, 2008). The one-stage reactor was operated at ambient temperature and at a *hydraulic retention time* (HRT) of 10 h with a digester system later incorporated at 35°C. The addition of a digester system to the UASB-septic tank had remarkably improved the removal efficiencies for all fractions of COD (total, suspended, colloidal and dissolved COD, VFA) (Mahmoud, 2008).

Recently, Mahmoud and co-workers have been investigating community-based UASB-septic tanks. The start-up of the two community UASB-septic tanks was reported by Al-Shayah and Mahmoud (2008). The identical reactors operated in parallel over six months under two different HRT (HRT of 2 d for one and 4 d for other). The incoming wastewater had a high total COD concentration (above 1 000 mg/L), with a large fraction consisting of suspended solids COD (about 54%). During start-up, the longer HRT reactor had marginal but significantly better removal efficiencies for total and suspended COD, BOD and TSS with dissolved and colloidal COD removals similar. The performance of both reactors was then evaluated over a year during winter (<18°C) (Al-Jamal and Mahmoud, 2009). As with the earlier study, the incoming domestic wastewater had a high total COD concentration (905 mg/L) with a large fraction of the total COD made up of suspended solids COD (approximately 40%). Statistically similar removal efficiencies were achieved for different COD fractions and TSS in both reactors with the only exception being suspended solids COD (Al-Jamal and Mahmoud, 2009). A community-based UASB reactor was also used by Vieira *et al.* (1994) to treat domestic wastewater from 235 houses in Sumaro, Brazil. The 63 m³ system was able to achieve average COD, BOD and TSS removal efficiencies of 74, 80 and 87% respectively.

2.1.4 POST-TREATMENT OPTIONS FOR ANAEROBIC SYSTEMS

It is well-known that anaerobic treatment produces an effluent that requires further treatment to comply with discharge regulations established by environmental agencies (Foresti, 2002; Chernicharo, 2006). The three main pollutants that require further treatment in a polishing step include remaining organic matter, nutrients (specifically nitrogen and phosphorus) and pathogenic organisms (Foresti, 2002; Chernicharo, 2006). Various post-treatment options have been proposed for effluent polishing after anaerobic treatment. These include facultative ponds, overland flow systems, activated sludge, submerged aerated biofilter, trickling filter, anaerobic filters (AFs), dissolved air floatation and constructed wetlands. Membrane technology has not been included in this section as it is still envisaged as an emerging technology with respect to anaerobic polishing systems (Chernicharo, 2006) (details of membrane technology are covered in Section 2.2). Energy-driven processes, such as activated sludge, dissolved air flotation and submerged aerated biofilm, have also not been included as they are not expected to be used for decentralised sanitation systems.

The purpose of this review is therefore to gain an understanding of the polishing technologies available for decentralised anaerobic systems; the pros and cons of which will be used to argue for use of membranes in this thesis. As the UASB process has dominated the anaerobic treatment of domestic wastewater over the last three decades, the majority of the review relates

to post-treatment after the UASB process. The few investigations dealing with ABR effluent polishing are covered in section 2.1.5.7.

2.1.4.1 Facultative Ponds

Facultative ponds are commonly used to polish effluents from anaerobic ponds. The ponds use symbiotic reactions between algae and bacteria to degrade organic matter (Polprasert and Agarwalla, 1994). The advantage of the system is that high pathogen removal efficiencies can be attained but these systems have a large land area footprint and the final effluent can contain algae (Chernicharo, 2006). In contrast to wastewater stabilisation ponds which treat raw wastewater, polishing ponds are used to reduce organic and suspended solids loads from efficient anaerobic systems. Hence, the limiting factor that usually determines the minimum detention time is not the organic load or suspended solids but the removal of pathogenic organisms (Chernicharo, 2006). Some UASB systems with facultative polishing ponds have been shown to comply with European effluent discharge standards for urban wastewater and WHO (World Health Organisation) guidelines for unrestricted irrigation (von Sperling and Mascarenhas, 2005) although this is not always the case (von Sperling *et al.*, 2002). Moreover, in some pond systems, high pathogen indicator removal rates only occur after a start-up period (von Sperling *et al.*, 2003).

2.1.4.2 Overland Flow System

This polishing step involves the flow of effluent over a downward inclined vegetation ramp. The vegetation acts as a filter removing nutrients and remaining organic matter from the digestion process. Biological oxidation and sedimentation are also thought to occur in the vegetation layer (US EPA, 1981 and 1984; Metcalf and Eddy, 1991). The remaining water from the overland flow system is neither evaporated nor absorbed and is disposed in a water body (Chernicharo, 2006). Overland flow systems have been used to polish UASB effluents. Good helminth removal was observed in the polished effluent (ca. 0.2 eggs/L) but only 2- to 3-log removal of faecal coliforms was observed (Coracucci Filho *et al.*, 2000 cited in Chernicharo, 2006; Chernicharo *et al.*, 2001).

2.1.4.3 Trickling Filter (aerobic)

A trickling filter consists of a tank containing packing material through which wastewater percolates downwards (Chernicharo, 2006). The wastewater is treated by biofilms which develop on the packing material as the wastewater flows to the bottom of tank. Although the systems can be cost-effective and easy to maintain, not much research has been directed at this polishing step with respect to anaerobic systems (von Sperling and Chernicharo, 2005). Some of the few studies that have been conducted with anaerobic systems, in particular hybrid UASB

process, have shown that satisfactory polishing can be achieved (COD, BOD and TSS concentrations of 120, 40 and 30 mg/L) (evidence cited in Chernicharo, 2006).

2.1.4.4 Anaerobic Filter

The concept of the anaerobic filter (AF) was developed by Coulter and co-workers and introduced by Young and McCarty in 1969 (van Haandel and Lettinga, 1994; Anderson *et al.*, 2003). The system relies on sludge entrapment by microbial attachment in the form of a biofilm on support material present in the reactor and between the interstices of support material (Lettinga and Hulshoff Pol, 1998). Wastewater is treated as dissolved pollutants are absorbed by the attached biofilm (Anderson *et al.*, 2003). Whilst early AF systems used rocks as the support material, synthetic materials such as plastics and reticulated foam particles are used today as they have higher void volumes and greater surface areas (Anderson *et al.*, 2003; Rittmann and McCarty, 2001). The cost of the support material, however, can be as high as the construction cost of the reactor itself (Speece, 1996). Another disadvantage is that clogging of bed structure can occur through accumulation of biosolids, influent suspended solid and precipitated minerals (Rittmann and McCarty, 2001). Hence, the use of the AF for the direct treatment of domestic wastewater or high solid content is not practical.

The application of AFs as a polishing step for high-rate anaerobic systems, such as the UASB, is common (Anh *et al.*, 2003). Satisfactory performance has been reported in pilot studies with UASB plants (Chernicharo and Machado, 1998) whilst some scoping experiments have been performed for ABRs treating blackwater (Nguyen *et al.*, 2007). AFs are often included in the design of *DEWATS* (DEcentralised WAstewater Treatment System) plants designed by the non-profit organization *BORDA* (Bremen Overseas Research and Development Association). In most of these plants the ABR forms the core treatment system (Gutterer *et al.*, 2009) (see Figure 2.4). Although many of these ABR-AF type systems have been implemented, scientific literature regarding the performance of the systems is scarce. In one of few articles published, James *et al.* (2006) examined the performance of ABR coupled to AF and an aerobic filter with domestic wastewater. The HRT of the ABR, AF and aerobic filter was 7.6 h, 7.2 h and 11.4 h respectively, with consecutive treatment efficiencies of 43%, 79% and 94% reported. In Vietnam, the performance of laboratory ABR and septic tank systems with and without AFs was evaluated (Nguyen *et al.*, 2007). The results from that study showed AF improved the performance of the treatment system (for more detail, refer to section 2.1.5.7).

2.1.4.5 Constructed Wetland

A constructed wetland is a treatment system that uses vascular plants (in most cases) to treat substrate in the water of a basin, pond or shallow canal (US EPA, 2000; Chernicharo, 2006). The control of flow direction, hydraulic detention and water level is often predetermined by the inclusion of an impermeable layer, either natural or synthetic, during construction (Chernicharo, 2006). Inert porous material such as gravel and stones can also be used as a filter bed (Chernicharo, 2006).

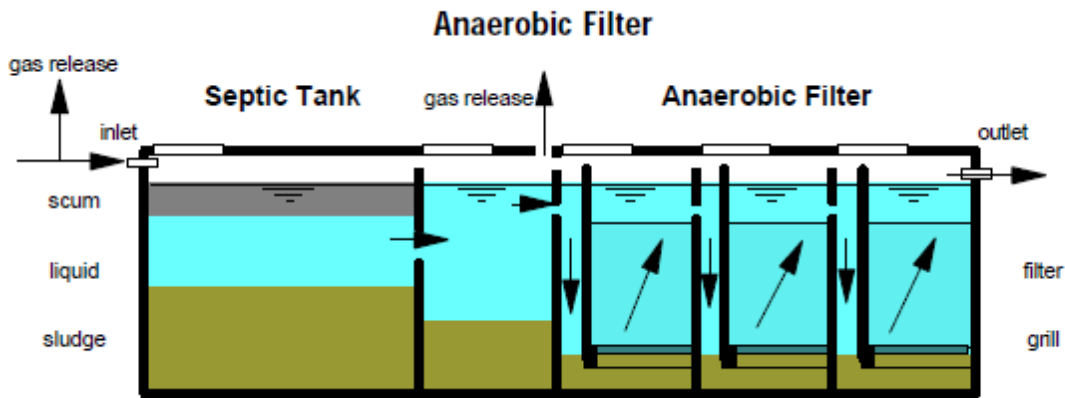


Figure 2.4: Schematic representation of anaerobic filter (AF) used in BORDA designed DEWATS plants (taken from Gutterer *et al.*, 2009). The AF is usually operated in the upflow mode after an ABR or an un-compartmentalised septic tank.

The processes that wastewater undergoes in a wetland polishing are numerous and include physical and biological which are often interrelated. These mechanisms include: settling of particulate and suspended material, filtration, chemical precipitation and transformation, adsorption and ion exchange at the plant-surface interface, breakdown and transformation of various products entering or generated as a by-product of the process (micropollutants, substrates, sediment and litter) and finally the disinfection of the water through predation and natural die-off of pathogenic microorganisms (US EPA, 2000). Not all wastewater streams can be treated in a wetland. Typically, wetlands are more appropriate for wastewaters with a low suspended solids concentration and COD concentrations below 500 mg/L (GTZ-GATE, 2001; Gutterer *et al.*, 2009).

Three types of wetlands treatment systems are commonly used for polishing. They include the overland treatment system, the vertical flow filter and the horizontal flow filter

(GTZ-GATE, 2001). The process in overland flow systems is similar to that outlined in section 2.1.4.2 with water distribution occurring through sprinklers or channels. As this type of wetland is more prone to clogging, extra vigilance and maintenance are required in this system (GTZ-GATE, 2001). In the vertical flow wetland process, wastewater is directed with the help of a distribution device from the top of the bed to the bottom. In the horizontal flow wetland process, wastewater flows from one side of the bed to the other. The vertical flow wetland can achieve higher treatment rates but require more stringent *charging* intervals (interval when the wetland is oxygenated during plug feeding) and is more difficult to operate and maintain than the horizontal flow wetland (GTZ-GATE, 2001).

The advantages of constructed wetlands are that they can reduce operational and power costs when coupled to an anaerobic system (Chernicharo, 2006). Disadvantages include a large requirement for land and a potential problem with pests. For a typical wetland polishing step after anaerobic digestion, von Sperling and Chernicharo (2005) estimated land requirements of approximately 2.4 to 4.0 m²/habitant. Flow in these wetlands should also occur subsurface as odour production is known to occur above ground (Chernicharo, 2006). Failure in constructed wetland treatment usually occurs slowly with clogging of the filter bed the most common cause of failure (GTZ-GATE, 2001).

There has been significant research directed at the use of constructed wetlands for anaerobic effluents, with most done on UASB reactor effluents. De Sousa *et al.* (2001) treated effluent from UASB treating domestic wastewater in four wetland polishing units containing coarse sand as the medium and operated with different hydraulic loads. Excellent faecal coliform (99.99%) and phosphorus (average of 90% for lowest loading) removals were measured. COD removal ranged from 79 to 85% whereas suspended solids removal varied from 48 to 71%. Nitrogen removal in the effluent was only partial with 45 to 70% for ammonia and 47 to 70% for TKN. Both vegetated and non-vegetated wetlands have been shown to significantly remove faecal coliforms from the UASB effluent with removal efficiencies better in vegetated wetlands (approximately 4-log units in vegetated and 3-log unit in the non-vegetated wetland operated with the same hydraulic load) (de Sousa *et al.*, 2003). Similar findings were made by Kaseva (2004) in an UASB treating domestic wastewater in Tanzania. Other studies such Barros *et al.* (2008) reported 2-log unit reductions in horizontal wetlands treating UASB effluent servicing a small community (30 people) with low COD, BOD and TSS concentration (<30 mg/L). El-Khateeb and El-Gohary (2003) have also reported good faecal coliform removals (4 log units).

BORDA-DEWATS plants often include constructed wetlands as polishing steps either using a single wetland or a series of horizontal and/or vertical wetlands (Gutterer *et al.*, 2009). Several of these ABR effluent polishing steps have been installed with ABR technology in southern Africa and southern Asia with varying degrees of success (Nguyen *et al.*, 2007; Muller, 2009; Singh *et al.*, 2009; Jenny and Ducñas, 2010) (refer to section 2.1.5.7).

2.1.5 THE ANAEROBIC BAFFLED REACTOR

This section provides a brief review of the development, performance and applications of the ABR.

2.1.5.1 Basic Design

The basic design of the reactor consists of a cascade of vertical baffles which compartmentalise the reactor. The design forces wastewater to flow through sludge beds at the bottom of each compartment (Figure 2.5) (Skiadas *et al.*, 2000). The micro-organisms within the reactor tend to rise and settle with gas production, and move horizontally at a relatively slow rate (Xing *et al.*, 1991; Nachaiyasit and Stuckey, 1997a). The design of the system therefore allows for wastewater to come into contact with a large amount of active biomass, providing high treatment rates.

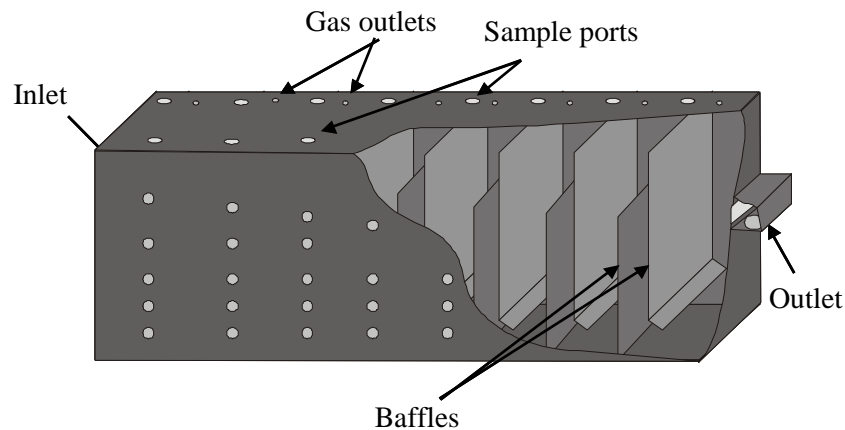


Figure 2.5: Schematic diagram of the ABR with cut-away, showing hanging and standing baffles (from Foxon *et al.*, 2004).

The compartmentalised design has numerous cited advantages (Barber and Stuckey, 1999; Bell, 2000). Among these is reduced biomass washout as solids simply migrate along the reactor length (Polprasert *et al.*, 1992). Another is the spatial separation of anaerobic microbial consortia (Barber and Stuckey, 1999; Foxon *et al.*, 2006). The latter feature has been shown to confer greater protection against toxic substances and changes to environmental parameters,

such as pH and temperature (Barber and Stuckey, 1999, Bell, 2000). Furthermore, it may enhance the hydrolysis of particulate organics in the front of the reactor due to a low pH, without affecting the methanogenesis phase (Langenhoff *et al.*, 2000).

2.1.5.2 Historical Overview of the Anaerobic Baffled Reactor

McCarty and co-workers were credited with the development of the ABR when they removed the rotating discs from a rotating biological contactor (RBC) (Bachmann *et al.*, 1983). Since then various modifications have been made to the initial design. Most of these modifications have been implemented to improve reactor performance, mostly through enhanced solid retention (Table 2.3) (Barber and Stuckey, 1999; Liu *et al.*, 2010). A few modifications, however, have been implemented in order to treat *difficult* wastewaters, such as those with a high particulate content (Boopathy and Sievers, 1991) or to reduce capital costs (Orozco, 1997).

Table 2.3: Historical modifications of the ABR (adapted from Barber and Stuckey, 1999).

Modification	Purpose	Reference
Addition of vertical baffles to plug-flow reactor	Solid retention enhanced	Fannin <i>et al.</i> , 1981
Downflow chambers narrowed	Retention in the upflow region increased	Bachmann <i>et al.</i> , 1983
Edges on baffles slanted	Mixing is enhanced	Bachmann <i>et al.</i> , 1983
Settling chamber included after last compartment	Solid retention enhanced	Tilche and Yang, 1987
Packing positioned at the top of each chamber	Washout of solids prevented	Tilche and Yang, 1987
Separated gas chambers included	Provided enhanced reactor stability by controlling gas measurement	Tilche and Yang, 1987
Enlarged first compartment	Improved treatment of wastewaters with a high solid content	Boopathy and Sievers, 1991
Reduction of compartments for domestic wastewater treatment	Reduction in capital cost without affecting reactor performance	Foxon <i>et al.</i> 2006

2.1.5.3 Start-up

The success of any anaerobic reactor is dependent on the start-up of the system. It is recognised as the most important step in reactor operation and its purpose is to establish an appropriate microbial culture that is best suited to the wastewater to be treated (Barber and Stuckey, 1999). Once this is established, the reactor operation can be quite stable (Barber and Stuckey, 1999).

The initial loadings should be low to prevent washout and/or overload of slow-growing anaerobic micro-organisms (Barber and Stuckey, 1999, Uyanik, 2003). Low gas and liquid

upflow velocities are also recommended to encourage flocculent and granular growth (Barber and Stuckey, 1999).

For anaerobic reactors, initial organic loadings rates (OLR) of up to 1.2 kg COD/m³ d are recommended (Henze and Harremoës, 1983; Speece, 1996). However, OLRs higher than 1.2 kg COD/m³ have been applied successfully in certain instances to some ABRs (Boopathy *et al.*, 1988; Boopathy and Tilche, 1991; Uyanik, 2003; Zheng *et al.*, 2009).

There are many procedures that can be implemented to promote stability of the system during start-up. These include reducing the OLR during start-up or split feeding (Uyanik, 2003), adjusting the pH in the first compartments (or those compartments which accumulate VFA) (Grobicki, 1989) and stimulating the growth of methanogens using metabolic substrates, such as acetate (Barber and Stuckey, 1999). Stepwise decreases in hydraulic loads have also been recommended by Barber and Stuckey (1997) who used this strategy to start-up a laboratory ABR treating a synthetic sucrose wastewater. The ABR was initially operated under a long retention time (80 h) and then the retention time was decreased in a stepwise fashion (whilst keeping the substrate concentration constant). This procedure did not only enhance reactor stability but also improved performance over another ABR fed with the same wastewater and started-up at the same time using a constant and low retention time (Barber and Stuckey, 1997).

2.1.5.4 Low-Strength Treatment

Although anaerobic digestion is better suited to high-strength wastewater treatment, various low-strength wastewaters have been successfully treated in an ABR (Witthauer and Stuckey, 1982; Polprasert *et al.*, 1992; Orozco, 1997; Langenhoff *et al.*, 2000; Langenhoff and Stuckey, 2000; Manariotis and Grigoropoulos, 2002; Hassouna and Stuckey, 2003). In certain instances, relatively high COD removal efficiencies of more than 90% have been achieved (Barber and Stuckey, 1999).

Temperature has been shown to negatively influence ABR performance in treating low-strength wastewater applications (Langenhoff and Stuckey, 2000; Feng *et al.*, 2008 and 2009). However, low temperature is not always detrimental to the process as COD removals of 60% and 70% can still be achieved at 10 and 20°C, respectively (Langenhoff and Stuckey, 2000). Moreover, performance decline cannot only be attributed to low temperature alone as other factors, such as the HRT, also influence reactor performance (Feng *et al.*, 2008).

For low-strength applications, low HRTs are required and are sometimes crucial for ABR performance and stability (Barber and Stuckey, 1999). However, irregular COD removal and

low sludge blankets (low active biomass) can occur if the HRT is too low (Witthauer and Stuckey, 1982). Seeding of reactor (3 g volatile suspended solids – VSS – per litre) before start-up has been suggested as means to overcome this problem (Whitthauer and Stuckey, 1982)

With respect to phase separation, low-strength wastewater applications can result in limited or no microbial separation between compartments in an ABR (Hassouna and Stuckey, 2003; Foxon *et al.*, 2006). Hassouna and Stuckey, (2003) found that microbial populations in each compartment were similar in ABR compartments when treating dilute wastewaters (Hassouna and Stuckey, 2003). Similarly, Foxon *et al.* (2006) using various microscopic techniques found that limited phase separation in a pilot ABR treating domestic wastewater.

In the previous two decades, most studies concerning the application of an ABR in treating low-strength wastewater have been performed on soluble wastewaters with no particulate content. Very little research was conducted into treating dilute particulate wastewaters such as domestic wastewater. This part of the section highlights some of the earlier laboratory studies to evaluate the potential for dilute particulate wastewater treatment. Information regarding ABR performance in treating domestic wastewater can be viewed later in section 2.1.5.7.

In one of the earlier studies, Langenhoff and co-workers sought to evaluate the performance of an ABR in treating dilute wastewater containing a colloidal component (Langenhoff *et al.*, 2000). Identical ABRs were compared and assessed in treating synthetic dilute soluble and colloidal wastewater. The colloidal wastewater was made up of blended dog food and rice that had an average particle size of greater than 500 μm . In contrast, the soluble feed was composed of semi-skimmed milk with a COD concentration of 500 mg/L. Both reactors were initially started with long HRT (HRT = 80 h) and then reduced gradually over time to 6 h. Both systems (with different feed) were able to achieve consistent COD removal efficiencies of greater than 80% at all HRTs tested with even a 40% removal achieved at a HRT of 1.3 h. Furthermore, Langenhoff *et al.* (2000) indicated that the digestion rates were similar between the two differently fed systems (as indicated by methane production) thereby indicating that hydrolysis was not rate limiting in the degradation of colloidal feed. However, in wastewaters containing more particulates such as domestic wastewater, this is not the case (Foxon *et al.*, 2006).

In a more recent study, Gopala Krishna and co-workers investigated the potential of ABR systems for domestic wastewater applications. However, a synthetic feed wastewater representative of domestic wastewater was used instead of domestic wastewater itself. In the

first study, the group studied an 8-compartment ABR treating a synthetic wastewater made out of cellulose and starch (40: 60) (Gopala Krishna *et al.*, 2007). The reactor was operated at HRTs of 20, 15, 10, 8 and 6h (corresponding OLR = 0.6, 0.8, 1.2, 1.5 and 2 kg COD/m³.d) over a period of 600 days. *Pseudo-steady-state* (defined by Gopala Krishna *et al.*, (2007) as insignificant variation in effluent COD for a specific period) was achieved at every HRT. Total COD and BOD removals were found to be greater than 88% for all HRTs studied. Compartment-wise COD (or BOD) profiles of the reactor showed that most of the COD was transferred to later compartments with an increase in the OLR indicating that compartmentalisation contributed to COD reduction. Compartment-wise pH and VFA profiles of the reactor at different HRT showed that a predominance of hydrolysis and acidogenesis phases at the front end of the reactor indicating that phase separation (of anaerobic processes) was occurring along the length of the reactor. The authors also performed tracer tests at each flow regime. The results showed the flow characteristics were an intermediate between plug and mixed flow conditions, and that the HRT did not influence the volume of dead space in the ABR.

The study was extended to treat a low-strength synthetic wastewater (500 mg COD/L) composed of sucrose and peptone (90: 10) (Gopala Krishna *et al.*, 2009). At pseudo-steady-state, the average total and soluble COD values were 50 and 40 mg/L, respectively at an 8 h HRT. Similarly, total and soluble COD values were 47 and 37 mg/L respectively at pseudo-steady-state at a 10 h HRT. The COD and BOD (3 days) removal efficiencies at 8 and 10 h HRT (OLRs from 1.5 to 1.2 kg COD/m³.d) were greater than 90%. Moreover, parameters of effluent quality measured showed low values of standard deviation indicating good reactor stability at pseudo-steady-state. Mass balance calculations yielded that more than 60% of incoming wastewater was converted to methane in the gas phase. Compartment-wise profiles at both HRT showed that most COD and BOD reduction occurred at the front end of the ABR. Moreover, a sudden drop in the pH value was coupled with the formation of VFA in the first compartment of the ABR from acidogenic and acetogenic phases. Thereafter, the pH increased and VFA concentration decreased along the length of the reactor. Evidence for phase separation was provided by qualitative scanning electron microscopy (SEM) micrographs of the compartment sludge beds.

2.1.5.5 Shock Loadings (Organic and Hydraulic)

In one of the earlier studies, Grobicki and Stuckey (1991) evaluated the influence of organic and hydraulic loadings on mass transfer and reaction rate limitations in an ABR. They found that the reactors recovered within 24 h after shock loadings to their pre-shock levels (Grobicki and Stuckey, 1991).

In the late 1990s, Nachaiyasit and co-workers conducted two parallel investigations examining the effects of organic and hydraulic shock loadings on ABR performance. In the first study, they the effect of organic shock loads in a laboratory-scale, 8-compartment ABR was examined (Nachaiyasit and Stuckey, 1997a). After operating this reactor for a month at a 20 h HRT, a temperature of 35°C and a feed concentration of 4 000 mg/L COD, the feed concentration was increased to 8 000 mg/L COD and 15 000 mg/L COD for 20 d each. Stable and relatively unchanged COD removal efficiencies were measured when the feed concentration was doubled whilst the recovery from the shock was rapid. This rapid recovery was attributed to the creation of a buffer zone in the front end of reactor which allowed greater absorption of the overload and prevented the exposure of the biomass at the end of the reactor to low pH values, thereby enhancing reactor stability (Nachaiyasit and Stuckey, 1997a). However, when the feed concentration was increased to 15 000 mg/L COD, the reactor displayed signs of *overload* with VFA detected in the effluent and lower COD removal efficiency observed (Nachaiyasit and Stuckey, 1997a).

In the second study, the effect of transient and stepwise increases in hydraulic loads on ABR performance was evaluated (Nachaiyasit and Stuckey, 1997b). Over a month, two identical laboratory-scale ABRs were operated at 20 h HRT, 4 000 mg/L COD at 35°C. COD removal efficiencies of 98% were achieved during this period. Hydraulic shocks with an HRT of 1 h, 5 h and 10 h were then applied to reactors for 3 h, 2 weeks and 3.5 weeks, respectively. The shocks resulted in a decrease in COD removal efficiency with biomass loss occurring at lower HRT. After the shocks were ceased, the reactor stability improved and recovered back to its baseline values (98% COD removal) (approximately 9 h after the higher shock loadings were ceased).

The resilience of the ABR was also demonstrated by Langenhoff and Stuckey (2000). The authors found that decreasing the HRT from 80 h to 10 h resulted in a temporary increase in effluent COD. However, this was short-lived and the reactor quickly recovered its removal efficiency (> 90%).

2.1.5.6 Effect of Temperature

Temperature, like pH, is known to have influence on the digestion process (Rittmann and McCarty, 2001). Nachaiyasit and Stuckey (1997c) evaluated this parameter on two 10 L ABRs fed with a totally biodegradable feed composed of a synthetic carbohydrate (sucrose) and protein (meat extract) substrate. During the preliminary operation at 20 h HRT, 4 000 mg/L COD at 35°C, COD removal efficiencies of 96% were achieved. The operating temperature of the ABRs was then reduced from 35 to 25°C. No significant change was

observed with COD removal efficiency ranging between 93 to 97% between the two reactors. A further temperature decline to 15°C resulted in a decline in COD removal efficiency (approximately 20%) after a month in both reactors. Both VFA and increased COD were detected in the effluent. The presence of VFA in the effluent lead the authors to believe that lower rates of metabolism and an increase in the K_s for VFA (at high K_s values, VFA cannot be degraded) was experienced at low temperatures. The increase in the effluent COD was attributed to either an enhanced production of *soluble microbial products* (SMP) or a decrease in cellular metabolism (Nachaiyasit and Stuckey, 1997c).

In a similar study, Langenhoff and Stuckey (2000) used a 10 L, 8-compartment ABR treating a dilute wastewater (500 mg COD/L). The reactor was initially started with a HRT of 80 h and at 35°C. The HRT was then progressively reduced to 10 h with COD removal in all tested HRT above 80%. However, when the temperature was reduced to 20°C and 10°C, the COD removals of 70% and 60%, respectively, could only be reached.

2.1.5.7 Application of Anaerobic Baffled Reactors in Sanitation

In Trenjo, Columbia, two 8-compartment ABRs (197 m³) were constructed to serve a population of less than 2 500 people. The wastewater stream was a combination of industrial dairy waste and domestic wastewater (organic loading rate of 0.85 kg/m³day) with average COD and suspended solids removal of 70% and 80% reported over a two-month period (Orozco, 1997, cited in Barber and Stuckey, 1999).

A variation of the ABR was implemented at Biancolina wastewater treatment facility, Bologna, Italy (Garuti *et al.*, 2000). This plant consisted of a 2-compartment ABR with a third anoxic compartment and a fourth compartment which operated as a sludge trap. In this system, the ABR was not designed to achieve complete COD removal but to serve as a pre-treatment step with the effluent entering into an aeration tank and then to a settling tank (Garuti *et al.*, 2000). The reactor was fed intermittently with a feed with an average COD concentration of 600 mg/L with total COD and TSS removal of 31% and 45% reported respectively over 4 months.

In KwaZulu-Natal, South Africa, a comprehensive pilot-scale study was performed on an 8-compartment ABR (3 000 L) (Foxon *et al.*, 2006; Foxon, 2009). The purpose of the investigation was to evaluate the use of ABR as a waterborne sanitation technology in peri-urban areas. The reactor was constructed out of mild steel and operated at two different wastewater treatment facilities. The first operation was at Umbilo Wastewater Treatment Works over a period of 409 d. The wastewater, composed of approximately 50% domestic and 50% industrial wastewater, was screened at the head of the works before being pumped to the pilot

reactor. In the second operation, the reactor was moved to Kingsburgh Wastewater Treatment Works which treated domestic wastewater with no industrial component (Foxon *et al.*, 2006). At the Kingburgh facility, the wastewater was screened at the head of the works and pumped to the pilot reactor. The reactor was operated at Kingsburg for three operating periods of 4, 4.5 and 6 months. The study revealed that reactor operation was fairly smooth despite occasional variations in flow and load, and biomass washout incidents (Foxon *et al.*, 2006). Reactor failure occurred only once during 5-year period, and was traced to organic overload from the illegal dumping of septic tank sludge in the influent to the wastewater treatment plant (Foxon *et al.*, 2006). Despite the sudden increase in organic load, the ABR showed rapid recovery after failure. The recovery was attributed to pseudo-plug-flow conditions in the ABR which resulted in the washout of acids and excess substrate from the organic overload with little loss in biomass.

Total COD removal was fairly constant in all operating periods, even during start-up when biomass concentrations in the reactor were low. At a hydraulic retention time of 22 h, effluent COD was found to be 190 mg COD/L and was further reduced to 130 mg COD/L at a retention time of 40 to 44 h. No nutrient removal was obtained in pilot ABR with ammonia concentrations increasing through reactor as a result of the liberation of organically bound nitrogen during digestion of complex organic material whilst phosphorus concentrations were largely unaffected by the digestion process. Moreover, the effluent still contained unacceptably high concentrations of all of pathogen indicators. Further treatment of the effluent would be required should any discharge or re-use strategy be realised (Foxon *et al.*, 2006; Pillay, 2006).

The use of the ABR as a sanitation technology has gained momentum in recent years especially in southern Africa and parts of south Asia. A number of decentralised household- or community-based sanitation treatment systems based on ABR technology have been installed by the German non-profit organisation, BORDA. The organisation specialises in designing the decentralised wastewater plants and training local communities on their usage. The construction of the system is often done with the aid of the local government and water authorities with community members involved in maintenance. The sanitation system, known as BORDA DEWATS, generally consists of following treatment steps (Figure 2.6) (Gutterer *et al.*, 2009):

- 1) primary treatment using settling tanks, biogas digester or sedimentation ponds
- 2) secondary treatment using an ABR with AFs or anaerobic and facultative pond systems
- 3) post-treatment in aerobic polishing ponds or gravel filters.

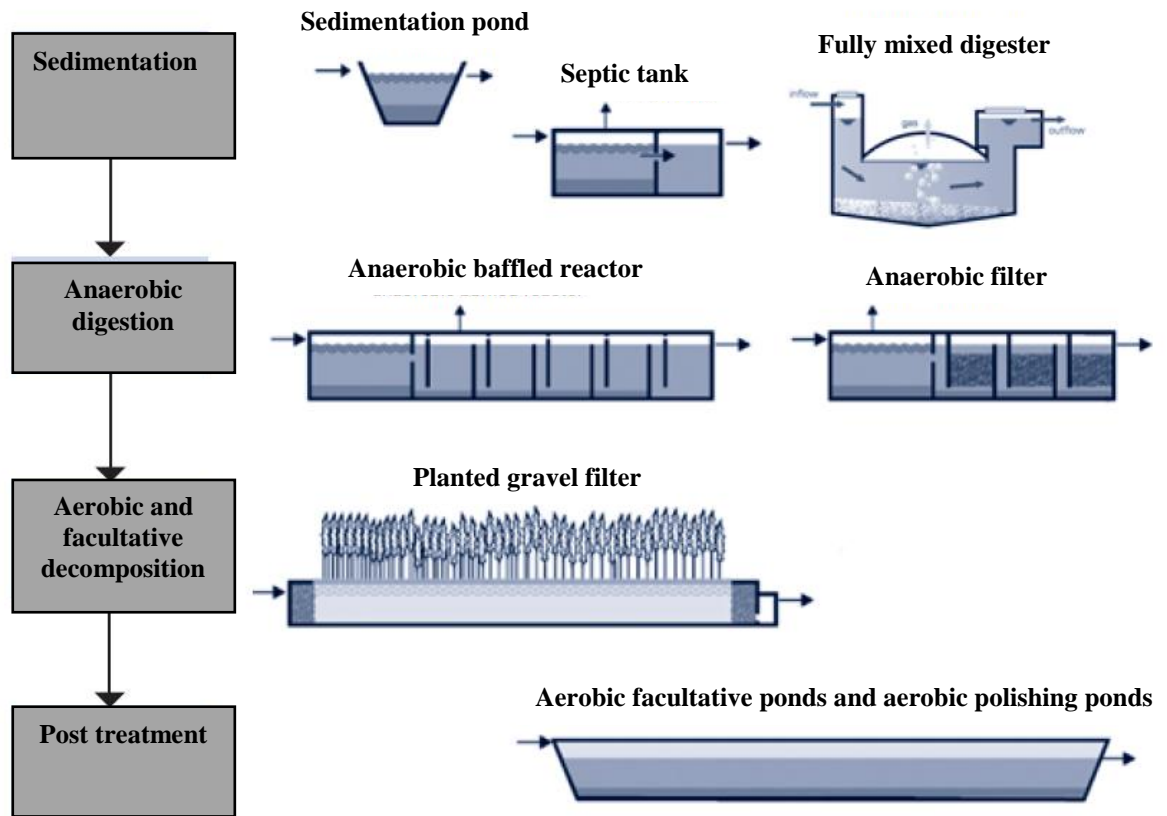


Figure 2.6: Schematic configuration of BORDA DEWAT plants. Picture taken from Gutterer *et al.* (2009).

The biogas that is generated in the biodigester is often harvested and used for cooking purposes (Figure 2.7a and b). The ABR may contain four or more compartments with baffles in the form of walls (brick masonry) (as in Singh *et al.*, 2009) or downflow pipes (Figure 2.7d). Effluent polishing usually occurs in a constructed wetland but this not always the case as shown in Reynaud *et al.* (2009). By 2003, an estimated 120 000 DEWATS units had been implemented in China, India and the Philippines (Panzerbieter *et al.*, 2005).

Interest in BORDA DEWATS plants has generated several laboratory and pilot-scale studies on these plants. The ABR forms the core treatment step in all of these studies with different treatment steps utilised before and after the ABR. Anh *et al.* (2003) investigated the performance of a combination of a settling tank, ABR and AFs treating blackwater from toilets. The laboratory-scale system (size not stated) produced average removal efficiencies of 73%, 71% and 75% for COD, BOD₅ and suspended solids, respectively. The authors suggested a decentralised system consisting of a settling chamber, 3 to 4 chamber ABR followed by 2 to 3 AF chambers. Secondary treatment of the effluent after the settling tank-ABR-AF train was also suggested before the final effluent could be discharged or re-used for irrigation.



a) Gas stove connected to biogas dome



b) Biogas dome in front of an ABR



c) Four chamber ABR in Indonesia



d) Downflow pipes used as baffles in AF



e) Prefabricated DEWATS system (biogas chamber and ABR)



f) Post-treatment in a plant gravel filter

Figure 2.7: Pictures of BORDA DEWATS plants worldwide. The pictures show different components of various DEWATS plants at community-scale (pictures by PRG, 2008 to 2010).

Nguyen *et al.* (2007) compared the performance of a conventional septic tank with an ABR with and without AF polishing. The study was divided into three parts: a laboratory-based study comparing the performance of a septic tank with an ABR, a full-scale study comparing performance of ABRs with and without AFs and lastly, the evaluation of vertical wetlands as a septic tank effluent polishing step.

In the laboratory study, a septic tank and ABR were made from individual plastic cylinders (approximately 50 L/cylinder) which represented the upflow chambers in both systems (Figure 2.8). The reactors were fed with blackwater from nearby toilets that was screened using a coarse filter (to avoid clogging of pipes), diluted to a desired COD range (approximately 500 mg/L), stored in a 1 000 L stainless steel mixing tank, and pumped to the laboratory systems. The ABR was able to achieve higher removals of COD and TSS than the septic tank under identical working conditions (Table 2.4). Optimum operational HRT for the ABR was in the range of 12 to 48 h with no improvements in the degree of treatment for all HRT values greater than 48 h. An increase in HRT (up to 48 h) led to the stabilisation of the digestion process.

Table 2.4: Average removal efficiencies reported by Nguyen *et al.* (2007) in a 2-compartment septic tank and a 6-compartment ABR treating blackwater and operated at different HRTs.

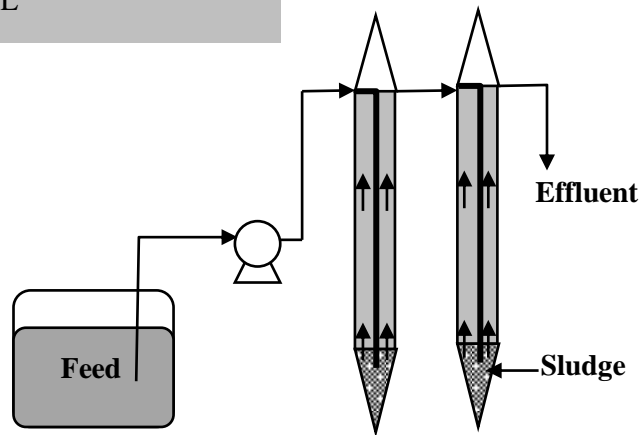
Parameter	Removal Efficiencies (%)							
	2-compartment septic tank ^a				6-compartment ABR ^a			
	HRT				HRT			
	<u>12</u>	<u>24</u>	<u>48^b</u>	<u>72</u>	<u>12</u>	<u>24</u>	<u>48^b</u>	<u>72</u>
COD	48	49	56-60	58	58	66	72-76	72
TSS	35	44	48-69	55	65	61	70-78	70

^a, each compartment is represented by an upflow cylinder; ^b, range of removal average efficiencies reported for two experiments at a HRT of 48 h.

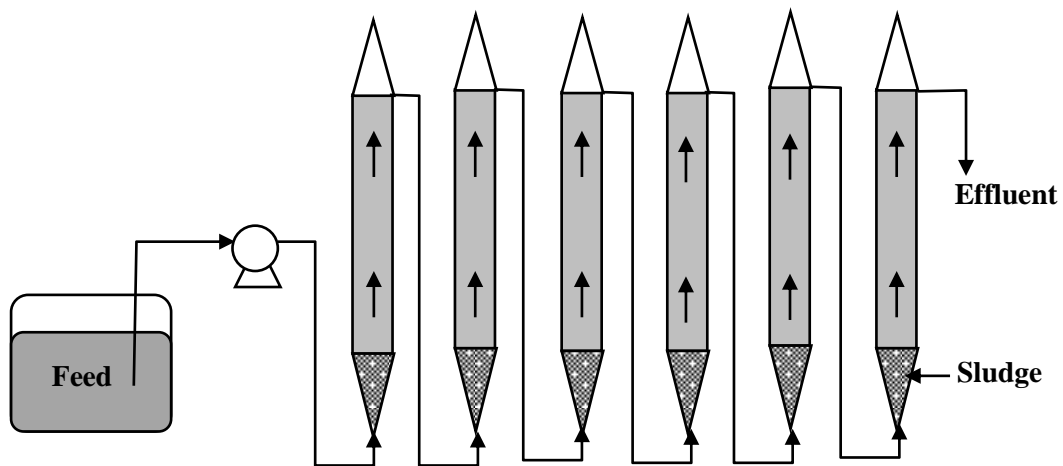
In comparison, a minimum HRT of 48 h was required in the septic tank below which significantly lower removals were observed (Table 2.4). Compartment-wise COD profiles through the ABR train showed that no improvement in COD removal was observed for more than four compartments. The addition of AF compartments containing plastic media improved the performance of both the septic tank and ABR. With regards to the septic tank, the average COD removal efficiency increased from 64 to 85%. This effect was less evident in the ABR followed by an AF polishing step, although average removal efficiencies of COD, BOD and TSS were the highest in this system (COD and TSS removals of 86 and 91% respectively).

Average feed wastewater characteristics:

- Total COD = 505 mg/L
- Filtered COD = 250 mg/L
- BOD = 196 mg/L
- TSS = 284 mg/L



(a) Two-compartment septic tank



(b) Six-compartment ABR

Figure 2.8: Schematic representation of the flow pattern in the laboratory systems used by Nguyen *et al.* (2007). Plastic cylinders represented the upflow region of each unit. (a) 2-chambered septic tank and (b) 6-compartment ABR. The systems were fed with blackwater from the same collection vessel.

The second part of the study investigated full-scale ABR applications at a household level and a community-based system (Nguyen *et al.*, 2007). For the former application, ten ABRs were constructed to serve individual buildings (homesteads, administrative buildings and neighbourhoods) in rural and urban areas. The incoming wastewater stream to the ABRs were

either blackwater, a mixture of washing (greywater) and blackwater, or combined sewer flow (Nguyen *et al.*, 2007).

For the community-based plant, a second full-scale ABR (17.6 m³) was constructed to serve a group of 20 households. This system treated a combination of domestic and livestock breeding wastewaters. The system consisted of a sedimentation chamber followed by 4-compartment ABR. The number of users on the plants varied from four people (at household level) to 360 people (at community-level). The influent wastewater for household- and community-level applications was highly variable with a high COD content (relative to other sources of domestic wastewater) (greater than 2 000 mg/L COD). Despite this, both systems were able to produce an effluent with relatively stable characteristics as indicated by the comparison of standard deviations of both the influent and effluent parameter concentrations (Nguyen *et al.*, 2007). The household ABR system showed satisfactory treatment efficiencies, with average removal efficiencies of 77%, 71% and 86% achieved for COD, BOD₅ and TSS, respectively. The treatment performance of the community-based ABR system was even greater, with average removal efficiencies of 88%, 88% and 94% achieved for COD, BOD and TSS, respectively. The values reported were higher than the average removal efficiencies reported in conventional septic tanks around the world. Some important operational issues were noted during the monitoring of the full-scale reactors. These include the greater accumulation of sludge and scum in the first compartment and reduced treatment performance after two years of operation which indicated that the sedimentation tank should be desludged on a bi-annual basis.

In the last part of the study, Nguyen *et al.* (2007) evaluated vertical-flow constructed wetlands as post-treatment step for both septic tanks and ABRs. The focus was to evaluate the treatment performance using two different types of filter material (for the wetlands) and the physiological effects of septic tank effluent on local plant species. A two-stage vertical-flow wetland was shown to meet most effluent local discharge guidelines (COD, BOD, TSS, total nitrogen, NH₄-N, total phosphorus) except for pathogen indicators (only 1-log removal was achieved).

In one of the more recent studies, Reynaud *et al.* (2009) evaluated a BORDA DEWATS plant in Java, Indonesia in relation to the dimensioning parameter used to construct the system (developed by Sasse, 1998). The system consisted of a biodigester (to harvest biogas), a 4-compartment ABR preceded by a settling tank followed by three AF compartments. The treatment system was connected to 68 households by a shallow sewer system with the blackwater component of 40 households entering the biodigester. The greywater component from the 40 households was then combined with domestic wastewater from an additional 28 households. Only the biodigester was seeded before the plant was started-up. The

investigation showed that prediction on the number of people connected to the plant was underestimated during the design process (277 compared to 200 people) whilst the average feed flow to the plant was 88% of the design flow due to an overestimation of the average per capita wastewater production (Reynaud *et al.*, 2009). This resulted in the plant being hydraulically under-loaded (in comparison to design) whilst being organically overloaded (139% of the design value). Nevertheless, the plant performed to design expectations. Suspended and particulate matter was efficiently reduced through the plant (TSS less than 0.1 mg/L) with particulate COD nearly identical to total COD (122 ± 12 mg/L) in the effluent. The removal for TSS and BOD met local discharge standards. The effluent contained a large fraction of biodegradable matter (as indicated by BOD concentrations) indicating the digestion process was not complete. The results were supported by alkalinity, pH and soluble COD measurements. According to Reynaud *et al.* (2009), the low conversion of soluble organics was attributed to the relatively recent start-up of the system (6 months operation) and lack of seeding. Based on the evidence provided by Reynaud *et al.* (2009), it could be assumed that hydrolysis was not complete in the system (biodegradable particulate COD passed through the system).

In Nepal, Singh *et al.* (2009) evaluated a BORDA DEWATS plant consisting of ABR with polishing in constructed wetlands. The system did not contain AF after the ABR as in Reynaud *et al.* (2009). Effluent flow from the ABR was directed to two parallel wetland systems each consisting of identical horizontal flow and vertical flow constructed wetlands connected in series. The DEWATS system was used to treat high-strength domestic wastewater ($>2\ 000$ mg COD/L, $>1\ 000$ mg/L for TSS and BOD₅) from 80 households in a 43 m³ABR and 300 m² of wetland (four wetlands). A summary of removal efficiencies through the entire plant is presented in Table 2.5. The ABR was able to remove 45%, 47% and 68% of influent BOD, COD and TSS. The two horizontal constructed wetlands were able to achieve average removal efficiencies of 24%, 27%, 51%, 58% and 69% for NH₄-N, total phosphorus, COD and TSS respectively. The average faecal coliform reduction was 69% (approximately 1-log unit). The effluent stream from the horizontal constructed wetlands was treated in the vertical constructed wetlands. The final average effluent concentrations was 38 mg TSS/L, 173 mg BOD₅/L, 319 mg COD/L, 45 mg NH₄-N/L, 17 mg total phosphorus/L and 6 000 coliform forming units (CFU)/100 mL.

Table 2.5: Removal of selected parameters through a BORDA DEWATS plant treating domestic wastewater in Nepal (adapted from Singh *et al.*, 2009).

Parameters	Raw Wastewater (mg/L)	Percentage Removal (%)			
		ABR	Horizontal Flow Constructed Wetland	Vertical Flow Constructed Wetland	Total
TSS	1506	68.3	69.3	57.6	95.9
BOD ₅	1594	45.3	57.5	44.9	90.1
COD	2914	47.2	51.4	45.7	90.0
NH ₄ -N	142	a	23.8	70.9	69.5
TP	24	a	27.3	0.0	26.1
FC	8E+05 ¹	a	68.8	73.7	97.5

TP, total phosphorus; FC, faecal coliforms; a, no removal observed; ¹, unit of measurement is Faecal Coliforms/100 mL.

In Egypt, Sabry (2010) evaluated a full-scale hybrid UASB-ABR based on their previous pilot studies. Sewage (details not specified) entered from the bottom of a septic tank (UASB process) and moved through a two-chambered ABR containing sieved gravel in the last chamber. The system was able to achieve COD, BOD and TSS removal efficiencies of 84%, 81% and 89%, respectively, with digestion in the ABR being the main mechanism of treatment during start-up and the early steady-state. After steady-state was achieved, most of the digestion occurred in the UASB-septic tank with the ABR performing as an organic matter removal and polishing step. The system also performed well under hydraulic and organic shock loads. The role of temperature in the digestion process was clearly shown with 9% drop in efficiency reported over the cooler winter period (22°C versus summer mean of 35°C). Effluent concentrations of TSS were not affected by the temperature which probably highlights the solids retention ability of the system.

Large-scale ABR processes have been used elsewhere in Egypt. In 2006, a full-scale ABR treatment plant was commissioned to serve a population of approximately 2 000 inhabitants (Moussa and Salem, 2008). According to Moussa and Salem (2008), the plant was able to reach the Egyptian discharge guidelines with removal efficiencies of 70%, 73% and 75% reported for BOD, COD and suspended solids. No mention is made in the report as to whether any polishing was required or was the actual effluent concentrations provided for different parameters. Probably critical to the operation of the plant was the training programme that was implemented within the community.

2.2 MEMBRANE FILTRATION

This section provides a description and the basic terminology relating to membrane filtration. The operation of anaerobic MBRs (AnMBR) is reviewed in section 2.3.

2.2.1 PROCESS DESCRIPTION

Membrane filtration is defined as the physical separation of components in a fluid mixture by a membrane (Evenblij, 2006). The physical barrier created by the membrane provides a selective barrier where the passage of certain components of a fluid mixture occurs, but others above a particular size or weight are rejected (Jacobs *et al.*, 2000; Judd, 2006). Thus, two streams are generated by the process with the pore size of the membrane defining its selectivity (Evenblij, 2006; Judd, 2006). The stream that is retained by the membrane is called the *retentate* or *concentrate* whilst the stream that passes through the membrane is called the *permeate* or liquid stream (Jacobs *et al.*, 2000; Odhav, 2004). The driving force for the separation of the two streams is brought about by pressure drop or differential pressure. The difference between these pressures is known as the *transmembrane pressure* (TMP).

Four key membrane separation processes can be defined by the size of the membrane pores and the type of separation they achieve. These are microfiltration (MF), ultrafiltration (UF), nanofiltration (NF) and reverse osmosis (RO) (Figure 2.9). As pore size also defines the degree of selectivity, membranes can be categorised according to their molecular weight cut-off (MWCO) and the pressure at which they operate (van der Roest *et al.*, 2002). These categories are explicitly linked with each other. For example, if the pore size of the membrane becomes smaller or the MWCO decreases, the pressure required for separation of permeate from other components in the fluid mixture generally increases.

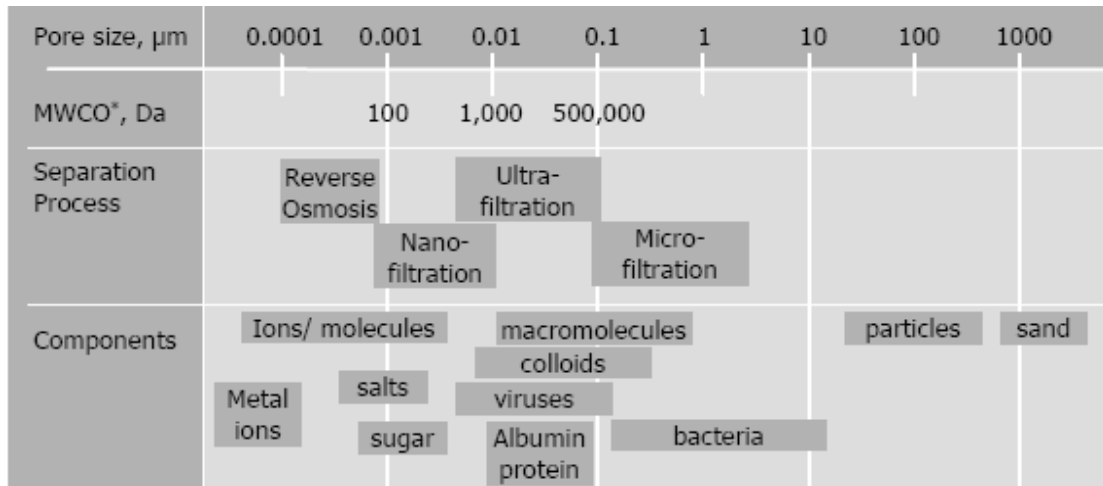


Figure 2.9: Classification of pressure driven membrane processes, * MWCO [molecular weight cut-off (Daltons)] (from Evenblij, 2006).

Ultrafiltration and microfiltration modules are the commonly used filtration processes used in MBR studies as their operating pressures are much lower than that of NF and RO. In both processes, separation of fluid components is based on size exclusion (Jacobs *et al.*, 2000), with

the interaction of constituents in the mixture and the membrane resulting in separation of components (Evenblij, 2006). The pores of microfiltration modules range from approximately 0.05 μm to 2 μm and the process is typically used to remove relatively large components in a fluid mixture, such as emulsified oils, suspended solids and macromolecules with molecular weights larger than 50 000 Daltons (Da) (van der Roest *et al.*, 2002). Ultrafiltration modules, on the other hand, have typically smaller pore sizes than microfiltration modules, ranging from approximately from 2 nm to 30 nm, and can separate macromolecules with MWCO greater than 5 000 Da (Jacobs *et al.*, 2000; van der Roest *et al.*, 2002). Although the separation range between the microfiltration and ultrafiltration process can overlap to large extent, typically higher levels of separation can be achieved in ultrafiltration membranes, particularly with regards to pathogenic micro-organisms (van der Roest *et al.*, 2002).

2.2.2 MEMBRANE MATERIALS

A variety of materials can be used to construct the membrane with the most common being organic and ceramic (Baker, 2000; Judd, 2006). These materials are available in a range of pore sizes and distributions, membrane configurations and formed through a variety of production techniques (Evenblij, 2006; Judd 2006). Membranes constructed from organic polymers, such as polyvinylidenedifluoride, polyethersulphone, polyethylene and polypropylene, are more commonly applied in wastewater treatment (Evenblij, 2006). According to Judd (2006), the material to be used should encompass the following characteristics: be mechanically strong, display some resistance to chemical and thermal attack and exhibit some resistance to membrane fouling. Cost is a major factor in determining the membrane material to be used in wastewater treatment. For instance, ceramic membranes are capable of higher working temperatures and pressures than organic membranes, but their use in wastewater treatment is limited due to their higher production costs which can be ten times more than their organic counterparts (Owen *et al.*, 1995).

2.2.3 MODULE CONFIGURATIONS

Membranes can be configured into different membrane modules using a number of forms such as sheets, hollow fibres and tubes (Mulder, 1996). Table 2.6 presents the applications of different forms of membranes (Baker, 2000).

Table 2.6: Membrane configurations and application in different separation processes (from Baker, 2000).

Membrane configuration	Abbreviation	Application			
		RO	NF	UF	MF
Spiral wound	SW	X	X	X	
Tubular	T		X	X	X
Hollow fibre inside-out	HO-IO	X	X	X	X
Hollow fibre outside-in	HO-OI			X	X
Plate and frame	PF			X	X

Hollow-fibre and tubular membranes are the only forms that can be operated in two different modes (Figure 2.10). The two modes, *inside/out* and *outside/in*, are used to describe the direction of permeate flow through the membrane. During the *inside/out* mode, the feed flows through the bore or cavity of the membrane. The direction of permeate flow occurs from the inner surface of the membrane to the outside of the fibre or tube. During the *outside/in* mode, the feed flows on the outside surface of the membrane with permeate flowing to the inside of the membrane or its cavity. In this case, smaller pore sizes are found on the outside surface of the fibre or tube (in contrast to *inside/out* mode which has smaller pore sizes on the inner surface). In addition to the different filtration modes, membranes may be encased (flow is confined to a certain volume) or have no casing (no restrictions for membrane movement with air and liquid not forced to pass the membranes) (Cabassud *et al.*, 2006).

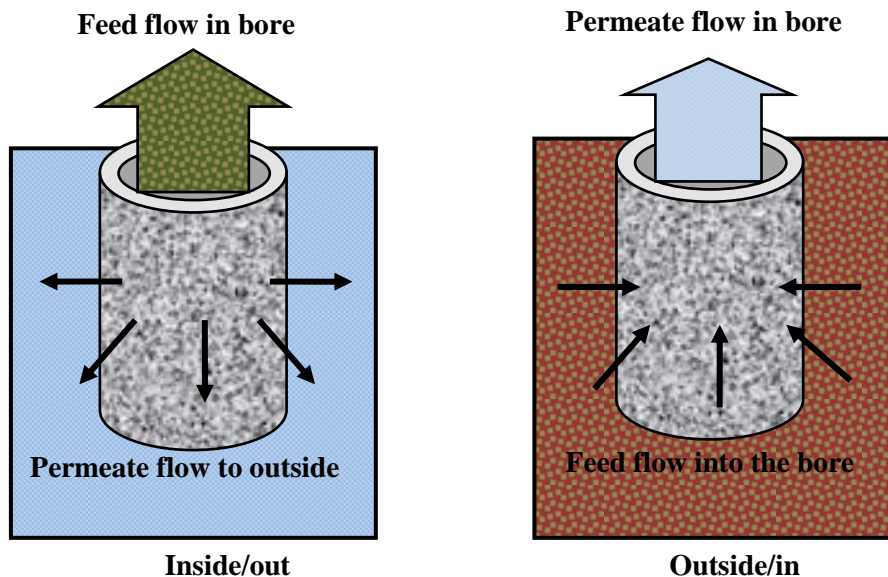


Figure 2.10: Filtration mode applicable to hollow fibre and tubular membranes. During inside/out mode, the feed flows in the bore of the membrane. During outside/in mode, the permeate flows inside the bore of the membrane.

2.2.4 PROCESS TERMINOLOGY

Flux (J) is the most often cited term used to describe the membrane filtration process. It describes the flow of the liquid through a membrane. As the liquid must pass through a membrane of a defined surface area, the flux is defined as *the flow of liquid through a specific surface area per unit time* (van der Roest *et al.*, 2002; Judd, 2006). The unit of flux differs among research groups around the world. For example, in Japan, the unit of flux is expressed in SI unit as $\text{m}^3/\text{m}^2\cdot\text{h}$ (van der Roest *et al.*, 2002). In contrast, the European standard for flux is $\text{L}\cdot\text{m}^{-2}\cdot\text{h}^{-1}$. For this thesis, the latter was chosen as the standard unit for flux as recommended by partner groups. For pure solvents, flux under laminar conditions is expressed using Darcy's Law (Lojkine *et al.*, 1992):

$$J_p = \frac{TMP}{\mu \cdot R_m} \quad \text{Equation 2.1}$$

where:

J_p : permeate flux [$\text{L}\cdot\text{m}^{-2}\cdot\text{h}^{-1}$]

TMP : transmembrane pressure [Pa]

μ : permeate viscosity [Pa.s]

R_m : clean membrane resistance [m^{-1}]

When the fluid being filtered is not pure (contains dissolved or suspended substances), the filtration law changes to include the resistance due to fouling, R_f .

$$J_p = \frac{TMP}{\mu \times (R_m + R_f)} \quad \text{Equation 2.2}$$

where:

R_f : fouling resistance [m^{-1}]

According to this model, the flux is a function of the TMP and is inversely proportional to the total resistance. The total resistance is the sum of individual resistances and can be determined experimentally through a series of pure water filtration experiments.

Temperature plays an important role in filtration characteristics as it has a strong influence on the viscosity of the permeate and concentrate (van der Roest *et al.*, 2002). For example, a temperature decrease can cause an increase in the viscosity of a fluid. Hence, a greater TMP will be required to achieve the required flux through the membrane resulting in lower membrane permeability. For this reason, most flux values are corrected to a standard temperature to eliminate the influence of permeate viscosity on flux (van der Roest *et al.*, 2002). This correction enables the assessment of membrane performance over several time periods. In most studies, the actual permeate temperature is corrected to a standard temperature of 20°C (Rosenberger and Kraume; 2002; Xu *et al.*, 2002; Rosenberger *et al.*, 2005 and 2006).

Values of TMP and flux alone provide very little information regarding the performance of membranes. However, if the flux is divided by the TMP, the specific flux (or *membrane permeability*) through a specific surface area for a particular pressure difference can be determined. The membrane permeability (L_p) of a membrane can be calculated as the ratio between the flux and TMP (**Equation 2.3**).

$$L_p = \frac{J_p}{TMP} = \frac{1}{\mu(R_m + R_f)} \quad \text{Equation 2.3}$$

where:

L_p : permeability [$L.m^{-2}.h^{-1}.Pa^{-1}$] or [$L.m^{-2}.h^{-1}.bar^{-1}$]

J_p : permeate flux [$L.m^{-2}.h^{-1}$]

TMP : transmembrane pressure [Pa]

For this thesis, permeability was presented in $L.m^{-2}.h^{-1}.Pa^{-1}$ instead of the routinely used units of $L.m^{-2}.h^{-1}.bar^{-1}$. The reason for the change was that the TMP was presented as Pa in this thesis instead of bar pressure units. The use of Pa pressure units is a standard practice among membrane researchers. The permeability graphs presented in this thesis were therefore flux ($L.m^{-2}.h^{-1}$) versus TMP (Pa) plots. Another reason for the choice of Pa over bar pressure units was that the TMPs used in this study were significantly lower (less than 0.1 bar or 10 kPa) than those reported in other energy-driven MBR systems where TMP operation above 100 kPa (1.0 bar) is common. Thus, the presentation of permeability units as $L.m^{-2}.h^{-1}.Pa^{-1}$ would be a better scale to interpret and evaluate data, especially for readers with no membrane reactor expertise. In the text of the thesis, where permeability results are presented and/or discussed, the

corresponding permeability values in $\text{L}\cdot\text{m}^{-2}\cdot\text{h}^{-1}\cdot\text{bar}^{-1}$ have been included in order to compare with other published work.

Membrane permeability is commonly used to assess the performance of the membrane process as it defines the condition of the membrane at a given time. This assists in the comparison in membrane performance between the different operating conditions at different times (van der Roest *et al.*, 2002). Moreover, it provides a useful tool by which to assess membrane performance over a specific time period, to evaluate membrane recovery and to predict cleaning requirements (van der Roest *et al.*, 2002). The permeability of the membrane is influenced by number of factors including the properties of membrane (pore size, porosity, hydrophobicity, and surface charge) and filtration conditions (TMP, aeration, module geometry, and sludge characteristics) (Chang *et al.*, 2002).

The specific flux (and therefore permeability) is significantly influenced by the presence of suspended and dissolved substances in the mixed liquor. The deposition of these components, on or within the pores, decreases the available area for filtration and is characterised by an increase in the resistance against permeate flow (Koros *et al.*, 1996; Leukes *et al.*, 2002) (Equation 2.3). This phenomenon is termed *membrane fouling*. Fouling can be classified as being *reversible* or *irreversible* depending on the manner in which fouling layer is removed. In reversible fouling, the fouling layer is removable from the membrane using physical cleaning, such as washing. In contrast, the internal fouling caused by adsorption of dissolved substances in membranes and pore blocking is classified as irreversible fouling. The latter requires chemical cleaning (Chang *et al.*, 2002). In reality, it is difficult to categorise fouling as not all cake layers can be removed using physical methods and not all adsorption is irreversible (Chang *et al.*, 2002). This had led to different definitions of reversible and irreversible fouling. To avoid such confusion, Meng *et al.* (2009) have suggested classifying the types of fouling into three categories: *removable fouling*, *irremovable fouling* and *irreversible fouling*. Removable fouling is defined as that which can be easily removed using a physical protocol and is caused by loosely-binding foulants (Meng *et al.*, 2009). Irremovable fouling, on the other hand, is defined as that which requires chemical intervention to remove strongly attached foulants and foulants stuck within pores whilst irreversible fouling is defined as that which cannot be removed by any cleaning (physical and chemical) regime (Meng *et al.*, 2009).

2.2.5 EMPIRICAL MODELS

Fouling is characterised by an increase in membrane resistance as manifested by a decrease in the permeate flux at constant TMP (Thomas *et al.*, 2000). In constant pressure filtration, fouling causes a sudden initial flux decline followed by a gradual decrease towards a steady-state or

pseudo-steady-state flux (Chang *et al.*, 2002). Four filtration models have been proposed to describe the initial flux decline and have their origins in early dead-end filtration studies [Grace, 1956 cited in Chang *et al.* (2002) and Judd (2006)] (Figure 2.11). These include: complete blocking, standard blocking, intermediate blocking and cake filtration (Judd, 2006).

The models imply a dependence of flux decline on the ratio of the particle size to pore size (Judd, 2006). The standard blocking and cake filtration models appear the best suited to describe the initial flux decline in the filtration of colloidal and protein solutions (evidence cited in Chang *et al.*, 2002; Judd *et al.*, 2006).

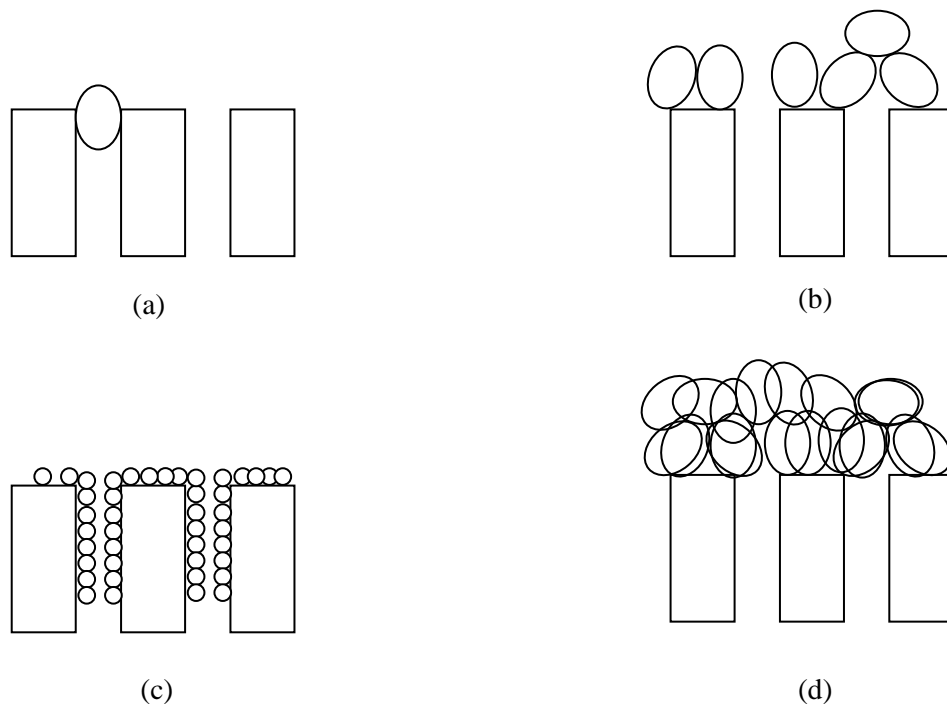


Figure 2.11: Fouling mechanisms: (a) complete blocking, (b) standard blocking, (c) intermediate blocking, (d) cake filtration (taken from Judd, 2006).

2.2.6 CONCENTRATION POLARISATION

Permeate flux decline can be described by either cake filtration theory, the osmotic pressure model or the *concentration polarisation* model (Yazdanshenas *et al.*, 2010). The concentration polarisation model is used to describe the process when solutes that are convectively driven to the membrane surface accumulate at the membrane surface within a boundary film created by the hydrodynamic conditions. This creates a concentration gradient with a higher solute concentration at the membrane interface than in the bulk solution (Yeh *et al.*, 1999). The higher concentration at the membrane interface will cause solutes to diffuse back into the bulk solution (Bowen and Jenner, 1995).

Film theory is often used to characterise concentration polarisation. According to the model, the longitudinal mass transport within the boundary layer is assumed to be negligible (Jonsson, 1986). Furthermore, solutes will continue to accumulate on the membrane surface until the back diffusion (from membrane surface) is equal to the forward convective transport to the membrane surface (Porter, 1990).

At steady state, the following solute mass balance above the membrane surface is (Bowen and Jenner, 1995):

$$J_c = D \frac{dc}{dy} + J_{cp} \quad \text{Equation 2.4}$$

Where:

D : diffusion coefficient of the solute

c : solute concentrations in the boundary layer

c_p : solute concentration in the permeate

Integration of equation 2.4 with boundary conditions ($c = c_m$ at $x = 0$; $c = c_b$ at $x = \delta$) gives the film model relationship:

$$J = k_s \ln \left(\frac{c_m - c_p}{c_b - c_p} \right) \quad \text{Equation 2.5}$$

Where:

k_s : mass transfer coefficient = D / δ

c_m : concentration at the membrane surface

The osmotic pressure model is not generally used in ultrafiltration applications (or membranes with larger pore sizes than an ultrafiltration module) to describe concentration polarisation as the macromolecules in solution are thought to have insignificant osmotic pressures (Porter, 1972; Sablani *et al.*, 2001). However, this is not entirely true as many researchers have found that macromolecules can have an appreciable osmotic pressure of the same order of applied pressure (Clifton *et al.*, 1984).

The *gel polarisation* model was the first model used to explain to describe concentration polarisation and it is often used to describe concentration polarisation effects in an ultrafiltration module (Porter, 1972). The basic assumption in the model is that the concentration of solutes at the membrane surface increases to a point where it can reach its solubility limit to form a gel

precipitate (Bowen and Jenner, 1995). This gel layer can form a dynamic secondary membrane on the membrane surface and can cause major resistance to flow and hydraulic permeability (Porter, 1972; Sablani *et al.*, 2001). This process is known as the *gel polarisation*. According to gel polarisation model, the gel layer is indicative of concentration polarisation reaching its maximum value with diffusion the only means of solutes moving back into the bulk fluid. It is therefore independent of pressure, bulk solution characteristics, fluid flow conditions or membrane characteristics. Therefore, an increase in TMP will only result in an increase in gel layer thickness and not the flux (Van Den Berg and Smolders, 1990).

2.2.7 MEMBRANE FOULING

Fouling has a significant impact on the cost-effectiveness of the filtration process as it reduces the permeate flux (Graham *et al.*, 1989; Pervov *et al.*, 1996 cited in Leukes, 2002). This is associated with an increase in the operational costs of the system and reduces the attractiveness of the technology. Due to the influence it has on the filtration process, it is understandable that most research has focussed on fouling with special emphasis placed on the constituents responsible for fouling to “enable their suppression, render them innocuous or assist in their removal” (Judd, 2007). Foulant studies in MBR literature are dominated by two categories: *characterisation* and *identification* (Judd, 2006 and 2007). Characterisation refers to the properties the fouling constituent demonstrates (usually in relation to membrane permeability) either *in situ* (within the MBR) or *ex situ* using a standard measurement (Judd, 2006 and 2007). Identification refers to the physical and/or chemical characterisation of the fouling constituent using extractive and concentration techniques prior to chemical analysis, including those used to characterise the biomass (Judd, 2006 and 2007).

Fouling constituents can be defined in three different ways, namely, *practical*, *mechanical* and *composition* (Table 2.7) (Judd, 2007). The practical definition is the most applied in MBR research and is based on pure water filtration before and after fouling (or cleaning). In such cases, fouling can be described as being either reversible or irreversible (Judd, 2007). The mechanical definition takes into consideration the manner in which the fouling constituents deposit on the membrane surface or within its pores (refer to section 2.2.5). The definition can be used to predict the filtration behaviour of a test solution provided that the mechanism does not change over time (Judd, 2007). Other more complex models have been developed for fouling below the *critical flux* (section 2.2.9) but these tend to be more qualitative than quantitative (Judd, 2007).

Table 2.7: Fouling definitions used in MBR study (modified* from Judd, 2006 and 2007).

Practical definition	Mechanism	Foulant composition
Removable: Removed by physical cleaning	Pore blocking or filtration model: Complete blocking	Size: Molecular, macro-molecular, colloidal, particulate
Irremovable: Removed by chemical cleaning	Standard blocking Intermediate blocking	Surface charge/chemistry: Positive or negative (cationic or anionic)
Irreversible: Cannot be removed by any cleaning regime	Cake filtration	Chemical type: Inorganic or organic Carbohydrate or protein (fractions of EPS ^a) Origin: Microbial, terrestrial or man-made Extracted or soluble EPS

^a Extracellular polymeric substances (EPS), * The terms removable, irremovable and irreversible, as defined by Meng *et al.* (2009), have used instead of reversible, irreversible and irrecoverable respectively.

The composition of the fouling constituent has attracted the most attention in MBR literature, specifically the size of foulant particles (Judd, 2006 and 2007). The mixed liquor in an MBR is usually fractionated into three main groups: suspended solids, colloids and solutes. These constituents are thought to influence fouling and are influenced by operating conditions, such as the sludge retention time (SRT). The mixed liquor is routinely fractionated into these three groups and characterised by a variety of approaches and techniques (Judd, 2006). For a review on the fouling propensity of each of these fractions, a number of articles and books can be consulted (Visvanathan *et al.*, 2000; Chang *et al.*, 2002; Judd, 2006 and 2007).

2.2.7.1 Mixed Liquor Suspended Solids

Much of the attention in the early stages of MBR development was centred on the role of mixed liquor suspended solids (MLSS) on membrane fouling (Chang *et al.*, 2002). An early study at the beginning of 1980s showed that membrane resistance increased linearly with MLSS concentration (Fane *et al.*, 1981 cited in Chang *et al.*, 2002). In the early 1990s, Yamamoto and co-workers demonstrated the importance of MLSS in bench-scale microporous hollow-fibre membrane experiments (flux decline rapidly after a 40 000 mg/L MLSS concentration) (Yamamoto *et al.*, 1989 cited in Chang *et al.*, 2002) and reported MLSS as the main factor affecting fouling in a hollow-fibre unit submerged in sequencing batch reactor treating tannery wastewater (Yamamoto and Win, 1991). Bae and Tak (2005) found that the MLSS fraction was the main foulant (other fractions were colloidal and solutes) in bench-scale MBR studies using a synthetic wastewater.

However, the relationship between the MLSS concentration and fouling is rather complex. Not all studies report a decrease in membrane performance with increasing MLSS concentrations (Defrance and Jaffrin, 1999, Hong *et al.*, 2002, Le Clech *et al.*, 2003). Hong *et al.* (2002) found, for example, that the MLSS concentrations between 3 600 and 8 400 mg/L did not have much influence on permeate flux in a submerged hollow-fibre system treating a synthetic wastewater. This problem is further exacerbated by the existence of a threshold above which MLSS becomes influential on membrane fouling. In Yamamoto and co-workers' early work, a negative influence on membrane performance was reported when the membrane feed was above 40 000 mg MLSS/L (Yamamoto *et al.*, 1989 cited in Chang *et al.*, 2002; Yamamoto and Win, 1991) whilst Lübbecke *et al.* (1995) reported a negative influence above 30 000 mg/L. Rosenberger *et al.* (2005), on the other hand, reported reduced fouling below 6 000 mg/L but increased fouling at MLSS concentrations above 15 000 mg/L. Between 8 000 to 12 000 mg/L, no significant effect was observed. Table 2.8 presents a summary of the influence of MLSS concentrations on membrane performance.

Table 2.8: Influence of changing MLSS concentration on MBR fouling (adapted from Judd, 2006).

MLSS shift (mg/L)	Details	Reference
<u>Fouling increase</u>		
0.09-3.7	Cake resistance: $21-54 \times 10^{11}$ and α : $18.5-0.7 \times 10^8 \text{m/kg}$	Chang and Kim (2005)
2.4-9.6	Total resistance: $9-22 \times 10^{11} \text{m}^{-1}$	Fang and Shi (2005)
7-18	Critical flux: 36-47 LMH (for SRT of 30-100 days)	Han <i>et al.</i> (2005)
2.1-9.6	Critical flux: 8-13 LMH	Bin <i>et al.</i> (2004)
1-10	Critical flux: 35-75 LMH	Madaeni <i>et al.</i> (1999)*
2-15	“Limiting flux”: 50-150 LMH	Cicek <i>et al.</i> (1998)*
1.6-22	“Stabilised flux”: 25-65 LMH	Beaubien <i>et al.</i> (1996)*
>10	Rate of filtration resistance: measured and correlated with parameters	Wu and Huang (2009)
<u>Fouling decrease</u>		
3.5-10	Critical flux >80, <60 LMH	Defrance and Jaffrin (1999)*
<u>No (or little effect)</u>		
4.4-11.6	No impact between 4 and 8g/L, slightly less fouling for 12g/L	Le-Clech <i>et al.</i> (2003)
4-15.1	Critical flux ↓ 25 to 22 LMH	Bouhabila <i>et al.</i> (1998)
3.6-8.4		Hong <i>et al.</i> (2002)

* submerged MBR; LMH, litres per metres squared per hour.

Due to such conflicting reports, it is has now become common place to report MLSS along with other sludge properties, such as sludge volume index (SVI), viscosity, capillary suction time, particle size and *extracellular polymeric substances* (EPS), and correlate all measured parameters with membrane performance. Yigit *et al.* (2008), for example, examined five different MLSS concentrations in single tank pilot MBR treating raw domestic wastewater. Four

different aeration velocities were used at each MLSS concentration with particle size distribution and EPS also measured during each step. Reid *et al.* (2008) tested a number of sludge properties from five full-scale activated sludge MBR plants. With respect to the MLSS concentration, an exponential relationship with viscosity was observed (Reid *et al.*, 2008). A similar finding was reported by Wu and Huang (2009) at MLSS concentrations above 10 000 mg/L.

2.2.7.2 Colloidal Particles

The term colloid is used to describe various species with particles smaller than 1 μm (Laabs *et al.* 2004). Colloids may consist of organic compounds such as micro-organisms, polysaccharides, gel-like material humic and fulvic acids or inorganic compounds such as clay, carbonate and iron oxyhydroxides (Buffle and Leppard, 1995). This submicron fraction in the suspended solids has been reported to correlate with membrane fouling. In an early study, Waite *et al.* (1999) found that cake accumulation rates similar on ultrafiltration membranes filtering hematite aggregates in stirred suspension (in the absence of a repulsion barrier) and those with a repulsion barrier. However, the former had specific resistances that are an order of magnitude lower. The difference in cake resistance was considered to stem from the size and fractal properties of the hematite assemblages with porosity increasing with the size of the aggregates (Waite *et al.*, 1999).

Jarusutthirak *et al.* (2002) isolated wastewater effluent into different fractions; colloids, hydrophobic and transphilic (hydrophilic non-humic natural organic matter) fractions. Size exclusion chromatography, Fourier transform infrared spectroscopy, specific ultraviolet A spectroscopy and total sugars determination were performed on each fraction. The colloidal fraction was reported as having a hydrophilic character and primarily composed of polysaccharides, proteins and/or aminosugars (monosaccharides having an amino group instead of an alcoholic hydroxy group). The hydrophobic and transphilic fractions possessed characteristics of humic substances. Each fraction isolated exhibited different characteristics in fouling of NF and UF membranes. The colloidal fraction showed the most negative influence on membrane performance which was primarily due to the effects of pore blockage. Less severe fouling and flux decline was observed in the filtration of hydrophobic and transphilic fractions. The polysaccharides and/or aminosugars from the colloids in wastewater effluent were found to play an important role in fouling of NF and UF membranes (Jarusutthirak *et al.*, 2002).

Itonaga *et al.* (2004) examined membrane fouling occurring in pilot MBRs with or without pre-treatment (coagulation/sedimentation) with emphasis on the influence of suspension viscosity and dissolved organic matter on membrane fouling. Membrane performance was

improved with the pre-coagulation/sedimentation step by controlling irreversible fouling and the formation of a thick cake layer. As it was difficult to directly relate membrane fouling to DOM detected in the membrane chamber, a series of laboratory-scale dead-end filtration experiments was carried out to determine which fractions in the biomass suspension had the greatest influence in the deterioration of membrane permeability. Based on the dead-end tests, it was shown that the colloidal fraction was main cause in the deterioration of membrane permeability (Itonaga *et al.*, 2004).

Laabs *et al.* (2004) investigated the effect of organic colloids using stirred cell tests. The colloidal fraction of wastewater effluent was isolated using a rotary-evaporation pre-concentration step followed by dialysis. A significant difference was found between flux curves of filtered and unfiltered colloid samples. Fourier transformed infra-red spectra analysis showed that the main compounds were polysaccharides and proteins. Further analysis using size exclusion analysis showed that the main component of organic colloids were polysaccharides.

Rosenberger and co-workers observed that two similar pilot MBRs treating the same feed wastewater and operated under similar operating conditions exhibited severe differences in membrane performance (Rosenberger *et al.*, 2006). The only difference between the pilot MBRs was the position of the denitrification zone; the first pilot MBR had a pre-denitrification step whilst the second MBR had a post-denitrification step. However, this constructional difference could not account for the observed differences in membrane performance. To elucidate the differences in performance between the pilot MBRs, Rosenberger and co-workers correlated membrane fouling rates and permeability with the activated sludge characteristics and the operating regimes of both MBRs. They found that the MLSS concentration and loading rates could not account for the different behaviour of the two parallel MBR plants. However, the liquid phase organic matter consisting of polysaccharides, proteins and organic colloids with molecular weights greater than 20 kDa was found to impact on fouling with higher fouling rates in the pilot MBR with a greater composition of this fraction (Rosenberger *et al.*, 2006). This fraction was therefore implicated in the observed differences in performance between the pilot plants and was also shown to be of microbiological origin.

Leiknes *et al.* (2006) investigated the effect of colloid particles on membrane fouling in a moving bed-biofilm reactor operated at two organic loading rates (HRT of 4 h and HRT of 1 h). COD fractionation of the mixed liquor was performed using graded series of pore sizes from 0.1 to 1.2 μm . Capillary suction time and time-to-filtrate analyses were performed together with particle size distribution during different stages of the process. Membrane fouling was more pronounced in the high loading rate (HRT of 1 h) which showed higher amounts of submicron

particles (<0.45 µm) (obtained from fractionated COD tests and particle size distribution analysis).

2.2.7.3 Extracellular Polymeric Substances

The role of solutes, in particular EPS, has received much attention as they are widely recognised as being the primary groups of compounds responsible for fouling (Chang and Lee, 1998; Jefferson *et al.*, 2000; Lee *et al.*, 2003; Judd, 2007; Amy, 2008; Meng *et al.*, 2009). EPS are heterogenous mixtures consisting of predominately of polysaccharides, proteins and nucleic acids (Bura *et al.*, 1998) found at or outside the cell surface and in between cells in a floc or aggregate (in the intercellular space) (Judd, 2007). These substances arise from cell lysis, natural bacterial secretion and hydrolysis products (Hernandez Rojas *et al.*, 2005). EPS are also known to be composed of nucleic acids, humic acids and phospholipids (Meng *et al.*, 2009).

In MBR studies, EPS are subdivided into two experimental categories: *bound* (or *extractable*) *EPS* and *soluble EPS* (or *soluble microbial products*, SMP) (Ye *et al.*, 2005). Bound EPS are usually derived from sheaths, condensed gel, capsular polymers, loosely-bound polymers, or attached organic matter (Nielsen and Jahn, 1999). In contrast, soluble EPS are composed of soluble, biodegradable macromolecules and are a product of bound EPS dissolution (Nielsen *et al.*, 1997) (Figure 2.12). The term SMP is often used as a synonym for soluble EPS in MBR studies (Meng *et al.* 2009). In this thesis, the term *soluble EPS* (and not SMP) will be used to describe the soluble organic fraction formed by bacterial metabolism in the mixed liquor and the product of bound EPS dissolution.

Using a variety of techniques, these two fractions are analysed for chemical composition (usually in the form of protein and carbohydrate assay) and correlated with the fouling propensity. The most common way to separate two forms of EPS is usually by centrifugation where the polymers in the supernatant are defined as slimes and the polymers bound to the pellet known as capsular polymers (Nielsen and Jahn, 1999).

Bound EPS tend to be harder to isolate than soluble EPS. In MBR research, both physical and chemical techniques are used to extract bound EPS. The extraction procedures include sampling and pretreatment (washing to remove soluble EPS and homogenising), extraction by an appropriate procedure, purification and analysis (Nielsen and Jahn, 1999). Physical extraction procedures involve the use of sonication and ultracentrifugation (Dignac *et al.*, 1998), cation exchange resin (Frølund *et al.*, 1996) and heating (Morgan *et al.*, 1990; Liu *et al.*, 2001; Lee *et al.*, 2003). Chemical extractions are usually more efficient than physical procedures and include the use of alkaline reagents, ethylenediamine tetraacetic acid (EDTA) and aldehydic

solutions with ultracentrifugation commonly employed during the purification phase (Nielsen and Jahn, 1999). Whatever the method chosen, the aim is to have a sample representative of the EPS bound to cells with the least amount of cell lysis, interruption and release of the EPS biopolymer. In reality, there is no standard extraction method that exists that meets these requirements (Nielsen and Jahn, 1999). Several authors, however, have tried to evaluate which of the methods are the best for extraction.

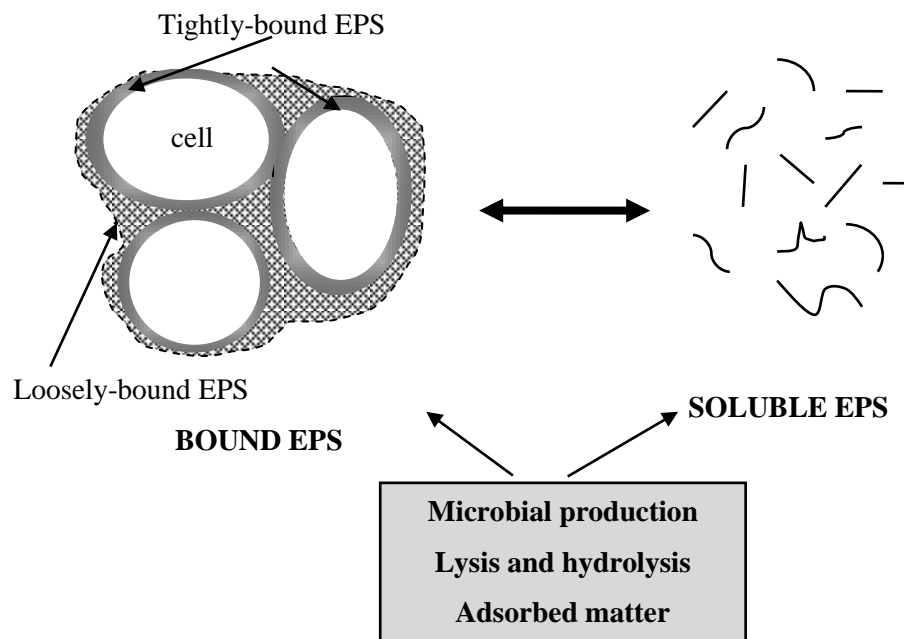


Figure 2.12: Definition of bound and soluble EPS. EPS may originate from bacterial synthesis, hydrolysis and lysis or from attachment (taken from Nielsen and Jahn, 1999).

Liu and Fang (2002) tested various extraction procedures on aerobic, acidogenic and methanogenic (anaerobic) sludge. The techniques that were used included EDTA (2% at 4°C for 3 h), cation exchange resin (4°C for 1 h) and formaldehyde (at 4°C for 1 h, with 1 N NaOH at 4°C for 1 h, with sonication at 60 W for 2.5 min) and physical separation using ultracentrifugation (which also served as the control). Formaldehyde with NaOH extracted the most EPS from all tested sludges with ultracentrifugation the least. The EPS was found to be composed predominantly of carbohydrate, proteins and humic acid with minor quantities of uronic acid and deoxyribonucleic acid (DNA). Using the formaldehyde-NaOH method, it was shown that there were differences in the sludge samples with respect to the most predominant constituent in the extracted EPS. In acidogenic sludge, carbohydrate was the most predominant whereas protein was predominant in aerobic and methanogenic sludge samples. Liu and Fang (2002) also used confocal laser scanning microscopy (CLSM) to quantify EPS in

a microbial community. The EPS content was measured by estimating the weight difference between the volatile solids (VS) and the total volume of microbial cells (determined after staining in the CLSM). The results showed that the CLSM was able to detect more bound EPS than the most effective chemical extraction method (formaldehyde-NaOH) indicating further optimization of extraction procedure is required (Liu and Fang, 2002).

Comte *et al.* (2006) compared four physical and three chemical extraction methods on two different activated sludge samples. The physical methods include sonication (40 W for 2 min), cation exchange resin (DOWEX 50×8 for 1 h at 4°C), sonication with cation exchange resin (40 W for 2 min with DOWEX 50×8 for 1 h at 4°C) and heating (80°C for 10 min). The three chemical methods included EDTA (2% for 3 h at 4°C), formaldehyde (1 h at 4°C) with 1 M NaOH (3 h at 4°C) and 10% glutaraldehyde (for 12 h at 4°C). A control in the form of centrifugation at 4 000 × g was also applied. Chemical extraction procedures were more efficient than physical ones. However, infra-red spectra analysis demonstrated that EPS contamination by extracting reagents occurred. Extraction procedures using glutaraldehyde and EDTA were shown to interfere with the biochemical analysis of the composition of EPS with glutaraldehyde totally preventing the measurement. The physical extraction methods showed a different qualitative composition with protein and carbohydrate as predominant compounds indicating that the process modified the nature of EPS extracted.

Pan *et al.* (2010) compared two physical methods (centrifugation and sonication) and three chemical methods (2% EDTA for 3, 36.6% formaldehyde for 1 h at 4°C, and 36.5% formaldehyde plus 1 M NaOH at 4°C) for the extraction of EPS from algal biofilm. Once the extraction procedure was performed, samples were ultracentrifuged, filtered and purified with a dialysis membrane. The results showed that pre-treatment using low intensity sonication nearly doubled the EPS yield without significant modification of the composition of EPS. The use of EDTA or extraction with formaldehyde-NaOH yielded the best results with respect to extracted EPS content but when analysed using carbohydrate and protein assays, the contents were low. Pan *et al.* (2010) also used three-dimensional excitation-emission matrix fluorescence to analyse all samples before and after dialysis (using a membrane with a MWCO of 3.5 kDa). Protein-like and humic acid-like substances were detected (based on fluorescence) in all of the EPS samples prepared using different methods with fulvic-like fluorescence detected only in the EPS extracted with formaldehyde-NaOH. Differences in peak location and intensity were observed among extraction methods. Moreover, dialysis was found to be an important factor influencing the yield, composition and fluorescence characteristics of EPS as it resulted in a shift in the location of some of the peaks and either reduced or enhanced fluorescence intensity (depending on the extraction method). In most cases, reduced fluorescence was observed indicating that

components with molecular weight of less than 3.5 kDa contained a substantial amount of fluorophores which were removed through dialysis. However, dialysis also enhanced fluorescence intensity in some cases (NaOH-formaldehyde and EDTA extraction methods). Pan *et al.* (2010) suggested that this may be due to interaction of the fluorophores with chemicals used during the extraction procedure or with the ultrasonication method, the binding of some fluorophores to dissociation or degradation products formed during sonolysis.

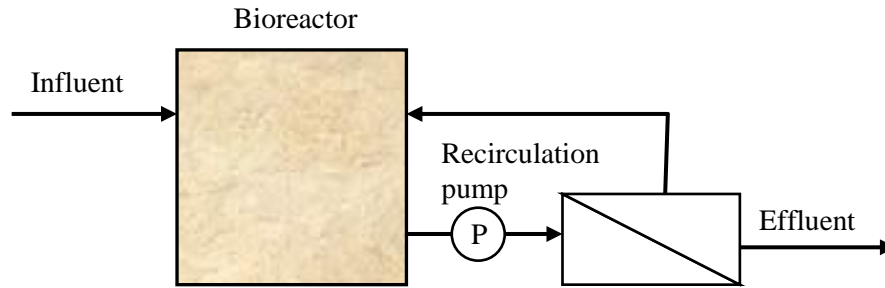
Whilst there is extensive literature that suggests that EPS is involved in fouling, the review above has shown that there is no standard procedure for extracting EPS with a variety of techniques used for extraction and characterisation. This makes comparison between published articles impossible. The issue is further complicated by the definition used to describe different fractions of EPS as it is not consistent between different researchers (Judd, 2006). For this reason, the influence of bound EPS and soluble EPS on membrane fouling is much debated, as is the comparison between results (Nuengjamnong *et al.*, 2005). For example, Kim *et al.* (1998) found that the filterability decreased with increasing soluble EPS in activated sludge. Nagaoka *et al.* (1996), on the other hand, reported that filterability decreased with increasing bound EPS. There are also differences in opinion to which fraction causes membrane fouling. Houghton *et al.* (2001) suggested that polysaccharides are the main fraction responsible for fouling. Masse (2004), on the other hand, postulated that proteins are the main EPS constituent controlling fouling. Consequently, different studies have identified different constituents with having the most influence on fouling.

The *EUROMBRA* Project sought to eliminate some of these problems by standardising the classification, extraction and analytical techniques of these various fractions. This in fact formed part of the first work package of the *EUROMBRA* Project. Through communication between the various partner groups, a common methodology handbook was developed by the Institut National des Sciences Appliquées (INSA Toulouse) and distributed among partners to be used in all MBR research (Cabassud *et al.*, 2006). In the booklet, a few commonly used extraction procedures were highlighted with the most recommended method established from literature and the availability of common equipment among research groups (to ensure that all groups could apply the same technique). Parts of the document describing experiments and data analysis have been reproduced in **Appendix III** and sections of **Appendix IV**.

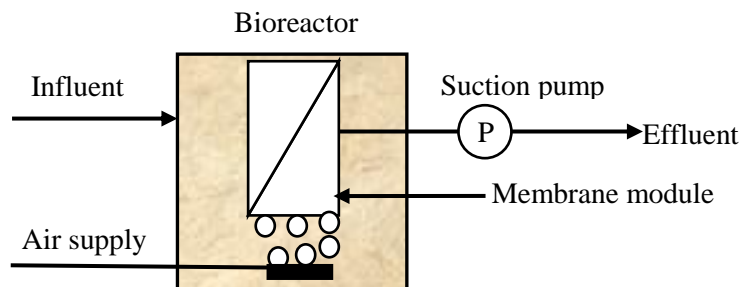
2.2.8 MEMBRANE CONFIGURATION

Membranes can be incorporated into a treatment process in two ways; *internal* (submerged) or *external* (side-stream). The terms internal and external refer to the position of the membrane with respect to the reactor. In the former, outside skin membranes are submerged in the reactor

and permeation occurs to the inside of the membrane (outside/in) (Figure 2.13). The driving force across the membrane is achieved by creating a negative pressure on the permeate side (Cicek, 2003).



(a) External membrane bioreactor



(b) Submerged membrane bioreactor

Figure 2.13: Schematic representation of a) submerged (internal) MBR and b) recirculated (external) MBR (from Ueda, 2001). The representation shows the set-up for an aerobic MBR. Aeration and air scouring would not occur inside an AnMBR.

In external configurations, the membrane is positioned external (outside) to the reactor with the option to either recycle the concentrate back to the reactor or to eliminate recycling step altogether in what is termed *dead-end filtration* mode. Both outside and inner-skin modules can be used in this application (Cicek, 2003). Submerged configurations are often preferred over external configurations due to the lower energy consumption and associated costs (van Dijk and Roncken, 1997; Rosenberger *et al.*, 2002, van der Roest *et al.*, 2002). This can, however, be offset by the higher demand for membrane surface area.

2.2.8.1 Dead-End versus Cross-Flow Operation

Membranes can be operated in two modes: *dead-end* and *cross-flow*. In dead-end operation, the flow of the membrane feed is perpendicular to the membrane and the only stream leaving the membrane is the permeate. In this mode there is no recycling of the concentrate (refer to Figure 2.14).

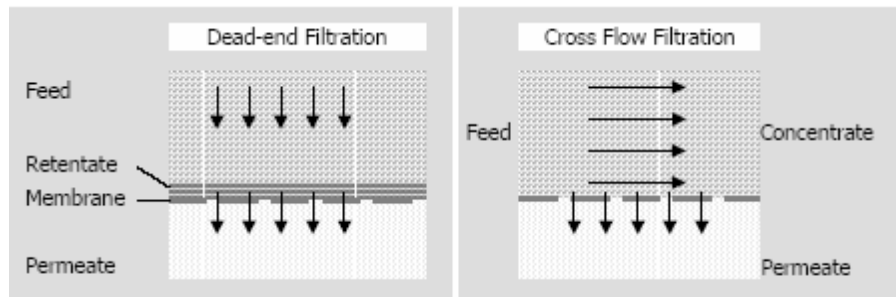


Figure 2.14: Schematic representation of dead-end and cross-flow filtration (from Evenblij, 2006).

In cross-flow operation, a part of the reject stream is recirculated over the membrane surface (Pillay and Jacobs, 2005). This serves to continuously scour and limit the fouling layer resulting in higher flux rates compared to dead-end filtration. However, higher operational costs are associated with the energy required to re-circulate the feed flow.

The choice between dead-end and cross-flow filtration is often determined by concentration of contaminants in the feed. Dead-end operation is usually used for mixtures with lower solids content whilst cross-flow operation is favoured for mixtures with higher solids content. Cost can also be a determining factor. Defrance and Jaffrin (1999) compared the different modes of filtration. The study found that constant flux operation is preferred to constant TMP operation as fouling was less severe with lower operating costs.

2.2.8.2 Constant Flux versus Constant Pressure

From an operational standpoint, membrane filtration is performed in two ways; with a constant transmembrane pressure (TMP) or constant flux. In some cases, a combination of the approaches may be used. In constant flux operation, the permeate production rate is maintained. This operation is usually characterised by an increase in the TMP over time to maintain a steady flux through the membrane as the fouling layer develops (Evenblij, 2006). In constant TMP, the differential pressure across the membrane is maintained. This operation is usually characterised by a decrease in flux over time. Constant flux operation is usually preferred over constant TMP

operation as there are fewer problems in interpreting data from constant flux operation (Aimar and Howell, 1989 cited in Field *et al.*, 1995; Defrance and Jaffrin, 1999).

2.2.9 CRITICAL AND SUSTAINABLE FLUX CONCEPTS

A useful concept, the critical flux (J_c) was introduced by Field *et al.* (1995) to describe and quantify the filtration characteristics of a fluid. The term was originally defined for microfiltration but has now found widespread application in various MBR processes. It was defined as a flux below which a decline of permeability with time does not occur (Field *et al.*, 1995; Howell, 1995). The idea behind the concept is that fouling would not occur under sub-critical fluxes but rather above the critical flux. However, sub-critical fouling has been observed in membrane filtration and membrane bioreactors (Cho and Fang, 2002, Ognier *et al.*, 2002; Le-Clech *et al.*, 2003). Inconsistent results among research groups have resulted in differences in opinion about the definition and notion of critical flux. For that reason, the definition of *critical flux* concepts was re-classified by Howell *et al.* (2004). Three different fluxes were identified which could be used to describe the filterability of a fluid. They are: (i) the *critical flux*, (ii) *transition flux* and (iii) the *sustainable flux* (Cabassud *et al.*, 2006).

The critical flux, originally proposed by Field *et al.* (1995), was re-defined as the permeate flux for which the force balance, between the repulsive forces of particles and the convective forces through the membrane, is equal to zero. Hence, it is the flux at which no fouling occurs. Above this flux, convective forces become higher than repulsive forces resulting in fouling (Cabassud *et al.*, 2006). It also represents the phase transition between a dispersed phase and a condensed phase where particles aggregate to form a deposit that adds to the fouling resistance (Cabassud *et al.*, 2006).

In cross-flow filtration systems, the critical flux is influenced by the cross-flow velocity. Critical conditions can therefore be evaluated using the permeate flux and the cross-flow velocity (Cabassud *et al.*, 2006). Then, for a given cross-flow velocity a critical flux can be defined and for a given permeate flux, a critical cross-flow velocity can be defined (Cabassud *et al.*, 2006). In dead-end filtration systems, when only a liquid sample is used, the convective flow is not counterbalanced by a cross-flow velocity. The deposit mass is thus proportional to the filtered volume. A critical permeate flux can therefore be determined for a filtered volume and a critical filtered volume for a critical permeate flux (Bessière *et al.* 2005, cited in Cabassud *et al.*, 2006).

The determination of the critical flux is difficult experimentally as fouling can occur rapidly, even under low TMP operation. Furthermore, it is difficult to predict the onset of fouling. For this reason, the term *transition flux* is often used to describe the fouling. The term refers to the

flux for which the plot of flux versus TMP for a real fluid differs from the straight line (Darcy's Law) for pure solvent and can be determined experimentally from the filtration of a real fluid (Figure 2.15) (Cabassud *et al.*, 2006). The concept, however, is heavily dependent on the precision of the instrumentation used in the filtration process (Cabassud *et al.*, 2006).

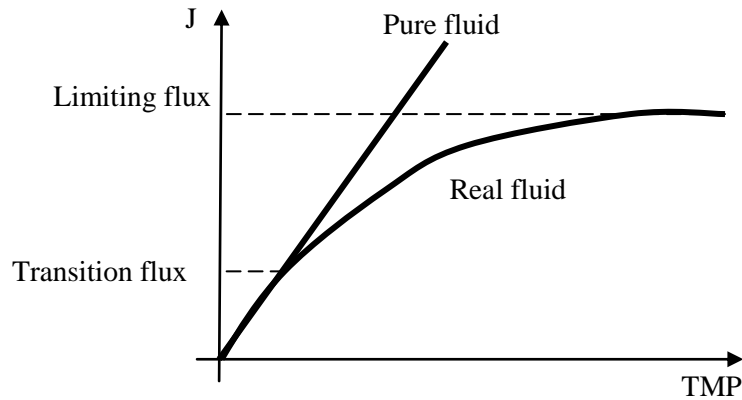


Figure 2.15: Comparison of transition flux and limiting flux with permeate flux against TMP for pure and real fluids (taken from Cabassud *et al.*, 2006).

The *limiting flux* on the other hand is the pressure independent plateau reached by flux in fixed TMP operation. In some cases, this value is close to critical flux at identical velocities (Defrance and Jaffrin, 1999).

The third concept, the *sustainable flux*, is the most practical of the concepts. It describes a range of fluxes which allow for stable operation over a long period and includes the cleaning operations or periodical filtration cycles used to control fouling. This concept is generally used in real systems and is often higher than critical and transition flux (Cabassud *et al.*, 2006).

2.2.10 MEMBRANE CLEANING

The design and operation of MBRs should be based on reducing the rate of fouling, using physical and chemical cleaning while accepting the inevitability of reduced flux due to fouling (Zhang *et al.*, 2007). Recent improvements in fouling control have meant longer membrane life and decreased costs (Chang *et al.*, 2002).

Cleaning is usually divided into two categories: physical and chemical cleaning. The cost associated with cleaning is related to the duration and frequency of the cleaning procedure. More frequent and longer cleaning regimes results in higher operational costs due to process downtime. In MBR studies, physical cleaning is usually performed as *backwashing* or *relaxation*. In backwashing, the flow through the membrane is reversed into the feed channel

(Judd, 2006). This technique is usually performed with submerged hollow-fibre membranes (Chang *et al.*, 2002). The efficiency of this technique is related to the nature of fouling. Stronger adhesion in pore blocking or cake layer formation, for example, results in less effectiveness (Chang *et al.*, 2002). Longer and less frequent backwashing has been reported to be better than shorter, more frequent backwashing (Jiang *et al.*, 2005). Air can also be used to backwash especially in aerobic MBRs. The technique has shown to be quite effective in improving flux [evidence cited in Chang *et al.* (2002) and Judd (2006)]. However, membrane integrity can be compromised due to partial drying of membranes (Judd, 2006).

In membrane relaxation, permeation is ceased for a certain period. The pressure relaxation encourages diffusive back transport of fouling constituents away from the membrane surface under a concentration gradient (Judd, 2006). The technique has been used in both submerged and side-stream aerobic (with enhanced shear through air scouring) and anaerobic systems to positive effect [evidence cited in Chang *et al.* (2002) and Judd (2006)].

Chemical cleaning is characterised by the use of chemical reagents to remove irremovable fouling. Alkaline and acidic cleaning solutions are used to clean organic and inorganic fouling constituents, respectively. Whilst sodium hypochloride (NaOCl) (0.01 to 0.5% v/v) is commonly used in chemical cleaning (Judd, 2006 and 2007), the cleaning procedure itself is usually provided by the membrane supplier.

2.3 ANAEROBIC MEMBRANE BIOREACTORS

The term MBR is commonly associated with activated sludge processes where the membrane replaces the sedimentation stage (Thomas *et al.*, 2000). Due to the predominance of aerated processes in wastewater treatment, far less literature exists with regards to the operation and design of anaerobic membrane systems (AnMBR). Moreover, most scientific research on AnMBR is centred on the treatment of high-strength industrial wastewaters.

With a better understanding of anaerobic processes gained over the last few decades, the coupling of membrane filtration can be seen as advantageous to the digestion process. First, it can be used to increase biomass concentration without increasing reactor volume. Second, it can enhance phase separation through retention of specific anaerobic consortia allowing better treatment efficiencies. Moreover, it can also produce a superior quality effluent. This is particularly important when anaerobic digesters are used as the primary treatment step as anaerobic digestion alone is not sufficient to meet many effluent discharge guidelines. Lastly, installation of membranes can allow intermediate toxin removal at a faster rate than other

anaerobic systems through retention of slow-growing anaerobic micro-organisms (Visvanathan *et al.*, 2000). The elimination of gas scouring, which can account for 20 to greater than 90% of the total cost, and lower sludge production (Gander *et al.*, 2000a) makes the system feasible but it is often offset by the challenge of operating membranes without gas scouring.

Typically, AnMBR research has mostly been confined to the treatment of high-strength wastewaters emanating from food industries (Oyanedel *et al.*, 2003; He *et al.*, 2005), alcohol processing (Ince *et al.*, 2000; Visvanathan *et al.*, 2000; Melamane *et al.*, 2007) and municipal sewage sludge (Aya and Namiki, 1992; An *et al.*, 2009). Whilst the process has been gaining popularity for a number of high-strength wastewaters, applications for domestic wastewater treatment have been limited. In this section, a review of applications in domestic wastewater treatment is presented.

In one of the earliest studies, Bailey *et al.* (1994) investigated a crossflow microfiltration membrane to treat the top liquor from a laboratory-scale UASB. Filtration over 17 d increased the suspended solids concentration in the reactor from 1 000 to 5 900 mg/L. The permeate quality was high with less than 50 mg suspended solids/L and an increase in COD removal (ranging from 98 and 99%) observed. It was postulated that the increase in performance was due to returning liquor that had been aerated from the top zone of the reactor (therefore aerobic digestion of residual COD) or due to increased biomass retention through membrane coupling.

Wen *et al.* (1999) studied a laboratory-scale anaerobic bioreactor coupled with a submerged hollow-fibre membrane treating domestic wastewater at ambient temperature. The plant was able to achieve high biomass retention (16 to 22.5 g/L) and high COD removals (97%) with an organic loading ranging from 0.5 to 12.5 kg.m⁻³.d⁻¹ and temperature fluctuations from 12 to 27°C. Intermittent membrane operation was found to influence membrane permeability with no membrane cleaning required over a two week period at an operational mode of 4 min pumping and 1 min relaxation.

Chu *et al.* (2005) evaluated the performance of an expanded granular sludge bed reactor with a submerged hollow-fibre membrane treating a synthetic domestic wastewater. The system was operated over a 7-month period at a HRT ranging from 3.5 to 5.7 h and constant temperatures ranging from 11 to 25°C. At temperatures above 15°C, the system achieved total COD and total organic carbon (TOC) removals greater than 85% and 83%, respectively. At 11°C, COD removal was shown to increase with an increase in HRT from 3.5 to 5.7 h. Filtration experiments with effluent and clean water revealed that cake layer resistance was the major resistance.

Chu *et al.* (2005) postulated that dispersed solids in the liquid fraction, as opposed to easily settleable granular sludge, adhered to the membrane surface through extraction. The authors stated that electron microscopic investigations showed that a fouling layer had developed on the surface of the membrane while fouling of pores was insignificant although no micrographs were shown in the published work. Values of VSS/TSS of the sludge on the membrane surface were 81 to 86% indicating high organic content. As a means to ameliorate fouling, the effect of upflow velocity on fouling was evaluated. Filtering at upflow velocities ranging from 3 to 8 m/h, Chu *et al.* (2005) found that membrane permeability increased with higher upflow velocities. However, the contribution of upflow velocity to the preservation of membrane permeability decreased after 10 d with little difference between upflow velocity used and the permeability measured. The authors suggested that this result was due to the adhesion of cells to the membrane surface and an increase in the thickness of the cake layer. To elucidate the role of EPS on membrane performance, the quantity of EPS per gram VSS was measured on the membrane surface and the granules in the expanded granular sludge bed reactor. It was found that the membrane surface contained more EPS per gram than granules indicating more EPS accumulation on the membrane surface. Fouling reduction using periodic backwashing with two 3 min cycles per day showed a 3 min on and 1.5 min off operation mode was the most cost-effective. Chemical cleaning with a 0.03% sodium hypochloride (NaOCl) solution was the most effective compared to a mixture of alkaline and acidic solutions.

Kocadagistan and Topcu (2007) evaluated a laboratory-scale anaerobic reactor coupled with a cross-flow microfiltration unit treating the municipal wastewater of Erzurum City, Turkey. The laboratory AnMBR system used in this study was operated in cold ambient temperatures (6°C, approximate average over several years) and was thought to be more useful than a potential large-scale conventional activated sludge plant which would not operate effectively under such conditions. The AnMBR experimental system consisted of one microfiltration module and an anaerobic reactor with a total working volume of 50 L. The plant was able to achieve high removal efficiencies (98, 81 and up to 99% for COD, PO₄-P and suspended solids, respectively) at high permeate fluxes (up to 450 L.m⁻².h⁻¹) with the suspended sludge and sludge micro-organism concentrations below detectable levels in the final effluent.

Saddoud *et al.* (2006) studied the performance of a pilot plant consisting of an anaerobic digester coupled to a cross-flow ultrafiltration membrane. The pilot plant treated domestic wastewater from two sources, Sfax and Ksour Essef regions in Tunisia. Treating wastewater originating from Sfax, the AnMBR did not reach its stationary phase as the anaerobic biomass was unable to adapt to the wastewater. Saddoud *et al.* (2006) attributed this result to fluctuations in domestic wastewater composition and a possible contamination by industrial discharge.

Treating wastewater originating from Ksour Essef, AnMBR operation was successful. In both cases, a total removal of all tested pathogens was achieved with the quality of treated wastewater reaching WHO guidelines for unrestricted irrigation. Phytotoxicity and the microtoxicity tests, using *Lepidiumsativum* and *Vibrio fischeri* respectively, demonstrated that wastewater originating from Sfax exhibited higher toxicity than that from Ksour Essef.

Grundestam and Hellström (2007) investigated the treatment of domestic wastewater by an AnMBR followed by RO. The main objectives of that study were to evaluate gas production, organic matter removal and nutrient recovery in the plant. The AnMBR was operated at 22°C and a HRT of 0.6 d. The AnMBR could achieve removal efficiencies of 92, 9 and 9% for TOC, nitrogen and phosphorus, respectively. Relatively stable gas production rates throughout the study period. The addition of RO to the AnMBR further increased removal efficiency to 99% for TOC, 91% for Kjeldahl nitrogen and about 99% for phosphorus. The addition of the RO unit to the AMBR produced a final effluent that could be used in agricultural activities. The concentrate produced from RO process had a similar nutrient concentration and heavy metal content to human urine (a nitrogen content of approximately 3 g N/L and less than 2 mg cadmium/kg P). However, an acidic solution was required to prevent precipitation and fouling of the RO unit. The authors estimated that the total electricity use for operation for the entire system was approximately 3 to 6 kilowatts/m³.

Saddoud *et al.* (2007) investigated the treatment of domestic wastewater in anaerobic reactor coupled to a cross-flow filtration membrane. The AnMBR was operated over 5-months in order for the system to reach pseudo-steady-state. The system was able to achieve removal efficiencies of 100%, 90% and 88% for TSS, soluble COD and BOD respectively. Biogas production increased with organic loading rate with nearly 30 L of biogas produced per day at an OLR of 2 g COD/L/day after 140 d. Approximately 70% of the biogas produced was in the form of methane and served as an indicator of good indicator of reactor performance. Filtration was characterized by an initial flux over 12 L.m⁻².h⁻¹ over the first 20 d followed by a stage of constant flux (9 L.m⁻².h⁻¹) over 110 d and a progressive flux decrease to the end of the experimentation despite an increase in the TMP applied. Similarly, biomass retention by the membrane allowed biomass concentration to progressively increase from 0.5 g/L MLSS to 10 g/L MLSS at the end of the study. Phytotoxicity tests performed with *Lepidiumsativum* showed that the permeate was non-phytotoxic. The treated wastewater stream met WHO and Tunisian quality guidelines for re-use in agriculture but further processing is required to remove residual nitrogen and phosphate for discharge into public domain.

Van Voorthuizen *et al.* (2008) conducted an interesting study comparing the performance of MBR treating blackwater under aerobic and anaerobic conditions. Two anaerobic systems were used. The first was an AnMBR with a submerged membrane and the other was an UASB reactor with filtration occurring external to the reactor. The same module was used in all reactors treating the same feed wastewater. Membranes were operated at constant flux (around $10 \text{ L.m}^{-2}.\text{h}^{-1}$) with the only difference in operating being the gas lifts used in each system (AnMBR, biogas used at velocity of 40 m/h; UASB, nitrogen used at 35 m/h and aerobic MBR, gassed at 29 m/h). The UASB-membrane reactor produced COD removal efficiencies comparable to the aerobic MBR (91%) but sludge production was noticeably lower. The AnMBR removed the least COD (86%) but had lower sludge production than aerobic MBR. Only minor nutrient removal occurred in all three systems with the level of nutrient conservation (total nitrogen and total phosphorus) high in the effluent. Differences were noted with respect to the nitrogen species in the effluent with more than 80% of the effluent nitrogen in the anaerobic systems consisting of ammonium whereas the nitrogen in the aerobic MBR effluent consisted mainly of nitrate. Total removal of suspended and colloidal matter was reported in all three systems but the effluent still contained relatively high concentrations of soluble COD. With respect to the filtration behavior, the three systems exhibited different fouling patterns which seemed to be linked to the concentration of colloidal matter in the feed. The aerobic MBR had the lowest fouling, followed by the membranes used for UASB effluent filtration and then anaerobic MBR.

Lew *et al.* (2009) investigated the treatment of domestic wastewater in a laboratory-scale anaerobic reactor coupled to an external microfiltration membrane operated in the dead-end mode. The system was fed with pre-settled domestic wastewater and operated at 25°C at three different backwash frequencies and different constant fluxes. Constant filtration flux was achieved without a pump by measuring the height between the anaerobic reactor and the membrane filtration unit (the difference in height between the anaerobic reactor and filtration unit provided the TMP). In all filtration experiments, the TMP was measured continuously until the height difference was 2 m. The system was able to achieve 88% COD removal efficiency and an accumulation of 350 mg TSS/L/day inert matter over a 6-month period. The evolution of fouling occurred in two stages for experiments with different backwashing frequency and constant fluxes: a slow linear phase followed by a rapid increase in TMP. Based on fouling rates during the slow linear phase, it was established that the highest backwash frequency (1 h) was the most appropriate in terms of energy savings and fouling amelioration. Particulates were shown to play an important role in fouling as indicated by the linear increase in TMP in relation to the amount of particulate matter reaching the membrane module. With respect to membrane

cleaning, a mixture of alkaline and acidic solutions gave the best results instead of individual solutions alone.

2.4 PATHOGEN REMOVAL BY MEMBRANE PROCESSES

One of the main drivers of membrane technology is their ability to provide an effective, non-hazardous alternative disinfection step (Shang *et al.*, 2005). As many MBRs incorporate membranes which have smaller pore sizes than bacteria, protozoan parasites and helminths, almost complete removal of these microorganisms have been reported by many researchers (Adham and Jacangelo, 1994; Côte *et al.*, 1997; Hirata and Hashimoto, 1998; Edwards *et al.*, 2001; Lonigro *et al.*, 2006).

High removals of pathogen indicator microorganisms have been achieved in various MBR plants. Gander *et al.* (2000b) reported a 5-log and 9-log reduction in total coliforms using a polysulphone membrane (0.4 mm pore size) and a polypropylene membrane (5 µm pore size) respectively. Ueda and Horan (2000) reported 2 to 6-log removal of phage in a bench-scale MBR (three flat-sheet polyethylene microfiltration membrane modules with a pore size of 0.4 mm) treating settled domestic wastewater. The same MBR plant demonstrated better removal of faecal coliforms and faecal streptococci (up to 7-log) than the conventional full-scale treatment plant treating the same settled sewage (2-log removal) (Ueda and Horan, 2000). Ottoson *et al.* (2006) also reported higher pathogen indicator (*E. coli*, Enterococci, somatic coliphages) removal in a pilot MBR operated in parallel (and treating the same sewage) to a conventional activated sludge process plant. However, the investigation also showed that the removal of viruses was similar to that of the tertiary treatment step in the activated sludge process plant indicating that viruses are not always as efficiently removed as bacteria. Whilst this result may have been expected considering the average nominal pore size of the membrane module (0.4 µm – which is larger than a virus), virus removal can occur even in microfiltration modules (with pore sizes larger than viruses)

In the study performed by Shang *et al.* (2005), a hollow-fibre module with a pore size of 0.4 µm showed poor virus (cultured stock of bacteriophage MS-2, size approximately 0.02 µm) removal when the module was submerged in a tank without biomass. However, once biomass was introduced the system, a biofilm developed on the membrane surface which substantially increased the removal of the virus. Similarly findings were noted by Lv *et al.* (2006) using a submerged MBR with two different pore size hollow-fibre membranes (0.1 µm and 0.22 µm) treating municipal wastewater. A virus (T4 phage) was introduced into the MBR and the rejection of this phage monitored through both membrane modules. When stable membrane

operation was achieved, both modules exhibited near complete removal of the phage. In the smaller pore size membrane (0.1 μm), the membrane alone (through its pore size) prevented the passage of the phage into the permeate line. However, in the larger pore size module, a cake/gel layer formed which played a significant role on phage removal possibly through adsorption. The deliberate removal of this fouling layer resulted in decreased phage removal efficiency. These results indicate the importance of maintaining a balance between allowing fouling layer development to occur and ensuring that the effluent flux or the increase in TMP is practical.

It is important to note the membrane module cannot always provide a disinfected product. Pathogens may pass through membranes when the membrane system integrity is compromised. The four main reasons for membrane failure are: (1) chemical oxidation through prolonged use of cleaning agents or frequent washings; (2) faulty installation and poor maintenance; (3) damage through abrasive or sharp-edged materials in the membrane feed; and (4) faulty membrane/module structure (Le-Clech *et al.*, 2005). Once damage occurs to the membrane, the disinfection process of the modules will be compromised and the faulty membrane/module should be replaced immediately (Le-Clech *et al.*, 2005).

2.5 CONCLUDING REMARKS

This section presents the conclusions of the literature survey, the challenges of this work and the technological gaps that would be addressed in this thesis.

2.5.1 ABR

The ABR has been shown to be a fairly robust on-site sanitation system. In the literature review, it has been shown that the ABR displays superior performance over conventional septic tanks (Foxon *et al.*, 2006, Nguyen *et al.*, 2007) and in one case, found to be the main treatment system in un-steady-state conditions in a hybrid UASB system (Singh *et al.*, 2009). Over 120 000 ABRs have been installed as part of BORDA DEWATS plants in Asia and southern Africa over the past decade to serve dense urban settlements on a household or community level (BORDA, 2005, Panzerbieter *et al.*, 2005; Eales, 2008). One of the major problems with some of these plants is that the ABR unit cannot achieve local water discharge regulations (pathogen indicators and nutrients) by itself. Whilst this not a problem confined to ABR technology or any other anaerobic or aerobic technology (almost all biological treatment systems require polishing), the choice of effluent polishing is problematic as the polishing system must also conform to the decentralised approach (that is, low-cost and low maintenance) for which the system is intended. Thus, complicated and energy-intensive polishing such as activated sludge, submerged aerated biofilm reactors or trickling filters cannot be used as their application would

defeat the initial purpose of the plant. In conventional BORDA DEWATS plants, a combination of anaerobic filters, constructed wetlands and/or ponds are used after an ABR for polishing. Whilst these systems are not energy intensive, they do require a large land area for construction which may not be available in a densely populated community. More importantly, the reliability of these systems to disinfect the effluent stream is debatable. A review of the literature has shown that in the most widespread anaerobic system, the UASB reactor, pathogen indicator removal varies, with many a polishing system not reaching international guidelines for discharge (1 000 CFU/mL) (section 2.1.4). A similar problem has been reported in some DEWATS plants (Anh *et al.*, 2003; Nguyen *et al.*, 2007).

2.5.2 MEMBRANES

In this thesis, the use of membrane technology following an ABR is considered. The process has well-known advantages including the potential to consistently produce a highly quality effluent stream (reduced pathogen load) at reduced land area footprint (compared to a wetland or pond). This potentially pathogen-free product rich in plant nutrients can then be recycled and used as a fertilizer replacement in community gardens. The main disadvantages of the technology are related to cost and inherent fouling phenomenon experienced in all membrane systems. With respect to cost, it is generally acknowledged that whilst membrane polishing systems are costly, the price of membranes is continually decreasing due to a greater understanding of the process and improved process design (Kennedy and Churchouse, 2005; Judd, 2006). Strategies, such as submerging membranes in the aeration tank to control fouling (Yamamoto *et al.*, 1989) and operation below the critical flux (Field *et al.*, 1995) have prolonged process operation.

2.5.3 CHALLENGE

One of the challenges in this thesis is to use membrane technology, considered a high-tech treatment system, in a low-cost manner. Any membrane polishing system incorporated with ABR technology for on-site sanitation must also conform to decentralised principles (low maintenance, no energy requirements). Thus, aeration cannot be used for fouling control and no pumps can be used to operate the system at constant flux. The membranes must then be operated at ultra-low hydrostatic pressures (using gravity) without air scouring (no energy). Whilst this strategy has been employed for decentralised drinking water solutions (Ueda and Hata, 1999; Peter-Varbanets *et al.*, 2009) and certain greywater applications (Huelgas and Funamizu, 2009 and 2010), there is scarce information regarding the application of membrane polishing technology in this manner for decentralised sanitation. To the author's knowledge, only one published article deals with a similar situation (septic tank with membranes operated at constant flux) and that was over 30 years ago (Grethlein, 1978).

Another challenge is to understand the membrane filtration behavior under anaerobic conditions, specifically in an ABR. While this has been investigated for several anaerobic systems (Liao *et al.*, 2007), no research has been performed on an ABR. Whilst the fouling mechanism may be similar to that of aerobic and anaerobic MBRs, the nature of the foulants is expected to differ as even with systems treating the same feed, differences in membrane fouling have been observed (Van Voorthuizen *et al.*, 2008). The conditions to which membranes will be exposed will be different to other systems; membranes will be installed after the last compartment of the ABR where the concentration of solids and biodegradable COD are expected to be low (refer to Table 2.9). Additionally, fouling behaviour may be different due to differences in process operating conditions, feed characteristics and membrane properties.

Table 2.9: Effluent concentrations from ABRs treating various wastewaters.

Wastewater treated	HRT (h)	Total COD	TS	VS	VFA	Reference
Domestic	22	212	225	127	nd	Foxon (2009)
Domestic	40-44	130	378	nd	0	Foxon (2009)
Synthetic	8	51	nd	nd	26	Gopala Krishna <i>et al.</i> (2007)
Synthetic	10	47	nd	nd	25	Gopala Krishna <i>et al.</i> (2007)
Combination of domestic, greywater and blackwater streams	nd	295	195*	nd	nd	Nguyen <i>et al.</i> (2007)

nd, not determined; *, TSS value.

2.5.4 TECHNOLOGICAL GAPS

Based on the review conducted, the study aims to fill the following technological gaps:

- evaluate the performance of an ABR treating a complex wastewater (defined as particulate wastewater that is not easily hydrolysable as with a soluble feed) representative of blackwater
- evaluate the performance of gravitational filtration systems (no energy) operated without gas scouring as a polishing step for anaerobic technologies, in particular the ABR.
- evaluate differences in membrane systems (different membrane types) treating ABR effluent
- evaluate differences in ultra-low pressure (less than 10 kPa) change on fouling behaviour
- characterise the fouling behaviour in a membrane-coupled ABR
- identify fouling constituents in an ABR based on two of the three recognised foulant definitions (practical and composition) using standardised techniques provided by *EUROMBRA*.

These gaps will be addressed by:

- designing and constructing a laboratory ABR to treat a complex particulate wastewater from VIP toilets
- operating membrane units after ABR treatment using gravitational pressures to drive the process
- two different module types will be assessed; a flat-sheet unit and a hollow-fibre unit and their performance evaluated in terms of flux-time relationships, and membrane permeability values before and after fouling (practical definition of fouling)
- evaluate membrane performance at different TMP to investigate the effects on flux-time relationships
- use *EUROMBRA* stipulated techniques to identify the nature of the foulant (chemical composition and size-fraction membrane filtration, that is, according to the compositional definition of fouling).

In the next chapter (**Chapter 3**), the design and operation of the laboratory membrane unit coupled to an ABR is presented.

CHAPTER 3 : DESIGN, CONSTRUCTION AND OPERATION OF LABORATORY SYSTEM

This chapter presents the development of an ABR followed by a membrane filtration step for laboratory-based studies. The design and operation of the laboratory ABR is presented in sections 3.1 and 3.2, respectively. Sampling of the feed for the laboratory system is presented in section 3.4 whilst the preparation of the feed wastewater for the system is presented section 3.5. Section 3.6 presents a comparison of the laboratory feed against actual sanitation wastewaters. A brief description of analytical techniques used and sampling points is presented in section 3.7. Section 3.8 describes operational and maintenance issues whilst section 3.9 provides a description of standard terminology used in this thesis.

3.1 DESIGN AND CONSTRUCTION OF ABR

The laboratory-scale ABR was designed according to recommendations highlighted in Foxon *et al.* (2006). The 8-compartment pilot ABR design used in Project K5/1248 (width: length: height ratio = 2: 6: 2) (Foxon *et al.*, 2006) was changed to a 4-compartment ABR with wider compartments. External dimension ratios of approximately 2: 3: 5 (width: length: height) were used in designing the laboratory system. According to Foxon *et al.* (2006), a larger width: height ratio design (a 40% increase in width in comparison to pilot ABR) is more suited for the treatment of domestic wastewater as it encourages better solids retention.

All compartments were constructed from stainless steel sheets and laser cut to specific dimensions (Laser CNC). The dimensions of the feed tank and compartment boxes are shown in Figure 3.1.

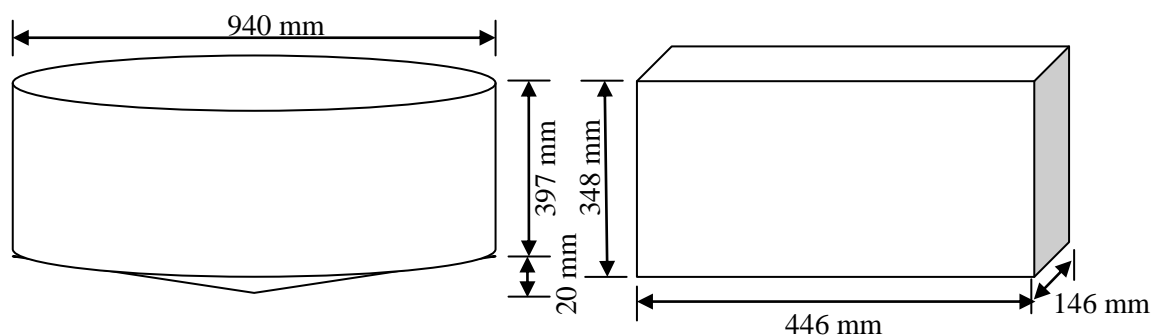


Figure 3.1: Schematic representation of the ABR plant showing external dimensions. The feed tank and the compartment boxes were built from 3 mm stainless steel sheets. Diagrams are not drawn to scale.

The reactor was also modularised into a large round feeding tank (approximately 240 L) and four compartment reactor *boxes* (approximately 22 L) connected in series (Figure 3.2). The rationale behind this modification was that compartments could be added to or removed from the basic design of four compartments. Previously built ABRs were typically a fixed design, a rectangular box that was divided by baffles into compartments, which did not allow compartments to be added or removed.

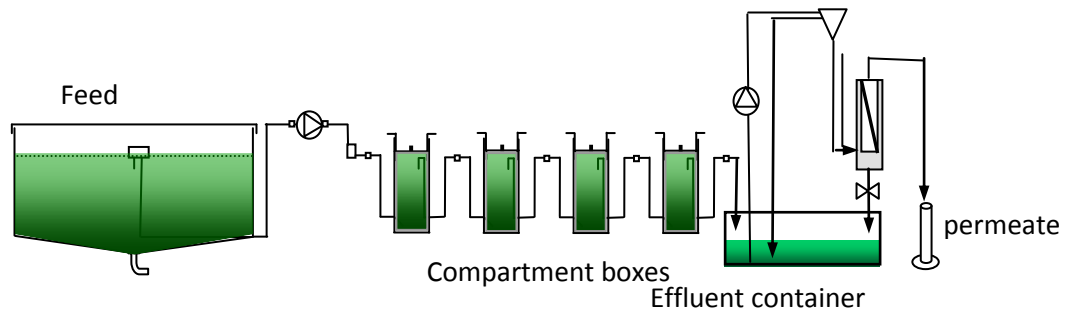


Figure 3.2: Schematic representation of laboratory ABR with membrane post-treatment.

The large round tank served as both a settling and feeding tank with the capacity to hold two days of feed. The feed tank was filled via a sampling port on feed tank lid using a bucket or a 95 L polyvinyl chloride (PVC) container. Wastewater was pumped from a floating pipe into a splitter box via a peristaltic pump (Watson-Marlow 320 Du/D). The wastewater then flowed through the ABR train consisting of a series of four reactor compartments (Figure 3.2). Inside each compartment were three upflow and three downflow pipes, representing standing and hanging baffles, respectively (Figure 3.3). This design removed the hanging and standing baffle design of the old pilot ABR design with the no clearly defined downflow section (Figure 3.4). Siphon breakers were also placed between each box to prevent air blockages in the pipes. Water-seal lids kept the reactor compartments anaerobic and allowed for the collection of biogas via a valve connected to plastic Tedlar® bags (Sigma-Aldrich).

The effluent generated from the ABR was collected in a large container (120 L). Initially, plastic containers were used but over time they became damaged due to the weight of the effluent (approximately 90 L/day). To solve this problem, a stainless steel effluent container was constructed with the capacity to hold a 2 d effluent volume. The effluent generated from the ABR was pumped via a peristaltic pump to an external (side-stream) membrane bioreactor. Excess effluent was decanted in a drainage system in the laboratory that connected to a sewer.

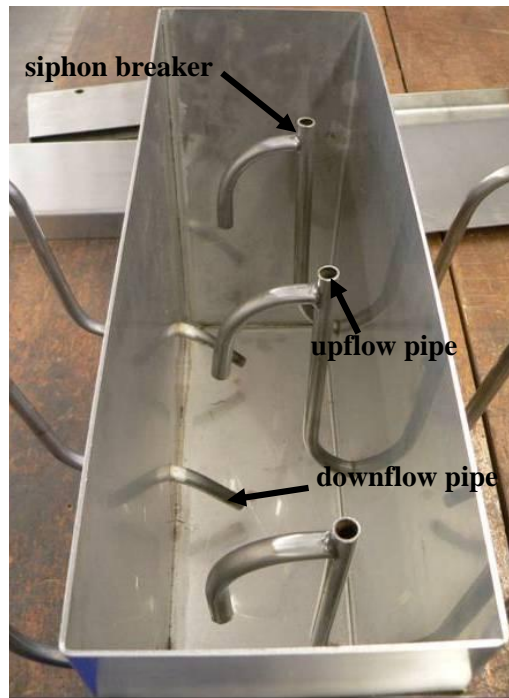


Figure 3.3: The inside view of the laboratory-scale ABR compartment. Downflow pipes act as hanging baffles whilst upflow pipes act as standing baffles. The siphon breaker acts to limit scum from moving to the next compartment and prevents the clogging the pipes.

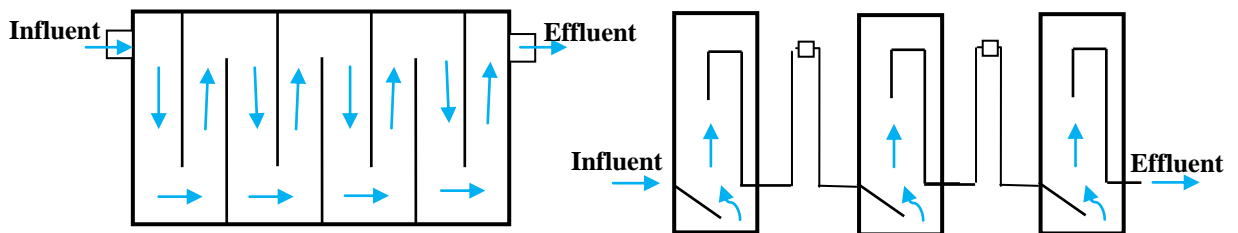


Figure 3.4: Schematic comparison of ABR designs from (a) Project K5/1248 (Foxon *et al.*, 2006) with (b) the laboratory ABR used in this thesis showing flow patterns. In Project K5/1248, the pilot ABR had hanging and standing baffles with clearly defined downflow and upflow regions. In contrast, the laboratory ABR used in this study removed the ‘downflow’ section of the old design; flow through sludge bed in each box compartment occurred through slanted pipes welded at the bottom of each box. The diagrams are not drawn to scale.

3.2 OPERATION OF ANAEROBIC BAFFLED REACTOR

This section describes the operating procedure of the laboratory ABR and the determination of hydraulic and organic loadings.

3.2.1 FEEDING MODE

The laboratory-scale ABR was operated in the semi-continuous mode with the feed wastewater loaded into the round feed tank batch-wise (every 1 to 2 d). Consequently, the concentrations in the feed tank were not constant.

Flow between the feed tank and compartment boxes was continuous. The peristaltic pump was switched off during feeding and restarted when the round feed tank was loaded with feed wastewater. Feeding was usually performed when the amount of wastewater in the feed tank was close to the upper level of accumulated sludge in the decanting cone of the feed tank. The effluent was collected continuously and the effluent tank emptied before feed wastewater loading and after the recording of effluent volume.

3.2.2 HYDRAULIC RETENTION TIME AND ORGANIC LOADING RATE

The flow rate through the ABR treatment train was kept relatively constant using a peristaltic pump. The hydraulic retention time (*HRT*) of the laboratory ABR was calculated using equation 3.1. The equation describes the average time that the wastewater resides in the plant.

$$HRT = \frac{V}{Q} \quad \text{Equation 3.1}$$

where:

HRT: hydraulic retention time (d)

V: Working volume of the reactor (the volume of the round feed tank and ABR train) (m³)

Q: Process flow rate (m³/d).

In this thesis, the working volume of the reactor used in Equation 3.1 represented the combined volumes of the round feed tank and the ABR train. This was done in order to include the possible effect that most of the COD removal and digestion in the plant occurs in the feed tank rather than in the compartment train (the theoretical *HRT* of a single box compartment was approximately 5 h but varied between 0 to 72 h in the feed tank).

The OLR is defined as the amount of organic matter, in either feed VS or COD, which must be treated by a certain volume of a reactor in a certain time (Equation 3.2).

$$OLR = \frac{\text{Feed COD} \times V}{HRT} = \text{Feed COD} \times Q \quad \text{Equation 3.2}$$

where:

Feed COD: The total COD of the feed wastewater (kg COD/d)

V: working volume of the reactor (m³)

HRT: hydraulic retention time (d)

Q: Process flow rate (m³/d)

The operating conditions of the laboratory ABR train are presented in **Appendix II** which presents details of performance of the system and effluent characteristics for membrane experiments.

3.3 MEMBRANE FILTRATION SYSTEM

Two membrane filtration units were designed and developed for ABR effluent post-treatment. The first system was designed to house hollow-fibre modules whilst the other was designed to house flat-sheet modules. In this section, details of each filtration system and the membrane modules used are presented.

3.3.1 HOLLOW-FIBRE UNIT

Two membrane modules, a microfiltration (MF) and an ultrafiltration (UF) membrane, were specifically manufactured by Polymem (France) for the *EUROMBRA* Project and delivered to UKZN in 2007 (Figure 3.5). The modules consisted of a bundle of polyethersulfone hollow-fibres. The active filtration area of the bundle was 1 m². Details of the membranes are provided in Table 3.1.

Table 3.1: Characteristics of hollow-fibre membranes used during study.

Membrane	Type	Area	MWCO	Model	Supplier
Ultrafiltration	Hollow-fibre	1 m ²	0.08µm	UF2522 S3	Polymem, Fr.
Microfiltration	Hollow-fibre	1 m ²	0.20µm	MF2522 S	Polymem, Fr.

Abbreviations: MWCO, molecular weight cut-off; UF, ultrafiltration; MF, microfiltration; Fr., France

The Polymem membrane module housing was constructed out of PVC. The membranes were removed and placed in storage solution in separate storage cylinders. A feed line was inserted near the base of the airtight membrane housing which was connected to a height-adjustable feed funnel (to change the hydrostatic pressure) via silicon tubing [8 mm internal diameter (i.d.)] (Figure 3.6). A clear PVC tube was placed between the feed funnel and the PVC casing to



Figure 3.5: Hollow-fibre ultrafiltration and microfiltration membrane modules provided by Polymem, France.

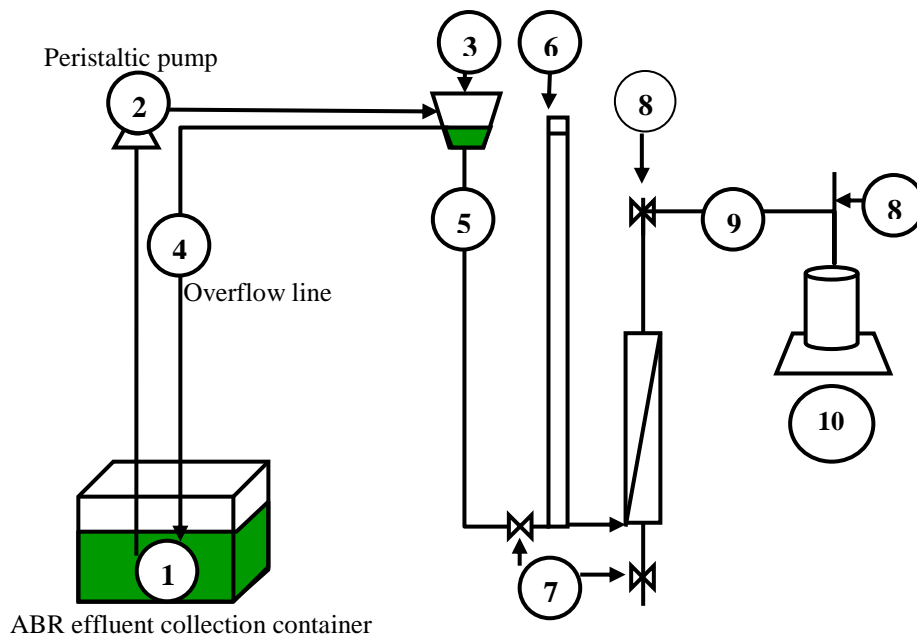


Figure 3.6: Schematic representation of the external MBR used in this study. (1) ABR effluent container, (2) peristaltic pump, (3) height-adjustable feed funnel, (4) feed funnel overflow, (5) membrane feed line, (6) water column stand pipe, (7) decant valves, (8) siphon breaker, (9) permeate line, (10) mass balance. The diagram is not drawn to scale.

determine the water column height on the feed side of the membrane. The laboratory ABR effluent was pumped from ABR effluent collection container to the encased membrane module. Flow occurred from the outside of the membrane fibres to the inside of the hollow-fibres and exited at an outlet pipe connected to silicon piping (8 mm i.d.). Permeate pipes were filled with water before filtration using the siphon breaker (Figure 3.6) to induce a siphon. Valves were placed on the bottom of the casing to drain the membrane concentrate and near the base of the casing to bleed trapped air (Figure 3.6). The volume of concentrate available to membrane area was 4.7 L.m^{-2} (volume of membrane unit = 4.7 L; area of membrane = 1 m^2).

3.3.2 FLAT-SHEET MEMBRANE UNIT

A flat-sheet membrane filtration system was designed and evaluated by Dr. S Pollet as part of his post-doctoral research study at the Pollution Research Group (PRG). Two types of flat-sheet modules were evaluated in this reactor: Kubota and a locally produced fabric membrane. The Kubota membrane was an A4 size plate-and-frame module that is commercially available (Figure 3.7) and was donated by Aquator, a local distributor of Kubota membranes in South Africa. The second type was a woven-fibre fabric membrane that was constructed to an A4 paper size by the Durban University of Technology (DUT) (Figure 3.7). The same module was used in another WRC-funded project which sought to provide potable water supply in rural communities through microfiltration. Details on the development and construction of this membrane module can be accessed in WRC Project K5/1598 (Pillay, 2009).

The difference between the two flat-sheet microfiltration modules is related to the type of material used in the construction of the module. The membrane material used in the Kubota module consists of a chlorinated polyethylene outside surface cast on a porous flat support media (van der Roest *et al.*, 2002) (Figure 3.8) whereas polyester filaments spun into fibres are used for the locally produced fabric modules (Figure 3.9). The fabric module has a distinct advantage over the other modules as its integrity is not compromised when the membrane is dried (the other modules have to be immersed in liquid or kept wet after filtration). The disadvantage of the module is that it has no clearly defined pore size due to the nature of the filter material (interwoven fabric). The nominal pore size of Kubota membrane sheet is $0.4 \mu\text{m}$.

The membrane modules were housed in a PVC filtration system (length \times width \times height of $245 \times 200 \times 510 \text{ mm}$) (Figure 3.10). The flat-sheet system was divided into two sections; a smaller compartment which was connected to a membrane housing compartment through a 25 mm spacer at the bottom of the box. The effluent from the ABR was pumped via a peristaltic pump (Watson-Marlow 323) to the smaller inlet compartment in which any solids would settle. An overflow was placed on the membrane housing side to maintain a constant liquid level in the



Figure 3.7: Pictures of the Kubota (left) and fabric (right) membranes (PRG, 2009).

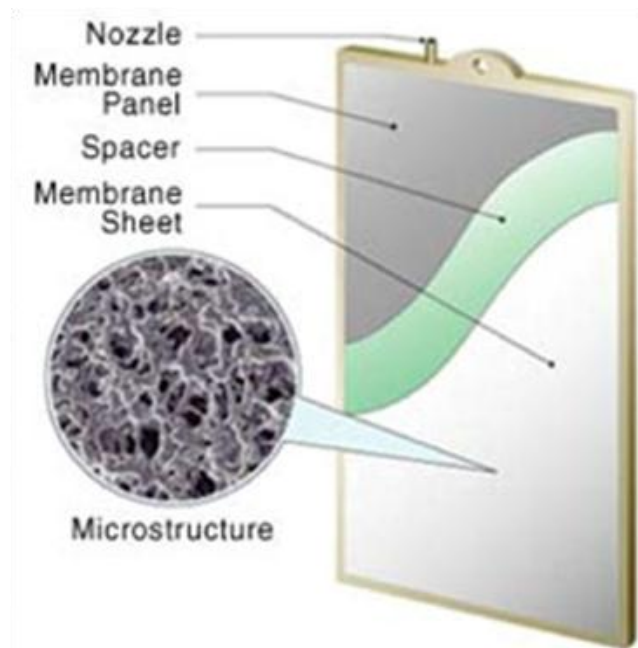


Figure 3.8: The microstructure detail of the Kubota membrane (Taken from: Ministry of the Environment - Global Environment Centre, 2007).

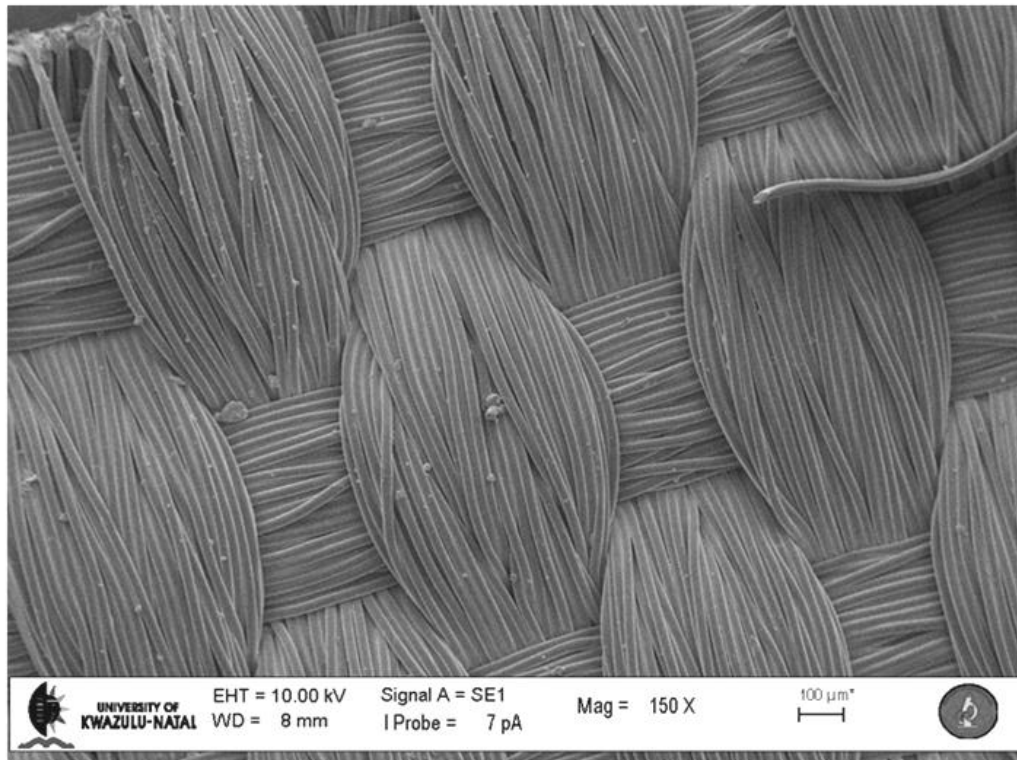


Figure 3.9: SEM image of the fabric membrane showing woven-fibres (PRG, 2010).

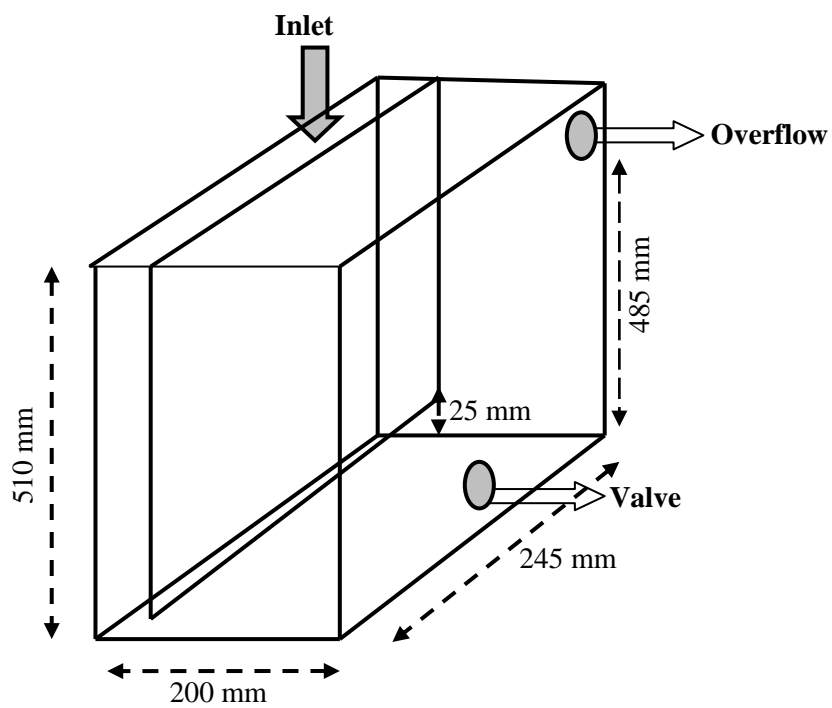


Figure 3.10: Schematic of the membrane pilot used to house flat-sheet membranes (PRG, 2009).

box. A decanting valve was also placed near the bottom of the membrane box to remove any settled material. Membranes were stored in distilled water between experiments.

Membranes were positioned at least 50 mm above the compartment bottom to avoid the possible filtration of settled material in the box. Active membrane filtration areas were approximately 0.090 m² for each woven flat-sheet membrane and 0.117 m² for each Kubota membrane. The filtration occurred on both sides of the membrane with fluid flow occurring from outside to the inside the membrane and exiting the membrane via an outlet pipe at the top of the frame. The volume of concentrate to membrane area was approximately 230 L.m⁻² (volume of membrane unit = 23 L; approximate area of membranes = 0.1 m²). Silicon tubing was connected to the outlet pipe and used to adjust the hydrostatic pressure.

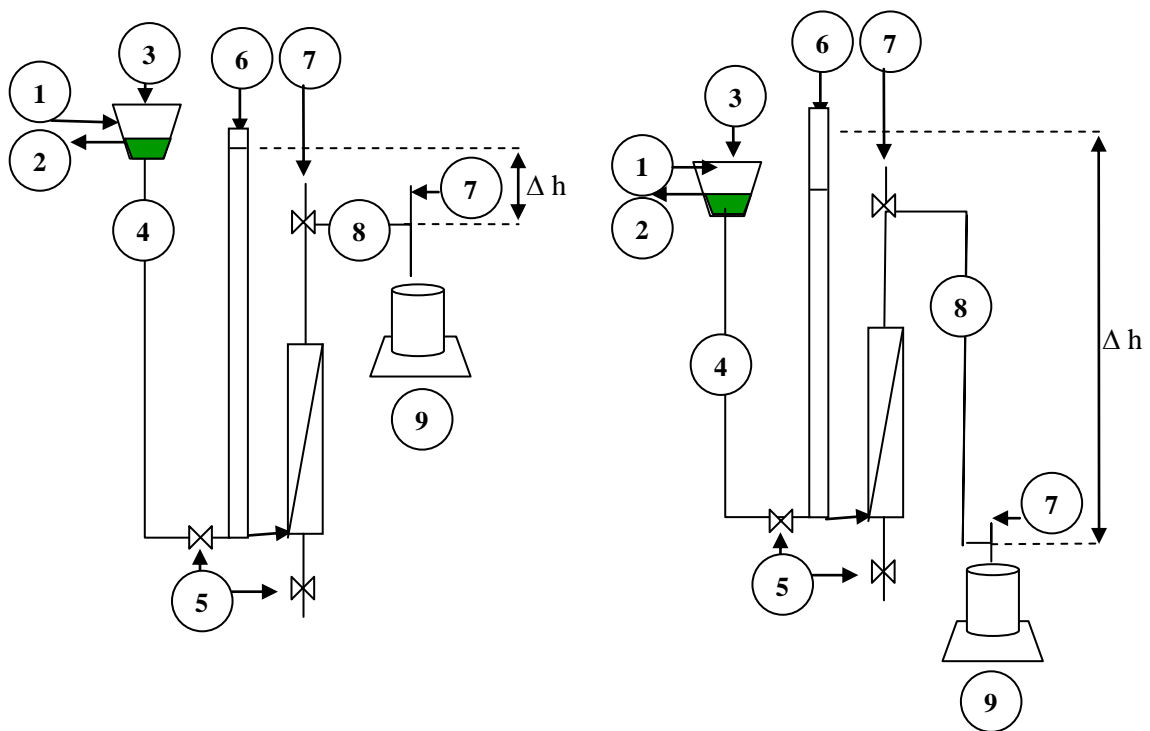
3.3.3 MEASUREMENT OF TMP IN MEMBRANE UNITS

This section describes the measurement of the hydraulic head and the calculation of TMP for the two membrane units.

Figure 3.11 presents an overview of the measurement of the hydraulic head for the hollow-fibre modules. The hollow-fibre unit was designed to have flexible water height configurations. Both the membrane feed funnel and the airtight membrane housing could be moved vertically in either direction. The hydraulic head was measured by calculating the height difference between the top of the permeate pipe to the water level in the stand pipe. During earlier trial clean water filtration tests, the hydraulic head was determined from the height difference between the bottom of the permeate pipe to the water level in the stand pipe. This led to an underestimation of the flux at a specific TMP, especially at pressures lower than 300 mm water head. This error in measurement (approximately 10 mm – 8 mm pipe bore and 2 mm wall size) was corrected before the first filtration experiments were reported in this dissertation.

Two configurations were used to measure the hydraulic head in the hollow-fibre unit. At hydraulic heads under 500 mm, the configuration shown in Figure 3.11a was used. This was due to the configuration being limited by the water column height available in the clear PVC stand pipe. When hydraulic heads over 500 mm water were required, the configuration in Figure 3.11b was used. The membrane housing unit was elevated up to the level of membrane feeding funnel and the permeate line lowered below the membrane housing. In all configurations, the hydraulic head was measured was assumed to be equal to the average pressure head across the membrane module. The permeate line of the hollow-fibre unit was placed over 5 L beaker. A T-piece was used at the end of the permeate line to act as a siphon

breaker. Furthermore, it prevented the permeate from adhering to the outside of the walls of the permeate pipe and dripping along the length of the pipe.



a) Configuration for under 500 mm water head b) Configuration for over 500 mm water head

Figure 3.11: Schematic representation of the configurations used to measure the hydraulic head in the hollow-fibre membrane unit. (a) Configuration used when hydraulic heads under 500 mm water were required. (b) Configuration used when hydraulic heads over 500 mm water were required. Key: (1) ABR effluent feed line, (2) feed funnel overflow, (3) height-adjustable feed funnel, (4) membrane feed line, (5) decant valves, (6) water column stand pipe, (7) siphon breaker, (8) permeate line, (9) mass balance. The diagram is not drawn to scale.

Figure 3.12 presents an overview of the measurement of the hydraulic head for the flat-sheet modules. Unlike the hollow-fibre unit, the flat-sheet unit could not be arranged into different height configurations by moving the feed line or membrane housing box. Furthermore, the membrane housing unit was not airtight with an overflow maintaining a constant water height in the box. Thus, the hydraulic head of the flat-sheet unit could only be significantly changed by adjusting the height of the permeate lines. At low hydraulic heads over than 400 mm water, the hydraulic head was determined by the difference between the height of the liquid level in box

(in relation to the floor) (the sum of labels *a*, *b* and *c* in Figure 3.12) from the height to the top of the permeate pipe (in relation to floor) (label *c* in Figure 3.12).

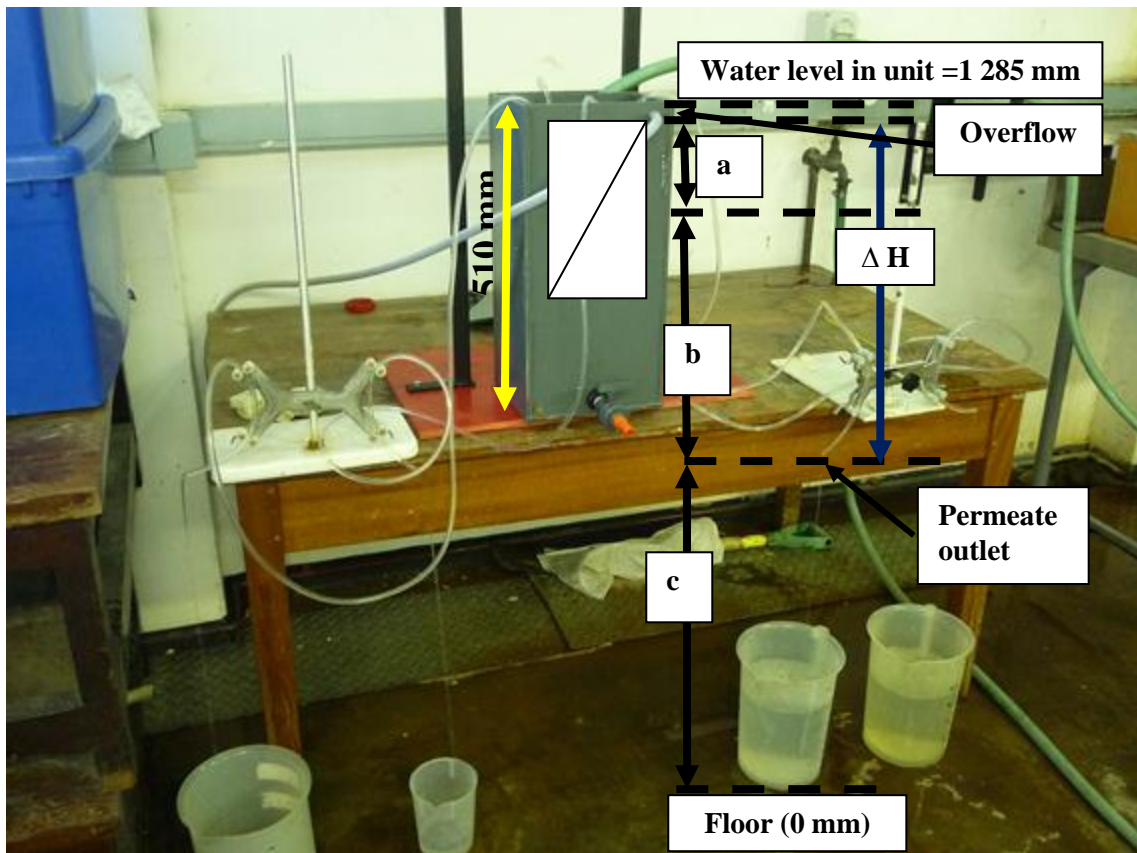


Figure 3.12: Photograph of the flat-sheet membrane unit during a clean water filtration test. The hydraulic head was determined by the difference in elevation from the permeate line to the middle of the membrane module. (a) Height from liquid level in box to the middle of the membrane module. (b) Height from middle of the membrane module to the permeate pipe. (c) Height from floor to permeate pipe.

When low hydraulic heads were used (under 400 mm water), the hydraulic head was measured from difference in height from the middle of the membrane module to floor (labels *b* plus *c*) and from the top of permeate outlet to the floor (label *c* in Figure 3.12). The reason for the difference in the measurement of the hydraulic head in the same membrane unit was due to the membrane modules being operated in an upright position. Under low hydraulic heads (400 mm), the average hydraulic head cannot be calculated from the top liquid level to the outlet of the permeate pipe due to the length of the membrane module (approximately 300 mm). For this reason, the average hydraulic head of the module was calculated from height difference from middle of the module to the permeate outlet.

The flat-sheet membrane unit was placed on a desk and not moved for the duration of the study. Thus, the height of the water level in the membrane unit was constant throughout the study (1 285 mm).

The methods used to the hydraulic head were not consistent throughout the study as different project team members were responsible for designing, feeding, sampling, measuring, analysing membrane data.

The TMP in both membrane units was calculated by assuming 1 000 mm of water head was equal 10 kPa and that the frictional losses along the length of the pipe were negligible. Theoretically, 1 000 mm of water head is equal to 9.8 kPa (pressure = density (1 000 kg/m³) × height (1 m) × gravitational field strength (9.81 N/kg)). Thus, the error in the assumption that 1 000 mm water head was equal to 10 kPa was minor.

3.4 FEED COLLECTION AND HANDLING

At the beginning of WRC Project K5/1661 (in 2006), the project team had to decide between commissioning a pilot reactor at a treatment facility and having a laboratory-based system. The team opted for a laboratory-scale system based on difficulties experienced with operating a pilot ABR at a treatment works. These included the distance travelled between the university and to the nearest treatment plant that treats domestic wastewater only (approximately 30 km) as well as the time taken between sampling at the treatment works and analysis in the laboratory.

A laboratory-based system was chosen for the following reasons. It could be easily monitored daily, laboratory analyses could be performed almost immediately after sampling whilst transport costs are kept to a minimum. However, the limitation of this strategy was that a relatively large and constant supply of feed wastewater (100 L/d) to the reactor was required. Wastewater was not easily assessable at the university nor was transporting large volumes of wastewater to the laboratory feasible. Initially, fresh faecal and urine samples were collected from students to feed the reactor but supply was not consistent or sufficient to maintain successful operation (continuous feeding). Consequently, the strategy shifted towards acquiring large amounts of faecal material which could be used to feed the system.

An opportunity arose to receive large volumes of sludge from another WRC-funded project dealing with VIP toilet processes, emptying and disposal (WRC Project K5/1630) (Foxon and Buckley, 2007). Periodic emptying of VIP toilets was being undertaken by the Ethekwini municipality in a specific area with the aid of contractors once the pits were full. The pit

contents are composed of faeces and urine, and can be therefore regarded as a source of blackwater. Other solid waste, such as plastic and glass, is also common in the pits. Although it is understood that the treatment of this sludge in an ABR and the resultant effluent interactions with the membrane may not necessarily be the same as that of actual domestic wastewater, this was the closest representation of feed material that could be used within the confines of the project.

3.4.1 SYNTHETIC BLACKWATER

The sludge of VIP toilets were used as a source of synthetic blackwater. To collect the VIP sludge, project team members would either drive to the area where pits were being emptied by contractors (Tongaat or KwaMashu) or obtain the sludge from a specific household in Marianhill (Figure 3.13). The latter required the approval and permission of the municipality and a local community liaison or leader through which communication between team members and the community was mediated. Once this was been established, project team members visited the household and with permission of the user, opened the pit and emptied the pit contents. This household was selected and sampled as the latrine had been previously emptied (samples were relatively fresher compared to a full pit), it did not contain any pit latrine additive and the sludge was more solid than other toilets surveyed and therefore easier to empty with a spade and store in containers. Non-desirable items, such as bricks, metal, plastic bags and hair, were found dispersed in the pit (Figure 3.14). Heavier items were removed at the sampling point and the sludge placed in plastic containers lined with plastic refuse bags (Figure 3.15a). Once full, the container was sealed with an airtight lid and disinfectant spray used to sterilise the outside of the containers and placed in the transport vehicle (Figure 3.15b). The surrounding area of the pits were also rinsed with soapy water and sprayed with a disinfectant.

Samples from Tongaat and KwaMashu were obtained from contractors at a nearby treatment works where VIP sludge from numerous households were being disposed of (Figure 3.16 and Figure 3.17). In certain instances, the non-faecal solid waste material was disposed of on-site.



a) Marianhill site



b) Tongaat site

Figure 3.13: A view of the housing settlements where VIP waste is collected. a) Marianhill, b) a township in Tongaat. Both areas are serviced with VIP toilets (PRG, 2007).



Figure 3.14: Contents of a VIP toilet in the Marianhill area. The pit consists of a semi-solid mixture of faeces and urine. Other non-desirable materials, such as glass, plastic and even tablets are found in the waste. Larger items, such as bricks and bottles, are removed from the toilet before sampling (PRG, 2007).



Figure 3.15: Sampling of a household VIP pit from Marianhill. a) Plastic buckets (100 L) with sealable lids are used to collect VIP sludge, b) the pit is sealed once sampling is complete by placing the concrete slab over the pit (PRG, 2007).



Figure 3.16: Pit emptying in Magwaveni, Tongaat (approximately 35 km from Durban). VIP sludge is manually removed from pit latrines and transported to a vehicle via refuse bins (PRG, 2007).



Figure 3.17: The bins are transported to a nearby wastewater treatment facility where the waste is screened and pumped into the head of works. It is at this point where samples for feeding the ABR were taken (PRG, 2007).

3.4.2 GREYWATER

Greywater was obtained from PRG test site at the Old Mutual Building at the University of KwaZulu-Natal, approximately 2 km from the research laboratory. Approximately 200 L of greywater was delivered daily to the test site by the eThekweni Municipality as part of another WRC Project (Jackson *et al.*, 2006). The greywater was collected from a nearby informal settlement, in the Cato Manor area. The greywater, which was collected in plastic drums (25 L) from various informal households, was poured into four water storage tanks (200 L each) at the test site (Figure 3.18a). A metal wire mesh acted as a screen on the top of the storage tanks preventing unwanted material from entering the containers (Figure 3.18b).

Every two days, greywater was collected from these tanks via a tap or bucket and poured into 25 L plastic drums. The outside of the drums were rinsed with tap water, sprayed with disinfectant and transported to the laboratory where they were stored in the cold room at 4°C. The greywater had a high organic strength (~ 1 000 mg COD/L), probably due to the lack of availability of water in those areas.



a) Greywater tanks



b) Screen on tanks

Figure 3.18: a) Greywater storage containers at the Old Mutual test site. The eThekweni Municipality delivered approximately 200 L of greywater to the site and poured it into the storage containers, b) Wire mesh on the storage container which prevents undesirable material from entering the containers (PRG, 2006).

During May to June 2007, greywater supply became erratic due to a number of factors, including less water consumed during winter months, repair of greywater storage tanks, and the temporary cancellation of greywater delivery due to the completion of that WRC greywater project. For this reason, the project team decided to eliminate the greywater component from the feed wastewater from the remaining period of the study. No steps were taken to replace the greywater component as the project team shifted focus to the treatment of a synthetic blackwater instead of domestic wastewater. The feed, without the greywater, would probably have less soluble and biodegradable COD in it.

3.5 FEED PREPARATION

Two types of synthetic wastewaters were used to feed the laboratory ABR; domestic wastewater made from diluted VIP sludge and greywater (section 3.5.1) and blackwater made from diluted VIP sludge only (section 3.5.2). The preparation of the feed wastewaters to the laboratory ABR is presented in this section.

3.5.1 SYNTHETIC DOMESTIC WASTEWATER

During the initial stages of the project (in 2006), a high-to-medium strength synthetic representation of domestic wastewater (1 000 mg COD/L) was made from the combination of greywater and VIP sludge (60: 40 ratio) and was used to feed the ABR (100 L/d). The

greywater was diluted with tap water (according to the COD concentration) and poured into the round feed tank of the ABR. The blackwater, represented by the VIP sludge, was screened to remove undesirable materials, such as plastic and broken glass. The sludge was mixed using a shovel and large bucket, and large unwanted objects were removed using gloves (Figure 3.19).



Figure 3.19: Sludge from VIP toilets that had been mixed with a shovel (large bucket). In the smaller bucket, undesirable material such as glass and plastic have been removed from the waste and placed in an autoclave bag for sterilisation. The pre-mixed VIP waste is further homogenised in a mechanical blender.

A small proportion of this mixture was further homogenised in a mechanical blender at low speed and smaller material, such as stones and small glass pieces, were removed using a sieve. This pre-screened, homogenised VIP sludge was then made up with tap water to a feed concentration of 1 000 mg COD/L in graduated plastic drums (25 L each) and poured into the ABR feed tank. Results from this stage of ABR operation have not been included in this thesis due to insufficient operation (plug feeding could only be performed as there was an erratic supply of greywater). However, specific bench-scale membrane investigations conducted on the effluent have been included in **Chapter 4**.

3.5.2 SYNTHETIC BLACKWATER

From June 2007, greywater supply became erratic. Due to the time constraints within the project, the project team undertook the decision to shift the focus of the study from the treatment of synthetic domestic wastewater to a synthetic blackwater. Further motivation for the shift in research direction was the problem of pit emptying and disposal of VIP contents. Faecal matter accumulates in the pits to a level where emptying is necessary. This presents several problems for municipalities. First, the removal of pit contents can be difficult, especially in

areas which are inaccessible to desludging equipment. Second, the disposal of pit contents has become a dilemma for many municipalities with many treatment works are not able to reach their discharge limits due to the increase in the organic load. Anaerobic pre-treatment in an ABR was seen as possible option for the treatment of VIP contents as the pit contents are concentrated due to the lack of availability of water.

During the early stages of the study (2007 to 2008), the feed concentration was determined by measuring the COD value of a pre-determined weight of homogenised VIP sludge (feed prepared according to section 3.5.1). A certain amount of VIP sludge was diluted in distilled water and a COD analysis performed. This COD value was then used to determine the mass of VIP sludge required for feeding the reactor a desired COD range. The sludge was diluted in tap water and placed in 25 L plastic drums and fed through the lid on the round feed tank of the ABR using a bucket.

The problem with this feed technique was that the sludge was a heterogeneous mixture of faecal, urine and other matter which resulted in a highly variable feed wastewater COD values. To solve this problem, the project team undertook the decision to change the manner in which the feed wastewater was prepared to a desired COD value. A well-mixed portion of VIP sludge (as prepared in section 3.5.1) was diluted in tap water to form a concentrated solution. The COD of this concentrate was then determined, diluted to a desired concentration in 25 L plastic drums and fed to reactor using a bucket. In 2008, a graduated PVC feed dispenser with a capacity of 95 L was constructed to ease the laborious feeding procedure. The concentrate (or diluted homogenised sludge) was placed in the graduated feed dispenser and made up to a desired COD value using tap water. A decant valve at the bottom of the dispenser connected to a hose pipe was used to dispense the feed wastewater into the round feed tank.

3.6 COMPARISON OF LABORATORY FEED WITH ACTUAL WASTEWATERS

Table 3.2 presents a comparison of data from the characterisation of actual sanitary wastewaters and of the VIP sludge used in this study. Three blackwater and two domestic wastewater data sources have been used to compare with the laboratory feed made from VIP sludge. The high variation in the laboratory feed concentration is due to the laboratory ABR plant being operated under a variety of organic loadings (VIP sludge diluted to various strengths) and is not due to the natural variation of physico-chemical parameters of the VIP sludge.

Although the laboratory feed used had a similar range of physico-chemical characteristics as the other wastewater sources, the biodegradability of the laboratory feed was less than other sources. Approximately 30% of the laboratory feed is biodegradable compared to the 50 to 70% reported in some blackwater sources (Elmitwalli *et al.*, 2001 de Graaf *et al.*, 2010). The implication of this result is that the laboratory ABR had been operated in conditions not suited to anaerobic digestion (high particulate content with low biodegradability). Under these conditions, the initiation or production of foulant species may occur (Rittmann and McCarty, 2001; Chrysi and Bruce, 2001; Aquino and Stuckey, 2003).

Table 3.2: Comparison of physico-chemical properties of sanitation wastewater in relation to the feed used in this study.

Parameter	Blackwater			Domestic wastewater		Lab feed
	1	2	3	4	5	
P _{tot}	21-58	25	11	4-12	4-15	
N _{tot}	130-180	180 ^a	41 ^a	20-70	20-85	
BOD	410-1 400	338	458	160-300 ^b	110-400	
COD	806 – 1 400	1 225	1 013	250-800	250-1 000	150-3 000
TS	920-4 320	437	715 ^c	390-1 230	350 -1 200	234-1 319
VS	420-3 660	529	401 ^d	95-315	105-325	25-1 017
pH	8.87-9.08	8.0	8.02			6.11-8.93

1, Palmquist and Hanæus (2005); 2, Metcalf and Eddy (2003); 3, Hocaoglu *et al.* (2010); 4, Al-Juiady *et al.* (2003); 5, Metcalf and Eddy (1991)

^a, TKN

^b, BOD₅

^c, TSS

^d, VSS

3.7 MATERIALS AND METHODS

This section describes the methods used to measure the performance characteristics of the laboratory ABR and the membrane units.

The laboratory ABR was operated over a period of 3 years (30 June 2007 to 4 October 2009) in which seven different operating periods were tested (details presented in **Appendix II**). Different project team members were responsible for feeding, sampling, measuring, analysing and collating data and hence, the methods used to measure certain performance characteristics were not consistent throughout the study. Table 3.3 presents a summary of responsibilities for feeding, sampling, analysing and interpreting data for each analysis and operating period. Table 3.4 lists people responsible for analysing different wastewater components. A detailed description of the physico-chemical methods used during each phase is presented in **Appendix IV** whilst the results from those campaigns are presented in **Appendix II**.

3.7.1 SAMPLING

Samples of the feed wastewater, feed tank overflow and outlet streams of the ABR were obtained and analysed to determine the extent of anaerobic digestion treatment through the system. Samples were collected in 500 mL glass Schott® bottles and analysed immediately or stored in the cold room at 4°C for further analyses.

Table 3.3: Table of responsibilities of feeding, sampling, analyses and data collation for the laboratory ABR treating diluted VIP sludge.

	Phase I	Phase II	Phase III	Phase IV	Phase V	Phase VI	Phase VII
Feeding	SP	SP	JK	JK	JK	JK	SP, POL
Sampling	SP	SP	JK	JK	JK	JK	SP, POL
Analyses	SP	SP	JK	JK, SP	JK, SP	JK, SP	SP, POL
Date capture	SP	SP	JK	JK	JK	JK	SP
Data analysis	SP	SP	JK	JK	JK	JK	SP

Key: JK, Joseph Kapuku; POL, Samuel Pollet; SP, Sudhir Pillay

Table 3.4: Table of responsibilities for different analytical method used during this study.

Parameter	Phase I	Phase II	Phase III	Phase IV	Phase V	Phase VI	Phase VII
COD _{total}	SP	SP	JK	JK	JK	JK	SP, POL
COD _(0.45µm)	SP	Nd	Nd	nd	nd	nd	nd
pH	SP	SP	JK	JK	JK	JK	SP
Temperature	nd	SP	JK	JK	JK	JK	nd
TS	SP	SP	JK	SP	SP	SP	SP
VS	SP	SP	JK	SP	SP	SP	SP
Proteins _(soluble)	nd	Nd	Nd	SP	SP	SP	SP, POL
Carbohydrates _(soluble)	nd	Nd	Nd	SP	SP	SP	SP, POL

Key: nd, not determined; JK, Joseph Kapuku; POL, Samuel Pollet; SP, Sudhir Pillay

3.7.2 FEED WASTEWATER

Grab samples were taken from the middle of the feed tank (Figure 3.20) or in some cases, from the feed dispenser (if the feed tank was nearly empty). The samples were withdrawn after the feed tank was loaded with a freshly made up feed wastewater.



Figure 3.20: Photograph of feed wastewater sample taken from the middle of the feed tank (PRG, 2008).

3.7.3 FEED TANK OVERFLOW

Grab samples were taken from splitter box to the laboratory ABR train (defined in this thesis as the *overflow* of the feed tank) to provide an indication on how wastewater components or measurements change from feed loading to the beginning of the ABR treatment train. The samples were withdrawn immediately after the feed loading and the starting of the peristaltic pump.

3.7.4 ABR EFFLUENT SAMPLES

The term *ABR effluent* used in this thesis refers to the composite samples taken from the effluent container from which the flow after the last compartment box of the ABR train collects (Figure 3.21). This fluid was used as the membrane feed in all subsequent membrane experiments.

3.7.5 MEMBRANE PERMEATE

In this thesis, the fluid that passed through the membrane was referred to as the *membrane permeate*. The flow rate through the membrane was calculated using a weighing balance-timer or a bucket-and-stopwatch approach whilst the permeate flux was calculated according to equation 2.2 (section 2.2.4). More details regarding data interpretation can be viewed in section A 3.4 in **Appendix III**.



Figure 3.21: Photograph of the laboratory ABR effluent from the collection container after the outlet pipe of the last ABR compartment (PRG, 2008).

3.8 OPERATIONAL AND MAINTENANCE ISSUES

This section provides details of the operation and maintenance of the ABR and the membrane filtration system. As two separate technologies were used, the maintenance and operational issues differed accordingly.

3.8.1 ABR

This section provides details related to health and safety issues regarding the use of the ABR and the maintenance of the ABR.

3.8.1.1 Personnel Safety

The ABR was operated in the lower level of the Biochemical Engineering laboratory of the School of Chemical Engineering. The work area was demarcated as a biological hazardous area. Health and safety preventative measures against biological and chemical hazards were introduced for each member of the laboratory. Inoculation against Hepatitis A and B strains, Tetanus and Typhoid was administered before sampling and experimentation. Bimonthly chemotherapy against helminth species was also administered.

3.8.1.2 Hazardous Operation

The ABR generated a large volume of wastewater that needed to be handled with care, contained and disposed of safely. Plastic containers (120 L) were placed under each reactor box

as preventative measure against spillages due to clogging or other mechanical problems. The effluent was contained in a large plastic container and later a stainless steel box. The effluent was decanted in a drainage system connected to a sewer line. Excess sludge was containerised and disposed of in a local wastewater treatment facility. Any spillages during feeding or effluent decanting were cleaned with Jik® (sodium hypochloride solution) and anti-bacterial soap. Work benches were disinfected daily with 10% ethanol or prior to use. The floors of the laboratory were cleaned bimonthly with detergent and a high-pressure hose pipe.

3.8.1.3 Maintenance

General maintenance of the ABR was required due to continuous operation. The Marprene® tubing for the peristaltic pump was changed after every couple of months due to wear. Once the tubing was changed, the pump was recalibrated for the required flows by calculating the flow rate at each motor speed using a bucket and stop watch.

Occasionally, when sludge built up in the system (compartment boxes and feeding container) the pipes connecting the system became clogged. The reactor was stopped and a piece of wire or flexible tubing placed in the pipes to remove clogged material. If this procedure did not successfully remove clogged material, the mixed liquor and sludge from compartment boxes was decanted into plastic storage containers and the pipes of boxes rinsed with a hose. Once the pipes were cleared, the compartments boxes were refilled to a third of their working volume using the sludge stored in the container. For the feed tank, desludging occurred through a valve at the bottom of the round tank. The sludge was decanted until 25 L of sludge was left (the volume of the cone at the bottom of the feed tank).

Excess sludge that had built-up to a level where desludging was necessary had to be disposed of. These events were logged and mentioned briefly in **Appendix II**. The excess sludge was bottled and kept in the cold room at 4°C until it could be transported to the treatment facility for disposal.

3.8.2 MEMBRANE UNITS

This section provides details related to health and safety issues regarding the use of the membrane units and the maintenance of the membranes.

3.8.2.1 Hazardous Operation

The feed lines on the module were easily secured to the feed funnel by connecting silicon tubing to PVC outlets. Two overflow drains were made on the feed funnel to maintain a constant level of water height and to prevent the overflow of effluent. The permeate was collected in plastic

drums (25 L) or in a beaker and disposed in the drain connected to sewer line. The work area, including the outside of the module and weighing balance, were cleaned with 10% ethanol before and after experiments.

3.8.2.2 Maintenance

After filtration experiments, the fouled modules were washed with tap water and soaked in a solution of distilled water. Polymem modules were stored between experiments in a preservative solution (10g/L of sodium bisulfate) to prevent the fibres from drying out. Flat-sheet modules required additional physical cleaning using gloved hands before they were stored in distilled water.

3.8.3 POWER OUTAGES

During the latter part of 2007 up until May 2008, South Africa experienced ‘rolling blackouts’ as electricity demand exceeded supply in the country. During certain parts of day and the week, an area would experience no electricity as part of the rotating strategy to supply electricity countrywide. These blackouts were extremely disruptive to the operation of the ABR system as the system had to be restarted after each blackout.

3.8.4 RELOCATION OF FACULTIES

In 2004, the University of KwaZulu-Natal was formed by the merger of the University of Natal and University of Durban-Westville. Science and engineering faculties were split to different areas within Durban, with the School of Chemical Engineering remaining at the Howard College Campus in Glenwood and the School of Chemistry relocated to Westville campus as part of the merger process. Equipment that was used at the School of Chemistry and the School of Biological and Conservation Science (high-speed centrifuge and spectrophotometer) was packed and relocated to the new building. As a consequence, there was a certain period where fractionation of solutions and EPS measurements could not be performed. In late 2008, the Pollution Research Group purchased a new centrifuge and spectrophotometer to perform these analyses.

3.8.5 CONSTRUCTION DISTURBANCES

The extension to the School of Chemical Engineering building from 2007 to 2009 was also disruptive as the new wing was built next to the laboratory. In certain instances, the laboratory plant had to be shut down as construction workers passed through the biohazardous zone demarcated in the laboratory. Furthermore, water and electricity cut-offs, and theft of equipment were also a common occurrence during this period.

3.9 TERMINOLOGY

Table 3.5 presents a description of standard terminology and the context in which it is used in this thesis whilst Table 3.6 presents the chapters in which the terminology has been used.

Table 3.5: Standard terminology and the context in which it is used in this thesis (Chapters 4 to 7).

Term	Description
ABR	
Pilot ABR	An 8-compartment ABR used in WRC Project K5/1248 (Foxon <i>et al.</i> , 2006).
Laboratory ABR	A 4-compartment ABR used in this thesis.
Sampling point	
Feed wastewater	The feed solution made up and emptied into the feed tank of the laboratory ABR.
Feed tank overflow	The upper portion of the feed tank wastewater that is pumped into the laboratory ABR.
ABR effluent	The composite sample from the overflow of compartment 4 of the laboratory ABR.
Membrane filtration time	
Short-term experiment	Membrane filtration experiment duration of between 1 and 24 h.
Mid-term experiment	Membrane filtration experiment duration of between 1 and 10 d.
Long-term experiment	Membrane filtration experiment duration of more than 10 d.
Membrane feeds	
Biological supernatant	Mixed liquor sludge sample which has been centrifuged at 10 000 g to remove colloids and suspended particles*.
Laboratory ABR effluent	The composite sample from the overflow of compartment 4 of the laboratory ABR.
Compartment 2 supernatant	The soluble component of mixed liquor from compartment 2 of the pilot ABR that was isolated by ultracentrifugation.
Compartment 3 supernatant	The soluble component of mixed liquor from compartment 2 of the pilot ABR that was isolated by ultracentrifugation.
Compartment 4 supernatant	The soluble component of mixed liquor from compartment 2 of the pilot ABR that was isolated by ultracentrifugation.
Anaerobic sludge supernatant	The soluble component of mixed liquor from a conventional anaerobic digester that was isolated by ultracentrifugation.
Activated sludge supernatant	The soluble component of mixed liquor from an aeration tank that was isolated by ultracentrifugation.
Settled effluent	Laboratory ABR effluent which has been allowed to settle for 48 h.
Supernatant of settled ABR effluent	The upper liquid portion of laboratory ABR effluent that has been allowed to settle for 48 h.
Soluble ABR effluent	Microfiltered laboratory ABR effluent
Operation	
Ultra-low pressure	Pressure operation below 10 kPa (1 000 mm water head)

*, Cabassud *et al.*, 2006.

Table 3.6: Location of standard terminology (Table 3.6) used in this thesis and the location of this terminology in thesis.

Term	Location
Sampling point	
Feed wastewater	Chapters 3, 4, 5, 6, 7 and Appendix II
Feed tank overflow	Chapters 3, 7 and Appendix II
ABR effluent	Chapters 3, 7 and Appendix II
Membrane filtration time	
Short-term experiment	Chapters 5, 6 and 7
Mid-term experiment	Chapters 5, 6 and 7
Long-term experiment	Chapters 5, 6 and 7
Membrane feeds	
Biological supernatant	Chapter 4
ABR effluent	Chapters 3, 4, 5, 6, 7 and Appendix II
Compartment 2 supernatant	Chapter 5
Compartment 3 supernatant	Chapter 4
Compartment 4 supernatant	Chapter 4
Anaerobic sludge supernatant	Chapter 4
Activated sludge supernatant	Chapter 4
Settled effluent	Chapters 5, 6 and 7
Supernatant of settled effluent	Chapters 5, 6 and 7
Soluble ABR effluent	Chapters 5, 6 and 7
Operation	
Ultra-low pressure	Chapters 5, 6 and 7

CHAPTER 4 : BENCH-SCALE EXPERIMENTS

Foulants can be fractionated into three size-specific groups, namely, suspended solids, colloidal and soluble macromolecules for investigative purposes (refer to section 2.2.7). To investigate the role of the soluble component of the biomass in fouling propensity, a test cell technique was developed and standardised among *EUROMBRA* partners. The purpose of the technique was to have a common qualitative tool for assessing and comparing the role of solutes on membrane fouling across a range of operating parameters and conditions. Key to interlinking research among partner groups was to have identical definitions for describing the filtration process, and common analytical techniques and instruments to characterise fouling behaviour and potential soluble fouling constituents.

An Amicon® dead-end filtration cell was operated in the Biochemical Engineering laboratory in the School of Chemical Engineering, University of KwaZulu-Natal (UKZN). The set-up and operation of the test cell formed part of a collaboration between UKZN and the Institut National des Sciences Appliquées of Toulouse (INSA), France. Analytical techniques were developed and provided by *EUROMBRA* (Cabassud *et al.*, 2006). The technique involved the fractionation of the soluble component of a sample of sludge mixed liquor through ultracentrifugation at 10 000 *g* at room temperature. This *biological supernatant*, which is free from suspended and colloidal fractions, is used to characterise the fouling propensity of the *soluble component of a sludge source only* (Cabassud *et al.*, 2006). In this way, a fouling signature is generated for a particular biomass under a specific operating condition. As the technique is standardised amongst partners, the fouling behaviour of a number of biomass sources (with different ages, treated wastewater) can be compared and linked to physico-chemical data to elucidate the possible foulant in the soluble phase. There are distinct advantages of using test cells in evaluating fouling propensity of different fluids. These include: short duration and replication of experiments, a small proportion of test solution utilised and the requirement for membrane area is small (Jimenez *et al.*, 2004).

The results from only UKZN are presented in this section. For a comparison of results from various partner groups, refer to the final *EUROMBRA* report (2010a) or alternately papers from partner groups (Teychene *et al.*, 2008 and 2011). This part of the study was conducted only during one of the aforementioned phases of ABR operation (Phase I, **Appendix II**). Other samples were taken from the pilot ABR which formed the basis of WRC Project K5/1248 (Foxon *et al.*, 2006) and the laboratory ABR treating a synthetic domestic wastewater composed of VIP sludge and greywater (refer to **Chapter 3**). The research presented in this chapter aims to: (i) evaluate fouling in test cells using the soluble liquid phase of different membrane feed

solutions, (ii) elucidate the fouling propensity of the soluble component of ABR fluid (including ABR compartments) in relation to other sources (to evaluate membrane suitability), (iii) determine the reproducibility of fouling tests and (iv) whether data are able to satisfy cake filtration theory (see section 4.1). Additionally, for the test cell technique to be commercially viable, the membrane must be reusable and should offer good reproducibility between samples. Parts of this section have been published in the scientific journal *Desalination* (Pillay *et al.*, 2008).

4.1 THEORETICAL BACKGROUND

The technique recommended by *EUROMBRA* partners is dependent on the cake filtration model to describe membrane fouling. One of the model's assumptions is that the macromolecules rejected form a cake on the membrane surface during filtration (Lodge *et al.*, 2004). This cake is then assumed to be the only mechanism that increases the resistance during the filtration test (Khirani *et al.*, 2006). In dead-end filtration, the empirical equation that describes the process is a simplified model of mass transfer across the membrane that is derived from Darcy's Law, that is:

$$J_p = \frac{\Delta P}{\mu \times (R_m + R_c)} \quad \text{Equation 4.1}$$

where J is the flux, ΔP is the TMP (which includes the pressure drop across the cake), μ is the viscosity and R_m (membrane resistance) and R_c (cake layer resistance) are the resistance in series.

The cake resistance (R_c) is described as the specific cake resistance (α), the total volume filtered (V) and the quantity of accumulated matter per unit volume of filtrate (C_s) (Abogrean *et al.*, 2003). R_c increases proportionally to the volume filtered (V) through the membrane and the dry cake mass:

$$R_c = \alpha m_c = \alpha C_s \frac{V}{A} \quad \text{Equation 4.2}$$

The specific cake resistance (α) describes the way the cake is built (Cabassud *et al.*, 2006). However, its value is difficult to determine as α is not the only unknown parameter (Cabassud *et al.*, 2006). C_s , the quantity of accumulated matter on the membrane per unit volume, is also unknown and difficult to obtain experimentally. As such, values of the product αC_s are often used to provide information on the cake structure or the quantity of deposited

material on the membrane surface and allows for the comparison of filter cake properties between different filtration experiments (Cabassud *et al.*, 2006).

The product of $\alpha.C_s$ is commonly used as part of the *modified fouling index* (MFI) in which microfiltration membranes are used to assess the fouling propensity of a feed solution (Schippers and Verdouw, 1980; Boerlage *et al.*, 2002; Khirani *et al.*, 2006; Sim *et al.*, 2011). When ultrafiltration membranes are used (to incorporate particles less than 0.45 μm that may have an effect on cake filtration), the index is referred as MFI-UF (Boerlage *et al.*, 2002; Abogrean *et al.*, 2003). The MFI value is determined from linear portion of the slope of t/V versus V from the general cake filtration model:

$$\frac{t}{V/A} = \frac{\mu R_m}{\Delta P} + \frac{\mu \alpha C_s}{2\Delta P} \frac{V}{A} \quad \text{Equation 4.3}$$

$$\text{with } MFI = \frac{\mu \alpha C_s}{2\Delta P}$$

The I index (which is also called the resistivity – Boerlage *et al.*, 1998) in the MFI is the product of the specific cake resistance (α) and the quantity of accumulated matter on the membrane per unit volume (C_s). According to Abogrean *et al.* (2003), the I index is assumed to be independent of pressure and is correlated with the concentration of matter in the feed wastewater.

$$I = \alpha.C_s \quad \text{Equation 4.4}$$

There are several assumptions with regards the MFI and the model from which the index is derived. The first is that the macromolecules that are rejected by the membrane form a cake and that is the only mechanism that induces a higher resistance during a filtration run. The other is that the cake is incompressible, that is, α has a time independent permeability and uniform cake porosity throughout the depth of the cake (Boerlage *et al.*, 2003). In practice, however, very few cases of incompressible cakes are observed (Brauns *et al.*, 2002; Abogrean *et al.*, 2003; Boerlage *et al.*, 2003). As such, filtration time (t/V) versus cumulative volume (V) curves that are constructed from experimental data are often not linear. The curve commonly has three regions. an initial upward convex slope which corresponds to pore blocking, a linear portion corresponding to cake filtration and a third portion corresponding to cake filtration with clogging and/or cake compression (Abogrean *et al.*, 2003; Boerlage *et al.*, 2003). (refer to Figure 4.1). Cake compression is due to presence of highly compressible material in the cake such as clays or microbial cells (Kawakastu *et al.*, 1993; Chellam and Jacanangelo, 1998). These substances reduce the porosity of the cake when pressure is applied above a certain point

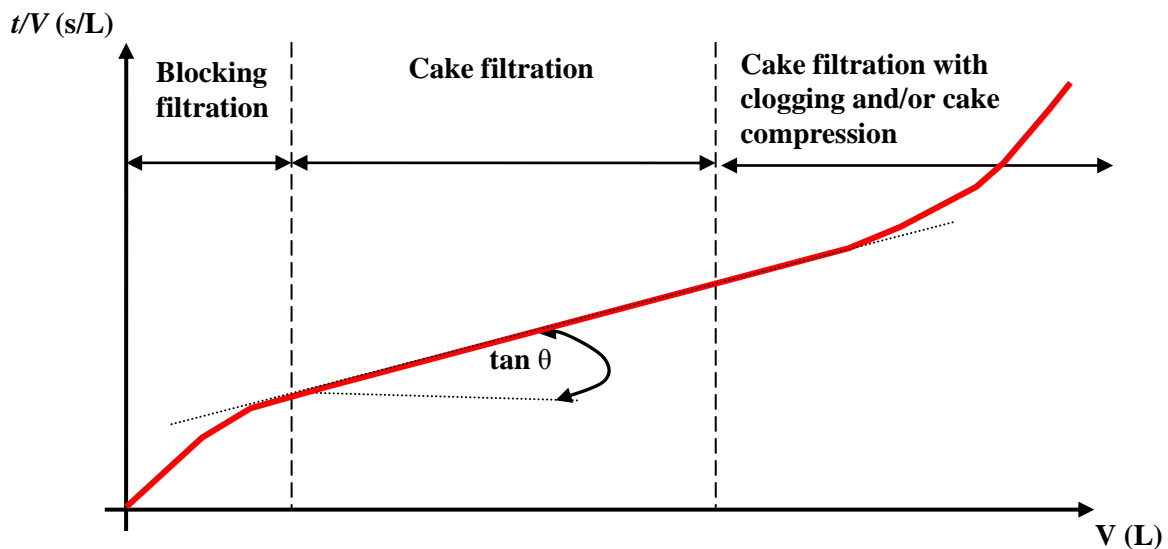


Figure 4.1: A typical non-linear t/V versus V curve showing three regions which correspond to pore blocking, cake filtration and cake filtration with clogging and/or cake compression (Boerlage *et al.*, 2003). It is common practice to determine the MFI from the gradient of the linear portion of the curve.

creating a non-uniform porosity distribution in the direction of flow which can result in erroneously higher MFI values (Boerlage *et al.*, 2003).

To negate the effect of compressibility of cake material on the MFI value, some researchers include an estimation of compressibility which assumes that the specific cake resistance increases as a power law function with pressure (Boerlage *et al.*, 2003; Lodge *et al.*, 2004). When the specific cake resistance data are logged and differentiated with $\log \Delta P$, a value for compressibility (s in equation 4.5) can be calculated (Lodge *et al.*, 2004).

$$\frac{d(\log \alpha)}{d(\log \Delta P)} = s \quad \text{Equation 4.5}$$

Other researchers, such as Brauns *et al.* (2002), suggested an alternative method to analysing data from a batch test as means to evaluate the fouling potential of different fluids. The method was established due to the non-linearity of t/V versus V plots used to obtain MFI values. The experimental procedure is similar to that required to obtain MFI values and involves a multi-value representation of the fouling potential which can be then be used to complement MFI values.

For this chapter, a compressibility coefficient has not been included into the analysis nor has other means to evaluate the fouling potential of different fluids. The stirred cell technique recommended by *EUROMBRA* partners was applied as recommended with limitations of the technique taken into account. Although, in a strict way, the non-linearity of t/V versus V plots can be viewed as inappropriate, no universal model is available to describe and predict the layer build up (Brauns *et al.*, 2002). This is due to the complexity of layer phenomenon which involves particles of different composition, size distribution, surface charge (Brauns *et al.*, 2002). Additionally, other factors such as membrane pore size and layer compressibility as a result of increased pressure difference across the layer have also been shown to influence MFI values (Brauns *et al.*, 2002; Lodge *et al.*, 2004).

4.2 SAMPLING AND HANDLING

Samples tested were from (1) a pilot ABR treating domestic wastewater, (2) a secondary anaerobic digester, (3) aeration tank and the effluent from the laboratory ABR treating (4) diluted VIP sludge or (5) a mixture of diluted VIP sludge and greywater. Grab samples of mixed liquor were obtained from compartments 2, 3 and 4 of a pilot ABR (3 000 L) from WRC Project K5/1248 (Foxon *et al.*, 2006). Samples were taken from the pilot ABR in August 2006 with reactor being offline since 2005. This sludge was therefore essentially inactive and may have contained significant amounts of dead biomass. The same sludge was used to seed the 5-compartment laboratory-scale ABR with an external membrane unit. Samples of the sludge column in the upflow region of each compartment were obtained using a specially designed sampling column, mixed in a bucket and sampled for analysis. Sludge samples were also obtained from a secondary anaerobic digester and from an aeration tank at Northern wastewater treatment plant for comparison. The facility treats a combination of industrial and domestic wastewater. Approximately 5 L of sludge was collected using a suitable collection bottle and labelled with biohazard signs [as recommended by occupational health and safety codes (Government Gazette, 2001)]. Effluent samples (compartment 4 overflow) were also taken from the laboratory-scale ABR treating a mixture of greywater and VIP sludge as well as diluted VIP sludge (from Phase I). All samples were stored in a cold room at 4°C prior to analysis.

4.3 METHODOLOGY

This section describes the experimental set-up used in test cell experiments (section 4.3.1), the preparation of membrane feed solutions (section 4.3.2), the operation of the test cell (section 4.3.3) and the analyses performed (section 4.3.4).

4.3.1 EXPERIMENTAL SET-UP

The test cell apparatus, known as a *fouling ability of flat sheet membrane* (FAFS) apparatus, was used to characterise the fouling propensity of the soluble fraction from each sludge source (Cabassud *et al.*, 2006) (Figure 4.2). The experimental set-up consisted of a pressure gauge, a pressurised vessel and an Amicon® dead-end filtration cell (model 8400, 400 mL). The apparatus was set-up according to instructions from *EUROMBRA* partners (Cabassud *et al.*, 2006) with a Masters student, Mr. V. Yvenat from INSA Toulouse assisting with experimental set-up and data capture. Ultrafiltration polyethersulphone membranes (AMICON PM10, 75 mm diameter discs) with an effective filtration area of 0.004 m² were used as the test membrane. The disc membranes have a *nominal weight mass limit* (NWML) of 10 kDa. Amicon® products were chosen as they were commercially available (and easily accessible) to all research partners.

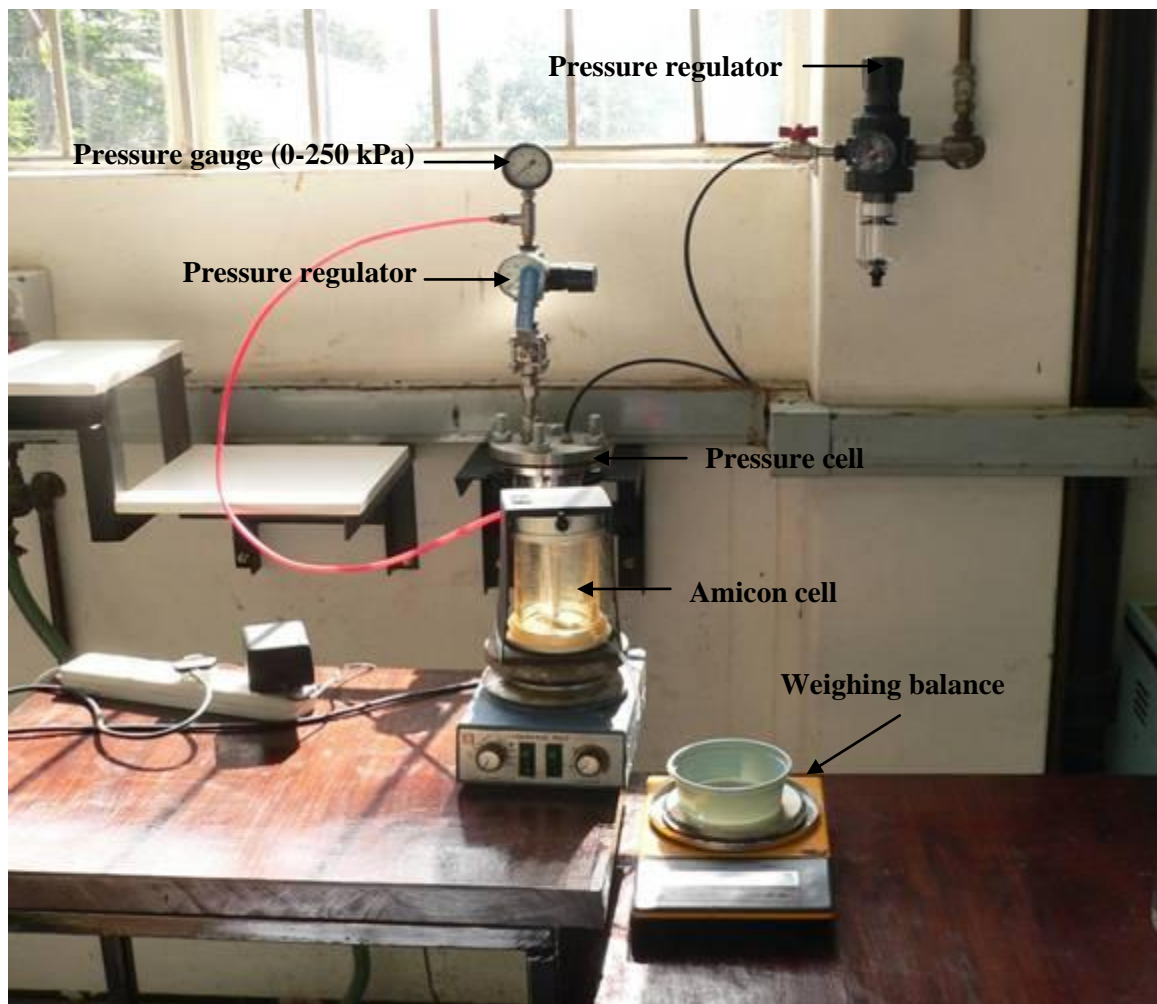


Figure 4.2: Picture of fouling ability of flat-sheet membrane apparatus (FAFS) recommended by *EUROMBRA* partners.

4.3.2 FRACTIONATION OF SOLUBLE PHASE

The sludge from each source was ultracentrifuged at 10 000 *g* for 15 min. This separated suspended solids and colloidal particles from the soluble phase. This technique was stipulated by *EUROMBRA* partners. The fluid obtained after ultracentrifugation was defined by partners as the *biological supernatant* (Cabassud *et al.*, 2006). It was this fluid that was used as the membrane feed in test cell filtration experiments.

4.3.3 OPERATION OF TEST CELL

The Amicon® cell containing the membrane was filled with the biological supernatant. The cell was closed and pressurised using an air compressor via a stainless steel pressure reservoir. The air pressure was controlled using two pressure regulators (0 to 1 000 kPa) and monitoring using a pressure gauge (0 to 250 kPa, Ashcroft). Membrane filtration was monitored in the dead-end mode.

The volume of permeate was measured continuously at fixed intervals by collecting the filtrate on a weighing balance. The temperature of the permeate was measured during each experiment to allow for temperature correction to 20°C (refer to section A3.4 in **Appendix III**).

The FAFS apparatus was operated under a range of constant TMP with each step lasting 10 min. This TMP-step method was employed for a range of pressures from 18 to 120 kPa with 50 kPa used as the reference pressure by which to evaluate the specific cake resistance. A detailed explanation of the protocol is presented in **Appendix III**.

A total of four Amicon® membranes were used for the study. Figure 4.3 illustrates the experiments performed on each membrane. Four sets of supernatant filtration experiments were performed in duplicate on the Amicon® membrane 1. The source of supernatant used in chronological order (from first experiment) were: compartment 2 ABR sludge, compartment 3 ABR sludge, compartment 4 ABR sludge and activated sludge. Clean water flux filtration experiments were performed before and after each filtration run. Additionally, chemical cleaning using 0.5 M NaOH was employed to restore membrane permeability after each run.

For Amicon® membrane 2, sludge was collected from a completely mixed anaerobic digester from a local treatment works. A single filtration run was performed with raw supernatant from the anaerobic sludge and three replicated runs with the supernatant from anaerobic sludge that was diluted with distilled water to a COD range similar to that of ABR effluent. Clean water flux filtration experiments were performed before and after each filtration run. Additionally,

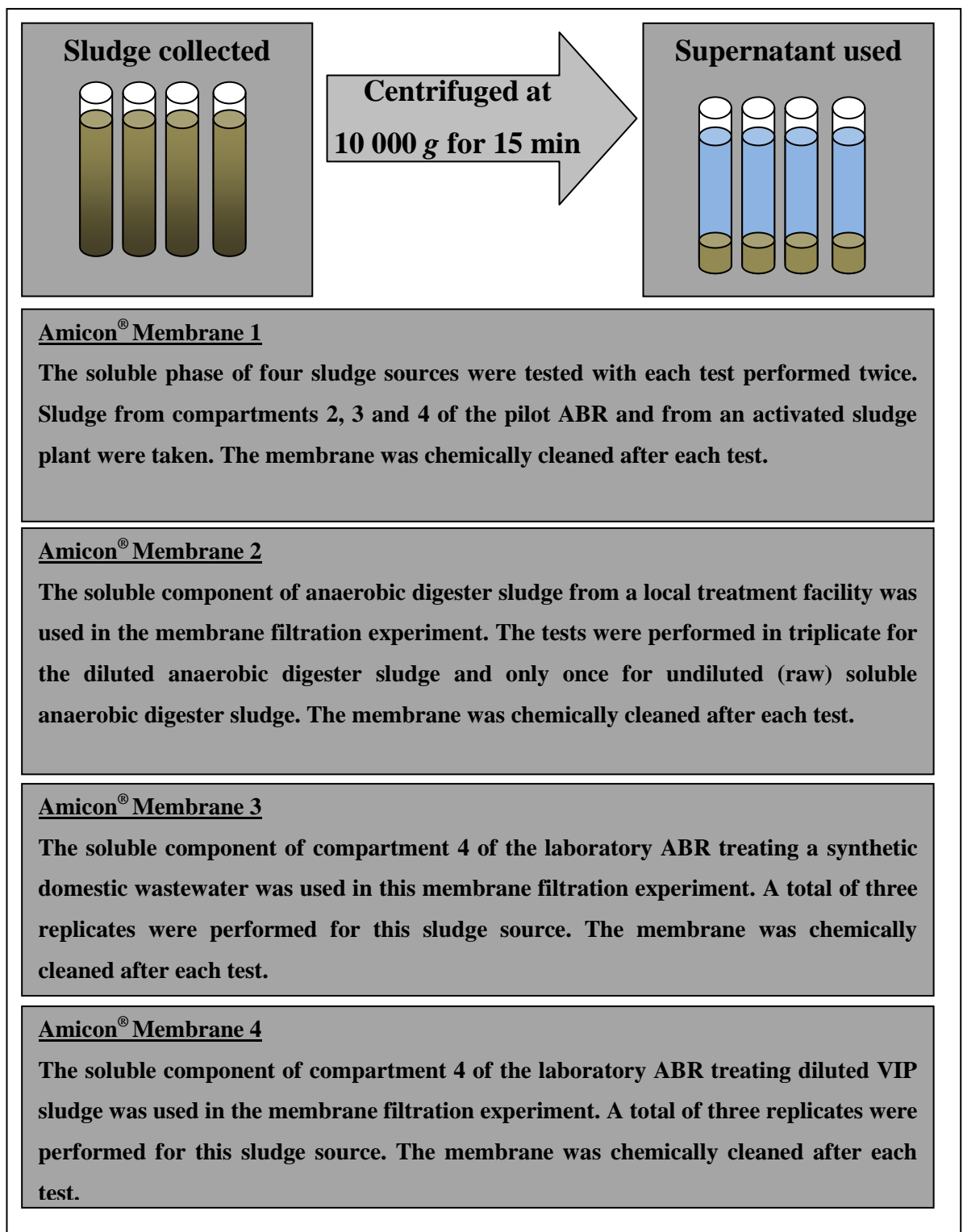


Figure 4.3: Breakdown of filtration experiments performed on Amicon® membranes using the soluble phase from different biomasses.

chemical cleaning using 0.5 M NaOH was employed to restore membrane permeability after each run.

For Amicon® membrane 3, effluent from the laboratory ABR treating a synthetic domestic wastewater (overflow of compartment 4 sludge) was ultracentrifuged and the supernatant used in three replicated filtration runs. For the fourth membrane, effluent from the laboratory ABR treating diluted VIP sludge (overflow of compartment 4 sludge) was ultracentrifuged and the supernatant used for three replicated filtration runs. For both membranes (three and four), clean water flux tests were performed before and after supernatant filtration with chemical employed thereafter to restore membrane permeability.

The resistance-in-series model (Darcy's law) was used to evaluate the fouling characteristics of each supernatant (refer to section 2.2.4 and **Appendix III**). The membrane resistance was determined by filtering distilled water at the beginning of the experiment and at the end. In this way, the resistance due to fouling was determined (refer to **Appendix III**). A combination of chemical (0.5M NaOH for 1 h) and physical cleaning (rinsing with distilled water) was used to remove the fouling layer after each run. All flux values were corrected to 20°C to account for changes in viscosity (equation 4.5). The units of measurement of flux and pressure used in this chapter are L.m⁻².h⁻¹ and kPa, respectively. Permeability has been presented in two units in this section; L.m⁻².h⁻¹.kPa⁻¹ and L.m⁻².h⁻¹.bar⁻¹ (only in text) to assist reader with no membrane expertise (refer to section 2.2.4). A detailed protocol of the technique is presented in **Appendix III**.

$$\mu_{(T_{exp})} = 1.002 \times \exp \left[3.056 \times \frac{(20 - T)}{(T + 105)} \right] \quad \text{Equation 4.5}$$

where:

T : temperature (°C)

μ : permeate viscosity

4.3.4 ANALYSES PERFORMED

The COD analyses were performed according to University of Cape Town (UCT) Open Reflux COD Method for wastewater (Lakay *et al.*, 2000). TSS and VSS analyses were performed according to Standard Methods (APHA-AWWA-WEF, 1998). Bound, soluble and loose extracellular polymers (EPS) were fractionated according to recommendations by Cabassud *et al.* (2006). Proteins and carbohydrates were quantified according to the

Frølund *et al.* (1996) and Dubois *et al.* (1956) methods, respectively. Reagent grade chemicals were used. **Appendix IV** presents a detailed description of the analytical methods used.

4.4 RESULTS AND DISCUSSION

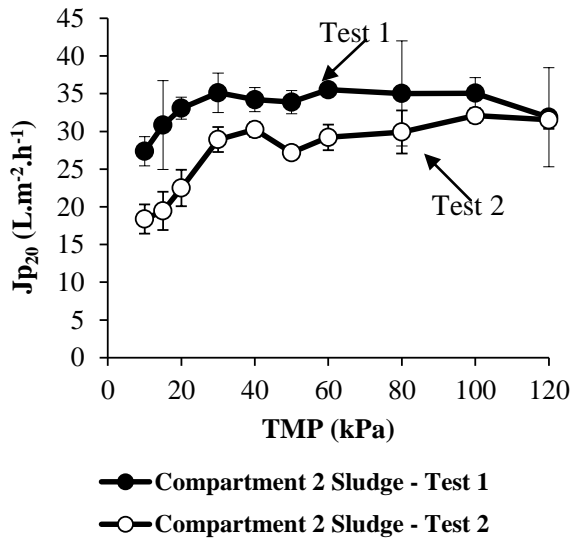
This section is divided into two sub-headings. The first subheading (section 4.4.1) presents the permeate flux data of different soluble membrane feed solutions. The second subheading (section 4.4.2) presents the values for the product of $\alpha.C_s$ for different membrane feed solutions

4.4.1 PERMEATE FLUX

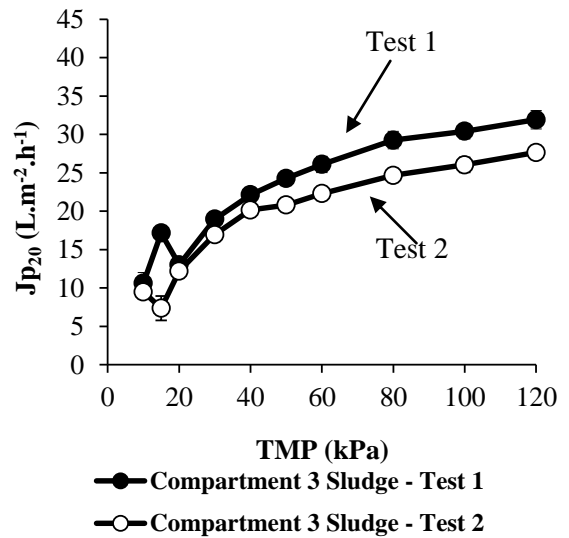
Figure 4.4 shows the permeate flux versus TMP for the soluble component of different sludge sources. Flux values were adjusted to 20°C to account for the effect of temperature on viscosity (equation 4.5). On the first membrane, the permeate flux of the soluble component of sludge from compartment 2, compartment 3, compartment 4 of the pilot ABR and finally the soluble component of activated sludge was determined. Each run was replicated twice for a range of pressures from 18 to 120 kPa with clean water flux tests performed before and after run and chemical cleaning before the start of a new filtration run.

The flux of the supernatant samples from compartment 2 of the pilot ABR is shown in Figure 4.4a. The flux increased to 30 kPa after which flux remained relatively constant ($\sim 30 \text{ L.m}^{-2}.\text{h}^{-1}$). For the supernatant samples of compartment 3, the slope of the permeate flux increased with decreasing slope at higher TMPs (Figure 4.4b). A similar pattern can be observed with respect to the filtration of supernatant from compartment 4 of the pilot ABR (Figure 4.4c) and activated sludge (Figure 4.4d). For each replicated run, permeate flux did not vary much indicating good reproducibility of flux results.

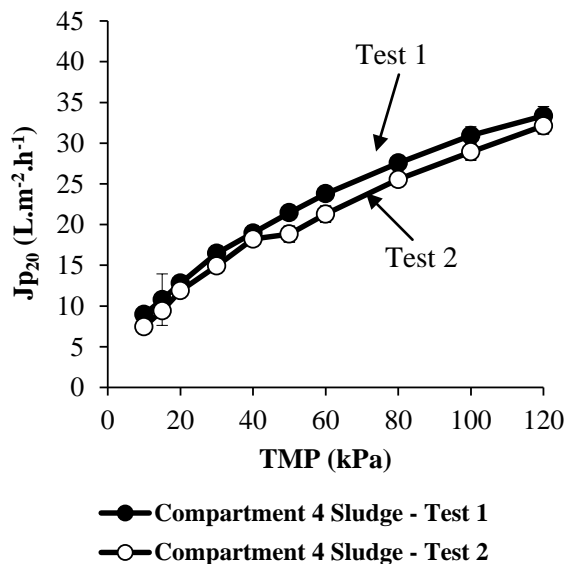
The permeate flux of diluted and undiluted supernatant from anaerobic digester sludge against TMP is plotted in Figure 4.5. The experiment was performed on a new membrane (Amicon® membrane 2). The COD value for the undiluted anaerobic sludge supernatant was substantially higher ($1281 \pm 28 \text{ mg/L}$) than that of an effluent from an ABR treating domestic wastewater (Foxon *et al.*, 2006) and thus the effect of solute build-up on the membrane is obvious. In order to have a representative sample of ABR effluent (in terms of COD), the supernatant was diluted with distilled water and used for subsequent membrane filtration tests. It was found that the dilution factor 1: 6 gave COD values similar to that of pilot ABR effluent treating domestic wastewater (Foxon *et al.*, 2006). Table 4.1 presents a summary of chemical characteristics of undiluted and diluted supernatant and the permeate that was produced.



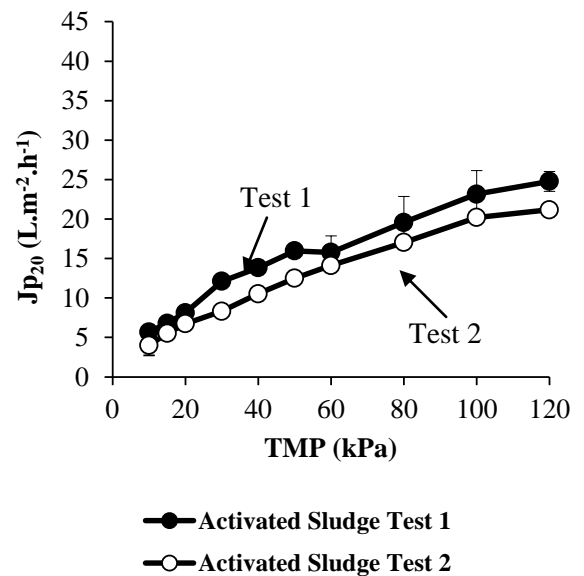
a) Compartment 2 of the pilot ABR



b) Compartment 3 of the pilot ABR

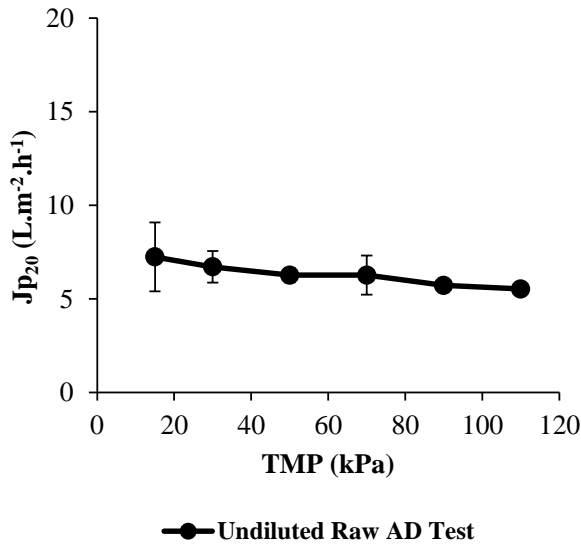


d) Compartment 4 of the pilot ABR

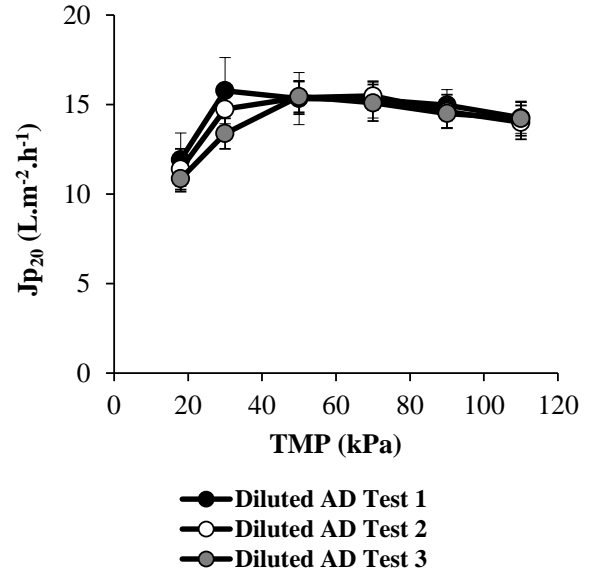


d) Activated sludge

Figure 4.4: Plots of flux at 20°C as a function of constant TMP for supernatant samples of (a) sludge from compartment 2 of ABR ($n = 2$), (b) sludge from compartment 3 of ABR ($n = 2$), (c) sludge from compartment 4 of ABR ($n = 2$), and (d) sludge from an activated sludge plant on Amicon® membrane 1 ($n = 2$). Error bars represent the standard deviation for each TMP step under dead-end conditions. In certain instances, the error bars are too small to be visible.



a) Raw anaerobic supernatant



b) Diluted anaerobic supernatant

Figure 4.5: Plots of flux at 20°C as a function of constant TMP for supernatant from (a) raw supernatant (1 281 mg COD/L) ($n = 1$) and (b) diluted supernatant from an anaerobic digester (258 mg COD/L) ($n = 2$) at a local wastewater treatment facility on Amicon® membrane 2. Error bars represent the standard deviation for each TMP step under dead-end conditions.

Table 4.1: Summary of chemical results obtained from membrane filtrations of diluted and undiluted anaerobic sludge supernatant.

	<u>Parameter</u>		
	COD mg/L (n)	Soluble Protein mg/L (n)	Soluble Carbohydrates mg/L (n)
Undiluted supernatant	1 281 ± 27.6 (3)	nd	nd
Permeate _(raw supernatant)	291 ± 35.0 (3)	nd	nd
Diluted supernatant	258 ± 27.1 (3)	68 ± 0.5 (3)	10 ± 0.8 (3)
Permeate _(diluted supernatant)	42 ± 20.3 (3)	19 ± 0.1 (3)	1 ± 1.4 (3)

nd, not determined.

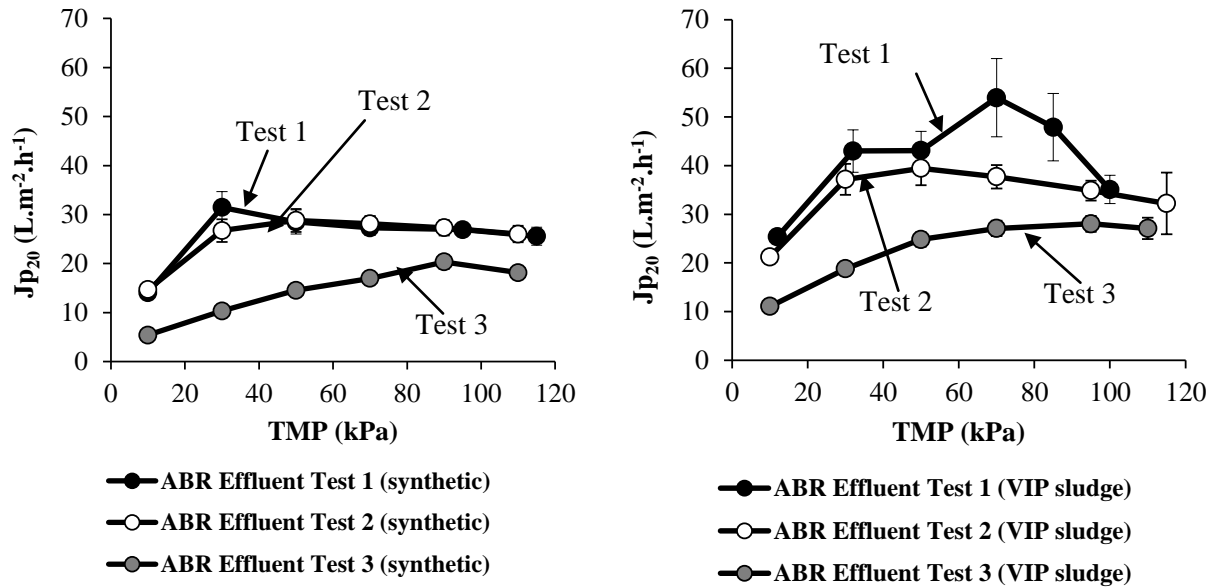
The COD removal efficiency achieved for undiluted supernatant and the diluted supernatant after filtration was 77% and 84%, respectively. Interestingly, the COD value for raw supernatant permeate was seven times higher than that of the diluted supernatant permeate which approximates the dilution factor used in the experiment.

Soluble EPS measurements were represented by the combination of protein and carbohydrate values within the water phase of the supernatant. The membrane was able to remove 73% of the proteins and 88% of the carbohydrates from the diluted supernatant sample. No measurements were made for undiluted supernatant EPS. In addition, EPS was not extracted from the sludge and quantified (bound EPS).

Nearly identical flux profiles were achieved during replicated runs of the diluted supernatant sample indicating good reproducibility. A gradual reduction in flux was noticed at higher TMP (> 50 kPa). Moreover, fluxes were noticeably lower than other supernatant sources.

The permeate flux of supernatant from the overflow of compartment 4 sludge from the laboratory ABR treating a synthetic domestic wastewater (membrane 3) and diluted VIP sludge (membrane 4) are shown in Figure 4.6a and b, respectively. The addition of greywater to the feed component to the ABR resulted in lower flux value over corresponding TMP. Furthermore, variation in the flux was observed especially after the third replicated run.

In the next section, the values for the product of $\alpha.C_s$ (the product of the specific cake resistance and the concentration of particles in feed solution) were determined to quantify the fouling propensities of each of the biological supernatant samples.



a) Effluent from ABR treating greywater and VIP sludge.

b) Effluent from ABR treating diluted VIP sludge only.

Figure 4.6: Plots of flux at 20°C as a function of constant TMP for supernatant from the laboratory ABR treating (a) synthetic domestic wastewater and (b) diluted VIP sludge on Amicon® membrane 3 and 4, respectively. Error bars represent the standard deviation for each TMP step under dead-end conditions.

4.4.2 DETERMINATION OF THE PRODUCT OF $\alpha.C_s$

The values for the product of $\alpha.C_s$ were determined from the slope of t/V and V filtration curves (Cabassud *et al.*, 2006; Teychene *et al.*, 2008). Four identical Amicon® membranes were used in experimentation. On Amicon® membrane 1, four experiments were performed (in chronological order) using the supernatant samples from compartment 2, 3 and 4 mixed liquor sludge of the pilot ABR and finally activated sludge (Figure 4.7). The values for the product of $\alpha.C_s$ were calculated for each of these sludge sources.

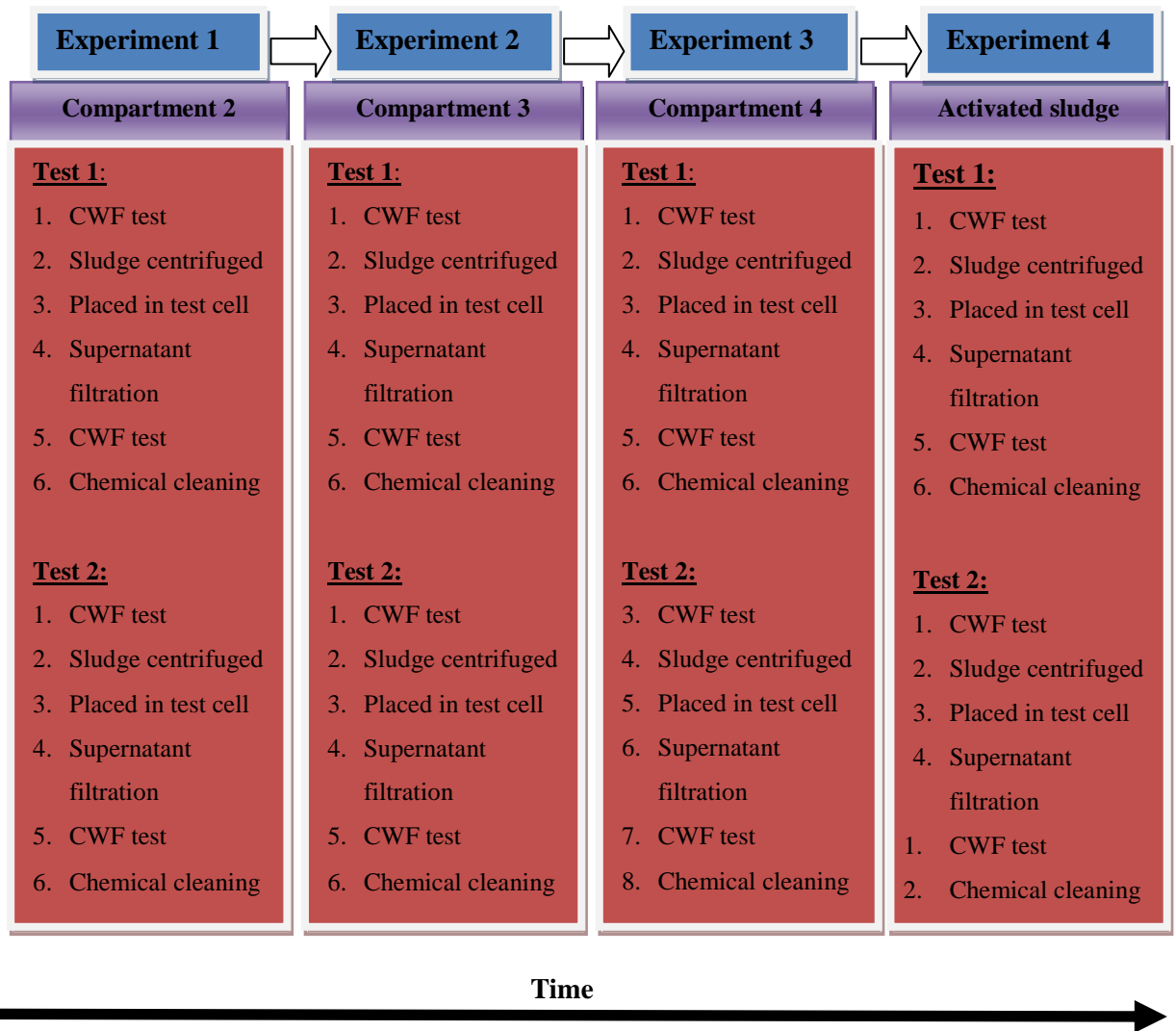


Figure 4.7: Timeline of filtration experiments performed on the Amicon® membrane 1 using supernatant from different sludge sources. For each experiment, duplicate filtration experiments were performed with chemical cleaning and clean water tests (CWF) performed after each supernatant filtration cycle.

Figure 4.8 presents the data for the calculation of the product of $\alpha.C_s$ from the t/V versus V plots for duplicated runs of compartment 2 supernatant from the pilot ABR. The exploitation of data is based on the theory presented in section 4.1 and the product of $\alpha.C_s$ that was calculated from the slope of graph was used to evaluate the fouling propensity of the filtration solution. In the first run, a non-linear curve of t/V versus V was observed with initial steep slope followed by gradual incline corresponding to pore blocking and cake filtration, respectively (refer to section 4.1). It is important to note that pore blocking in this experiment was not due to particle deposition on the membrane pores as particulate and colloidal material were removed through the ultracentrifugation step. The blocking was probably due to adsorption and/or sedimentation

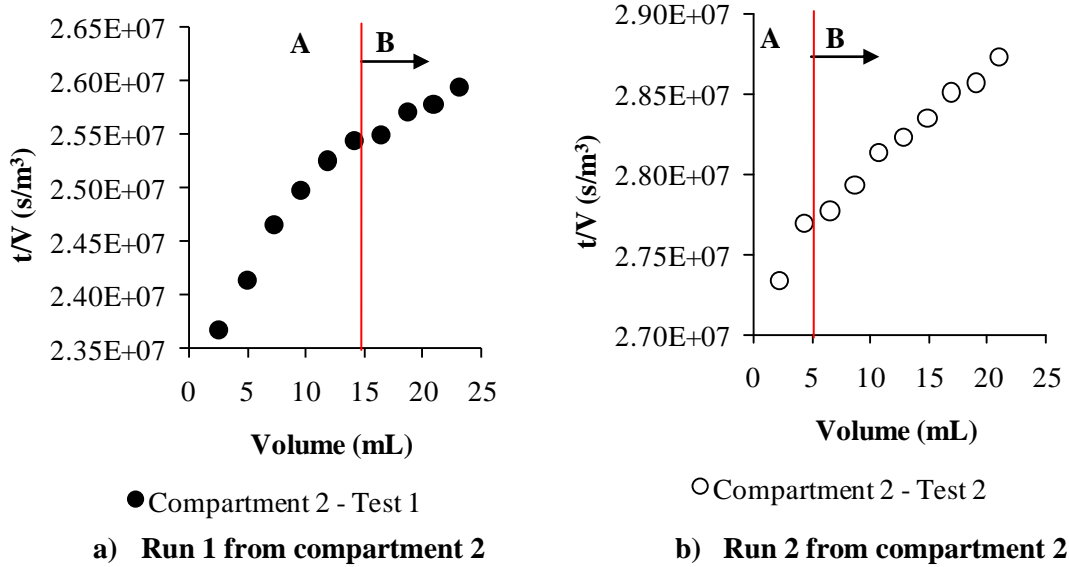
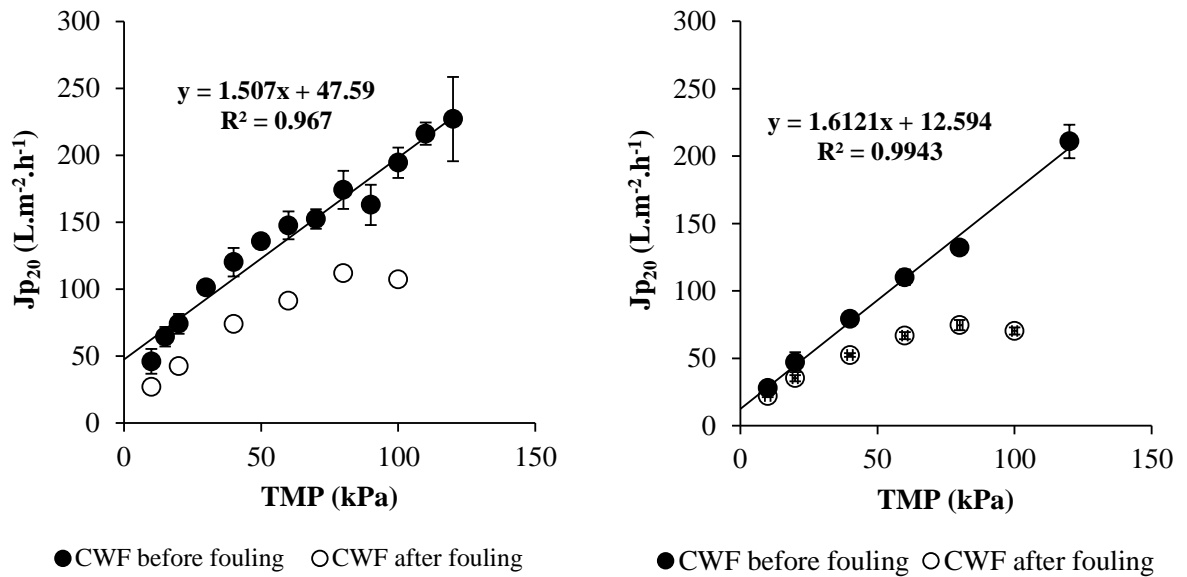


Figure 4.8: Plots of t/V versus V for (a) Run 1 and (b) Run 2 of the membrane filtration of supernatant from compartment 2 of the pilot ABR at 50 kPa. Regions A and B on each graph represent approximate location of blocking and cake filtration, respectively.

of soluble macromolecules in the feed on the membrane surface even though low stirring was applied.

A linear extrapolation was constructed from the last six data points on the graph which corresponds to the initial cake filtration phase ($R^2 = 0.98$). Instead of reporting a single value based on the product of $\alpha \cdot C_s$, the lower and upper range (95% confidence level) of values for this index has been reported in this section for comparative purposes due to non-linearity of t/V versus V curves (lower, $4.8 \times 10^{10} \text{ m/s}^2$; upper, $7.0 \times 10^{10} \text{ m/s}^2$). In a similar manner, a linear regression analysis was performed from the second to the last data point of t/V versus V plot of the second run ($R^2 = 0.99$). The lower and upper values (95% confidence level) for the second run were 5.8×10^{10} and $7.1 \times 10^{10} \text{ m/s}^2$, respectively. The linear regression analysis performed on the data has been included in **Appendix III**.

Clean water flux tests before and after supernatant filtration clearly showed that the layer on the membrane was compressible (Figure 4.9) as TMP increased, the permeate flux started to decline in both runs. As no particles or soluble macromolecules were present in the clean water, the effect is likely to be due to the cake layer becoming compressed over the membrane reducing the passage of flow.



a) CWF before and after Run 1

b) CWF before and after Run 2

Figure 4.9: Plots of clean water flux (CWF) before and after compartment 2 supernatant filtration for (a) Run 1 and (b) Run 2. Each point represents the average flux for a specific TMP whilst error bars represent the standard deviation for that point. In some instances the error bars are too small to be visible.

Figure 4.10 presents a photograph of the fouling layer that developed after filtration of supernatant from compartment 2 of the pilot ABR. The layer was evenly distributed over the membrane and was easily sloughed off with distilled water (and thereafter chemically cleaned with a solution of 0.5 M NaOH). The restoration of permeability to near its original state is confirmed by the comparison of the clean water flux at the start of Run 1 [$1.51 \text{ L.m}^{-2}.\text{h}^{-1}.\text{kPa}^{-1}$ ($151 \text{ L.m}^{-2}.\text{h}^{-1}.\text{bar}^{-1}$)] and Run 2 [$1.61 \text{ L.m}^{-2}.\text{h}^{-1}.\text{kPa}^{-1}$ ($161 \text{ L.m}^{-2}.\text{h}^{-1}.\text{bar}^{-1}$)] respectively (Figure 4.9).

Figure 4.11 presents the data for the calculation of the product of $\alpha.C_s$ for the supernatant samples from compartment 3 of the pilot ABR. For the first run, a typical plot with three regions was generated (refer to section 4.1). The first region corresponds to pore blocking and is probably due to adsorption of soluble constituents on the membrane surface.



Figure 4.10: Picture of the fouling layer after compartment 2 supernatant membrane filtration. The fouling layer was thin and easily removed by rinsing and chemical cleaning.

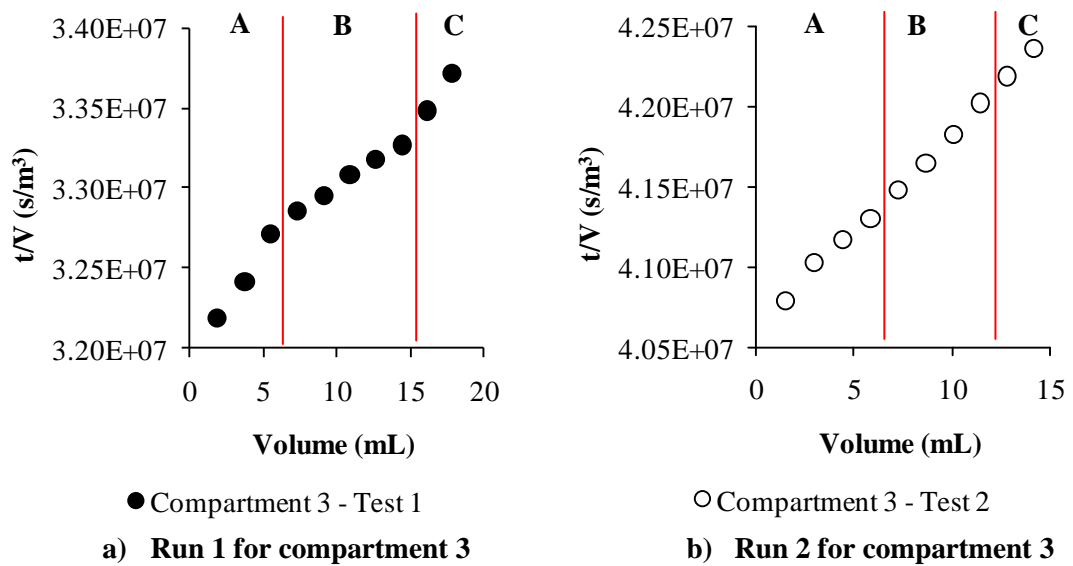


Figure 4.11: Plots of t/V versus V for (a) Run 1 and (b) Run 2 of the membrane filtration of supernatant from compartment 3 of the pilot ABR at 50 kPa. Regions A, B and C on each graph represent the approximate location of blocking filtration, cake filtration and cake filtration with blocking and/or compression, respectively.

The lower and upper range of the values for the $\alpha.C_s$ product were generated from the second and third regions of the plot ($R^2 = 0.99$) with values of 5.8×10^{10} and $7.2 \times 10^{10} \text{ m/s}^2$ (Figure 4.11a). Significantly the last region corresponding to cake filtration and cake clogging and/or compression is clearly shown (denoted as region C on Figure 4.11) but has been included in the calculation of the product of $\alpha.C_s$ limits due to the non-linearity of the plot. As the data is generated from a short interval (10 min), the results indicate that the layer on the cake is highly compressible. This was further substantiated by clean water flux after the filtration of the supernatant (with the fouling layer intact) which clearly shows that the slope of the flux decreases at higher TMP (Figure 4.12).

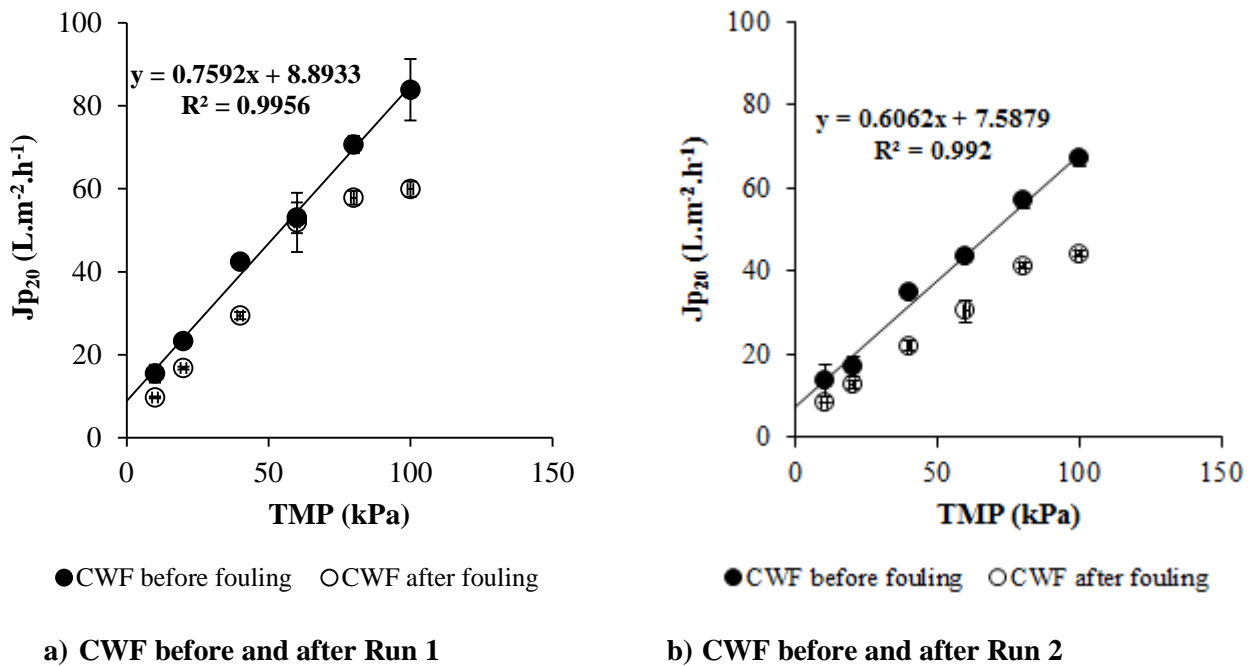


Figure 4.12: Plots of clean water flux (CWF) before and after membrane filtration of compartment 3 supernatant for (a) Run 1 and (b) Run 2. Each point represents the average flux for a specific TMP whilst error bars represent the standard deviation for that point. In some instances the error bars are too small to be visible.

For the second run, a similar plot to the first run was observed except that the three regions were less distinct (Figure 4.11b). The lower and upper range of the product of $\alpha.C_s$ was calculated by determining the gradient from the fourth point to the last point in the t/V versus V plot (see **Appendix III**) (lower, 13×10^{10} and upper, $13 \times 10^{10} \text{ m/s}^2$). As with the first run, the clean water flux immediately after supernatant filtration showed that the layer was compressible at high TMP (Figure 4.11b). The results were substantiated by clean water tests after supernatant filtration which showed compressibility of the fouling layer at high TMP (Figure 4.12).

The clean water flux tests between runs also demonstrated that the fouling was more severe than previous experiments. Membrane permeability was shown to drastically decrease from the first experiment to second [from greater than $1.5 \text{ L.m}^{-2}.\text{h}^{-1}.\text{kPa}^{-1}$ ($150 \text{ L.m}^{-2}.\text{h}^{-1}.\text{bar}^{-1}$) to under $0.8 \text{ L.m}^{-2}.\text{h}^{-1}.\text{kPa}^{-1}$ ($80 \text{ L.m}^{-2}.\text{h}^{-1}.\text{bar}^{-1}$). The reasons for the decrease in the permeability are unknown as the previous chemical cleaning regime was shown to restore permeability to near its original state. Possible explanations include lack of contact time in cleaning solution and strong adsorption of soluble macromolecules on membrane surface implying the presence of a different chemical or biological fouling agent compared to the first experiment.

Figure 4.13 shows the fouling layer that developed on the membrane during the filtration of the supernatant from compartment 3 of the pilot ABR. The layer was yellow-brown in colour and not well distributed on the membrane surface. The layer consisted of a thick, viscous gel-like substance which could not be easily removed by rinsing. The layer had to be physically scraped off and chemically cleaned with a solution of 0.5 M NaOH. It is interesting to note that the sludge sample was taken from compartment of the pilot ABR in which bioaggregates or granules developed. These granules were formed by a selection pressure for certain groups of anaerobic micro-organisms which are bound together by extracellular polymers (EPS) (Foxon *et al.*, 2006).



Figure 4.13: Picture of the fouling layer after compartment 3 supernatant membrane filtration. The fouling layer was viscous and gel-like and could not be easily removed by rinsing and chemical cleaning.

It was hypothesised that the fouling layer was primarily composed of EPS as EPS-producing *Methanosaeta* microorganisms have been shown to predominate in this compartment (Foxon *et al.*, 2006). The results are substantiated by EPS analyses which show comparatively higher EPS quantities in this supernatant, especially soluble carbohydrates (Table 4.2).

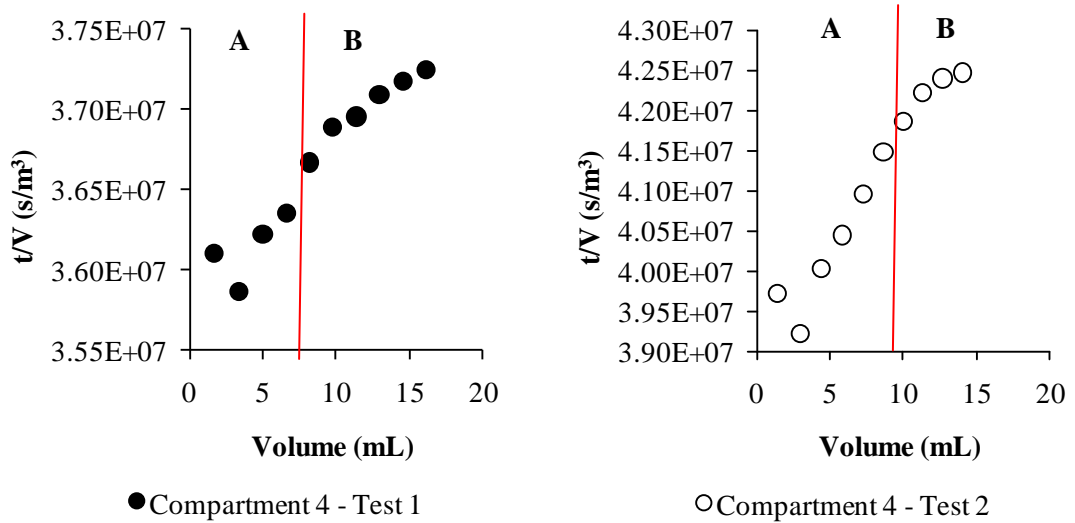
Table 4.2: Physico-chemical results of the different soluble fractions of each sludge source.

Parameter	Unit	Compartment.2	Compartment.3	Compartment.4	AD sludge	Activated sludge	ABR Effluent ¹	ABR Effluent ²
COD _(t)	mg/L	94 ± 10	88 ± 0	65 ± 10	258 ± 17	437 ± 42	219 ± 23	154 ± 22
Carbohydrate _(s)	mg/L	9 ± 0.1	14 ± 0.3	3 ± 0.2	10 ± 0.8	2 ± 0.1	6 ± 2.7	8 ± 0.1
Carbohydrate _(b)	mg/L	31 ± 0.3	20 ± 0.9	33 ± 0.3	-	4 ± 0.1	-	-
Carbohydrate _(l)	mg/L	2 ± 0.4	7 ± 0.2	7 ± 0.3	-	5 ± 0.3	-	-
Proteins _(s)	mg/L	61 ± 1.2	60 ± 0.7	30 ± 0.4	87 ± 0.6	19 ± 0.5	46 ± 3.3	69 ± 5.2
Proteins _(b)	mg/L	106 ± 0.9	86 ± 0.7	139 ± 0.5	-	12 ± 1.3	-	-
Proteins _(l)	mg/L	36 ± 0.5	34 ± 0.1	33 ± 0.4	-	20 ± 0.3	-	-
TSS*	mg/L	2 308 ± 23	2 350 ± 52	1 444 ± 50	-	15 ± 0.3	-	-
VSS*	mg/L	78 ± 3.4	91 ± 6.4	41 ± 12.0	-	0.2 ± 0.1	-	-

Note: [†], mean data from 3 reps of diluted anaerobic digester sludge tests; *, values obtained from sludge samples; (t), total; (s), supernatant obtained after ultracentrifugation; (b), sludge-bound EPS extracted using cation-exchange resin; (l), loose bound EPS obtained after ultracentrifugation, washing with buffer, and another ultracentrifugation step. TSS, VSS, bound and loose EPS measurements represent the values of the raw sludge sample and not the supernatant.¹, ABR treating greywater and diluted VIP sludge; ², ABR treating diluted VIP sludge only.

Figure 4.14 presents data for the calculation of the product of $\alpha.C_s$ for the supernatant samples from compartment 4 of the pilot ABR. For the first run, blockage of pores by soluble macromolecules is observed in the t/V versus V plot (region A) followed by cake filtration (region B). An estimate of the lower and upper range (95% confidence level) values for the product of $\alpha.C_s$ was made by constructing a linear extrapolation from the last five points on the Figure 4.14a. This was calculated to be to 4.6×10^{10} and $7.2 \times 10^{10} \text{ m/s}^2$ for the lower and upper range respectively.

For the second run in the membrane filtration of compartment 4 supernatant, the product of $\alpha.C_s$ was calculated by constructing a linear regression of the last four data points on the t/V versus V graph in Figure 4.14b ($R^2 = 0.92$). The slope decreases near the end of the plot indicating that an asymptote may exist. The decrease towards a plateau is the approximate location of cake filtration from which the lower and upper limits of the product of $\alpha.C_s$ were calculated (lower, 8.7×10^{10} ; upper, $28 \times 10^{10} \text{ m/s}^2$).



a) Run 1 for compartment 4

b) Run 1 for compartment 4

Figure 4.14: Plots of t/V versus V for (a) Run 1 and (b) Run 2 of the membrane filtration of supernatant from compartment 4 of the pilot ABR at 50 kPa. Regions A and B on each graph represent approximate location of blocking and cake filtration, respectively.

Figure 4.15 presents the clean water flux tests before and after the membrane filtration of compartment 4 supernatant. There is little discernible difference between the flux before and after supernatant filtration in both runs indicating that the attachment of fouling agent is probably reversible. However, a steady decrease in the membrane permeability has been noted over time. As the number of filtration experiments increased on the membrane, the permeability of the membrane also decreased from $1.51 \text{ L.m}^{-2}.\text{h}^{-1}.\text{kPa}^{-1}$ ($151 \text{ L.m}^{-2}.\text{h}^{-1}.\text{bar}^{-1}$) in the first experiment on this membrane to $0.76 \text{ L.m}^{-2}.\text{h}^{-1}.\text{kPa}^{-1}$ ($76.0 \text{ L.m}^{-2}.\text{h}^{-1}.\text{bar}^{-1}$) in the third experiment and finally to approximately $0.51 \text{ L.m}^{-2}.\text{h}^{-1}.\text{kPa}^{-1}$ ($51.3 \text{ L.m}^{-2}.\text{h}^{-1}.\text{bar}^{-1}$) in this experiment. The results indicate that the membrane was gradually becoming irreversibly fouled. Moreover, the chemical cleaning procedure employed between the different filtration experiments was not effective as in previous filtration regimes.

Figure 4.16 shows a picture of the fouling layer that developed from these runs. The fouling layer produced after filtration of compartment 4 supernatant was not as prominent as observed with other tests and is probably due to a lower concentration of organic content (Table 4.2).

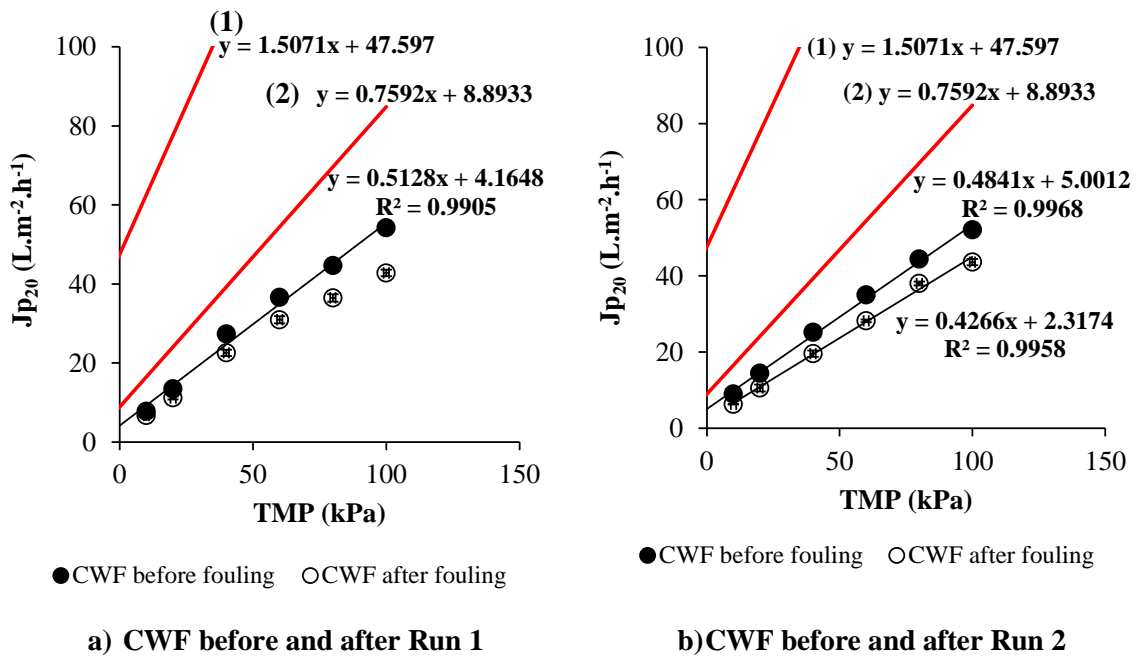


Figure 4.15: Plots of clean water flux (CWF) before and after membrane filtration of compartment 4 supernatant for (a) Run 1 and (b) Run 2. Each point represents the average flux for a specific TMP whilst error bars represent the standard deviation for that point. In some instances the error bars are too small to be visible. For comparison, the CWF for the virgin membrane (1) and at the beginning of the compartment 2 supernatant test (2) have been included.



Figure 4.16: Picture of the fouling layer after membrane filtration of compartment 4 supernatant. The fouling layer was thin and evenly distributed around the membrane.

Figure 4.17 presents data for the calculation of the product of $\alpha.C_s$ for the supernatant samples from the activated sludge plant from a local treatment facility. These experiments were the last performed on the first Amicon® membrane. For the first run, a linear extrapolation was constructed from the last four data points corresponding to the approximate location of cake filtration (region B). From the gradient, the lower and upper range of the product of $\alpha.C_s$ was calculated (based on a 95% confidence level) to be 9.5×10^{10} and $19 \times 10^{10} \text{ m/s}^2$ respectively. For the second run, a linear extrapolation was constructed from the last seven data points corresponding to the approximate location of cake filtration (region B). From the gradient, the lower and upper range (95% confidence level) of the product of $\alpha.C_s$ was calculated to be 18×10^{10} and $24 \times 10^{10} \text{ m/s}^2$, respectively.

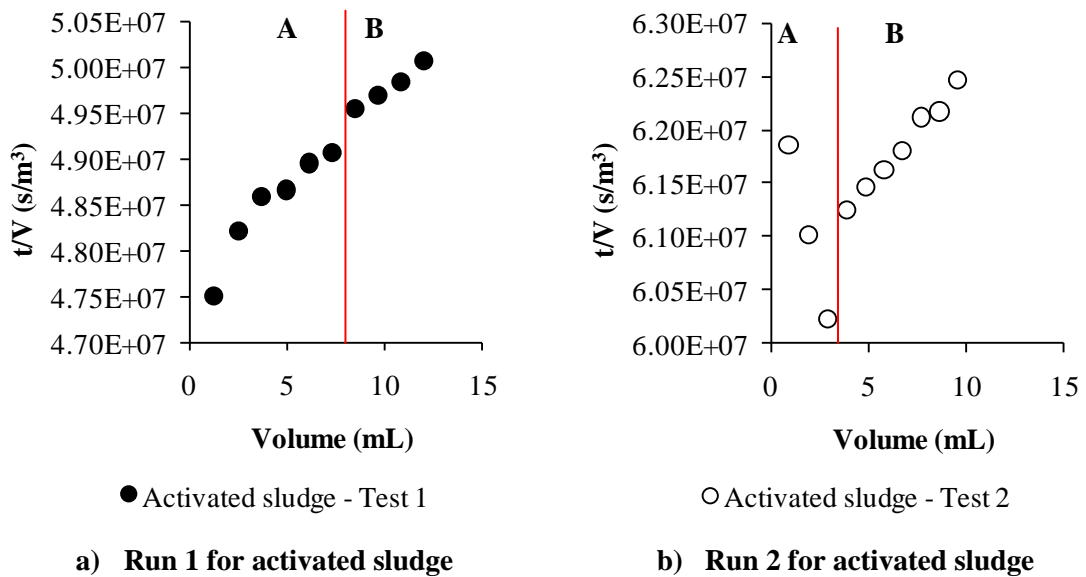


Figure 4.17: Plots of t/V versus V for (a) Run 1 and (b) Run 2 of the membrane filtration of supernatant from an activated sludge tank at 50 kPa.

Figure 4.18 presents the clean water flux tests before and after activated sludge supernatant tests for both runs. Permeability decline due to fouling is clearly shown by the gradient of the slope of flux versus TMP. For the first run, permeability decrease due to fouling was 60%. For the second run, this amounted to 52%. Unlike previous clean water tests performed after supernatant filtration, no compressibility was observed at higher TMP.

The fouling layer that developed after filtration of the soluble component of activated sludge is shown in Figure 4.19. The layer was relatively thin and evenly distributed fouling layer and was easily removed by combination of distilled water rinses and chemical cleaning.

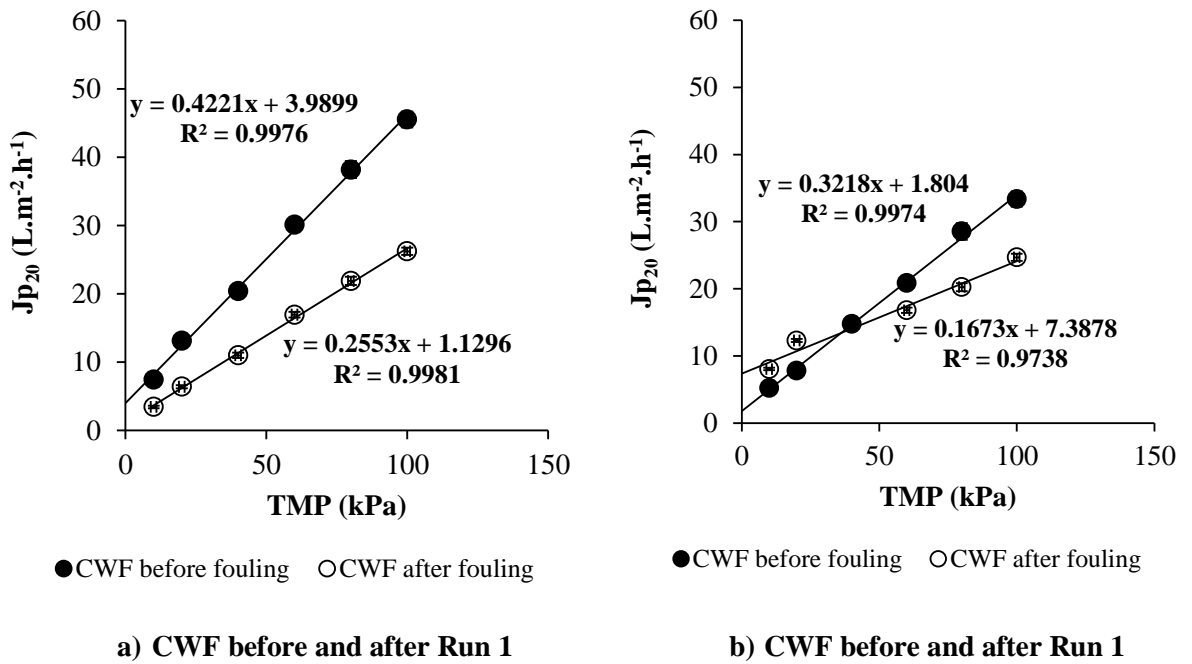


Figure 4.18: Plots of clean water flux (CWF) before and after membrane filtration of activated sludge supernatant for (a) Run 1 and (b) Run 2. Each point represents the average flux for a specific TMP whilst error bars represent the standard deviation for that point. In some instances the error bars are too small to be noticed.



Figure 4.19: Picture of the fouling layer after membrane filtration of the soluble component of activated sludge. The fouling layer was thin and evenly distributed around the membrane.

On Amicon® membrane 2, two experiments were performed using the supernatant of mixed liquor sludge from a secondary anaerobic digester. For the first experiment, one filtration run was performed using the supernatant of the anaerobic sludge (no replicates). For the second, three filtration runs were performed on diluted anaerobic sludge from the same source (Figure 4.20).

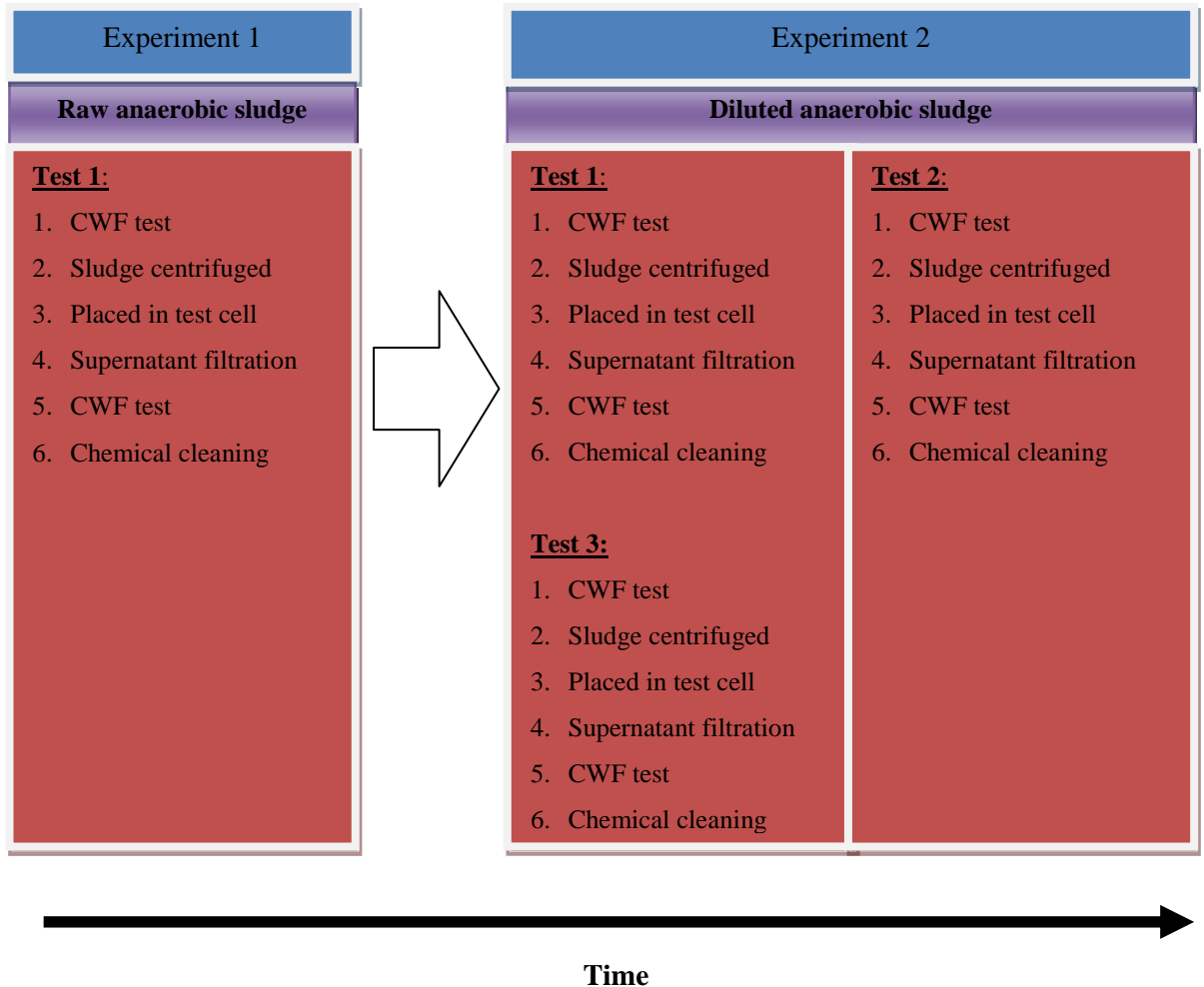


Figure 4.20: Timeline of filtration experiments performed on Amicon® membrane 2 using supernatant from an anaerobic digester. For the first experiment, only one run was performed. For the second experiment, triplicate experiments were performed with chemical cleaning and clean water tests (CWF) performed after each supernatant filtration cycle.

The t/V versus V plot for the filtration of undiluted supernatant of sludge from a secondary anaerobic digester is shown in Figure 4.21. The data were generated from a new Amicon® membrane (membrane 2) with only one run performed (no replicates). The lower and upper limits of the product of $\alpha.C_s$ were calculated to be (based on a 95% confidence level) 297×10^{10} and $496 \times 10^{10} \text{ m/s}^2$, respectively. Only one filtration run was performed as the flux data showed the liquor to induce a high fouling propensity.

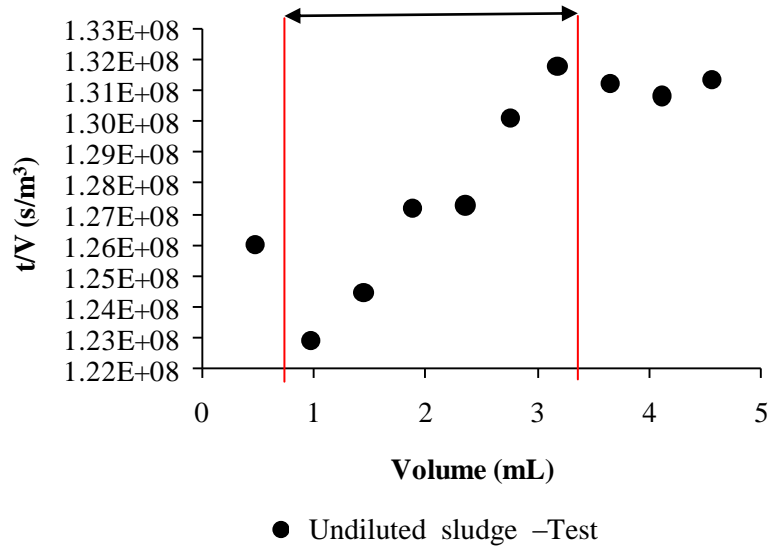


Figure 4.21: Plots of t/V versus V for the membrane filtration of supernatant from an anaerobic digester at 50 kPa. The area highlighted in the plot shows the points which were used to calculate the lower and upper limits of the product of $\alpha.C_s$.

The clean water tests that were performed before and after filtration of the anaerobic supernatant are presented in Figure 4.22. The permeability determined from the slope of flux versus TMP was calculated to be $0.82 \text{ L.m}^{-2}.\text{h}^{-1}.\text{kPa}^{-1}$ ($82.0 \text{ L.m}^{-2}.\text{h}^{-1}.\text{bar}^{-1}$). Compressibility of the fouling layer was observed with the clean water flux after fouling convexing upwards at higher TMP.

Figure 4.23 presents the t/V versus V graphs for diluted anaerobic sludge from an anaerobic digester. For the first run, the lower and upper range (95% confidence level) of the product of $\alpha.C_s$ was calculated from the last eight data points. The values were $67 \times 10^{10} \text{ m/s}^2$ for the lower range and $78 \times 10^{10} \text{ m/s}^2$ for the upper range. For the second run, the product of $\alpha.C_s$ was calculated from the last seven data points with a lower and upper range (95% confidence level) of 34×10^{10} and $46 \times 10^{10} \text{ m/s}^2$, respectively. For the third run, the product $\alpha.C_s$ was calculated

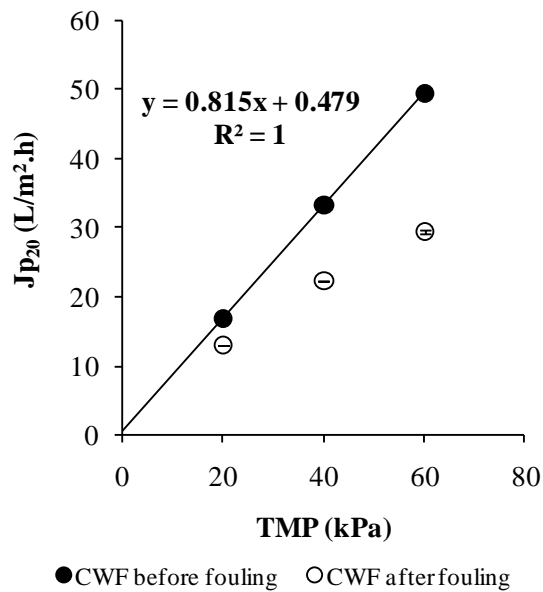
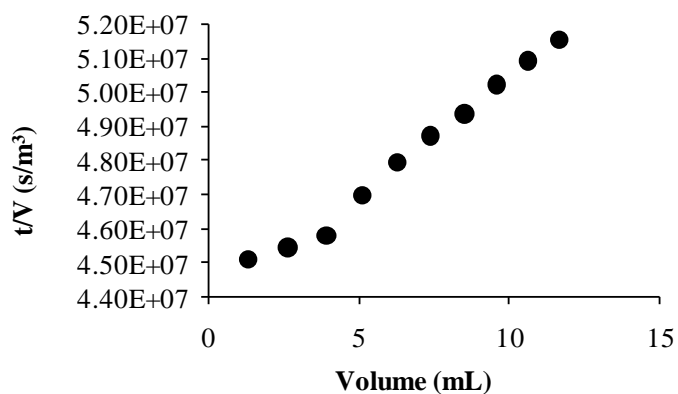


Figure 4.22: Plots of clean water flux (CWF) before and after membrane filtration of anaerobic sludge supernatant. Each point represents the average flux for a specific TMP whilst error bars represent the standard deviation for that point. In some instances the error bars are too small to be visible.

from the last seven data points with a lower and upper range (95% confidence level) of 39×10^{10} and 47×10^{10} m/s², respectively.

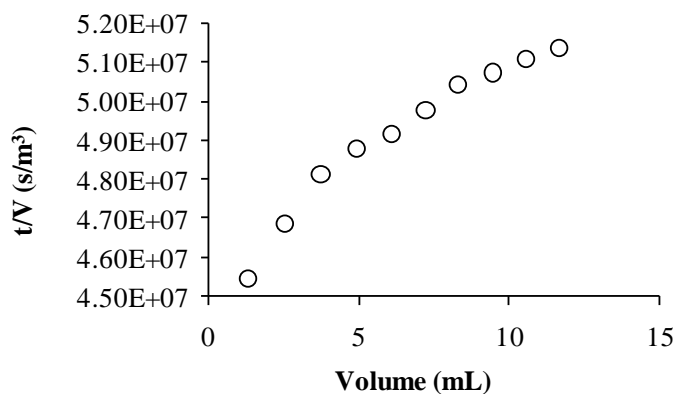
The clean water tests performed before and after the first filtration using diluted anaerobic sludge are shown in Figure 4.24. At the start of the experiment, the initial permeability of the membrane was $0.71 \text{ L.m}^{-2}.\text{h}^{-1}.\text{kPa}^{-1}$ ($71.0 \text{ L.m}^{-2}.\text{h}^{-1}.\text{bar}^{-1}$) with a 24% decrease in permeability due to fouling. For the second run, a 58% decline in permeability observed after fouling from an initial permeability was $0.82 \text{ L.m}^{-2}.\text{h}^{-1}.\text{kPa}^{-1}$ ($82.0 \text{ L.m}^{-2}.\text{h}^{-1}.\text{bar}^{-1}$). For the third run, the initial permeability was $0.81 \text{ L.m}^{-2}.\text{h}^{-1}.\text{kPa}^{-1}$ ($81.0 \text{ L.m}^{-2}.\text{h}^{-1}.\text{bar}^{-1}$) with permeability declining by 51% after fouling. Chemical cleaning between filtration runs was effective as indicated by nearly identical permeabilities before each supernatant challenge.

On the Amicon® membrane 3, triplicate filtration experiments were performed using effluent from the laboratory ABR treating a synthetic wastewater (composed of VIP sludge and greywater). The effluent therefore represents the overflow from compartment of this particular ABR system. The data for the calculation of the product of $\alpha.C_s$ of the effluent from the laboratory ABR treating a synthetic wastewater (greywater and diluted VIP sludge) is presented in Figure 4.25. The tests were performed on Amicon® membrane 3 with the tests performed in



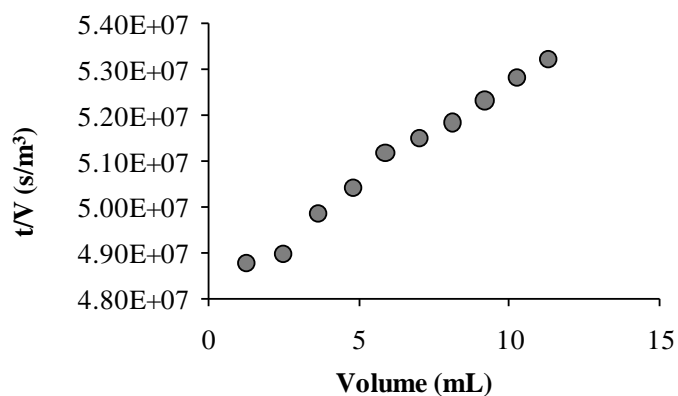
● Diluted anaerobic sludge - Test 1

a) Run 1



○ Diluted anaerobic sludge - Test 2

b) Run 2



● Diluted anaerobic sludge - Test 3

c) Run 3

Figure 4.23 Plots of t/V versus V for (a) Run 1, (b) Run 2 and (c) Run 3 of the membrane filtration of diluted supernatant from an anaerobic digester at 50 kPa on Amicon® membrane 2.

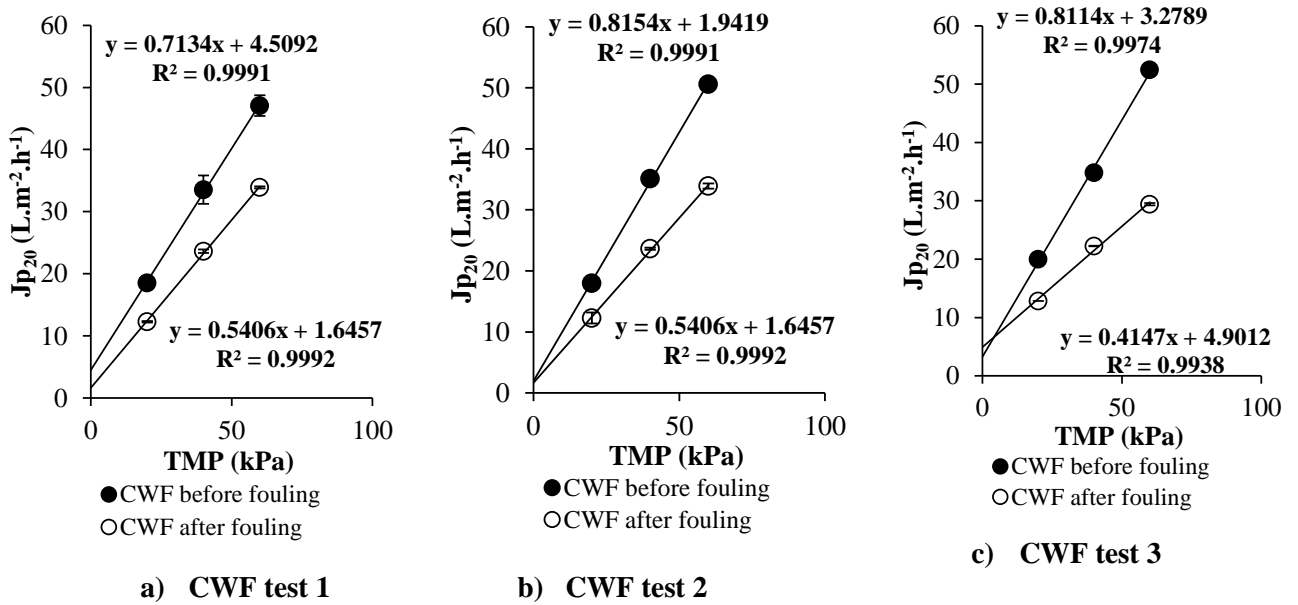
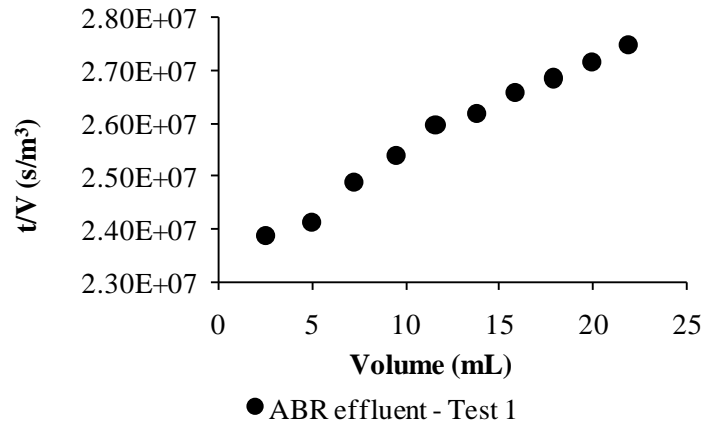


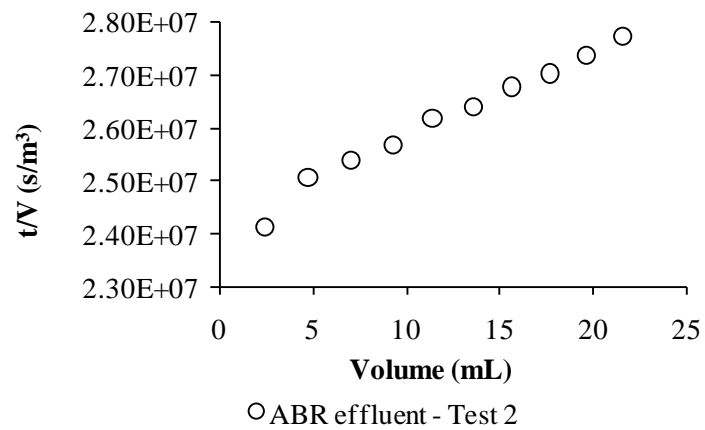
Figure 4.24: Plots of clean water flux (CWF) before and after membrane filtration of diluted anaerobic sludge supernatant. Each point represents the average flux for a specific TMP whilst error bars represent the standard deviation for that point. In some instances the error bars are too small to be visible.

triplicate. The data generated from t/V versus V curves were relatively linear (R^2 value ranging from 0.98 to 0.99). For the first run (Figure 4.25a), the product of $\alpha.C_s$ was calculated to be $20 \times 10^{10} \text{ m/s}^2$ with a lower and upper range (95% confidence level) of 17×10^{10} and $22 \times 10^{10} \text{ m/s}^2$, respectively. For the second run (Figure 4.25b), the product of $\alpha.C_s$ ($20 \times 10^{10} \text{ m/s}^2$) was calculated from the second point onwards with a lower and upper range of values of 15×10^{10} and $17 \times 10^{10} \text{ m/s}^2$, respectively. For the third run, the product of $\alpha.C_s$ ($40 \times 10^{11} \text{ m/s}^2$) was calculated from the third point onwards in Figure 4.25c. The lower and upper confidence range of values for the product of $\alpha.C_s$ was 32×10^{10} and $39 \times 10^{10} \text{ m/s}^2$. As shown in earlier filtration tests, the data becomes less reproducible after the second replicate experiment (refer to Table 4.3 for the number of data points used to calculate the product of $\alpha.C_s$ and for a summary of data).

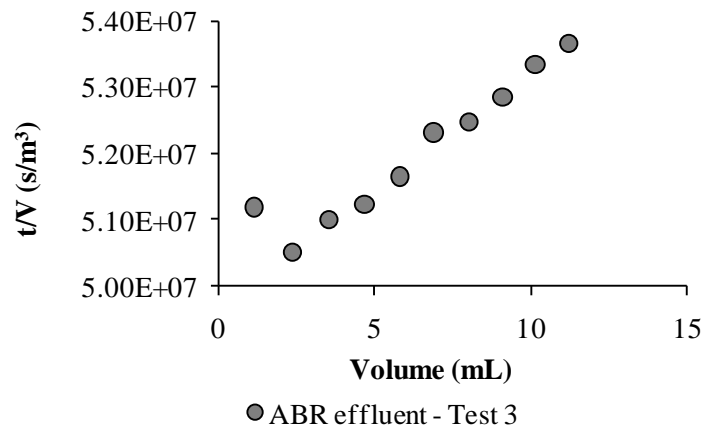
Evidence for the reproducibility of filtration tests decreasing after the second duplicate can be viewed in Figure 4.26 where permeability of the membrane decreased by 67% after the second test despite the same chemical cleaning regime shown to effective in the previous run. The results suggest only a limited number of replicates may be performed on each membrane.



a) Run 1



b) Run 2



c) Run 3

Figure 4.25: Plots of t/V versus V for (a) Run 1, (b) Run 2 and (c) Run 3 of the membrane filtration of supernatant from an ABR treating a synthetic domestic wastewater at 50 kPa on the Amicon® membrane 3.

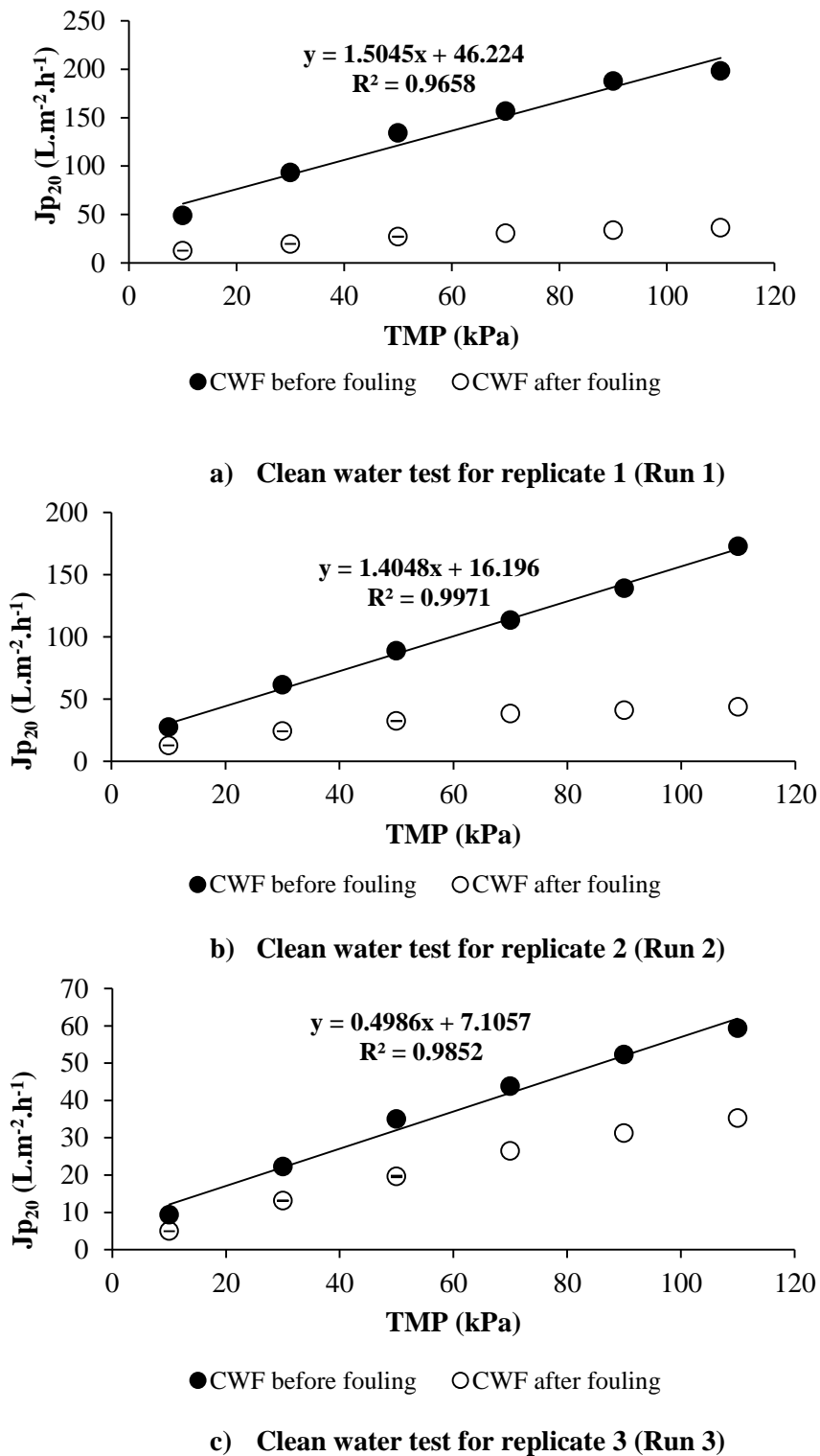


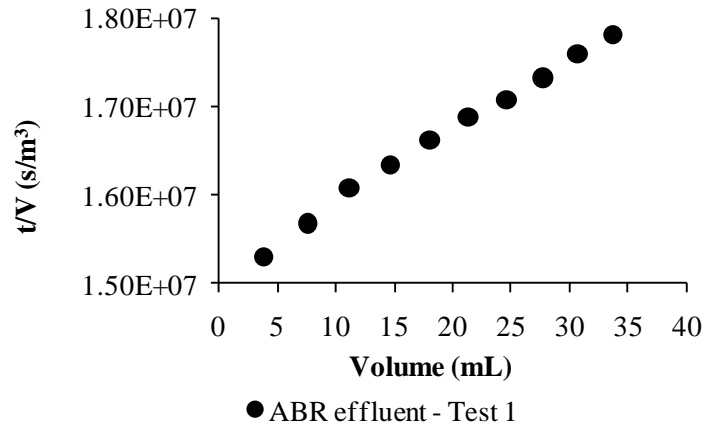
Figure 4.26: Plots of clean water flux (CWF) before and after membrane filtration of supernatant from an ABR treating a synthetic domestic wastewater on Amicon® membrane 3. Each point represents the average flux for a specific TMP whilst error bars represent the standard deviation for that point. In some instances the error bars are too small to be visible.

The final Amicon® membrane (4) was used to evaluate the fouling potential of the effluent from the laboratory ABR treating diluted VIP sludge only. The sample therefore represents the liquor from the overflow of compartment 4 of that system. Figure 4.27 presents data for the calculation of the product of $\alpha.C_s$ for replicated tests using the effluent.

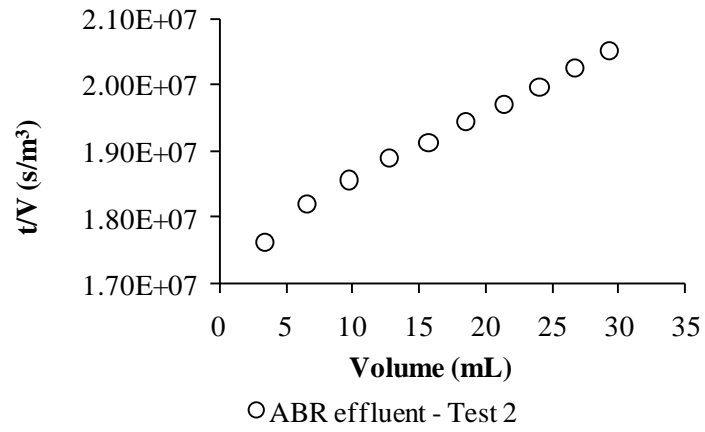
For the first run, the graph was relatively linear ($R_2 = 0.99$) for all data points. The lower and upper range (95% confidence interval) for the product of $\alpha.C_s$ was calculated to be 7.8×10^{10} and $8.8 \times 10^{10} \text{ m/s}^2$. For the second run, the lower and upper range for the product of $\alpha.C_s$ (95% confidence level) was calculated to 9.7×10^{10} and $10 \times 10^{10} \text{ m/s}^2$. For the third run, the lower and upper range of data set correlating to the linear region was calculated to be 17×10^{10} and $19 \times 10^{10} \text{ m/s}^2$.

The clean water tests performed after effluent filtration from an ABR treating diluted VIP sludge are presented in Figure 4.28. A highly compressible fouling layer had developed in all test runs as shown in clean water tests performed after effluent filtration. As with previous runs, the reproducibility of the cleaning regime diminished after the third filtration run.

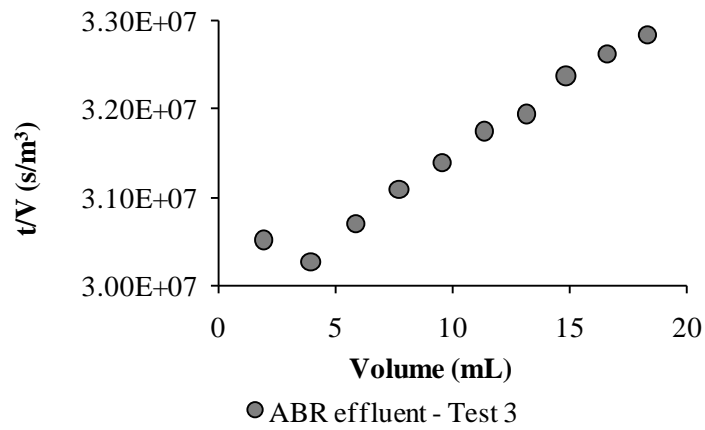
In the next section, the results emanating from this chapter are discussed.



a) Run 1

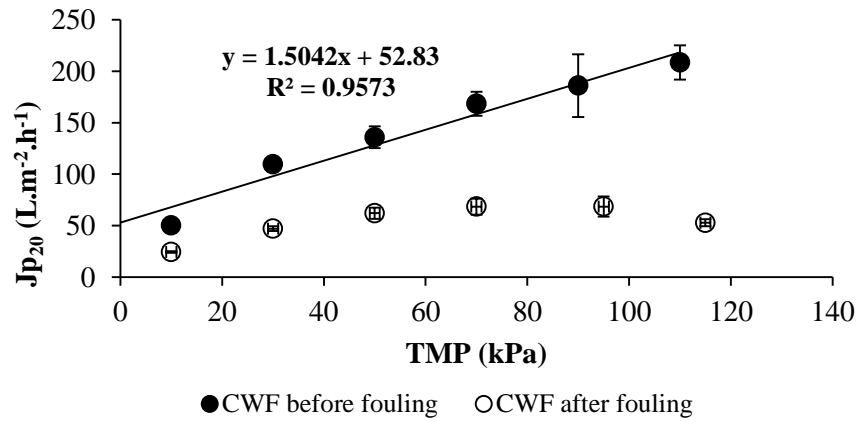


b) Run 2

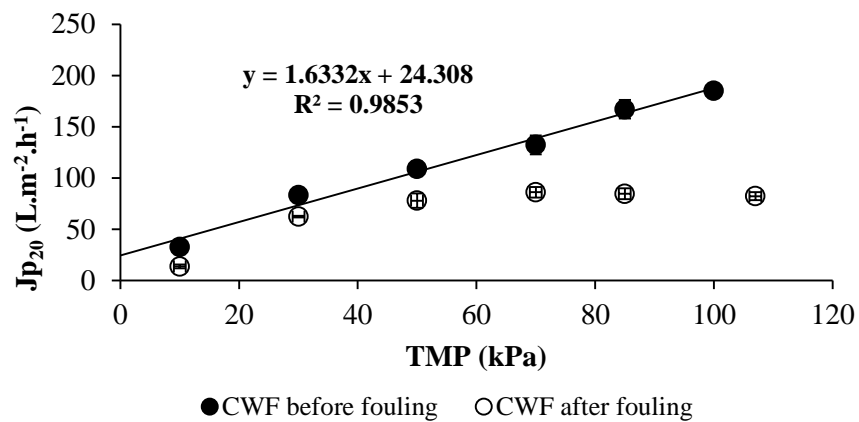


c) Run 3

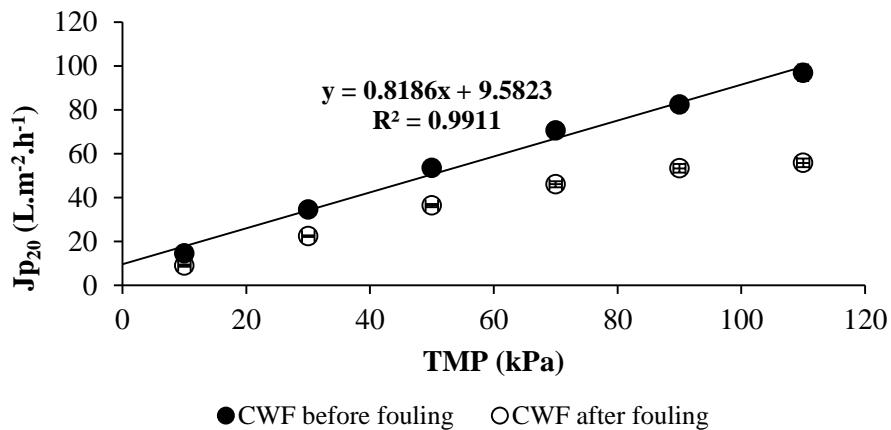
Figure 4.27: Plots of t/V versus V for (a) Run 1, (b) Run 2 and (c) Run 3 of the membrane filtration of supernatant from an ABR treating diluted VIP sludge at 50 kPa on the Amicon® membrane 4.



a) Clean water test for replicate 1 (Run 1)



b) Clean water test for replicate 1 (Run 1)



c) Clean water test for replicate 1 (Run 1)

Figure 4.28: Plots of clean water flux (CWF) before and after the membrane filtration of supernatant from an ABR treating diluted VIP sludge on Amicon® membrane 4. Each point represents the average flux for a specific TMP whilst error bars represent the standard deviation for that point. In some instances the error bars are too small to be noticed.

4.5 DISCUSSION

A test cell technique recommended by *EUROMBRA* partners was used to evaluate the fouling propensity of the soluble component of different sludge sources. The measurements are based on the calculation of the product of $\alpha.C_s$ from the slope of t/V versus V curves. Although most of the data gathered were non-linear (in contrast to cake filtration theory), the lower and upper range of values of the product of $\alpha.C_s$ (based on 95% confidence levels) at 50 kPa (reference TMP) have been presented in Table 4.3. By doing so, it enables the comparison of fouling propensity between different solutions.

Table 4.3: Lower and upper confidence values (95% confidence level) for the product of $\alpha.C_s$ at 50 kPa (reference TMP).

Amicon® membrane	Sample	Replicate	Lower ($\times 10^{10} \text{ m/s}^2$)	Upper ($\times 10^{10} \text{ m/s}^2$)	No. of points*
1	Compartment 2 – pilot ABR	1	4.9	7.0	6
		2	5.8	7.1	8
	Compartment 3 – pilot ABR	1	5.8	7.2	7
		2	13	13	6
	Compartment 4 – pilot ABR	1	4.6	7.2	5
		2			4
	Activated sludge	1	9.5	20	4
2		18	24	7	
2	Anaerobic sludge	1	296	496	6
	Diluted anaerobic sludge	1	67	78	8
		2	34	46	7
		3	39	47	7
3	Lab ABR Effluent 1	1	17	22	10
		2	15	17	9
		3	32	39	8
4	Lab ABR Effluent 2	1	7.8	8.8	10
		2	9.7	10	9
		3	17	19	9

*, refers to the number of data points used to calculate the product of $\alpha.C_s$.

Based on the ranges presented in Table 4.3, it can be observed that the first four runs with supernatant from compartments 2, 3 and 4 of the pilot ABR are similar. Moreover, the values for the product of $\alpha.C_s$ were lower than of other supernatant samples which were probably a reflection of conditions at which samples were taken. Sampling was done when the pilot ABR was offline for nearly a year after the last feeding to the system. The reason for the sampling was that the laboratory ABR had not been built yet. The organic content (as determined by COD values) was low but all compartment samples contained a considerable amount of proteinaceous compounds (as determined by assays) which probably lead to formation of gel-like fouling layers (despite the lack of reactor feeding) in these samples. This gel-like layer was prominent

in the compartment 3 supernatant samples which were taken from the compartment in the ABR which contained bioaggregates or granules of anaerobic micro-organisms bound by EPS (refer to Foxon, 2009) (Figure 4.29). The presence of these compounds in the fluid probably results in a compressible fouling layer as observed in t/V versus V plots and clean water tests performed after compartment 3 supernatant filtration tests.

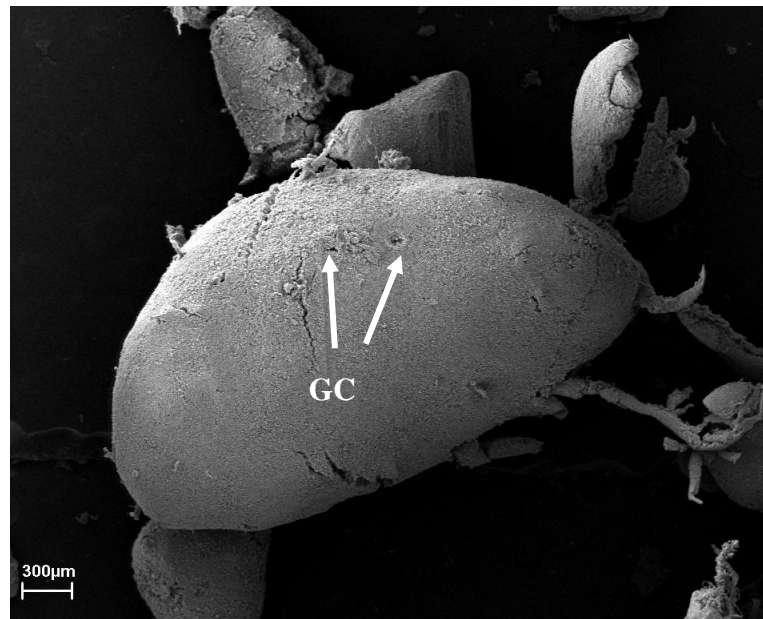


Figure 4.29: SEM micrograph from compartment 3 of pilot ABR treating domestic wastewater reproduced from WRC Project K5/1248 (Foxon *et al.*, 2006). The granules surface is covered with gas cavities (GC) which lead to inner structure bound by EPS containing different metabolic groups (Pillay *et al.*, 2006).

The lower and upper range values of the product of $\alpha.C_s$ for supernatant samples from an aeration tank were similar but slightly higher than that of pilot ABR compartment samples. The fouling layer that developed was not as gelatinous as that from the ABR and is probably a reflection of different biomass conditions and subsequent supernatant characteristics (especially protein concentration). Nevertheless, the result suggests that the fouling propensities of the pilot ABR compartment and activated sludge supernatant samples are similar.

Supernatant samples from diluted anaerobic sludge had the highest propensity for fouling based on the lower and upper limit of the product of $\alpha.C_s$ (nearly triple of that calculated from other solutions). Although this sample had a lower organic content than activated sludge supernatant samples (as measured by COD), the propensity for fouling is much higher (as evidenced by

lower and upper limits of the product of $\alpha.C_s$). Thus, the chemical composition of solution plays an important role in fouling and not just the overall concentration. As can be seen in Table 4.2, diluted anaerobic supernatant samples had a higher proportion of soluble proteinaceous and carbohydrate concentration in solution than the activated sludge supernatant samples tested which may have resulted in a higher fouling potential.

The calculation of the product of $\alpha.C_s$ from t/V versus V filtration curves from the laboratory ABR treating different feeds showed that higher fouling propensity was observed from the laboratory ABR treating a synthetic domestic wastewater (greywater and diluted VIP sludge) than from the reactor treating diluted VIP sludge only. This may be explained by the presence of other soluble organic compounds in the solution (supernatant from ABR treating a synthetic wastewater had a higher COD concentration). However, when the lower and upper range of values for the product of $\alpha.C_s$ from the laboratory ABR treating both types of wastewaters were compared with the data set from other tests, not much difference was observed (with the exception of diluted anaerobic digester supernatant samples). The results indicate that the fouling propensity in an ABR system (specific to the feedwater fed to the system) is not significantly higher than that of aerobic and other anaerobic technologies and fits well with other data from different sludge sources (Yang *et al.*, 2006; Lesage *et al.*, 2008; Teychene *et al.*, 2008).

4.6 CONCLUSIONS

A recommended test cell technique was used to evaluate the fouling propensity of the soluble component of different sludge sources. One of the advantages of using the test cell technique is that it can be easily set-up and standardised among different research groups (as the equipment is commercially available) and reduces the time and cost for membrane experimentation as it eliminates the need for elaborate membrane pilot plants.

The fouling propensity of a particular feed solution is then determined by calculating the product of $\alpha.C_s$ from a simplified model of cake filtration theory. The data therefore gives vital information on the severity of fouling from soluble constituents in the mixed liquor. Using this technique, the effluent and some compartments of ABR systems (one laboratory and one pilot reactor) were compared with other biological treatment systems. The results indicated that the filterability or fouling propensity of the soluble component of ABR fluids is not vastly different from other sources.

One of the major shortcomings of this technique is the inappropriateness of a simplified cake filtration model to describe experimental data. This study showed that there were difficulties in both the interpretation and the selection of the values for the product of $\alpha.C_s$ due to the non-linearity of data. This made statistical validation of fouling propensity between solutions difficult. It is hypothesised that the presence of fouling agents in the solution forms a compressible layer (as substantiated by clean water flux tests) that results in non-linear curves. Consequently, experimental data do not agree well with the general cake filtration model. Whilst it is acknowledged that modifications have been made to the model to compensate for these type of effects (refer to section 4.1), this objective fell outside the scope of this thesis with the method applied as recommended.

Another disadvantage of the technique is related to the cost of set-up and membrane material. Whilst the technique may be cheaper to implement than a pilot membrane plant, the equipment is still costly (Table 4.4). The results in this thesis show that reproducibility of data diminishes after two supernatant filtration tests. Thus, if multiple tests are required, high costs can be incurred (based on membrane price, approximately ZAR 158 per membrane). Recommendations for the improvement of the technique can be viewed in **Chapter 8** whilst the general conclusions from this chapter are presented in **Chapter 7**.

Table 4.4: Cost of experimental equipment used to evaluate fouling propensity. Cost based on 2006 prices (US\$ 1 = ZAR 7.8) and excludes value-added tax. Cost of pressure reservoir and weighing balance has not been included.

Item	Description	Cost (ZAR)
Amicon® stirred cell	Stirred cell model 8400	13 193
Amicon® PM discs	Ultrafiltration membranes 76 mm, 10 pieces	1 582

The next chapter (**Chapter 5**) presents laboratory-based membrane filtration experiments performed with the hollow-fibre unit containing Polymem modules. The hollow-fibre modules were constructed by Polymem (France) and delivered to UKZN as part of the *EUROMBRA* Project.

CHAPTER 5 : HOLLOW-FIBRE FILTRATION

The previous chapter (**Chapter 4**) presented the results from bench-scale membrane experiments performed with an Amicon® test cell. In this chapter, the performance of Polymem hollow-fibre modules treating the effluent of the laboratory ABR is presented. Two Polymem modules were used in membrane filtration experiments; a microfiltration module and an ultrafiltration module (refer to section 3.2 for a description of modules). Filtration was performed over the various phases of ABR operation (see **Appendix II**). The overall objective of these experiments was to evaluate the performance of hollow-fibre modules treating ABR effluent. This chapter is divided into eight sections:

- *short-term filtration* (defined as filtration performed for 1 to 24 h, refer to section 3.9) to establish a suitable TMP by which to operate modules under gravity (section 5.1)
- short-term filtration at constant TMP (section 5.2)
- *long-term filtration* (defined as filtration performed for longer than 10 d, refer to section 3.9) at constant TMP (section 5.3)
- *medium-term filtration* (defined as filtration performed over 1 to 10 d, refer to section 3.9) to evaluate differences between ultrafiltration and microfiltration modules (section 5.4)
- short-term filtration using TMP relaxation (section 5.5)
- medium-term filtration of the non-settleable portion of ABR effluent (section 5.6)
- medium-term filtration of the soluble component of the ABR effluent (section 5.7)
- section 5.8 presents a summary of the experiments performed in this chapter.

5.1 SHORT-TERM TMP-STEP EXPERIMENTS

This section presents the details of a series of short-term membrane filtration experiments using the effluent from the laboratory ABR treating diluted VIP sludge. The aims of these specific membrane experiments are presented in section 5.1.1, the methodology is presented in section 5.1.2 and the results and discussion presented in section 5.1.3. A summary of this series of experiments is presented in section 5.1.4.

5.1.1 INTRODUCTION

Short-term fixed TMP-step experiments were performed with Polymem hollow-fibre modules. The technique was recommended by *EUROMBRA* partners and adapted by our research group to evaluate the modules using *ultra-low* (less than 10 kPa) hydrostatic driving forces. In this technique, low increment step increases in the TMP were applied on the membranes to determine a suitable hydrostatic pressure to drive the filtration process. The procedure is

analogous to constant flux step procedure used to determine the critical flux in MBR systems (Le Clech *et al.*, 2003) except that TMP is kept constant. Ultra-low driving pressures were chosen as operating TMP as field-based ABR-membrane systems are expected operate under a gravitational pressure heads of less than 1 m water head (10 kPa) (excavation deeper than the height of an ABR will incur higher construction and pumping costs, and is inconvenient). At present, there is a distinct lack of knowledge related to the selection of an optimal hydrostatic pressure under these conditions. The objective of this study was thus to determine an operating TMP that provides a compromise between higher fluxes and stable long-term operation. The specific aims of this experiment were:

- Establish the *limiting flux* of Polymem modules using the TMP-step method suggested by *EUROMBRA*. This value is the plateau reached by flux independent of TMP and has been shown to be similar to the *critical flux* value in fixed TMP operations (Defrance and Jaffrin, 1999). Although fouling mechanisms differ in constant flux and constant TMP operations (Defrance and Jaffrin, 1999), it was hypothesised that constant pressure operation below this flux may result in less fouling in a similar manner to operation below the *critical flux*.
- Examine the effect of increased feed organic loading on the value of the *limiting flux*.
- Compare the performance of ultrafiltration and microfiltration hollow-fibre modules treating the same feed wastewater.
- Use the practical definition of fouling (section 2.2.7) to determine the nature of the foulants in laboratory ABR effluent.

5.1.2 METHODOLOGY

This section presents the details of methodology used in constant TMP membrane filtration experiments with the Polymem membrane modules treating laboratory ABR effluent.

5.1.2.1 Membrane Feed

Effluent from the laboratory ABR treating diluted VIP sludge was pumped directly from the effluent tank (containing a 2 d supply) or collected in plastic drums and stored. Filtration was performed during the corresponding operations: Phase I, Phase III, Phase V and Phase VI (refer to **Appendix II**). Only a single batch of effluent (approximately 200 L) was used from each phase of ABR operation as a compromise was required between the number of filtration experiments performed and prolonging membrane lifespan. The average of the total COD of the ABR effluent during these operations ranged between 300 to 1 500 mg COD/L and was similar to that measured in the batch collection. No filtration experiments were performed during Phases II and IV. Phase II was dedicated to optimising ABR operation whilst no filtration experiments were performed during Phase IV due to time constraints.

5.1.2.2 Membrane Units

Polymem microfiltration (MF) and ultrafiltration (UF) modules were used during batch dead-end filtration experiments. Storage chemicals were removed from the membranes prior to use by filtering distilled water overnight (approximately 18 h). The experimental set-up is described in more detail in section 3.2. All filtration experiments were performed in the Biochemistry Engineering laboratory at the University of KwaZulu-Natal.

5.1.2.3 Filtration Experiment

The filtration experiments were performed in batches at constant TMP. The general procedure is similar to that recommended for batch test cell experiments (refer to **Chapter 4**) with the exception that it is used for the determination of an optimum operating TMP (which has never been dealt with according to the author's knowledge). The general procedure is summarised in Figure 5.1.

Step 1

Filtration of distilled water was performed at the beginning of the experiment to determine the initial membrane resistance (R_m). The membrane unit was opened and filled with distilled water. Trapped air bubbles were removed by displacing air with distilled water. The filtration of distilled water was performed at constant TMP for at least three different TMP values with each filtration cycle lasting a minimum of 10 min. The TMP was manually regulated between experiments by adjusting the water column height on the feed side of the membrane module.

Step 2

Distilled water was removed from the membrane unit using decant valves or opening the membrane unit and replacing it with ABR effluent. Trapped air bubbles were removed using valves and replaced with ABR effluent. Filtration of ABR effluent was performed at progressively increasing constant TMP with each cycle lasting a minimum of 10 min.

Step 3

The remaining ABR effluent and concentrate from filtration was carefully decanted from the membrane housing unit. The module was carefully lifted so as to not disturb the fouling layer and placed undisturbed in a separate dry membrane housing unit. The experimental membrane housing unit was washed with detergent and rinsed with distilled water. The membrane was then placed back into the housing unit and carefully immersed in distilled water so as to not disturb the fouling layer. Air bubbles were removed using decanting valves. The time between

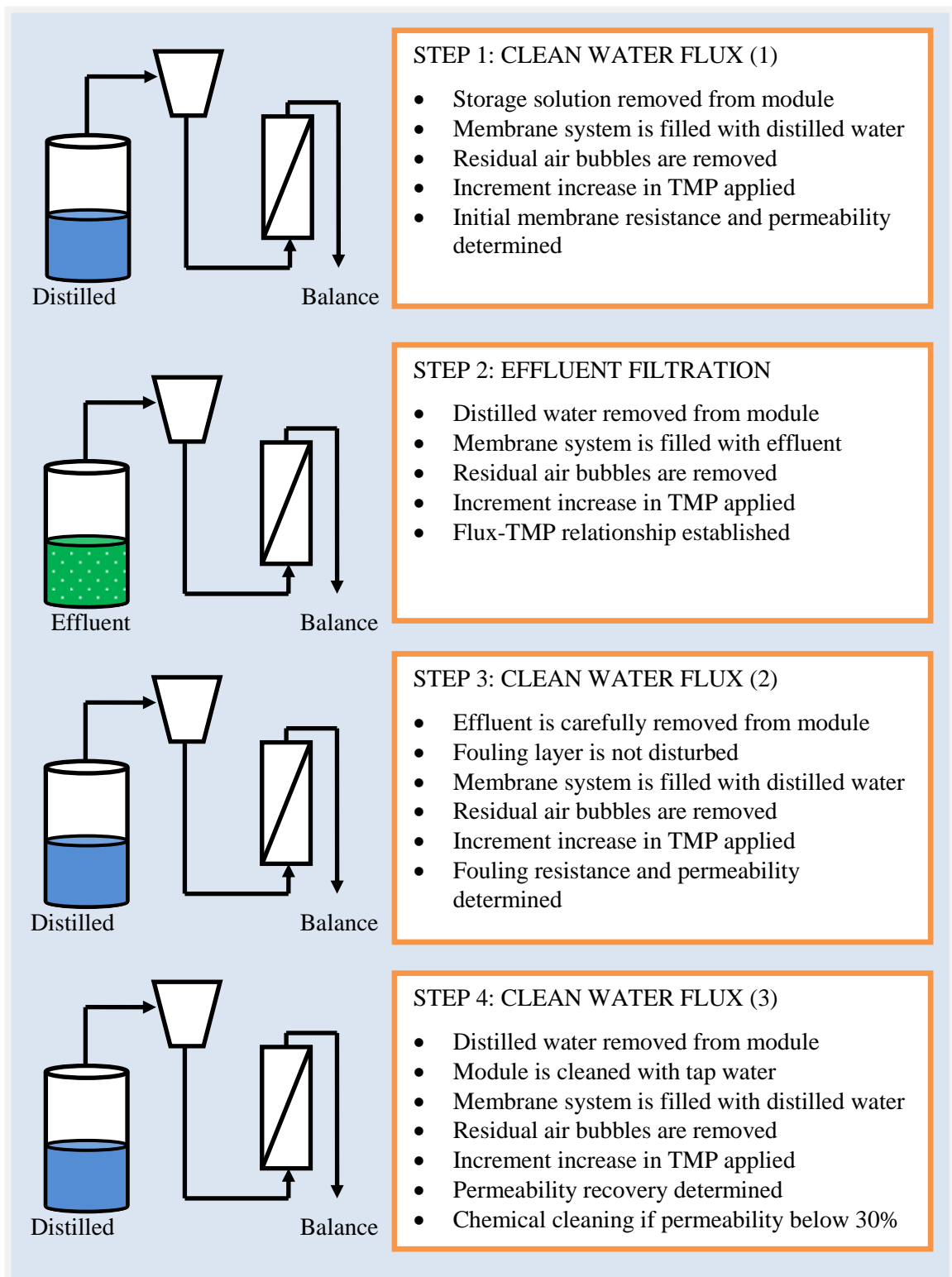


Figure 5.1: Schematic representation of the protocol used for assessing Polymem performance based on practical definition of fouling (refer to section 2.2.7).

removing the module from the housing unit and cleaning was kept to a minimum (approximately 3 min) to prevent drying of the membrane fibres. The feed funnel, permeate pipe and feed pipe were cleaned with detergent and rinsed with distilled water.

Once the feed funnel, permeate pipe and feed pipe were reattached to the membrane unit, the membrane system was filled with distilled water with a constant supply provided by a peristaltic pump (Watson-Marlow 323 Du/D) connected to a storage drum (25 L). The TMP was set by adjusting the water column height on the feed side of the membrane unit (see **Appendix III**). Filtration of distilled water was then performed at progressively increasing TMP. This set of experiments provided the resistance due to fouling (R_f).

Step 4

The module was removed from the housing after the second distilled water filtration and the fouling layer removed by rinsing the membrane under a stream of tap water. Residual tap water was removed by immersing the module in distilled water. The housing unit was once again cleaned using detergent and rinsed with distilled water. The module was then placed back into the housing unit and filled with distilled water. Trapped air bubbles were removed using decanting valves. A third set of distilled water filtration was performed at progressive increases in TMP. This set of experiments provided the efficiency of the cleaning procedure as indicated by membrane resistance and permeability results.

Step 5

A fourth set of distilled water experiments was required after chemical cleaning if the membrane permeability at the start of the experiment was significantly different to that after physical cleaning (not included in Figure 5.1). This value was approximately 70 to 80% of the virgin flux. The results from this series of clean water membrane filtration experiments would provide a practical definition of fouling (refer to section 2.2.7) in this system.

5.1.2.4 Data Acquisition and Interpretation

The permeate mass was monitored using an Ohaus Adventurer Pro balance. A timer was used to determine the length of the experiment. The temperature of the permeate was measured using a mercury thermometer. All measurements were manually recorded. The resistance-in-series model was used to calculate the permeate flux. The data exploitation is elaborated further upon in **Appendix III** (section A 3.4). Permeability values have been presented in two pressure units; $L \cdot m^{-2} \cdot h^{-1} \cdot kPa^{-1}$ (plots and text) and $L \cdot m^{-2} \cdot h^{-1} \cdot bar^{-1}$ (text only) (see section 2.2.4).

5.1.2.5 Physico-Chemical Analyses

The determination of COD was performed according to the UCT Open Reflux COD Method for wastewater (Lakay *et al.*, 2000). TS, VS and pH analyses were performed according to Standard Methods (APHA-WEF-AWWA, 1998). Soluble protein and carbohydrate were measured according to the Frølund *et al.* (1996) and Dubois *et al.* (1956) methods, respectively. Details of analytical protocols can be viewed in **Appendix IV**.

5.1.3 RESULTS AND DISCUSSION

In this chapter, the term effluent refers to the overflow of compartment 4 of the laboratory ABR (refer section 3.9 for terminology). It was this fluid that was used as the feed to the membrane plant. A summary of ABR effluent conditions used for filtration experiments is shown in Table 5.1.

Table 5.1: Summary of ABR effluent characteristics during short-term TMP-step filtration. Polymem ultrafiltration and microfiltration modules were tested using the TMP-step method during these phases. The values represent the average and standard deviation (except pH value which is represented as a median) with numbers in parentheses representing the sample replicates.

	Phase I	Phase III	Phase V	Phase VI
COD	257 ± 115 (34)	307 ± 77 (14)	447 ± 78 (13)	1 305 ± 365 (9)
pH	7.3 (6)	7.4 (14)	7.6 (13)	7.7 (9)
TS	266 ± 87 (10)	477 ± 126 (5)	208 ± 64 (9)	314 ± 61 (4)
VS	99 ± 46 (7)	159 ± 75 (5)	41 ± 14 (8)	nd
Protein _(soluble)	nd	69 ± 21 (2)	23 ± 4.1 (13)	16 ± 3.1 (7)
Carbohydrate _(soluble)	nd	2.3 ± 0.2 (2)	2.9 ± 0.4 (13)	2.9 ± 0.3 (7)

nd, analysis not performed.

5.1.3.1 Phase I Effluent

During Phase I, the average feed COD entering the ABR was 679 ± 341 mg/L with an average effluent COD of 257 ± 115 mg/L achieved after digestion. Specific short-term constant TMP filtration experiments were performed on Polymem modules using ultra-low hydrostatic driving forces. The variation of flux over the transient increasing increments of constant TMP is presented in Figure 5.2. Each point on the graph represents the average flux at each constant TMP. The filtration curves of Polymem ultrafiltration and microfiltration modules are characterised by an initial linear flux increase with TMP followed by an asymptote towards a flux independent plateau (Figure 5.2) (Cabassud *et al.*, 2006). However, the flux independent plateau (*limiting flux*) was not reached. Thus, only predicted values for the limiting flux is noted for this set of data. For the microfiltration module, a limiting flux was not observed below $15 \text{ L.m}^{-2}.\text{h}^{-1}$ at TMP less than 6 kPa. For the Polymem UF module, the *limiting flux* was not observed below approximately $10 \text{ L.m}^{-2}.\text{h}^{-1}$ at TMP less than 6 kPa.

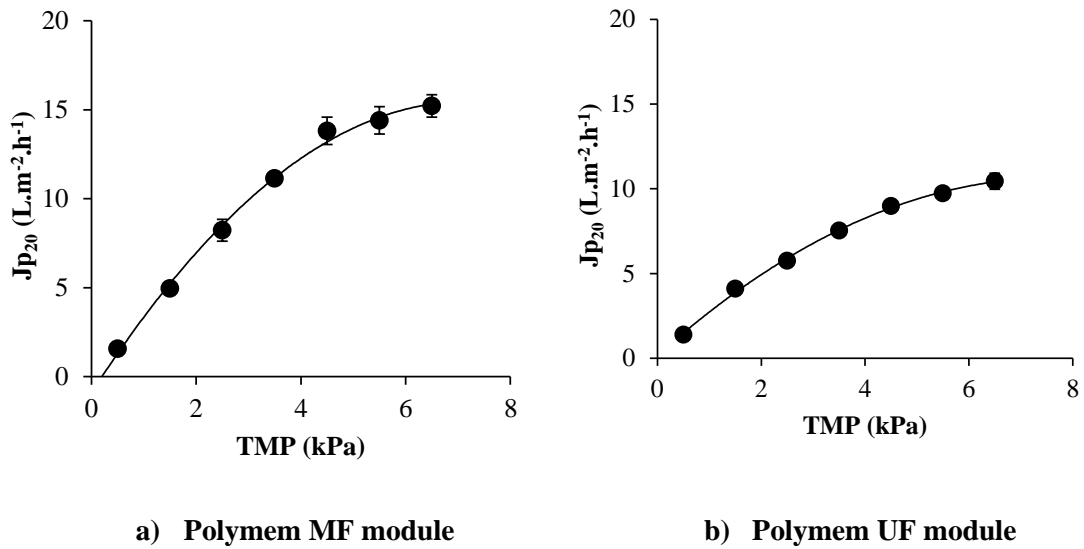


Figure 5.2: Variation of flux with pressure during Phase I effluent for a) flux-TMP graph of the Polymem MF module and b) flux-TMP graph of the Polymem UF module. Each data point (●) represents the average flux over each pressure step. The error bars represent the standard deviation for each TMP step. In some instances, the error bars are too small to be visible.

The fouling resistance (R_f) for the microfiltration module over each TMP-step is shown in Figure 5.3 (for the calculations refer to section A 3.4 in **Appendix III**). The R_f was calculated using equation 2.2 with R_t and R_m determined by the clean water flux tests before and after fouling. Filtration at the lowest TMP showed a gradual decrease in R_f as filtration time proceeded. It is unclear why fouling resistance decreased. Possible explanations include a minor pressure drop across the membrane which limits the adherence of the fouling layer or wettability issues related to the membrane material. As each increment increase in TMP step is applied, a gradual increase in R_f is observed followed by a rapid increase after 4 kPa. Moreover, the R_f is shown to asymptote near the end of a filtration run at higher TMP with R_f becoming less dependent on time (areas circled in Figure 5.3). This area was not used in the calculation of fouling velocity (in Figure 5.5). It is probable that during this part of the run that the fouling layer is experiencing an equilibrium-type effect with the rate of build-up equalling that at which foulant diffuses or sloughs off into the bulk solution.

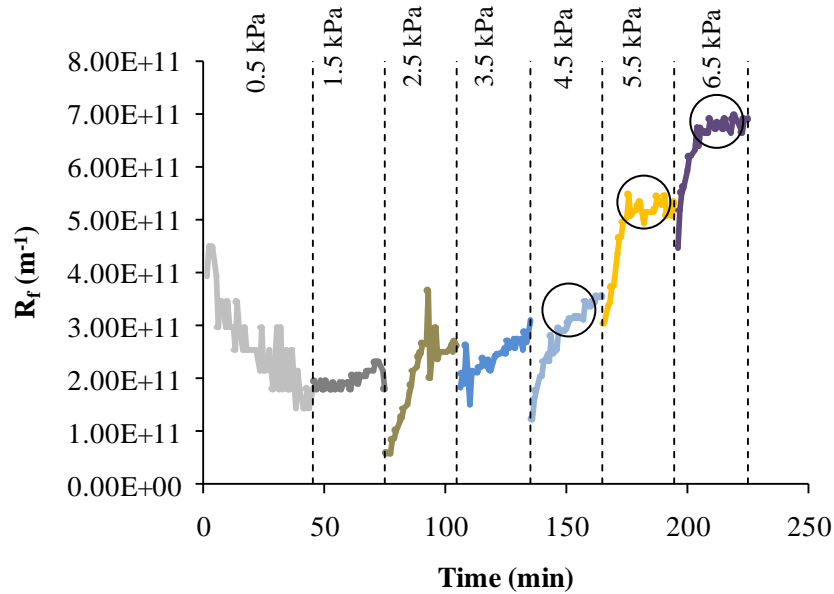


Figure 5.3: Fouling resistance (R_f) as a function of TMP over progressive increases in TMP for the Polymem MF module during Phase I. The encircled areas represent the asymptote of R_f for a particular TMP step.

The fouling resistance (R_f) for the ultrafiltration module over each TMP-step is shown in Figure 5.4. At the lowest TMP used (1 kPa), the R_f starts at higher rate than other TMP and gradually increases as time progresses. The higher R_f at the lowest TMP is probably a consequence of low pressure driving force just sufficient to overcome internal resistances (such as in the permeate pipes) to establish flow. This would probably reflect as higher R_f as shown in Figure 5.4. As was the case in the microfiltration module, R_f increases gradually with a steeper increase observed at higher TMP (above 5 kPa) coupled with an asymptote of fouling resistance data at longer filtration times.

The fouling velocity (fouling rate) for Polymem microfiltration and ultrafiltration modules over the TMP are presented in Figure 5.5 as a function of time. The calculation is based on the slope of R_f over time for a constant TMP (see **Appendix III**). Not included in the calculations are data where R_f becomes increasing independent on time at higher TMP (see Figure 5.3 and Figure 5.4). Whilst no clear pattern can be observed with fouling velocity over TMP for the microfiltration module (Figure 5.5a), it is visually apparent from the raw data set in Figure 5.3 that fouling rate increases more rapidly at TMP values over 4 kPa. For the ultrafiltration module, this is more apparent (Figure 5.5b) with a steep increase noted after 5 kPa. The results suggest that fouling layer exerts a greater influence at TMP greater than 4 kPa for this particular feed.

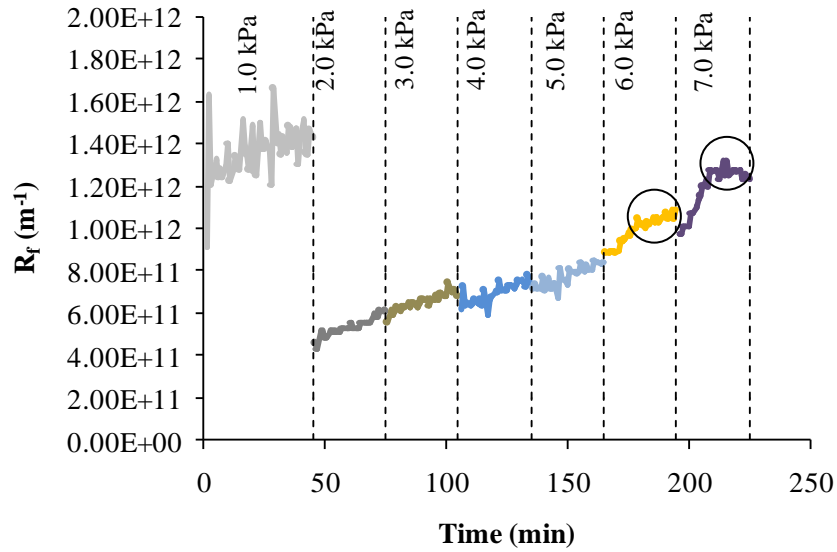


Figure 5.4: Fouling resistance (R_f) as a function of TMP over progressive increases in TMP for the Polymem UF module during Phase I. The encircled areas represent the asymptote of R_f for a particular TMP step.

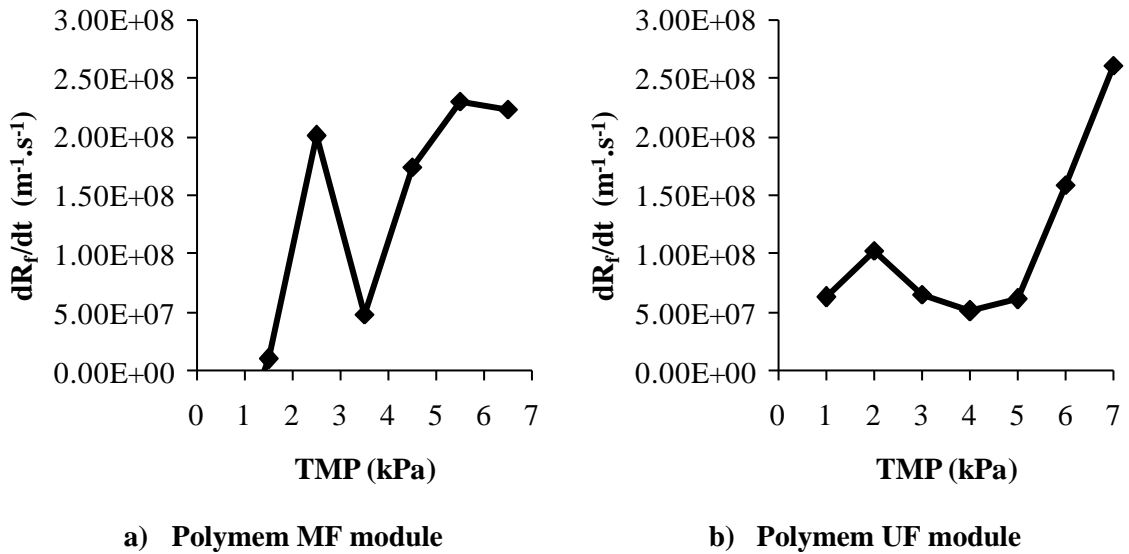


Figure 5.5: Fouling velocity (or fouling rate) for Polymem MF and UF modules as a function of TMP during Phase I. The points were calculated by from the slope of R_f over filtration time. Outliers have been excluded from plot.

The *practical approach* was used to evaluate fouling in terms of permeability before and after filtration. This was determined by the performing clean water flux determination before and after fouling. (Figure 5.6) The permeability of the virgin Polymem module was $4.0 \text{ L.m}^{-2}.\text{h}^{-1}.\text{kPa}^{-1}$ ($400 \text{ L.m}^{-2}.\text{h}^{-1}.\text{bar}^{-1}$). After fouling, this was reduced by 16% to $3.41 \text{ L.m}^{-2}.\text{h}^{-1}.\text{kPa}^{-1}$ ($341 \text{ L.m}^{-2}.\text{h}^{-1}.\text{bar}^{-1}$). By simply placing the module under running tap water, the permeability of the module was restored beyond its original virgin state at a higher value ($4.79 \text{ L.m}^{-2}.\text{h}^{-1}.\text{kPa}^{-1}$ or $479 \text{ L.m}^{-2}.\text{h}^{-1}.\text{bar}^{-1}$; data rounded to three-significant numbers). It is unsure why the permeability increased to a higher level than the virgin state but it was postulated that improper removal of membrane storage fluid or other contaminants in the membrane system may have been present during the first clean water run.

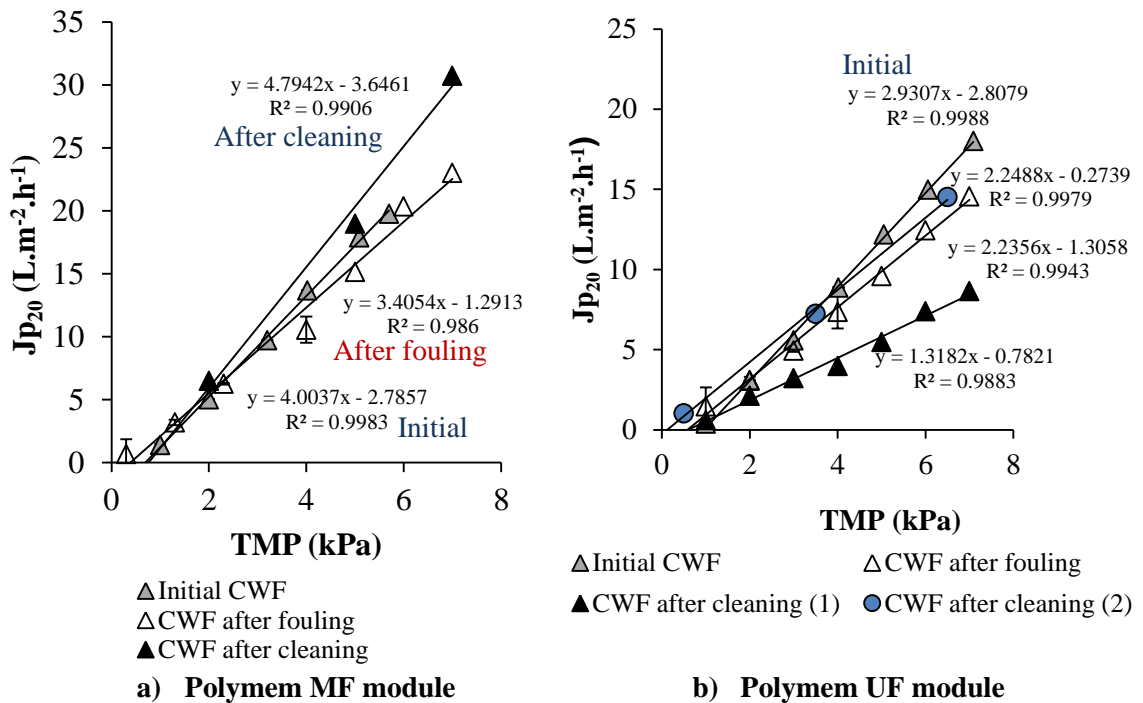


Figure 5.6: Variation of clean water permeate flux (CWF) with TMP during Phase I for a) Polymem MF module and b) Polymem UF module. The data points (Δ) represent the average clean water flux over a specific TMP whilst the error bars represent the standard deviation for a specific period. In some instances, the error bars are too small to be visible.

For the Polymem UF module, the permeability of the virgin module was $2.93 \text{ L.m}^{-2}.\text{h}^{-1}.\text{kPa}^{-1}$ ($293 \text{ L.m}^{-2}.\text{h}^{-1}.\text{bar}^{-1}$). After effluent filtration, permeability decreased by 24% to $2.24 \text{ L.m}^{-2}.\text{h}^{-1}.\text{kPa}^{-1}$ ($224 \text{ L.m}^{-2}.\text{h}^{-1}.\text{bar}^{-1}$). Clean water flux determination after tap water cleaning revealed that the permeability of the module had been further reduced to 55% of its original permeability. To validate the results, a second cycle of tap water cleaning was performed and a repeat of the

clean water flux determination performed. The results showed that the subsequent cleaning restored permeability close to that of the initial permeability [$2.23 \text{ L.m}^{-2}.\text{h}^{-1}.\text{kPa}^{-1}$ ($223 \text{ L.m}^{-2}.\text{h}^{-1}.\text{bar}^{-1}$)] with a 23% reduction in permeability observed from initial clean water flux to last one. Thus, removable fouling accounted for nearly 80% of the fouling with approximately 20% irremovable and/or irreversible fouling.

5.1.3.2 Phase III Effluent

During Phase III, the average feed wastewater COD concentration of the laboratory ABR was $1560 \pm 433 \text{ mg/L}$ with an average effluent COD of $310 \pm 75 \text{ mg/L}$ exiting the reactor. The variation of flux with constant TMP during this phase is shown in Figure 5.7.

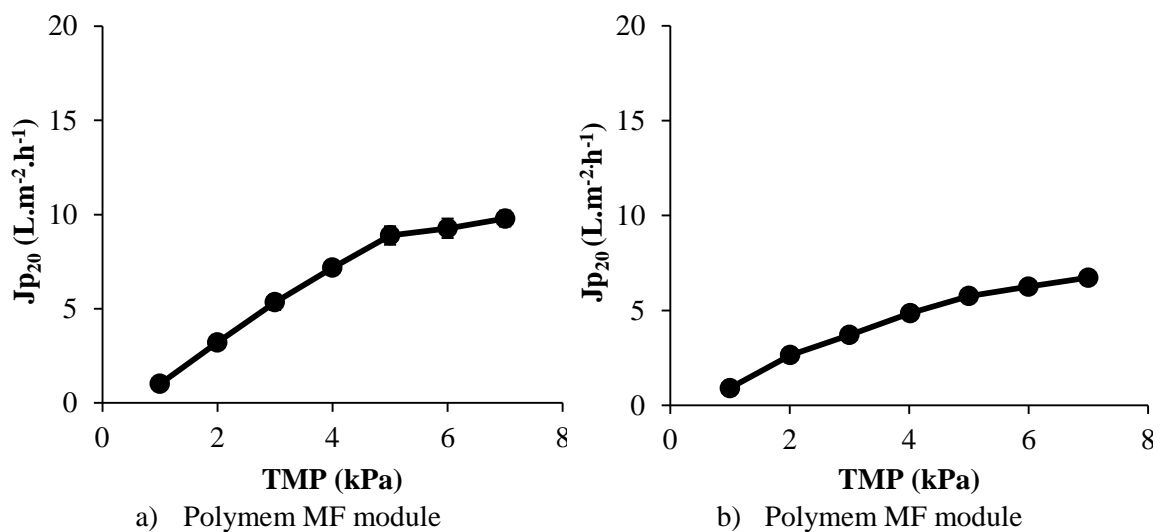


Figure 5.7: Variation of flux with pressure during Phase III for a) flux-TMP graph of the Polymem MF module and b) flux-TMP graph of the Polymem UF module. Each data point (●) represents the average flux over each pressure step. The error bars represent the standard deviation for each TMP step. In some instances, the error bars are too small to be visible.

As with Phase I effluent, the flux for both Polymem modules asymptotes towards the *limiting flux* but never actually reaches a flux independent plateau. For the Polymem microfiltration module, the *limiting flux* does not occur below $12 \text{ L.m}^{-2}.\text{h}^{-1}$ at TMP less than 6 kPa. At pressures below 4 kPa, there is a linear increase in the permeate flux with pressure. For the Polymem ultrafiltration module, the *limiting flux* was not observed below $7 \text{ L.m}^{-2}.\text{h}^{-1}$ at TMP less than 6 kPa.

The fouling resistance for Polymem microfiltration and ultrafiltration modules as a function of time for Phase III effluent are presented in Figure 5.8 and Figure 5.9, respectively.

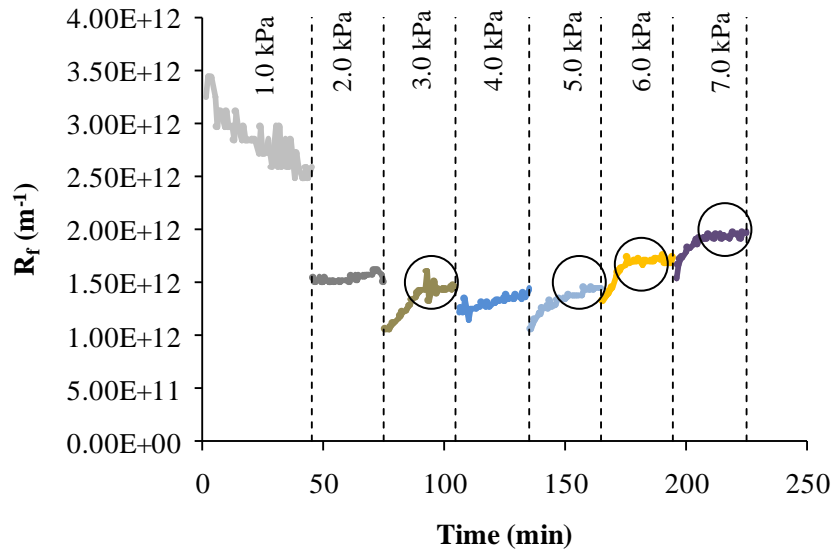


Figure 5.8: Fouling resistance (R_f) as a function of TMP over progressive increases in TMP for the Polymem MF module during Phase III. The encircled areas represent the asymptote of R_f for a particular TMP step.

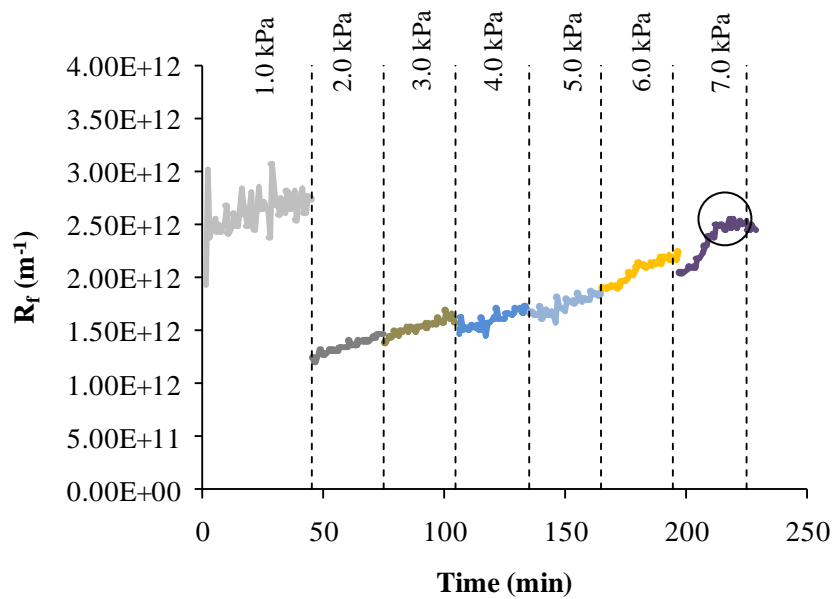


Figure 5.9: Fouling resistance (R_f) as a function of TMP over progressive increases in TMP for the Polymem UF module during Phase III. The encircled area represents the asymptote of R_f for a particular TMP step.

For the Polymem microfiltration module, the R_f pattern was similar to that of Phase I effluent with R_f decreasing at 1 kPa TMP followed by a gradual increase as time progressed (and a higher TMP). The fouling resistance in the Polymem ultrafiltration module, on the other hand, gradually decreased at the same TMP (1 kPa). Moreover, there were differences in how the R_f established itself at the onset of the next (and higher) TMP-step. Whilst there was continuity in which the R_f increased between TMP-steps for the ultrafiltration module, the onset of the next TMP-step in the microfiltration module resulted in a slight decrease in R_f followed by an asymptote towards a stable fouling rate. This pattern was shown only in the highest TMP applied for the ultrafiltration module (7 kPa) and was not included in the fouling velocity calculations in Figure 5.10.

The rate at which fouling occurs for both modules is shown in Figure 5.10 a and b, respectively. The diagrams did not include those points on previous graphs (Figure 5.8 and Figure 5.9) which asymptote towards a constant R_f .

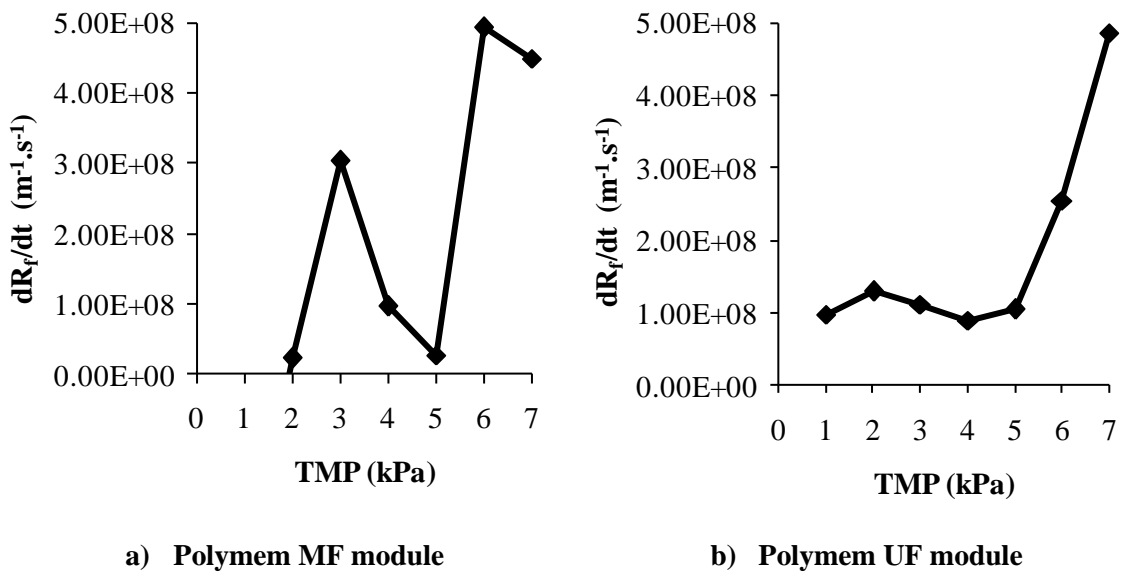


Figure 5.10: Fouling velocity (or fouling rate) as a function of TMP for Polymem MF and UF modules during Phase III. The points were calculated by determining the slope of R_f over filtration time. Outliers have been excluded from plot.

With respect to the microfiltration module, no clear pattern can be observed from fouling velocity over TMP. A negative fouling velocity was observed under 2 kPa as fouling was shown to decrease during this filtration period (refer to Figure 5.8) and was thus not included in Figure 5.10. For the Polymem ultrafiltration module, fouling rate was similar from 1 to 6 kPa with a sharp increase noted afterwards.

Clean water flux determination was performed on both modules before and after effluent filtration. The graphs are presented in Figure 5.11. The permeability of microfiltration module was $4.27 \text{ L.m}^{-2}.\text{h}^{-1}.\text{kPa}^{-1}$ ($427 \text{ L.m}^{-2}.\text{h}^{-1}.\text{bar}^{-1}$) before effluent filtration. Fouling reduced the permeability by 8% to $3.93 \text{ L.m}^{-2}.\text{h}^{-1}.\text{kPa}^{-1}$ ($393 \text{ L.m}^{-2}.\text{h}^{-1}.\text{bar}^{-1}$). Tap water washing restored the permeability of the module to $4.36 \text{ L.m}^{-2}.\text{h}^{-1}.\text{kPa}^{-1}$ ($436 \text{ L.m}^{-2}.\text{h}^{-1}.\text{bar}^{-1}$). Thus removable fouling accounted for 100% of fouling with no irremovable fouling.

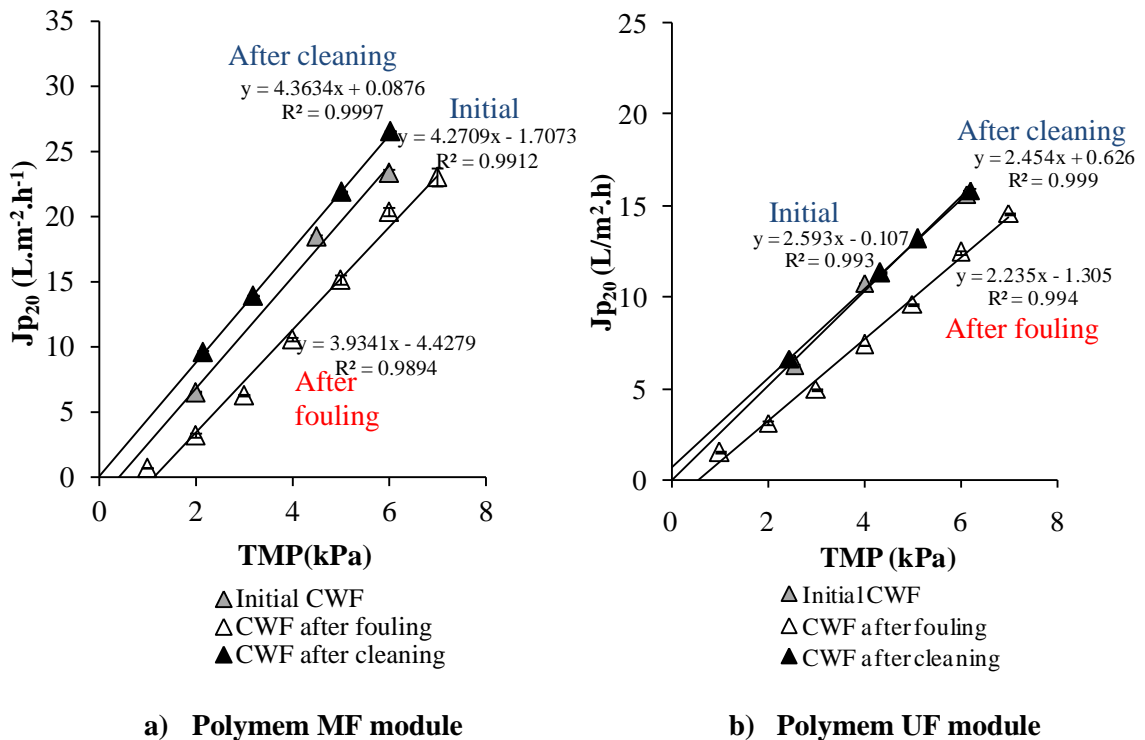


Figure 5.11: Variation of clean water permeate flux (CWF) with TMP during Phase III for a) Polymem MF module and b) Polymem UF module. The data points (Δ) represent the average clean water flux over a specific TMP whilst the error bars represent the standard deviation for a specific. In some instances, the error bars are too small to be visible.

For the ultrafiltration module, the initial permeability was reduced from $2.59 \text{ L.m}^{-2}.\text{h}^{-1}.\text{kPa}^{-1}$ ($259 \text{ L.m}^{-2}.\text{h}^{-1}.\text{bar}^{-1}$), to $2.24 \text{ L.m}^{-2}.\text{h}^{-1}.\text{kPa}^{-1}$ ($224 \text{ L.m}^{-2}.\text{h}^{-1}.\text{bar}^{-1}$), representing a 14% decrease in permeability. Tap water cleaning restored permeability to near its original state with only a slight reduction (5%) observed between initial permeability and after cleaning. Thus, only a small portion of fouling is irremovable (5%).

5.1.3.3 Phase V Effluent

During Phase V, the average feed COD entering the ABR was 1 500 mg/L. An average effluent COD of 457 ± 72 mg/L was achieved after digestion. The flux-TMP curves for Polymem microfiltration and ultrafiltration modules are presented in Figure 5.12. For the Polymem microfiltration module, the *limiting flux* was approximately $8 \text{ L.m}^{-2}.\text{h}^{-1}$ at TMP over 2 kPa. However, the transition to the *limiting flux* and the TMP at which it occurs could not be deduced from the flux-TMP graph. An initial linear increase in the flux is not observed at this phase with flux remaining relatively constant at pressures above 2.5 kPa. The grey rectangle (\square) indicates the area in which the *transition flux* could occur (Figure 5.12). For the Polymem ultrafiltration module, the *limiting flux* was determined to be approximately $7.5 \text{ L.m}^{-2}.\text{h}^{-1}$. The TMP at which this plateau is reached is approximately 5 kPa.

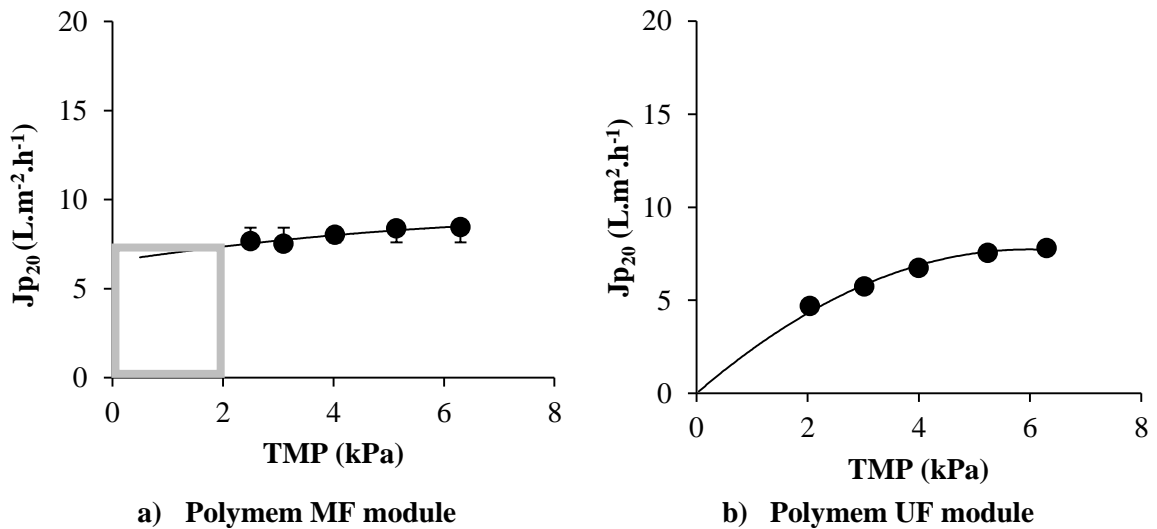


Figure 5.12: Variation of flux with pressure during Phase V for a) flux-TMP graph of the Polymem MF module and b) flux-TMP graph of the Polymem UF module. Each data point (\bullet) represents the average flux over each pressure step. The error bars represent the standard deviation for each TMP step. In some instances, the error bars are too small to be visible.

The R_f during each TMP is plotted as a function of time for Polymem microfiltration and ultrafiltration modules in Figure 5.13 and Figure 5.14, respectively. For the microfiltration module, it can be observed from Figure 5.13 that the fouling layer progressively builds up after each TMP-step increase. In contrast to previous experiments, there is no levelling of R_f during a particular TMP step. The pattern in the Polymem ultrafiltration module was similar to the microfiltration one with R_f steadily increasing during and after each TMP-step.

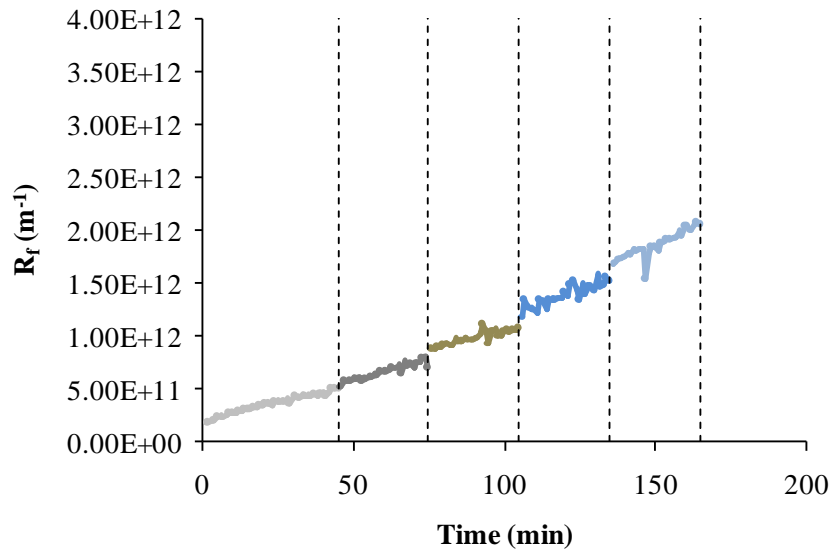


Figure 5.13 Fouling resistance (R_f) as a function of TMP over progressive increases in TMP for the Polymem UF module during Phase V.

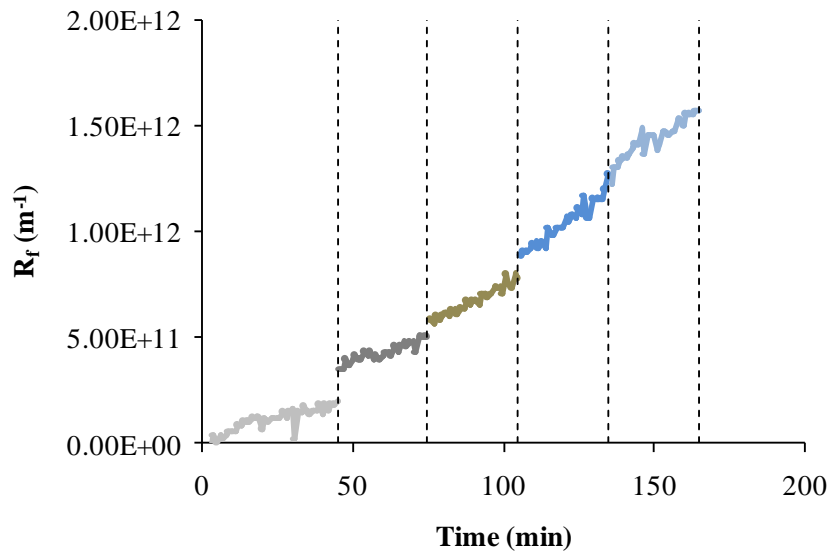


Figure 5.14: Fouling resistance (R_f) as a function of TMP over progressive increases in TMP for the Polymem UF module during Phase V.

Figure 5.15 presents the fouling velocity of the microfiltration and ultrafiltration modules treating an ABR with an average COD concentration of approximately 500 mg/L. For the microfiltration module, the fouling rate increased rapidly after 4 kPa. In the ultrafiltration module, increases in a step-wise manner with each increment TMP increase.

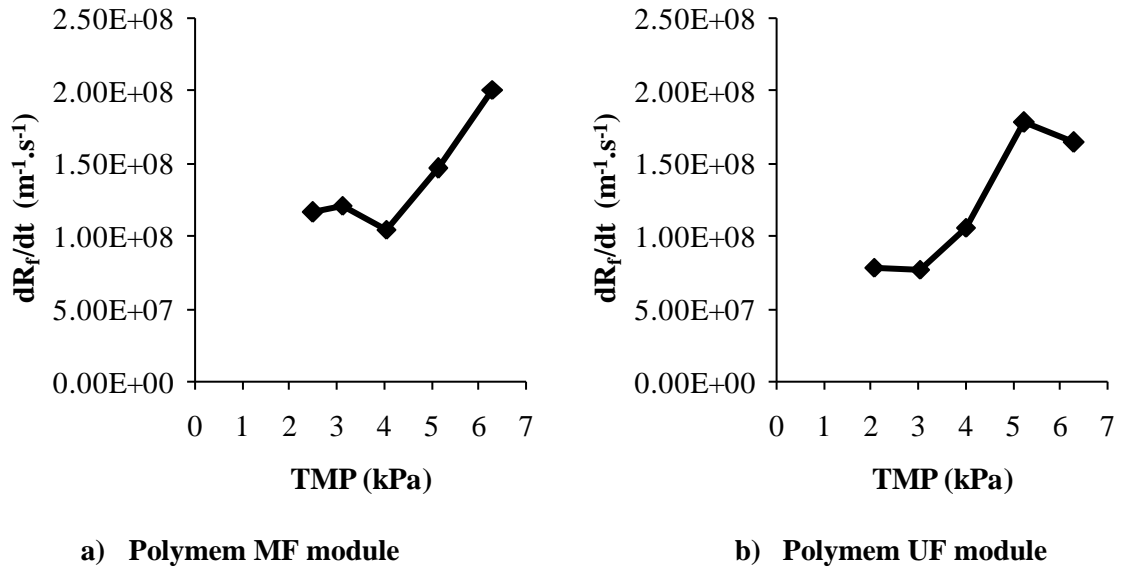


Figure 5.15: Fouling velocity (or fouling rate) for Polymem MF and UF modules as a function of TMP during Phase V. The points were calculated by determining the slope of R_f over filtration time.

The permeability of the modules was determined by clean water filtration before and after fouling. The results revealed a similar pattern as to previous experiments in which the initial permeability is restored after cleaning the module under a tap (Figure 5.16a). For the microfiltration module, permeability decreased by 31% from $4.36 L.m^{-2}.h^{-1}.kPa^{-1}$ ($436 L.m^{-2}.h^{-1}.bar^{-1}$) to $3.00 L.m^{-2}.h^{-1}.kPa^{-1}$ ($300 L.m^{-2}.h^{-1}.bar^{-1}$). After tap water rinsing, membrane permeability was restored to its initial state (Figure 5.16a). In the ultrafiltration module, fouling reduced the permeability of the membrane by 24%. Cleaning with tap water restored membrane permeability up to 84% of its initial permeability [$2.07 L.m^{-2}.h^{-1}.kPa^{-1}$ ($207 L.m^{-2}.h^{-1}.bar^{-1}$) versus $2.46 L.m^{-2}.h^{-1}.kPa^{-1}$ ($246 L.m^{-2}.h^{-1}.bar^{-1}$)]. The results indicate that fouling during the TMP-step experiments was largely removable.

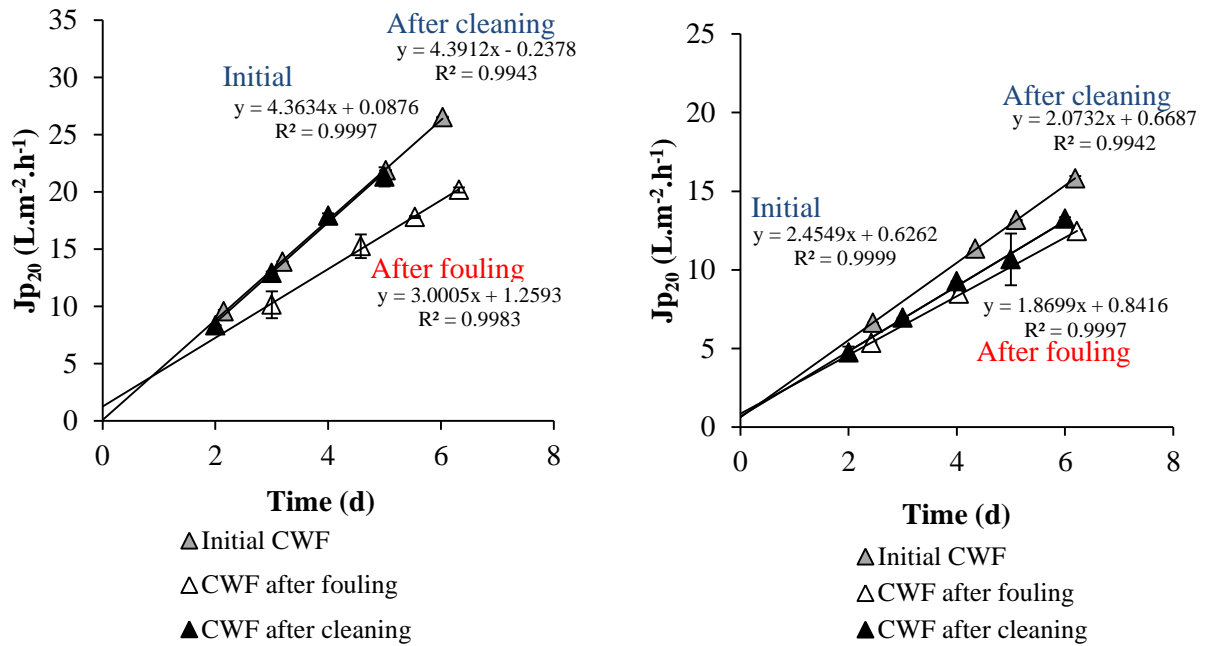


Figure 5.16: Variation of clean water permeate flux (CWF) with TMP during Phase V for a) Polymem MF module and b) Polymem UF module. The data points (Δ) represent the average clean water flux over a specific TMP whilst the error bars represent the standard deviation for a specific period. In some instances, the error bars are too small to be visible.

5.1.3.4 Phase VI Effluent

During Phase VI, the ABR treated a high-strength feed with an average total COD concentration of 3 000 mg/L. The effluent had an average total COD concentration of $1\,408 \pm 205$ mg/L. The TMP-step experiments performed on the effluent are presented in Figure 5.17. For the Polymem microfiltration module, the *limiting flux* was found to be approximately $10 \text{ L.m}^{-2}.\text{h}^{-1}$ at TMP exceeding 2 kPa. The pressure at which the flux is independent on TMP is lower than that those approximated during Phase I and III. For the ultrafiltration module, the flux asymptotes towards a *limiting flux* at TMP exceeding 6 kPa.

Figure 5.18 presents the R_f with progressive TMP increases over time for the microfiltration module. The R_f decreases with time for TMPs step 2 to 5 kPa towards indicating that there an equilibrium-type effect may occur at the fouling layer-bulk fluid interface.

Figure 5.19 presents the R_f with progressive TMP increases over time for the ultrafiltration module. The R_f increases steadily increases from one TMP to the next. Unlike the

microfiltration module, there is no drop in R_f during incremental TMP increases. The results indicate that fouling layer build-up differs between the two modules.

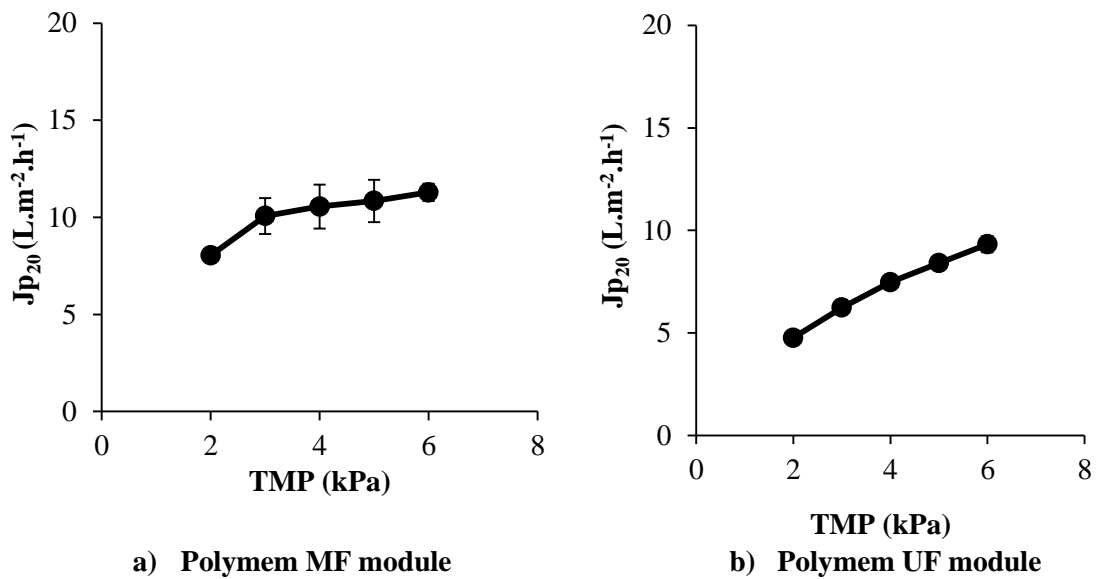


Figure 5.17: Variation of flux with pressure during Phase VI for a) flux-TMP graph of the Polymem MF module and b) flux-TMP graph of the Polymem UF module. Each data point (●) represents the average flux over each pressure step. The error bars represent the standard deviation for each TMP step. In some instances, the error bars are too small to be visible.

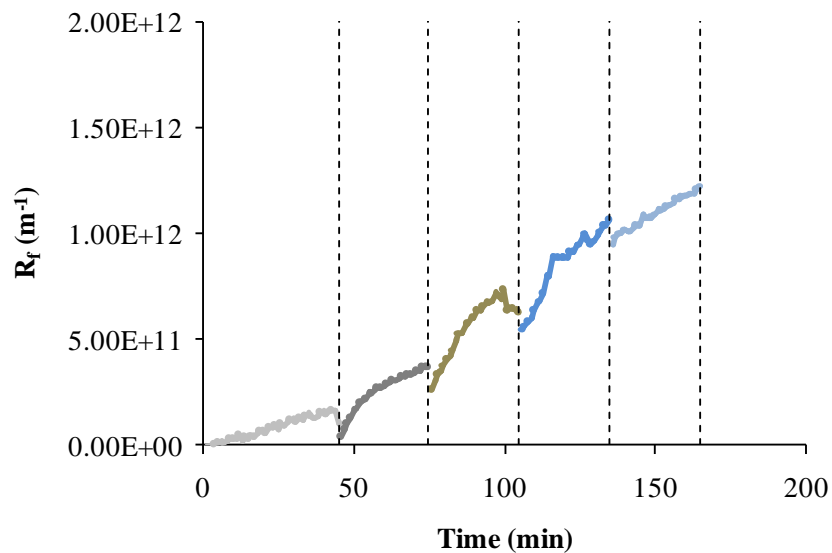


Figure 5.18: Fouling resistance (R_f) as a function of TMP over progressive increases in TMP for the Polymem MF module during Phase VI.

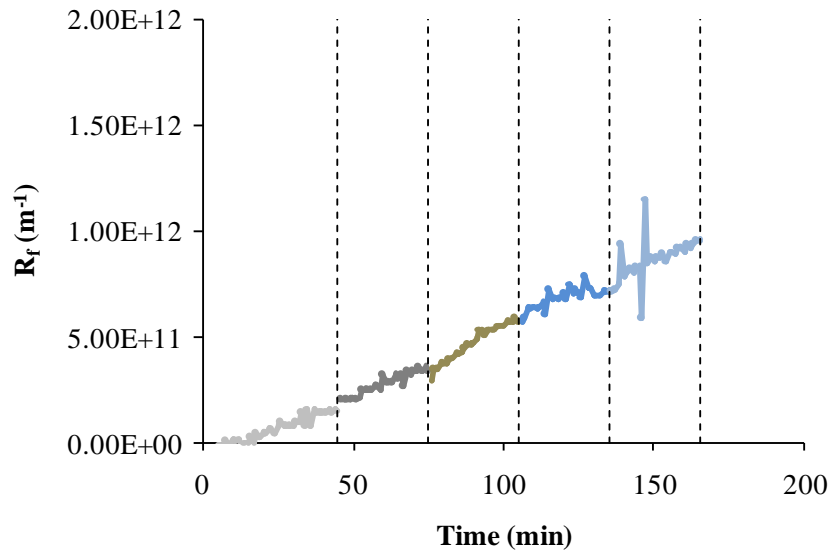


Figure 5.19: Fouling resistance (R_f) as a function of TMP over progressive increases in TMP for the Polymem UF module during Phase VI.

The fouling velocity of the microfiltration and ultrafiltration modules treating an ABR effluent with an average COD concentration of approximately 1 500 mg/L is presented in Figure 5.20.

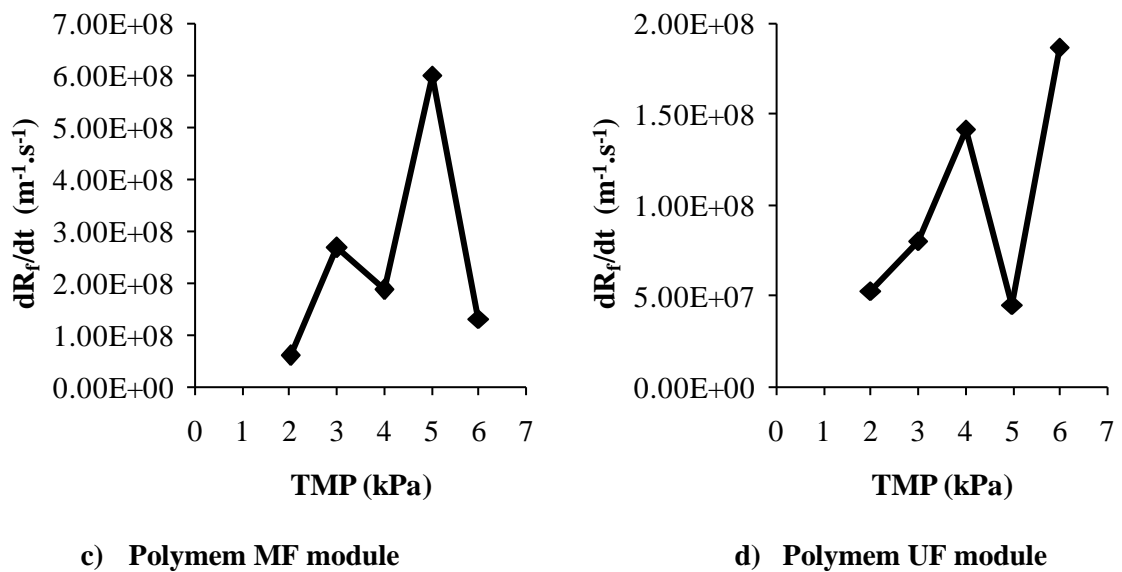


Figure 5.20: Fouling velocity (or fouling rate) for Polymem MF and UF modules as a function of TMP during Phase VI. The points were calculated by determining the slope of R_f over filtration time.

The fouling rate in the microfiltration module is much faster than the ultrafiltration module during batch tests at high membrane feed concentrations with peaks in fouling velocity occurring after 4 kPa.

The permeabilities of both modules before and after effluent filtration are presented in Figure 5.21. With the microfiltration module, permeability decreased from 4.39 L.m⁻².h⁻¹.kPa⁻¹ (439 L.m⁻².h⁻¹.bar⁻¹) to 3.61 L.m⁻².h⁻¹.kPa⁻¹ (361 L.m⁻².h⁻¹.bar⁻¹) (17% reduction in permeability after fouling). For the ultrafiltration module, fouling decreased permeability by 16% from 2.47 L.m⁻².h⁻¹.kPa⁻¹(247 L.m⁻².h⁻¹.bar⁻¹) to 2.07 L.m⁻².h⁻¹.kPa⁻¹ (207 L.m⁻².h⁻¹.bar⁻¹).

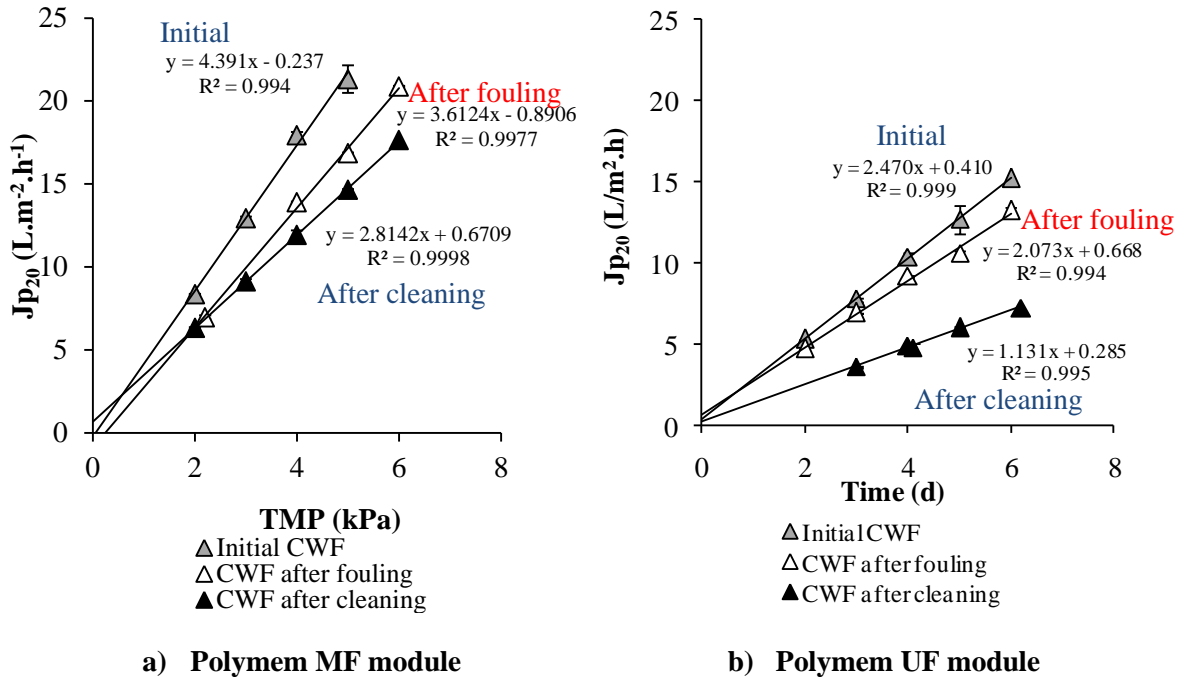


Figure 5.21: Variation of clean water permeate flux (CWF) with TMP during Phase VI for a) Polymem MF module and b) Polymem UF module. The data points (Δ) represent the average clean water flux over a specific TMP whilst the error bars represent the standard deviation for a specific period. In some instances, the error bars are too small to be visible.

However, unlike previous clean water flux determination experiments, the cleaning procedure did not restore the permeability to near its original state in both modules. In fact, the permeability after fouling was higher than that after cleaning. The decline in permeability after cleaning was hypothesised to be the result of prolonged storage. After determining the permeability after fouling, the module was cleaned with tap water and placed immediately into storage solution. The permeability after cleaning was then determined at the beginning of the next set of filtration experiments approximately 5 months later.

5.1.4 SUMMARY OF TMP-STEP EXPERIMENTS

Figure 5.22 shows a comparison between permeate fluxes over TMP at different COD concentrations. No conclusive evidence was observed on the relationship between the permeate flux and COD with flux profiles similar among modules at the different COD ranges tested.

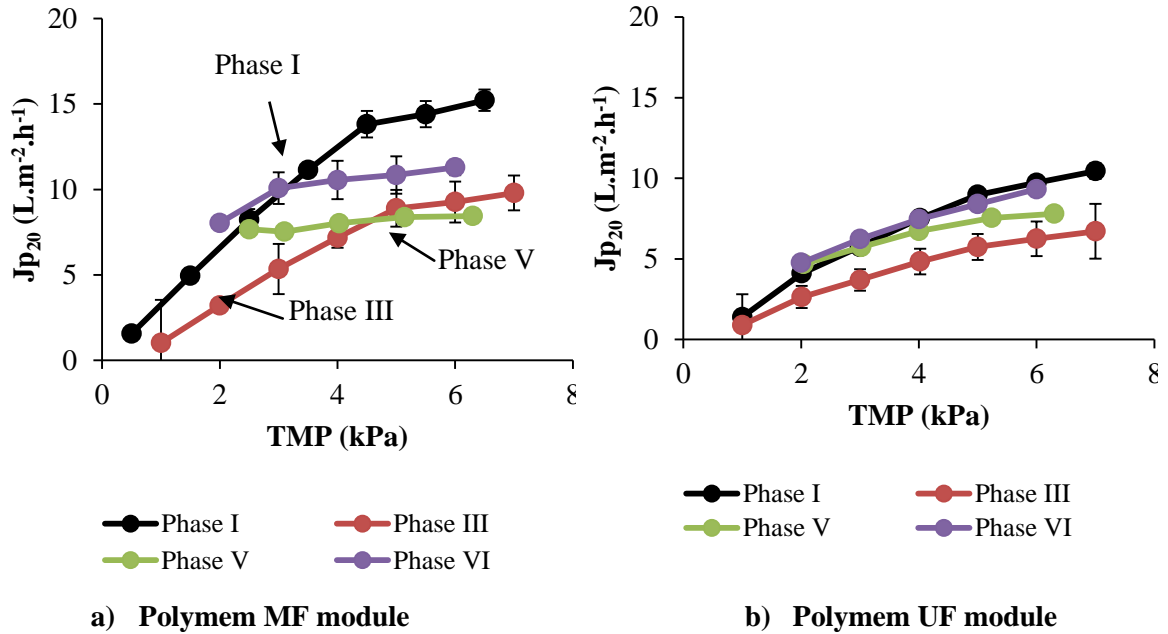


Figure 5.22: Permeate versus TMP for Polymem microfiltration and ultrafiltration modules during TMP step experiments at different feed COD concentrations. Each point represents the average flux over each TMP whilst error bars represent the standard deviation. In some instances, the error bars are too small to be noticed.

Moreover, the hypothesis that operation below the limiting flux could result in less fouling could not be evaluated as this threshold could not be reached at most of the TMP tested. However, valuable data on maximum fluxes that could be achieved at ultra-low hydrostatic pressures (less than 6 kPa) was reported. For microfiltration modules, this was approximately 15 L.m⁻².h⁻¹ whilst a maximum flux of approximately 10 L.m⁻².h⁻¹ could be achieved in the ultrafiltration modules, respectively). This result however only applies to effluents with a COD concentration below 1 500 mg/L.

The evolution of fouling resistance during each phase is summarised for both modules in Figure 5.23. In both modules, higher COD filtration results in a more pronounced effect of the TMP on the fouling resistance. At effluent COD concentrations below 400 mg/L, fouling is

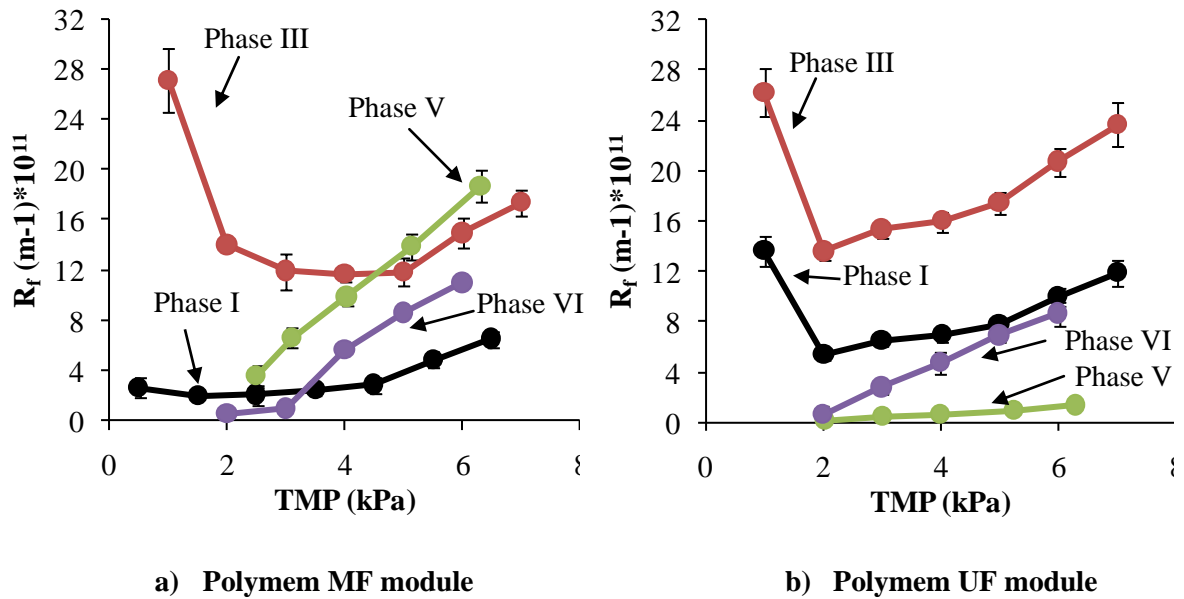


Figure 5.23: Plot of average fouling resistance (R_f) versus TMP for Polymem microfiltration and ultrafiltration modules. The errors bars represent the standard deviation for each TMP step.

relatively constant between 2 and 4 kPa. However, at COD concentrations above 400 mg/L (Phases V and VI), there is a linear increase in fouling resistance with pressure implying that fouling is progressive under such conditions. Based on the results, filtration with hollow-fibre modules (Polymem) is best suited for ABR effluent COD concentrations below 400 mg/L. Moreover, fixed TMP operation should be performed at pressures below 4 kPa to limit excessive foulant build-up.

Perhaps the most important result obtained from these tests is the recoverability of permeability at various feed conditions with only a simple mechanical wash required between experiments (Figure 5.24). Figure 5.25 presents the relationship between the ABR effluent total COD in each phase and membrane permeability. The results show that the total COD had little effect on permeability decrease and suggests that most of the foulants were removable and did not become lodged and/or adsorbed into the membrane surface.

The change in membrane permeability over all experiments is presented in Figure 5.26. In the microfiltration module, fouling was not severe with permeability recovering to near original pre-filtration state after each series of experiments (Figure 5.26a). Fouling was largely reversible with only a 30% reduction in permeability observed across all phases. A single chemical cleaning event occurred between Phase I and Phase III of the TMP-step experiments.



- a) Module is removed from housing b) The fouling layer is easily washed out with tap water c) Cleaned module immersed in distilled water

Figure 5.24: Photographs of the Polymem ultrafiltration module being cleaned after fouling experiment.

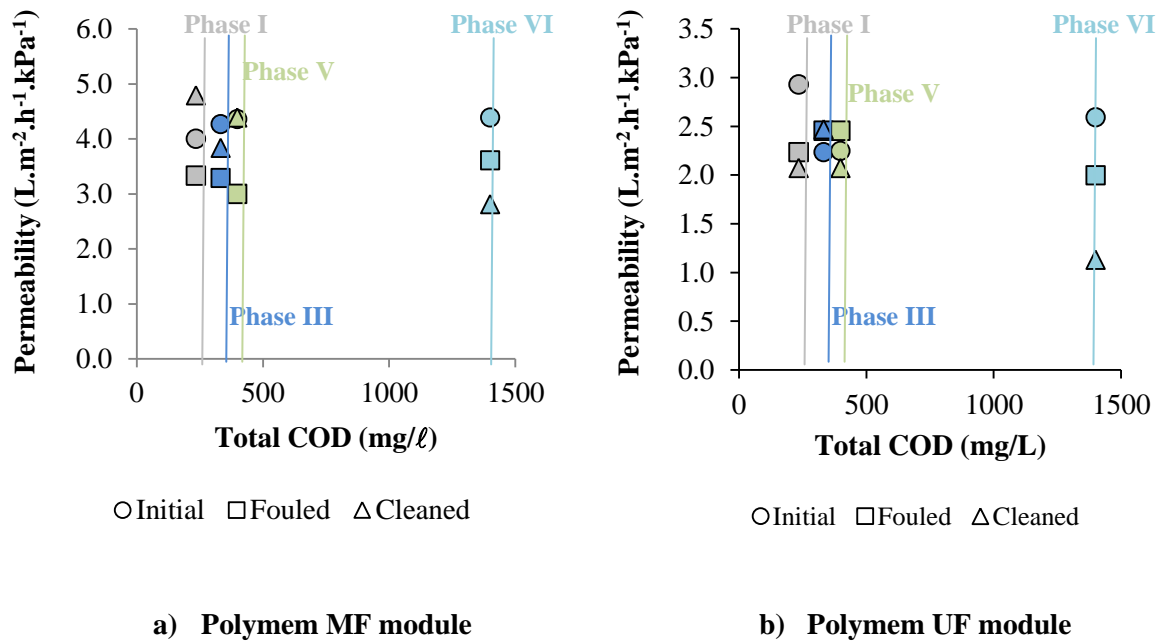


Figure 5.25: Relationship between membrane permeability and total COD during each series of experiments for the Polymem microfiltration and ultrafiltration module.

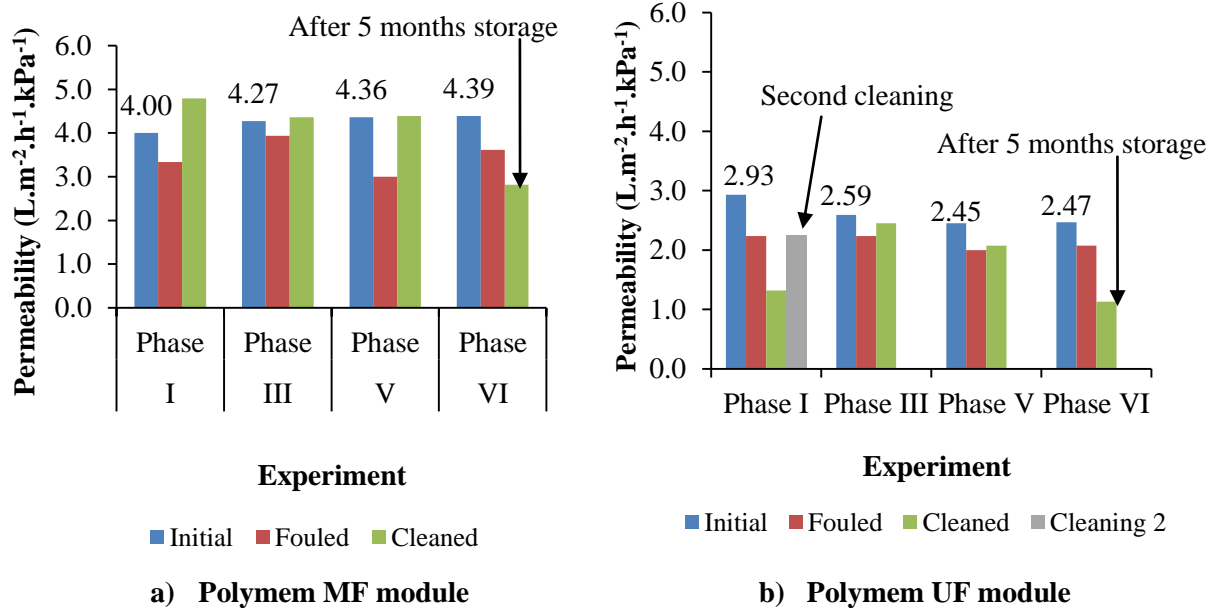


Figure 5.26: Comparison of membrane permeability of the Polymem microfiltration and ultrafiltration module during various phases of membrane testing.

During this period, a short-term filtration experiment was performed at fixed TMP to evaluate the removal efficiency of the module (section 5.2). Although permeate reduction was not below 80% of its original level, chemical cleaning was still employed to bring permeability to its pre-filtration state.

Permeability recovery in the ultrafiltration module showed a similar pattern as the microfiltration module (Figure 5.26b). Fouling was shown to be largely reversible with only tap water scouring used to restore permeability to near its ‘virginal’ state. The results imply that foulants may be loosely-bound particulates given the intrinsic rejection properties of the modules.

During Phase I, a second set of physical cleaning under tap water was required as the permeability of cleaned ultrafiltration module was lower than that measured immediately after fouling. Another observation that could not be explained was the drastic decline in permeability after cleaning in the last phase. As mentioned earlier, the clean water flux measurements after the cleaning procedure was determined after the module was stored in a chemical storage solution for 5 months (section 5.3). A similar observation was made with respect to the microfiltration module. The results indicate that the permeability of the modules is affected by long-term storage in the recommended chemical solution.

5.2 SHORT-TERM FILTRATION AT CONSTANT TMP

This section presents the results from short-term Polymem filtration experiments conducted at constant TMP and using effluent from the laboratory ABR treating diluted VIP sludge. The aims of this experiment are presented in section 5.2.1. The methodology used in this experiment is detailed in section 5.2.2. Section 5.2.3 presents the results and the discussion from this set of experiments whilst the conclusions are presented in section 5.2.4.

5.2.1 INTRODUCTION

A short-term membrane experiment of less than 10 h was used to examine fouling behaviour at low fixed pressure filtration of 4 kPa (400 mm water head). The hydrostatic driving force of 4 kPa was used in this experiment based on results obtained from section 5.1 which showed that operation below 4 kPa and 400 mg COD/L may result in reasonable operation. The purpose of this series of experiments was to determine the treatment performance of the membrane (in terms of COD) and examine the evolution of fouling over a few hours.

5.2.2 METHODOLOGY

Membrane Feed

Effluent from the ABR treating diluted VIP sludge during Phase I was pumped directly from the effluent tank to the module.

Membrane Units

Polymem microfiltration and ultrafiltration modules were simultaneously operated over 4 h using a hydrostatic driving force of 400 mm (4 kPa). Clean water flux was performed before filtration according to the procedure described in section 5.1.

Data Acquisition and Interpretation

The mass of the permeate was recorded using an Ohaus Adventurer Pro balance. A timer was used to determine the length of the experiment. The temperature of the permeate was measured using a mercury thermometer. All measurements were manually recorded. The resistance-in-series model was used to calculate the permeate flux (refer to **Appendix III**).

Physico-Chemical Analyses

Total COD were performed according to the UCT Open Reflux COD Method for wastewater (Lakay *et al.*, 2000). The soluble COD was fractionated by filtering the effluent through Whatman 0.45 µm filters.

5.2.3 RESULTS AND DISCUSSION

Short-term filtration at constant TMP is presented in Figure 5.27. For both modules, a constant hydraulic driving force of 4 kPa (400 mm water head) was used for 4 h.

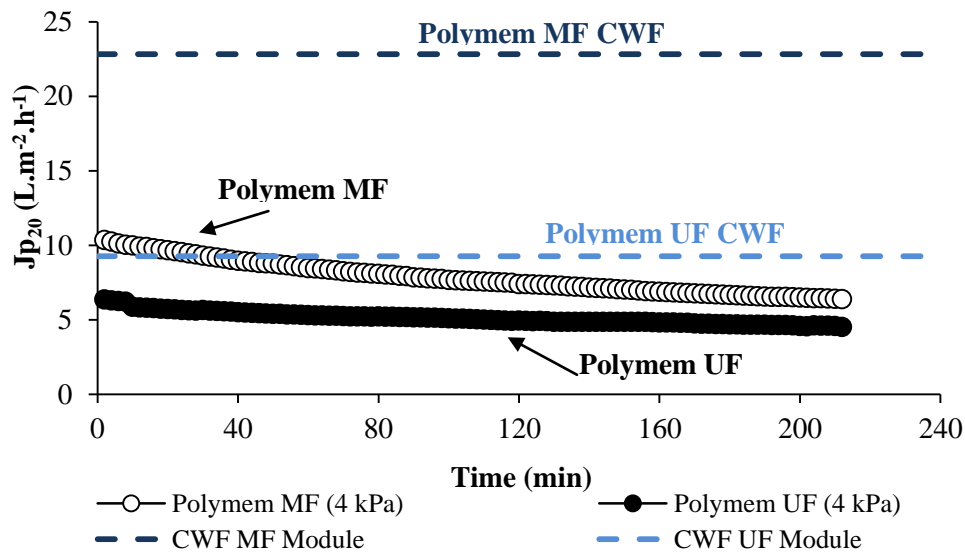


Figure 5.27: Variation in flux at a constant TMP of 4 kPa over 4h for Polymem MF and UF modules treating laboratory ABR effluent. The dashed lines (---) represent the calculated average clean water flux (CWF) before effluent filtration at 4 kPa.

The evolution of fouling was similar in both modules. The Polymem microfiltration module has a higher starting flux which gradually decreased during filtration. Permeate flux decreased from $11 L \cdot m^{-2} \cdot h^{-1}$ to $9 L \cdot m^{-2} \cdot h^{-1}$ during 1 h followed by a gradual flux decline to approximately $6 L \cdot m^{-2} \cdot h^{-1}$. The Polymem ultrafiltration module had a lower starting flux ($7 L \cdot m^{-2} \cdot h^{-1}$) than the microfiltration module peaking during the first 10 min of filtration, followed by a sharp decline to a plateau of approximately $5 L \cdot m^{-2} \cdot h^{-1}$ after 200 min. Interestingly, the microfiltration module had not reached this pseudo-steady-state after 4 h of filtration. The initial results implied that the permeate flux for both membranes could intersect over time. In such cases, the ultrafiltration module would be preferred over microfiltration for decentralised applications due to higher parameter removals, such as COD and indicator micro-organisms (based on the selectivity of the membrane pore size), at similar permeate rates.

Figure 5.28 presents the removal of COD through the entire laboratory plant (from feed tank to membrane permeate). The feed concentration to the ABR was $1\,304 \text{ mg/L}$. This was reduced to 234 mg/L through the ABR which amounted to COD removal of 82%. Membrane modules were able to further enhance COD reduction to 34 mg/L and 18 mg/L in microfiltration and

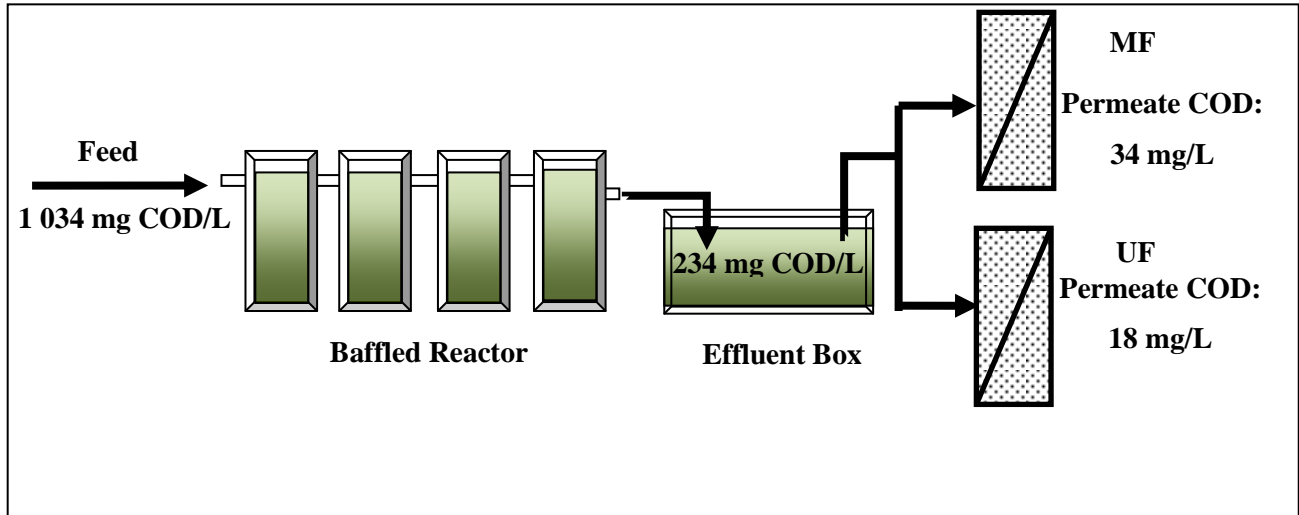


Figure 5.28: Schematic representation of the total COD concentration through the membrane coupled ABR during 4 h filtration.

ultrafiltration modules, respectively. This reduction was within the discharge limit for COD into surface water (DWAF, 1996).

Clean water flux tests were performed before and after effluent filtration to determine the effect of fouling. The results for microfiltration and ultrafiltration modules are presented in Figure 5.29a and b, respectively. The permeability for the microfiltration module was determined to be $4.79 \text{ L.m}^{-2}.\text{h}^{-1}.\text{kPa}^{-1}$ ($479 \text{ L.m}^{-2}.\text{h}^{-1}.\text{bar}^{-1}$) before effluent filtration. This was reduced to $3.29 \text{ L.m}^{-2}.\text{h}^{-1}.\text{kPa}^{-1}$ ($329 \text{ L.m}^{-2}.\text{h}^{-1}.\text{bar}^{-1}$) after fouling. Physical cleaning via tap washing restored membrane permeability to $3.84 \text{ L.m}^{-2}.\text{h}^{-1}.\text{kPa}^{-1}$ ($384 \text{ L.m}^{-2}.\text{h}^{-1}.\text{bar}^{-1}$) representing a 20% decline from the initial permeability. Chemical cleaning was employed to restore permeability to its 'virginal' state. A solution of 2 000 ppm chlorine was made and the module immersed in this solution for less than 2 h (as recommended by manufacturer). The module was then rinsed with tap and distilled water and stored in distilled water (instead of preservative solution). The permeability of chemically cleaned module was assessed at the beginning of Phase III TMP-step experiments and was found to be $4.27 \text{ L.m}^{-2}.\text{h}^{-1}.\text{kPa}^{-1}$ ($427 \text{ L.m}^{-2}.\text{h}^{-1}.\text{bar}^{-1}$) (6 months storage).

The initial permeability of the ultrafiltration module was determined to be $2.25 \text{ L.m}^{-2}.\text{h}^{-1}.\text{kPa}^{-1}$ ($225 \text{ L.m}^{-2}.\text{h}^{-1}.\text{bar}^{-1}$) before effluent filtration. After filtration, this was reduced to $1.85 \text{ L.m}^{-2}.\text{h}^{-1}.\text{kPa}^{-1}$ ($185 \text{ L.m}^{-2}.\text{h}^{-1}.\text{bar}^{-1}$). After physical cleaning, membrane permeability returned above the initial permeability [$2.59 \text{ L.m}^{-2}.\text{h}^{-1}.\text{kPa}^{-1}$ ($259 \text{ L.m}^{-2}.\text{h}^{-1}.\text{bar}^{-1}$)]. The results indicated that membrane fouling is removable with only physical cleaning required to restore membrane permeability.

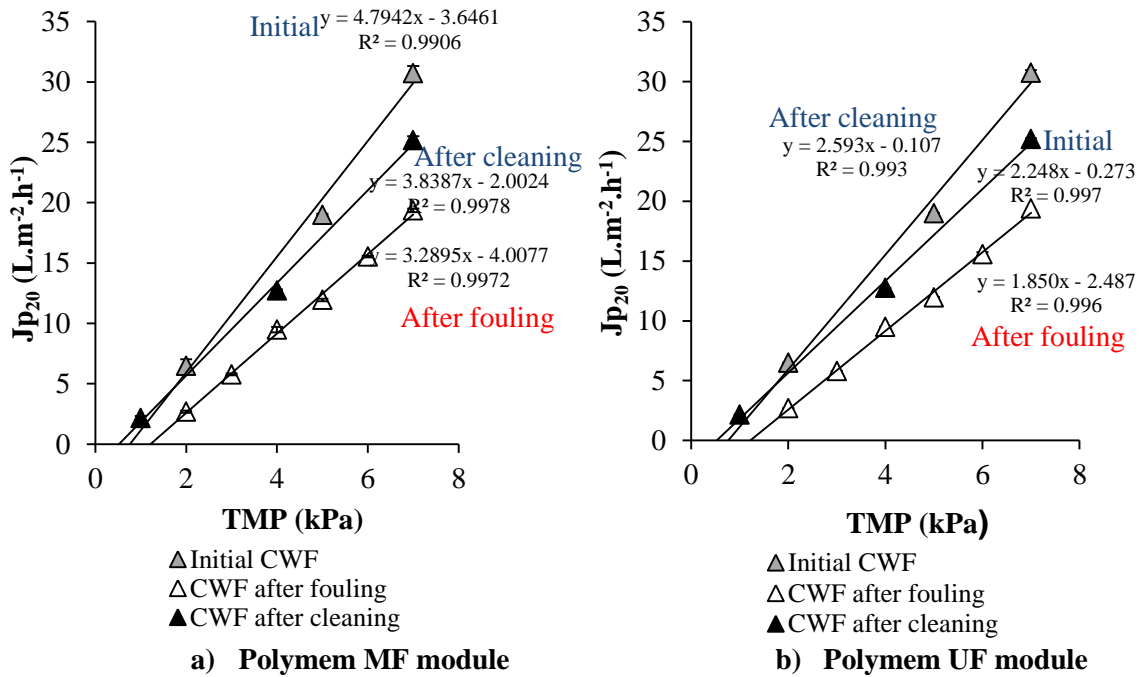


Figure 5.29: Variation of clean water permeate flux (CWF) with TMP during Phase VI for a) Polymem MF module and b) Polymem UF module. The data points (Δ) represent the average clean water flux over a specific TMP whilst the error bars represent the standard deviation for a specific period.

5.2.4 CONCLUSIONS

The short-term filtration results suggest that stable filtration is achieved during 4 h filtration intervals in both modules. After an initial decline, the flux reaches a stabilisation period of operation. With the ultrafiltration module, this is achieved at a faster rate than the microfiltration one. Fouling does occur as indicated by the difference in clean water flux at the beginning of the experiments and after effluent filtration. Moreover, fouling was largely removable as indicated by restoration of permeability after filtration.

Total COD is reduced from 1 304 mg/L to 234 mg/L in the effluent and subsequently further reduced through filtration to under 40 mg/L. This amounts to a COD removal efficiency of 82% from feed to effluent and greater than 85% from effluent to permeate. The ABR is able to produce a wastewater with a low COD concentration when coupled to membrane filtration. Moreover, it is anticipated that complete bacterial and parasite removal can be achieved using these modules (based on their MWCO) whilst allowing the passage of nutrients in the effluent [which has been shown not to be detrimental to soil conditions in a parallel study (Bame *et al.*, 2009)]. Membrane filtration therefore has the potential to overcome the major

limitation of ABR technology in sanitation, that is, to provide sufficient effluent polishing to an acceptable discharge limit.

5.3 LONG-TERM FILTRATION AT CONSTANT TMP

This section presents describes the long-term membrane filtration experiments with the Polymem ultrafiltration module conducted at constant TMP. Laboratory ABR effluent from Phase VII was used as the membrane feed. Section 5.3.1 presents the aims of this section. The methodology is presented in section 5.3.2. The results from this section are discussed in 5.3.3 and the conclusion from this series of experiments is presented in section 5.3.4. This set of experiments was performed simultaneously with the flat-sheet unit containing Kubota and fabric membrane modules to compare membrane performance between the two module types (hollow-fibre versus flat-sheet) (section 6.1).

5.3.1 INTRODUCTION

Long-term constant pressure filtration was performed with Polymem ultrafiltration module with the aim of establishing how long the membranes can be operated before cleaning is required and evaluating the flux-time relationship over time.

5.3.2 METHODOLOGY

Membrane Feed

Effluent from the laboratory ABR treating diluted VIP sludge during Phase VII was pumped directly from the effluent tank to the membrane unit. Only the Polymem ultrafiltration module was operated over a long-term period during Phase VII as there was insufficient effluent to operate the flat-sheet system simultaneously with both hollow-fibre modules (**Chapter 6**).

Membrane Modules

The Polymem ultrafiltration module was operated using a hydrostatic driving force of 3 kPa (300 mm water head). The operating pressure was pre-determined by TMP-step experiments which showed that operation below 4 kPa may provide reasonable flux (provided that the COD was below 400 mg/L). Clean water flux was performed before effluent filtration to determine the initial membrane permeability and resistance. The calculations have been elaborated upon in **Appendix III**.

Data Acquisition and Interpretation

The permeate mass was determined using an Ohaus Adventurer Pro balance. A laptop connected to the balance was used to record data using data logging software. The software was

created in Microsoft Excel using Visual Basic (Microsoft 2007) with the ability to record mass data every 2 s. The temperature of the permeate was manually measured using a mercury thermometer. The resistance-in-series model was used to calculate the permeate flux (**Appendix III**) and the data plotted as a 12-point moving average.

Physico-Chemical Analyses

Total COD were performed according to the UCT Open Reflux COD Method for wastewater (Lakay *et al.*, 2000).

5.3.3 RESULTS AND DISCUSSION

The filtration of ABR effluent using the ultrafiltration module over time is presented in Figure 5.30. Flux values are presented as a 12-point moving average over time. The flux was characterised by a rapid decline during the first 3 d followed by a relatively stable pseudo-steady-state operation (approximately $0.2 \text{ L.m}^{-2}.\text{h}^{-1}$). On day 23, a mechanical problem with the feeding peristaltic pump occurred. The water column of the feeding side of the membrane dropped below the permeate side resulting in no driving force across the membrane surface. Inadvertently, this caused a relaxation of the TMP across the membrane. This relaxation resulted in a higher flux and reduced fouling resistance once feeding resumed and the TMP was re-established (from $0.1 \text{ L.m}^{-2}.\text{h}^{-1}$ to $0.3 \text{ L.m}^{-2}.\text{h}^{-1}$). This period of higher flux was only sustained for a short period after which flux returned to its original pseudo-steady-state plateau.

On day 32, filtration was stopped due to impractically low flux (average permeate flux was $0.01 \text{ L.m}^{-2}.\text{h}^{-1}$). To restore membrane filtration, the TMP to the system was temporarily relaxed (approximately 6 h) by stopping feed flow to the module. Thereafter, TMP was re-established with filtration resuming at $0.3 \text{ L.m}^{-2}.\text{h}^{-1}$. This period of filtration was not maintained and was characterised by a rapid decrease of permeate flux with air influx from the permeate side of the module.

On day 35, the project team undertook the decision to increase the driving force through the membrane by increasing the TMP to 6 kPa. Flux through the membrane resumed at $0.5 \text{ L.m}^{-2}.\text{h}^{-1}$ and quickly reached a plateau up of approximately $0.3 \text{ L.m}^{-2}.\text{h}^{-1}$ until day 45 when an accidental TMP relaxation event occurred through a mechanical pump problem. This event was associated with an increase in flux to $0.5 \text{ L.m}^{-2}.\text{h}^{-1}$ which subsequently decreased gradually until no permeate flow was achieved. At this point, the ultrafiltration module was removed from the housing unit and subjected to clean water flux experiments to evaluate the resistance to fouling and the efficiency of membrane cleaning.

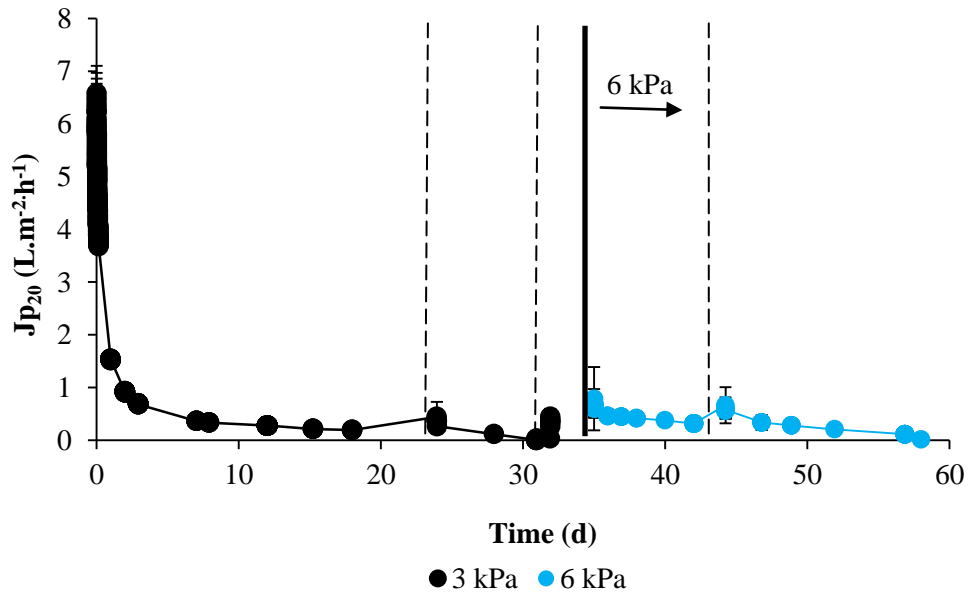


Figure 5.30: The evolution of flux over time for the Polymem UF module treating ABR effluent. Data points (● and ●) represent a 16-point moving average of the flux at a specific time whilst error bars represent the standard deviation for each point. The module was operated at constant TMP at 3 kPa (●) for 34 d after which the TMP was increased to 6 kPa (●). Horizontal dashed lines (---) represent potential performance-affecting incidents such as TMP relaxation whilst the solid vertical black line (—) represents the transition from 3 kPa to 6 kPa.

The results show that the Polymem ultrafiltration module is unable to maintain a stabilised flux over a long period of time. Complete fouling or maintenance is required before 30 d of operation flux. Furthermore, the increase in the driving force across the membrane does not increase permeate production. During this run, the ultrafiltration module was able to remove approximately 74% of the total COD in the effluent (average effluent concentration = 342 mg COD/L; average permeate concentration = 91 ± 47 mg/L, $n = 10$).

The initial permeability of the ultrafiltration module was determined by filtering distilled water over increasing constant TMP (Figure 5.31). Also included in the graph are the permeabilities after fouling and after tap water cleaning. Permeability decreases by as much as 68% from $1.13 \text{ L.m}^{-2}.\text{h}^{-1}.\text{kPa}^{-1}$ ($113 \text{ L.m}^{-2}.\text{h}^{-1}.\text{bar}^{-1}$) to $0.37 \text{ L.m}^{-2}.\text{h}^{-1}.\text{kPa}^{-1}$ ($37 \text{ L.m}^{-2}.\text{h}^{-1}.\text{bar}^{-1}$) due to fouling. Physical cleaning with tap water was able to restore permeability to within 15% [$0.96 \text{ L.m}^{-2}.\text{h}^{-1}.\text{kPa}^{-1}$ ($96.0 \text{ L.m}^{-2}.\text{h}^{-1}.\text{bar}^{-1}$)] of the initial clean water permeability.

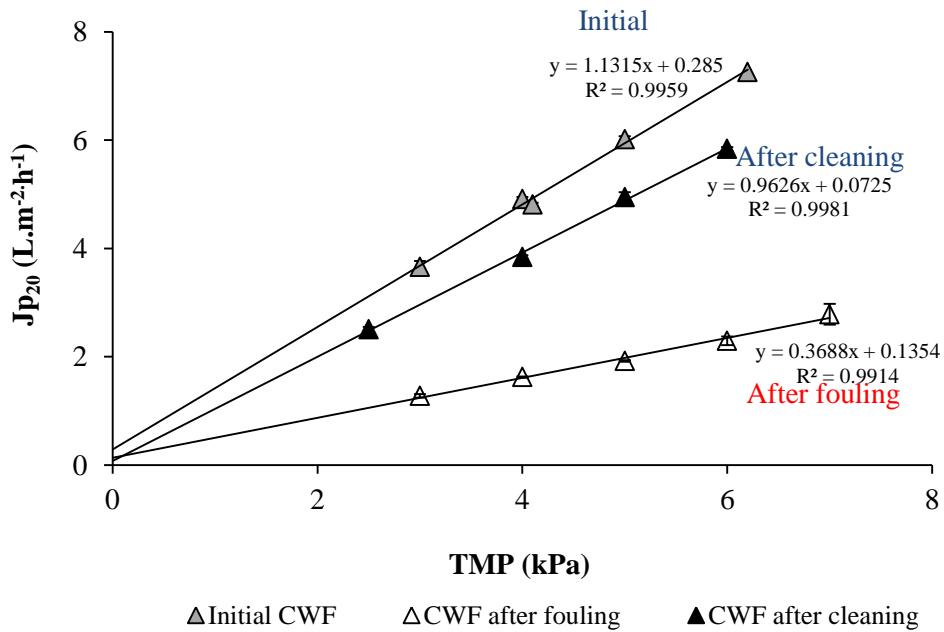


Figure 5.31: Variation of clean water permeate flux (CWF) before and after effluent filtration and after physical cleaning (Polymem UF module). The data points (Δ) represent the average clean water flux over a specific TMP whilst the error bars represent the standard deviation for a specific period.

5.3.4 CONCLUSIONS

The results indicate that stabilised flux cannot be achieved in the Polymem ultrafiltration module. User intervention is required early in the service of this module. An increase in the driving force across the membrane did not change the fouling pattern observed in this module with fouling shown to be largely removable (as indicated by clean water flux tests). In the next section, a series of experiments were performed to evaluate whether there were any differences in Polymem ultrafiltration and microfiltration fouling mechanisms.

5.4 MEDIUM-TERM FILTRATION OF ABR EFFLUENT

This section presents a comparison between Polymem microfiltration and ultrafiltration performance over a medium-term (10 d). Long-term filtration was not considered to this set of experiments as no improvement in flux was expected after 10 d (based on the results obtained in section 5.3 which showed that flux does not increase after this period). The aims of this series of experiments are presented in section 5.4.1. Section 5.4.2 presents the methodology and section 5.4.3 discusses the results from this section. The conclusions for this series of experiments are presented in section 5.4.4.

5.4.1 INTRODUCTION

A medium-term filtration experiment was performed over 10 d to compare the flux profiles of Polymem microfiltration and ultrafiltration modules. The objective of the experiment was to determine whether there were any differences in filtration characteristics between hollow-fibre ultrafiltration and microfiltration modules treating laboratory ABR effluent. The filtration was kept at 10 d as no change in the flux is expected after that time.

5.4.2 METHODOLOGY

Membrane Feed

The Polymem microfiltration module was operated after the long-term ultrafiltration experiment (section 5.3). Both modules could not be operated simultaneously as there was insufficient effluent. The permeate from the microfiltration module was used to supply the soluble component of the effluent to the Polymem ultrafiltration module (section 5.7) and the flat-sheet system in later experiments (section 6.3). Effluent from the ABR treating diluted VIP sludge during Phase VII was pumped directly from the effluent tank to the membrane filtration unit.

Membrane Modules

The Polymem microfiltration module was operated using a hydrostatic driving force of 3 kPa (300 mm water head). The operating pressure was pre-determined by TMP-step experiments. Clean water flux was performed before effluent filtration to determine the initial membrane permeability and resistance. The protocol has been further elaborated upon in **Appendix III**.

Data Acquisition and Interpretation

The permeate mass was determined using an Ohaus Adventurer Pro balance. A laptop connected to the balance was used to record data using data logging software. The software was created in Microsoft Excel using Visual Basic (Microsoft 2007) with the ability to record mass data every 2 s. The temperature of the permeate was manually measured using a thermometer. The resistance-in-series model was used to calculate the permeate flux.

5.4.3 RESULTS AND DISCUSSION

Figure 5.32 presents the flux-time curve of the Polymem microfiltration module treating ABR effluent. The permeate flux of the Polymem ultrafiltration treating ABR effluent has also been included in Figure 5.32 for comparison. It must be noted, however, that the modules were not operated simultaneously (microfiltration was performed after ultrafiltration during Phase VII of ABR operation). The flux was characterised by a sharp decline from 11 L.m⁻².h⁻¹ to 1.0 L.m⁻².h⁻¹ in 2 d followed by a period of stabilisation (approximately 0.5 L.m⁻².h⁻¹) until day 9. The flux curve is a typical characteristic of constant TMP operation and is nearly identical to that of the

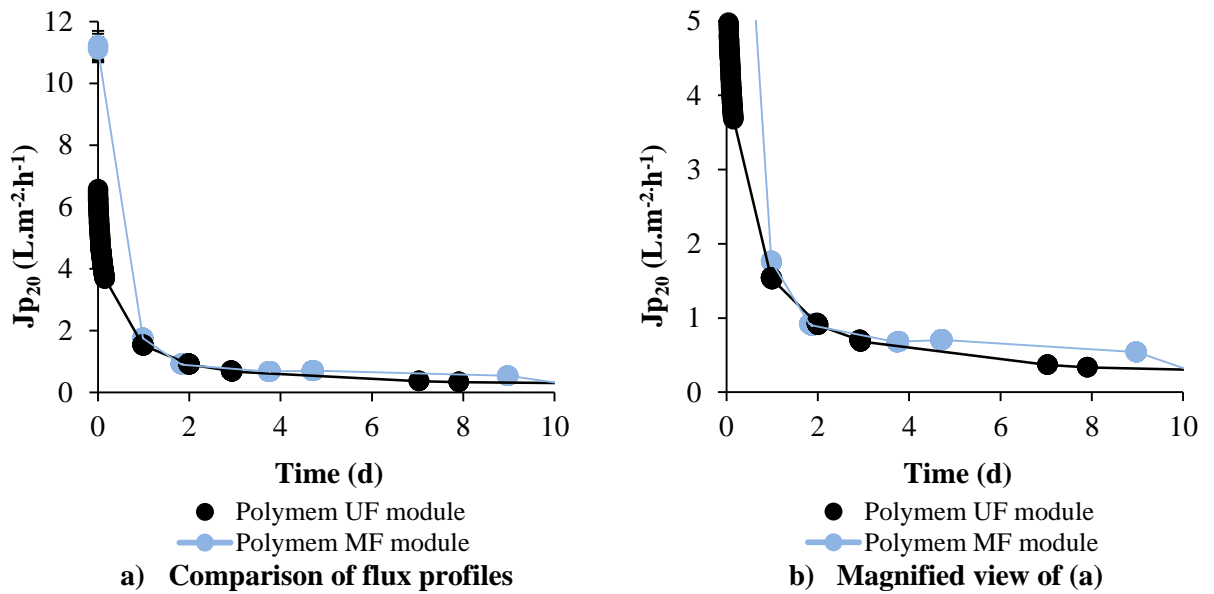


Figure 5.32: The simultaneous variation of flux against time for the Polymem microfiltration module treating ABR effluent at 3 kPa. Data points represent a 16-point moving average of the flux over a specific time.

ultrafiltration module. However, the permeate flux declined to $0.06 \text{ L.m}^{-2}.\text{h}^{-1}$ after day 9 indicating that the module had become fouled beyond normal operation. The module was removed from the housing unit and subjected to clean water flux determination as no further improvement in flux was expected. The results indicate that the fouling dominates the flux of both modules with a similar fouling layer developing in both modules (pictures not shown).

5.4.4 CONCLUSIONS

The results from this section revealed that there was no difference in fouling characteristics between hollow-fibre ultrafiltration and microfiltration modules treating laboratory ABR effluent. As filtration time increases, a cake-like fouling layer develops on the module to a point where the modules become fouled beyond normal operation. In the next section, TMP relaxation was evaluated as a strategy to prolong the flux decline in the hollow-fibre modules.

5.5 SHORT-TERM FILTRATION USING TMP RELAXATION

One of the strategies used by membrane operators to control fouling is to relax the driving force across the membrane. This section discusses the use of TMP relaxation to reduce fouling in the Polymem microfiltration module. The aim of this set of experiments is presented in section 5.5.1. Section 5.5.2 presents the methodology and section 5.5.3 presents the discussion for this series of experiments. The conclusions for this section are presented in section 5.5.4.

5.5.1 INTRODUCTION

A short-term filtration experiment was designed to evaluate if TMP relaxation across the membrane reduces fouling. This technique is routinely used in MBR operations and was envisaged to improve membrane performance. The hypothesis was derived from long-term filtration experiments which showed that permeate flux recovers after an incidental TMP relaxation (section 5.3).

5.5.2 METHODOLOGY

Membrane Feed

Laboratory ABR effluent from Phase VII was used as the membrane feed. The effluent was pumped from the effluent container to the feed funnel of the membrane system and the Polymem microfiltration module operated at 3 kPa.

Membrane Module

Only the Polymem microfiltration module was used in this experiment as the ultrafiltration module was used in a parallel experiment (sections 5.6 and 5.7). However, as the modules display similar flux profiles for the same feed solution it was envisaged that the flux-time curves of the ultrafiltration module would be similar to that of the microfiltration one. The module was operated for 360 min at 3 kPa with the TMP relaxed for 1 min for every 9 min of filtration. Relaxation was performed by cutting off the feed supply to the module via a valve. The relaxation protocol was only applied during the initial stage of fouling as that is when the flux decline is the greatest.

Data Acquisition and Interpretation

The permeate mass was determined using an Ohaus Adventurer Pro balance. A laptop connected to the balance was used to record data using data logging software. The software was created in Microsoft Excel using Visual Basic (Microsoft 2007) with the ability to record mass data every 2 s (Pollution Research Group). The temperature of the permeate was manually measured using a mercury thermometer. The resistance-in-series model was used to calculate the permeate flux (**Appendix III**). The flux test was performed once as it was envisaged as a scoping trial to examine the effectiveness of the fouling control strategy and to determine whether the early flux pattern could be improved by relaxing the TMP across the module.

5.5.3 RESULTS

Figure 5.33 presents the real-time flux for the Polymem microfiltration module treating ABR effluent. For comparison, the real-time flux of the same module treating ABR effluent without relaxation is also included (same curve as presented in Figure 5.27).

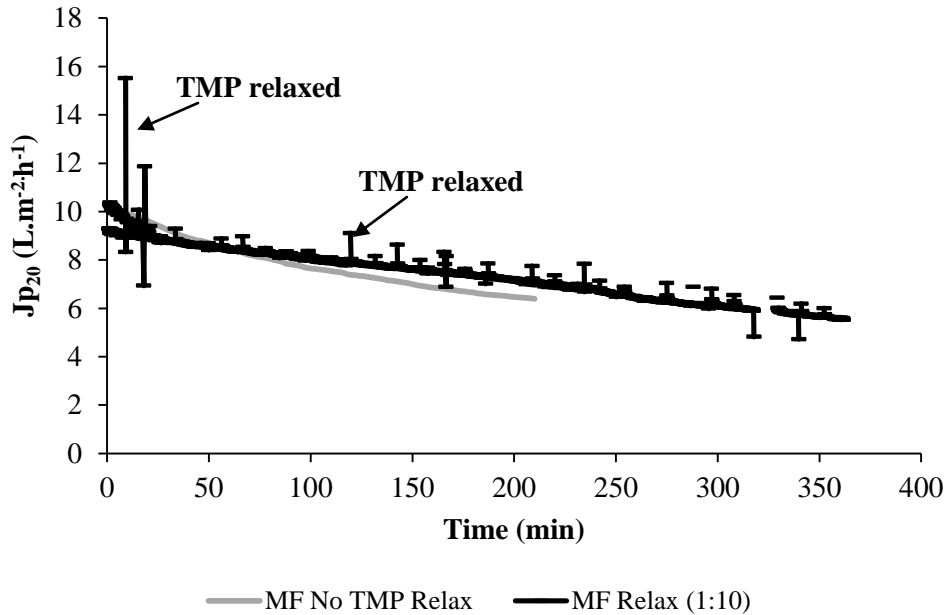


Figure 5.33: Real-time flux for the Polymem microfiltration module operated with and without TMP relaxation.

The strategy with TMP relaxation is nearly identical to that without. There are periods when the TMP is relaxed where the flux increases immediately after the restoration of pressure. However, the flux still declines almost immediately to level similar to that when operated without relaxation. The results clearly show that TMP relaxation does not influence the performance of the module over a period of 6 h. Longer periods of relaxation were not considered since TMP relaxation was not thought to be appropriate for decentralised technologies.

5.5.4 CONCLUSIONS

A short-term experiment was conducted to evaluate if TMP relaxation can improve Polymem hollow-fibre performance in treating laboratory ABR effluent. The experiment was not carried out over a long period but instead focussed on initial stage of filtration where a sharp decline in flux is observed. As no improvement in the flux is predicted through flux relaxation, it can be deduced that TMP relaxation is unlikely to be a useful strategy in decentralised membrane systems.

The next section presents a series of membrane filtration experiments performed using a size-compositional approach. The aim of this series of experiments was to elucidate the fraction in laboratory ABR effluent responsible for fouling in the hollow-fibre modules.

5.6 MEDIUM-TERM FILTRATION OF SETTLED ABR EFFLUENT

In this section, the results from Polymem ultrafiltration of the non-settleable fraction of the laboratory ABR effluent are presented. The aims of this set of experiments are presented in section 5.6.1. The methodology for this experiment is presented in section 5.6.2. The results discussed in section 5.6.3 and the conclusions from this series of experiments presented in section 5.6.4. The experiments presented in this section were performed simultaneously with the flat-sheet unit containing Kubota and fabric modules (section 6.2).

5.6.1 INTRODUCTION

The objective of this study was to determine whether particle deposition on the membrane surface was the main mechanism of fouling. The hypothesis was derived from TMP-step experiments which showed that fouling in Polymem modules was largely reversible with final clean water permeabilities similar to that of the virgin membrane (section 5.1). It was hypothesised that particulates larger than the pore size of the membrane bind loosely to the membrane surface to form a fouling layer. As this fouling layer is loosely attached to the membrane surface, it can be easily sloughed off under a stream of tap water.

5.6.2 METHODOLOGY

Experimental Design

To test the hypothesis, laboratory ABR effluent, fresh laboratory ABR effluent was collected in batches and topped up in a separate tank over a 48 h period at room temperature. The effluent was then allowed to settle for 24 h to separate the settled fraction from the non-settled fraction. The supernatant of this fluid was used as the membrane feed. The same membrane feed was used to evaluate the hypothesis of settleable particulate fouling in flat-sheet modules (section 6.2).

Membrane Modules

Only the Polymem ultrafiltration module was used to test the hypothesis as previous filtration experiments in section 5.4 have shown Polymem microfiltration and ultrafiltration modules displaying similar flux-time curves. Furthermore, there was insufficient filtrate (supernatant of settled effluent) to operate the Polymem microfiltration module simultaneously with the

flat-sheet system. The module was operated at 3 kPa for a period of 8 d as would not change thereafter.

Data Acquisition and Interpretation

The permeate mass was determined using an Ohaus Adventurer Pro balance. A laptop connected to the balance was used to record data using data logging software. The software was created in Microsoft Excel using Visual Basic (Microsoft 2007) with the ability to record mass data every 2 s (Pollution Research Group). The temperature of the permeate was manually measured using a glass mercury thermometer. The resistance-in-series model was used to calculate the permeate flux. The mathematical formula for this parameter is presented in **Appendix III**. Flux values are presented as a 16-point moving average over time to provide a smooth curve.

5.6.3 RESULTS AND DISCUSSION

Figure 5.34 presents a comparison of flux over time for the Polymem ultrafiltration module treating laboratory ABR effluent and the supernatant from settled laboratory ABR effluent. This experiment was performed simultaneously with flat-sheet membranes using the same feed solution (section 7.2).

The flux values of settled supernatant and laboratory ABR effluent (no pre-treatment) results in nearly identical flux-time curves. The results indicate that there is no significant difference in the fouling characteristics of the membrane feed solutions and hence settleable particulates do not play an important role in fouling in the hollow-fibre modules. The filtration experiment was stopped after 8 d as no further improvement in the flux was expected.

The permeability of the module before and after filtration is presented in Figure 5.35. It can be deduced from the graph that the fouling layer has the same properties as that observed with the filtration of untreated effluent in that fouling is reversible. After running the module under a stream of tap water and successive rinses in distilled water, the permeability of the module was restored to near its pre-filtration state.

5.6.4 CONCLUSIONS

The results from this section revealed that settleable particulates in the laboratory ABR effluent did not play a role in the fouling behaviour of the hollow-fibre ultrafiltration module. This series of experiments was continued further to investigate the role of soluble compounds in the effluent in membrane fouling. Details of the experiment are presented in the following section.

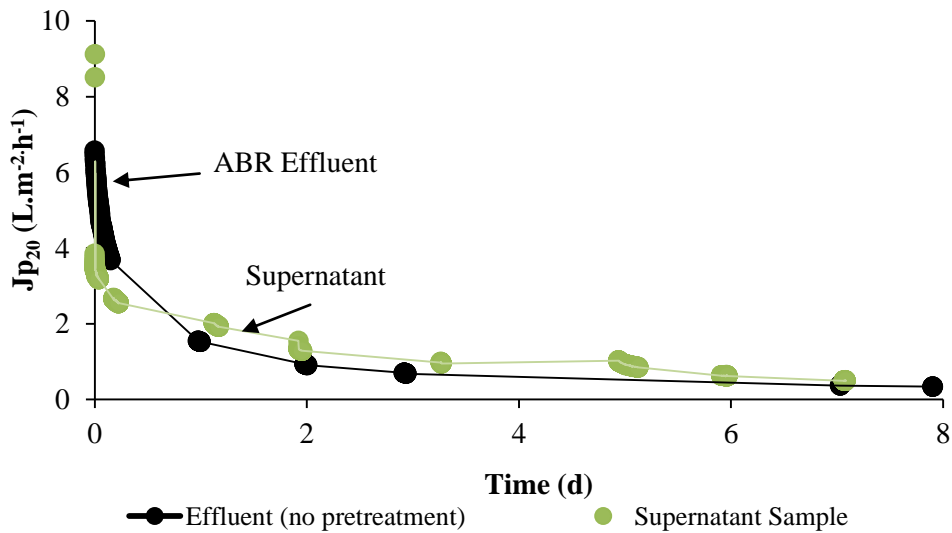


Figure 5.34: The simultaneous variation of flux against time for the Polymem ultrafiltration module treating laboratory ABR effluent and the supernatant of settled ABR effluent. Data points represent the flux (presented as 12-point and 16-point moving average for the ABR effluent and the supernatant of settled ABR effluent, respectively) over a specific time.

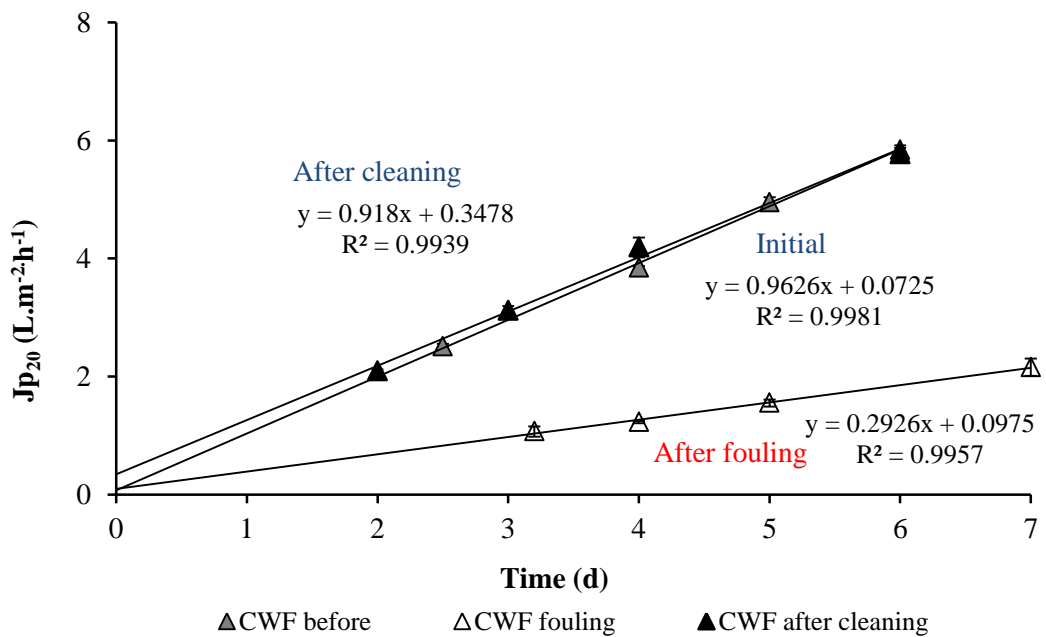


Figure 5.35: Variation of clean water permeate flux (CWF) before and after supernatant filtration and after physical cleaning. The data points (Δ) represent the average clean water flux over a specific TMP whilst the error bars represent the standard deviation for a specific period.

5.7 MEDIUM-TERM FILTRATION OF SOLUBLE ABR EFFLUENT

In this section, the results from membrane filtration of the soluble fraction of the laboratory ABR effluent are presented. The aims of this set of experiments are presented in section 5.7.1. The methodology for this experiment is presented in section 5.7.2 and the results discussed in section 5.7.3. The conclusions from this section as discussed in section 5.7.4. The experiments presented in this section were performed simultaneously with the flat-sheet unit containing Kubota and fabric modules (section 6.3).

5.7.1 INTRODUCTION

This experiment was designed to elucidate the role of the soluble component of the effluent on filtration characteristics. The hypothesis was derived from the previous experiment (section 5.6) which implied that the non-settleable fraction of the effluent is involved in fouling.

5.7.2 METHODOLOGY

Experimental Design

To test the hypothesis, the laboratory ABR effluent from Phase VII was microfiltered through the Polymem microfiltration module and the permeate produced used as the feed for the ultrafiltration module. Consequently, only constituents that are smaller than 0.2 μm would affect the filtration characteristics of the ultrafiltration module.

Membrane Modules

Only the Polymem ultrafiltration module was used to test the hypothesis as there was insufficient membrane feed (soluble effluent) to operate the Polymem microfiltration module simultaneously with the Polymem ultrafiltration module and flat-sheet system. The module was operated at 3 kPa for a period of 4 d. The experiment was not replicated as there was a compromise between conflicting requirements of performing multiple tests on a module and the deterioration of membrane integrity over time. The project team chose to a single test that performed using batches of microfiltered effluent that was collected over four days instead of a single batch.

Data Acquisition and Interpretation

The permeate mass was determined using an Ohaus Adventurer Pro balance. A laptop connected to the balance was used to record data using data logging software. The software was created in Microsoft Excel using Visual Basic (Microsoft 2007) with the ability to record mass data every 2 s. The temperature of the permeate was manually measured using a thermometer.

The resistance-in-series model was used to calculate the permeate flux. Flux values are presented as a 16-point moving average over time to provide a smooth curve.

5.7.3 RESULTS

Figure 5.36 presents the flux-time profile of the ultrafiltration module treating the soluble component of the ABR effluent. For comparison, the filtration curves of the supernatant from settled effluent and effluent without pre-treatment have been included in Figure 5.36. Unlike previous filtration experiments, a rapid flux decline is not observed in the first two days. Flux remains relatively stable from the start of filtration up until day 4 (approximately $3 \text{ L.m}^{-2}.\text{h}^{-1}$). The graph suggests that fouling is minimal in comparison to other tests and similar to clean water flux performed before soluble effluent filtration ($3.1 \text{ L.m}^{-2}.\text{h}^{-1}$). Moreover, the soluble component does not play an important role in fouling in this system.

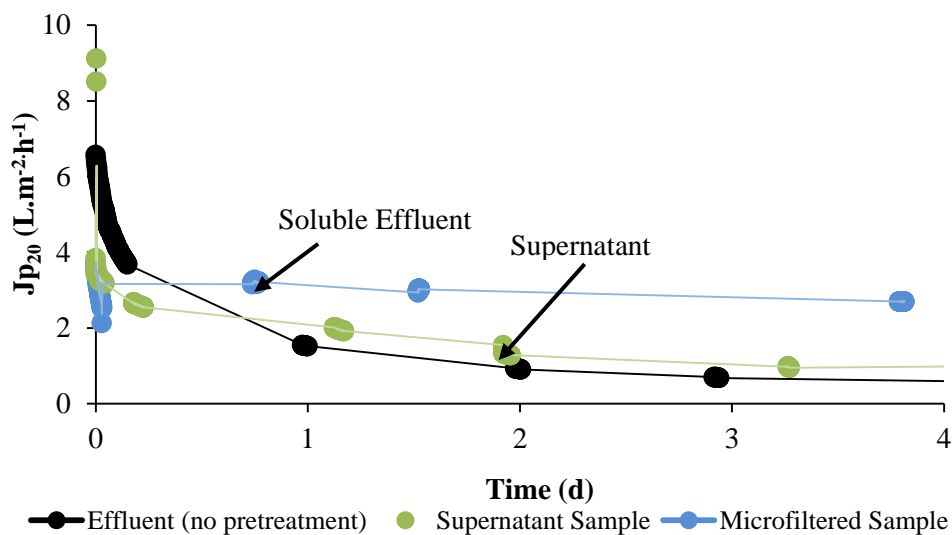


Figure 5.36: The simultaneous variation of flux against time for the Polymem ultrafiltration module treating (a) the soluble component of ABR effluent, (b) untreated ABR effluent and (c) the supernatant of settled ABR effluent. Data points represent the average flux over a specific time. Error bars represent the standard deviation for flux over a time period.

5.7.4 CONCLUSIONS

The results of the flux-time experiment for microfiltered laboratory effluent at a pressure of 3 kPa show that no rapid decrease in the flux is observed over the first 2 d as observed for the other medium-term experiments. The results indicate that the foulant constituent(s) in the effluent have been removed from by microfiltration and that the foulant(s) are not settled material or soluble in nature. It has been hypothesised that colloidal and suspended particulates may play a role in fouling in this system.

5.8 SUMMARY OF HOLLOW-FIBRE FILTRATION EXPERIMENTS

A series of filtration experiments were performed with Polymem hollow fibre modules. The first set of experiments was specifically by the *EUROMBRA* group. The experiments involved short-term filtration (few hours) at various constant transmembrane pressures (TMP) to evaluate the limiting flux of each module. The collective filtration experiments at constant TMP were referred to as TMP-step experiments. Although not the same as the critical flux (performed at constant flux operation), operation below the limiting flux was hypothesised to limit fouling and define the TMP at which to operate the modules.

The TMP-step experiments were performed at varying organic feed concentrations to the ABR. The resulting effluent concentrations ranged from 1 000 to 3 000 mg COD/L. The TMP-step experiments revealed that the organic loading has only a slight effect on the limiting flux of each module with a 400 mm hydrostatic head (4 kPa) identified as a suitable operational TMP provided effluent COD concentrations below 400 mg/L favourable for membrane filtration. Moreover, effluent COD concentration has little effect on permeability recovery after fouling whilst fouling was largely removable (as indicated by clean water permeabilities tests before and after fouling). Based on the findings, it was initially hypothesised that large loosely-adhered particulates may be causing fouling.

A long-term filtration experiment was carried out on ultrafiltration module using the effluent from the ABR. This experiment was conducted simultaneously with flat-sheet membrane filtration (section 6.1). The ultrafiltration module operated at constant TMP (3 kPa) showed a rapid decline in flux during the initial stages of filtration (2 d) followed by a plateau of approximately $0.2 \text{ L.m}^{-2}.\text{h}^{-1}$. The flux profile is a typical characteristic of constant TMP operation. However, a period of constant flux could not be maintained in the ultrafiltration module. The ultrafiltration module was stopped due to unreasonable flux and severe fouling after 30 d. A similar trend was observed in short-term filtration studies with the hollow-fibre microfiltration module (Polymem).

Incidental TMP relaxation events only slightly improved flux recovery but this was trend could not be maintained even in a short-term filtration test designed to examine the effects of TMP relaxation of membrane performance (section 5.5). The results suggest that fouling in hollow-fibre units is severe (results in unreasonable flux) but largely reversible.

Detailed medium-term filtration experiments (few days) were conducted on the effluent using mechanical approach to identifying possible foulants. Using this mechanistic approach, the effluent was fractionated according to size of constituents in solution. First, the filtration of the supernatant fraction of settled effluent (non-settleable) fraction was performed on the ultrafiltration module. The results showed that the filtration of this fraction was nearly identical to that of untreated (not fractionated) effluent. To test the influence of suspended and colloidal particulates on fouling, the effluent was filtered through the Polymem 0.2 μm microfiltration module. The permeate that was generated was used as the membrane feed for the ultrafiltration module. The results revealed that the majority of fouling constituents were removed and that the soluble phase of the ABR effluent did not contribute to fouling.

In the next chapter (**Chapter 6**), the results from constant TMP experiments using flat-sheet membrane modules are presented. The membrane filtration experiments presented in **Chapter 6** were performed simultaneously with those presented in sections 5.3, 5.6 and 5.7. The aims of the experiments presented in **Chapter 6** were to elucidate the fouling constituent based on size-fractionation ABR effluent filtration whilst the purpose of the investigations was to compare the fouling mechanisms between flat-sheet and hollow-fibre modules. Concluding statements about the mechanism of fouling and the nature of the foulant(s) can be viewed in **Chapter 7** (section 7.8).

CHAPTER 6 : FLAT-SHEET FILTRATION

The previous chapter presented the results from hollow-fibre module treating laboratory ABR effluent. In that chapter it was shown that hollow-fibre modules develop a cake-like fouling layer which develops to a point where fouling is beyond normal operation. This fouling layer is hypothesised to be due to the suspended and colloidal fraction in the laboratory ABR effluent and is easily removed by rinsing.

In this chapter, membrane filtration experiments were performed on two types of flat-sheet modules; Kubota and fabric modules. Detailed descriptions of the modules can be viewed in section 3.3.2. The experiments were performed together with Dr. S Pollet, a post-doctoral student at the PRG, UKZN. Dr. Pollet designed the flat-sheet filtration system and participated in data collection. The experimental set-up has been previously described in **Chapter 3**. Effluent from the laboratory ABR that was used in this part of the study was from Phase VII (refer to section A 2.8 in **Appendix II**). Filtration experiments were divided in three parts:

- *long-term* filtration experiment using ABR effluent (section 6.1)
- *medium-term* filtration experiment using the supernatant from settled ABR effluent (section 6.2)
- *medium-term filtration* experiment using microfiltered ABR effluent (refer to section 3.9 for definitions of membrane feeds and time-scales of experiments) (section 6.3).

The purpose of these investigations was to determine how long the flat-sheet membranes could operate without maintenance and elucidate the mechanism of fouling in this system by understanding the nature of foulant (size and chemical composition). Parts of this chapter have been published in the *Journal of Water Practice and Supply* (Pillay *et al.*, 2010) (**Appendix VI**).

6.1 LONG TERM FILTRATION WITH ABR EFFLUENT

This section presents the long-term membrane filtration experiments with Kubota and fabric modules operated at constant TMP and treating laboratory ABR effluent from Phase VII. This set of experiments was performed simultaneously with those presented in section 5.3 (long-term hollow-fibre experiments) and using the same membrane feed. This section is divided into three subheadings. In section 6.1.1, the aims and objectives for this set of experiments are stated. Section 6.1.2 presents the methodology and section 6.1.3 discusses the results from this series of experiments. The conclusions arising from this section are presented in section 6.1.4.

6.1.1 INTRODUCTION

The overall objective of this investigation was to evaluate the performance of flat-sheet modules treating effluent from a laboratory ABR fed a synthetic blackwater (diluted VIP sludge). Specific aims were: (i) to investigate how long could membranes be operated at constant TMP without maintenance, (ii) evaluate if TMP has an influence on filtration characteristics and (iii) to identify possible fouling constituents based on physico-chemical analyses.

6.1.2 METHODOLOGY

Membrane Feed

Membrane modules were gravity-fed with laboratory ABR effluent from Phase VII. The average physico-chemical composition of the feed wastewater and effluent are presented in Table 6.1.

Membrane System

Two pairs of microfiltration modules were used in the filtration experiment, Kubota and fabric modules. The Kubota module is an A4 sized flat-sheet membrane with a defined pore size (0.4 μm). The fabric module is a locally produced flat-sheet membrane that is constructed from polyester filaments that are spun into fibres and woven into fabric. Detailed descriptions of the modules are given in section 3.2.

Table 6.1: Feed and effluent characteristics for Phase VII (4 June 2009 to 5 October 2009). Calculations of averages and standard deviations are presented for all measurements except for the pH value which is reported as a median value. The number in parenthesis represents the number of samples over the operating period.

Parameter	Unit	Feed wastewater (<i>n</i>)			ABR effluent (<i>n</i>)		
		Min	Max	Average	Min	Max	Average
COD _(total)	mg/L	2 000	2 000	2 000 \pm 0 (19)	105	1004	331 \pm 199 (20)
pH		6.1	8.3	8.0 (12)	7.1	8.1	7.9 (12)
TS	mg/L	203	717	434 \pm 176 (10)	157	449	336 \pm 110 (5)
VS	mg/L	27	157	76 \pm 45 (10)	37	68	56 \pm 12 (5)
Proteins _(soluble)	mg/L	-	-	nd	4.5	104	63 \pm 31 (23)
Carbohydrates _(soluble)	mg/L	-	-	nd	0.5	16	3.2 \pm 4.2 (11)
Mean HRT	3.6 d			Total flow treated	5 571 L		

nd, not determined. Soluble protein and carbohydrate concentrations were not measured for the feed wastewater as this phase was concerned more membrane operation.

Experimental Design

Two operating pressures were chosen for filtration, 3 kPa and 6 kPa. The selection of the 3 kPa operating pressure was based on filtration experiments with the hollow-fibre units (Polymem) (section 5.1.4) which indicated that operation below 4 kPa may induce less fouling (depending on the COD concentration of the membrane feed). A TMP of 6 kPa was chosen as the upper limit of operation based on probable excavation heights available after the ABR. This set of membrane filtration experiments was performed simultaneously with that of the Polymem hollow-fibre ultrafiltration module using the same membrane feed (laboratory ABR effluent). In this way, the filtration characteristics of the different modules could be compared.

Filtration Experiment

The initial permeability of each module was determined prior to effluent filtration by filtering tap water. The modules were soaked in tap water (for a day) before use and placed in a holder in the membrane box (Figure 6.1). The membrane feed box was filled and supplied with tap water connected to a hose pipe. An overflow drain at the top of the box maintained a constant level of water in the box.

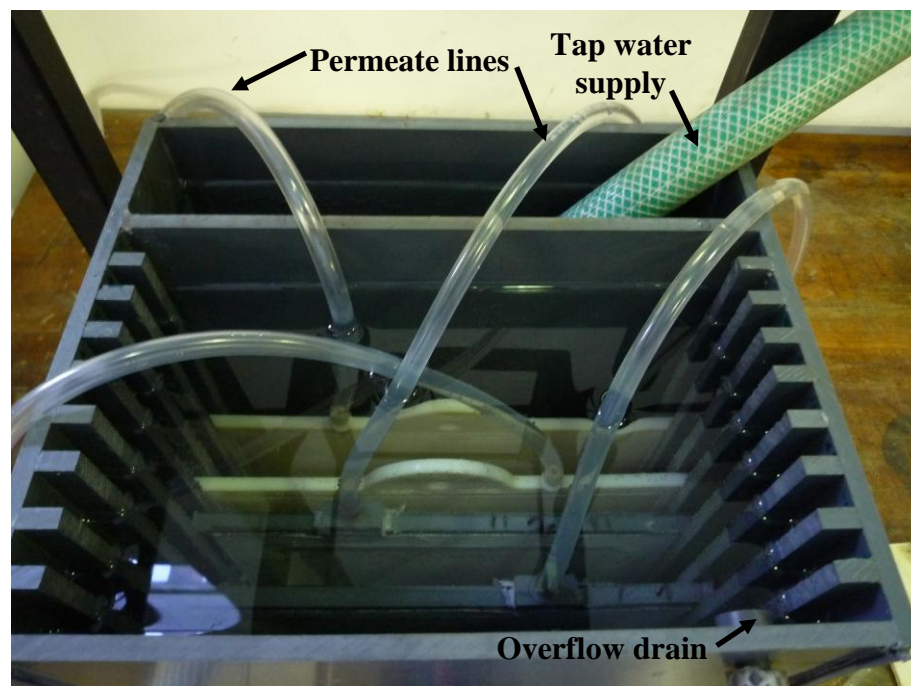


Figure 6.1: Photograph of the inside of the membrane feed box showing modules immersed in tap water. The permeate pipes, hose supplying tap water and overflow drain are also shown in photograph (PRG, 2009).

Prior to filtration of tap water, the permeate lines were filled with tap water to prime the filtration process. Clamps were placed on the end of the permeate line and opened at the start of

each run. The filtration of tap water was performed at constant TMP for at least three different TMPs and the permeability of the module determined using equation 2.3 (section 2.2.4).

Once the clean water flux was determined, the permeate lines were clamped and the tap water in the membrane box decanted and replaced with ABR effluent. The membrane box was constantly fed with laboratory ABR effluent using a peristaltic pump (Watson-Marlow 323) with an overflow pipe draining back to the effluent container (Figure 6.2). This ensured that the contents of the membrane feed box remained mixed and discouraged settling. Filtration of ABR effluent was performed at two different TMP for each module and the data analysed using the resistance-in-series model (section A 3.4 in **Appendix III**). A lid was placed over the membrane box to prevent contaminants from entering the system.

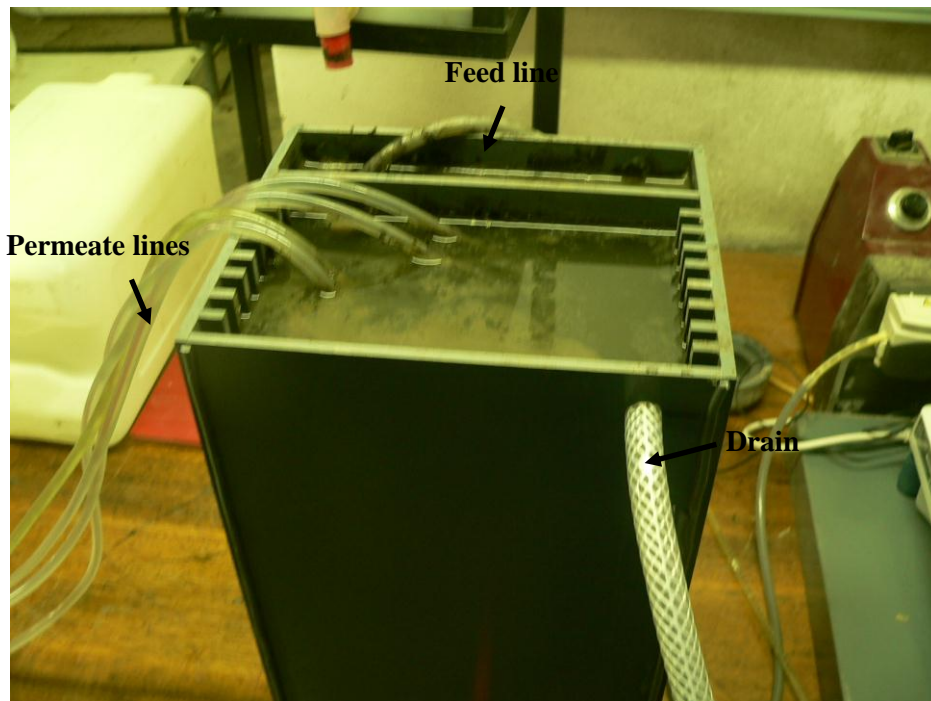


Figure 6.2: Photograph of the flat-sheet system showing permeate lines, membrane feed line and overflow. Unlike the Polymem system (Chapter 5), the flat-sheet system was not completely airtight (PRG, 2009).

After effluent filtration, the clean water flux after fouling was determined by filtering tap water through progressive increases in TMP. The fouling layer was then removed by gloved hands and rinsed in a pre-defined aliquot of distilled water for subsequent chemical analysis. The solution was then placed in the cold room (4°C) prior to analyses. The chemical composition of the fouling layer presented in this chapter represents those fouling agents which could be physically removed from membrane surface and not those strongly adhered or lodged in membrane surface or pores.

Data Acquisition and Interpretation

The flow rate was calculated by using a bucket and stopwatch method. The TMP calculations have been presented in section 3.3.3. As filtration occurs on both sides of a flat-sheet module, the area on one side of each module was calculated and multiplied by two to give to the effective filtration area. The resistance-in-series equation was used to calculate the permeate flux with flux corrected to 20°C to account for changes in viscosity. A detailed description of data analysis can be viewed in section A 3.4 in **Appendix III**.

Physico-Chemical Analyses

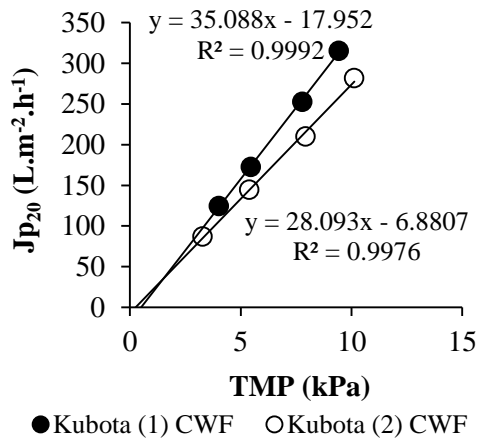
Total COD measurements were made according the University of Cape Town (UCT) Open Reflux COD Method for wastewater (Lakay *et al.*, 2000). Soluble protein and carbohydrate measurements were made according to the Frølund *et al.* (1996) and Dubois *et al.* (1956) methods, respectively.

6.1.3 RESULTS AND DISCUSSION

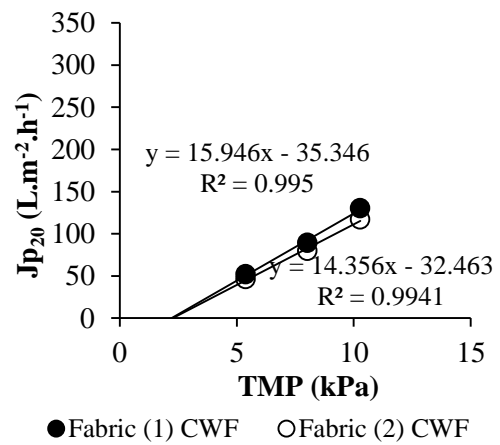
The initial clean water flux and permeabilities were measured for the ‘virgin’ modules before effluent filtration. Figure 6.3 presents the clean water flux for two Kubota and two fabric modules over constant TMP. The permeability of the two Kubota modules was 35.1 (351) and 28.1 L.m⁻².h⁻¹.kPa⁻¹ (281 L.m⁻².h⁻¹.bar⁻¹) (data rounded to three-significant figures). In contrast, the fabric modules had initial permeabilities from 14.4 to 16.0 L.m⁻².h⁻¹.kPa⁻¹ (1 440 to 1 600 L.m⁻².h⁻¹.bar⁻¹).

For the long-term experiment, the flat-sheet modules were operated over a period of 80 consecutive days (from 9 June 2009 to 27 August 2009) during Phase VII of ABR operation. Effluent generated by the ABR during this phase was gravity-fed to the membrane filtration system (Table 6.1).

Figure 6.4 represents the evolution of flux over time for both flat-sheet modules. Both module types exhibit a similar flux profile with a sharp decline observed at the start of filtration with a plateau after 3 d. The initial fluxes for the Kubota modules were 15 and 34 L.m⁻².h⁻¹ at 3 and 6 kPa, respectively. For the fabric modules, the initial fluxes were 4 and 29 L.m⁻².h⁻¹ at 3 and 6 kPa, respectively (Figure 6.4a). In order to compare the four filtration curves, the first 10 d have been magnified in Figure 6.4b.



a) Kubota modules



b) Fabric modules

Figure 6.3: Variation of clean water flux (CWF) with TMP for Kubota and fabric modules before laboratory ABR effluent filtration. The data points represent the average flux over a specific time period.

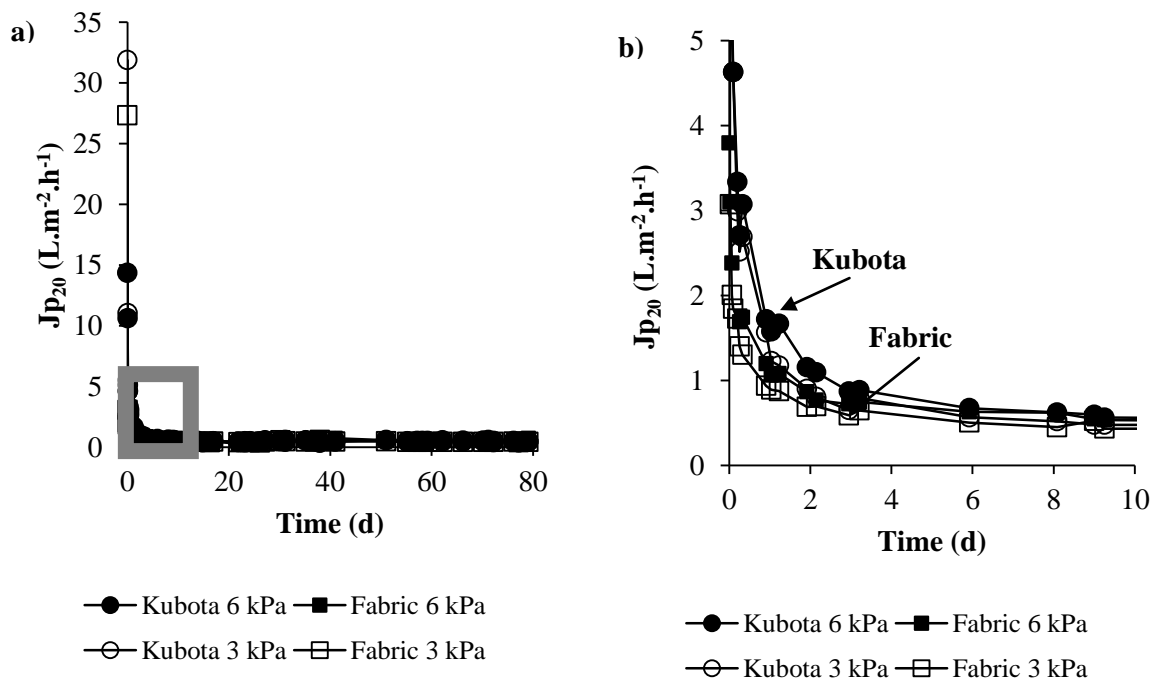


Figure 6.4: The simultaneous variation of flux versus time for Kubota and fabric modules treating laboratory ABR effluent. a) Flux-time profile of modules over 80 d. b) Magnified view of area marked by □ in (a). Data points represent the actual flux at a specific time.

During operation of the laboratory ABR at Phase VII, there were only slight differences in flux observed between Kubota and fabric modules with the Kubota modules producing a slightly higher flux than the fabric modules during the first day. The flux of Kubota module operated at 6 kPa was initially higher than that of other modules but decreased to a similar level after 3 d of filtration. After 8 d of ABR effluent filtration, the fluxes were stable and nearly identical for all modules (approximately $0.5 \text{ L}\cdot\text{m}^{-2}\cdot\text{h}^{-1}$) and did not change significantly for the remaining days (see Figure 6.5).

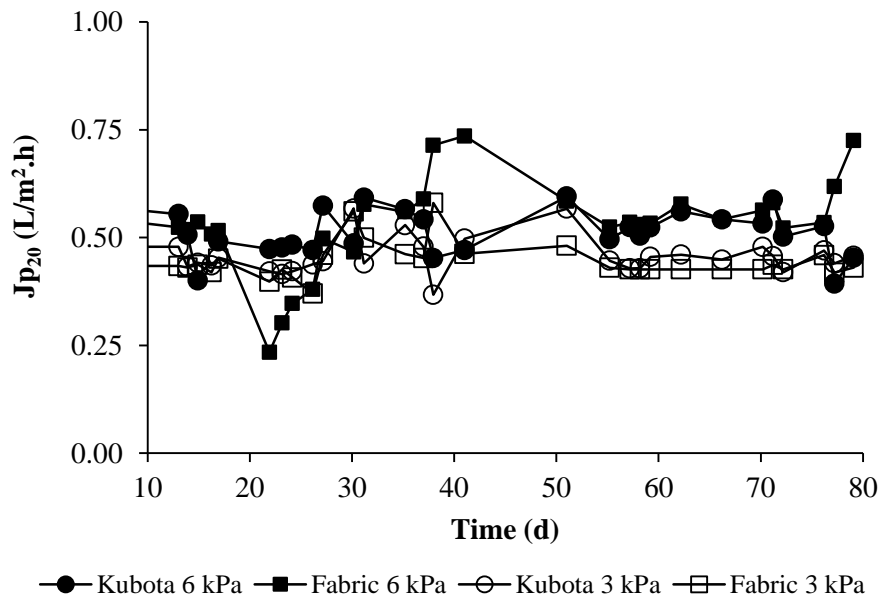


Figure 6.5: A magnified view of the simultaneous variation of flux versus time for Kubota and fabric modules treating laboratory ABR effluent. The plot shows the steady-state flux for each TMP and module tested.

The operating pressure was shown to have no significant effect on flux-time relationships. Since only slight differences in flux were observed at different operating pressure for each module, TMP was deemed to be not significant (for the TMP ranges tested) (Figure 6.5).

Cumulative permeate volumes were calculated by assuming that the flow rates were constant between the days that flow was measured (Table 6.2). The purpose of the calculations was to compare the volumes produced by each module type and for each pressure. Furthermore, it assisted in the interpretation of data obtained from the determination of the mass of substances attached to the membrane surface after fouling. The disadvantage of the assumption used in the calculation was that it was assumed that flux did not decline between two sampling dates. Thus, the calculated values presented in this thesis are probably higher than actual cumulative volumes.

Calculated cumulative volumes were equal to 1 137, 1 304, 944 and 1 102 L.m⁻² for Kubota 3 kPa, Kubota 6 kPa, fabric 3 kPa and fabric 6 kPa, respectively. The differences between these volumes after 80 d of filtration were slight between each module type and each operating pressure (within 20% of each other). The results suggest that it may not be necessary to work at a pressure lower than 6 kPa for this type of filtration. Moreover, the results imply that the steady-state flux is independent of TMP based on equation 2.2. During the initial stage of filtration, the resistance increases to a higher value at higher TMP so that ultimately the flux at 3 kPa is more or less equal to the flux at 6 kPa. The results suggest that at low TMPs the flux is a function of the fouling characteristics only and independent of TMP and the membrane type (but obviously dependent on the foulant concentration and shear rate). This conclusion cannot be extended to higher TMPs than 6 kPa or membranes with smaller pore sizes. Moreover, this may not apply to effluents with significantly different physico-chemical characteristics.

Table 6.2: Calculated cumulative volumes of Kubota and fabric modules operated at 3 and 6 kPa over 80 d*.

	Kubota 3 kPa	Kubota 6 kPa	Fabric 3 kPa	Fabric 6 kPa
<u>Total (L.m⁻²)</u>	1 137	1 304	944	1 102
<u>First 8 d (L.m⁻²)</u>	173	206	130	154
<u>Last 72 d (L.m⁻²)</u>	614	649	580	644

*, The volume produced takes into consideration the effective filtration area of each module.

At the end of the experiment, the permeability decrease due to fouling was measured by filtering tap water. The results are presented as flux versus pressure in Figure 6.6.

As can be deduced from Figure 6.6, membrane permeabilities have strongly decreased by over 90% (in relation to the clean water flux). Fouling was severe during the filtration and induced a very low permeability at the end of the experiment. Furthermore, a simple mechanical wash with tap water was not sufficient to remove the layer (in contrast to the Polymem modules in **Chapter 5**). The fouling layer that had developed had a darkish brown hue and had to be manually removed by gentle scraping using gloves. Figure 6.7 shows the fouling layer that had developed on Kubota and fabric modules.

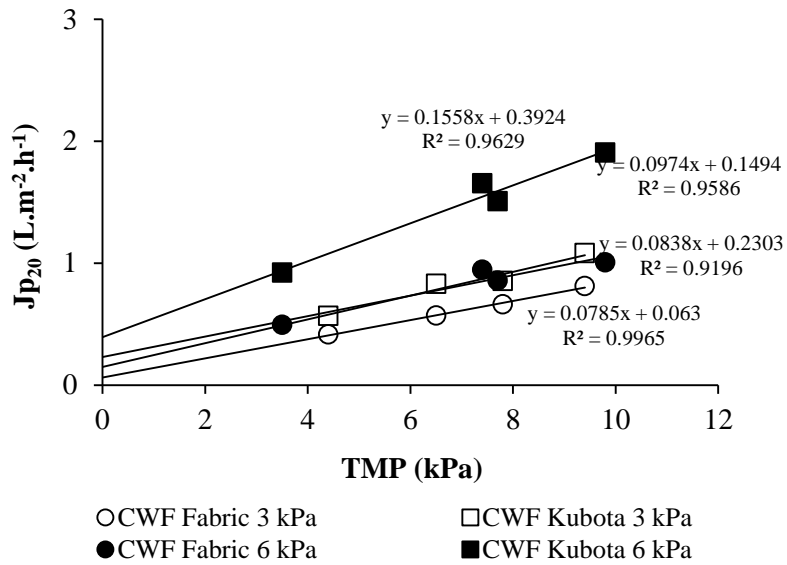


Figure 6.6: Variation of clean water flux (CWF) with TMP for Kubota and fabric modules after laboratory ABR effluent filtration. The data points represent the average flux over a specific time period.

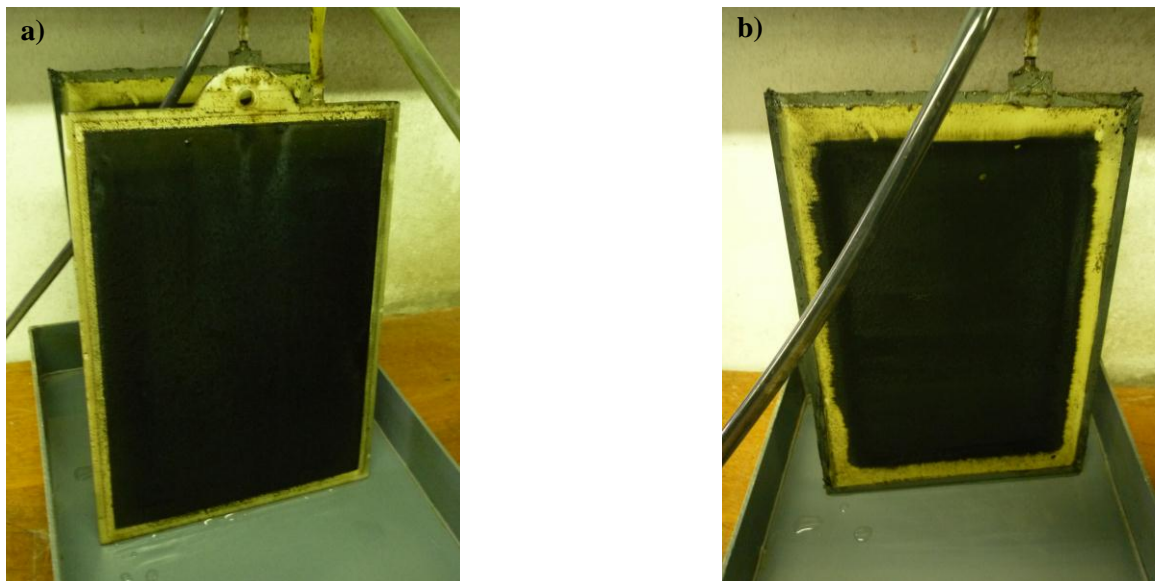


Figure 6.7: Photographs of the fouling layer on a) Kubota module and b) fabric module after laboratory ABR effluent filtration. The fouling layer had a gel-like structure and was difficult to remove using physical cleaning techniques (PRG, 2009).

Chemical analyses

Samples of ABR effluent, membrane box bulk fluid and permeate from each membrane were taken for chemical analysis at different times: day 1, 7 and 17 corresponding to dates 9 June 2009, 16 June 2009 and 26 June 2009, respectively. On 27 July 2009, the chemical composition of the fouling layer was determined. The results of each of these sampling days will be discussed in this section. The time of these samplings in relation to the flux-time curve are presented in Figure 6.8.

Chemical oxygen demand (COD), soluble protein and soluble carbohydrate measurements were performed during these specific days. Details of the analytical protocols have been presented in **Appendix IV**.

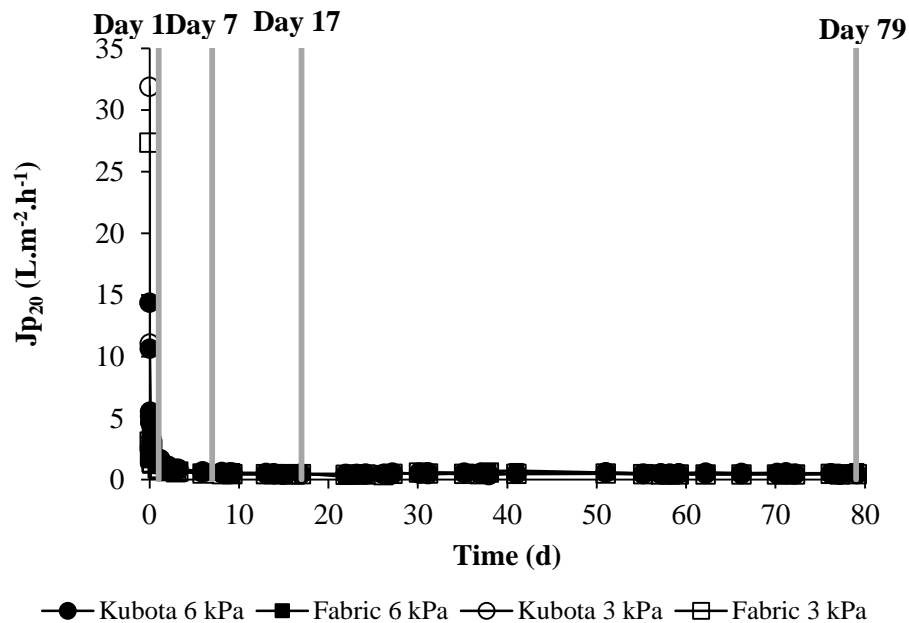


Figure 6.8: The simultaneous variation of flux versus time for Kubota and fabric modules treating laboratory ABR effluent. Effluent and permeate samples were collected on day 1, 7 and 17 (grey solid lines) and were analysed for total COD, soluble protein and soluble carbohydrate. On day 79 the fouling layer was removed and analysed for protein, carbohydrate and COD content.

The results of the chemical analyses are presented in Table 6.3. On day 1 (9 June 2009), the average total COD concentration in the ABR effluent was 667 mg/L. The Kubota module was able to reduce the effluent COD to 158 and 140 mg/L at 3 and 6 kPa, respectively. In contrast, the fabric modules were able to reduce effluent COD to 68 and 181 mg/L at 3 and 6 kPa, respectively. The flat-sheet modules performed similarly with regards to COD removal, with

COD removals greater than 70% (and less than 200 mg/L) achieved through filtration. The fabric module operated at 3 kPa was able to achieve the highest COD removal (90%). The results indicate that COD removal is very efficient through the flat-sheet modules during the first day of operation.

Table 6.3: Chemical composition of ABR effluent, membrane box and permeate samples from Kubota and fabric modules operated at 3 and 6 kPa for days 1, 7 and 17. Analyses were performed in duplicate or triplicate (unless otherwise stated).

Day	Parameter	Unit	ABR Effluent	Membrane Box	<u>Kubota</u>		<u>Fabric</u>	
					3 kPa	6 kPa	3 k Pa	6 kPa
1	COD	mg/L	667 ± 385	705 ± 40	158 ^a	140 ± 26	68 ± 20	181 ± 29
	Protein	mg/L	66 ± 1.6	61 ± 0.1	14 ± 0.1	13 ± 5.2	18 ± 0.6	21 ± 0.5
	Carbohydrate	mg/L	2.8 ± 0.2	3.2 ± 0.6	0.9 ± 0.2	0.9 ± 0.2	0.9 ± 0.3	1.4 ± 0.2
7	COD	mg/L	445 ± 30	381 ± 25	190 ± 82	142 ± 51	138 ± 10	118 ± 66
	Protein	mg/L	49 ± 1.3	nd	53 ± 1.9	43 ± 0.5	56 ± 2.5	53 ± 1.2
	Carbohydrate	mg/L	2.0 ± 0.2	nd	0.8 ± 0.1	0.9 ± 0.1	1.1 ± 0.2	1.7 ± 0.3
17	COD	mg/L	nd	281 ± 76	59 ± 0	45 ± 6	41 ± 27	nd
	Protein	mg/L	66 ± 0.2	62 ± 0.2	37 ± 0.4	39 ± 0.5	37 ± 2.8	40 ± 1.5
	Carbohydrate	mg/L	3.0 ± 0.3	2.8±0.2	0.9 ± 0.3	0.7 ± 0.2	0.9 ± 0.4	1.1 ± 0.2

^a, only one replicate performed on sample.

nd, not determined.

The COD concentration did not differ greatly between the ABR effluent container to membrane box bulk fluid. The membrane box is fed with effluent from the ABR effluent container which is intermittently topped up by the ABR (Figure 6.9). The overflow from the membrane flowed back into the ABR effluent container. Accordingly, the COD from the ABR container and membrane bulk fluid should be similar (as shown in these results) although some change over time would be expected (as the container is intermittently topped up) and as the amount of material rejected by the membrane modules increases (although no significant amount of biomass was observed at the bottom of membrane feed box over 80 d).

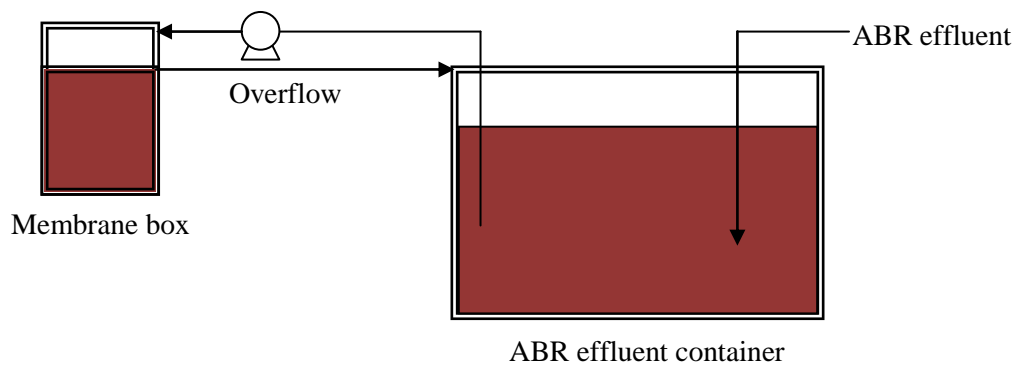


Figure 6.9: Flow diagram showing the feeding system to the membrane from the laboratory ABR effluent container.

With regards to the protein concentration on day 1, the ABR effluent had a soluble protein concentration of 66 mg/L with a similar value measured in the membrane feed box bulk fluid (61 mg/L). The results indicate that no biological modification of the fluid occurs in terms of proteins between the ABR effluent collection point and the membrane feed box bulk fluid. All membranes rejected more than 69% of protein in the membrane box bulk fluid (protein concentration is below 22 mg/L) indicating efficient removals through the modules during the first day of operation. Kubota modules rejected more proteins (minimum of 80%) than the fabric ones (maximum of 72%) irrespective of operating pressure used. This difference can probably be attributed to the structure of the membrane material in each module type. The porous structure of Kubota membranes seems to reject more proteins than the woven fabric which has more space between the fibres, at least during the first day of operation but these differences are small (and therefore thought to be not significant).

With regards to the soluble carbohydrate concentration on day 1, the laboratory ABR effluent had a concentration of 2.8 mg/L with a similar value measured in the membrane box (3.2 mg/L) which suggests that no modification of the biological fluid occurs from the effluent to the membrane box in terms of carbohydrates. Kubota and fabric modules display similar soluble carbohydrate rejection properties with removals of higher than 54% observed in all modules. Although carbohydrate removal is efficient through the membrane, very low concentrations have been observed in the feed wastewater and effluent (**Appendix II**). The results indicate that nearly half of the soluble carbohydrates present in effluent pass through both types of flat-sheet modules and hints at some sort of size fractionation (or selectivity) of carbohydrates occurring during filtration.

On day 7 (16 June 2009), the ABR effluent had a COD concentration of 445 mg/L. After filtration, the COD concentration is below 200 mg/L in all modules with COD removal similar to that of day 1. The results suggest COD removal is relatively constant during filtration.

With regards to the soluble protein concentration, the laboratory ABR effluent contained 49 mg/L. After filtration, no rejection of proteins occurs on the membrane (the soluble protein concentration ranges from 43 and 56 mg/L). Surprisingly, protein rejection does not seem to occur at this stage of filtration. The results suggest that protein molecules are not being held back by the fouling layer and may be due to concentration polarisation effects on the membrane surface (this is further elaborated upon in section 7.8).

With regards to the soluble carbohydrate concentration, the laboratory ABR effluent had a concentration of 2.0 mg/L. After filtration, the soluble carbohydrate concentration is between 0.8 and 1.7 mg/L which corresponds to removals of 15 and 60%. Kubota modules displayed better removal efficiencies than fabric modules irrespective of the TMP applied. However, this difference was too small to be attributed to any physical separation process.

Laboratory ABR effluent COD measurements were not made for day 17 as it was considered to be the same as bulk fluid in the membrane box. The COD value of the bulk liquor in the membrane box was 281 mg/L. Permeate COD values for Kubota and fabric modules were much lower than previous days (less than 60 mg/L) with the exception of the permeate of the fabric module operated at 6 kPa on which no COD measurements were made. Although the COD value of the effluent is not known, the average COD removal from the membrane box for Kubota modules and the fabric module (6 kPa only) was higher than 80%. The results imply that COD removal may have improved over time and could be related to the development of the fouling layer on the module surfaces.

With regards to the soluble protein and carbohydrate concentrations, no differences in rejection were observed with respect to the type of module used or the operating pressure. Moreover, the effluent (66 mg/L) and bulk fluid of the membrane box (62 mg/L) had similar concentrations.

Interestingly, rejection is the highest during the initial filtration stage (day 1). The results suggest that a higher proportion of proteinaceous compounds are being retained on the membranes during the initial stage of filtration. These findings become more relevant with respect to the mechanism of fouling later in this thesis (section 7.8).

The results indicate that the membrane feed in the membrane box was nearly identical to that of ABR effluent. The implications of this result suggest that there is no biological modification in the fluid from effluent tank to the flat-sheet unit. In addition, the highest rejection of COD and proteins occurs during the first day of experiment. Low soluble concentrations are present in the effluent and the permeate samples, and is probably a reflection of the feed wastewater composition (low carbohydrate concentration in the feed).

To elucidate the nature of constituents attached to the membrane surface, COD, protein and carbohydrate measurements were made on the fouling layer. Once filtration was stopped, the fouling layer was manually removed by gentle scraping using gloves and diluted with an aliquot of distilled water. Chemical analyses were then performed on the mixed liquor. The results of the chemical analyses of the cleanings are presented in Table 6.4 in terms of mass deposited per membrane surface per area. The cumulative filtered volume has also been included in Table 6.4. The chemical results only take into account the material that could be removed by hand from the membrane surface and not material adsorbed on the membrane.

Table 6.4: Chemical composition of manually removed fouling layer from Kubota and fabric modules operated at 3 and 6 kPa for day 79. Analyses were performed in duplicate or triplicate (unless otherwise stated). Cumulative volumes of permeate were calculated using flow rates between sampling days and divided by the effective filtration area for each module.

Day	Parameter	Unit	<u>Kubota</u>		<u>Fabric</u>	
			3 kPa	6 kPa	3 k Pa	6 kPa
79	Cumulative Volume	L.m ⁻²	1 137	1 304	944	1 102
	COD	g/m ²	37 ± 14	46 ± 18	60 ± 12	44 ± 9
	Protein	g/m ²	0.8 ± 0.01	0.8 ± 0.01	0.9 ± 0.01	0.8 ± 0.00
	Carbohydrate	g/m ²	0.9 ± 0.2	0.9 ± 0.2	0.9 ± 0.3	1.4 ± 0.2

The masses of protein and carbohydrate retained per unit area on each module were quite similar. Moreover, only slight differences in the mass of COD per unit area were observed between modules with fabric modules retaining slightly more organic material on their surface than Kubota ones and could be possibly due to measuring and sampling uncertainties. The overall results fits into the theory (page 6-7) that the resistance that controls the flux is related to pore blocking and therefore the results are unsurprising in that the mass of external foulants is not different between modules.

Based on the results, the chemical composition of the foulant could not be deduced (as protein and carbohydrate composition of fouling layers were similar). Consequently, the project team initiated another set of filtration experiments based on the filtration of size-fractionated effluent. The experiments were derived from Polymem filtration trials which suggested that particle deposition may be the main mechanism of fouling (section 5.1).

6.1.4 CONCLUSIONS

The results from this series of experiments indicated that a different mechanism of fouling was occurring in flat-sheet modules treating laboratory ABR effluent compared to hollow-fibre modules (**Chapter 5**). Long-term filtration experiments showed that Kubota and fabric microfiltration modules show a period of stabilised flux (less than $0.5 \text{ L.m}^{-2}.\text{h}^{-1}$) with irremovable gel-like fouling layers developing. Although chemical analysis of the fouling did not reveal the chemical composition of the fouling layers, the results indicated that a higher proportion of proteins were being retained on the flat-sheet microfiltration modules during the early stages of filtration implicating these compounds in flat-sheet membrane fouling.

In the next section, the results from a series of membrane filtration experiments performed on size-fractionated laboratory ABR effluent are presented to elucidate the fraction responsible for fouling in the flat-sheet unit.

6.2 MEDIUM-TERM FILTRATION OF SUPERNATANT FROM SETTLED ABR EFFLUENT

This section presents the results from medium-term flat-sheet microfiltration of the supernatant from settled laboratory ABR effluent. This set of experiments was performed simultaneously with the hollow-fibre ultrafiltration module in section 5.6. This section is divided into three subheadings. The aims and objectives of this series of experiments are presented in section 6.2.1. Section 6.2.2 presents the methodology and section 6.2.3 discusses for this the results for this series of experiments. The conclusions arising from this section are presented in section 6.2.4.

6.2.1 INTRODUCTION

The objective of this study was to determine whether particle deposition on the membrane surface was the main mechanism of fouling. The hypothesis was derived from hollow-fibre membrane experiments which showed that permeabilities return to near virginal state after placing the module under a stream of tap water (sections 5.1 to 5.3).

6.2.2 METHODOLOGY

Experimental Design

Effluent from Phase VII of ABR operation was collected and allowed to settle for 48 h in large cylindrical containers (approximately 200 L). The top layer of the fluid in a settling tank was used as the filtrate, that is, the supernatant of the settled effluent. The same membrane feed was used in simultaneous hollow-fibre experiments in section 5.6.

Membrane Modules

Kubota and fabric modules were operated at 3 and 6 kPa, respectively. The duration of the experiment was deduced from the previous experiment which showed that a rapid decrease flux was observed over the first 2 d, thereafter there is a gradual reduction in flux until day 8 after which the flux remains constant. As no further changes in the flux were expected after that time, it was deemed unnecessary to continue filtration for a longer period of time. A clean water flux determination was performed before and after supernatant filtration.

Data Acquisition and Interpretation

The flow rate was calculated by measuring time required to fill a certain volume. The TMP was calculated as the height difference between the outlet of the permeate pipe and the middle of the membrane module. The resistance-in-series equation was used to calculate the permeate flux with flux corrected to 20°C to account for changes in viscosity (section A 3.4 in **Appendix III**).

Physico-Chemical Analyses

Total COD measurements were made according the UCT Open Reflux COD Method for wastewater (Lakay *et al.*, 2000). Soluble protein and carbohydrate measurements were made according to the Frølund *et al.* (1996) and Dubois *et al.* (1956) methods, respectively (**Appendix IV**).

6.2.3 RESULTS AND DISCUSSION

Clean water permeabilities were measured for each of the four modules before the filtration test. Each module had a different permeability. The results are presented in

Figure 6.10 as permeate flux versus TMP. The clean water flux of the Kubota module did not pass through the origin and probably represents an error in the analysis.

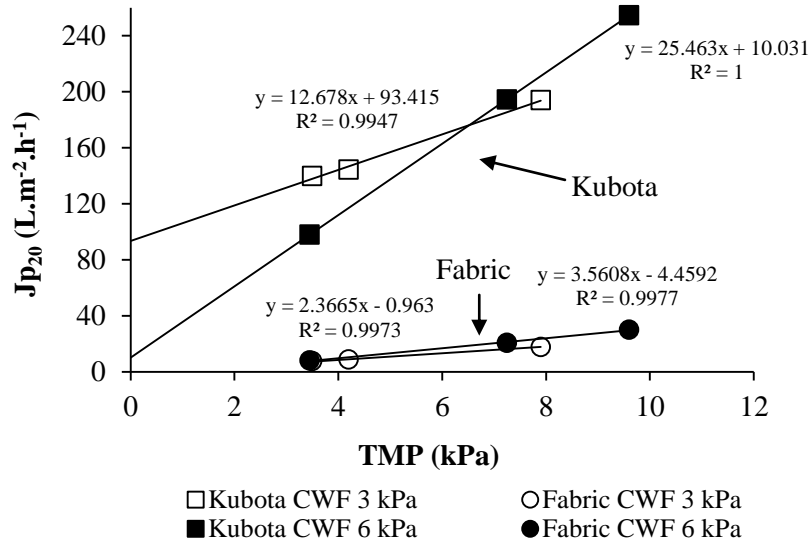


Figure 6.10: Variation of clean water flux (CWF) with TMP for Kubota and fabric modules before laboratory ABR effluent filtration. The data points represent the flux over a specific time period.

The permeabilities of the Kubota membranes were equal to 25.5 (255 L.m⁻².h⁻¹.bar⁻¹) and 12.7 L.m⁻².h⁻¹.kPa⁻¹ (127 L.m⁻².h⁻¹.bar⁻¹) whilst fabric modules were equal to 2.37 (237 L.m⁻².h⁻¹.bar⁻¹) and 3.56 L.m⁻².h⁻¹.kPa⁻¹ (356 L.m⁻².h⁻¹.bar⁻¹). No chemical cleaning was employed before experimentation and thus initial permeabilities for this experiment are lower than that of the first effluent filtration experiment.

The modules were operated over a period of 8 consecutive days using the supernatant from ABR. Figure 6.11a presents the evolution of flux over time using the supernatant from settled effluent. The initial fluxes were 135 and 93 L.m⁻².h⁻¹ for Kubota and 5 and 3 L.m⁻².h⁻¹ for fabric at 3 and 6 kPa, respectively. The flat-sheet modules exhibit a similar flux profile with an initial decline followed by a period of low stabilised flux. In order to compare the four filtration curves, the graphs presented in Figure 6.11a have been reproduced, magnified and presented at a maximum flux of 5 L.m⁻².h⁻¹ is presented in Figure 6.11b.

The results indicate that the flux is not dependent on the pressure applied across the membrane. Moreover, there were only slight differences in the flux between Kubota and fabric modules with the Kubota modules able to achieve a higher permeate flux in the initial stages of filtration. However, after 7 d the flux levels out to a similar plateau as that of fabric modules (0.5 L.m⁻².h⁻¹ for the combined fabric modules and 0.7 and 0.9 L.m⁻².h⁻¹ for Kubota membranes at 6 and 3 kPa, respectively).

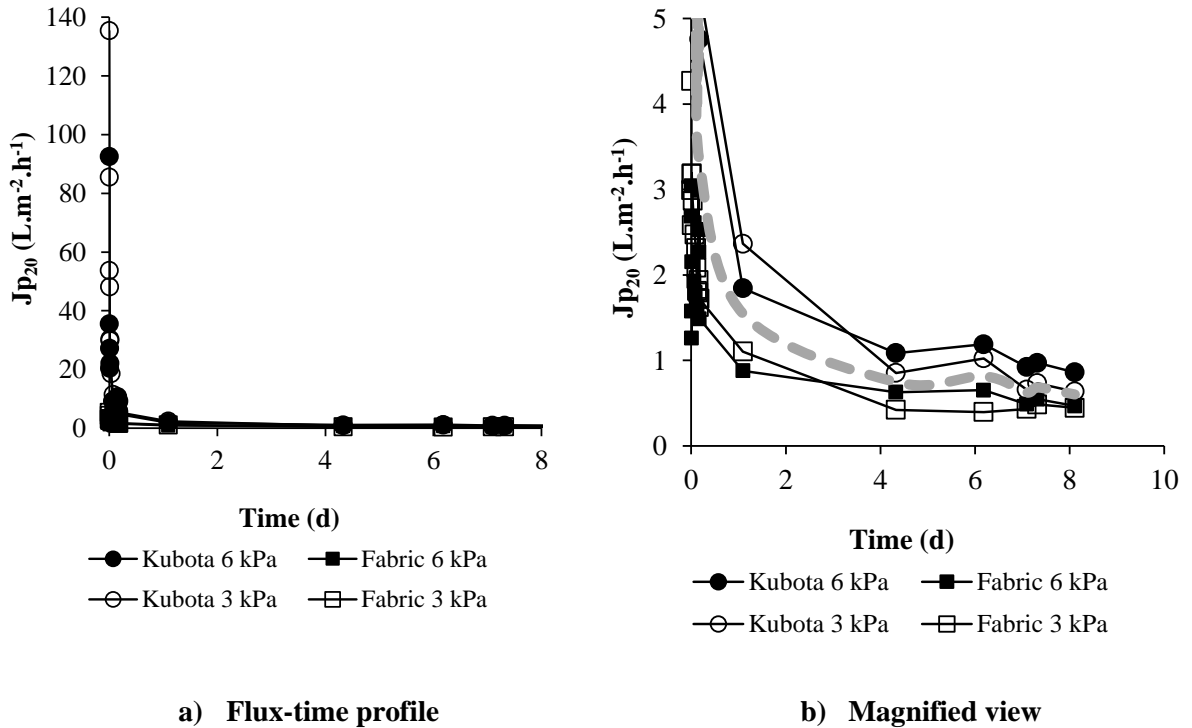


Figure 6.11: The simultaneous variation of flux versus time for Kubota and fabric modules treating the supernatant from settled laboratory ABR effluent. a) Flux-time profile of flat-sheet modules over 8 d. b) Magnified view of (a) with flux presented a maximum of $5 \text{ L.m}^{-2}.\text{h}^{-1}$. The thick grey dashed line represents the combined average flux of flat-sheet modules during the 8 d filtration test. Data points represent the actual flux at a specific time.

The cumulative permeate volumes were calculated with the same assumption as for the first experiment (section 6.1.3) and are presented in Table 6.5. Calculated values for cumulative volumes over 8 d were equal to 207, 216, 147 and 177 L.m^{-2} for Kubota 3 kPa, Kubota 6 kPa, fabric 3 kPa and fabric 6 kPa, respectively. The volumes generated from the modules were similar to that generated from filtration with unfractionated laboratory ABR effluent indicating a similar pattern of fouling behaviour. Differences between these volumes after 8 d of supernatant filtration are low for a given membrane, with Kubota membrane modules producing a greater volume than fabric modules. The difference in calculated volume produced over 8 d corresponds to an approximately 20 to 30% increased permeate production with Kubota modules.

Table 6.5: Calculated cumulative volumes of Kubota and fabric modules operated at 3 and 6 kPa over 8 d treating the supernatant from settled ABR effluent. Cumulative volumes of permeate were calculated using flow rates between sampling days and divided by the effective filtration area for each module. For comparison, the cumulative volumes of the modules treating ABR effluent from section 7.1 have also been included.

Kubota 3 kPa	Kubota 6 kPa	Fabric 3 kPa	Fabric 6 kPa
<u>Volume (L.m⁻²) for first 8 d treating supernatant from settled ABR effluent</u>			
207	216	147	177
<u>Volume (L.m⁻²) for first 8 d treating ABR effluent</u>			
173	206	130	154

Chemical analyses

The results of the chemical analyses of day 7 (9 June 2009) are presented on Table 6.6.

Table 6.6: Chemical composition of settled ABR supernatant, membrane box and permeate samples from Kubota and fabric modules operated at 3 and 6 kPa for day 7 (9 June 2009). Analyses were performed in duplicate or triplicate (unless otherwise stated).

Day	Parameter	Unit	Supernatant	Membrane Box	<u>Kubota</u>		<u>Fabric</u>	
					3 kPa	6 kPa	3 k Pa	6 kPa
7	COD	mg/L	399 ± 3	375 ± 86	66 ± 6	43 ± 19	58 ± 7	73 ± 18
	Protein	mg/L	144 ± 3.7	145 ± 2.8	27 ± 0.4	28 ± 0.9	30 ± 3.8	30 ± 0.7
	Carbohydrate	mg/L	nd	7.3 ± 0.4	0.8 ± 0.1	1.1 ± 0.1	0.9 ± 0.3	1.1 ± 0.6

nd, not determined.

With regards to the COD concentration, all modules removed the COD below 73 mg/L after membrane filtration (80% removal). Kubota modules on average removed more COD than fabric ones.

With regards to the soluble protein concentration, the supernatant of the settled ABR effluent had a concentration of 144 mg/L with a nearly identical value measured in the membrane box. After filtration, the protein concentration was below 30 mg/L. Protein rejection was similar between modules and at different operating pressures with a minimum removal of 79% removal of total soluble protein.

With regards to the soluble carbohydrate concentration, the membrane feed box had an average concentration of 7.3 mg/L. The carbohydrate concentration of the settled ABR effluent was not

determined. There was no significant difference in carbohydrate rejection between modules and at different operating pressures. The results suggest that the rejection of soluble carbohydrates in the flat-sheet modules is similar.

At the end of the experiment, the clean water permeability after fouling was measured for only the modules operated at 3 kPa (Figure 6.12). Clean water determination was not performed on the modules operated at 6 kPa as filtration at higher TMP was shown to be similar to that at 3 kPa. Consequently, the modules operated at 6 kPa were removed from the laboratory membrane system and stored.

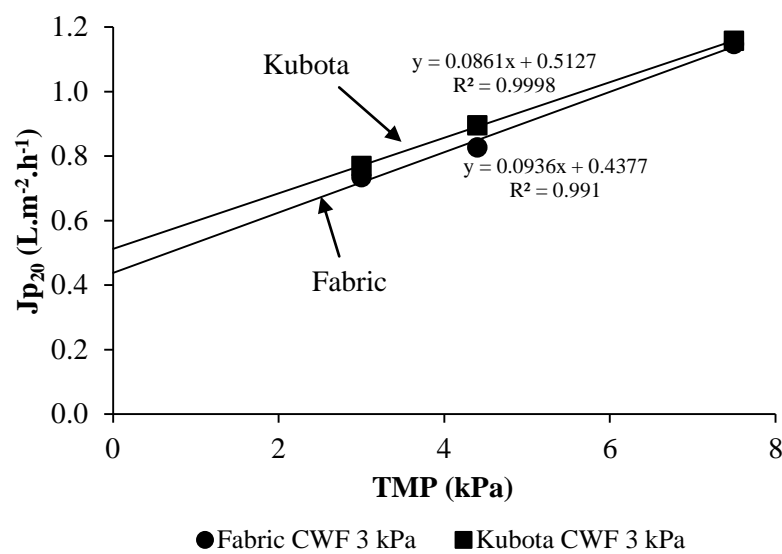


Figure 6.12: Variation of clean water flux (CWF) with TMP for Kubota and fabric modules after filtration of supernatant from settled laboratory ABR effluent. The data points represent the average flux over a specific time period.

In relation to the initial permeability before filtration, a sharp decline is observed in both Kubota and fabric modules with permeability decline greater than 95% observed for both modules. As was the case with the first effluent filtration experiment, fouling was severe and induced a very low permeability at the end of the experiment. Moreover, the fouling layer could not be removed by simply running the module under a stream of tap water (as shown in **Chapter 5**). The fouling layer had to be physically removed by gentle scraping using gloves over the membrane surface.

The removed fouling layer was diluted in a pre-defined aliquot of water and subjected to chemical analyses. The results of the analyses are presented in Table 6.7.

Table 6.7: Chemical composition of the fouling layer from Kubota and fabric modules operated at 3 and 6 kPa (10 June 2009). Analyses were performed in duplicate or triplicate (unless otherwise stated).

Day	Parameter	Unit	Kubota		Fabric	
			3 kPa	6 kPa	3 k Pa	6 kPa
8	Cumulative Volume*	L.m ⁻² (7 days)	207	216	147	177
	COD	g/m ²	11 ± 2	22 ± 3	25 ± 1	28 ± 5
	Protein	g/m ²	0.4 ± 0.2	0.3 ± 0.2	0.4 ± 0.0	0.6 ± 0.0
	Carbohydrate	g/m ²	0.3 ± 0.0	0.2 ± 0.0	0.3 ± 0.0	0.3 ± 0.0

*, The volume produced takes into consideration the effective filtration area of each module.

Total COD, soluble protein and soluble carbohydrate measurements are presented as mass per unit area to determine the quantity of these constituents retained on the membrane surface. The cumulative filtered volume for each membrane has also been indicated on Table 6.7. Kubota modules were able to produce nearly 30% more volume per m² of permeate than fabric modules based on calculated values for cumulative permeate production.

As was the case with the first flat-sheet experiment (section 6.1), the masses of soluble protein and carbohydrate deposited on the membranes are quite similar even at different operating pressures. The COD mass per unit area, however, is slightly higher for the fabric modules (25 and 28 g/m² at 3 and 6 kPa, respectively compared to Kubota modules, 11 and 22 g/m² at 3 and 6 kPa, respectively). The results suggest that the fabric modules may retain a higher organic content on their surface than Kubota modules.

6.2.4 CONCLUSIONS

The results from this series of detailed experiments revealed that the filtration of supernatant from settled effluent yields similar fluxes to that of untreated effluent. It can be therefore deduced that the role of settleable particles in fouling in the laboratory ABR treating diluted VIP sludge is minimal.

This series of experiments was continued further to investigate the role of soluble compounds in the effluent in membrane fouling. Details of the experiment are presented in the following section.

6.3 MEDIUM-TERM FILTRATION OF SOLUBLE ABR EFFLUENT

The results presented in this section follow the experiments performed in section 6.2. This section presents the results from the flat-sheet microfiltration of Polymem microfiltered laboratory ABR effluent. The rationale behind microfiltering the laboratory ABR effluent was to remove the suspended and colloidal fraction (smaller than 0.2 μm) and evaluate their influence of fouling behaviour in the flat-sheet unit. This set of experiments was performed simultaneously with the ultrafiltration hollow-fibre module (section 5.7). The aims and objectives of this section are presented in section 6.3.1. Section 6.3.2 presents the methodology and section 6.3.3 discusses the results from this series of experiments. The conclusions from this experiment are presented in section 6.3.4.

6.3.1 INTRODUCTION

This experiment was conducted to elucidate the role of soluble constituents on fouling in flat-sheet modules. The design of the experiment was based on the previous filtration experiment (section 6.2) which showed that settleable particles did not play an important role in fouling. The specific aims of this experiment were: (i) to examine the effect of the soluble component of the effluent on flux-time relationships in flat-sheet modules, (ii) to determine the effect of operating pressure on module performance and (iii) identify foulants based on specific chemical analyses.

6.3.2 METHDOLOGY

Experimental Design

Laboratory ABR effluent from Phase VII (see **Appendix II**) was collected and microfiltered through the Polymem microfiltration module with a nominal pore size of 0.2 μm . In doing so, all suspended and colloidal particles (above 0.2 μm) were removed from the effluent. Hence, the flat-sheet modules were exposed only the soluble components of the effluent.

Membrane Modules

Kubota and fabric modules treating microfiltered laboratory ABR effluent were operated at 3 and 6 kPa, respectively. The length of the experiment was deduced from the first experiment which showed that a rapid decrease in flux was observed over the first 2 d followed by a plateau of steady-state flux after 8 d. Both modules operated at 6 kPa were removed from the system after 1 d as the pressure was shown not to influence filtration characteristics. Clean water flux determinations were performed before and after supernatant filtration (refer to section A 3.4 in **Appendix III**).

Data Acquisition and Interpretation

The flow rate was calculated by measuring time required to fill a certain volume. The TMP was calculated as the height difference between the outlet of the permeate pipe and the middle of the membrane module. The resistance-in-series equation was used to calculate the permeate flux with flux corrected to 20°C to account for changes in viscosity (see **Appendix III**).

Physico-Chemical Analyses

Total COD measurements were made according to the UCT Open Reflux COD Method for wastewater (Lakay *et al.*, 2000). Soluble protein and carbohydrate measurements were made according to the Frølund *et al.* (1996) and Dubois *et al.* (1956) methods, respectively (see **Appendix IV**).

6.3.3 RESULTS AND DISCUSSION

The clean water permeabilities were measured for the four modules before effluent filtration. The results from that test are presented in Figure 6.13 as flux versus TMP. The clean water permeabilities of the Kubota modules were equal to approximately $24.0 \text{ L.m}^{-2}.\text{h}^{-1}.\text{kPa}^{-1}$ ($2400 \text{ L.m}^{-2}.\text{h}^{-1}.\text{bar}^{-1}$) (similar to first filtration experiment, section 6.1). In contrast, the clean water permeability of the fabric modules were approximately $2.00 \text{ L.m}^{-2}.\text{h}^{-1}.\text{kPa}^{-1}$ ($200 \text{ L.m}^{-2}.\text{h}^{-1}.\text{bar}^{-1}$), significantly lower than that of the first experiment (section 6.1).

The results indicate that fabric modules may retain more fouling constituents on their surface than the Kubota modules. This may be due to the material used in the construction of the membranes. Kubota modules have a uniform and smooth membrane surface whilst fabric modules, due to the nature of the material used in their construction, are less uniform in terms of pore size. Hence, it is possible that more foulants could be lodged in-between the fibres of the fabric than on the smoother surface of the Kubota and are therefore more difficult to remove using physical cleaning.

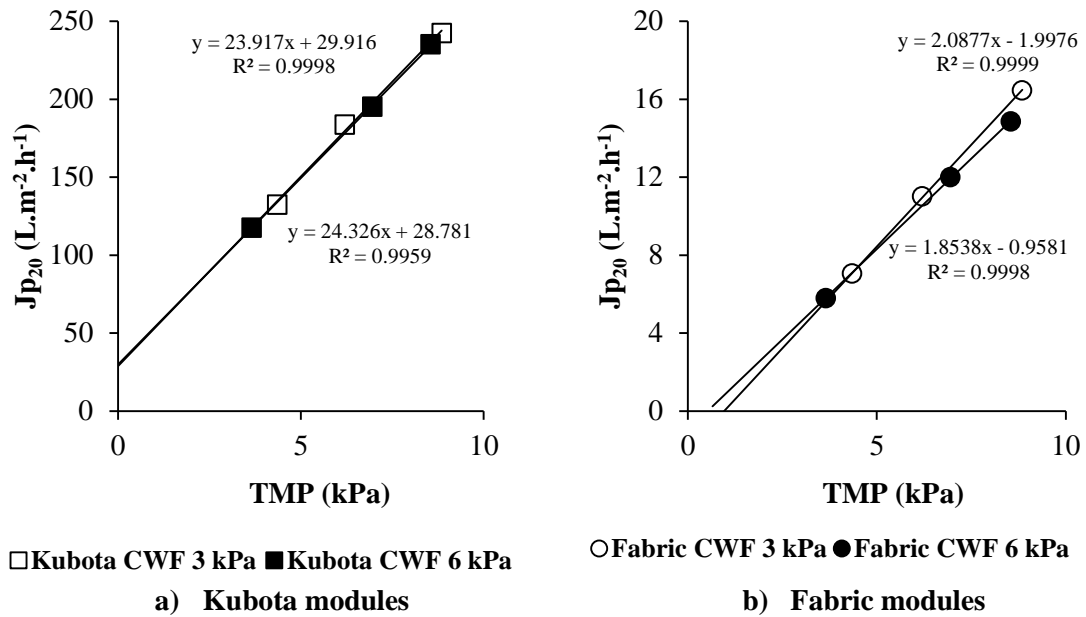


Figure 6.13: Variation of clean water flux (CWF) with TMP for Kubota and fabric modules before microfiltered ABR effluent filtration. The data points represent the average flux over a specific time period.

The modules were operated as a gravity-fed system over a period of 8 d using microfiltered effluent. In other words, the modules *only treated the soluble component of the ABR effluent* with no solid or colloidal fraction (at least up to 0.2 μm). The flux-time graph of the experiment is presented in Figure 6.14. The Kubota modules had a higher starting-up flux (104 $\text{L.m}^{-2}.\text{h}^{-1}$ and 187 $\text{L.m}^{-2}.\text{h}^{-1}$ at 3 and 6 kPa, respectively) than the fabric modules (5 $\text{L.m}^{-2}.\text{h}^{-1}$ and 9 $\text{L.m}^{-2}.\text{h}^{-1}$ at 3 and 6 kPa, respectively). On day 1, the membrane box was damaged after it accidentally fell down. A side panel was broken during the fall which required repair. An indication of the time at which the pilot was damaged is shown in Figure 6.14. The incident has been included into the graph to show the difference between the start-up fluxes before and after the incident. The start-up fluxes of the modules were at least four times higher at the beginning of the experiment than after the incident. The flux for Kubota modules before the incident was 10 and 11 $\text{L.m}^{-2}.\text{h}^{-1}$ at 3 and 6 kPa, respectively. For the fabric modules, the flux was 3 and 11 $\text{L.m}^{-2}.\text{h}^{-1}$ before the incident at 3 and 6 kPa, respectively.

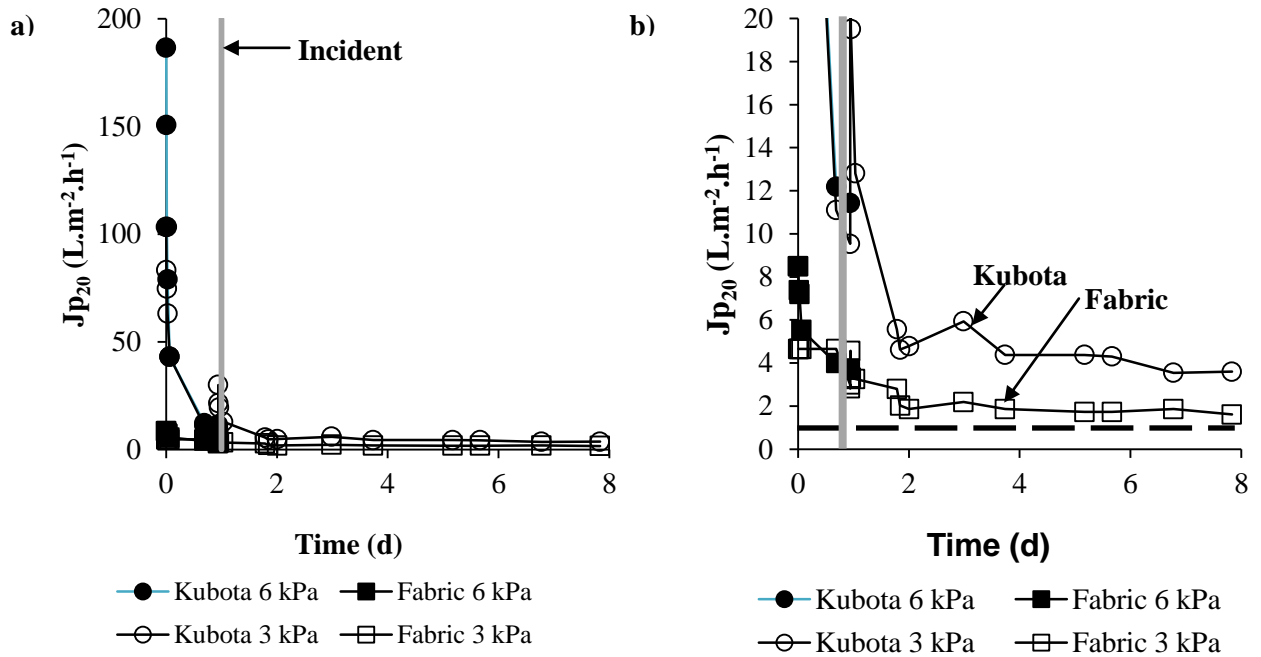


Figure 6.14: The simultaneous variation of flux versus time for Kubota and fabric modules treating the soluble component of the laboratory ABR effluent. a) Flux-time profile of modules over 8 d. b) Magnified view of (a) with flux presented at a maximum of 20 $L.m^{-2}.h^{-1}$. The vertical grey line (—) represents the time of the incident whilst the horizontal dashed black line (---) represents the flux plateau from previous experiments. Data points represent the actual flux at a specific time.

Whilst the side panel was repaired, the modules were stored in a solution of microfiltered effluent. The experiment was then restarted but with only one module of each type at 3 kPa (one Kubota and one fabric module at 3 kPa). Modules used at 6 kPa were removed from the system as initial flux data during the filtration of microfiltered effluent showed similar trends to those modules operated at 3 kPa. As flow rates were similar at both operating pressures, there was no need to continue operating at different pressures for each module type.

The restart of the filtration resulted in a higher flux in Kubota and fabric modules than prior to the incident. This could have been due to the relaxation of pressure across the membrane, possible back diffusion of foulants into the storage solution or the dislodging of the fouling layer during the fall. Nevertheless, the flux decreased rapidly in one day after the restart to a plateau similar to one that could have been reached had the incident not occurred.

The stabilised flux plateau reached by the flat-sheet modules was higher than that achieved in previous experiments (approximately 4 and 2 L.m⁻².h⁻¹ in Kubota and fabric modules, respectively). This represents a permeate production increase of greater than 100%. The results imply that reduced fouling has occurred through the removal of suspended and colloidal matter. Interestingly, a significant decline in flux still occurred in both modules during the initial stage of filtration. The pattern suggests that severe fouling was still occurring. This coupled with comparatively lower flux rates when compared to the initial clean water fluxes suggest that the soluble component of the effluent plays an important role in fouling. It can therefore be deduced that soluble components and/or non-settleable constituents were responsible for fouling in this membrane system.

With respect to the permeate production, Kubota modules were able to produce more permeate than the fabric module over the 8 d. Calculated cumulative permeate volumes were equal to 1 150 L.m⁻² for Kubota and 393 L.m⁻² for fabric modules at 3 kPa, respectively, representing nearly 400% increase in productivity in Kubota modules over the fabric ones.

Chemical analyses

The results of the chemical analyses of day 1 (22 September 2009) of the microfiltered effluent experiment are presented in Table 6.8. With regards to the COD concentration, the soluble component of the effluent had concentration of 43 mg/L with no further removal occurring after filtration with flat-sheet modules. This result was expected as the Polymem microfiltration module has a smaller pore size than Kubota and fabric modules. The result shows that a second microfiltration step does not remove any residual COD.

Table 6.8: Chemical composition of microfiltered laboratory ABR effluent, membrane box and permeate samples from Kubota and fabric modules operated at 3 and 6 kPa for day 7 (9 June 2009). Analyses were performed in duplicate or triplicate (unless otherwise stated).

Day	Parameter	Unit	Microfiltered effluent	<u>Kubota</u>		<u>Fabric</u>	
				3 kPa	6 kPa	3 k Pa	6 kPa
1	COD	mg/L	43 ± 0	43 ± 9	43 ± 13	41 ± 5	41 ± 38
	Protein	mg/L	43 ± 0	8 ± 0.3	8 ± 0.7	8 ± 0.3	8 ± 1.2
	Carbohydrate	mg/L	4 ± 0.25	4 ± 0.1	4 ± 0.1	4 ± 0.2	4 ± 0.1

nd, not determined.

In contrast, soluble protein concentration decreases after a second filtration through fabric and Kubota modules. The soluble component of the effluent had a concentration of 43 mg/L before

flat-sheet filtration. After filtration, this was reduced to 8 mg/L in the Kubota and fabric modules suggesting that protein is being retained by the membrane modules. As carbohydrate concentrations remain relatively constant across the flat-sheet modules, it is hypothesised that proteins may play a role in fouling in this system.

The clean water permeability after fouling was determined and is presented in Figure 6.15. The permeabilities of the modules that were removed from the system are also shown on the graph (represented as Kubota 6 kPa and fabric 6 kPa).

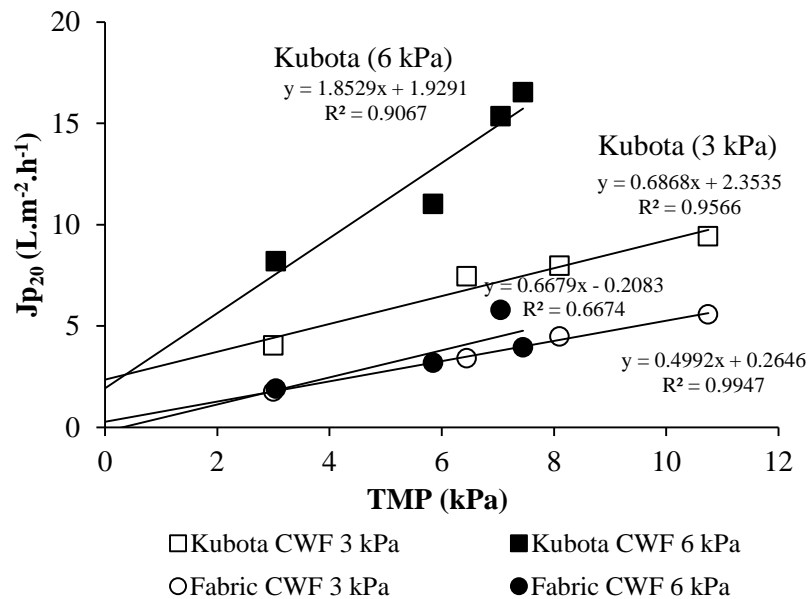


Figure 6.15: Variation of clean water flux (CWF) with TMP for Kubota and fabric modules after laboratory ABR effluent filtration. The data points represent the flux over a specific time period.

The final permeabilities of the Kubota and fabric modules operated at 6 kPa were equal to 1.86 (186 L.m⁻².h⁻¹.bar⁻¹) and 0.69 L.m⁻².h⁻¹.kPa⁻¹ (69.0 L.m⁻².h⁻¹.bar⁻¹). These modules were operated only for 1 d. The final permeabilities of the Kubota and fabric modules operated at 3 kPa (7 d) were equal to 0.67 (67.0 L.m⁻².h⁻¹.bar⁻¹) and 0.50 L.m⁻².h⁻¹.kPa⁻¹ (50.0 L.m⁻².h⁻¹.bar⁻¹).

Although a decline in permeability was observed in both module types, the difference between the fabric modules was not large. The results indicate that fabric modules are easier to foul than Kubota ones. Moreover, most of the fouling occurs during the first day of filtration.

The results of the chemical analyses of the cleaning completed on the last day, day 7 (9 September 2009) are presented in Table 6.9.

Table 6.9: Chemical composition of the fouling layer from Kubota and fabric modules operated at 3 and 6 kPa for day 7 (9 September 2009). Analyses were performed in duplicate or triplicate (unless otherwise stated). The volume produced takes into consideration the effective filtration area of each module.

Day	Parameter	Unit	Kubota		Fabric	
			3 kPa	6 kPa	3 k Pa	6 kPa
7	Cumulative Volume	L.m ⁻²	1 150	381 ^a	393	99 ^a
	COD	g/m ²	1.4*	0.8 ± 0.2	1.2 ± 0	2.1 ± 0.1
	Protein	g/m ²	0.7 ± 0.0	1.1 ± 0.1	0.4 ± 0.0	1.3 ± 0.3
	Carbohydrate	g/m ²	0.01 ± 0.0	0.06 ± 0.0	0.03 ± 0.0	0.44 ± 0.0

^a, Only one day of filtration

*, Only one sample analysed.

Calculated values for cumulative volumes were equal to 1 150, 381, 393 and 99 L.m⁻² for Kubota 3 kPa, Kubota 6 kPa, fabric 3 kPa and fabric 6 kPa, respectively. The values presented for modules operated at 6 kPa represent the calculative cumulative flow over 1 d. Kubota modules are able to produce significantly more permeate than fabric modules.

The total COD, soluble carbohydrate and protein concentration per unit area is relatively similar among modules. There was no clear difference in chemical composition between modules operated at a longer time (Kubota and fabric modules at 3 kPa) and those operated for only a day indicating that the fouling layer develops during the initial stage of filtration. Proteineaceous compounds constituent nearly half of the total COD present on the surface on the flat-sheet modules implicating these compounds in fouling of this system.

6.3.4 CONCLUSIONS

The results from this section indicate that the soluble component of the laboratory ABR effluent is involved in fouling in the flat-sheet unit. Proteinaceous compounds are thought to play a role in the fouling layer developed based on chemical analyses.

6.4 SUMMARY OF FLAT-SHEET FILTRATION

A flat-sheet system was evaluated as a possible post-treatment step for ABR. Long-term filtration with Kubota and fabric microfiltration modules showed that a period of stabilised low flux (less than 0.5 L.m⁻².h⁻¹). The fouling pattern in both modules is typical of constant TMP operation with a rapid initial decline in flux followed by a stabilised period. Operating pressure

has no influence on filtration characteristics. Fouling is severe and irremovable in both modules as indicated by the decline in permeability after filtration.

Detailed medium-term experiments were performed with the aim of identifying the foulant based on size-specific filtration. To understand the role of settleable particulates in fouling, supernatant from settled ABR effluent was filtered and compared to untreated effluent. Nearly identical flux-time curves were produced from the two sets of experiments which suggested that settleable particulates do not contribute to fouling. To understand the role of the soluble component of fouling, microfiltered ABR effluent was fed to the flat-sheet membrane unit. The results indicated that an improvement in flux was attained but this flux was still much lower than the clean water flux before soluble effluent filtration. Moreover, the fouling layer that had developed was more difficult to physically remove. Through progressive experimentation, it was deduced that the non-settleable and soluble constituents in the ABR effluent contributed to membrane fouling in the flat-sheet system. Chemical analyses of the fouling layer after microfiltering the laboratory ABR effluent indicated that proteins may be involved in the fouling mechanisms observed in the flat-sheet unit.

In the next chapter, the main discussions and conclusions emanating from this thesis are presented (**Chapter 7**). The results are discussed in context of the observed fouling mechanisms in membrane filtration systems treating the effluent from an ABR. More specific detail related to the mechanism of fouling in **Chapter 6** can be viewed in section 7.8.

CHAPTER 7 : DISCUSSION AND CONCLUSIONS

7.1 INTRODUCTION

In the previous chapter, the results from the flat-sheet microfiltration unit treating laboratory ABR were discussed. In this chapter, the experiments performed with a laboratory ABR coupled to membrane filtration systems are discussed and summarised. The purpose of this chapter is to summarise the findings of membrane experiments and assess the applicability of membrane technology for ABR effluent polishing. The contents of **Chapters 2 to 6** are summarised and the research questions posed in the thesis answered to provide conclusions to this study.

7.2 TECHNOLOGICAL GAP

Chapter 2 presented a review of literature regarding anaerobic technology, more specifically the ABR and membrane filtration technology. The ABR was shown to be a robust sanitation option for decentralised applications. However, the review highlighted the lack of published work regarding the availability of a suitable effluent polishing step for anaerobic technologies; a critical feature which limits the wider spread use of the technology. Membrane technology was considered in this thesis as a possible post-treatment system. Although there are many articles published with respect to membrane filtration technology for decentralised drinking water and greywater applications, not much information is available with regards to the post-treatment of anaerobic effluents using gravity-driven (no energy) filtration. Moreover, the membrane processes that determine performance will be different to other aerobic and anaerobic technologies. This work therefore represents a novel application of a high-technology application in a low-cost manner for effluent polishing in a decentralised anaerobic system.

7.3 DESIGN AND OPERATION OF THE PLANT

Chapter 3 presented the design and construction details of the laboratory ABR and membrane filtration apparatus. The design of the ABR was modularised and included a large round feeding tank from which wastewater was pumped through ABR compartments. The modularised design used small piping (maximum inner diameter of the peristaltic pump were 8 mm) between the feeding tank and ABR compartments which limited the treatment of wastewaters with a high particulate content. Diluted sludge from VIP latrines was used as a ‘synthetic’ feed wastewater. Samples were collected from a specific household and from pit emptying contractors, stored in the laboratory and processed during feeding. Continuous ABR operation was sometimes difficult to due to power shortages, pump problems and building construction, events that are not likely to influence field ABR systems. Two membrane types were evaluated for membrane fouling; hollow-fibre modules and flat-sheet microfiltration modules. The hollow-fibre modules

were constructed by Polymem and included a microfiltration and an ultrafiltration module. Two types of flat-sheet microfiltration modules were evaluated for membrane performance; a standard A4 size plate and frame Kubota module and a locally developed fabric module manufactured by the Durban University of Technology (DUT). The major difference between the flat-sheet modules was related to material used in the manufacturing process; Kubota modules have an average pore size of 0.4 μm while fabric modules do not have a defined pore size. Fabric modules are also the more robust membrane type due to its resilience to drying (unlike Polymem and Kubota modules) after which the fouling layer can be peeled off.

There were similarities and differences between the design and operation of the two membrane units. In both membrane units, the membrane was operated in an upright position and at constant TMP. The differences between the membrane units were a result of different people responsible for designing and operating the systems. The hollow-fibre unit was an airtight unit which did not allow for the routine measurement of the concentrate in the membrane casing. If the valves on the casing were to be opened for sampling, it would have caused TMP relaxation across the module and a possible disturbance of the fouling layer. Thus, the bulk liquid concentration of the membrane unit could only be measured at the end of an experiment. The airtight design with the flexible height configurations did, however, make the measurement of TMP across the membrane easier than the hollow-fibre unit.

Unlike the hollow-fibre unit, the flat-sheet unit was not airtight. A lid was used to prevent contaminant from entering the membrane unit. The TMP of the module could only be changed significant by adjusting the height of the permeate lines. The design, however, did allow for the routine measurement of the bulk liquid concentration in the membrane unit.

Another difference between the membrane units was the volume of concentrate available per membrane area in each unit. The flat-sheet unit had a working volume of approximately 24 L with the average flat-sheet membrane in the module approximately 0.1 m^2 (volume per membrane area = 240 $\text{L}\cdot\text{m}^{-2}$). In contrast, the hollow-fibre unit had a working volume of approximately 5 L with a membrane area of 1 m^2 available for filtration (volume per membrane area = 5 $\text{L}\cdot\text{m}^{-2}$). Thus, there was more volume of concentrate available in the flat-sheet unit than the hollow-fibre unit.

7.4 OPERATION OF ABR SYSTEM

In **Appendix II**, the performance of the laboratory ABR treating a complex synthetic particulate wastewater representative of blackwater was evaluated. One of the major drawbacks of the

study was related to the feed wastewater characteristics. The laboratory ABR was fed with diluted VIP sludge which contained a high concentration of solids and a low biodegradability content. Bakare (2011) measured the biodegradability of the upper surface of pit latrine sludge to be approximately 30%; a similar value calculated using a rough estimation of the COD mass balances in this ABR system (Kapuku, 2011). The feed was chosen as a representation of blackwater as it was logistically simpler to collect than actual domestic wastewater (or blackwater) and was thought to be more representative than a soluble synthetic feed. When soluble synthetic wastewaters are treated in an ABR, distinct phase separation can occur in the ABR and methanogenesis can be the rate-limiting step as the substrates in the wastewater are easily assimilated by anaerobic microorganisms (refer to section 2.1.5). However, domestic wastewater or blackwater treatment is more difficult in an ABR due to particulates in the wastewater. For these types of wastewater, partial or limited phase separation occurs in the ABR with hydrolysis (breakdown of particulates) often being the rate-limiting step. Therefore, the VIP sludge represented the closest available source of a sanitation wastewater for this study. The limitation of this approach is that membrane experiments could not be extrapolated to field conditions.

The design of the system was not suited to the treatment of a high particulate wastewater emanating from the feed. Clogging of the overflow pipes with solids and other material (such as maggot eggs, pieces of cloth used as toilet paper) prevented the overflow of the feed wastewater from the round feed tank to ABR compartments. Moreover, the feed characteristics did not allow low speed stirring for the same reason (the inner diameter of the pumping tubes was too small even though the largest commercially available tubing size was used for this particular pump). When stirring was applied, suspended solids clogged the pump to the ABR train. Retention of solids in the first round feed tank was shown to be a major mechanism of organic removal with nearly half of total COD removed this way (**Appendix II**). While a similar problem has been observed in BORDA DEWATS plants, the results nevertheless highlight the design limitation of the ABR system used in this study.

7.5 QUANTIFYING FOULING PROPENSITY IN TEST CELLS

A bench-scale test cell membrane filtration apparatus was used in **Chapter 4** to evaluate the fouling propensities of the soluble fractions of different sludge sources. The technique was recommended by *EUROMBRA* partners as a standardised parameter with its main objective to provide a quick examination of fouling strength of a particular feed solution. This technique could then be used to determine an appropriate pre-treatment requirement for membranes without the need to conduct a laborious and expensive pilot-scale study. The aims of **Chapter 4**

were to explore the use of the recommended test cell technique for the evaluation of fouling propensity of *only the soluble constituents* in different membrane feed solutions. Emphasis was placed on the comparison of fouling propensity of the soluble component of ABR fluids in relation to each other and other sources (aerobic and other anaerobic mixed liquor samples). It envisaged that the experiments would yield more information on the suitability of treating ABR effluents with membranes and whether membrane modules could be submerged within compartments of the ABR as it is done in submerged aerobic MBRs. Lastly, the experiments aimed to provide a critical analysis of the technique in relation to the reproducibility of results and suitability of the cake filtration model (see section 4.1) to interpret fouling in the test.

The use of test cells in membrane fouling studies is common (Jarusutthirak *et al.*, 2002; Jimenez *et al.*, 2004; Lodge *et al.*, 2004; Cho *et al.*, 2005; Khirani *et al.*, 2006; Wang *et al.*, 2007; Arabi and Nakhla, 2008; Huang *et al.*, 2008; Lesage *et al.*, 2008; Teychene *et al.*, 2008; Jamal Khan *et al.*, 2009). The most common type (and the brand used in this study) is the Amicon® stirred batch ultrafiltration cell (evidence cited in Jimenez *et al.*, 2004) with filtration performed at constant pressure using a reference flat-sheet membrane (Huang *et al.*, 2008). Fouling in the apparatus is described by cake filtration theory which is assumed to be the dominant process in fouling with the macrosolutes rejected by the membrane forming a cake layer under dead-end filtration (Huang *et al.*, 2008). From this model, a membrane fouling index (commonly called MFI or its variants or the product of $\alpha.C_s$, can then be calculated from experimentally determining and fitting t/V and V values (Boerlage *et al.*, 1998; Huang *et al.*, 2008), thereby providing a representation of fouling propensity. One of the major limitations of this approach that has been noted in this study is the non-linearity of t/V versus V plots which made the measurements of values of the product of $\alpha.C_s$ difficult to interpret and therefore limited statistical evaluation between test solutions. This is not an unusual occurrence as many other authors have also noted a similar problem in the filtration of mixed liquors (Boerlage *et al.*, 2003; Yim and Song, 2005; Park *et al.*, 2006). In such cases, modifications to the existing model and/or protocol have been made to account for other influences (Brauns *et al.* 2002; Jimenez *et al.*, 2004; Huang *et al.*, 2008; Sim *et al.*, 2011), such as membrane compaction and a dominant pore blocking mechanism which has been shown to occur in these experiments. However, such modifications were not made in this study as it was thought not to fall within the scope of this research and the technique was applied as recommended (with limitations acknowledged). Furthermore, most of the models developed were for mixed liquors and not exclusively the soluble component (free of colloids and solids) of the feed.

It must be also noted that there were cases when data or protocol modification were not required in other *EUROMBRA* related studies using a similar set-up (Teychene *et al.*, 2008). The results indicate that there are other factors (such as membrane type, filtration time, feed solution) that could affect results. For example, numerous authors have conducted filtration experiments over a longer length of time. In Abogrean *et al.* (2003), at least 300 L of cumulative filtrate volume was used in the calculation of the MFI-UF value (calculated from t/V versus V plots). In Boerlage *et al.* (2002), a stable region in specific cake resistance value (determined by plot of MFI-UF versus time) was only achieved after at least 20 h for tap water whilst at least 2 h was required for dilute canal water (Boerlage *et al.*, 2003). The experimental set-up was similar to test cell technique used in this thesis. Keskinler *et al.* (2004) found that at least 5 min was required to achieve linear relationship in the plot of t/V versus V and that this was the case in all filtration experiments performed. With respect to published works, the findings in this thesis indicate that the cake filtration model has been applied to the part of curve where pore blocking (section 2.2.5 and section 4.1) is the more pronounced mechanism of fouling. Filtration times should have therefore been longer to include the cake filtration mechanism or analysed from the onset of linearity of t/V versus V plots. Furthermore, the nature and concentration of different soluble EPS in the test solutions were different to other partners (lower than other partner groups).

As t/V versus V data were mostly non-linear, the lower and upper ranges (based on a 95% confidence level) of the values for the product of $\alpha.C_s$ were calculated. Although not ideal, it made comparison between solutions isolated from different sludge sources possible. The results revealed that solutions from the starved pilot ABR (from Project K5/1248, Foxon *et al.*, 2006) had the lowest fouling propensity. This result was expected as the reactor had not been fed for a year (samples were taken as the laboratory ABR had not been constructed at that time). However, highly compressible solute gel-like cake layers formed in these compartments samples especially compartment 3. Although the COD value of the solution was low, it still contained a high proportion of soluble proteinaceous compounds which probably formed part of the gel-like layer which developed. This layer was difficult to remove manually. The high proportion of proteins in solution may be due to biomass decay (from starvation) which releases soluble EPS (soluble microbial products) faster than they are assimilated (Noguera *et al.*, 1994). Nevertheless, the results suggest that using membranes to treat an effluent from the compartments at the front end of the ABR may not be advisable.

The soluble fraction of the sludge from a conventional anaerobic digester was shown to have the highest fouling propensity (based on lower and upper range values for the product of $\alpha.C_s$). The fouling propensity of the soluble fraction of the effluent (or the overflow from compartment 4)

of the laboratory-scale ABR treating the two types of wastewaters were comparable to that from an activated sludge indicating that the ABR system does not produce an effluent with a higher fouling propensity than an activated sludge plant. It is important to note that conditions in the ABR would have been stressed due to some degree of starvation or limited substrate conditions as the feed wastewater had a low fraction of biodegradable COD (**Appendix II**). Although this parameter was not extensively examined here, literature suggests that the production of EPS may occur as a protective mechanism under nutrient-limited or starvation conditions and that it (starvation) is sometimes necessary for the initiation of the EPS production process (Rittmann and McCarty, 2001; Chrysi and Bruce, 2002; Aquino and Stuckey, 2003; Li *et al.*, 2006). Moreover, a portion of the soluble EPS produced in starved reactors may occur through biomass decay (as discussed earlier) (Noguera *et al.*, 1994; Aquino and Stuckey, 2003). Despite the fact that the laboratory ABR is expected to contain a high proportion of these soluble compounds, fouling propensity did not differ much from the other samples (except from the anaerobic digester samples).

The results from this study provided valuable information towards the improvement and development of a standardised fouling parameter that is based on cake filtration theory. According to the author's knowledge, the *EUROMBRA* project into which this study fed provided the first attempt to develop a standardised fouling parameter and apply it over a range of case studies. The technique does have limitations (as discussed earlier) with most of the problems relating to the complexity and range of the mechanisms involved in fouling which make any effort to provide a simple model for fouling characterisation difficult. Recommendations for improvement in the technique are presented in **Chapter 8**.

7.6 HOLLOW-FIBRE MEMBRANE PERFORMANCE

The results of a series of filtration experiments with Polymem hollow fibre modules were presented in **Chapter 5**. In many of the medium-term tests, the experiments were not replicated as there was a compromise between conflicting requirements of performing multiple tests on a module and the deterioration of membrane integrity over time. The project team chose to do a single test that was performed using batches of membrane feed (settled or microfiltered) and collected over four or more days instead of a single batch to improve the significance of the experimental results. In one of the instances, the membranes were operated in series (microfiltered first in Polymem module then other modules) to ensure that the fouling trends were similar.

A unique set of experiments was performed at various constant and low transmembrane pressures (TMP) to evaluate the limiting flux of each module using the protocol described in **Appendix II**. The collective filtration experiments at constant TMP were referred to as TMP-step experiments. Although the value of the limiting flux is not as informative as the critical flux (performed at constant flux operation) and not expected to yield less fouling below this parameter, valuable information regarding the TMP threshold at which to operate the modules in field-scale decentralised systems was gathered.

From TMP-step experiments performed at varying COD concentration to the ABR (total COD between 1 000 to 3 000 mg/L), it was shown that the COD concentration had only a slight influence on the flux of each module. Operation below 4 kPa (400 mm hydrostatic head) was identified as a potentially suitable operational TMP (provided effluent COD concentrations are also below 400 mg/L). Moreover, fouling during short-term operation in this system (hollow-fibre unit) was found to be largely removable with clean water permeabilities being restored to their pre-effluent filtration state. Based on the findings, it was initially hypothesised that pore blocking by large particulates may be the dominant fouling mechanism.

A long-term filtration experiment was carried out on an ultrafiltration module treating effluent from the ABR at low hydrostatic pressures (3 kPa). A rapid decline in flux was observed during the initial stages of filtration (2 d) followed by a plateau ($0.2 \text{ L}\cdot\text{m}^{-2}\cdot\text{h}^{-1}$) which was not sustained. Maintenance was required relatively early during the service of the membrane with excessive fouling occurring after 30 d. The fouling layer was largely removable using tap water rinsing with the trend similar to that observed during short-term TMP-step filtration experiments.

Detailed medium-term filtration experiments (a few days) were conducted on the laboratory ABR effluent using a compositional approach to identifying possible foulants. The laboratory ABR effluent was fractionated according to size of constituents in solution. First, the filtration of the supernatant fraction of settled effluent (non-settleable) fraction was performed on the ultrafiltration module. The results showed that the flux of this fraction was nearly identical to that of effluent without any pre-treatment. To examine the influence of suspended and colloidal particulates on fouling, the laboratory ABR effluent was microfiltered through 0.2 μm Polymem module. The permeate that was generated was used as the membrane feed for the ultrafiltration module. The results revealed that the majority of fouling constituents were removed and that the soluble fraction of the effluent had a lower fouling propensity than the colloidal-solute fraction. These experiments were performed in parallel with flat-sheet microfiltration membranes. The conclusion is that the main source of fouling for the hollow-fibre unit was in the suspended and

colloidal phase, that is, the fraction which was not removed by settling but was removed by a 0.2 μm microfiltration membrane.

7.7 FLAT-SHEET MEMBRANE PERFORMANCE

Chapter 6 presented the results from a flat-sheet membrane system using two types of microfiltration modules. Although the filtration tests were performed only once, it was performed over four days to minimise the lack of data replication. Stabilised filtration was achieved in both Kubota and fabric modules operated at 3 and 6 kPa, respectively. The fouling pattern in both modules is typical of constant TMP operation with a rapid initial decline in flux followed by a stabilised period. Operating pressure was shown to have no influence on filtration characteristics with gel-like fouling observed in both modules types regardless of the operating TMP. Stabilised flux values were achieved over 80 d for both module types (in contrast to hollow-fibre modules).

Detailed medium-term experiments were performed with the aim of identifying the foulant based on size-specific filtration. To understand the role of larger settleable particulates in fouling, supernatant from settled ABR effluent was used as the membrane feed and the results compared to effluent with any pre-treatment. Nearly identical flux-time curves were produced from the two sets of data which suggested that settleable particulates did not contribute to fouling. To understand the role of the soluble component of fouling, microfiltered effluent was used as the membrane feed. Improvement in flux was observed but it was still much lower than the clean water flux before soluble ($\geq 0.2 \mu\text{m}$ particle free) effluent filtration. Through progressive experimentation, it was deduced that the non-settleable and soluble constituents in the ABR effluent contributed to membrane fouling in the flat-sheet system. The effect of the soluble EPS constituents was also investigated. However, no significant trends were observed with respect to the cause of fouling.

7.8 EFFECT OF PORE SIZE AND SURFACE MORPHOLOGY ON FOULING LAYER DEVELOPMENT

The results presented in this dissertation were different to those reported by other partner groups in the *EUROMBRA* Project. Most of the outcomes of the *EUROMBRA* Project were based on investigations using conventional aerated MBRs (*EUROMBRA*, 2010b). For example, at the Final MBR-Network Workshop in Berlin in 2009, in the session “Membrane Fouling and Control”, most of the results presented were in relation to laboratory and full-scale aerated membrane systems and the impact of aeration rates on membrane performance. Other topics included the development of fouling resistant membrane types and cleaning solutions

(EUROMBRA, 2010 – downloadable deliverable and workshop documents available on website: <http://www.mbr-network.eu/mbr-projects/downloads-common.php>). The study performed at UKZN was unique, not only in that no aeration was used to scour membranes but also the mode of membrane operation (low and constant TMP), the type of wastewater treated, the pre-treatment step (in an ABR) and the type of modules used (Polymem modules made specifically for on-site waterborne systems, locally produced fabric modules). In such cases, the results were not comparable to other groups and thus the fouling trends and findings observed in this dissertation are unique to other partner groups.

The results from **Chapters 6 and 7** revealed that there are two different fouling mechanisms occurred in the laboratory system. In the hollow-fibre system (Polymem modules), the fouling is so severe that user intervention is required in less than a month to restore a reasonable flux. The fouling layer that develops, however, can be easily washed off and permeability restored using a combination of physical cleaning techniques. In the flat-sheet system (Kubota and fabric modules), fouling is not severe with low steady-state flux easily maintained without any user intervention. There are also physical differences in the fouling layer that develops between module types. Hollow-fibre modules developed a sludge-like cake layer on their membrane surface whilst flat-sheet formed a gel-like layer despite both module types receiving the same effluent under identical operating conditions.

The differences in fouling observations between hollow-fibre and flat-sheet modules are hypothesised to be related to the physical characteristics of membranes and not the biochemical properties of the membrane feed for the following reasons. First, identical membrane feed solutions were used for experiments. Second, the bulk liquid conditions (as determined by COD) in the membrane reactors were similar to effluent for both membrane types (although this could not be statistically validated because of a limited number of samples). And finally, the same material, polyethersulphone, was used to construct the outer skins of the Polymem and Kubota modules possibly eliminating the effects of surface chemistry, such as hydrophobicity, between the modules. Moreover, it could not explain why the fabric modules exhibited similar fouling layer development to the Kubota module (which is made from woven polyester fibres).

At first, it was hypothesised that difference in fouling behaviour is related to the pore size (based on clean water permeabilities with hollow-fibre modules). The importance of pore size in membrane fouling has been noted by other authors (Nghiem and Hawkes, 2007; Jin *et al.*, 2010). The hollow-fibre modules had smaller nominal pore sizes (0.2 µm microfiltration module and 0.08 µm pores in the ultrafiltration module) than flat-sheet microfiltration modules (at least 0.4 µm). A different fouling layer may develop if the foulants,

possibly colloids or suspended solids in the bulk fluid, are larger than the pore size of the hollow-fibre modules but smaller than flat-sheet modules. In such a scenario, a loosely-attached fouling layer will develop on the hollow-fibre modules which can then be easily removed (as demonstrated by clean water filtration tests). Conversely, these foulants could become more embedded and harder to remove from the pores of the flat-sheet modules. Although this hypothesis can convincingly explain the observed fouling behaviour, this hypothesis alone could not account for the formation of a gel-like fouling layer and the influence of soluble component on membrane fouling on the flat-sheet modules (hollow-fibre modules had a visually different fouling layer with the soluble component less influential in fouling). The results suggest that there may be other factors, besides pore size, influencing fouling layer development.

SEM micrographs were taken of the surfaces of the membranes to provide a better insight to interactions occurring on the membrane surface-bulk fluid interface. All modules were rinsed in tap water before viewing (the micrographs do not show fouling layers) and were prepared for viewing by freeze-fracturing membrane material in liquid nitrogen. Freeze-fracturing was used in sample preparation as the samples became compressed during dissection. Micrographs of Polymem module have not been presented in this section as the ultrafiltration module was used in most hypotheses testing. The micrograph in Figure 7.1 shows a fibre from a Polymem ultrafiltration module. A cross-section of the fibre reveals that the fibres do not have a uniform structure throughout their depth (Figure 7.2). A porous and less dense structure is observed closer to interior of the fibre where the permeate flows is collected and the denser side closer to the feed side of the membrane (or that which is exposed to the ABR effluent) (Figure 7.3). The outer skin of the hollow-fibre is smooth with a number of relatively evenly distributed pores (Figure 7.4). The pores have a defined shape with and are normal to the outer surface of the hollow-fibre (distinct shape) (Figure 7.5). In contrast, the fabric modules are constructed from polyester filaments that are spun into a fibre (thread) which is then woven into fabric to form a physical barrier (Figure 7.6 and Figure 7.7). The membrane does not have well-defined outer skin or pores like the other modules tested making an estimation of the selectivity of module difficult. Kubota modules are made from the same material (polyethersulphone) as the Polymem hollow-fibres. The membrane surface is porous and does not have well-defined pores (Figure 7.8 and Figure 7.9).

The following conclusions can be made from visual observations of the surface morphology of the membranes. Polymem modules have a smoother outer surface with more well-defined pores. The pores are evenly distributed on the surface, unlike the Kubota modules which has an uneven distribution of pores. The fabric module has a unique surface morphology compared to

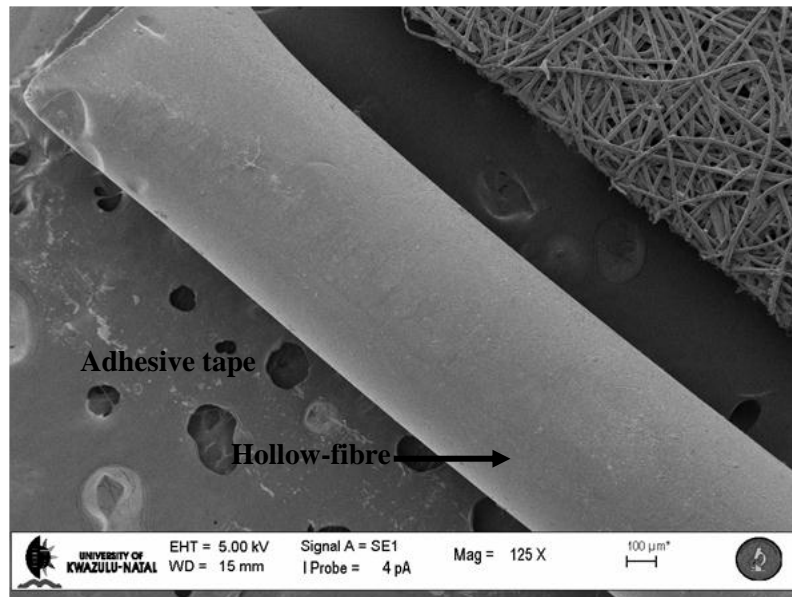


Figure 7.1: SEM micrograph showing surface view of a single hollow-fibre from the Polymem ultrafiltration module operated at constant TMP (Chapter 5). The module was cleaned with tap water before SEM examination. The area in the background is the adhesive used to place the fibre on an aluminium stub for SEM viewing (PRG, 2010). Magnification = 125 ×.

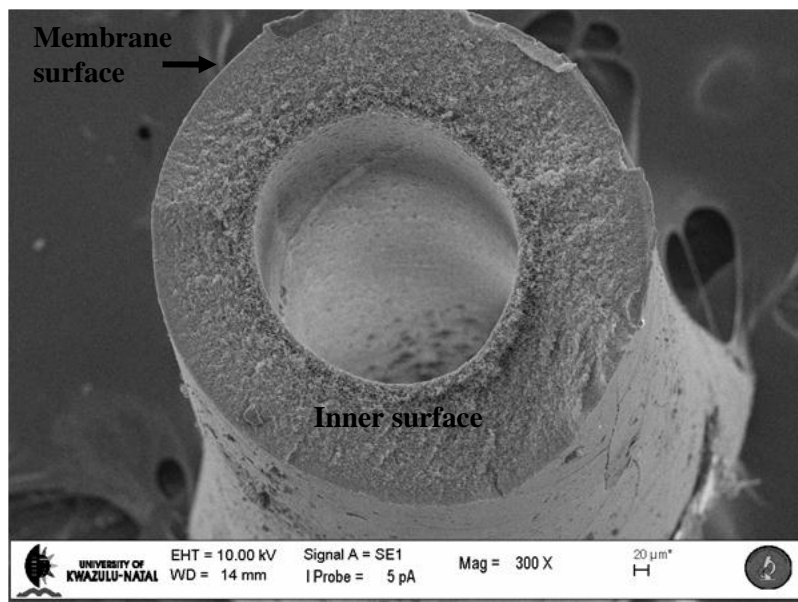


Figure 7.2: SEM micrograph showing cross section view of inner morphology of a freeze-fractured hollow-fibre from the Polymem ultrafiltration module operated at constant TMP. The module was cleaned with tap water before SEM examination (PRG, 2010). Magnification = 300 ×.

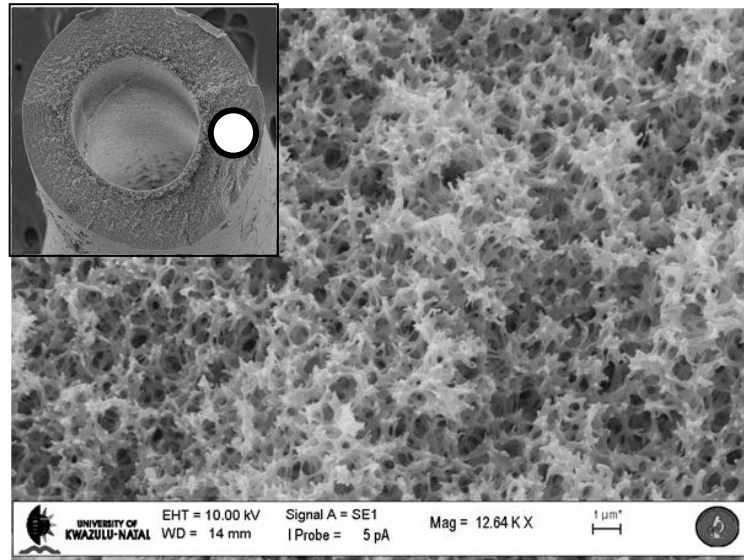


Figure 7.3: SEM micrograph showing high-magnification ($\times 12\,640$) of the inner surface of a single hollow-fibre from the Polymem ultrafiltration module. The insert located on the top left corner of micrograph shows the approximate location (encircled area) on the hollow-fibre from which this micrograph was taken (PRG, 2010).

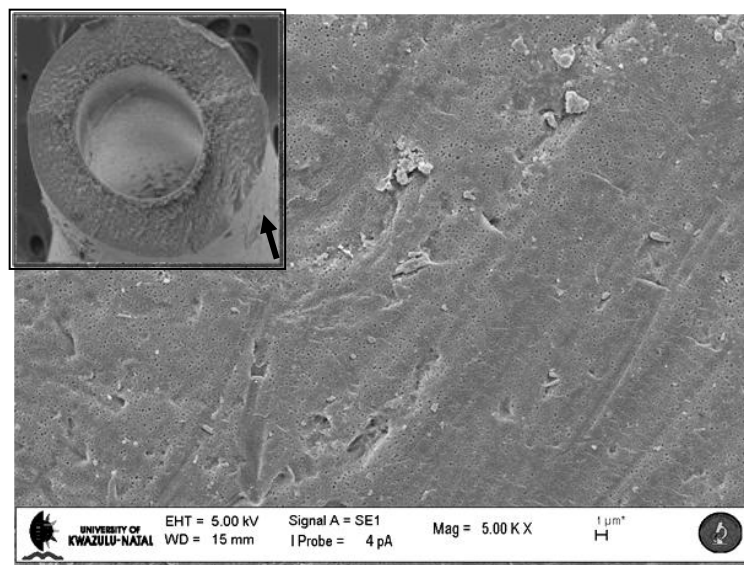


Figure 7.4: SEM micrograph showing the smooth outer surface skin with relatively evenly distributed pores (nominal pore of $0.08\ \mu\text{m}$) of a single hollow-fibre from the Polymem ultrafiltration module (PRG, 2010). The insert located on the top left corner of micrograph shows the approximate location (shown by arrow) on the hollow-fibre from which this micrograph was taken. Magnification = $\times 5\,000$.

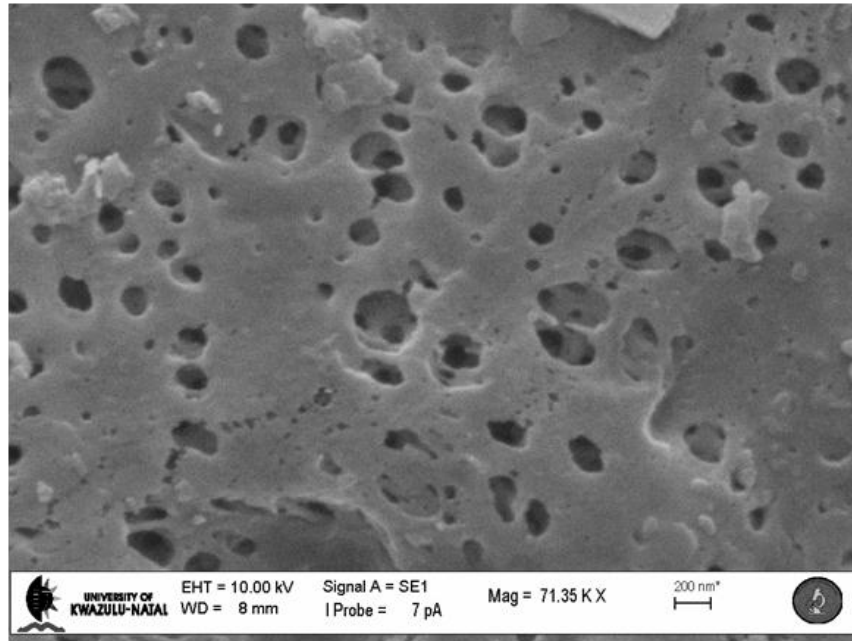


Figure 7.5: SEM micrograph showing high-magnification ($\times 71\,350$) of the inner surface of a single hollow-fibre from the Polymem ultrafiltration module. The SEM micrograph shows the pore structure on the membrane surface on the Polymem ultrafiltration module (PRG, 2010). Manufacturer stated pore size = $0.08\ \mu\text{m}$.

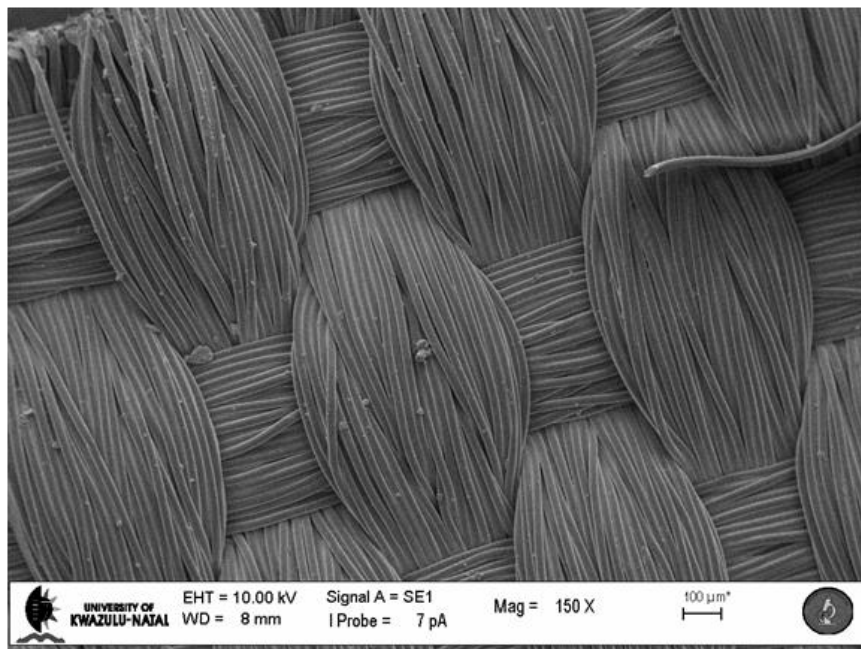


Figure 7.6: SEM micrograph of surface view of a fabric microfiltration membrane constructed by the Durban University of Technology. The membrane was constructed from spun polyester filaments and used in filtration experiments in Chapter 6 (PRG, 2010). Magnification = $150\times$.

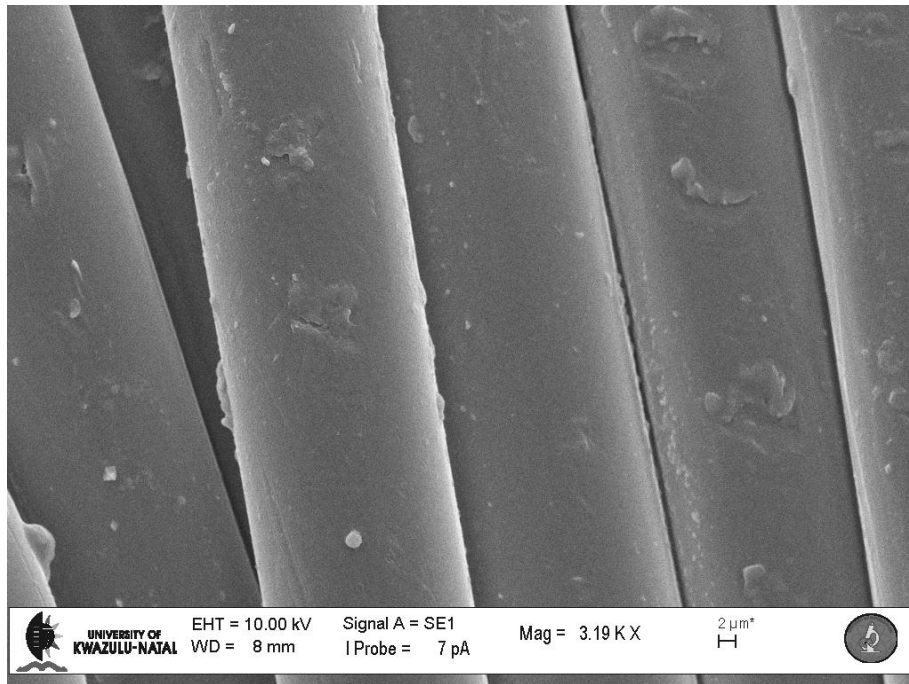


Figure 7.7: SEM micrograph showing a filament strand of the spun fibres making up the microfiltration fabric membrane (made by DUT) at high magnification (3 190 ×) (PRG, 2010). Much more space exists between strands than the other modules.

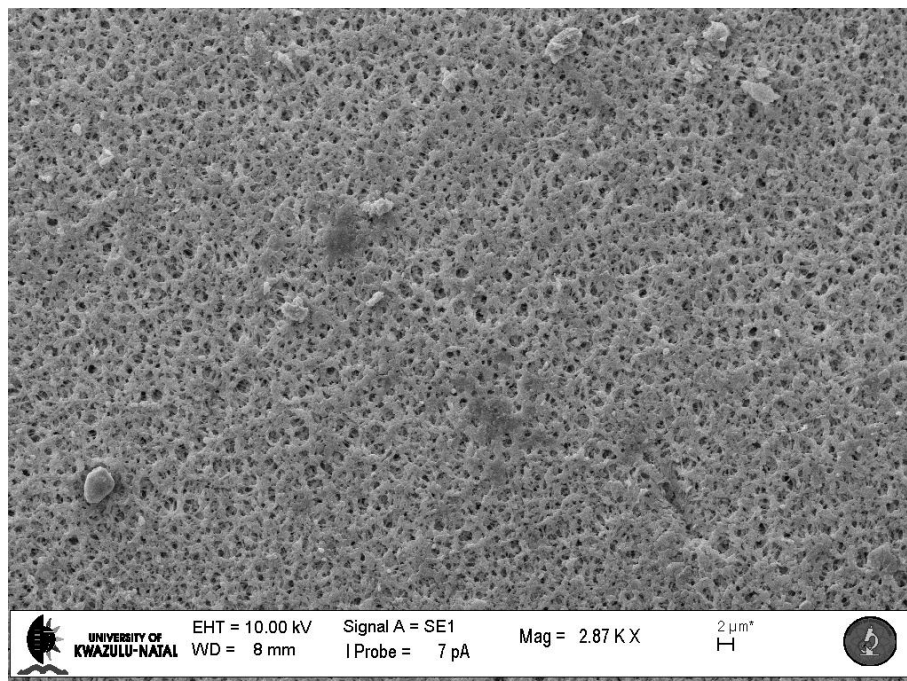


Figure 7.8: SEM micrograph of the surface topography of a cleaned microfiltration Kubota membrane (Chapter 6) (PRG, 2010). The surface is more porous than the Polymem modules. Manufacturer stated pore size = 0.4 µm. Magnification = 2 870 ×.

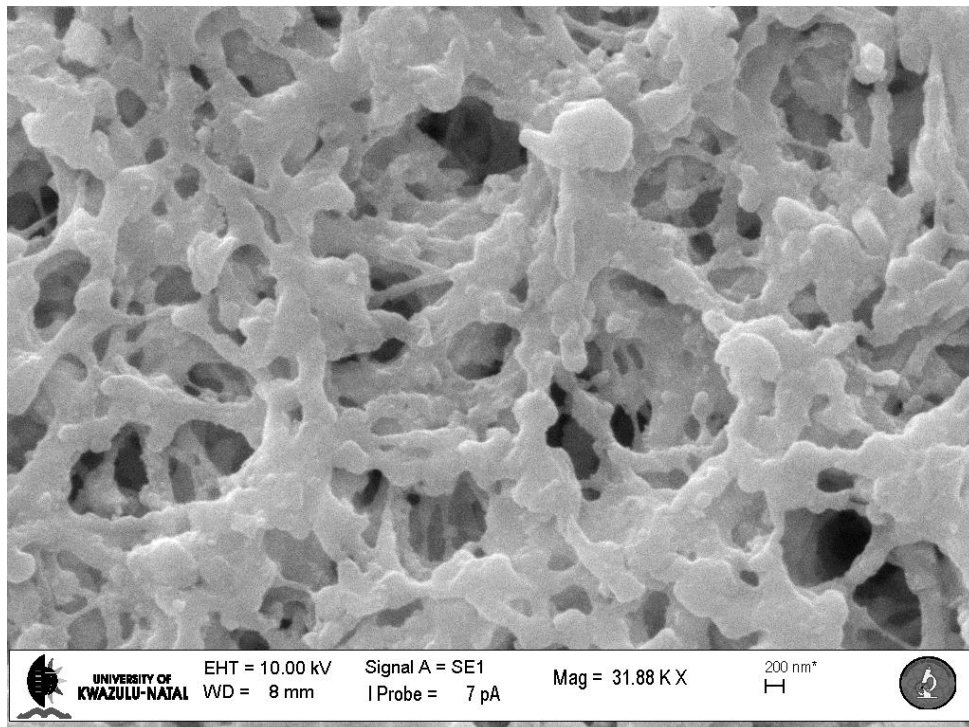


Figure 7.9: SEM micrograph showing a high-magnification of the surface topography of a cleaned microfiltration Kubota membrane. Magnification = 31 880 ×.

the other modules. There are no well-developed pores on the surface as the module is made from woven threads of polyester filaments and not from an organic polymer film. The module is likely to be more porous than hollow-fibre modules as there are large spaces between fibres (Figure 7.7). Kubota modules have more porous and rougher surface than Polymem modules. Moreover, it has larger pores sizes with less distinct shape.

Based on the visual observations and membrane filtration results, the following hypothesis was developed to explain differences in fouling layer development between membrane types (Figure 7.10). When pressure is applied, the various constituents of the bulk fluid are transported to the membrane surface. The rejection of the colloidal fraction, defined in this study to be greater than a nominal size of 0.2 μm (based on filtration experiments using microfiltered effluent), and its interaction with the membrane surface are critical to the type of layer that develops. Pore blockage by this colloidal fraction is the dominant process in the hollow-fibre membranes evaluated. Intermediate blocking and adsorption into the pores was shown (through clean water tests) to have little impact. The process is governed by the surface structure of these particular modules which dictates which process dominates. The smooth outer membrane skin with sparsely located pores limits colloidal fraction from entering and becoming lodged and/or adsorbed within pore spaces. Moreover, the well-defined round pores normal to

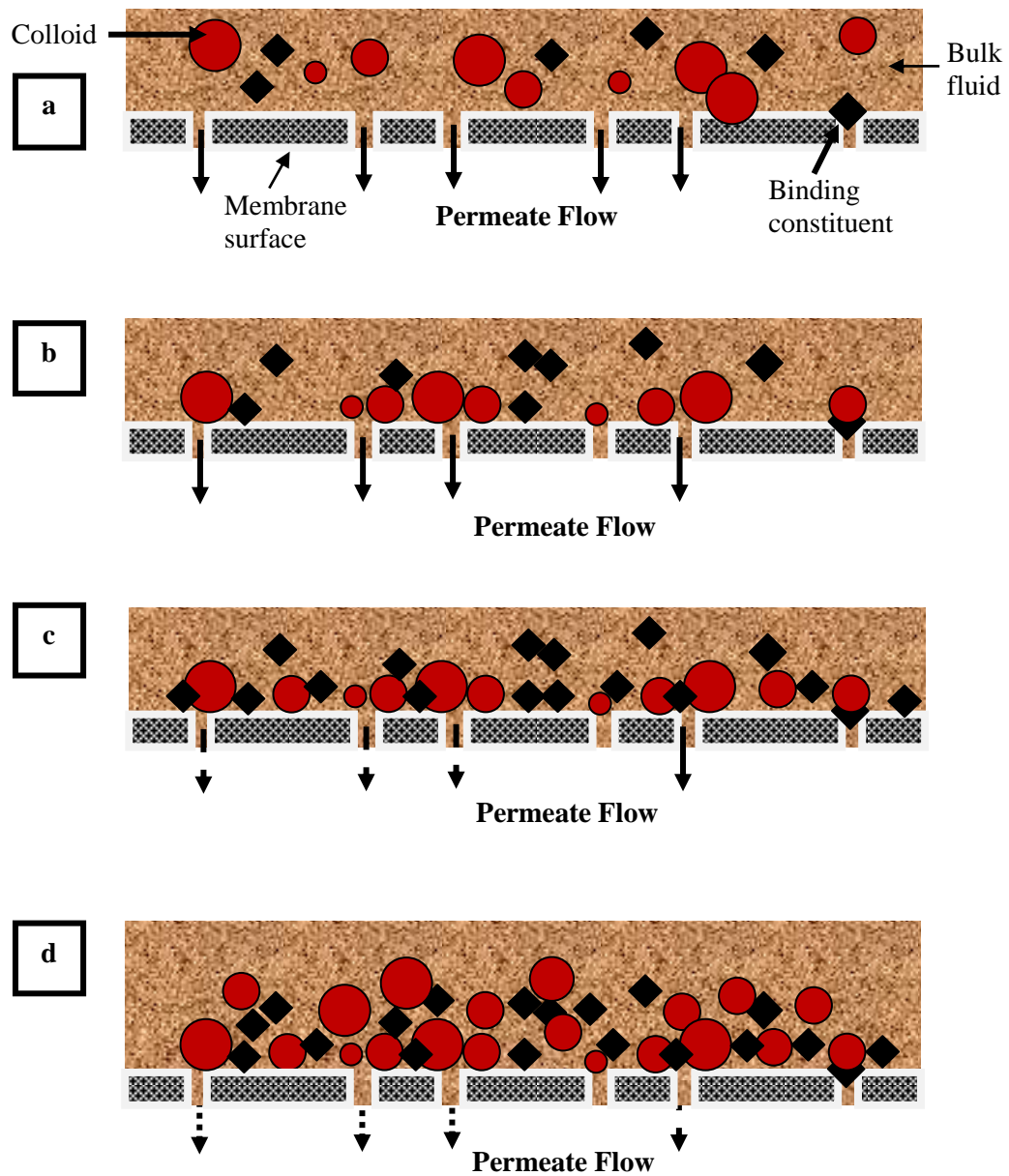


Figure 7.10: Proposed mechanism of fouling layer development in hollow-fibre modules treating effluent from an ABR treating complex particulate wastewater. (a) Pressure applied with flux at its highest. (b) Colloids loosely-adhered to pores which are normal to the outer surface of the module, decrease in flux. (c) Colloids and aggregates held together by soluble binding constituent and permeate flow is restricted. (d) Build-up of cake until flow becomes impeded.

outer surface present less surface area (than flat-sheet modules) for attachment or adsorption of these colloidal particles. The next step is the binding of soluble constituents to these colloidal particles to form a cake layer which continually builds up as more aggregates bind. These binding constituents are included in the hypothesis as flat-sheet modules have been shown to develop a thick, sticky gel-like layer after the filtration of supernatant from settled effluent and microfiltered effluent. Based on the chemical composition of the fouling layers presented in **Chapter 6**, it is plausible that proteinaceous substances are involved in this binding process. Although it is possible for sloughing off to occur when the cake layer grows to a certain point (Peter-Varbanets *et al.*, 2009), no such event was observed. The passage of fluid becomes progressively restricted by further pore blockage and/or reduced passage through a thicker cake.

Eventually, too little fluid is transported across the membrane surface making flux unreasonable such that user intervention is required. The proposed mechanism of fouling in hollow-fibres has been validated by SEM micrographs of the surface structure and clean water permeability tests between experiments. As the fouling layer is weakly attached (not within the pores) to the membrane surface, it can be easily removed by a physical cleaning method.

The fouling development that occurs in the flat-sheet modules is presented in Figure 7.11. Unlike hollow-fibre modules, colloidal particles are thought to become lodged or adsorbed into the larger pores of flat-sheet modules. This process is also facilitated by a porous and rougher membrane surface which increases the surface area for contact and adherence. Lodged/adsorbed colloids are not easily removed by physical methods. A binding constituent in the bulk solution, postulated to be proteinaceous compounds (based on chemical analyses), aids with the development of a fouling layer. This layer, however, does not build up to a thick sludge-like cake layer but instead forms a gel-like layer on the membrane surface, possibly through aggregation of colloids (Riedl *et al.*, 1998). The higher pore density on the flat-sheet modules may also act to encourage gel layer development as soluble compounds could easily form a network across the surface (in contrast to Polymem modules which have pores further apart). Indeed, gel fouling layers have been found to form a cross-linked three-dimensional network of deposited particles (Lapasin and Pricl, 1995).

Such gels are thought to develop due to concentration polarisation which was discussed in **Chapter 2** (section 2.2.6). The concentration of solutes and macromolecules accumulate at the surface of the membrane surface forming a concentration gradient from the surface on the membrane to the bulk fluid. When the concentration at the surface exceeds that required for gel-formation, a gel-like layer precipitates on the membrane surface forming a 'secondary membrane' (Porter, 1972). This layer both can alter the resistance of the membrane and act as a

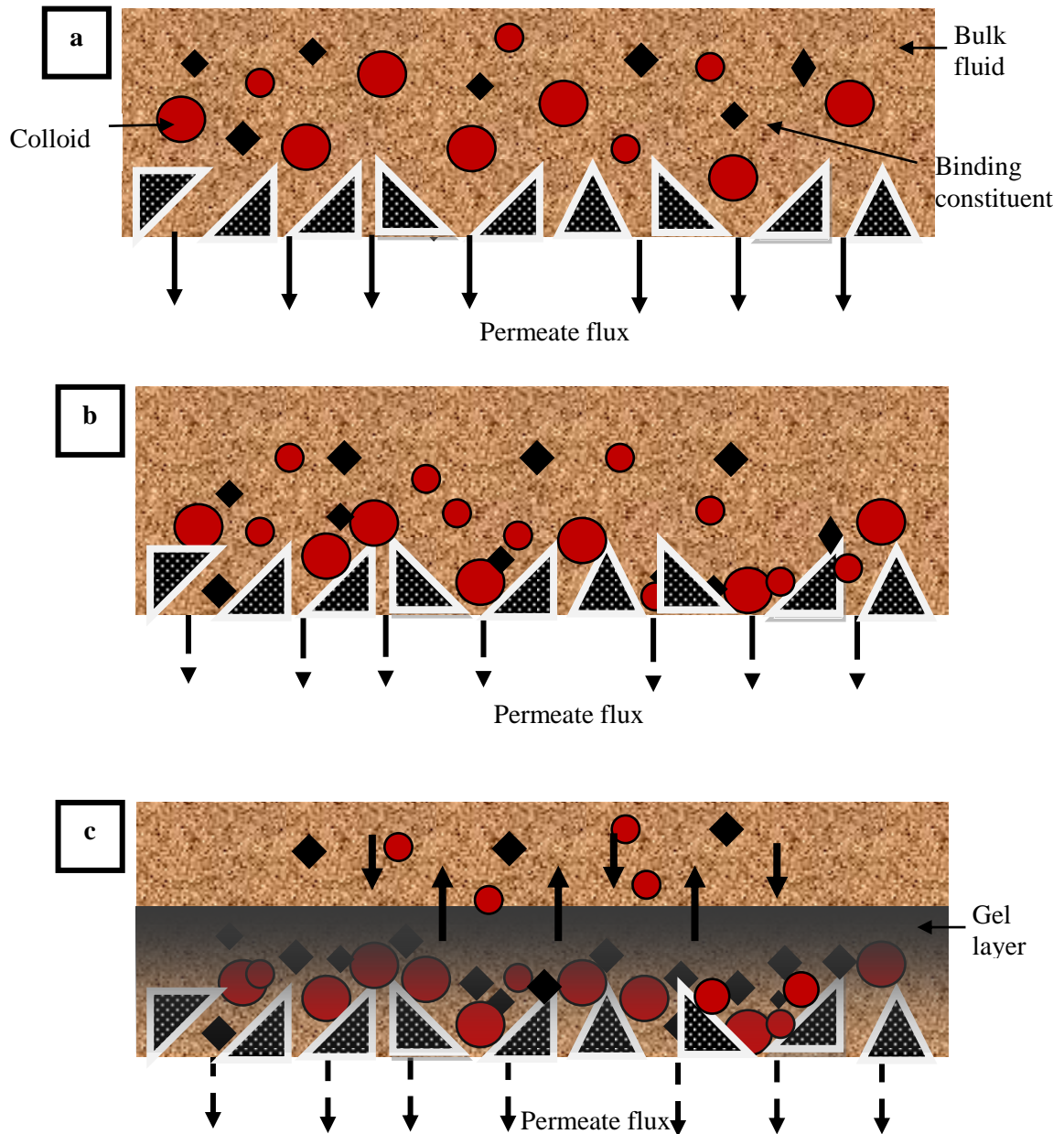


Figure 7.11: Proposed mechanism of fouling layer development in flat-sheet modules treating effluent from an ABR treating complex particulate wastewater. (a) Bulk fluid transported to membrane under TMP. (b) Adsorption and/or pore blocking of rough membrane surface by colloids. The porous nature of membrane surface also facilitates adherence of foulants through greater surface area. (c) Binding of protein layer and subsequent concentration polarisation gel-like layer formed. Transport through the layer occurs through diffusion (Judd, 2006).

sieve (Ingham *et al.*, 1979). Although this layer is difficult to remove, it has useful benefits in that it increases the selectivity of the membranes (see section 2.4).

The gel polarisation model is often used to describe the permeate flux decline when a gel-layer forms. Early research using ultrafiltration membranes treating macrosolutes and colloids showed that the steady-state flux reaches an asymptote limiting value flux value known as the limiting flux (evidence cited in Bowen and Jenner, 1995). Any further increase in TMP did not result in an increase in flux which cannot be explained by the film model of concentration polarisation (Bowen and Jenner, 1995). According to the gel polarisation model, once the accumulated solutes reach their solubility limit, it will precipitate into a gel that will have a constant concentration. The gel will continue to grow thicker with any increase in applied pressure. Moreover, it will be independent on the bulk concentrations, hydrodynamic conditions or membrane characteristics (including permeability) (Bowen and Jenner, 1995). When a 100% solute rejection, the concentration polarisation equation (equation 2.5) can be rewritten as:

$$J_{lim} = k_{sl} \ln \left(\frac{c_g}{c_b} \right)$$

Where:

c_g : constant gel concentration (which replaces c_m - concentration at membrane surface)

J_{lim} : limiting flux

The gel layer is dependent on solute characteristics and the mass transfer co-efficient. Thus, the improved flux can only be achieved by decreasing the boundary thickness or increasing the mass transfer co-efficient.

The results presented in this dissertation suggest that some of the assumptions of the gel polarisation model have been met in the flat-sheet unit. Pressure, has indeed, been shown to have no effect on the permeate flux. In all flat-sheet membrane filtration experiments, it was shown that similar steady-state fluxes are achieved irrespective of the applied pressure. Furthermore, the different permeabilities of the Kubota and fabric modules did result in different steady-state fluxes.

Using the same model, the lack of gel formation in the Polymem modules could be due to the lack of solute transport to the membrane surface to cause precipitation into a gel. By calculating the cumulative flow (per membrane area) based on the assumption that flux did not decrease between flux measurement days, it was observed that there was 25 to 80 more flow passing through flat-sheet modules than the hollow-fibre module over the same operating period. The

higher convective flow towards the flat-sheet membranes with more concentrate available per unit membrane area could have initiated the formation of a gel layer. However, the total COD analysis of the fouling layers after the filtration of microfiltered effluent showed that there was more COD/m² attached to the hollow-fibre unit (8 g/m²) compared to the flat-sheet modules (approximately 1 g/m²). Given that there was a greater accumulation of substances (per membrane area) on the hollow-fibre unit than on the flat-sheet membrane, it would be expected that gel polarisation would also occur in this system. The results indicate that there are other factors limiting the precipitation of the gel on the hollow-fibre modules. SEM images of the membrane surface indicate that the smaller and more defined pore size with greater distance between pores could possibly limit the accumulation of macrosolutes on the membrane surface.

To conclude, it was hypothesised that the continued flux in the flat-sheet microfiltration modules results in formation of a concentration polarisation which occurs through the build-up of solutes to a point where precipitation or gel layer occurs (gel polarisation). The flow through the gel layer is not completely impeded and as a result, the gel does not back diffuse into the bulk fluid. The formation of this gel layer in the flat-sheet modules probably also explains why the protein passage increases after gel formation (due to concentration polarisation effects) (see **Chapter 6**). In the hollow-fibre modules, the flow is impeded more than the flat-sheet modules. Consequently, polarisation does not occur to the same extent and therefore there is no gel precipitation. The pore size and shape has been shown to influence these characteristics.

In the next section (section 7.9), the main findings of this section are placed in context to literature. The purpose of section 7.9 is to highlight the novelty of the mechanism of fouling shown in this thesis.

7.9 CONTEXT OF OBSERVED FOULING BEHAVIOUR IN RELATION TO LITERATURE

The findings of this study indicate that membrane surface roughness and pore shape (and to a lesser extent pore size) governs the fouling behaviour in membranes treating effluent from an ABR fed with low biodegradability particulate wastewater. Rougher surface structure and larger pore size are thought to be responsible for a gel-like fouling layer whilst smoother surfaces with smaller pores result in a sludge-cake layer which results in an unreasonable flux but is easier to remove. Similar findings have been made by Jin *et al.* (2010). In that study, four ceramic membranes constructed from the same material but with different pore sizes were examined for membrane performance. The membrane with the roughest surface and largest pores had the

highest fouling whilst the opposite was true for the membrane with the smoothest and smallest pore size.

Using a size-compositional approach to determine the nature of the foulant, the effluent was divided into two sized-based fractions: supernatant from settleable effluent and pre-filtered effluent. Colloids and other soluble macromolecules (nominally less than 0.2 μm) were implicated in fouling. Similar findings have been made by others (Bouhabila *et al.*, 2001; Howe and Clark, 2002). Like this study, these authors fractionated the membrane feed into different physical components. In Bouhabila *et al.* (2001) synthetic wastewater was divided into three different fractions: sludge, colloids and solutes and solutes only. The results from the membrane filtration studies showed that suspended solids were only partially responsible for fouling with the main contributor being the colloids and solutes which contributed to nearly 75% of the fouling. Howe and Clark (2002) also highlighted the importance of colloids and to a lesser extent the solutes. In that study, membrane filtration was performed on particulate matter, colloids and DOM.

Particulates larger than 0.45 μm were found to have no discernible impact on fouling. In contrast, the colloidal fraction (ranging between 3 and 20 nm) was implicated to have the greatest fouling tendencies with a lesser effect observed with the DOM fraction (colloidal-free membrane filtration). Like that study, the results presented here indicate the importance of colloid adsorption in fouling.

The adsorption and/or blocking of pores by colloids (above 0.2 μm) are hypothesised to be the initiation mechanism for the development of fouling layers in this system (taking into account the membrane surface structure and, pore size and shape). Moreover, the strength of the binding and/or adsorption manner dictates the type of fouling layer that will develop.

This is not the first study to report different fouling layer development on different membranes types treating identical wastewaters. Riedl *et al.* (1998) reported a similar observation treating apple juice under dead-end conditions in a test cell operated at 344 kPa and using with four different membrane types (polyethersulphone, polyvinylidene fluoride, polysulphone and nylon) with same nominal pore size (0.2 μm). The nylon membranes were found to develop a thin (relative to other membranes) and tightly-bound fouling layer of apple juice aggregates almost immediately after filtration with a secondary layer forming thereafter from the adherence of colloids. The additional binding of the colloids further increased the development of the fouling layer by aggregating to form a gel-like layer. A similar observation was made with polysulphone membranes. In contrast, thicker but less dense particulate-like fouling layers were

observed on polyethersulphone and polyvinylidene fluoride membranes. The fouling layers on these membranes developed at slower rate and had less resistance per unit thickness than the thin layer that had developed on the nylon and polysulphone membranes. Despite similar types of fouling layer development reported in this thesis, the findings presented in Riedl *et al.* (1998) contradict the results presented here with respect to the effect on surface roughness. Riedl *et al.* (1998) observed that smoother membranes developed the denser gel-like fouling layer whilst rougher surface membranes resulted in more open fouling layers. Moreover, the TMP used was higher in the test cell experiments than observed in this thesis and probably the chemical nature of the foulant.

The formation of gel-like fouling layers has also been reported by Lee *et al.* (2004). In that work, a test cell apparatus with various microfiltration and ultrafiltration membranes treated natural water under low pressures (26 to 97 kPa, with differences in pressure applied to most membranes). Lee *et al.* (2004) observed that microfiltration membranes were more prone to fouling than ultrafiltration ones. Microfiltration fouling was thought to occur through pore blockage and adsorption of natural organic matter by smaller molecules with the flux recovery after fouling lower than ultrafiltration membranes. Ultrafiltration membranes, on the other hand, showed evidence of gel-like fouling layer development. Lee *et al.* (2004) also supported the notion that membrane surface roughness plays an important role in fouling and that it is probably more important than hydrophilic/hydrophobic character of the membranes. The findings of Lee *et al.* (2004) are contradictory to those reported here (microfiltration membranes formed gel-like fouling layers and ultrafiltration membranes sludge-like layers). Whilst different membrane feed water and membranes were used, the influence in pore shape in fouling layer development (as shown in this study) was not investigated.

Test cell experiments were also performed by Laabs *et al.* (2004) (refer to section 2.7.2.2). In that work, wastewater was fractionated into different colloid fractions. Membrane filtration was then performed on microfiltration and ultrafiltration membranes under low-pressure membrane filtration. In a similar manner to what was observed in this study, colloids formed a cake layer on the membrane surface when the raw sample (colloids not removed by pre-filtration) was filtered with this cake were easily removed during backwashing. However, the macromolecular component of the colloids isolated from pre-filtration caused severe fouling by the formation of a gel-like fouling that was difficult to remove. It was hypothesised that the polysaccharides in the colloids isolated were responsible for the formation of this layer. The findings in this study, however, shows significantly higher protein concentrations in the membrane feed. Polysaccharides are generally low in concentration, probably a reflection of the ABR feed

wastewater characteristics, are therefore not implicated in this work. Furthermore, very low concentrations were measured on the fouling layers of the flat-sheet modules.

To conclude, the results presented in this work show that pore shape may be a defining characteristic for the type of fouling layer that develops because of its influence on the adsorption of colloids. To the author's knowledge, no previous work has highlighted such differences in fouling layer development with respect to that specific membrane surface property. In this work, it has also been hypothesised that pore shape is more influential than surface roughness as it initiates the process and governs the type of layer that develops. The results also show that different conditions for the formation of gel-like layer exist in relation to other published work. The main findings of this research need to be replicated to increase the significance and the confidence of the conclusions derived from the experiments.

7.10 IMPLICATIONS OF STUDY FOR DEWATS APPLICATION

The last and probably the most important question to be answered in relation to the work presented here is:

What are the implications of this research for DEWATS process?

This study showed that use of membrane technology as polishing step is dependent on the reactor conditions (which in turn depend on other factors such as feed wastewater characteristics, organic and hydraulic loadings and environmental parameters) and the physical (and probably chemical) characteristics of the membrane. Whilst this is not a new concept, the results indicate that a trial-and-error process must be implemented for a particular plant if membrane technology is going to be used.

In simpler words, there probably exists no single membrane type which could be applied for all DEWATS technologies. This is due to the variable nature of membrane feed which is influenced by ABR operating conditions. Even within the compartments of an ABR, conditions are not same and thus potentially different foulants may be produced. For instance, Barker *et al.* (2000) found that high molecular weight soluble EPS (> 300 kDa) were produced in the middle compartments of an ABR treating low-strength synthetic wastewater composed of semi-skimmed milk. These heteropolysaccharide (sugars and volatile acids) compounds were more easily degraded under aerobic conditions (86% degradable) than anaerobic conditions (4%) and consisted of 22% of the effluent COD. In contrast, low molecular weight compounds (< 1 kDa) originated from the first compartment of the ABR and formed the highest portion of

effluent COD (36%). These compounds, some of which consisted of aromatics, alcoholic and carboxylate groups, were also more easily degraded under anaerobic conditions (33%). Soluble EPS production was also shown to change with temperature and HRT. Lower temperatures resulted in more soluble EPS production probably due to reduced metabolism of soluble EPS at lower temperatures whilst soluble EPS production increased with increasing HRT (probably due to increased decay at longer HRT) (Barker *et al.* 2000).

Langenhoff *et al.* (2000) showed the effects of different feed wastewaters on soluble EPS production in the ABR. In that work, laboratory ABRs were fed with two types of synthetic wastewaters; a soluble feed wastewater composed of milk and a colloidal feed wastewater composed of dog food and rice. The effluent of the reactor fed with soluble wastewater was primarily composed of VFA (which were detected in small amounts) whilst the other fed with colloidal feed had significant quantities of soluble EPS and slightly lower COD removals. Unlike Barker *et al.* (2000) decreases in HRT resulted in higher soluble EPS production which highlights the variability of potential soluble foulant compositions that can be found in ABR systems.

Nevertheless, this study has shown that stabilised flux values of $0.5 \text{ L.m}^{-2}.\text{h}^{-1}$ can be achieved in an ABR system (with respect to flat-sheet microfiltration membranes). Schmidt (2010) has reported slightly higher stabilised flux values ($2 \text{ to } 3 \text{ L.m}^{-2}.\text{h}^{-1}$) using the same woven-fibre microfiltration modules. The modules were operated at ultra-low hydrostatic pressures (approximately 4 kPa) treating effluent (200 to 500 mg COD/L) from three different BORDA DEWATS plants in Lesotho (the data are available to Pollution Research Group but have not been published elsewhere or presented in this thesis due to ownership rights).

The low flux values indicate that it may be impractical to use membrane technology for larger-scale (community-type) where large volumes of treated wastewater will be generated as the required membrane area would be large and therefore costs disproportionately higher. Instead, membrane technology is more appropriate on a household level, small community or institutions where water is not used throughout the day and the volumes of wastewater are low. Alternatively, a portion of the effluent from a large community-based system could be treated by membrane technology. In such cases, different qualities of treated wastewater would be produced by the DEWATS process with the higher quality membrane effluent re-used for activities where more stringent guidelines are required.

Depending on the quality of treated wastewater required, a multi-membrane system may be used. The fabric modules developed by Pillay (2009) are robust and can be allowed to dry – a

feature which makes them distinct from other membrane types. This feature is well-suited to decentralised requirements where maintenance issues must not be too complicated. These modules can therefore act as pre-filter (microfilter) for other more selective membrane types (such as ultrafiltration) based on data presented in this thesis (and applies only to the hypothesis presented here which states that the pore shape influences fouling behaviour). However, the fabric modules ability to provide a constant barrier against potential pathogens has not yet been evaluated.

With respect to evaluating the suitability of membrane technology for a particular DEWATS plant, medium-term constant TMP tests as performed in this thesis could be replicated in the field. The advantage of these tests is that the suitability of membrane filtration for a potential BORDA DEWATS plants could be evaluated over a short period.

7.11 MAIN CONCLUSIONS

This section lists the main conclusions from this work:

- The laboratory ABR was not well designed to the feed wastewater characteristics (alternatively, this could be stated as the feed wastewater characteristics were not suited for the design of the ABR). The feed wastewater, made from diluted VIP sludge, had a low biodegradability content. Consequently, the large non-biodegradable portion built-up in the reactor which sometimes required desludging or clogged overflow pipes to the ABR train. To account for this effect of this process, the feeding/settling tank was included in the calculation of the HRT. The main mechanism of treatment occurred through solids retention and accumulation.
- A standardised test cell technique was used to determine the fouling propensities of the soluble fraction of different sludge sources. The results showed that the samples from starved pilot ABR had the lowest fouling propensity whilst the sample from a conventional anaerobic digester had the highest propensity. Gel-like fouling layers developed from compartment 3 (and to lesser extent from compartments 2 and 4) of the starved ABR which contained biogranules. Although these solutions had low fouling propensities, the layer was highly compressible. The tests also showed that the effluent from a laboratory ABR had similar fouling propensities to other samples (both aerobic and anaerobic) tested. The results could not be statistically validated due to non-linearity of data indicating that improvements to the technique are required.
- Different fouling mechanisms were observed between hollow-fibre and flat-sheet modules treating identical membrane feed (that is, the ABR effluent). This difference was hypothesised to be the result of membrane surface-bulk fluid interactions with

irremovable gel layer formation in the flat-sheet modules and removable ‘cake-like’ fouling in the hollow-fibre modules. The differences observed were thought to be the results of differences in membrane pore shape and surface topography.

- Trial-and-error membrane experiments must be performed for each DEWATS unit as membrane fouling will be dictated by effluent composition which can vary due to the compartmentalised design and operating parameters of the ABR.
- Flux-time experiments revealed that gravitational membrane filtration units coupled to an ABR have low permeate rates (less than $1 \text{ L.m}^{-2}.\text{h}^{-1}$). Consequently, membrane technology is not envisaged for large community-based systems as the area required for membranes will be too large.

In the next chapter (**Chapter 8**), the recommendations for future research are highlighted.

CHAPTER 8 : RECOMMENDATIONS

In the previous chapter, the main findings from this thesis were presented. In this chapter, the recommendations arising from this thesis are presented. The recommendations have been divided into two subheadings: recommendations related to use of a standardised test cell technique in **Chapter 4** (section 8.1) and recommendations for future research (section 8.2).

8.1 STANDARD TEST CELL TECHNIQUE

This section describes recommendations for the improvement of a standardised test cell technique to evaluate the fouling propensity of a variety of mixed liquor sources: It is proposed that method specified by *EUROMBRA* partners must undergo further method development if the method is to be incorporated into routine MBR analysis. One of the suggestions is to include other well-known empirical models be used to describe fouling mechanism in the test cell. For example, Mahesh Kumar and Roy (2008) used the cake filtration model, standard pore blocking model and the complete pore blocking model to determine the filtration mechanism occurring a test cell treating suspended yeast cells. Keskinler *et al.* (2004) performed a similar analysis on yeast cells using all four models highlighted in section 2.2.5. Whilst it is understood that most of these models take into account the influence of colloids (and other particulates), the models could be applied in a similar manner to the filtration of the soluble fraction to elucidate the mechanism of filtration. If pore blocking is shown to be the dominant mechanism of fouling, the length of the filtration time could be increased until the cake filtration model is more dominant (the product of $\alpha.C_s$ is uniform or until the onset of linearity in t/V versus V plots). The precision and accuracy of the procedure must also be assessed.

8.2 FUTURE RESEARCH

This section provides recommendations for future research.

A repetition of the membrane fouling experiments in **Chapters 5** and **6** is required at different conditions and loads to verify the hypothesis constructed in **Chapter 7**.

This study was limited by the unavailability of domestic wastewater as a feed source to the ABR. Consequently, membrane experiments could not be extended to field conditions. Preliminary results by BORDA suggest that a pseudo steady-state flux can be achieved over a 3 month operation with fabric modules treating effluent from a DEWATS train (no polishing step). It is proposed that membrane experiments in this thesis be repeated on a DEWATS plant (containing an ABR) treating domestic wastewater (see **Appendix V**). Medium-term (as defined

in this thesis) filtration experiments could be used replicated for field-based systems worldwide and used as a testing strategy to evaluate the suitability of membrane modules.

Fabric modules have been identified as a suitable membrane module for BORDA DEWATS applications based on its robustness (ability to dry and scrub). The module could potentially be used as a pre-treatment step for more selective membrane types (such as ultrafiltration) or serve as an additional barrier to the DEWATS process. However, as the pore size is not defined, a pathogen indicator challenge is required to establish the module's disinfection properties before it can be implemented. Pathogen removal could not be evaluated for this module as the membrane filtration experiments were performed in an open environment in the laboratory (no fixed or enclosed membrane piping system as would occur in field-based systems). Thus, any samples taken for pathogen indicator analyses would have been susceptible to contamination.

APPENDIX I: LIST OF EUROMBRA PARTNERS

Table I.1: List of participants in the *EUROMBRA* Project.

Participant name	Short name	Country
Norwegian University of Science and Technology ^a	NTNU	Norway
Cranfield University	CU	U.K.
Rheinisch-Westfaelische Technische Hochschule Aachen	RWTH	Germany
Instituto de Biologia Experimental e Biológica	IBET	Portugal
Institut National des Sciences Appliquées	INSA	France
University of Montpellier	UM	France
Delft University of Technology	TU Delft	Netherlands
Swiss Federal Institute for Environmental Science and Technology	EAWAG	Switzerland
Università degli Studi di Trento	UNITN	Italy
University of Technology	Sydney UTS	Australia
University of KwaZulu-Natal	UKZN	South Africa
POLYMEM S.A	POLYMEM	France
KOCH Membrane Systems	GmbH KMS	Germany
MILLENNIUMPORE LIMITED	MILL U.K	U.K.
FlowConcept	GmbH FlowConcept	Germany
WATERSCHAP HOLLANDSE DELTA	WHD	Netherlands
ERFTVERBAND	EV	Germany
UNESCO-IHE Institute for Water Education	UNESCOIHE	Netherlands

^a, Project co-ordinator

APPENDIX II: OPERATION OF THE ANAEROBIC BAFFLED REACTOR

This annexure presents the results from the operation of the laboratory ABR treating a synthetic blackwater (diluted VIP sludge). The ABR was operated over several time periods with specific membrane filtration experiments performed over each time period (**Chapters 4 to 6**). The results of the ABR operation within these specific operating periods are presented in this annexure.

A 2.1 INTRODUCTION

This part of South African Water Research Commission (WRC) Project K5/1661 had the following objectives: (i) evaluating the performance of the ABR treating a synthetic blackwater and (ii) evaluating the ABR as a pre-treatment step for the disposal of VIP waste. It must be noted, however, that the primary objective of this thesis was to provide detailed studies of the performance of membranes in conjunction with ABR technology. As such, this study was not performed with aim of establishing the mechanism of digestion in the ABR as this has been previously elucidated in a report to the WRC (of South Africa) (Report K5/1248) (Foxon *et al.*, 2006; Foxon, 2009). In that report, it was revealed that the ABR primarily functioned as a solids retention device with particulate material retained through settling in the first compartment (Foxon *et al.*, 2006, Foxon, 2009). It was also shown the upflow velocity in the ABR chambers has a major influence of the digestion process with a more stable anaerobic population and partial phase separation of acidogenic and methanogenic communities observed at low upflow velocities (Foxon, 2009).

Nevertheless, preliminary results regarding the performance of the ABR in treating complex particulate wastewater has been generated as a by-product of the main objective and included in this annexure. More in-depth investigations relating to the performance of the ABR have been presented in Kapuku (2011) as part of a MSc Eng. study. The laboratory ABR was operated over a period of 828 d, beginning in 30 June 2007 and ending on the 5 October 2009. The ABR was operated under seven different operating periods (Figure II.1). Phase I and II were conducted at varying feed concentration whilst Phases III to VII was conducted at specific feed concentrations through the study period. During Phases III to VI, the ABR was operated by a MSc Eng. student (Kapuku, 2011). The aim of the MSc Eng. study was to investigate the effect of transient increases in organic loading on ABR performance. More specific analyses related to ABR system can be viewed in that document (Kapuku, 2011).

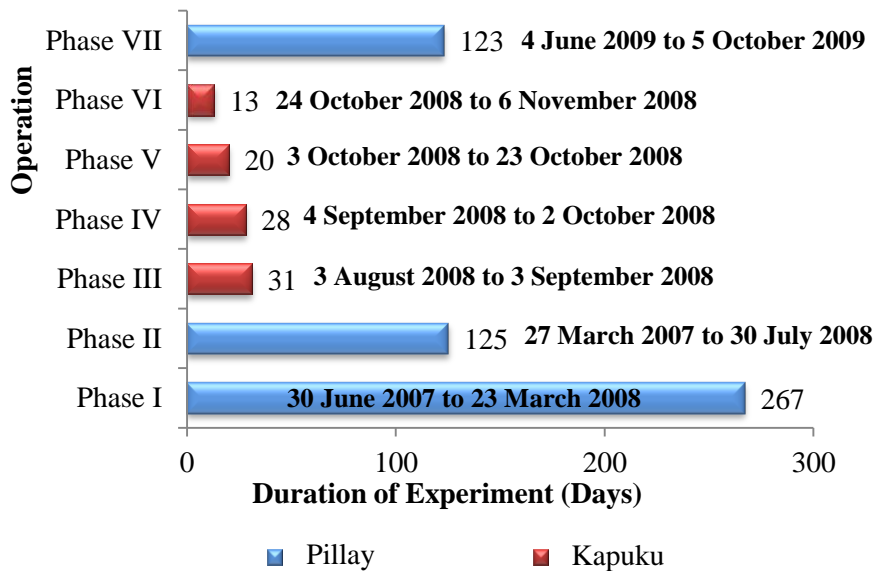


Figure II.1: Time-line of study showing different periods of operation for the laboratory ABR from 30 June 2007 to 5 October 2009. Phases III to VI were performed by Kapuku (2011).

Specific membrane experiments were conducted during most of the ABR phases, the details of which are presented in Table II.1

Table II.1: Details of membrane investigations.

Operation	Personnel Involved	Description of Membrane Experiments Performed
Phase I	S Pillay	Test cell experiments, short-term filtration with Polymem system
	V Yvenat	Set-up and evaluation of Amicon test cell (Chapter 4)
	CA Rouse	Filtration with Amicon test cell (Chapter 4)
	D Naicker	Filtration with Amicon test cell (Chapter 4)
Phase II	S Pillay	No membrane experiments performed
Phase III	S Pillay	TMP-step experiment (Chapter 5)
Phase IV	S Pillay	TMP-step experiment (Chapter 5)
Phase V	S Pillay	TMP-step experiment (Chapter 5)
Phase VI	S Pillay	TMP-step experiment (Chapter 5)
Phase VII	S Pillay	Long, mid and short-term filtration with all modules (Chapter 5,6)
	S Pollet	Long, mid and short-term filtration with flat-sheet modules (Chapter 6)

A 2.2 PHASE I

This section presents the first operation of the laboratory ABR (Phase I) treating diluted VIP sludge. The treatment of greywater and VIP mixture has not been included in this section due to insufficient data for the purpose of analysing reactor performance over a substantial period of time. This section comprises of two subheadings: section A 2.2.1 presents the flow conditions and incidents, and section A 2.2.1 presents the performance of the laboratory ABR.

A 2.2.1 FLOW RATE, DOWN-TIME AND INCIDENTS

During Phase I (average HRT of 3.4 d), a total of 18 900 L of feed wastewater (diluted VIP sludge) was treated over a 267 d with 52 d of ABR downtime (Figure II.2). Maintenance issues and electrical faults contributed 19 d of the total downtime.

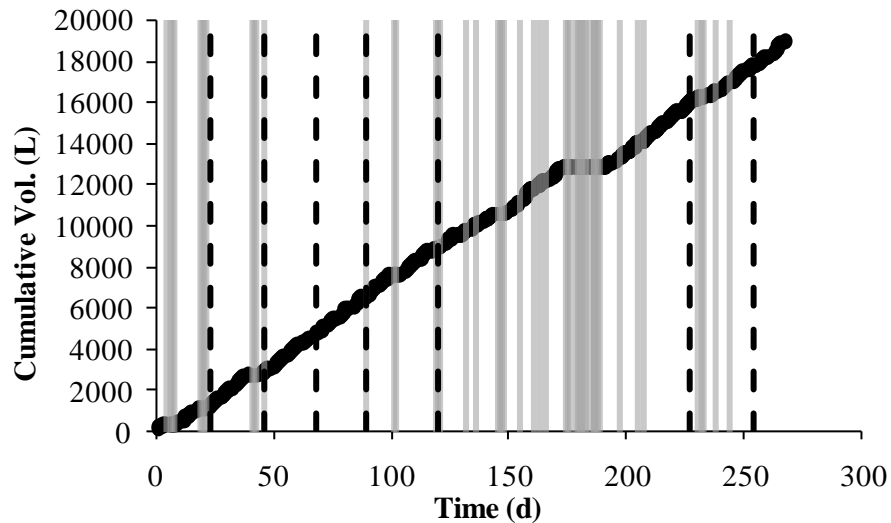


Figure II.2: Cumulative flow treated, incidents and downtime during Phase II (30 June 2007 to 23 March 2008). Grey areas represent reactor downtime whilst dashed lines (---) indicate potentially performance-affecting incidents such as desludging.

A total of seven desludging and scum removal events were required. These were limited to the feed tank from which a total of 217 L and 40 L of sludge and scum were removed, respectively. No desludging was required for the compartment boxes (ABR train).

A 2.2.2 ABR PERFORMANCE

During Phase I, the total COD concentration measured in the feed tank varied from 150 to 1 034 mg/L with an average concentration of 679 mg/L reported over 267 d (Table II.2). Soluble COD made up approximately 66% of the total COD of the feed tank wastewater. Total solids (TS) and volatile solids (VS) in the feed tank ranged between 309 to 1 069 mg/L and 132 to 500 mg/L, respectively. Digestion in the ABR produced an effluent with an average COD, TS and VS of 257, 266 and 99 mg/L. This equated to COD, TS and VS removal efficiencies of 62, 62% and 68%, respectively.

Table II.2: Feed and effluent characteristics for Phase I (30 June 2007 to 23 March 2008). Calculations of averages and standard deviations are presented for all measurements except for the pH value, which is reported as a median value. The number in parenthesis represents the number of samples over the operating period.

Parameter	Unit	Feed wastewater (<i>n</i>)			ABR Effluent (<i>n</i>)		
		Min	Max	Average	Min	Max	Average
COD _(total)	mg/L	150	1 034	679 ± 341 (25)	101	733	257 ± 115 (34)
COD _(0.45 μm)	mg/L	169	904	449 ± 244 (6)	86	105	94 ± 8 (4)
pH		7.12	7.32	7.23 (6)	6.98	7.42	7.27 (6)
TS	mg/L	309	1 069	705 ± 235 (10)	103	380	266 ± 87 (10)
VS	mg/L	132	500	311 ± 130 (8)	44	172	99 ± 46 (7)
Mean HRT	3.4 d	2.4 (min)	5.9 (max)		Total flow treated		18 900 L

Random samples of feed wastewater and effluent were measured for pH. The results show that the pH of the system is maintained through the system. In terms of anaerobic processes, it suggests that the feed wastewater characteristics either do not have acid or alkalinity-generating potential, or that the wastewater has a high alkalinity. In the next section, the operation from Phase II is presented.

A 2.3 PHASE II

This section presents the details of Phase II of the laboratory ABR operation. Diluted VIP sludge was used as the feed wastewater to the ABR. This section comprises of two subheadings: section A 2.3.1 presents the flow conditions and incidents, and section A 2.3.2 presents the performance of the laboratory ABR.

A 2.3.1 FLOW RATE, DOWN-TIME AND INCIDENTS

During Phase II (average HRT of 2.9 d), a total volume of 4 241 L of feed wastewater was treated over 125 d (27 March 2008 to 30 July 2008) with a total of 58 d of reactor downtime (Figure II.3). Maintenance issues and electrical problems contributed to 8 d of the total downtime. Erratic flow patterns were mostly due to power cuts that were experienced in the country at the time. No major performance affecting incidents, such as excessive sludge accumulation or sludge washout, were recorded during this phase.

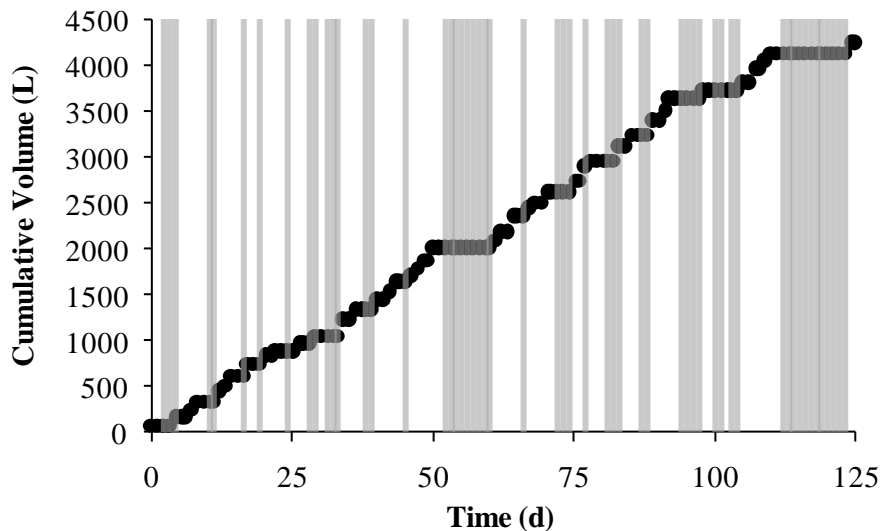


Figure II.3: Cumulative flow treated, incidents and downtime during Phase II (27 March 2008 to 30 July 2008). Grey areas represent reactor downtime.

A 2.3.2 ABR PERFORMANCE

Phase II was characterised by the treatment of a highly variable feed wastewater. Total COD ranged from 923 mg/L to 2 691 mg/L (Table II.3). TS and VS concentrations ranged from 341 to 1 319 mg TS/L and 209 and 1 017 mg VS/L, respectively. The variable nature of the feed was probably due to manner in which the feed wastewater was prepared during this phase (section 3.5.2). A certain amount of VIP sludge was diluted in distilled water and a COD analysis performed. This COD value was then used to calculate the amount of mass of VIP sludge required for feeding. The problem with this technique was that the sludge is a heterogeneous mixture of faecal and other matter which resulted in highly variable feed COD results. This procedure was changed in later phases of ABR operation.

Table II.3: Feed and effluent characteristics for Phase II (27 March 2008 to 30 July 2008). Calculations of averages and standard deviations are presented for all measurements except for the pH values which are reported as a median values. The number in parenthesis represents the number of samples over the operating period.

Parameter	Unit	Feed wastewater (n)			ABR Effluent (n)		
		Min	Max	Average/Median	Min	Max	Average/Median
COD(total)	mg/L	923	2 691	1 561 ± 432 (42)	150	615	303 ± 98 (41)
pH		7.70	8.93	8.35 (42)	7.08	7.92	7.48 (41)
Temperature	°C	17.0	24.6	20.4 ± 1.9 (42)	16.8	22.7	19.8 ± 1.6 (41)
TS	mg/L	341	1 319	844 ± 341 (15)	175	613	376 ± 138 (7)
VS	mg/L	209	1 017	611 ± 281 (15)	53	255	137 ± 75 (7)
Mean HRT	2.9 d	1.7 (min)	5.4 (max)		Total flow treated		4 241 L

Despite the high variability of feed wastewater, the ABR produced an effluent with an average COD, TS and VS of 303 ± 98 , 376 ± 138 and 137 ± 75 mg/L (Table 4.3). This equated to COD and TS and VS removal efficiencies of 81, 56, and 78%, respectively. The value of pH remained near 7 after digestion with only a slight decrease observed from feeding wastewater to effluent (median pH value for feed wastewater and effluent was 8.35 and 7.48, respectively, which was notably higher than the previous phase). In the next section, the operation and results of laboratory ABR from Phase III is presented.

A 2.4 PHASE III

This section presents the details of Phase III of the laboratory ABR operation. Diluted VIP sludge was used as the feed wastewater. This operational phase formed part of a series of experiments that evaluated the influence of increased organic loadings on the laboratory ABR performance and was conducted by Kapuku (2011) as part of his MSc Eng. degree. This section comprises of two subheadings: section A 2.4.1 presents the flow conditions and incidents, and section A 2.4.2 presents the performance of the laboratory ABR.

A 2.4.1 FLOW RATE, DOWN-TIME AND INCIDENTS

For Phase III (average HRT of 3.2 d), a total volume of 1 373 L was treated over 31 d (3 August 2008 to 3 September 2008), with 11 d of reactor downtime (Figure II.4). On day 14 (17 August 2008), the sludge in the feed tank built up to a level where the peristaltic pump was

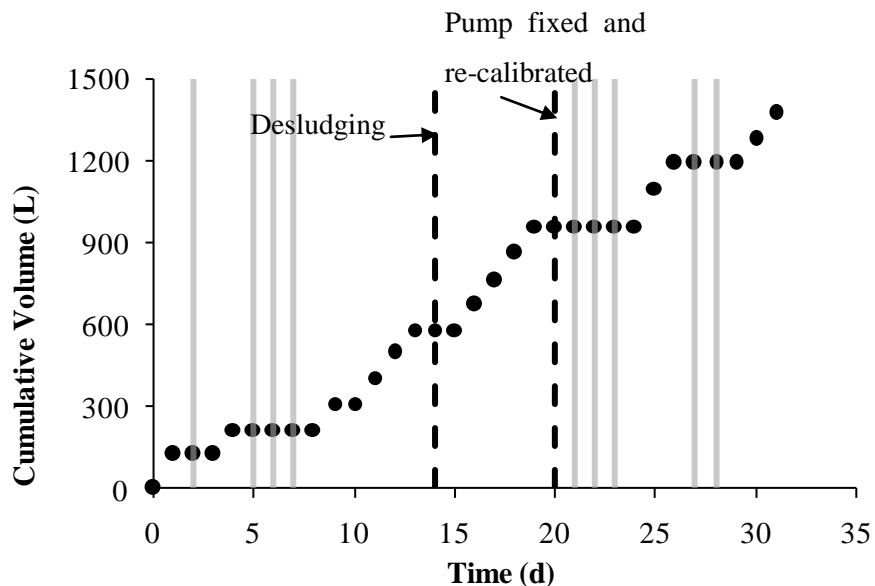


Figure II.4: Cumulative flow treated, incidents and downtime during Phase III (3 August 2008 to 3 September 2008). Grey areas represent reactor downtime whilst dashed lines (---) indicate potentially performance-affecting incidents such as desludging.

becoming continuously blocked. Subsequently, the sludge in the tank was removed to the level at the conical base of the feed tank (25 L left in feed tank). On day 21, mechanical problems were experienced with the pump. The pump was removed, tubing replaced and flow rate calibrations performed during days 24 to 26 (26 to 28 August 2008).

A 2.4.2 ABR PERFORMANCE

During Phase III (an average HRT of 3.2 d), the COD of the feed wastewater was maintained at 1 000 mg/L by changing the manner in which the feed solution was made up. Instead of measuring the COD of a certain mass of VIP sludge and diluting to it a desired COD value, a concentrated solution was made up by homogenising large quantities of sludge with tap water. The COD value of this slurry was then determined before feeding and diluted to form a feed wastewater of 1 000 mg/L. The only exception was on day 30 when a feed solution of 1 500 mg/L was made. This resulted in an increase in the average COD feed wastewater concentration to 1 034 mg/L (Table II.4).

Table II.4: Feed and effluent characteristics for Phase III (3 August 2008 to 3 September 2008). Calculations of averages and standard deviations are presented for all measurements except for the pH value, which is reported as a median value. The number in parenthesis represents the number of samples over the operating period.

Parameter	Feed wastewater (n)				ABR Effluent (n)		
	Unit	Min	Max	Average/Median	Min	Max	Average/Median
COD(total)	mg/L	1 000	1 500	1 034 ± 129 (15)	113	409	307 ± 77 (14)
pH		8.14	8.60	8.30 (15)	6.57	7.58	7.40 (14)
Temperature	°C	17.6	20.0	18.8 ± 0.8 (15)	18.0	21.0	19.6 ± 0.9 (14)
TS	mg/L	234	954	482 ± 196 (12)	343	637	477 ± 126 (5)
VS	mg/L	158	613	340 ± 133 (12)	70	252	159 ± 75 (5)
Proteins (soluble)	mg/L	-	-	nd	27	55	69.3 ± 21 (2)
Carbohydrates (soluble)	mg/L	-	-	nd	2.1	2.4	2.3 ± 0.2 (2)
Mean HRT	3.2 d	3.1 (min)	3.3 (max)		Total flow treated	1 373 L	

nd, not determined. The relocation of the School of Biological Science to Westville campus meant that a spectrophotometer was not readily available for use. Grab samples of the effluent were taken to the School of Chemistry for analysis.

The TS concentration in the feed was highly variable (234 to 954 mg/L) with an average of 482 mg/L. The VS concentration ranged from 158 to 613 mg/L with an average of 340 mg/L. The ABR was able to reduce COD, TS and VS to 307, 477 and 159 mg/L, respectively. This equated to average removals of 70 and 53% for COD and VS, respectively, with TS removal negligible (1%). The average soluble protein and carbohydrate concentration in the effluent was 69 and 2 mg/L, respectively. Whilst significant amounts of protein were found in the effluent, carbohydrate measurements were typically low (Table II.4). Only effluent samples were measured for this parameter as there were difficulties in obtaining a spectrophotometer for EPS measurements due to the relocation of equipment.

In the next section, the operation and results from Phase IV of the laboratory ABR treating diluted VIP sludge is presented.

A 2.5 PHASE IV

This section follows the experiments performed in the previous section (A 2.4) to evaluate the effect of increased organic loading on the performance of the laboratory ABR (Kapuku, 2011). In this

phase, the feed wastewater (diluted VIP sludge) concentration was increased from 1 000 mg COD/L (from section A 2.4) to 1 500 mg/L. This section comprises of two subheadings: section A 2.5.1 presents the flow conditions and incidents, and section A 2.5.2 presents the performance of the laboratory ABR.

A 2.5.1 FLOW RATE, DOWN-TIME AND INCIDENTS

During Phase IV (average HRT of 3.3 d), a total of 1 411 L of feed wastewater was treated over 28 d (from the 4 September 2008 to 2 October 2008) in the ABR (Figure II.5). Reactor downtime accounted for 8 d of total operation. On day 10 (13 September 2008), the COD apparatus was not working. Consequently, the feed concentration to the ABR could not be calculated. Feeding resumed on day 13 (17 September 2008) but the inlet and outlet pipes of the first compartment box became clogged and required cleaning. The sludge in the box compartment was emptied in an airtight storage container and pipes cleaned with hose. The box was re-seeded with the stored sludge to a third of its working volume. Excess sludge was stored in a separate container and disposed of at a local treatment works.

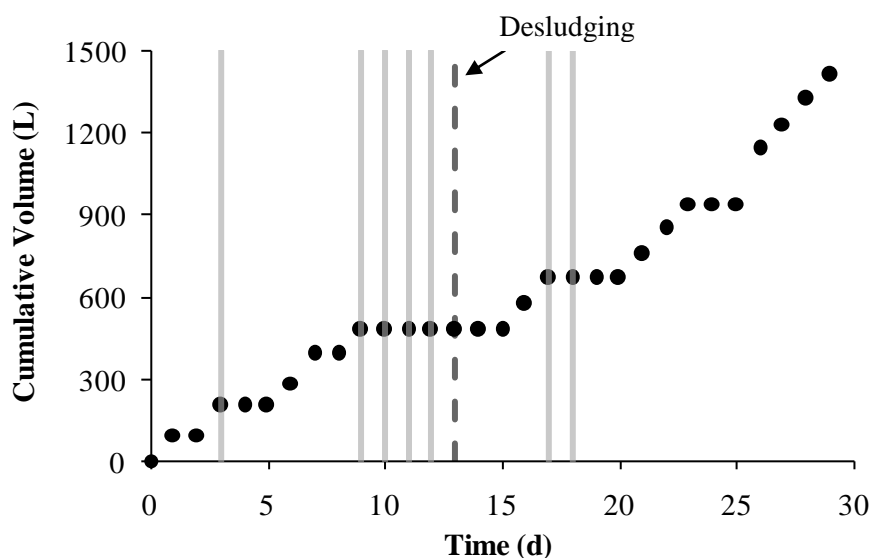


Figure II.5: Cumulative flow treated, incidents and downtime during Phase IV (4 September 2008 to 2 October 2008). Grey areas represent reactor downtime whilst dashed lines (---) indicate potentially performance-affecting incidents such as desludging.

A 2.5.2 ABR PERFORMANCE

During Phase IV (an average HRT of 3.3 d), the COD of the feed was kept constant at 1 500 mg/L (Table II.5). No solids measurements were made for the feed wastewater as there were electrical problems related to the muffle furnace. The construction of a new wing in the School of Chemical Engineering (UKZN) resulted in a disconnection of electrical supply where the furnace was located.

Table II.5: Feed and effluent characteristics for Phase IV (4 September 2008 to 2 October 2008). Calculations of averages and standard deviations are presented for all measurements except for the pH value, which is reported as a median value. The number in parenthesis represents the number of samples over the operating period.

Parameter	Unit	Feed wastewater (<i>n</i>)			ABR Effluent (<i>n</i>)		
		Min	Max	Average/Median	Min	Max	Average/Median
COD _(total)	mg/L	1 500	1 500	1 500 ± 0 (14)	240	396	334 ± 44 (14)
pH		7.92	8.32	8.10 (14)	7.18	7.74	7.44 (14)
Temperature	°C	18.6	20.0	19.0 ± 0.5 (14)	19.5	20.9	20.4 ± 0.5 (14)
TS	mg/L	-	-	nd	122	1219	476 ± 380 (9)
VS	mg/L	-	-	nd	22	210	95 ± 74 (9)
Proteins _(soluble)	mg/L	-	-	57.5* (1)	27.4	55.2	36.7 ± 9.8 (7)
Carbohydrates _(soluble)	mg/L	-	-	3.6* (1)	2.6	3.4	2.3 ± 0.8 (7)
Mean HRT	3.3 d	3.1 (min)	4.3 (max)		Total flow treated		1 411 L

nd, not determined. Problems with electricity supply; *, only one grab sample taken.

The furnace could not be relocated to another part of the building as it required an extractor to remove fumes from the samples (which set off the fire alarm). Thus, only a limited number of samples could be processed during the time period and this was limited to effluent samples only. The soluble protein and carbohydrate concentration in the feed wastewater was 58 and 4 mg/L (only one grab sample measurement was made).

The ABR was able to reduce the COD of feed wastewater to an average of 334 mg/L (78% reduction of COD) in the effluent. The average effluent concentration of TS and VS were 476 and 95 mg/L, respectively. The TS and VS measurements were made on effluent samples that were stored in the cold room at 4°C and analysed during the next phase (Phase V: 4 October to 24 October 2008). Hence, some degradation of solids could have occurred during storage resulting in a probable underestimation of true values. With respect to soluble protein and carbohydrate

concentrations in the effluent, higher concentrations of soluble protein were found in the effluent than carbohydrates.

A 2.6 PHASE V

This section follows the experiments performed in the previous section (A 2.5) to evaluate the effect of increased organic loading on the laboratory ABR performance (Kapuku, 2011). In this phase, the feed wastewater (diluted VIP sludge) concentration was increased from 1 500 mg COD/L (from section A 2.5) to 2 000 mg/L. This section comprises of two subheadings: section A 2.6.1 presents the flow conditions and incidents, and section A 2.6.2 presents the performance of the laboratory ABR.

A 2.6.1 FLOW RATE, DOWN-TIME AND INCIDENTS

During Phase V (average HRT of 3.2 d), a total of 1 192 L of feed wastewater was treated over a 20 days (3 October 2008 to 23 October 2008) with 5 d of ABR downtime (Figure II.6). No performance affecting incidents were recorded during this period. On day 8 (10 October 2008), the laboratory was fumigated over 2 d and necessitated reactor downtime.

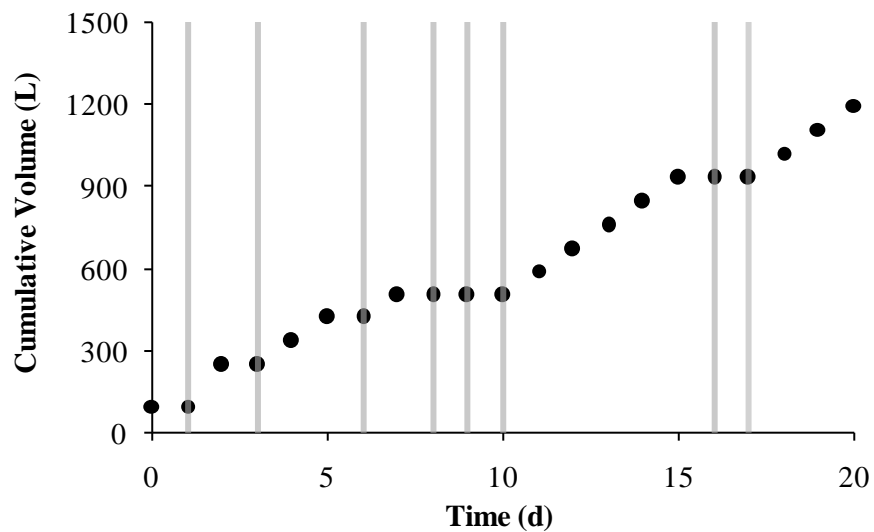


Figure II.6: Cumulative flow treated, incidents and downtime during Phase V (3 October 2008 to 23 October 2008). Grey areas represent reactor downtime whilst dashed lines (---) indicate potentially performance-affecting incidents such as desludging.

A 2.6.2 ABR PERFORMANCE

The feed wastewater COD concentration at Phase V (average HRT of 3.2 d) was kept constant at 2 000 mg/L (Table II.6). The TS concentration of the feed wastewater was highly variable and ranged between 235 to 818 mg/L with an average of 506 mg/L. The VS concentration of the feed wastewater ranged from 25 to 218 mg/L with an average of 104 mg/L. The ABR produced an effluent with an average COD, TS and VS of 447, 208 and 41 mg/L. This equated to an average removal efficiency of 77, 59 and 61% for COD, TS and VS, respectively.

Table II.6: Feed and effluent characteristics for Phase V (3 October 2008 to 23 October 2008). Calculations of averages and standard deviations are presented for all measurements except for the pH value, which is reported as a median value. The number in parenthesis represents the number of samples over the operating period.

Parameter	Unit	Feed wastewater (<i>n</i>)			ABR Effluent (<i>n</i>)		
		Min	Max	Average/Median	Min	Max	Average/Median
COD _(total)	mg/L	2 000	2 000	2 000 ± 0 (12)	315	575	447 ± 78 (13)
pH		7.84	8.38	8.08 (12)	7.32	7.75	7.55 (13)
Temperature	°C	18.9	21.0	20.2 ± 0.6 (12)	19.8	21.8	21 ± 0.5 (13)
TS	mg/L	235	818	506 ± 213 (6)	116	302	208 ± 64 (9)
VS	mg/L	25	218	104 ± 80 (6)	19	60	41 ± 14 (8)
Proteins _(soluble)	mg/L	13	58	42 ± 13 (12)	15	28	23 ± 4 (13)
Carbohydrates _(soluble)	mg/L	1.7	3.9	3.1 ± 0.6 (12)	2.4	3.5	2.9 ± 0.4 (13)
Mean HRT	3.2 d	2.2 (min)	3.8 (max)		Total flow treated	1 192 L	

The soluble protein concentration of the feed wastewater ranged from 13 to 58 mg/L with an average of 42 mg/L. Approximately 44% of the soluble protein was removed through the reactor with an average effluent soluble protein concentration of 23 mg/L detected. Soluble carbohydrate concentrations were typically low in the feed wastewater (1.7 to 3.9 mg/L with an average of 3.1 mg/L) with only no discernible change occurring through the reactor (average soluble carbohydrate concentration of 2.9 mg/L).

A 2.7 PHASE VI

This section follows the experiments performed in the section A 2.6 to evaluate the effect of increased organic loading on the laboratory ABR performance (Kapuku, 2011). In this phase, the feed wastewater (diluted VIP sludge) concentration was increased from 2 000 mg COD/L (from section A 2.6) to 3 000 mg/L. This section comprises of two subheadings: section A 2.7.1 presents the flow conditions and incidents, and section A 2.7.2 presents the performance of the laboratory ABR.

A 2.7.1 FLOW RATE, DOWN-TIME AND INCIDENTS

During Phase VI (average HRT of 3.4 d), a total of 765 L of feed wastewater was treated over 13 d (24 October 2008 to 6 November 2008) with 4 d of ABR downtime (Figure II.7). Although no performance-affecting incidents were recorded during this period, 135 L of sludge had to be removed from the feed tank before experimentation. Excess sludge from the previous regimes had built up to a level at which desludging was necessary to prevent clogging of the feeding pipe. This event was not thought to not influence the performance of the reactor during this phase.

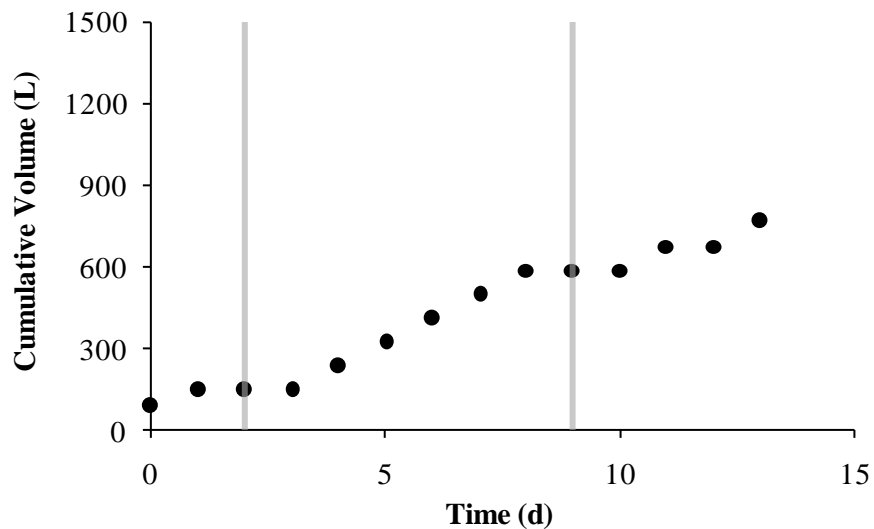


Figure II.7: Cumulative flow treated, incidents and downtime during Phase VI (24 October 2008 to 6 November 2008). Grey areas represent reactor downtime whilst dashed lines (---) indicate potentially performance-affecting incidents such as desludging.

A 2.7.2 ABR PERFORMANCE

During Phase VI (an average HRT of 3.4 d), the ABR was fed the highest concentration of COD (average 3 000 mg COD/L). The TS and VS of the feed wastewater could not be processed in the time period due to difficulties with the desiccator. The soluble protein concentration of the feed wastewater ranged from 21 to 54 mg/L with an average of 35 mg/L (Table II.7). The soluble carbohydrate concentration of the feed wastewater ranged from 2.5 to 4.5 mg/L with an average concentration of 3.4 mg/L. Despite the high feed wastewater COD concentration (in relation to other phases), the soluble protein and carbohydrate concentration in the feed was similar to that of other Phases.

Table II.7: Feed and effluent characteristics for Phase VI (24 October 2008 to 6 November 2008). Calculations of averages and standard deviations are presented for all measurements except for the pH value, which is reported as a median value. The number in parenthesis represents the number of samples over the operating period.

Parameter	Feed wastewater (<i>n</i>)				ABR Effluent (<i>n</i>)		
	Unit	Min	Max	Average	Min	Max	Average
COD _(total)	mg/L	3 000	3 000	3 000 ± 0 (7)	1 016	1 643	1 305 ± 365 (9)
pH		7.98	8.26	8.09 (7)	7.54	7.78	7.67 (9)
Temperature	°C	20.0	21.3	20.8 ± 0.5 (7)	20.6	21.9	21.1 ± 0.6 (9)
TS	mg/L	-	-	nd	246	394	314 ± 61 (4)
VS	mg/L	-	-	nd	-	-	nd
Proteins _(soluble)	mg/L	21	54	35 ± 12 (6)	13	22	16 ± 3 (7)
Carbohydrates _(soluble)	mg/L	2.5	4.5	3.4 ± 0.7 (6)	2.6	3.4	2.9 ± 0.3 (7)
Mean HRT	3.4 d	3.3 (min)	3.9 (max)		Total flow treated		765 L

nd, not determined. Malfunctioning equipment did not allow for the analysis of more samples during this phase.

The average effluent COD concentration was relatively higher than previous runs with an average COD of 1 305 mg/L (Table II.7). This equated to an average removal efficiency of 57%. The soluble protein was reduced to 22 mg/L in the effluent representing 54% removal efficiency. In contrast, soluble carbohydrate measurements remained relatively unchanged from the feed wastewater to the effluent.

A 2.8 PHASE VII

The results in this section present the operation of the laboratory ABR treating diluted VIP sludge with an average COD concentration of 2 000 mg/L. The feed wastewater concentration to the feed tank was kept constant to limit variations in the physico-chemical characteristics of the laboratory ABR effluent. During this phase, the laboratory ABR was operated and maintained by Mr. S Pillay. A series of membrane filtration experiments were conducted with the hollow-fibre unit (**Chapter 5** - section 5.3, section 5.6 and section 5.7) and the flat-sheet unit (**Chapter 6**) using the laboratory ABR effluent from this Phase.

A 2.8.1 FLOW RATE, DOWN-TIME AND INCIDENTS

During Phase VII (average HRT of 3.6 d), the ABR treated a total of 5 571 L of feed wastewater over a 123 d (4 June 2009 to 5 October 2009) with 41 d of ABR downtime (Figure II.8). On day 17 and 54, desludging of the feed tank was required. From day 87, the reactor was intermittently fed with feed wastewater to produce sufficient effluent for membrane filtration experiments (Chapter 5 and Chapter 6).

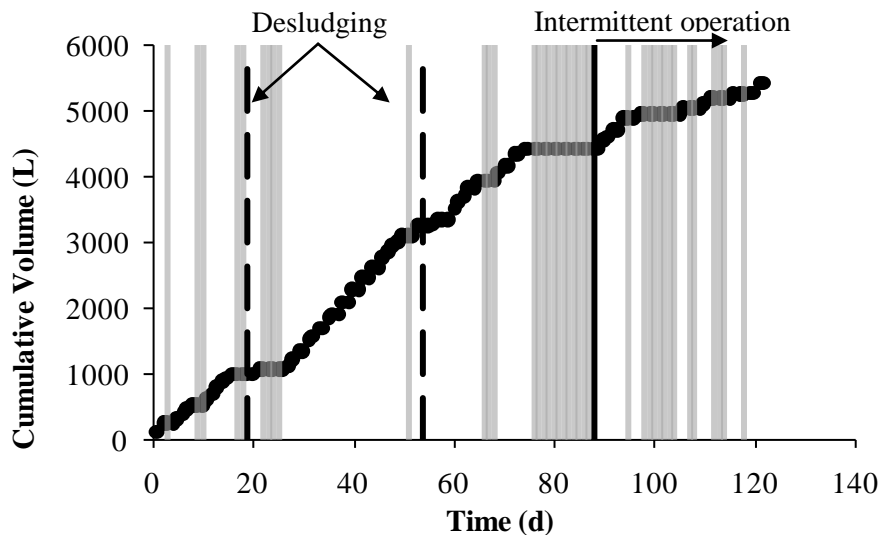


Figure II.8: Cumulative flow treated, incidents and downtime during Phase VII (4 June 2009 to 5 October 2009). Grey areas represent reactor downtime whilst dashed lines (---) indicate potentially performance-affecting incidents such as desludging.

A 2.8.2 ABR PERFORMANCE

During Phase VII (an average HRT of 3.6 d), the feed COD concentration to the ABR was kept constant at 2 000 mg/L (Table II.8). A highly variable TS concentration was measured in the feed (203 to 717 mg/L) with an average of 434 mg/L. The VS concentration ranged from 27 to 157 mg/L with an average of 76 mg/L.

The ABR was able to produce an effluent with an average COD, TS and VS of 331, 336 and 56 mg/L. This equated to an average removal efficiency of 82, 23 and 26% for COD, TS and VS, respectively.

Table II.8: Feed and effluent characteristics for Phase VII (4 June 2009 to 5 October 2009). Calculations of averages and standard deviations are presented for all measurements except for the pH value, which is reported as a median value. The number in parenthesis represents the number of samples over the operating period.

Parameter	Unit	Feed wastewater (<i>n</i>)			ABR Effluent (<i>n</i>)		
		Min	Max	Average	Min	Max	Average
COD _(total)	mg/L	2 000	2 000	2 000 ± 0 (19)	105	1 004	331 ± 199 (20)
pH		6.11	8.29	8.02 (12)	7.11	8.12	7.85 (12)
TS	mg/L	203	717	434 ± 176 (10)	157	449	336 ± 110 (5)
VS	mg/L	27	157	76 ± 45 (10)	37	68	56 ± 12 (5)
Proteins _(soluble)	mg/L	-	-	nd	5	104	63 ± 31 (23)
Carbohydrates _(soluble)	mg/L	-	-	nd	0.5	15.6	3.2 ± 4.2 (11)
Mean HRT	3.6 d	3.0 (min)	9.8 (max)		Total flow treated		5 571 L

nd, not determined. Soluble protein and carbohydrate concentrations were not measured for the feed as this phase concerned more with membrane operation.

A 2.9 SUMMARY OF RESULTS

Table II.9 presents a summary of feed wastewater and effluent COD values during the different phases of ABR operation. Also included in Table II.9 is the percentage removal of COD from the feed to the effluent.

Table II.9: Average measurements of COD for feed wastewater (COD in) and the effluent (COD out) of the ABR train at various phases of laboratory ABR operation.

Operation (Phase)	HRT (days)	COD in (average mg/L)	COD out (average mg/L)	Removal (%)
I	3.4	679	257	62
II	2.9	1 561	303	81
III	3.2	1 034	307	70
IV	3.3	1 500	334	78
V	3.2	2 000	447	78
VI	3.4	3 000	1 305	58
VII	3.6	2 000	331	83

During Phases I and II, the feed wastewater to ABR was not consistent despite the effort of the project team to maintain a constant COD concentration. This resulted in a highly variable COD feed wastewater concentration being treated by the ABR. After Phase II, the project team decided to change the manner in which the feed concentration was determined. Instead of measuring the COD per gram of VIP sludge before feeding and diluting the sludge to a desired COD concentration, a solution of concentrated VIP slurry was made using tap water. The COD of this slurry was then determined and diluted to a specific COD concentration. The result was a more consistent feed COD concentration being fed to the ABR in subsequent experiments.

During Phases III to VI, the feed concentration to the ABR was increased step-wise from 1 000 mg COD/L to 3 000 mg COD/L to observe the effect of organic loading on ABR and membrane performance (refer to **Chapter 5** for membrane results) (Kapuku, 2011). Despite the increase in organic loading, fairly stable operation was achieved in Phases III to V with COD removal efficiencies greater than 70% achieved. Similar COD removal efficiencies have been reported in ABRs treating blackwater under similar hydraulic regimes in Vietnam (Anh *et al.*, 2003 and 2007). At the highest organic loading, approximately half of the COD concentration in the feed reduced through the digestion process (57%). Despite reduction in the removal efficiency of the reactor, the removal efficiency was fair considering the strength and the biodegradability (approximately 30%) of the feed source. The latter has been determined in laboratory tests as part of another WRC study (Bakare, 2011).

Table II.10 presents a summary of TS measurements in the feed wastewater and effluent during the different phases of ABR operation. Also included in the table is the percentage removal of TS from the feed to the effluent.

Table II.10: Average measurements of TS for feed (TS in) and effluent (TS out) during various phases of laboratory ABR operation.

Operation (Phase)	HRT (days)	TS in (average mg/L)	TS out (average mg/L)	Removal (%)
I	3.4	705	266	62
II	2.9	844	376	56
III	3.2	482	477	1
IV	3.3	-	476	-
V	3.2	506	208	59
VI	3.4	-	314	-
VII	3.6	434	336	23

The no clear pattern with respect to TS and the HRT can be observed with removal efficiencies ranging from as low as 9% up to 59% using HRT ranging from 2.9 to 3.6 d.

Table II.11 presents a summary of VS measurements in the feed wastewater and effluent during the different phases of ABR operation. Also included in Table II.11 is the percentage removal of VS from the feed to the effluent.

Table II.11: Average measurements of VS for feed (VS in) and effluent (VS out) at various phases of laboratory ABR operation.

Operation (Phase)	HRT (days)	VS in (average mg/L)	VS out (average mg/L)	Removal (%)
I	3.4	311	99	68
II	2.9	611	137	78
III	3.2	340	159	53
IV	3.3	-	95	-
V	3.2	104	41	61
VI	3.4	-	-	-
VII	3.6	76	56	26

Total VS removals varied from each operation (26 to 78%) with no distinct trend observed between the HRT and removal efficiency.

In ABR technology, the major mechanism of treatment is the retention of solids in the front end of the ABR (Foxon *et al.*, 2006, Foxon, 2009). A similar mechanism occurs in this system as indicated in Figure II.9. The graph shows that the effluent and overflow (the wastewater passing from the feed tank to the first compartment box) follow the same trend throughout the study. The results suggest that effluent COD concentration at the end of the ABR train is dependent on the COD concentration of the flow from feed tank into the compartments, that is, that most of the COD removal occurs in the feed tank (Figure II.10).

This pattern is more clearly illustrated in Figure II.10 which shows a magnified view of the COD concentration during Phase III to VI. This is the time period in which the feed wastewater organic strength was increased in step-wise manner up until the end of Phase VI (day 495, 6 November 2008). The graph clearly shows that the dependence of the effluent COD concentration on the overflow (the flow from the leaving the feed tank and entering the splitter box).

The results indicate that a large percentage of the feed COD entering the reactor is removed in feed tank. As the system is not mixed (due to the presence of large particulate matter that clogs the pump), it can assumed that the COD reduction between the feed tank and compartments occurs through the retention of solids in the feed tank. Kapuku (2011) provided a more comprehensive analysis of the process in this ABR system. In that study, it was shown that solids retention was the major mechanism of COD removal, particularly in the feed tank where no mixing could be added to the design. Moreover, the feed wastewater was shown to have a lower biodegradability content than domestic wastewater. A COD mass balance across the system (determined from Phases III to VI) showed that only 30% of the total, incoming wastewater was converted to methane. The results were comparable to biodegradability tests performed on fresh VIP samples by Bakare (2011).

Figure II.11 illustrates the COD removal through the treatment train; from the feed tank to the first compartment of ABR train and from the first compartment of the ABR train to the effluent. During Phase I, 10% of the total COD in the feed was removed in the feed tank through settling. The ABR train were able to reduce the COD from the overflow of the feed tank by a further 58%. During

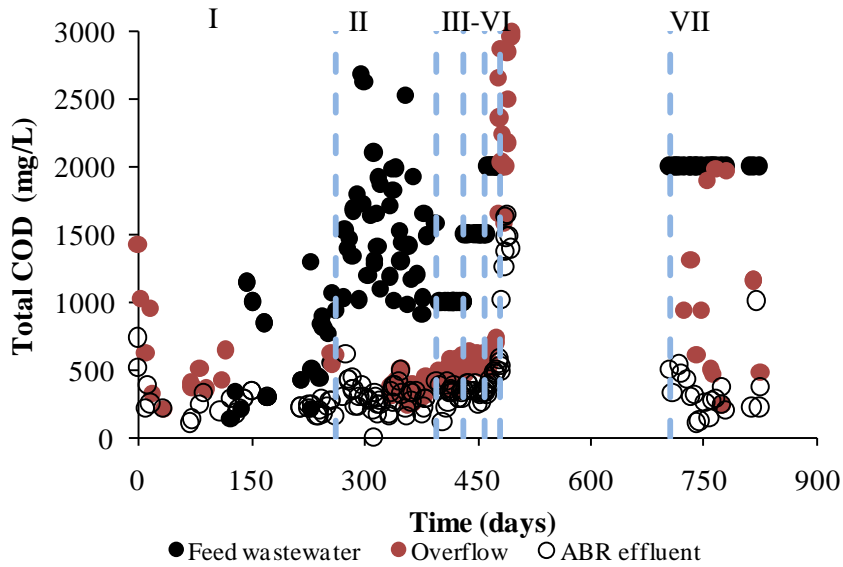


Figure II.9: Feed, overflow and effluent total COD concentrations for the laboratory ABR treating a synthetic blackwater (diluted VIP sludge) from 30 June 2007 to 5 October 2009. The light blue dashed line (---) represents the transition in operating parameters.

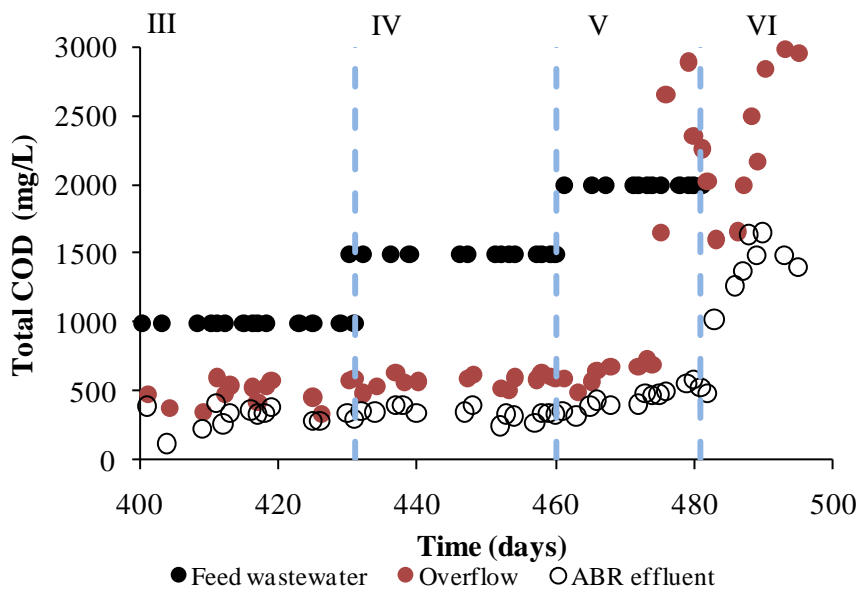


Figure II.10: Phases III to VI in Figure 4.9 showing feed, overflow and effluent total COD (tCOD) concentrations for the laboratory ABR treating a synthetic blackwater (diluted VIP sludge) from 2 August 2008 to 6 November 2008. The light blue dashed line (---) represents the transition in operating parameters.

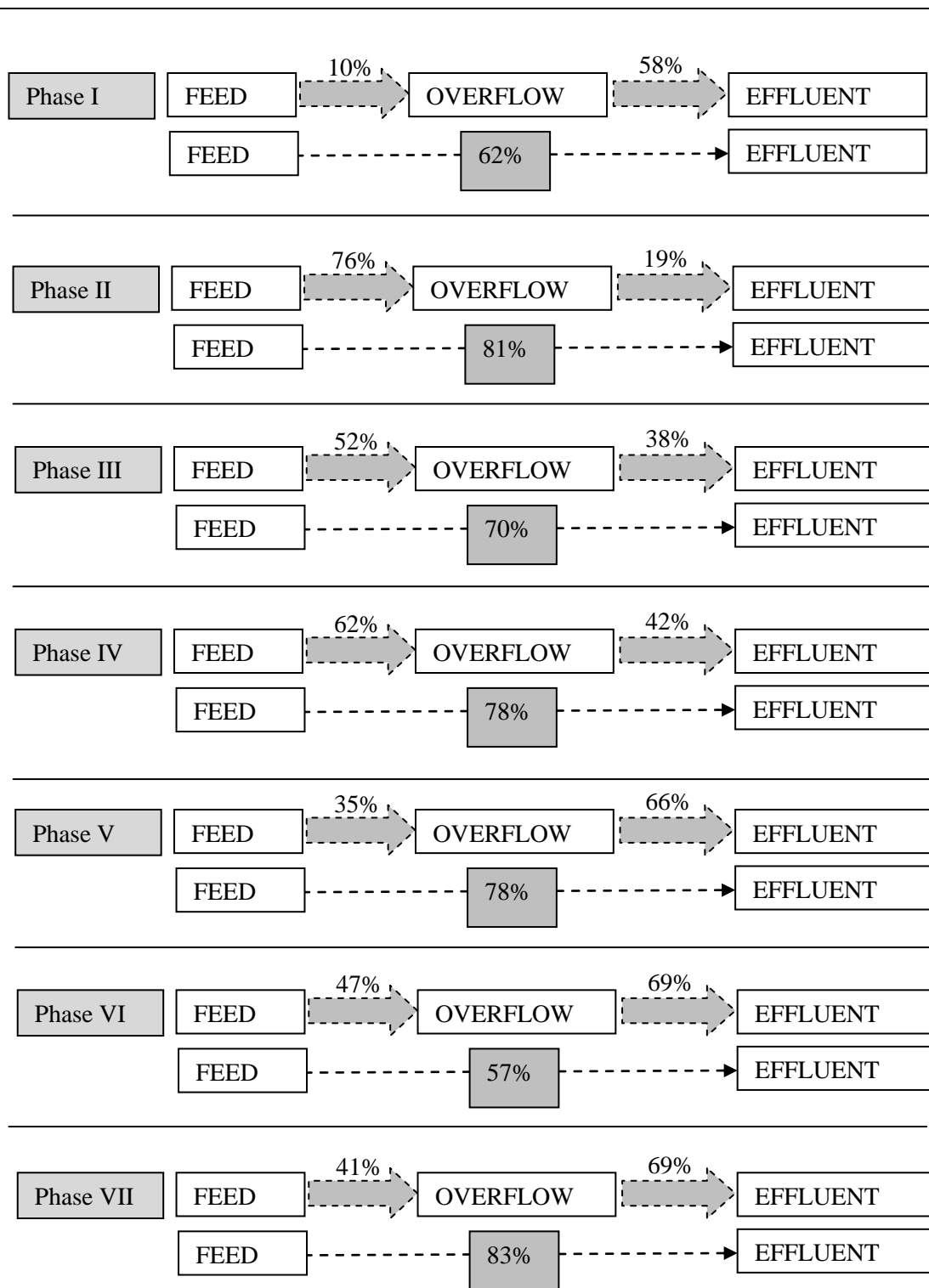


Figure II.11: The removal of COD from the feed tank to overflow (flow from feed tank to compartments) to effluent. The percentage values above grey arrows indicate percentage COD removal from either feed tank to overflow or overflow to effluent. The percentage value in grey box represents the COD removal from feed to effluent.

Phase II, as much as 76% of the total feed wastewater COD was removed in the feed tank. The ABR train was able to reduce the total COD of flow from the feed tank by a further 19%. A similar pattern was observed during Phases III and IV were nearly half of feed wastewater COD was removed through settling in the feed tank (Phases III, 52%; Phase IV, 62%). Phases V and VII, both conducted using a constant feed concentration of 2 000 mg/L, achieved the most COD removal through the ABR train.

The feed tank in this laboratory system displays similar attributes to those of settling tanks and biogas domes in BORDA designed DEWATS plants. In the BORDA DEWATS plants, a combination of blackwater and greywater or each stream enters a settling tank or biogas domes where the flow is distributed and enters an ABR. Figure II.12 shows pictures of biogas and settling used in some BORDA DEWATS plants. In some cases, it has been reported that most of the digestion occurs in the biogas dome or settling tank (Reynaud *pers. comm.*, 2010; Reynaud *et al.*, 2010), similar to the experiences in this study.



Figure II.12: Photographs of the biogas dome from a DEWATS plant in Indonesia (PRG, 2007) and China (BORDA, 2007).

Despite similar experiences observed in BORDA DEWATS plants, the results indicate a weakness in the design of the laboratory ABR and the experimental design. With respect to the design of ABR, large particulates settled in the feed tank and could not be pumped to the ABR train due to the physical nature of the feed wastewater solution. Fly larvae, maggots and larger faecal material clogged the piping when the system was mixed. As mechanical mixing could not be added to design of the feed tank, settling of particulate COD occurred in the reactor, which sometimes contributed much as 60% of the total feed COD concentration. To avoid clogging, periodic desludging was necessary.

Another experimental design weakness noted in this thesis is the use of VIP sludge as a synthetic feed source. Whilst it is common to use synthetic feed wastewater to replicate conditions in the treatment of domestic wastewater, Kapuku (2011) has shown VIP sludge fed to the ABR to be poorly biodegradable (30%). Similar values were achieved in a separate study into VIP sludge treatment and disposal (Bakare, 2011). The results indicate that most of the digestion is occurring in the feed tank before it enters the ABR train. It can therefore be concluded that the equipment design did not fit the experimental concept. Consequently, comparative results for the treatment of domestic wastewater in the ABR-membrane filtration system cannot be recorded as the outcomes should be different.

APPENDIX III: FOULING ABILITY OF FLAT SHEET MEMBRANE APPARATUS

A general description of the *fouling ability of flat-sheet membrane system* (FAFS) apparatus is presented below. The test cell technique was used to evaluate the fouling propensity of the soluble fraction of mixed liquor only. The technique was recommended by *EUROMBRA* partners and the set-up of experimental system in our laboratories formed part of technology transfer between UKZN (South Africa) and the Institut National des Sciences Appliquées de Toulouse (INSA Toulouse, France). Mr. Valetin Yvenat from INSA Toulouse assisted with data collection and instrument set-up. The interpretation of data was provided by Cabassud *et al.* (2006) as part of a work package and deliverable within the *EUROMBRA* Project which sought to standardise data exploitation between group members. The same filtration models used for the FAFS apparatus were also applied to data from the hollow-fibre (**Chapter 5**) and flat-sheet modules experiments (**Chapter 6**).

A 3.1 APPARATUS AND EQUIPMENT

- Amicon stirred cell model 8400 (Microsep, catalog number 5124).
- Centrifuge (Beckman J2-21 with JA10 rotor).
- Compressed air.
- Glass beakers.
- Magnetic stirrer (Ikamag RCT).
- Mass balance (Mettler AE 1690).
- Plastic box for storing membranes (local supplier).
- Pressure gauge (0 to 400 kPa) (Ashcroft).
- Pressure regulator × 2 (0 to 1 200 kPa) (Parker pneumatic).
- Sludge sample collection bottles (5 L, cleaned solvent bottles).
- Stainless steel pressurised reservoir (2 L) (built by laboratory technicians).
- Stop watch.
- Mercury glass thermometer (0 to 100° C).

A 3.2 REAGENTS AND MATERIALS

- Amicon PM10 ultra-filtration membranes, polyethersulphone 10 000 NWL (Microsep, catalog number 13112).
- Distilled water or MilliQ water (obtained from School of Biological and Conservation Science, UKZN).

-
- Reagent grade NaOH (Merck).

A 3.3 PROCEDURE

A general description of the procedure used for each test is described below. In the description, the term *clean water* is used as an analogy for MilliQ water or distilled water.

Procedure:

1. Centrifuge sludge at 10 000 g for 15 min and carefully decant the supernatant into a storage container. Store in cold room at 4°C or use immediately.
2. If the sample was in the cold room, allow the liquor to reach room temperature. Record the liquid temperature.
3. Rinse the fresh/cleaned membrane by letting it float shiny side up in clean water for 5 min.
4. Place the membrane on the membrane support (shiny side up), position the o-ring around the perimeter of the membrane and seal the unit with the cylindrical vessel.
5. Fill the filtration cell with 350 mL of clean water.
6. Close the Amicon® cell and connect to pressure reservoir.
7. Adjust pressure using the regulator to the required pressure.
8. Once the required pressure is reached and is constant, record the mass on the balance.
9. Record the permeate mass every minute for 10 min. If possible, record the permeate temperature every minute for 10 min.
10. Repeat steps 7 to 9 at higher pressures to obtain a plot of flux against TMP for clean water.
11. Release the pressure using the pressure regulator.
12. Open the filtration cell, remove the membrane filter and rinse it in a beaker with clean water for 10 min.
13. Empty the contents of the filtration cell into a sluice or toilet.
14. Remove membrane from beaker and place it on the membrane support (shiny side up), position the o-ring around the perimeter of the membrane and seal the unit with the cylindrical vessel.
15. Fill the filtration cell with 350 mL of the test solution and record the temperature.
16. Close the Amicon® cell and connect to pressure reservoir.
17. Adjust the pressure using the regulator to the required pressure.
18. Once the required pressure is reached and is constant, record the mass on the balance.
19. Record the permeate mass every minute for 10 min. If possible, record the permeate temperature every minute for 10 min.
20. Repeat steps 17 to 19 at higher pressures to obtain a plot of flux against TMP for the soluble fraction of the sludge.

-
21. Release the pressure using the pressure regulator.
 22. Open the filtration cell and carefully remove the membrane filter using gloves so as to not disturb the fouling layer.
 23. Empty the contents of the filtration cell into a sluice. Alternatively, chemical analyses can be performed on the concentrate prior to disposal.
 24. Clean the filtration cell with tap water and detergent to remove any debris and rinse with distilled water.
 25. Place the fouled membrane back on the membrane support (fouling layer up), position the o-ring around the perimeter of the membrane and seal the unit with the cylindrical vessel.
 26. Carefully fill the filtration cell with 350 mL of clean water by running the water along the sides of the vessel to prevent the disruption of the fouling layer.
 27. Close the Amicon® cell and connect to pressure reservoir.
 28. Repeat steps 7 to 9 to determine the resistance due to fouling.
 29. Remove the membrane filter from the beaker and transfer to another beaker containing clean water.
 30. Rinse the membrane in a glass beaker for 10 min and gently remove the fouling layer with gloves
 31. Transfer membrane to a glass beaker with 0.5M NaOH for 10 min.
 32. Repeatedly rinse membrane with clean water to remove excess NaOH.
 33. Store membrane in a sealed container (preferably glass) containing clean water until further analysis.

A 3.4 DATA INTERPRETATION

This section presents the mathematical analyses used in constant transmembrane (TMP) membrane filtration experiments. The data interpretation and exploitation was stipulated by *EUROMBRA* partners in *Deliverable 1: Common Methodologies* (Cabassud *et al.*, 2006).

A 3.4.1 TRANSMEMBRANE PRESSURE (TMP) EVALUATION

For each experiment, the module was operated under constant TMP instead of constant flux. The TMP across the membrane in the Amicon® filtration cell was obtained calculating the difference in the pressure reading on the pressure gauge and the permeate pressure (which is equal to the atmospheric pressure). Thus, the TMP can be calculated using the following equation:

$$\text{TMP} = P_{\text{cell}} - P_{\text{permeate}} \quad \text{(Equation A 3.1)}$$

A 3.4.2 DETERMINATION OF MEMBRANE PERMEABILITY

The mathematical analysis of membrane performance was performed according to Cabassud *et al.* (2006). The initial membrane permeability (L_{p0}) and the clean membrane hydraulic resistance (R_m) were determined before each set of experiments. These parameters are obtained through the determination of the TMP-permeate flux relationship during the filtration of clean water (MilliQ, distilled or tap water). Filtration tests were performed only at constant TMP.

For each constant TMP operation, the permeate flux at 20°C was determined using the following equation:

$$J_{p(20^\circ C)} = \frac{\Delta V}{S \cdot \Delta t} * \frac{\mu_{(T_{exp})}}{\mu_{(20^\circ C)}} \quad \text{(Equation A 3.2)}$$

where:

$J_{p(20^\circ C)}$: permeate flux at 20°C (L.m⁻².h⁻¹) or (m.s⁻¹)

ΔV : permeate volume obtained during the experiment time Δt (m³)

Δt : experiment time (s)

S : filtration area (m²)

$\mu_{(T_{exp})}$: permeate viscosity at experimental temperature (Pa.s)

$\mu_{(20^\circ C)}$: permeate viscosity at reference temperature (Pa.s)

The viscosity at temperature T is required to calculate L_{p0} . The influence of temperature on viscosity was calculated using the following equation (Cabassud *et al.*, 2006):

$$\mu_{(T_{exp})} = 1.002 \times \exp \left[3.056 \times \frac{(20 - T)}{(T + 105)} \right] \quad \text{(Equation A3.3)}$$

where:

T : temperature (°C)

μ : permeate viscosity

From the slope of flux (J) versus TMP, the initial membrane permeability (L_{p0}) at 20°C and the membrane resistance (R_m) can be determined using Darcy's Law (Figure III.1):

$$J_{p(20^{\circ}C)} = \frac{TMP}{\mu_{(20^{\circ}C)} \times R_m} = L_{p_0} \times TMP \quad \text{(Equation A 3.4)}$$

where:

L_{p_0} : membrane initial permeability ($L \cdot m^{-2} \cdot h^{-1} \cdot Pa^{-1}$) or ($L \cdot m^{-2} \cdot h^{-1} \cdot bar^{-1}$)

R_m : clean membrane resistance (m^{-1})

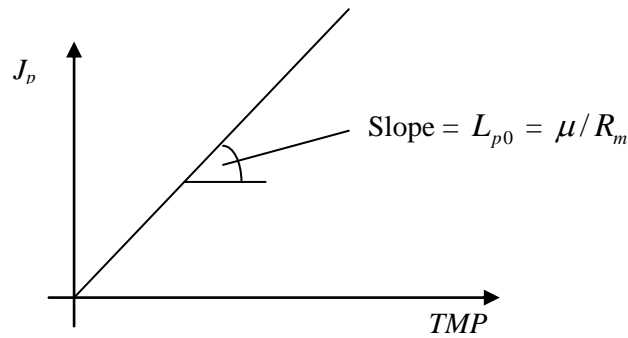


Figure III.1: Determination of the permeability (L_{p_0}) from the graph of flux (J) versus TMP (from Cabassud *et al.*, 2006).

The units for flux and pressure presented in this thesis are $L \cdot m^{-2} \cdot h^{-1}$ and Pa, respectively. Permeability has therefore been presented in $L \cdot m^{-2} \cdot h^{-1} \cdot kPa^{-1}$ in both plots and text through this thesis. However, in many membrane related studies the permeability of a system is expressed as $L \cdot m^{-2} \cdot h^{-1} \cdot bar^{-1}$. For this reason, permeability in $L \cdot m^{-2} \cdot h^{-1} \cdot bar^{-1}$ has also been included in the text in order to make comparison with published work easier.

A 3.4.3 DETERMINATION OF THE FOULING RESISTANCE

The first step is to calculate the viscosity of the permeate flux at 20°C equation A 3.3.

The permeate flux at 20°C is then determined using equation A 3.2.

R_m has been previously calculated with filtration tests using clean water (MilliQ, distilled water or tap water) (equation A 3.4) whilst the TMP is constant and determined by the user.

The resistance of fouling can then be calculated using the equation below which includes the temperature correction for the permeate flux at 20°C (reference temperature for the *EUROMBRA* Project):

$$J_{p(20^{\circ}C)} = \frac{TMP}{\mu_{(20^{\circ}C)} \times (R_m + R_f)}$$

where:

$J_{p(20^{\circ}C)}$: permeate flux at 20⁰ C (L.m⁻².h⁻¹) or (m.s⁻¹)

TMP : transmembrane pressure

$\mu_{20^{\circ}C}$: permeate viscosity at 20°C (Pa.s)

R_m : clean membrane resistance (m⁻¹)

R_f : fouling resistance (m⁻¹)

For each progressive increase in constant TMP, a decrease in the permeate flux should lead to an increase of the fouling resistance. Figure III.2 shows a typical fouling resistance evolution plot over time (Cabassud *et al.*, 2006).

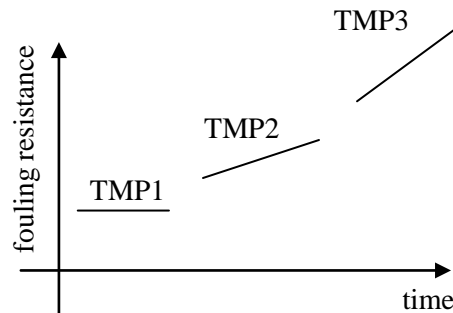


Figure III.2: Evolution of the cake resistance and TMP over time (from Cabassud *et al.*, 2006).

A 3.4.4 DETERMINATION OF FOULING VELOCITY

The fouling velocity (V_c) is defined as the variation in the cake (or fouling) resistance with time (Cabassud *et al.*, 2006). This velocity can be calculated by extrapolation of the plot of R_f against time.

$$V_c = \frac{dR_f}{dt}$$

(Equation A 3.5)

where:

V_c : fouling velocity (m⁻¹.h⁻¹)

R_f : fouling resistance (m⁻¹)

t : time (s)

The calculation of the fouling velocity is based on an assumption that the variation of the fouling resistance is linear during each 10 min step period and is thus calculated as an average of the values of the fouling resistance at the beginning and the end of each 10 min filtration step.

$$V_{average} = \frac{\Delta R_f}{\Delta t} = \frac{R_{f(end)} - R_{f(start)}}{t_{(end)} - t_{(start)}}$$

(Equation A 3.6)

The fouling velocity can be then be calculated for each constant TMP for a particular liquor.

By plotting the fouling velocity against the TMP, a unique fouling signature is generated for a liquor from a particular sludge source (see Figure III.3). In this manner, the fouling propensity of the soluble fraction from different groups from the *EUROMBRA* Project could be compared.

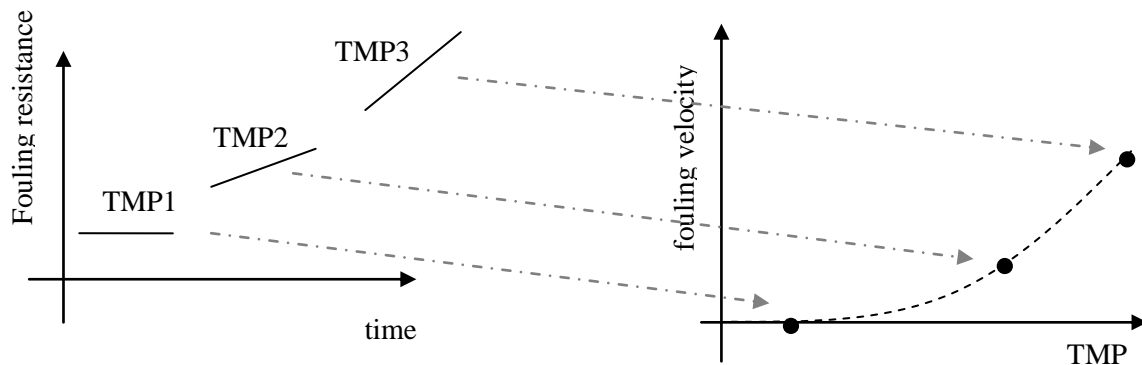


Figure III.3: A typical plot of fouling velocity against constant TMP which can used to compare the fouling potential of biological fluids from different sludge sources (from Cabassud *et al.*, 2006).

In this thesis, the fouling velocity curves from stirred cell tests and Polymem membrane step tests were not presented. The reason was that fouling resistance did not increase for each progressive TMP increase, making comparison between fouling velocity curves difficult. Furthermore, the reproducibility of the data was not good between the replicates of the same fluid (Chapter 4).

A 3.4.5 DETERMINATION OF THE PRODUCT OF $\alpha.C_s$ UNDER CONSTANT TMP

The specific cake resistance (α) is a commonly used parameter to quantify the membrane fouling (Cho *et al.*, 2005; Ye *et al.*, 2005). Its determination can be calculated as using equation A 3.8.

$$\frac{dt}{dV} = \frac{\mu}{S \times TMP} \times \left(\alpha \frac{C_s \times V}{S} \right) + R_m$$

(Equation A 3.7)

In most cases, the value of C_s cannot be experimentally obtained. As a result, only values of the product of $\alpha.C_s$ can be used. For an operation at constant TMP, the following equation (Equation A 3.8) is used to determine the $\alpha.C$ product.

$$\frac{t}{V} = \frac{\alpha \mu C_s V}{2.S^2.TMP} \cdot V + \frac{\mu R_m}{S.TMP}$$

(Equation A 3.8)

By plotting t/V against V , the value of the $\alpha.C_s$ product can be obtained from the value of the corresponding linear regression (Cabassud *et al.*, 2006). However, as shown in **Chapter 4**, the model assumes that there is a linear relationship between t/V versus V plot which is not always observed experimentally.

In the next section, the linear regression analysis used to determine product of $\alpha.C_s$ is presented.

A 3.5 LINEAR REGRESSION ANALYSIS OF t/V VERSUS V PLOTS

This section presents the analysis from the linear regression of t/V versus V plots of supernatant from various sludge sources. The lower and upper limits of the linear regressions plots in this section were to evaluate the fouling propensity of different soluble supernatant sources.

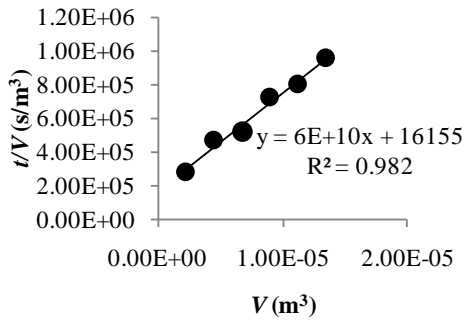
Figure III.4 presents the data for linear regression for supernatant samples from the pilot ABR on Amicon® membrane 1.

Figure III.5 presents the data for linear regression for supernatant samples from the activated sludge plant on Amicon membrane 1.

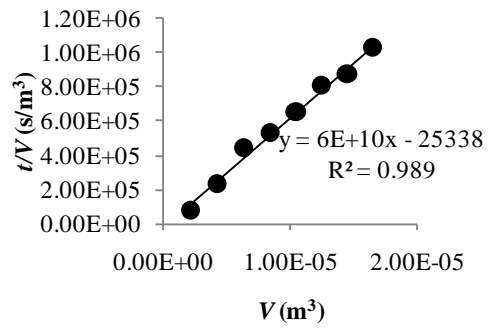
Figure III.6 presents the data for linear regression for supernatant samples from the conventional anaerobic digester on Amicon® membrane 2.

Figure III.7 presents the data for linear regression for supernatant samples from the laboratory ABR plant. Figure III.7a to c represent the data for the laboratory ABR treating a synthetic wastewater (diluted VIP waste and greywater) on Amicon® membrane 3. Figure III.7d to f represent the data for the laboratory ABR treating a diluted VIP waste on Amicon® membrane 4.

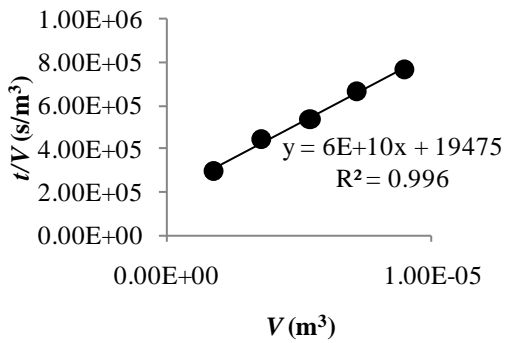
In the next annexure, details of the analytical methods used in this thesis are presented.



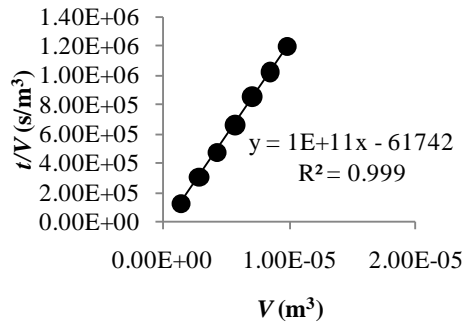
a) Compartment 2 of pilot ABR – Test 1



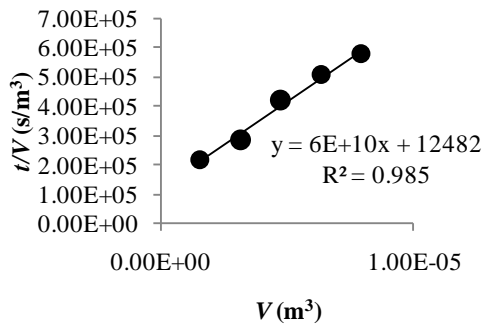
b) Compartment 2 of pilot ABR – Test 2



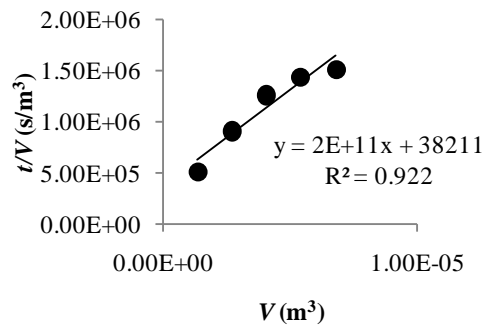
c) Compartment 3 of pilot ABR – Test 1



d) Compartment 3 of pilot ABR – Test 1

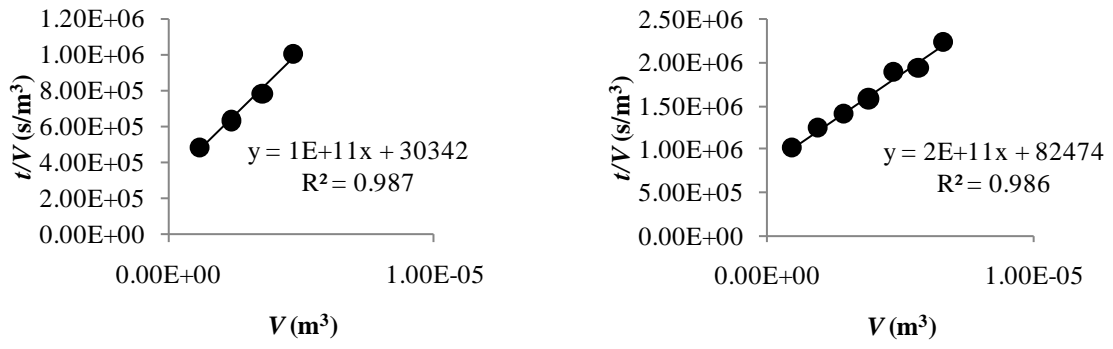


e) Compartment 4 of pilot ABR – Test 1



f) Compartment 4 of pilot ABR – Test 2

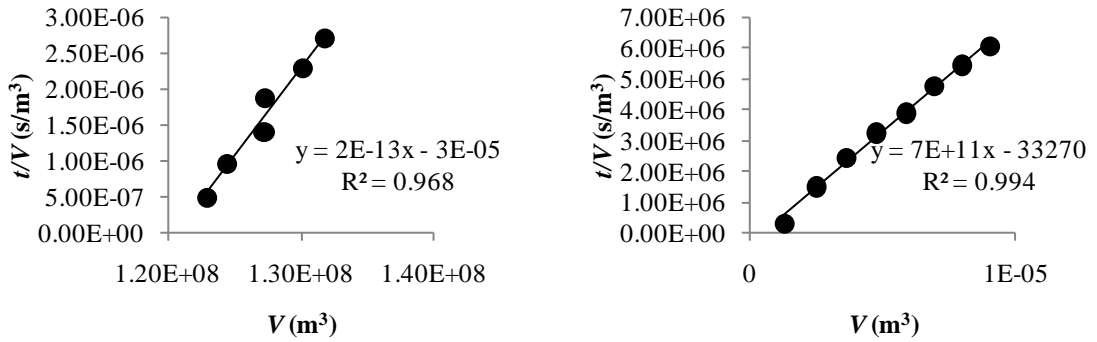
Figure III.4: Linear regression of points from t/V versus V plots in Chapter 4 for the pilot ABR supernatant samples on Amicon membrane 1.



a) Activated sludge – Test 1

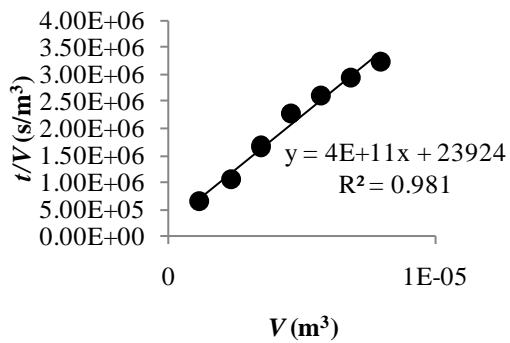
b) Activated Sludge - Test 2

Figure III.5: Linear regression of points from t/V versus V plots in Chapter 4 for the activated sludge samples on Amicon membrane 1.

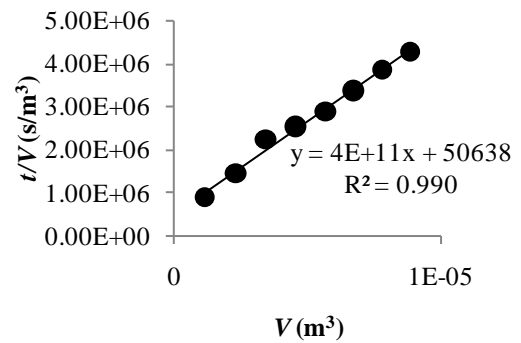


a) Raw undiluted anaerobic sludge

b) Diluted anaerobic sludge – Test 1

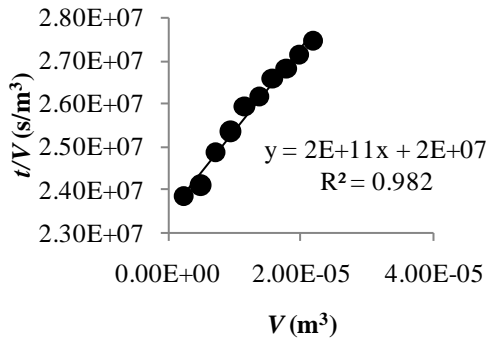


c) Diluted anaerobic sludge – Test 2

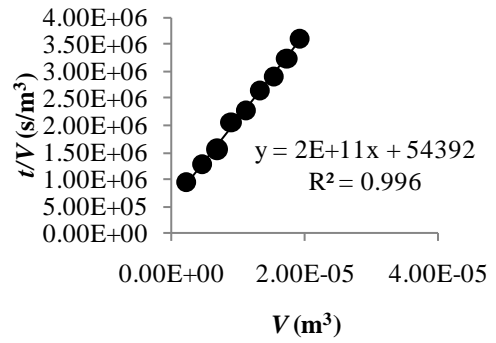


d) Diluted anaerobic sludge – Test 3

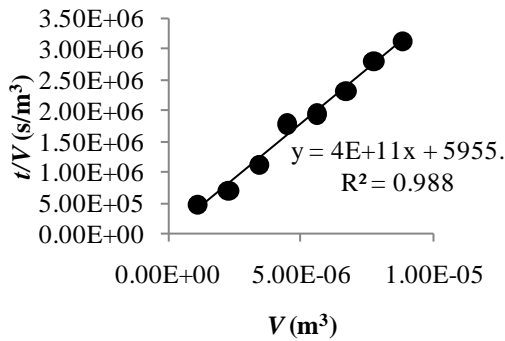
Figure III.6: Linear regression of points from t/V versus V plots in Chapter 4 for the activated sludge samples on Amicon membrane 2.



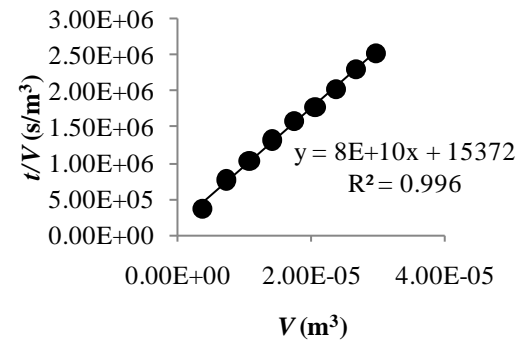
a) Synthetic wastewater – Test 1



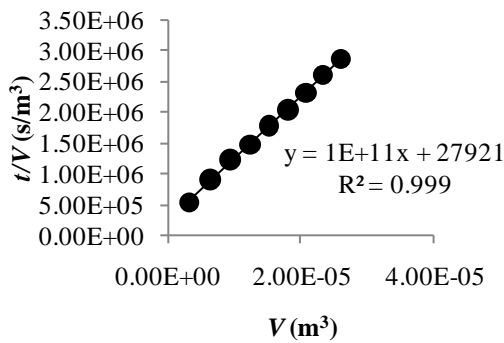
b) Synthetic wastewater – Test 2



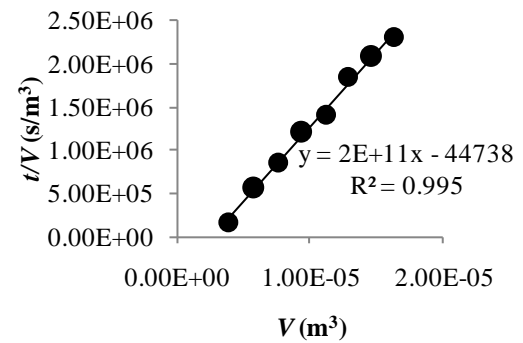
c) Synthetic wastewater – Test 3



d) Diluted VIP sludge – Test 1



e) Diluted VIP sludge – Test 2



f) Diluted VIP sludge – Test 3

Figure III.7: Linear regression of points from t/V versus V plots in Chapter 4 for the effluent samples from the laboratory ABR. Plots (a) to (c) represent samples from the ABR treating a synthetic domestic wastewater on Amicon membrane 3. Plots (d) to (f) represent samples from the ABR treating a synthetic domestic wastewater on Amicon membrane 4.

APPENDIX IV: ANALYTICAL METHODS

This section provides a detailed description of the analytical techniques used in this work.

A 4.1 pH

The value of pH has significant influence on the balance of the anaerobic process. For this reason, it is often measured to provide an indication of the reactor environment and performance. Furthermore, it can serve as an early warning signal of digester failure as changes in this parameter occur faster than others. The method used for determining this parameter is relatively simple and inexpensive. The pH value can be obtained from electronic pH meters. In this work, samples were taken from the top of the effluent and feed tank. The pH was immediately read with Metro Ohm pH meter model 744 (calibrated with standard solution, pH 4.0 and pH 7.0). Analysis of pH profile in compartments at various feeding regimes has been reported in Kapuku (2011).

A 4.2 TEMPERATURE

The temperature was recorded by placing a glass mercury thermometer in the liquor.

A 4.3 CHEMICAL OXYGEN DEMAND (COD)

The COD is the amount of oxygen necessary to oxidize the organic matter in a sample. The method presented used in this thesis is the University of Cape Town (UCT) Open Reflux COD Method for wastewater (Lakay *et al.*, 2000). The method is an adaptation of Standard Method 5220B (APHA-AWWA-WEF, 1998) with smaller volumes of reagent used in the UCT method.

A 4.3.1 PRINCIPLE

A mixture of chromic and sulphuric acid is boiled which oxidizes the organic matter in the sample (APHA-AWWA-WEF, 1998). The sample is refluxed in strongly acidic solution with a known excess of potassium dichromate ($K_2Cr_2O_7$). Following digestion, the remaining unreduced dichromate is titrated with ferrous ammonium sulphate (FAS) to determine the chromate consumed. The oxidisable organic matter is then calculated in terms of oxygen equivalent (APHA-AWWA-WEF, 1998).

A 4.3.2 APPARATUS

- Flat-bottomed Erlenmeyer flasks.
- Ground-glass 24/40 neck and 300 mm Liebig condenser with 24/40 ground-glass joint.

-
- Hotplate.
 - Timer (capable of stopping after 2 h).
 - Burette.

A 4.3.3 SAMPLE HANDLING AND STORAGE

Collect samples in glass bottles. If storage is unavoidable, preserve by acidification to $\text{pH} \leq 2.0$ using concentrated sulphuric acid (H_2SO_4 , Merck 95-98%). Shake or stir samples containing settleable solids to ensure representative sampling. Dilute samples containing high COD to reduce the error inherent in measuring small sample volumes. For soluble COD measurements, a mixed liquor sample is filtered through $0.45 \mu\text{m}$ Whatmann filters (47 mm cellulose nitrate) and the COD test performed on the filtrate.

A 4.3.4 PREPARATION OF REAGENTS

Potassium Dichromate ($\text{K}_2\text{Cr}_2\text{O}_7$)

- Dry standard reagent grade potassium dichromate (Merck) 0.25 N (0.0417M) in the oven at 103°C for 2 h.
- Cool in desiccator. Weigh out 12.2588 g.
- Dissolve in a 1 000 mL volumetric flask. Mix thoroughly.

Sulphuric Acid/Silver Sulphate Reagent ($\text{H}_2\text{SO}_4/\text{Ag}_2\text{SO}_4$)

- Add 15 g of silver sulphate crystals or powder (Merck) to 2.5 L of concentrated sulphuric acid (Merck, 95 to 98%).
- Place on a magnetic stirrer and stir well for 2 d.

Mercuric Sulphate (HgSO_4)

- Used to remove chlorides which give a higher COD result.
- 0.04 g crystal or powder (Merck).

Ferrous Ammonium Sulphate [$\text{Fe}(\text{NH}_4)_2(\text{SO}_4)_2 \cdot 6\text{H}_2\text{O}$]

- Dissolve 98g of ferrous ammonium sulphate (Associated Chemical Enterprises, ACE) in distilled water.
- Add 20 mL concentrated sulphuric acid (Merck, 95 to 98%). Cool and dilute to 1 000 mL.

Ferriin Indicator

- Dissolve 1.485 g 1:10 phenantroline monohydrate (ACE) and 0.695 g. ferrous sulphate (FAS, ACE) in distilled water and dilute to 100 mL.
- Add 2 to 3 drops in COD flask before titration.

Standard Preparation:

- Pipette 5 mL of potassium dichromate solution into an Erlenmeyer flask.
- Dilute to 50 mL with distilled water. Add 15 mL concentrated sulphuric acid (Merck, 95 to 98%).
- Cool and titrate against FAS with 2 to 3 drops of ferriin indicator.

Quality Control: Potassium Hydrogen Phthalate (KHP)

- Lightly crush and then dry KHP (Merck) to a constant weight at 120°C.
- Dissolve 0.425 g in distilled water and dilute to 1 000 mL.
- This solution has a theoretical COD of 500 mg/L. Use 10 mL of this solution in the COD test. For COD concentrations over 1 000 mg/L, dilution is necessary as samples are too concentrated – sample turns green upon addition of acid reagent.
- Solution can be stored in the refrigerator up to 3 months in the absence of biological growth.

A 4.3.5 PROCEDURE

1. Add approximately 0.04 g (2 match heads) of mercuric sulphate to a dry 250 mL Erlenmeyer flask.
2. Add 5 glass beads.
3. Add 10 mL sample. If the sample is concentrated, make an appropriate dilute and pipette 10 mL in COD flask.
4. Add 10 mL distilled water to another flask (blank).
5. Add 5 mL potassium dichromate solution.
6. Add 15 mL sulphuric acid reagent (with silver sulphate).
7. Pour acid down the wall of the flask while flask is tilted. If sample is too concentrated it will turn green which indicates that the sample needs to be diluted.
8. Immediately attach flask to the jacket condenser. Flasks must be level on heating pad.
9. Digest samples for 2 h. Ensure that the water flow rate in the condensers is swift to allow for reflux.
10. Cool samples with the condensers still in position.

-
11. Pour approximately 80 mL of distilled water through the top opening of each of the condensers into the sample mixture.
 12. Titrate FAS against the sample using 2-3 drops of ferroin indicator.
 13. The colour will change from green/orange to reddish/brown.
 14. Take reading on burette.
 15. Repeat procedure for quality control solution (KHP) on a bimonthly basis.
 16. Calculation:

$$\text{COD (mg/L)} = \frac{[\text{Blank (mL)} - \text{Titration (mL)}] \times 8\,000 \times \text{MFAS} \left(\frac{\text{mol}}{\text{L}}\right)}{\text{Sample volume (mL)}}$$

(Equation A 4.1)

A 4.4 TOTAL SOLIDS (TS)

This section presents the procedure for the determination of total solids (TS) in wastewater samples. In section A 4.4.1, the principle behind TS determination is presented. Section A 4.4.2 lists the apparatus used for TS determination and, the sampling handling and storage procedure is presented in A 4.4.3. Section A 4.4.4 lists the steps for the procedure and the calculations used for TS determination.

A 4.4.1 PRINCIPLE

In this procedure, a pre-weighed porcelain dish is placed in an oven to evaporate the moisture in a known aliquot of sample. The increase in weight over the empty dish is known as the total solids concentration.

A 4.4.2 APPARATUS

- Porcelain crucibles.
- Oven capable of reaching 105°C.
- Muffle furnace.
- Heat-protective gloves and tong.
- Desiccator containing a porcelain plate placed on dried silicon particles.
- Weighing balance (four decimal places).

A 4.4.3 SAMPLE HANDLING AND STORAGE

Glass bottles were used to store samples. When analysis could not be done immediately, samples were stored at 4°C to minimise degradation of solids.

A 4.4.4 PROCEDURE:

1. Heat a porcelain crucible in a muffle furnace for 2 h at 550°C.
2. Allow to cool in a desiccator (approximately 4 h).
3. Weigh empty crucible on a four decimal balance.
4. Dispense a certain aliquot of sample into crucible.
5. Place in an oven at 105°C until all moisture has evaporated (weight stays constant).
6. Place in a desiccator to cool (usually 1.5 h).
7. Weigh crucible containing dried sample.
8. Place weighed samples back in desiccator for further (volatile solids) analysis.
9. Calculation:

$$\text{Total Solids (mg/L)} = \frac{\text{Crucible weight after 105°C (mg)} - \text{Weight of dry crucible (mg)}}{\text{Sample Volume (L)}}$$

(Equation A 4.2)

A 4.5 VOLATILE SOLIDS (VS)

This section presents the procedure for the determination of volatile solids (VS) in wastewater samples. Section A 4.5.1 presents the principle behind the technique. Section A 4.5.2 lists the apparatus used in VS determination, and the sampling handling and storage procedure is presented in section A 4.5.3. Section A 4.5.4 lists the steps for the procedure and the calculations used for VS determination.

A 4.5.1 PRINCIPLE

The residue from the determination of total solids is ignited to constant weight at 550°C. An ignition period of 45 min was used in experimentation.

A 4.5.2 APPARATUS

- Porcelain crucibles.
- Muffle furnace.
- Heat-protective gloves and tong.
- Desiccator containing a porcelain plate placed on dried silicon particles.
- Weighing balance (four decimal places).

A 4.5.3 SAMPLE STORAGE AND HANDLING

The crucibles containing samples are stored in a desiccator after total solids determination.

A 4.5.4 PROCEDURE:

1. Complete total solids determination.
2. Remove crucible from desiccator and place in a muffle furnace for 45 min at 550°C.
3. Cool for 4 h in a desiccator.
4. Weigh crucible with ash sample.
5. Calculation:

$$\text{Volatile Solids (mg/L)} = \frac{\text{Crucible weight after 550}^\circ\text{C (mg)} - \text{Weight of crucible after 105}^\circ\text{C (mg)}}{\text{Sample Volume (L)}}$$

(Equation A 4.3)

A 4.6 TOTAL SUSPENDED SOLIDS (TSS)

This section presents the procedure for the determination of total suspended solids (TSS) in wastewater samples. Section A 4.6.1 presents the principle behind the technique. Section A 4.6.2 lists the apparatus used for TSS determination and, the sampling handling and storage procedure is presented in section A 4.6.3. Section A 4.6.4 lists the steps for the procedure and the calculations used for TSS determination.

A 4.6.1 PRINCIPLE

In this procedure, a well-mixed sample is filtered through a weighted glass fibre filter. The filter with the residue is placed in an oven and dried at 103°C to 105°C. The increase in weight of the filter is known as the total suspended solids concentration (APHA-AWWA-WEF, 1995).

A 4.6.2 APPARATUS

- Porcelain crucibles.
- Glass-fibre filters.
- Filtration apparatus (vacuum pump, Büchner holder and flask).
- Oven capable of reaching 105°C.
- Muffle furnace.
- Heat-protective gloves and long-handle metal tongs.
- Desiccator containing a porcelain plate placed on dried silicon particles.
- Weighing balance (four decimal places).

A 4.6.3 SAMPLE HANDLING AND STORAGE

Glass bottles were used to store samples. When analysis could not be done immediately, samples were stored at 4°C to minimise degradation of solids.

A 4.6.4 PROCEDURE:

1. Heat a porcelain crucible in a muffle furnace for 2 h at 550°C.
2. Dry glass-fibre filter at 105°C in an oven.
3. Allow crucibles to cool for 4 h in a desiccator.
4. Weigh empty crucible.
5. Allow filters to cool in desiccator and weigh.
6. Filter a certain aliquot of sample through glass-fibre filter.
7. Place the filter inside a crucible and put in an oven at 105°C until all moisture has evaporated.
8. Place in a desiccator to cool.
9. Weigh crucible containing filter with dried residue.
10. Place weighed samples back in desiccator for further analysis.
11. Calculation:

$$\text{Total Suspended Solids (mg/L)} = \frac{\text{Crucible+filter weight after 105°C (mg)} - \text{Weight of dry crucible (mg)}}{\text{Sample Volume (L)}}$$

(Equation A 4.4)

A 4.7 VOLATILE SUSPENDED SOLIDS (VSS)

This section presents the procedure for the determination of total suspended solids (VSS) in wastewater samples. In section A 4.7.1, the principle behind the technique is presented. Section A 4.7.2 lists the apparatus used for VSS determination and, the sampling handling and storage procedure is presented in section A 4.7.3. Section A 4.7.4 lists the steps for the procedure and the calculations used for VSS determination.

A 4.7.1 PRINCIPLE

The residue from the determination of total suspended solids is ignited in a furnace to constant weight at $550 \pm 50^\circ\text{C}$. A time of 20 to 30 min ignition is usually enough for a stable reading. The remaining solids in the crucible represent the fixed total dissolved solids whilst weight loss is the volatile solids.

A 4.7.2 SAMPLE HANDLING AND STORAGE

After completion of TSS determination, keep crucibles in the desiccator and use for VSS analyses.

A 4.7.3 APPARATUS

- Porcelain crucibles.
- Glass-fibre filters.
- Muffle furnace.
- Heat-protective gloves and long-handle metal tongs.
- Desiccator containing a porcelain plate placed on dried silicon particles.
- Weighing balance (four decimal places).

A 4.7.4 PROCEDURE

1. Complete total suspended solids determination.
2. Remove crucible from desiccator and place in a muffle furnace for 45 min at 550°C.
3. Cool for 4 h in a desiccator.
4. Weigh crucible with ash sample.
5. Place in a desiccator to cool.
6. Weigh sample.
7. Calculation:

$$\text{Volatile Suspended Solids (mg/L)} = \frac{\text{Crucible+filter weight after 550}^\circ\text{C (mg)} - \text{Weight of crucible+filter after 105}^\circ\text{C (mg)}}{\text{Sample Volume (L)}}$$

(Equation A 2.5)

This method was only used during the first part of study (refer to Table 4.2 in section 4.5.2). The reason for the discontinuation of the procedure was that replacement glass-fibre filters bought during the later stages of the project were not suitable for ignition. The recommended filters, Whatman glass-fibre filters (grade 934-AH), were out of stock. Replacement glass-fibre filters were suggested by suppliers according to product code of the Whatman grade 934 AH glass-fibre filters. Unfortunately, the replacement filters showed some ignition in the furnace (550°C) resulting in erroneously negative values for VSS. Moreover, they were not same pore size of the Whatman grade 934-AH glass-fibre filters.

A 4.8 EPS EXTRACTION AND DETERMINATION

A 4.8.1 SEPARATION OF SOLUBLE FRACTION

The soluble and bound EPS in the mixed liquor is separated using high-speed ultracentrifugation at 10 000 g at room temperature. The procedure was recommended by the *EUROMBRA* group based on a survey of equipment between partners and formed part of a work package within the project. In-house experiments were performed by INSA Toulouse to compare differentiate between different separation methods (Cabassud *et al.*, 2006) with

ultracentrifugation chosen as the organic components are isolated by mass with no interference from a support medium such as a prefiltration step (Teychene *et al.*, 2008). Figures IV.1 shows some of the steps for the separation and extraction process.

A 4.8.2 EXTRACTION OF BOUND EPS

Two methods were recommended as part of common methodology manual; cation exchange and sonication (Cabassud *et al.*, 2006). The cation exchange was the most recommended method with the methodology of Frølund *et al.* (1996) used. The general method detailed in Cabassud *et al.* (2006) is presented below.

Reagents and Materials

1. Buffer solution at pH 7.0 (2 mM Na₂HPO₄, 4 mM NaH₂PO₄, 9 mM NaCl and 1mM KCl).
2. Cation exchange resin (Dowex® Marathon, Sigma-Aldrich).
3. High-speed centrifuge capable of 10 000 g.
4. Magnetic stirrer with RPM control.

Extraction Procedure:

1. Determine VSS of sample.
2. Weigh out cation exchange resin to 70 to 75 g per VSS of sludge sample.
3. Equilibrium of cation exchange in buffer solution.
4. Centrifuge a 200 mL sludge sample at 10 000 g for 15 min at 15°C.
5. Carefully remove the centrifuge tubes from the centrifuge, decant the supernatant without disturbing the pellet and place in a storage bottle (store in refrigerator or analyse immediately). This supernatant represents the soluble fraction of sludge or the *biological supernatant* (Cabassud *et al.*, 2006)
6. Fill the centrifuge tube with 200 mL of buffer solution, close the cap and shake the bottle to resuspend pellet.
7. Centrifuge sample at 10 000 g for 15 min at 15°C.
8. Carefully remove the supernatant. This liquid fraction represent the ‘washings’ of sludge and is used to determine the loosely-bound EPS fraction. Store supernatant in a refrigerator or analyse immediately.
9. Fill the centrifuge tube with 200 mL of buffer solution, close the cap and shake the bottle to resuspend pellet.
10. Transfer the content of centrifuge tube to a glass beaker and add 70 to 75 g per VSS of the equilibrated solution.
11. Stir solution for 2 h at 600 RPM.

-
12. Allow solution to settle and re-centrifuge at 10 000 *g* for 15 min at 15°C.
 13. Carefully remove the supernatant which contains the extracted cell-bound EPS.

The extraction and chemical analysis of bound EPS was only performed for the test cell experiments. The centrifuge (Beckman J2-21) that was used for the separation and extraction of EPS fractions was packed and then re-located to the Westville campus as part of the merger process of the former University of Natal and University of Durban-Westville into the University of KwaZulu-Natal. Although a centrifuge was purchased later in the project, the availability of appropriate glass fibre filters for VSS analysis was limited.

In the next section, the methodology for protein determination is presented.



a) Aliquots of 200 mL sludge samples



b) High-speed centrifuge with temperature control (Beckman J2-21).



c) Supernatant representing soluble fraction



d) Pellet after decanting



e) Pellet resuspension with buffer



f) Supernatant with loose-bound EPS

Figure IV.1: Picture guideline of the separation process used in this project. Not included in the guide is the extraction process with cation exchange resin.

A 4.9 PROTEIN CONCENTRATION

Two methods were recommended by Cabassud *et al.* (2006) to determine the concentration of proteins in wastewaters; the modified Lowry method (Frølund *et al.*, 1996) and the bincichonic acid method (Smith *et al.*, 1985). The modified Lowry method was used as the project team had practical experience with the use of this technique.

A 4.9.1 APPARATUS

- Spectrophotometer.
- Glass curvettes.
- Vortex mixer.
- Automated pipettes (0.3 to 3.0 mL) with pipette tips.
- Test tubes with test tube rack.

A 4.9.2 SAMPLE HANDLING AND STORAGE

Store samples in glass bottles in refrigerator and analyse within a day.

A 4.9.3 REAGENTS

Reagent A: 143 mM NaOH and 270 mM Na₂CO₃

- Weigh out 5.72 g of sodium hydroxide (NaOH) pellets.
- Weigh out 28.62 g of sodium carbonate (Na₂CO₃).
- Dissolve in 1 L distilled water.

Reagent B: 57 mM Copper Sulphate (CuSO₄)

- Dissolve 9.12 g of copper sulphate (CuSO₄) in distilled water.

Reagent C: 124 mM Sodium Tartrate (Na₂C₄H₄O₆)

- Dissolve 24.06 g of sodium tartrate (Na₂C₄H₄O₆) in distilled water.

Reagent D

- Mixture of reagents A, B and C in the ratio of 100: 1: 1.
- Mixture has to be done immediately before analysis (cannot store).

Reagent E

- Folin-Ciocalteu reagent (Merck).

Bovine Serum Albumin (BSA)

- Make a serial dilution of aqueous BSA (96% purity, Merck) for calibration curve.
- Use pre-filtered buffer solution for dilutions.

A 4.9.4 PROCEDURE

- Pipette 1.5 mL of sample into test tube (3 replicates).
- Pipette 1.5 mL of buffer solution into a separate test tube (3 replicates).
- Add 2.1 mL of reagent D into each test tube and vortex until thoroughly mixed.
- Leave at room temperature for 10 min.
- Add rapidly 0.3 of reagent E and vortex sample.
- Leave at room temperature for 45 min
- Measure absorbance of sample against blank at 750 nm.

A 4.9.5 CALIBRATION CURVE

The calibration plots of BSA equivalents against absorbance at 750 nm are shown in Figure IV.2. The first was made for the spectrophotometer in the School of Biological and Conservation Science, University of KwaZulu-Natal (Spec 1). The other two plots were made for the Merck photometer that was purchased for the Pollution Research Group. Similar calibration curves were obtained from Merck spectrophotometer at the beginning of 2009 (Spec 2) and the end of 2010 (Spec 3) indicating good reproducibility of results.

A 4.10 CARBOHYDRATE CONCENTRATION

Two methods were recommended by Cabassud *et al.* (2006) for carbohydrate determination; the Dubois *et al.* (1956) method and the anthrone method (Dreywood, 1946; Morris *et al.*, 1948). The Dubois *et al.* (1956) method was used as it was found to be much easier to perform than the anthrone method.

A 4.10.1 APPARATUS

- Spectrophotometer.
- Glass cuvettes.
- Vortex mixer.
- Automated pipettes (0.3 to 3.0 mL) with pipette tips.
- Test tubes with test tube rack

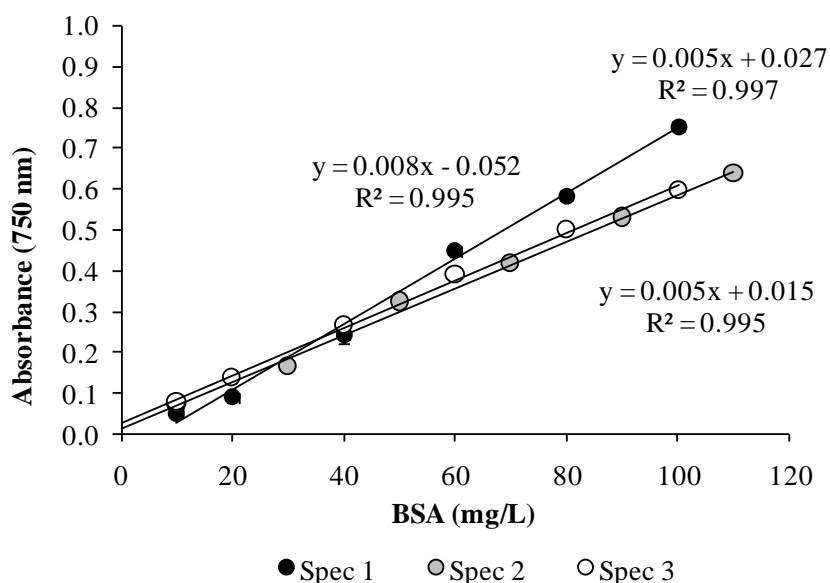


Figure IV.2: Plot of BSA concentration against absorbance at 750 nm (spec 1, spectrophotometer at the School of Biological and Conservation Science; spec 2 and 3 represent readings from Merck spectrophotometer).

A 4.10.2 SAMPLE HANDLING AND STORAGE

Store samples in glass bottles in refrigerator and analyse within a day.

A 4.10.3 REAGENTS

Phenol Solution

Dissolve 100 g of phenol crystals in 1 L of distilled water (5% w/v solution).

Sulphuric acid

Reagent grade (95 to 98%, Merck).

Calibration solution

Make a serial dilution of D-Glucose anhydrous (Merck).

A 4.10.4 PROCEDURE

1. Pipette 1 mL of sample into a test tube (perform replicates).
2. Pipette 1 mL of blank (buffer solution) into another test tube (perform replicates).
3. Add 1 mL of phenol solution into test tubes and vortex.
4. Rapidly add 5 mL of sulphuric acid. Be careful as the test tube heats very quickly.
5. Allow to stand for 15 min at room temperature.

6. Vortex test tubes again.
7. Allow to stand for 30 min at room temperature.
8. Vortex test tube again. An additional vortex step has been added to Cabassud *et al.* (2006) before measurement as the acid is quite viscous and forms waves when dispensing into curvette.
9. Measure absorbance at 490 nm against blank.

A 4.10.5 CALIBRATION CURVE

Two calibration plots were made using a serial dilution of D-glucose (Figure IV.3). The first (Spec 1) was for the spectrophotometer used at the School of Biological and Conservation Science. The second plot was from the Merck spectrophotometer used in the Biochemical Engineering laboratory at the Pollution Research Group.

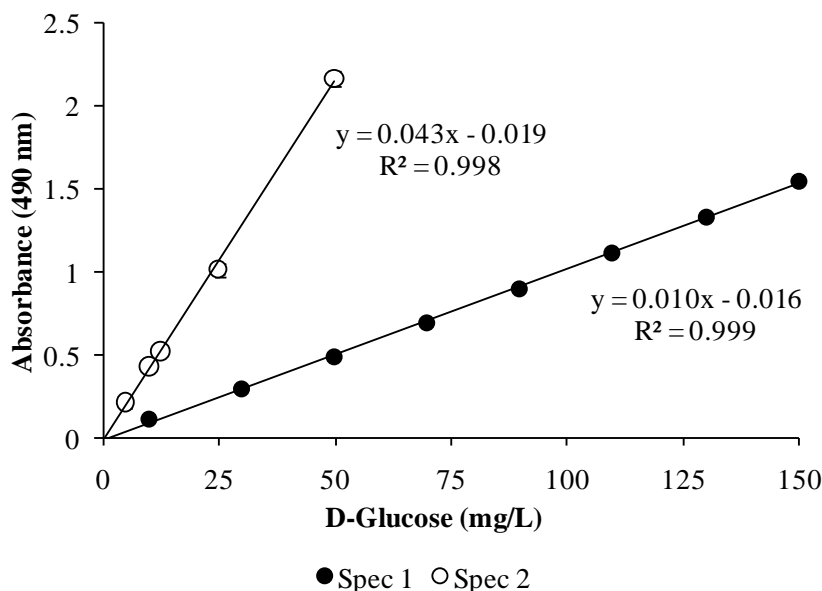


Figure IV.3: Plot of D-glucose versus absorbance at 490 nm for two different spectrophotometers (Spec 1, School of Biological and Conservation Science; Spec 2, Merck spectrophotometer at our laboratory).

There was a difference between the standard curves produced by each spectrophotometer. Each curve was replicated three times with very little deviation between replicates. The results indicate that there are differences in the reading between the spectrophotometers used. No correction was applied to differentiate between the two spectrophotometers.

APPENDIX V: NEWLANDS-MASHU PLANT

This section provides a brief history behind Water Research Commission (WRC) Project K5/2002 *The Evaluation of an Experimental DEWATS plant*. A field-based BORDA DEWATS was built to evaluate the treatment performance of the process under different loadings. A membrane chamber was included as part of the treatment train with the results from this thesis used to design the gravity-driven membrane unit. This project therefore represents the culmination of numerous studies at the Pollution Research Group into ABR technology including this work.

A 5.1 INTRODUCTION

The Pollution Research Group has been tasked with research activities of a technical demonstration DEWATS plant designed by BORDA. The design of the treatment plant is based on a technical report written by Sasse (1998) that has been used since the early 1990's to construct plants for the treatment of a variety of wastewaters including domestic wastewater in Southern Asia, South East Asia and parts of southern Africa (more content can be viewed in: <http://www.BORDA-net.org/modules/cjaycontent/index.php?id=29>). BORDA is also involved the training of various personnel to facilitate the dissemination of knowledge on the design, implementation and maintenance of DEWATS plants. Although many of these plants have been built and operated successfully, there has been very little performance monitoring and scientific evaluation of the processes in the plant as the main purpose of these plants is compliance monitoring.

In February 2009, a *Memorandum of Understanding* was signed between BORDA and the eThekweni Water and Sanitation division for a demonstration DEWATS plant. BORDA provided the designs for the demonstration plant and maintenance and operational guidelines whilst the eThekweni Municipality provided the construction costs. The Pollution Research Group was tasked by BORDA to co-ordinate the research activities for the demonstration plant and will be financed by the Water Research Commission (of South Africa) (Project K5/2002 - contract signed in March 2010). In July 2010, construction of plant was completed (without electrical installations) with the supervision of the eThekweni Water and Sanitation and the plant commissioned in October 2010 (Figure V.1).

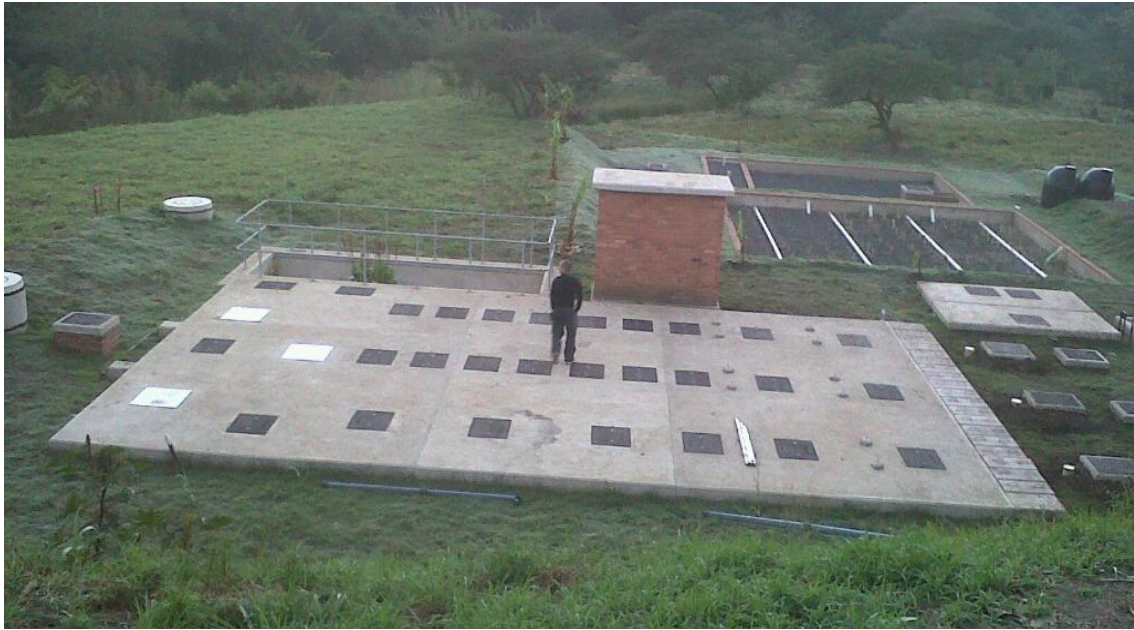


Figure V.1: Photograph of the site showing the experimental Newlands-Mashu plant designed by BORDA (PRG, 2010).

A 5.2 THE BORDA NEWLANDS-MASHU PLANT

The plant was constructed by a contractor, Small Civils, on a site on 71 John Dory Road (latitude = 29.7739, longitude = 30.9745) in Newlands-Mashu, Durban. The site is being used by a non-profit organisation, the *Newlands Mashu Permaculture Learning Centre* (NMPLC), to assist small-scale growers, emerging farmers and grower groups in producing agriculture products and providing practical assistance and support to run food programs in the area. The land was selected by the eThekweni Municipality based on the availability of land for construction and potential to re-use the treated wastewater in current horticultural activities at the site.

A trunk sewer connected to approximately 86 households in a residential area supplies approximately 40 m³/d to the plant. The incoming wastewater is treated by several treatment consecutive steps and processes. The wastewater enters a settling tank (which also functions as a biogas collector) in which grit and settling occurs. The wastewater then flows to three ABR treatment trains. All three trains are equal in length. Two of the trains have an identical number of ABR compartments (7) whilst a third train has less compartments (4) which are longer (Figure V.2). This larger chambered train was specifically included during the design and construction phase to evaluate the effects of lower upflow velocities on reactor performance. The rationale behind the change in design is based on the findings of Foxon (2009) who showed that lower upflow velocities improve reactor performance.

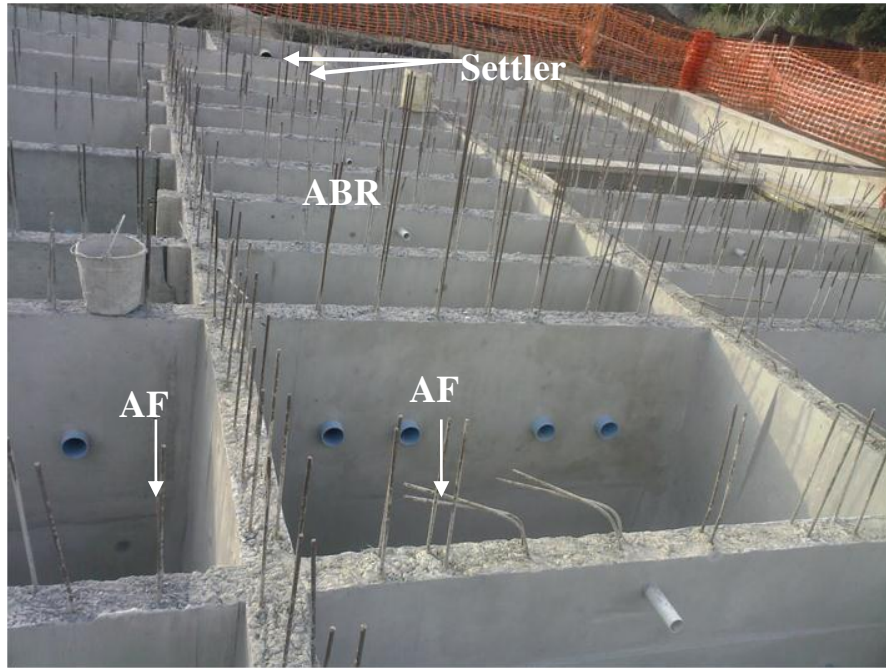


Figure V.2: Inside of the DEWATS plant showing the settler, three ABR trains and AF compartments (nearest compartments). The larger sized ABR compartments can be seen in the left of the picture (fewer walls) (PRG, 2010).

Each chamber or compartment has a set of downflow pipes as shown in Figure V.3. The plastic pipes have an internal diameter of 110 mm. The pipes have a siphon breaker to allow grease to float and prevent blockages. The flow to the next compartment occurs through a series of outlets that have been adjusted so that the water level is the same throughout each chamber. After the ABR, the flow moves through two successive anaerobic filters. A concrete slab with holes was laid just above the surface and the chamber filled with filter material (Figure V.3). The AF process is thought to provide enhanced removal of residual COD.

After the AF chambers all of the flow or parts can be distributed to two different polishing steps. The first consists of two types of constructed wetlands, a horizontal flow constructed wetland and a vertical flow constructed wetland that can be operated and tested individually. Alternatively, portions or all of the effluent can enter a membrane evaluation sump designed by Dr. S Pollet based on results presented in this thesis (Figure V.4). The sump has two chambers; a dry side where permeate can be collected and a wet side where membranes will operated under gravity. The sump was excavated to same depth as the settler-ABR-AF with 1 m of gravitational driving force available (from wet chamber to dry chamber) to drive membrane filtration. All flows from the sump can be directed back into the trunk sewer. A valve placed on the bottom of the wet chamber allows for the draining of the collected effluent.



Figure V.3: Downflow pipes in the AF chamber. Concrete slabs have been placed at the bottom and filled with graded material.



Figure V.4: Membrane evaluation sump designed by Dr. S Pollet. The sump has two sides; a wet side for immersing membrane modules and a dry side for collecting permeate. The sump was designed to the water level of the effluent pipes after the AFs and excavated to the depth of the settler-ABR-AF. Membranes will operate under a gravitational head in the wet chamber.

Medium-term filtration experiments presented in this thesis will be replicated in the experimental DEWATS plant by the Durban University of Technology. A flat-sheet housing unit containing woven-fibre modules has been designed to provide preliminary data on the flux-time relationships of these modules at different stages in the DEWATS process (Figure V.5). Hence, this experimental membrane system will not be installed in the membrane sump. The pressure for membrane filtration in this system would be provided by a peristaltic pump that would maintain a constant water head in the system (similar to the design used in this thesis).

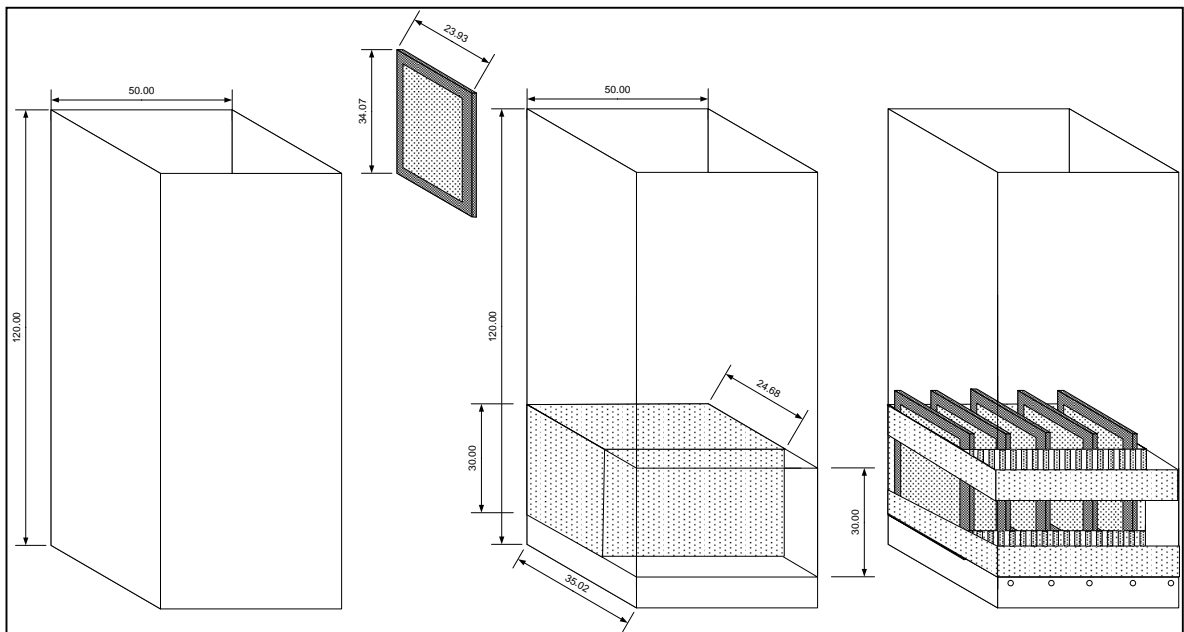


Figure V.5: Flat-sheet microfiltration housing unit designed by the Durban University of Technology. The experimental membrane unit will contain the same woven-fibre modules used in this thesis. The units of measurements in the diagram are cm. Picture courtesy of Prof. VL Pillay (Durban University of Technology).

As of July 2011, there has been no electrical installations implemented at the test site and thus no data for this membrane unit has been presented in this thesis. However, some preliminary operational data and results from the anaerobic (ABR-AF) and constructed wetland processes of the Newlands-Mashu DEWATS plant can be viewed in Pillay *et al.* (2011b).

APPENDIX VI: TECHNOLOGY TRANSFER

This section contains a summary of technology transfer items arising from this work. These include conference proceedings, publications and international and local collaboration.

A 6.1 CONFERENCE PROCEEDINGS

PILLAY S, YVENAT V, CABASSUD C, FOXON KM. AND BUCKLEY CA (2007) The characterisation of anaerobic feed solutions for flat sheet membranes. In: *Proceedings of the Water Institute of South Africa (WISA) Membrane Technology Division (MTD)*, Mabalingwe Nature Reserve, Limpopo, South Africa.

PILLAY S, FOXON KM AND BUCKLEY CA (2007) Anaerobic baffled reactor/membrane bioreactor (ABR/MBR) for on-site sanitation in low income areas. In: *Proceedings of the International Water Association (IWA) Specialist Membrane Conference*, Harrogate, Yorkshire, United Kingdom.

PILLAY S, FOXON KM AND BUCKLEY CA (2008) Performance of an anaerobic baffled reactor-membrane bioreactor treating blackwater, In: *Proceedings of the WISA Biennial Conference 2008*, Sun City, Limpopo, South Africa.

PILLAY S, FOXON KM AND BUCKLEY CA (2008) The treatment of blackwater using a combined anaerobic baffled reactor-membrane bioreactor (ABR-MBR). In: *Proceedings of the WISA Appropriate Technologies Conference 2008*, Fourways, Gauteng, South Africa.

PILLAY S, POLLET S, FOXON KM AND BUCKLEY CA (2010) A combination of an anaerobic baffled reactor with membrane filtration for decentralised wastewater treatment. In: *Proceedings of the IWA DEWATS Conference*, Surabaya, Indonesia.

PILLAY S, POLLET S, FOXON KM AND BUCKLEY CA (2010) Membrane processes in an anaerobic baffled reactor treating synthetic blackwater. In: *Proceedings of the WISA Biennial Conference 2010*, ICC Durban, South Africa.

A 6.2 PUBLICATIONS

PILLAY S, FOXON KM AND BUCKLEY CA (2008) Anaerobic baffled reactor/membrane bioreactor (ABR/MBR) for on-site sanitation in low income areas. *Desalination* **231** 91-98.

PILLAY S, POLLET S, FOXON KM AND BUCKLEY CA (2010) A combination of an anaerobic baffled reactor with membrane filtration for decentralised wastewater treatment. *Water Practice and Supply* 5.

A 6.3 INTERNATIONAL COLLABORATION

Mr. Valentin Yvenat, a student from INSA Toulouse (France), joined the Pollution Research Group (UKZN) as part of his degree requirements. He assisted with the set-up of the stirred cell apparatus and data collection on the filtration of supernatant from a secondary completely mixed anaerobic reactor. The experimental set-up was similar to that used by INSA for fouling propensity tests.

Mr. Diego Avesani, a Masters graduate from UNITN Trento (Italy), joined the project team in May 2008 to assist in the development of a biochemical model for the laboratory ABR system. Mr. Avesani spent 4 months in South Africa learning modelling programmes and operating ABR systems. Mr. Avesani was assisted by Dr. K Foxon and Dr. G Gugliemi in the model developed. The results of that work can be viewed in Pillay *et al.* (2011a).

The *Bremen Overseas Research and Development Association* (BORDA) has sent Mr. Sudhir Pillay to view full-scale plants in Lesotho, Indonesia and India. BORDA also provided scoping woven-fibre membrane filtration tests treating effluent from a DEWATS plant in Lesotho (Schmidt, 2010). The woven-fabric modules were identical to that used in this thesis and was delivered to BORDA by the Department of Chemical Engineering, Durban University of Technology. Mr.S Pillay was financed by BORDA to attend the IWA conference on DEWATS technology in Surabaya, Indonesia and to attend an engineering training course of design and construction of BORA DEWATS plants in Bangalore.

A 6.4 LOCAL COLLABORATION

The eThekweni Municipality has been actively involved in this project and have assisted in delivering greywater to the university, sampling for VIP waste and identifying sites for the full-scale DEWATS plant.

The Department of Chemical Engineering, DUT, has supplied woven-fibre modules for testing. The modules were constructed at that institution and delivered to the Pollution Research Group for membrane testing courtesy of Prof. VL Pillay.